ORDER

6820.10

VOR, VOR/DME, AND VORTAC SITING CRITERIA

APRIL 17, 1986

DEPARTMENT OF TRANSPORTATION
FEDERAL AVIATION ADMINISTRATION

Distribution: Selected Airway Facilities Field and Regional offices; ZAF-601
Initiated By: APM-420

FOREWORD

This order provides guidance and reference material to be used in certain practical applications of the very high frequency omnidirectional radio range (VOR), VOR distance measuring equipment (VOR/DME), and VOR tactical air navigation (VORTAC) in the Federal Aviation Administration's (FAA's) National Airspace System. It deals with the procedures and techniques that apply to the initial evaluation, selection, and acquisition of sites for these navigational aids. It also deals with site improvement and the minimization of performance degradation due to multipath. Finally, it provides guidance for the consolidation of buildings and antenna structures when such consolidation involves VOR, VOR/DME, or VORTAC installations.

Where the facilities consolidation program requires the relocation, consolidation, or establishment of a new VOR, VOR/DME, or VORTAC installation, this order provides technical guidance for the selection and acquisition of a site for the installation. It also provides technical guidance for improving the performance of VOR, VOR/DME, or VORTAC installations where performance degradation can be attributed to site conditions.

The guidance provided in this order applies to new establishments, relocated facilities, and consolidated facilities as specified by the facilities consolidation program. The guidance may also be applied to existing installations where performance is degraded to unacceptable levels by siting factors.

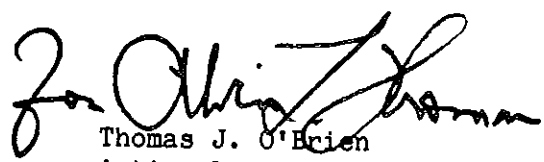

Thomas J. O'Brien
Acting Director, Program Engineering
and Maintenance Service

METRIC CONVERSION FACTORS

Approximate Conversions to Metric Measures

Symbol	When You Know	Multiply by	To Find	Symbol
	LENGTH			
in	inches	*2.5	centimeters	cm
ft	feet	30	centimeters	cm
yd	yards	0.9	meters	m
mi	miles	1.6	kilometers	km
	AREA			
in^2	square inches	6.5	square centimeters	cm^2
ft^2	square feet	0.09	square meters	m^2
yd^2	square yards	0.8	square meters	m^2
mi^2	square miles	2.6	square kilometers	km^2
	acres	0.4	hectares	ha
	MASS (weight)			
oz	ounces	28	grams	g
lb	pounds	0.45	kilograms	kg
	short tons (2000 lb)	0.9	tonnes	t
	VOLUME			
tsp	teaspoons	5	milliliters	ml
Tbsp	tablespoons	15	milliliters	ml
fl oz	fluid ounces	30	milliliters	ml
c	cups	0.24	liters	l
pt	pints	0.47	liters	l
qt	quarts	0.95	liters	l
gal	gallons	3.8	liters	l
ft^3	cubic feet	0.03	cubic meters	m^3
yd^3	cubic yards	0.76	cubic meters	m^3
	TEMPERATURE (exact)			
°F	Fahrenheit temperature	5/9 (after subtracting 32)	Celsius temperature	°C

*1 in = 2.54 (exactly). For other exact conversions and more detailed tables, see NBS Misc. Publ. 286, Units of Weights and Measures, Price $2.25, SD Catalog No. C13.10:286.

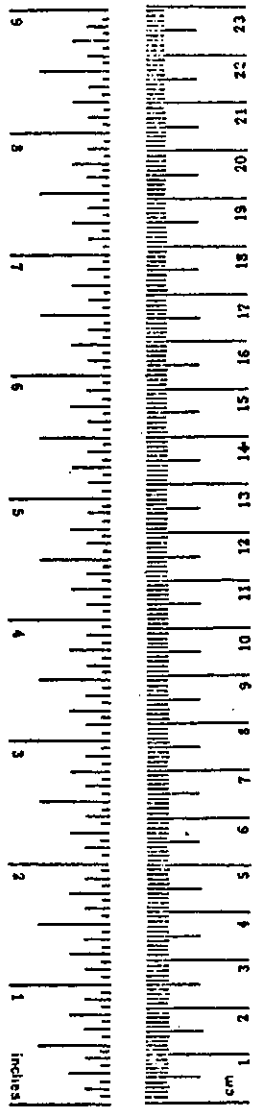

Approximate Conversions from Metric Measures

Symbol	When You Know	Multiply by	To Find	Symbol
	LENGTH			
mm	millimeters	0.04	inches	in
cm	centimeters	0.4	inches	in
m	meters	3.3	feet	ft
m	meters	1.1	yards	yd
km	kilometers	0.6	miles	mi
	AREA			
cm^2	square centimeters	0.16	square inches	in^2
m^2	square meters	1.2	square yards	yd^2
km^2	square kilometers	0.4	square miles	mi^2
ha	hectares (10,000 m^2)	2.5	acres	
	MASS (weight)			
g	grams	0.035	ounces	oz
kg	kilograms	2.2	pounds	lb
t	tonnes (1000 kg)	1.1	short tons	
	VOLUME			
ml	milliliters	0.03	fluid ounces	fl oz
l	liters	2.1	pints	pt
l	liters	1.06	quarts	qt
l	liters	0.26	gallons	gal
m^3	cubic meters	35	cubic feet	ft^3
m^3	cubic meters	1.3	cubic yards	yd^3
	TEMPERATURE (exact)			
°C	Celsius temperature	9/5 (then add 32)	Fahrenheit temperature	°F

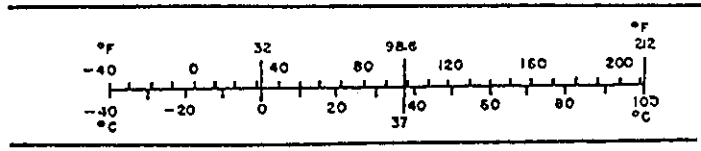

TABLE OF CONTENTS

LIST OF FIGURES

Page

LIST OF TABLES

CHAPTER 1. GENERAL

1. PURPOSE. This order provides guidance and reference material to be used in certain practical applications of the very high frequency omnidirectional radio range (VOR), VOR with distance measuring equipment (VOR/DME), and VOR with tactical air navigation (VORTAC) in the Federal Aviation Administration's (FAA's) National Airspace System (NAS). The order deals with the procedures and techniques that apply to the initial evaluation, selection, and acquisition of sites for these navigational aids. It deals with site improvement and the minimization of performance degradation due to multipath. Finally, the order provides guidance for the colocation of equipments and antenna structures when such colocation involves VOR, VOR/DME, or VORTAC installations.

2. DISTRIBUTION. This order is distributed to division level in the Program Engineering and Maintenance and Systems Engineering Services, in the Offices of Airport Standards and Flight Operations, and the Aviation Standards National Field divisions in Washington headquarters; to branch level in the regional Airway Facilities divisions and to the Airway Facilities sectors, sector field offices, sector field office units, and sector field units.

3. CANCELLATION. Order 6700.11, VOR/VORTAC Siting Criteria dated August 7, 1968, is canceled.

4. BACKGROUND. The first two chapters in this order provide an introduction and an overview of the subject matter. Chapters 3, 4, and 5 deal with site evaluation, acquisition, and improvement, respectively. These are intended to be the "how-to-do-it" chapters. Chapters 6, 7, and 8 represent in-depth presentations of technical information useful in the siting process. Chapters 6 and 7 present results from analysis of wave propagation and interference. These results have been used in summary fashion or by reference in the earlier chapters. Chapter 8 presents information on computer simulation models that have proven to be useful in the applications of interest here.

5. DEFINITIONS.

a. VOR, as its name indicates, is a navigational aid that operates in the very high frequency (vhf) band of the radio spectrum and that radiates uniformly in azimuth. Specifically, this facility operates between 108 MHz and 118 MHz and provides azimuth guidance to the pilot in the form of a visual display. There are two general types of VOR systems being used by the FAA, namely, the conventional VOR and the Doppler VOR.

b. DME is used for measuring the slant range between the aircraft and the facility. It operates in the 960- to 1215-MHz portion of the radio spectrum.

c. VOR/DME refers to associated VOR and DME systems. VOR and DME are the International Civil Aviation Organization (ICAO) standard for navigation.

d. Tactical air navigation (TACAN) was developed by the military, which accounts for the term "tactical." It operates in the same frequency range as DME and provides omnidirectional azimuth information primarily for military users of the NAS and distance information to all users of NAS. The distance measuring portion of the TACAN is compatible with the DME described above.

e. VORTAC refers to associated VOR and TACAN navigational facilities providing both azimuth and distance information to all users of the NAS.

f. The systems to be considered are presented in table 1-1. The VORTAC combination of systems is also referred to as the VOR/DME/TACAN system and is the short distance navigation system providing navigational signals to properly equipped civil and military aircraft (see also figure 1-1). For further details refer to FAA Order 9840.1, U.S. National Aviation Standard for the VOR/DME/TACAN Systems, September 9, 1982.

TABLE 1-1. SUMMARY DEFINITIONS OF SHORT DISTANCE NAVIGATION SYSTEMS

Designation	Type of Facility
VOR	vhf navigational facility, omnidirectional azimuth only
DME	uhf navigational facility, distance only
TACAN	uhf navigational facility, omnidirectional azimuth and distance
VOR/DME	associated VOR and DME navigational facilities
VORTAC	associated VOR and TACAN navigational facilities

6. APPLICATION. The criteria set forth in this order apply only to new establishments or relocated facilities. Changes to existing facilities for the sole purpose of obtaining compliance with this criteria are not required.

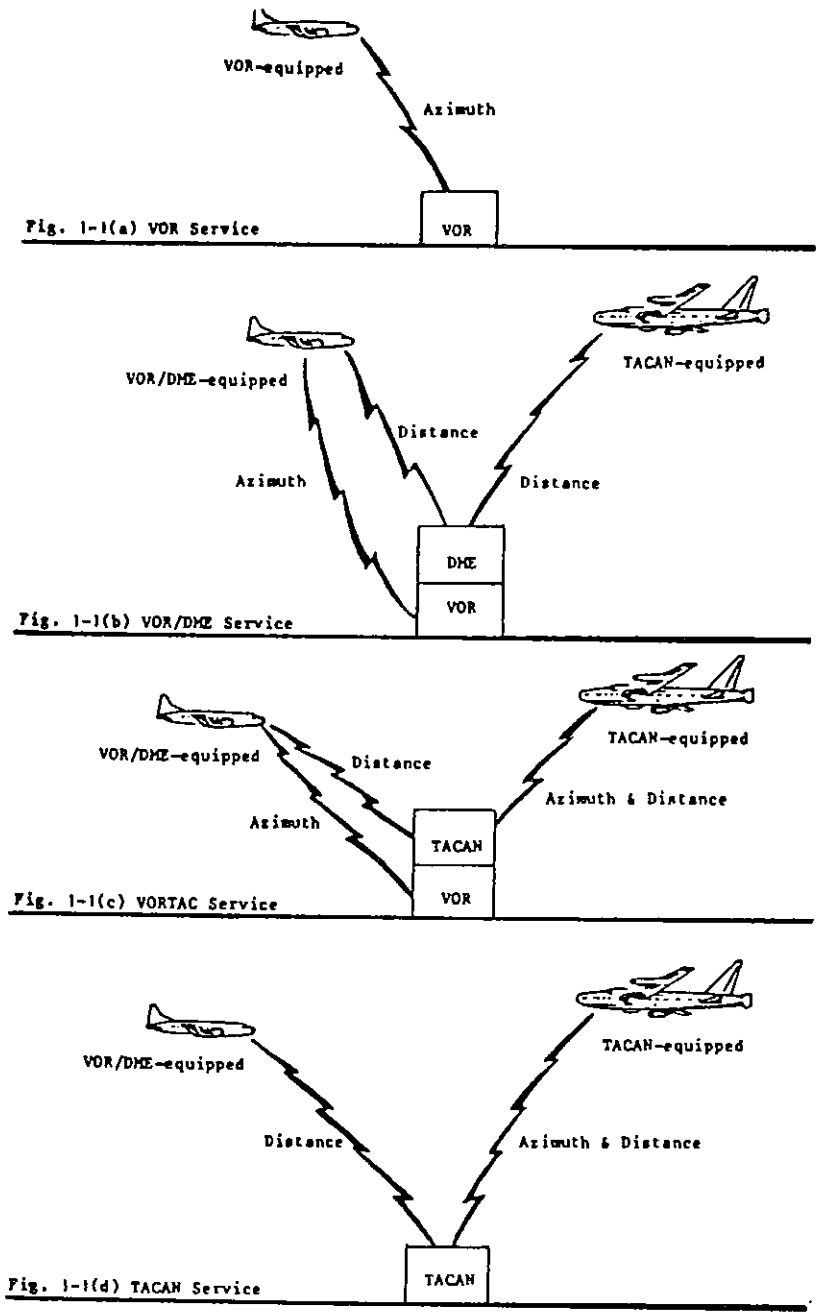

FIGURE 1-1. SHORT RANGE NAVAID GROUND STATION ARRANGEMENTS

7. SYSTEM CONCEPTS.

a. VOR.

(1) Both conventional VOR and Doppler VOR operate in the 108- to 118-MHz frequency band. Both VORs provide separate 30-Hz am and fm signals to the airborne avionics for phase comparison to determine the azimuth of the aircraft from the VOR site at a given time. The phase difference between the two 30-Hz modulation components is equal to the azimuth (in degrees clockwise from magnetic North) from the VOR site.

(2) Conventional VOR provides a 9960-Hz subcarrier modulated with a fixed-phase 30-Hz fm and a 30-Hz am whose phase is lagging the 30-Hz fm component proportional to the azimuth of the avionics from the VOR. Doppler VOR provides a 9960-Hz subcarrier modulated with a fixed 30-Hz am and a 30-Hz fm advancing counterclockwise, which also produces a phase difference proportional to the azimuth of the avionics from the VOR.

(3) The aircraft avionics is indifferent to whether its input signal is conventional or Doppler VOR. The avionics simply recovers the 30-Hz am and the 30-Hz fm, determines how much the am lags the fm, and displays that phase difference as azimuth from the VOR.

b. Conventional VOR.

(1) The VOR operates on the principle that measurement of the phase difference between two signals can be employed to determine azimuth if one of the signals maintains a fixed phase through 360 degrees and serves as a reference, and the phase of the second signal is made to vary as a direct function of azimuth. In practice, two 30-Hz signals are used and are termed the "reference phase" signal and the "variable phase" signal.

(2) The analogy used to describe VOR is that of a light bulb in the center of a large circle with 360 light bulbs each one degree apart on the circumference. The center bulb and the one due north are pulsed to light at the same time; then each bulb clockwise is pulsed to light in turn so that in 1/30th of a second the complete circle of bulbs is traversed and, once more, the center bulb and the north bulb light simultaneously. An observer, located on the north radial, would establish his direction by observing that the two bulbs in his line of vision were illuminated simultaneously. An observer on another radial would establish his azimuth by measuring the time delay between the illumination of the two bulbs in his line of vision.

(3) A pair of dipole antennas placed close together along the north-south line in a common equatorial plane and fed with electromagnetic (em) energy of equal amplitude but opposite phase will radiate a cosine pattern in that plane.

Consider such a pair of dipoles oriented along a northwest-southeast line. If the radio frequency (rf) carrier is modulated with a sinusoid of angular frequency, then the radiated pattern can be expressed as:

$$e_{NW-SE} = E_1 \cos \Theta \cos W_m t$$

A second pair of dipoles mounted concentric and coplanar with the first pair but aligned along the northeast-southwest line can, with proper adjustment be made to provide the pattern:

$$e_{NE-SW} = E_1 \sin \Theta \sin W_m t$$

The resultant field is a double sideband suppressed-carrier signal, with the sidebands in phase quadrature:

$$e = e_{NW-SE} + e_{NE-SW} = E_1 \left[\cos \Theta \cos W_m t - \sin \Theta \sin W_m t\right]$$

$$= E_1 \cos \left[W_m t + \Theta\right]$$

Thus the envelope of the carrier has a phase delay that varies one degree electrically for each degree of physical azimuth. To eliminate the symmetry, which causes a 180-degree ambiguity, an omnidirectional signal of constant amplitude is added to yield the final field amplitude of:

$$e_{TOT} = E_o + E_1 \cos (W_m t + \Theta)$$

which yields a limacon rotating at the angular frequency W_m. See figure 1-2.

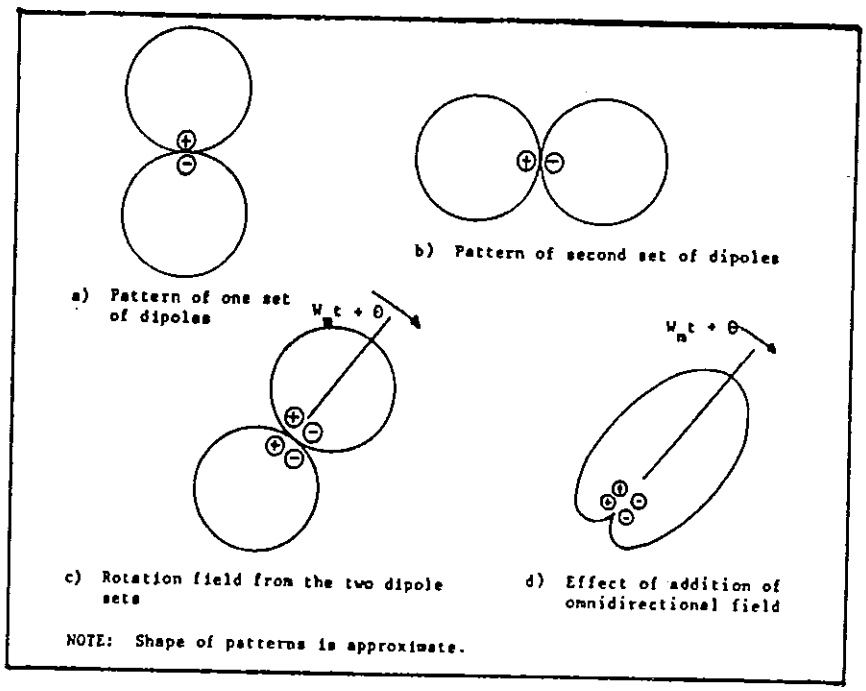

FIGURE 1-2. COMPONENTS OF THE VOR RADIATION PATTERN

(4) In conventional VOR, the variable-phase 30-Hz signal is radiated as a double sideband suppressed carrier (DSB-SC) modulation. The composite modulated signal, made up of a carrier and two sidebands in quadrature, is structured as three separate signals radiated independently which are combined in the receiver detector. This technique of space modulation is susceptible to multipath interference, since each radiated signal component may take a slightly different path to the receiver. Space modulation contrasts with the more conventional modulation techniques wherein the complete composite signal is created within the transmitting equipment, and the components travel together to the receiver.

(5) In the 4-loop antenna array, the modulated rf carrier containing the 30-Hz reference signal is fed, through a bridge network, to each of the four loops in phase. This provides the desired composite carrier circular (omnidirectional) radiation pattern. For the variable-phase signal, two separate sets of 30-Hz sidebands are generated by a rotating capacitor goniometer. The phase of one sideband varies as the sine of the goniometer angle. The phase of the second varies as the cosine of the goniometer angle. In the most recent equipment, the goniometer has been replaced with solid-state circuitry which performs the same function. The combination of the relationship of sideband signals and antenna geometry results in a radiated signal whose phase angle is a direct measure of azimuth as illustrated in figure 1-2 and the associated discussion. In the aircraft, presuming no distortions from multipath, the phases of the reference and the variable signals are compared to determine a line of position along which the phase difference is constant.

(6) Phase coherence in the 30-Hz reference and variable signals is obtained in the older equipment through electromechanical coupling and, in more recent equipment, through solid-state circuitry.

c. Doppler VOR.

(1) The Doppler VOR, DVOR uses a completely different method from that of conventional VOR for generating the azimuth information but, nevertheless, may be used with the conventional VOR aircraft receiver. If a distant radiating source is rotating sufficiently rapidly to create a noticeable Doppler shift, an aircraft properly instrumented can determine when the radiating source is in line with the aircraft and the center of rotation by the disappearance of the Doppler shift.

(2) The generation of the radiated variable-frequency DVOR signal is usually explained in terms of an analogy. Imagine a single radiating antenna located at the end of a 22-foot beam and rotating about a central point at the rate of 30 revolutions per second (rps). At the midfrequency of the 108- to 118-MHz VOR band, 113 MHz, this rotational motion causes a frequency deviation of +/-480 Hz due to the Doppler effect. An antenna located at the center of rotation radiates a signal which differs in frequency by 9960 Hz from the center frequency of the rotating radiator. The beating of these two frequencies in the receiver produces a 9960-Hz subcarrier which is frequency modulated at a 30-Hz rate by the +/-480-Hz deviation in the radiation from the rotating antenna. The deviation ratio of 16 of the 30-Hz fm is the variable signal in DVOR which fm capture effect protects from the interfering effects of multipath or noise.

(3) In the DVOR, the antenna field which simulates the single rotating antenna is made up of 50 separate antennas equally spaced in a circle of 22-foot radius. The 50 antennas are fed em energy sequentially to simulate the rotation. In older models of DVOR, the energy distribution is by means of an electromechanical distributor rotating at 30 rps. More recent models achieve the same effect with solid-state circuitry and electronic switching.

(4) The 30-Hz am reference phase signal for DVOR is carried as DSB-SC modulation on the carrier frequency and radiated from a centrally located antenna. The signal is less susceptible to multipath than is the equivalent DSB-SC space modulated signal in conventional VOR. The DVOR 30-Hz reference signal, however, should be carefully filtered in the airborne receiver if the best performance is to be achieved from DVOR.

(5) DVOR exists in the double sideband Doppler VOR (DSBDVOR) and single sideband Doppler VOR (SSBDVOR) versions. If the rotating distributor feeds rf energy simultaneously to oppositely located circumferential antennas, a double sideband Doppler signal is produced. Tests have revealed that DSBDVOR is much less susceptible to errors due to a coaxially located VOR and TACAN antennas than is SSBDVOR and, hence, may be superior for some applications.

(6) A summary comparison of the basic characteristics of conventional VOR and DVOR is contained in table 1-2. The conventional VOR and DVOR sites are generally similar but readily distinguished because of the multiple DVOR sideband antennas. See figures 1-3 and 1-4.

TABLE 1-2. SUMMARY COMPARISON OF BASIC CHARACTERISTICS OF CONVENTIONAL VOR AND DVOR

Parameter	Conventional VOR	Doppler VOR
Reference Signal	30-Hz fm, β of 16, modulation of 9960-Hz subcarrier	30-Hz, DSB-SC amplitude modulation of rf carrier
Variable Signal	30-Hz, DSB-SC amplitude modulation of rf carrier	30-Hz fm, β of 16 modulation of 9960-Hz subcarrier
Rotation of Intelligence	Peak amplitude rotates clockwise at rate of 30 rps	Peak frequency deviation rotates counter-clockwise at rate of 30 rps
Counterpoise	52' or 21' diameter	SSBDVOR - 150' diameter DSBDVOR - 100' diameter

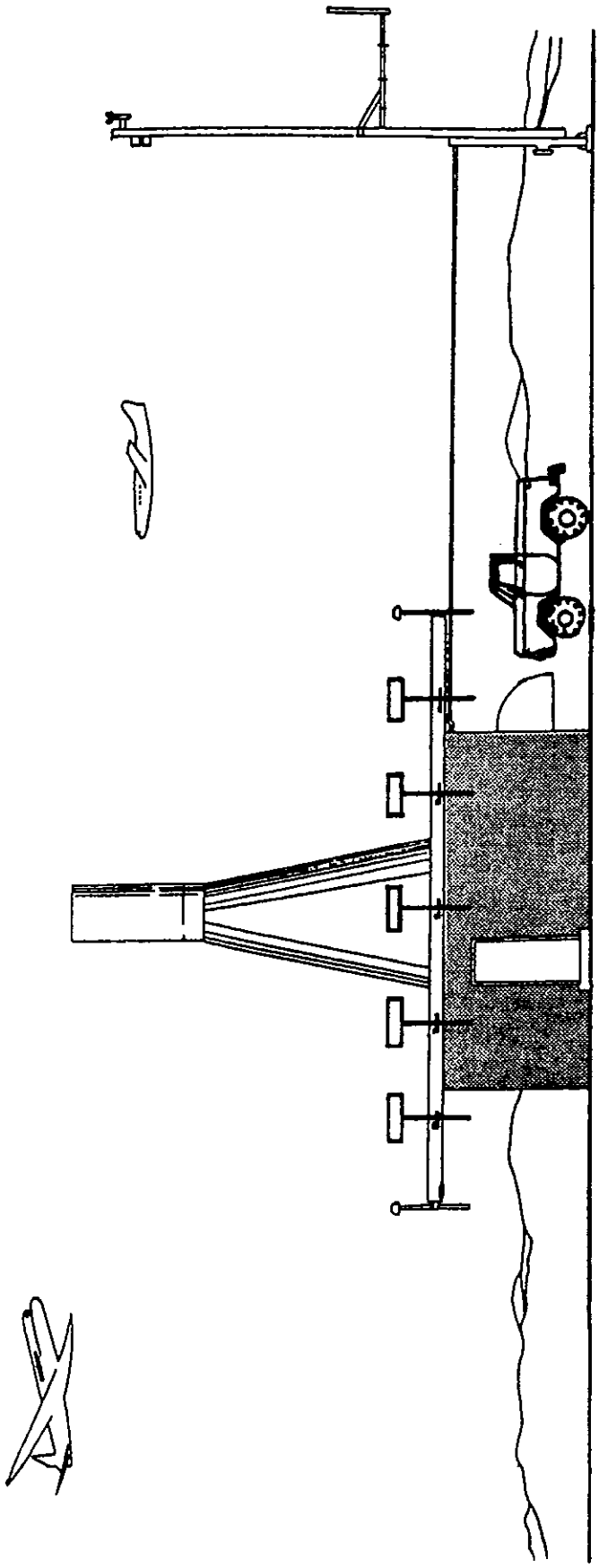

FIGURE 1-3. TYPICAL INTEGRAL VORTAC FACILITY

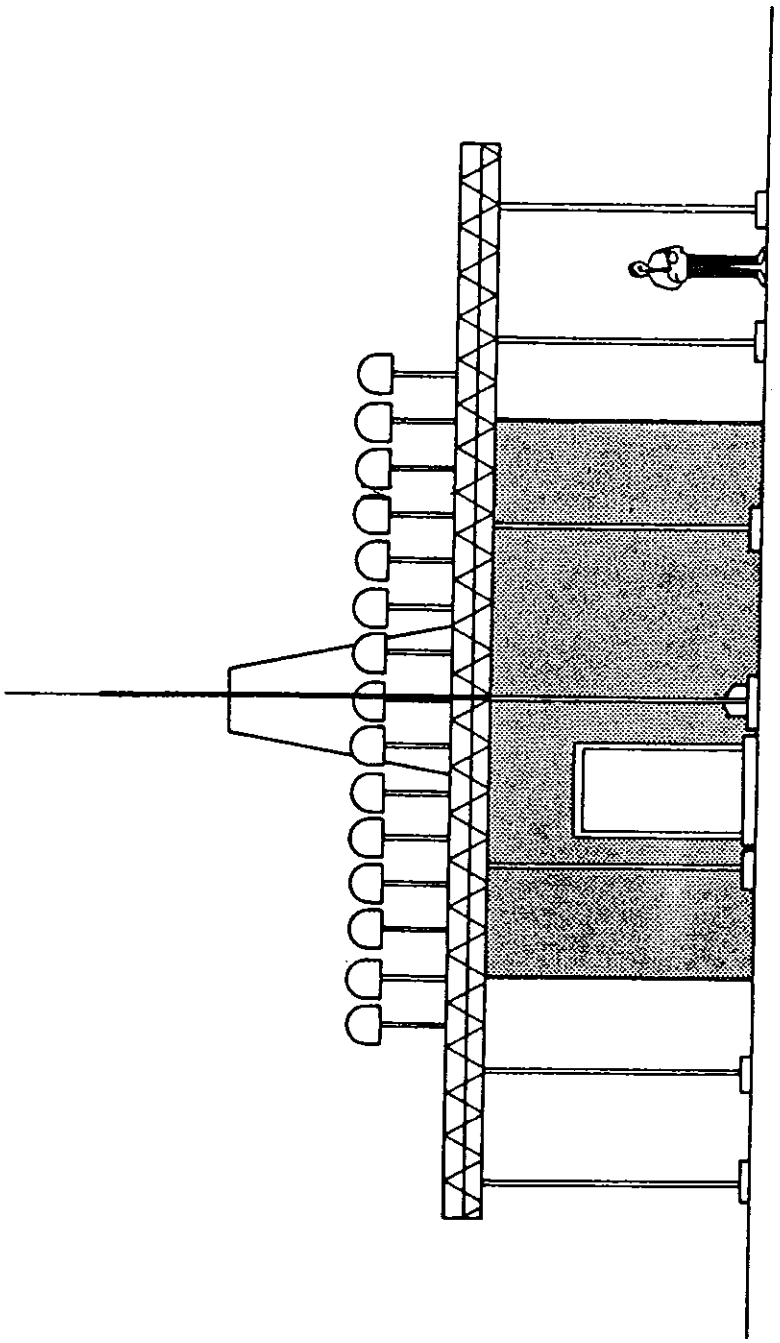

FIGURE 1-4. TYPICAL DVOR FACILITY

d. DME.

(1) The DME operates in the 960- to 1215-MHz band to enable a properly equipped aircraft to determine its slant range to the DME site by measurement of the travel time of pulse-modulated radio waves. The aircraft transmits a radio signal to a ground station. The ground station transmits a response signal to the aircraft on a second frequency, and the DME equipment in the aircraft measures the time interval between the transmission of the interrogation signal and the reception of the reply signal. Knowing that the time delay for the round trip is proportional to distance and allowing for the delay in the ground-based equipment, the airborne instrument displays the slant distance on the distance indicator.

(2) The x-mode interrogation signal from the aircraft itself consists of two pulses spaced 12 microseconds apart, each pulse being 3-1/2 microseconds in width. The reply is very similar: an identical pair of pulses having the same pulse width and spacing but on a different frequency 63 MHz from the interrogation signal (see figure 1-5). There are a hundred DME channels allocated in the frequency range of 1041 to 1150 MHz. These are in 1-MHz steps and, of course, there are likewise 100 reply frequencies which are in the two bands, 978 to 1020 MHz and 1157 to 1215 MHz, the frequency difference being in all cases 63 MHz between the aircraft transmitted frequency and the reply frequency. These frequency channels, incidentally, are paired on a channel-for-channel basis with the ILS (108-112) or VOR (112-118) navigation channels between 108 and 118 MHz.

(3) The pulse replies from the ground station are mixed with many others which are replies to other aircraft. The appropriate replies must be distinguished and identified at the aircraft by their phase coherence with the original interrogation pulses.

(4) The DME antenna generally is mounted above and coaxially with the VOR antenna in the center antenna housing on the VOR counterpoise (figure 1-6).

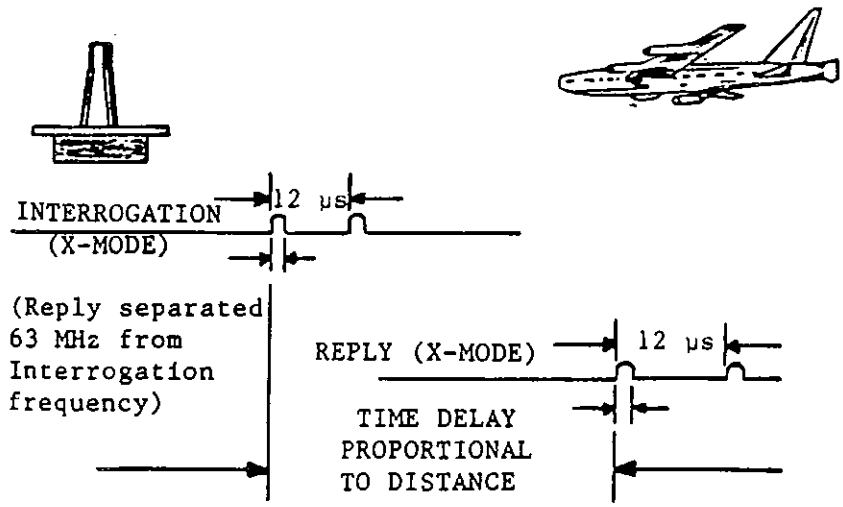

FIGURE 1-5. DME X-MODE PULSE CHARACTERISTICS

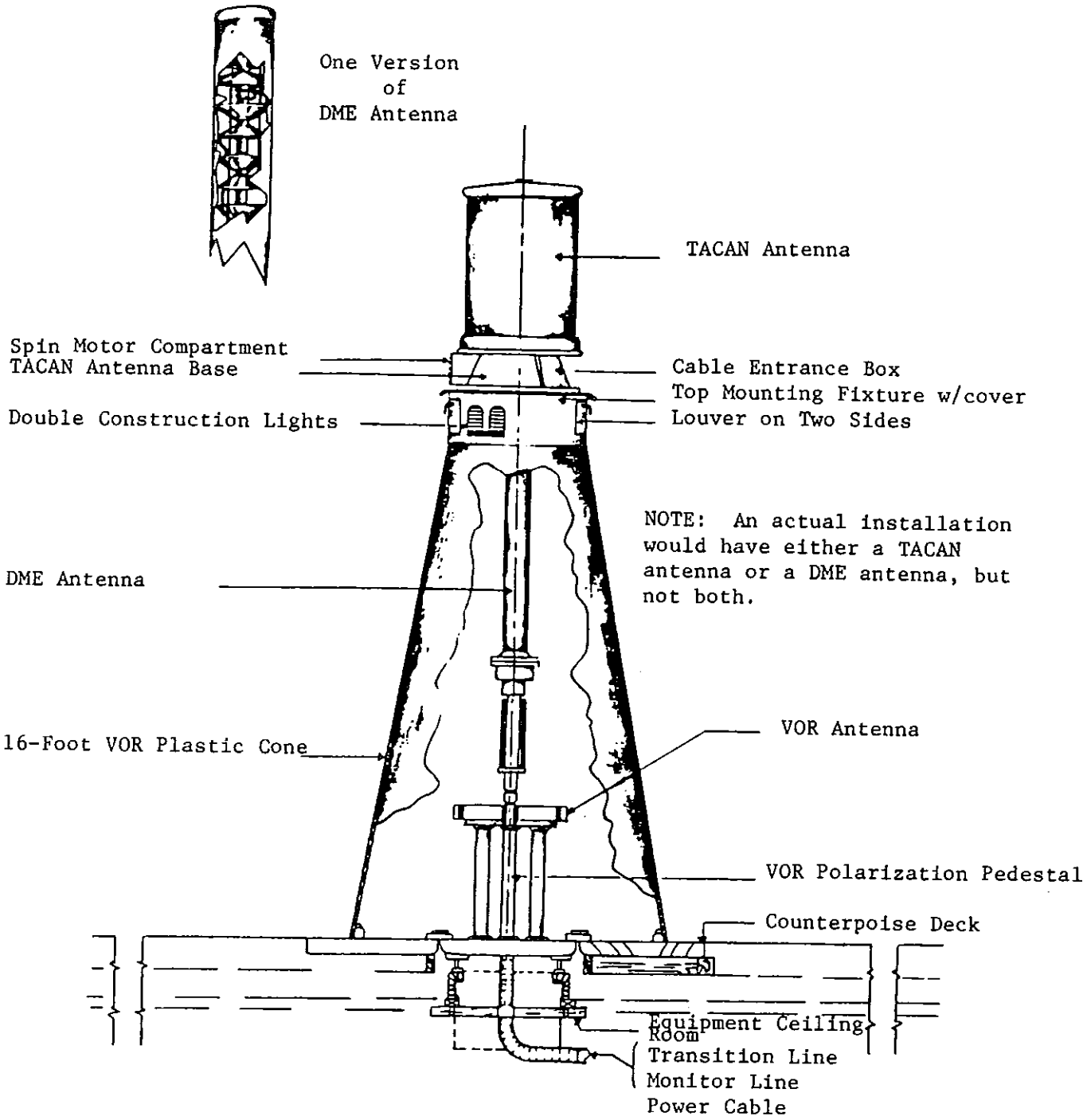

FIGURE 1-6. HOUSING FOR COAXIALLY MOUNTED NAVAID ANTENNAS

e. The TACAN Azimuth Determining Subsystem.

(1) The azimuth-determining TACAN subsystem, operating in the same frequency range as DME, utilizes a single radiated pattern rotating at 15 rps to provide a signal variable with azimuth in a scheme similar to that of conventional VOR. Superimposed upon this pattern is one rotating at 135 rps which provides a fine structure for a more accurate determination of azimuth than could be obtained from the 15-rps signal alone. The 15-Hz and 135-Hz signals appear as amplitude modulation of the train of DME pulse pairs. See figure 1-5. When such pulse pairs are not sufficiently frequent to support the am signals, additional randomly spaced pulse pairs called squitter pulses must be generated. A reference signal, called the North reference burst, is transmitted for each revolution of the director elements. Eight additional signals, called auxiliary reference bursts, are transmitted between North reference bursts, dividing each North reference burst cycle into nine equal parts. Since the coded characteristics of the different signals are not relevant to siting problems, they are not presented herein. For details on the signal coding, see MIL-STD-219A, Standard Tactical Air Navigation (TACAN) Signals.

(2) The 15-Hz and 135-Hz modulation signals are developed by mechanically rotating passive elements within the TACAN antenna assembly. See figure 1-7. The resulting radiation pattern developed in terms of the various contributing elements in the radiating antenna structure is shown graphically in figure 1-8. For a more detailed discussion, refer to the text by Greco and Reed entitled, TACAN - Principles and Siting Criteria published in 1968 by the Naval Electronic Systems Test and Evaluation Facility (renamed Naval Electronic Systems Engineering Activity, Code 0242, St. Inigoes, MD 20684).

(3) Figure 1-9 illustrates the bearing location of a receiver with respect to the TACAN beacon. The TACAN antenna assembly is aligned so that the omnidirectional reference burst is emitted when the maximum of the cardiod pattern is pointed to the geographic east. Figure 1-9 is a simplification to the extent that the 135-Hz fine structure is suppressed. As shown in the figure, the observer located due north of the TACAN antenna receives the coded reference burst on the 15-Hz sinusoid on its negative slope halfway between the maximum and minimum points.

(4) In practice, most TACAN airborne equipments utilize the North reference burst and the 15-Hz am to determine the azimuth of the TACAN transmitter within a 40-degree section ("coarse" bearing), and then utilize the auxiliary reference bursts and the 135-Hz am to determine the actual station azimuth within the 40-degree sector ("fine" bearing). The "fine" bearing provides a 9-to-1 improvement over the "coarse" 40-degree sectors in determining the azimuth.

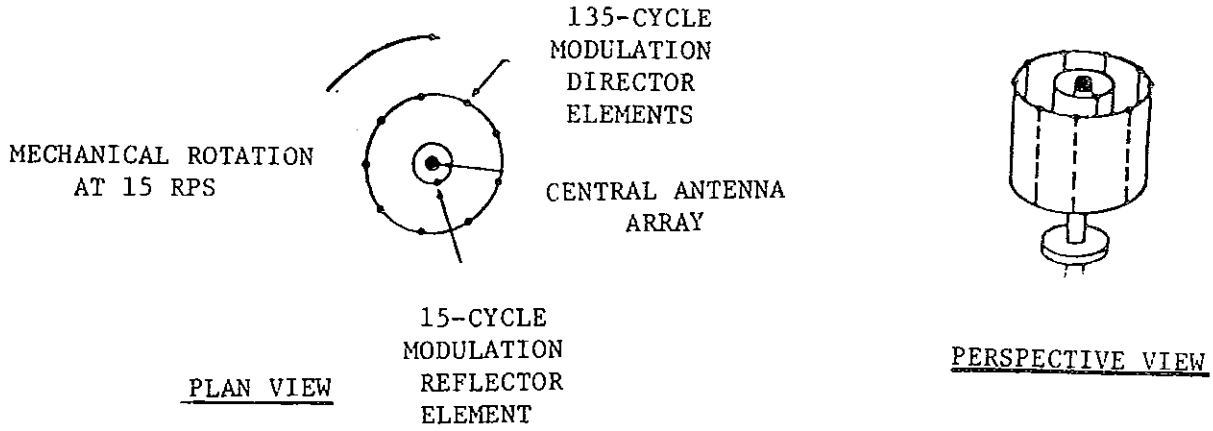

FIGURE 1-7. THE TACAN ANTENNA CONCEPT

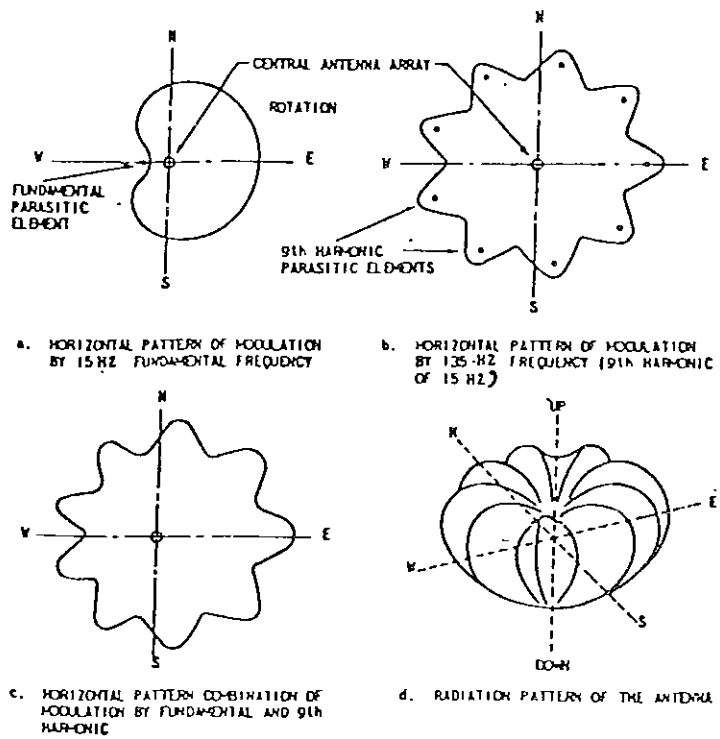

FIGURE 1-8. COMPONENTS OF THE TACAN RADIATION PATTERN

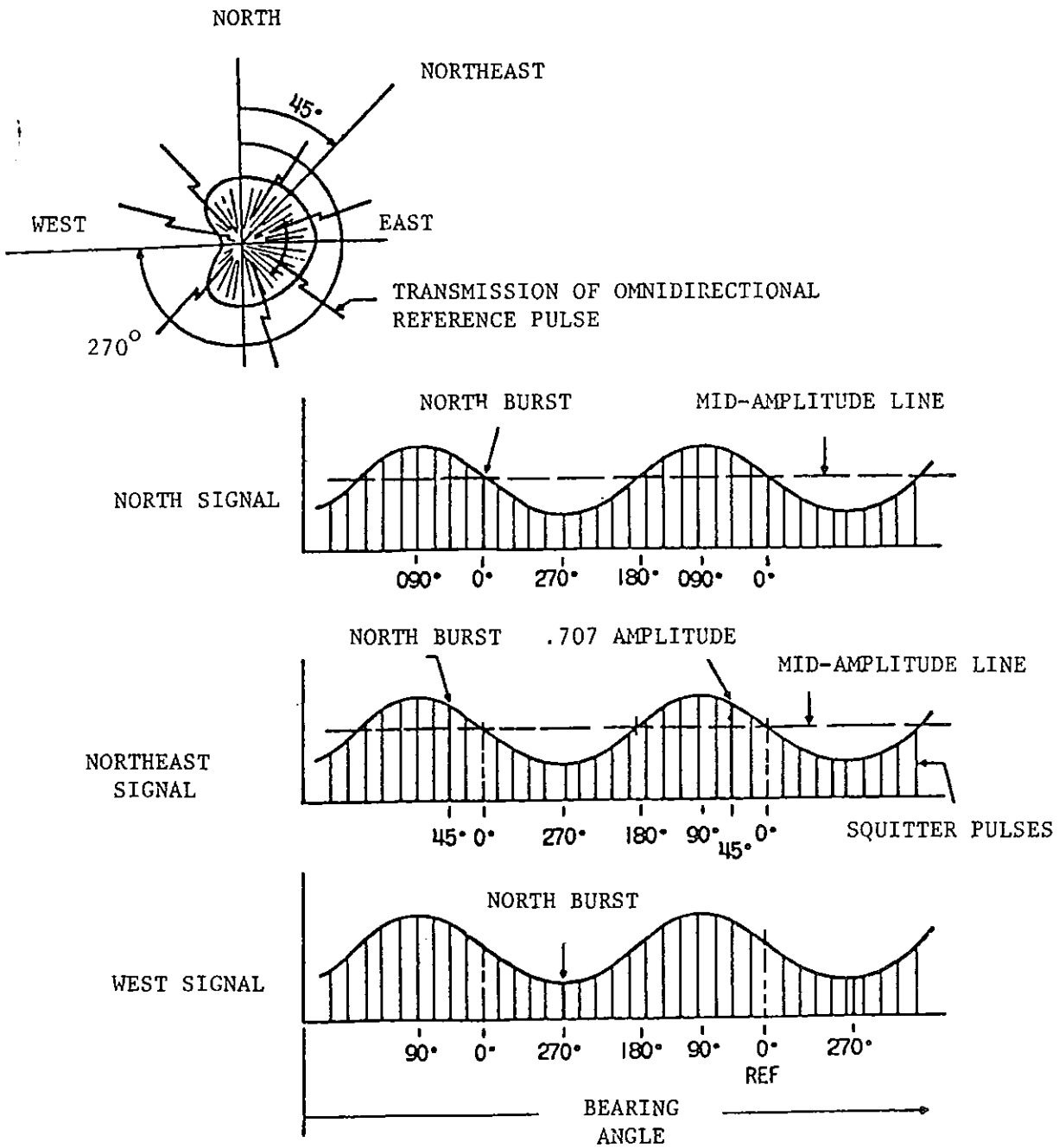

FIGURE 1-9. ILLUSTRATING GEOGRAPHIC BEARING FROM BEACON

CHAPTER 2. OVERVIEW OF LOCATION AND COVERAGE CONSIDERATIONS

8. GENERAL. This chapter provides general background on the subject of the siting of VOR, VOR/DME, and VORTAC as an introduction to chapters 3, 4, and 5 which deal with site evaluation, acquisition, and improvement, respectively.

a. When a TVOR or VORTAC is installed on an airport, the facility should be located, if possible, in an area adjacent to the intersection of the principle runways in order to provide approach guidance to the ends of these runways. To prevent the facility from being an obstruction to aircraft, it should not be located closer than 500 feet to the centerline of any runway or 250 feet to the centerline of a taxiway. Additionally, no part of the facility shall penetrate any surface defined in paragraphs 77.25, 77.28, or 77.29 of the Federal Aviation Regulations.

b. When located off an airport, consideration shall be given to selecting a site so that one or more of the course radials will provide an approach procedure to the primary bad weather runway in accordance with chapter 4 or chapter 5 of FAA Order 8260.3B, United States Standard for Terminal Instrument Procedures.

c. TVOR/VORTAC facilities on airports come under paragraph 77.15(c) of the Federal Aviation Regulations and do not require submission of a Notice of Construction or Alteration.

d. All of the navaids under consideration use either the phase difference between sinusoids of the same modulating frequency, or the time difference between pulses, or in the VORTAC azimuth determination a hybrid of the two. DVOR may be considered a special case of phase difference determination. In brief, the information is contained in the modulation rather than in the carrier. The modulation is at a much lower frequency than is the carrier. It follows that phase, amplitude, or frequency distortion of the modulation will usually cause performance errors, and similarly, momentary phase, amplitude, or frequency distortions of the rf carrier are not ordinarily of concern. An exception to this statement is noted below.

e. The one situation where interactions at rf are of critical importance is that where the combination of the direct ray and the interfering ray due to longitudinal multipath results in destructive interference causing a null in the radiation pattern at a specific elevation angle. The complete destruction of the carrier destroys the modulation information as well.

f. Lateral multipath can, in certain of the navaids, cause rays emitted from the navaid ground station at different azimuth angles to meet and combine at the airborne equipment. The combination of two different modulating signals yields a resultant generally containing false bearing information.

g. Note that longitudinal multipath cannot ordinarily cause errors in the modulating intelligence except, as mentioned, when it causes the serious weakening of the total signal. Similarly, lateral multipaths cannot cause nulls in the vertical radiation pattern. Figure 2-1 illustrates the two different categories of multipath. The objective of successful siting is that of avoiding the harmful effects of either type of multipath within the required coverage volume of the navaid.

h. The DME and TACAN radiations are vertically polarized. By contrast, VOR and DVOR radiations are horizontally polarized. For vertical polarization there is an angle of incidence on a smooth earth at which the reflected component, the longitudinal multipath, vanishes. This is the angle of incidence at which the radiation refracted into the ground and the reflected radiation, if it existed, would be at right angles (see figure 2-2). Related to the Brewster's angle effect is the much smaller coefficient of reflection from the ground for vertically polarized rays compared to horizontally polarized rays.

i. As shown in figure 2-3, the longitudinal multipath can result from reflection from the counterpoise and from the earth. Additionally, the diameter of the counterpoise can be selected so as to set a lower limit to the grazing angle of the radiation illuminating the earth.

j. In the material which follows and in the remainder of the order, certain parameters associated with the radiated energy will be useful. These parameters are summarized in table 2-1. Note that the quantities provided are often only approximates. For site evaluation and improvement activities, the quantities of table 2-1 will usually be found to be both convenient and sufficient. In applications requiring greater accuracy, the actual wavelength should be used and antenna heights should be determined by measurement.

k. As illustrated in figure 2-4, reflection can be specular or diffuse. Specular reflection provides a stronger signal in a specific direction than does diffuse reflection. Hence, if specular reflection causes undesirable interference, the interference can be expected to be relatively strong. Diffuse reflection from a rough surface is unpredictable in its effects. If the reflecting area is sufficiently large it can cause multipath problems. See figure 2-5 for an example of directional reflection due to periodicity in the roughness.

l. Judgement is required to determine whether or not a particular ground will be seen as rough or smooth by the electromagnetic energy. The criterion that is usually used is the Rayleigh criterion. See figure 2-6 and note that for small grazing angles a very irregular ground can act as a smooth reflective surface.

m. The brief review of the discussion of multipath is summarized in table 2-2.

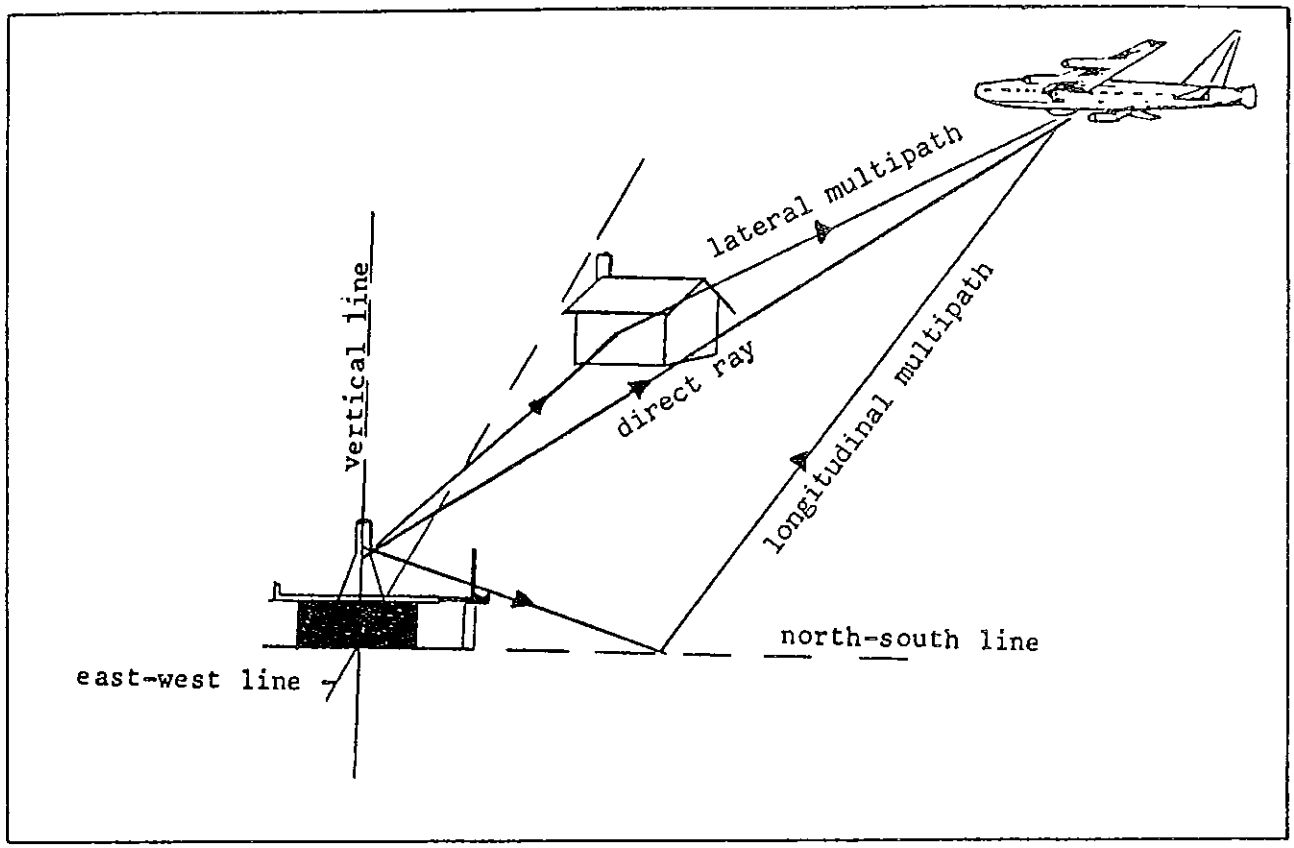

FIGURE 2-1. TYPES OF MULTIPATH

Type of Earth	Brewster's Angle at 1000 MHz (Approx)
Marshland	10°
Average	15°
Desert	30°

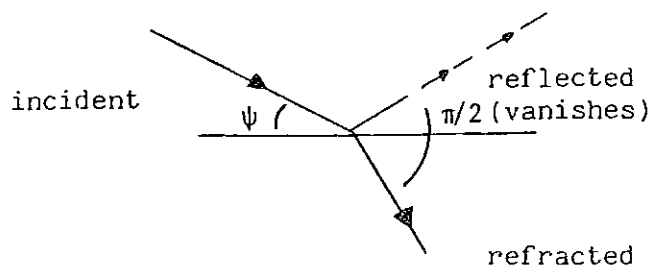

FIGURE 2-2. THE VANISHING OF REFLECTIONS AT BREWSTER'S ANGLE

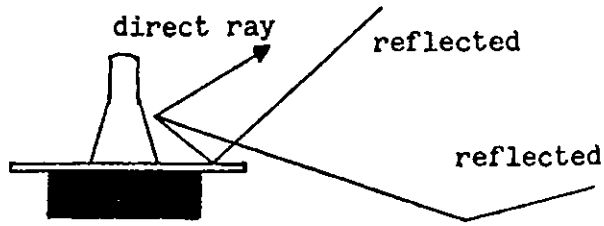

FIGURE 2-3. TWO LEVEL LONGITUDINAL MULTIPATH

TABLE 2-1. USEFUL PARAMETERS IN SITE EVALUATION

System	rf Carrier	Nominal rf Wavelength	Polarization	Ht Above Counter-poise*	Modulation	Max. Freq. of Modulation
VOR/ DVOR	108-118 MHz	8 ft	Horizontal	4.0 ft	Sinusoid (DSB-SC)	10,540 Hz
DME	962-1213 MHz	1 ft	Vertical	11.5 ft	Pulse	1 MHz**
TACAN	962-1213 MHz	1 ft	Vertical	20.5 ft	Pulse & Sinusoid	1 MHz**

* Height of effective radiating center above counterpoise. The figures given here are only approximate and should be checked for a specific installation. Counterpoise height is usually 12' but it also may vary; typical diameters are 52 feet and 21 feet (VOR), 150 feet (SSBDVOR), and 100 feet (DSBDVOR).

** Estimated on the basis of pulse rise time of 2.5 + 0.5 - 1.0 microseconds.

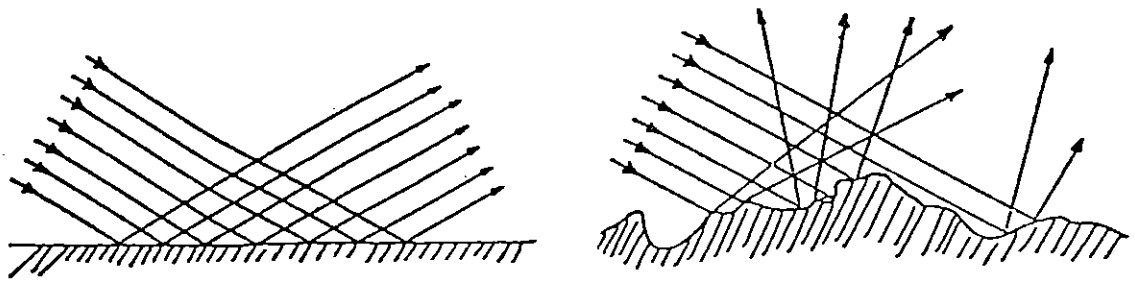

SPECULAR REFLECTION

DIFFUSE REFLECTION

FIGURE 2-4. EFFECTS OF TERRAIN IN PRODUCING SPECULAR & DIFFUSE REFLECTION

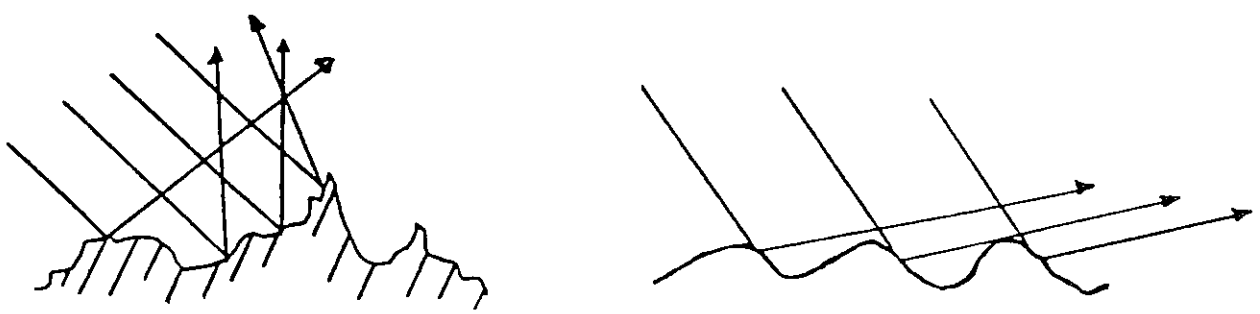

NON-UNIFORM ROUGHNESS

ROUGHNESS WITH A PERIODIC STRUCTURE (INTERFEROMETER EFFECT)

FIGURE 2-5. EFFECT OF PERIODICITY IN SURFACE ROUGHNESS

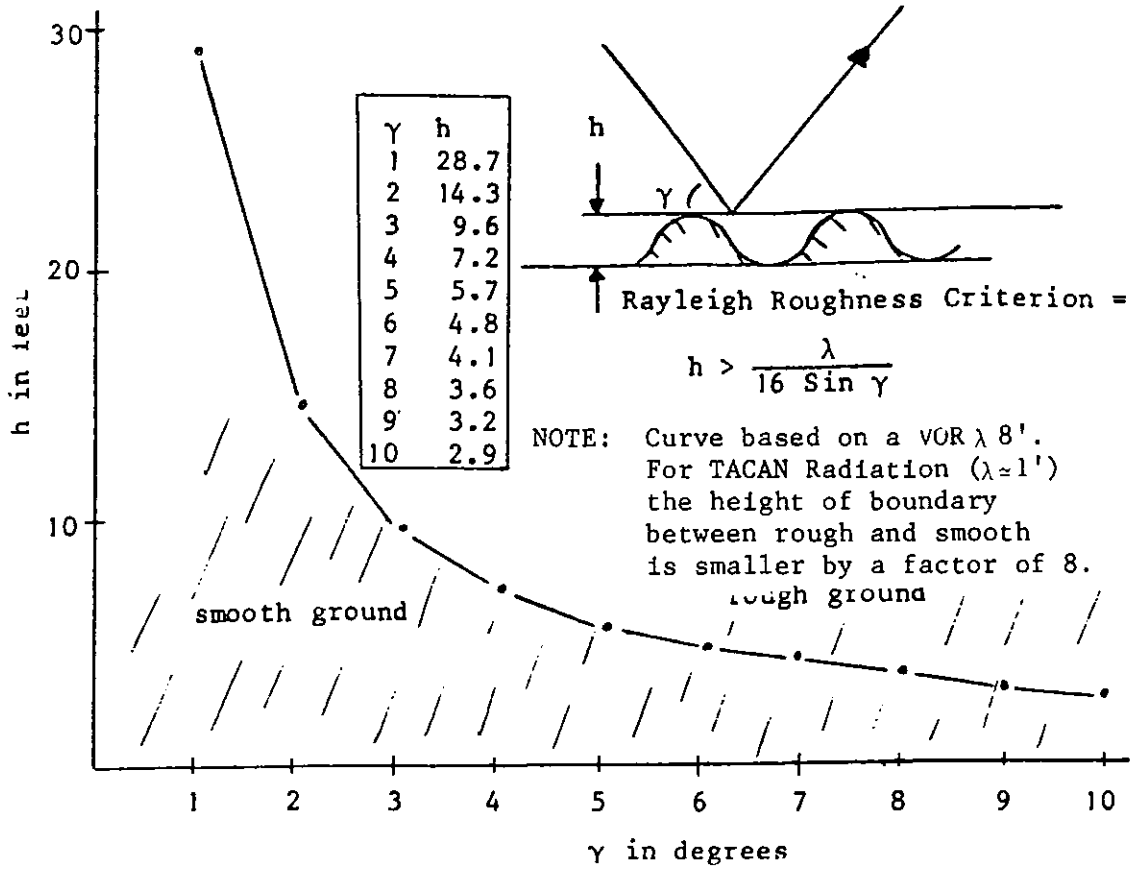

FIGURE 2-6. THE RAYLEIGH ROUGHNESS CRITERION

TABLE 2-2. TYPES OF MULTIPATH AND REFLECTION

Type or Parameter	Consideration
Longitudinal	Causes nulls in the vertical radiated pattern
Lateral	Causes interference in modulated information
Horizontal Polarization	Angular location of destructive longitudinal multipath is a matter of geometry
Vertical Polarization	Brewster angle effect eliminates some longitudinal multipath
Specular	Strong interference at specific angles
Diffuse	Interference weaker generally but occurs over a wide range of angles than does specular reflection

9. CONSIDERATIONS OF VERTICAL MULTIPATH.

a. General. Vertical multipath causes nulls in the vertical pattern of radiation and this in turn causes loss of signal in the airborne receiver. Hence, it is important in site analysis to identify those features that may lead to excessive multipath problems. Because of the different wavelengths, geometries, and problem details, vertical multipath for VOR, DME, and TACAN are considered separately.

b. Vertical Multipath in VOR.

(1) Refer to figure 2-3. Vertical multipath in VOR can result from reflection from the counterpoise and from the ground. Counterpoise reflections cause a null in the vertical pattern at an elevation angle of approximately 60 degrees. Since primary interest is in elevation angles of less than 10 degrees, this is of little importance. The elevation angles at which destructive multipath takes place due to ground reflection can be determined (see figure 2-7) from:

$$E(\gamma) = \cos [\gamma + kh \sin \gamma] - \sin [\gamma - kh \sin \gamma]$$

$$= 1/2 \cos \gamma \sin [kh \sin \gamma]$$

where the first term represents the antenna radiation pattern and the second term, the effect of the multipath.

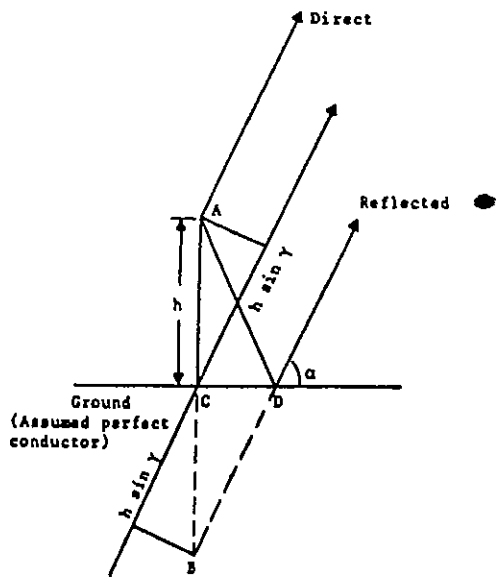

A = Source of radiation.

B = Apparent source of reflected radiation.

C = Source of combined radiation as seen by distant receiver.

D = Point of reflection.

FIGURE 2-7. VERTICAL MULTIPATH

The pattern has nulls where

$$\sin [kh \sin \gamma] = 0$$

$$\gamma = \sin^{-1} \left[\frac{n\lambda}{2h}\right]$$

when n = 1, 2, ...

(2) The usual 52-foot diameter counterpoise prevents DME antenna rays at angles greater than about 24 degrees from illuminating the ground. Similarly, the counterpoise prevents TACAN antenna rays greater than about 38 degrees from illuminating the ground. Because of the short wavelength of the TACAN and the height of the TACAN and DME antennas above the counterpoise, longitudinal multipath cannot be entirely prevented. As an example, DME destruction multipath will occur at about 1/2 degree if the ground is only 30 feet below ground level at the antenna site. See figure 2-8.

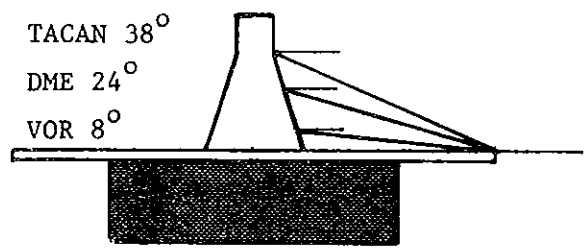

FIGURE 2-8. SHOWING EFFECT OF THE COUNTERPOISE IN LIMITING GROUND ILLUMINATION

c. Consideration of Longitudinal Multipath for DME and TACAN.

(1) It is readily seen from paragraph 5.b.(1) that for the shorter wavelengths of DME and TACAN there will be many more possibilities for destructive longitudinal multipath than there were for VOR. The vertical pattern has nulls when

$$\gamma_n = \sin^{-1} \left[\frac{n\lambda}{2h}\right]$$

$$n = 1, 2, 3, ...$$

For a given h and for the smaller wavelength there is a greater range of the integer n before $[n\lambda/2h] > 1$, and for each such integer there is an angle γ_n at which a null can occur.

(2) From figure 2-8, the counterpoise provides less angular blocking of DME and VORTAC rays from the ground. Hence, destructive longitudinal multipath can occur for a greater range of vertical angles for these two navaids.

(3) The first Fresnel zone for DME and TACAN is much smaller than for VOR. The width and length are reduced to approximately 1/3 the values for VOR and the total area is reduced by a factor of approximately 8. (See Chapter 3, figure 3-3.)

(4) The single favorable factor, of those discussed, which would make it more difficult to have destructive longitudinal multipath with DME and TACAN, is that greater ground smoothness is required for these shorter wavelength navaids. Note, for example that at nine degrees, a ground height variation of only 0.4 foot or about 5 inches makes the ground too rough for specular DME or TACAN reflection.

10. CONSIDERATIONS OF LATERAL MULTIPATH.

a. Lateral multipath involves the mutual interference between signals radiated at two different azimuth bearings. One is the direct ray. The second, the interfering ray, contains different navigational information than does the direct ray. The mix of the two modulations in the airborne receiver results in incorrect information being presented to the pilot.

b. In an idealized environment in which the ground based antenna site was surrounded by a smooth earth, it would be possible to have destructive longitudinal multipath. It would not, however, under these circumstances, be possible to have destructive lateral multipath. The requirement for lateral multipath to exist is that there be obstacles in the radiation field that accept radiation at one azimuth angle and reflect it off in a different direction either in a specular or a diffuse fashion.

c. Obstacles will exist in the radiation field and may consist of buildings that cannot be removed, telephone wires, power lines, and antennas for other FAA equipments. This order provides information on how to determine the effects caused by obstacles and how to minimize or eliminate such effects.

CHAPTER 3. SITE EVALUATION

11. GENERAL.

a. This chapter provides information to aid in the process of evaluating a site as a candidate location for any combination of the VOR, TACAN, and DME. It also provides information which may be used to evaluate the effect that physical changes proposed in the area of a site may be expected to have on the performance of existing navigational aids. Such changes can occur as areas evolve from rural to urban characteristics. Additionally, antenna systems of various kinds may be brought into the vicinity of the VORTAC/DME site as part of site consolidation efforts. The presence of these additional facilities can impact on navaids performance. This chapter also deals with the practical application of the technical material available in chapters 6, 7, and 8 to the problem of site evaluation. These chapters should be consulted for additional details.

b. In this order, the antenna systems are considered only as metallic objects in the radiation field of the navigational aids. Considerations of the mutual electromagnetic interference problems that may develop as a variety of radiators are brought into close geographic proximity are beyond the scope of this order.

12. CONSIDERATIONS OF LONGITUDINAL MULTIPATH.

a. General.

(1) Ground slope and ground smoothness in the vicinty of the VOR site determines the extent to which the ground will sustain reflections that, by interfering with the direct rays, cause nulls in the vertical radiated pattern. Since there are always some vertical angles for which such destructive interference can exist, the beam is shaped to avoid illuminating the ground. VOR and DVOR radiation is inhibited from illuminating the ground by the presence of the counterpoise. This is true only for a small area less than 10 to 20 feet from the VOR. The DME radiation pattern is shaped to attenuate ground illumination through use of multiple radiating elements. The site itself is not to be expected to completely inhibit destructive reflection. Considerable judgement is required in selecting sites with satisfactory properties, and no simple rules exist for concluding that one site is superior to another insofar as longitudinal multipath is concerned.

(2) The site evaluator should determine how far from the radiating antenna position his interest should extend. There is no simple answer. Areas close to the antenna location are relatively more important than distant areas because the close-in Fresnel zones are smaller. A distant rough area will, however, look smooth to the radiation traveling at a small grazing angle. This makes it easier for the large Fresnel zone to exist. A possible rule of thumb is that primary attention should be focused on the first 1,000 feet, with secondary attention given to the surrounding mile. In addition, a cursory examination of the first five miles is required to ensure the identification of geographic areas that might cause particular difficulty.

(3) Any site can be made to be satisfactory in its longitudinal multipath performance provided that sufficient care is taken in the selection and installation of the radiating system. Although such systems are nonconventional, it is possible to use site modifications such as oversized counterpoises or additional grounding elements. Accordingly, the investigator may consider preparing qualified recommendations for sites. One site, for example, may be attractive for a number of reasons but be characterized by unusually poor ground conductivity which could result in an abrupt discontinuity in electric field boundary conditions at the perimeter of the counterpoise. A recommendation regarding this site which identified the potential problem and its implication for wavefront binding would allow the next level of management to make tradeoffs between technical, financial, and acquisition problems in choosing between alternative possibilities.

b. Longitudinal Multipath and the VOR Equipment.

(1) It was pointed out in chapter 2, in connection with figure 2-7 and the associated discussion, that nulls in the vertical radiation pattern of the VOR will appear where:

$$\sin \left[kh \sin \gamma_n \right] = 0$$

where $$\gamma_n = \sin^{-1} \left[\frac{n\lambda}{2h} \right]$$

$$n = 1, 2, \ldots.$$

Using this relationship one may develop an approximate range within which the surrounding terrain can sustain destructive multipath. See figure 3-1.

(2) Note from figure 3-1 that, in order to minimize the possibility of longitudinal multipath from the VOR antenna, the ground in the vicinity of the VOR site must be level or must fall away gently from the ground level at the base of the antenna structure. If the ground falls away too sharply, geometry necessary for destructive multipath may exist. If the ground falls away precipitously, however, it becomes impossible to have destructive multipath because the counterpoise prevents ground illumination at angles of depression greater than 8 degrees. Finally, if the ground falls away and slopes away from the VOR, the ground slope can direct the multipath away from the direct ray. Note that the results of figure 3-1 are based on the assumption that the ground is level in the area of ground reflection. The action of a slope in reflecting energy downward cannot be relied upon since the reflection can be expected to be partly diffuse and partly specular in many cases. Regardless of how fast the terrain falls away from the VOR, there will be some terrain visible to the VOR within the service volume which will support vertical multipath.

(3) While there is no clear-cut boundary around the VOR site beyond which one is not required to be interested in the terrain, as the distance from the site increases, the terrain features become less important. As distance from the VOR site increases, the size of the first Fresnel zone increases. Since contributions from most of the first Fresnel zone are required to obtain substantial multipath, it is evident that there is smaller probability of finding a reflecting area as large as the first Fresnel zone at a large distance from the VOR site than is the case closer in. The growth of the VOR Fresnel zone with distance is shown in figure 3-2.

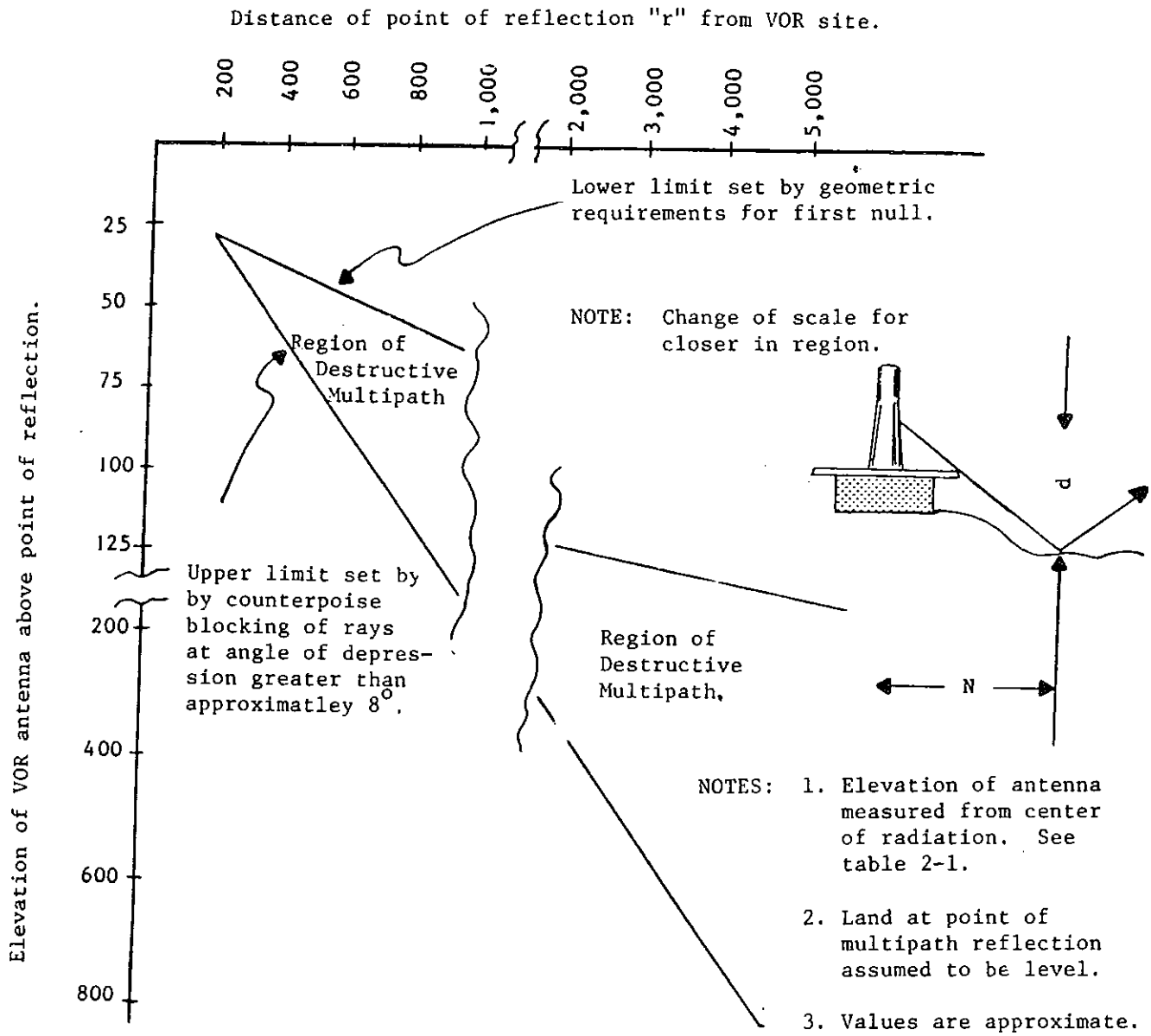

FIGURE 3-1. GROUND SLOPE CONSIDERATIONS

(4) Figure 3-3 illustrates this point in more detail and shows that the first Fresnel zone for small angles of reflection is several miles in length at a distance of a mile from the VOR site. Considerable judgement is required when using this figure, since the Rayleigh criterion shows that, at shallow grazing angles, even very rough terrain can look smooth to the incident radiation (see figure 2-6). The large Fresnel zones required may in fact exist.

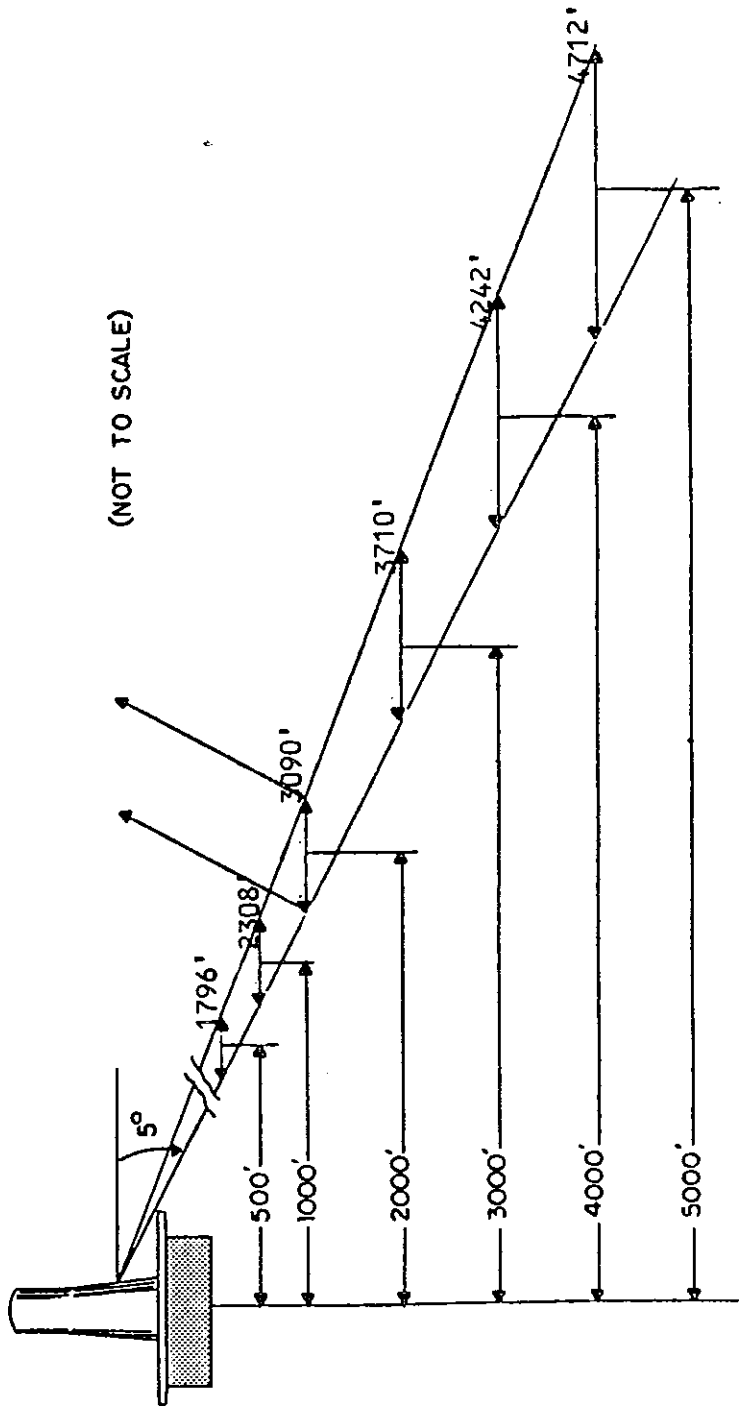

FIGURE 3-2. GROWTH OF VOR FRESNEL ZONE LENGTH WITH DISTANCE

Distance of Reflection Area from VOR Site in Feet	Range of Angles of Reflection	Dimensions of Fresnel Zone	
		Range of Widths (Feet) (W)	Range of Lengths (Feet) ($X_1 + X_2$)
1000	3.8° to 8°	175 - 183	1,377 - 3,197
2000	2.6° to 8°	251 - 258	1,904 - 6,743
3000	2.2° to 8°	302 - 316	2,314 - 9,579
4000	2.0° to 8°	345 - 365	2,661 - 11,871
5000	1.7° to 8°	389 - 409	2,978 - 15,936
6000	1.5° to 8°	428 - 448	3,257 - 20,086

$$W = 2\sqrt{\frac{\lambda h}{\sin \gamma}} \qquad X_1 = \frac{-\lambda \cos \gamma + \sqrt{\lambda^2 \cos^2 \gamma + 4 h \lambda \sin \gamma}}{2 \sin^2 \gamma}$$

$$X_2 = \frac{+\lambda \cos \gamma + \sqrt{\lambda^2 \cos^2 \gamma + 4 h \lambda \sin \gamma}}{2 \sin^2 \gamma}$$

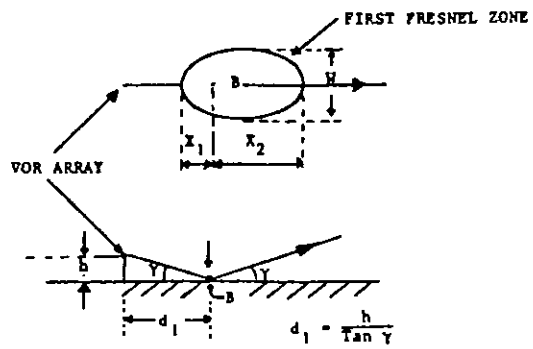

FIGURE 3-3. RANGE OF SIZES FOR FIRST FRESNEL ZONE

c. Longitudinal Multipath and the DVOR Equipment.

(1) The effect of longitudinal multipath on DVOR equipment performance will be discussed in terms of a comparison between VOR, SSBDVOR, and DSBDVOR. The diameter of the counterpoise is different for the three different pieces of equipment. The height above the counterpoise of the radiating center of the antennas is four feet in all three cases. The VOR antenna, for purposes of the discussion of longitudinal multipath, can be considered to be located at the center of the counterpoise. The DVOR antennas which generate the azimuth information are located in a circle of 22-foot radius, concentric with the counterpoise center. Additionally, the VOR signal containing the

azimuth information is a form of amplitude modulation called space modulation. Refer to figure 1-2 and the associated discussion. For both variations of DVOR, the azimuth information is carried as fm modulation with a deviation ratio, β, of 16.

(2) The DVOR azimuth information-bearing signal should be less susceptible to multipath interference because of the well-known fm threshold effect. By contrast, the VOR azimuth signal, since it involves three separately radiated amplitude-modulated signals, should be comparatively more vulnerable to multipath interference. The DVOR requires a larger counterpoise than does VOR. From any azimuth, the different antennas in the 22-foot DVOR circle experience different amounts of counterpoise, which results in a cyclic modulation on the radiated signal. In the nonlinear elements in the airborne receiver, this undesirable modulation can be transferred to other signals. The larger DVOR counterpoises diminish this asymmetrical effect, and DSBDVOR is less susceptible to the asymmetrical effects of the counterpoise than is SSBDVOR.

(3) The counterpoise's primary purpose is the sharp attenuation of the vertical radiation pattern for angles of radiation negative with respect to the horizon. The counterpoise weakens the radiated field in the direction of the horizon (see figure 3-4). There is some evidence that for every 15 feet in VOR counterpoise diameter, there is a loss of range at 1,000-foot altitude of approximately 15 miles. Since the same effect should exist in DVOR, it is reasonable to expect the DVOR low altitude coverage to be less than that of VOR.

(4) It may be thought that the large DVOR counterpoise could itself be a reflecting surface for multipath signals. At angles of 30 degrees or more, the Fresnel zone dimensions are 20 feet or less in their longest dimension. The DVOR geometry will not sustain destructive longitudinal multipath. Presuming a good conducting counterpoise which is properly grounded, longitudinal multipath should not be a problem with DVOR installations.

(5) The reduced range of the DVOR as compared with VOR suggests that DVOR is more appropriate for terminal area applications. See table 6-1 and the associated discussion. This does not preclude the use of DVOR for enroute applications when it is determined that the DVOR will satisfy and/or improve coverage requirements. A second characteristic of DVOR supports this conclusion. The simulated doppler signal decreases with the cosine of the angle of elevation so that at 60 degrees above the horizon, the effective β of the fm modulation is only 8 rather than 16. Some airborne receivers will release the malfunction flag at this low a value of β. Additionally, because of this cosine behavior, the cone of confusion whose center is directly above the navaid site is much larger in angular extent for DVOR than for VOR.

d. Longitudinal Multipath and the TACAN Equipment.

(1) Three factors make the analysis of longitudinal multipath effects for DME and TACAN differ from those of VOR:

(a) The wavelength for DME and TACAN is much shorter than for VOR (see table 2-1) making the Fresnel zone much smaller but requiring greater surface smoothness for specular reflection.

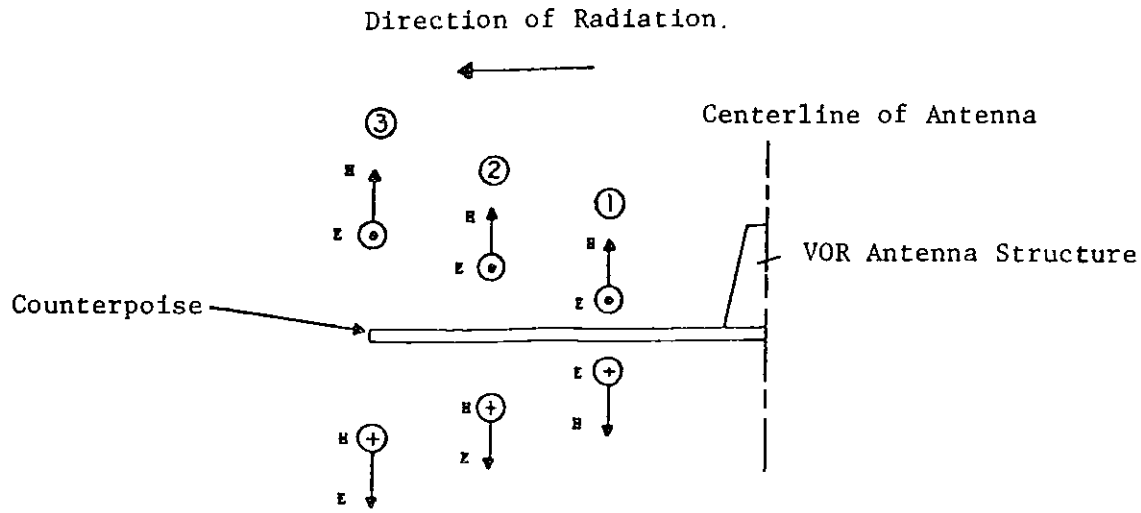

NOTES:

⊙ Indicates vector pointing out of page.

⊕ Indicates vector pointing into page.

FIGURE 3-4. RADIATED AND REFLECTED ELECTRIC FIELD AT COUNTERPOISE

(b) The DME and TACAN radiations are vertically polarized, whereas that of VOR is horizontally polarized. Ground reflections are generally much weaker for vertical polarization. See figure 6-1.

(c) The effect of the counterpoise is weaker for DME and TACAN because the antennas are mounted higher above the counterpoise, both in number of wavelengths and in absolute distance, than is the VOR antenna.

(2) These factors and their effects upon longitudinal multipath are summarized in table 3-1.

(3) The smaller dimensions of the Fresnel zone for TACAN are seen by developing a figure (similar to figure 3-2) which shows the growth of the Fresnel zone with distance, figure 3-5.

(4) Consider now the ground smoothness characteristic. At 5 degrees, the variation in ground elevation within the Fresnel zone should be less than 6 feet for the ground to be considered smooth to the VOR radiation. For the TACAN or DME, however, at the same angle the variation would have to be less than 9 inches (see figure 2-6). Hence, although the smaller Fresnel zone areas of TACAN and DME make it easier to produce longitudinal multipath, the greater ground smoothness required partly compensates for the reduced area.

TABLE 3-1. LONGITUDINAL MULTIPATH: TACAN COMPARED WITH VOR

NOTE: For purposes of this comparison DME may be associated with TACAN

Parameter	Differences	Effect
λ	λ (VOR)≈8 feet λ (TACAN)≈1 foot	Total area of Fresnel zone reduced by a factor of 8 for TACAN compared to VOR thus facilitating TACAN longitudinal multipath. Ground must be much smoother in the Fresnel zone area to sustain specular reflection for TACAN as compared to VOR.
Polarization of Radiation	VOR-Horizontally Polarized TACAN-Vertically Polarized	Vertically polarized radiation of TACAN is much less strongly reflected from the ground than is horizontally polarized radiation.
Height of Radiator Above Counterpoise	VOR - 4 feet TACAN - 20.5 feet	Below the horizon radiation from TACAN is not as sharply attenuated by the counterpoise as is that of VOR. Additionally, counterpoise is less effective in its blocking action. See figure 2-8.

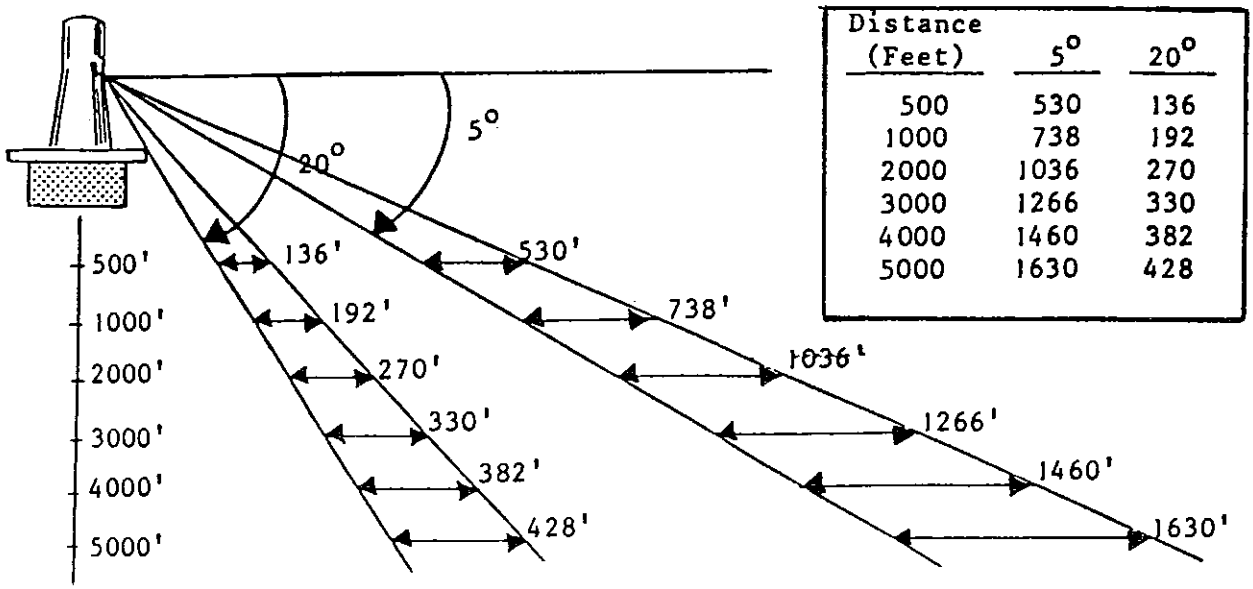

Distance (Feet)	5°	20°
500	530	136
1000	738	192
2000	1036	270
3000	1266	330
4000	1460	382
5000	1630	428

NOTE: Compare with figure 3-2.

FIGURE 3-5. Growth of TACAN/DME Fresnel Zone Length with Distance

(5) The use of vertical polarization for TACAN and DME aids in reducing the ground reflection, particularly in the angular region of the Brewster's angle. Unfortunately the Brewster's angle varies over a range of 5 to 30 degrees for various types of terrain and, in a particular geographic area, will vary with the season. Nevertheless, the effect is generally favorable to reducing longitudinal multipath. See detailed discussion in paragraph 23.f, chapter 6.

(6) The counterpoise is much less effective for TACAN and DME than it is for VOR. On the other hand, the antennas of TACAN and DME are multiple-element radiators designed to shape the pattern of radiation in the vertical plane so that energy directed toward the ground is sharply attenuated.

(7) A smooth, flat ground surface within approximately 25 feet of the navaids antenna complex will sustain longitudinal multipath from the DME at the angle of 24 degrees if the surface is smooth to within about two inches over a range of 27 feet. In most cases, the radiation at 24 degrees below the horizon will be sharply attenuated; however, the smooth, flat surface characteristic in the vicinity of the antenna complex is to be avoided.

13. CONSIDERATIONS OF LATERAL MULTIPATH.

a. General.

(1) Lateral multipath involves the mutual interference between signals radiated at two different azimuth angles from the same antenna. These signals contain different azimuth information in their modulations.

The resultant signal, if the interference is sufficiently strong, will contain erroneous azimuth information. The interference effects arise from the combining of two modulations which are not of the same phase angle.

(2) Existing sources of lateral multipath, such as permanent structures, often cannot be removed. The investigator should consider the option of preparing qualified recommendations for such sites, identifying the potential sources of multipath and his reasons for believing that such sources may be problems. Using the techniques for minimizing lateral multipath discussed in chapter 6, the cost and probability of success of such techniques can be factored into the overall evaluation.

b. Lateral Multipath and the VOR Equipment.

(1) Lateral multipath is caused generally by objects and structures rather than by the ground itself. Hence, a discussion of lateral multipath includes such objects as long wires, trees, cylinders, planes, and combinations of these. The general guidance provided here is supplemented by additional technical material provided in chapter 7 and, for wires and cylinders, by computer simulation techniques described in chapter 8.

(2) The previous discussion of Fresnel zones reveals that it is angular size, measured from the antenna site, rather than absolute dimensions. This is significant in determining the effect of a reradiating surface. Thus from figure 3-2, a ground surface of 1800 feet in extent can be as large in its effect as a surface extending over a mile at a longer distance. Hence, an appropriate measure of objects in the VOR field is the angle subtended by such objects at the VOR antenna.

(3) A second important consideration in evaluating the potential effect of objects in the VOR field is the azimuth at which the possible lateral multipath will be experienced. At some installations, notably terminal areas, some azimuths are relatively more important than others. It is characteristic of lateral multipath that the effect is most pronounced at azimuths other than the one at which the causing object is located.

(4) A useful reference for comparison purposes is the TACAN antenna monitor and support mast. This monitor structure will always be present in those situations where the navaids antenna complex is already installed and the site is being evaluated for possible modification. It subtends an angle of approximately 1.4 degrees at the VOR antenna and, as a reflecting re-radiator, causes a scalloping error in the VOR of about 0.2 degree at azimuths ±55 degrees from its location. See paragraph 25.b. for a more detailed discussion of directional re-radiators. Directional re-radiators of the same angular width as the TACAN antenna monitor, even though at a greater distance, can be expected to cause similar scalloping effects.

(5) Figure 3-6 is a qualitative guide to estimating the possible effect in causing lateral multipath of objects in the area of the VOR antenna. Several conclusions may be drawn from an examination of the figure, but judgement must be used in the application of these conclusions:

(a) Single trees and objects of similar angular dimensions can cause substantial lateral multipath if located within a few hundred feet of the VOR antenna. Because the VOR radiation is horizontally polarized, it is the angular extent of the tree in the horizontal plane that is significant. The height of the tree, however, enables it to project above the plane of the counterpoise.

(b) Cleared forest areas can cause scalloping.

(c) VOR does discriminate against objects which may cause severe lateral multipath.

(6) Specular reflectors and other directional reflectors have maximum scalloping amplitudes when the angle of incidence is in the region of 55 degrees. The half-power scalloping amplitudes occur for angles of 35 and 73 degrees. See figure 7-7 and the associated discussion in chapter 7.

(7) The scalloping amplitude for diffuse radiators is maximum when the azimuth of the re-radiator and the azimuth of the aircraft are at 90 degrees one to another. See figure 7-10 and the associated discussion in chapter 7.

c. Lateral Multipath and the DVOR Equipment

(1) Lateral multipath is known to involve interference for the 30-Hz modulating signal which carries the azimuth information. Lateral multipath of the reference signal cannot cause problems since the direct and multipath signals are essentially in the same phase and hence add constructively. In the

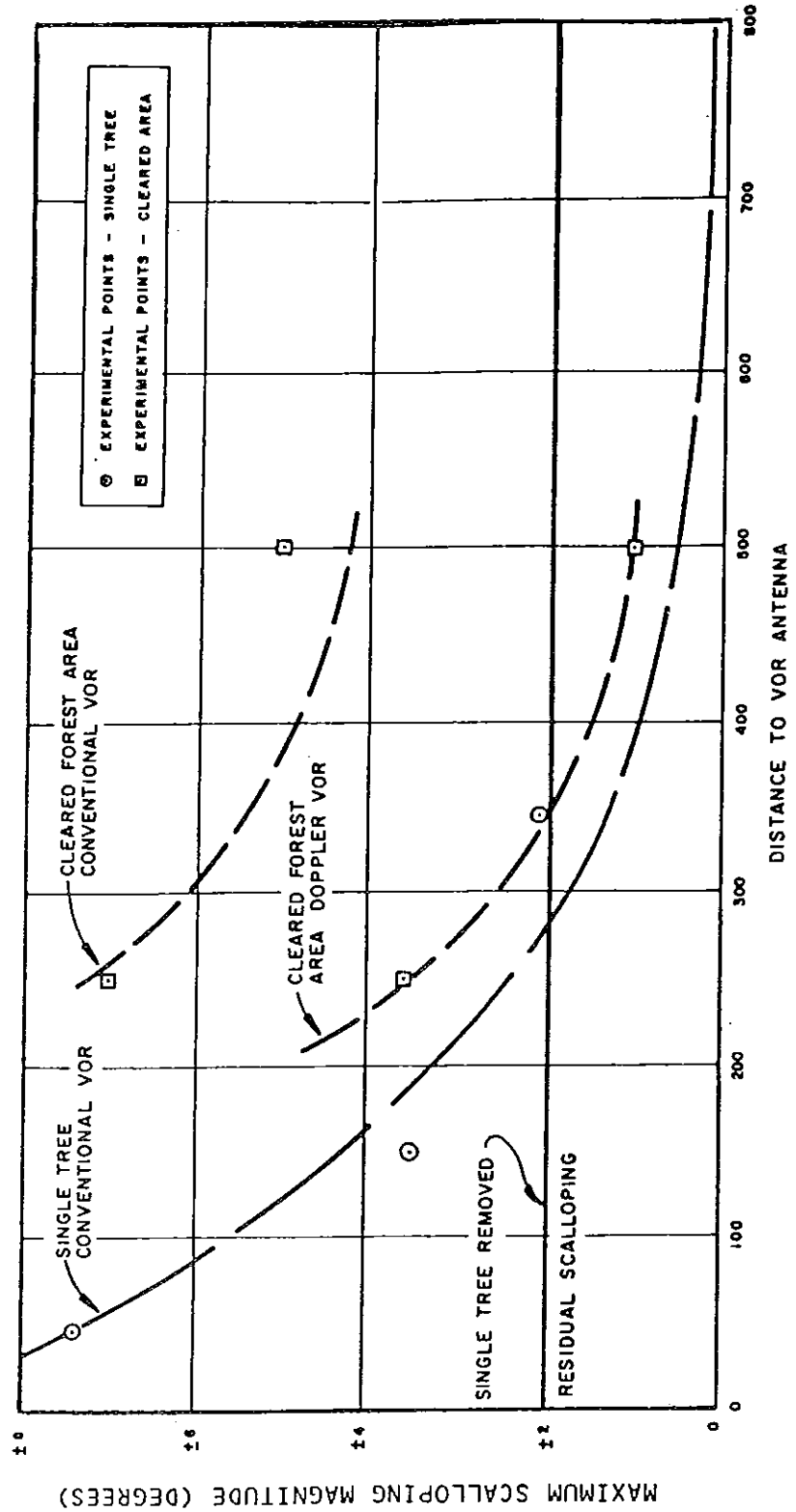

FIGURE 3-6. MAXIMUM SCALLOPING AMPLITUDE CAUSED BY SINGLE TREE AND BY FOREST

doppler VOR, the variable azimuth information is protected from interference because of the nature of fm modulation. It follows that DVOR is inherently resistant to lateral multipath.

(2) Site evaluation involves the identification of potential problems associated with the site and the recognition of approaches to the resolution of such problems. For sites with severe multipath problems, the DVOR may appear to be a reasonable candidate solution. DVOR has specific characteristics that should be taken into account in the development of such recommendations. The doppler shift decreases directly with the cosine of the angle of elevation, resulting in a large "cone of confusion" centered on the 90-degree angle of direct overhead. The very large DVOR counterpoise serves to reduce low angle coverage. The amount of the reduction is a function of the site elevation over average terrain in the direction of propagation. Finally, the cost and complexity of DVOR makes this equipment the practical candidate only for those sites for which few other alternatives exist. DVOR was developed originally for terminal areas, and its use has been largely restricted to such locations.

d. Special Considerations for Mountain Top Sites.

(1) It is usual to locate the VOR counterpoise directly at ground level at mountain top sites. One reason for this practice is that the low conductivity of the ground at such sites requires particular emphasis upon the best obtainable electrical connectivity between the ground and the counterpoise. A second reason is that the radiating wavefront tends to cling to the counterpoise at the counterpoise perimeter and so bend downward and direct some energy into the ground. The effect is less serious when the antenna is not elevated.

(2) Siting a VOR on a mountain top several thousand feet above surrounding terrain may result in VOR bearing errors which exceed flight check tolerances. Even with the large counterpoise on mountain top VORs, portions of the valleys may be illuminated by the VOR antenna. When this occurs, vertical lobing (longitudinal multipath) of the signal will cause nulls in the VOR vertical radiation pattern. When aircraft fly through these vertical nulls, the direct signal from the VOR is reduced compared to the reflections (lateral multipath) received from surrounding objects. This may result in bearings which are out of flight check tolerance and subsequent restrictions or shutdown of the VOR. If this condition exists, little or no improvement will be gained by installing a DVOR. A DVOR will provide significant signal improvement when lateral multipath is from relatively close objects; however, at mountain top sites where the source of the multipath may be several miles away, little improvement is gained.

e. Lateral Multipath and TACAN.

(1) Lateral multipath is more readily generated for the TACAN than for VOR because the shorter wavelength of TACAN requires a smaller Fresnel zone.

(2) Vertical wires that cause only slight multipath problems for the horizontally polarized VOR signal can cause substantial problems for the vertically polarized TACAN signal. Conversely, horizontal wires that cause serious multipath problems for VOR may have a much smaller effect on TACAN.

f. Wind Turbine Generators. The recent growth of alternative energy sources has led to an increasing number of wind turbine generators and to increasing complaints of electromagnetic interference from these generators. A study at the University of Michigan (D. Sengupta and T. Senior, "Electromagnetic Interference by Wind Turbine Generator," Report No. 014438-2-F, March 1978) indicates that VOR and DVOR facilities will experience no significant degradation of performance due to the presence of wind turbine generators if the generators are sited in accordance with FAA standard guidelines for objects near VOR and DVOR facilities.

14.-15. RESERVED.

CHAPTER 4. SITE SELECTION AND ACQUISITION

16. PROCEDURE FOR SITE SELECTION.

a. General. The selection of a suitable site for a navigation facility (VOR, VOR/DME, TACAN, or VORTAC) is primarily a function of performance and cost. No candidate site shall be selected that does not satisfy the minimum performance requirement at a cost commensurate with the benefit to be received. Primarily, this order provides the siting engineer with techniques for estimating site performance and the effect on performance of various corrective measures. This chapter presents a methodology for selecting a VOR, VOR/DME, TACAN, or VORTAC site which meets the performance requirements of the system and the cost limitations of the program. Although detailed performance or cost estimates are beyond the scope of this order, a good first approximation is required for site selection and acquisition. See figure 4-1 for a flowchart of the selection process.

b. Initial Locality. The general location of a navigation facility (VOR, VOR/DME, TACAN, or VORTAC) is initially determined by its type; whether it is a terminal facility or an en route facility (see paragraph 21.b). The location of a terminal facility is constrained by the actual location of the airport and by the orientation of the primary instrument landing runway. The location of en route facilities is determined largely by the location of the airways which they serve and, to a lesser extent, by the distance to other facilities serving the same airways.

c. Office Survey.

(1) Once the general location has been determined, candidate sites may be identified from topographic maps readily obtained from the U.S. Geological Survey of the Department of the Interior. These map studies will identify, as accurately as possible, the coordinates of the candidate sites and the locations of triangulation points or other control points. These points will permit establishment of an accurate baseline and verification of coordinates in the field.

(2) The initial office survey should develop a candidate site and several alternative sites, if possible. This will save the cost and time of additional field trips if the primary candidate is determined to be unsuitable or unavailable. Maps of each area should be acquired, and if the installation is to be within an existing facility, all available engineering drawings describing the site should also be assembled. Other information that does not require a site visit may also be compiled at this time. This includes some or all of the following:

(a) Ownership characteristics of the land, particularly name and address of owner(s); easements, rights-of-way, or other use limitations; and zoning or use restrictions imposed by the local political jurisdictions.

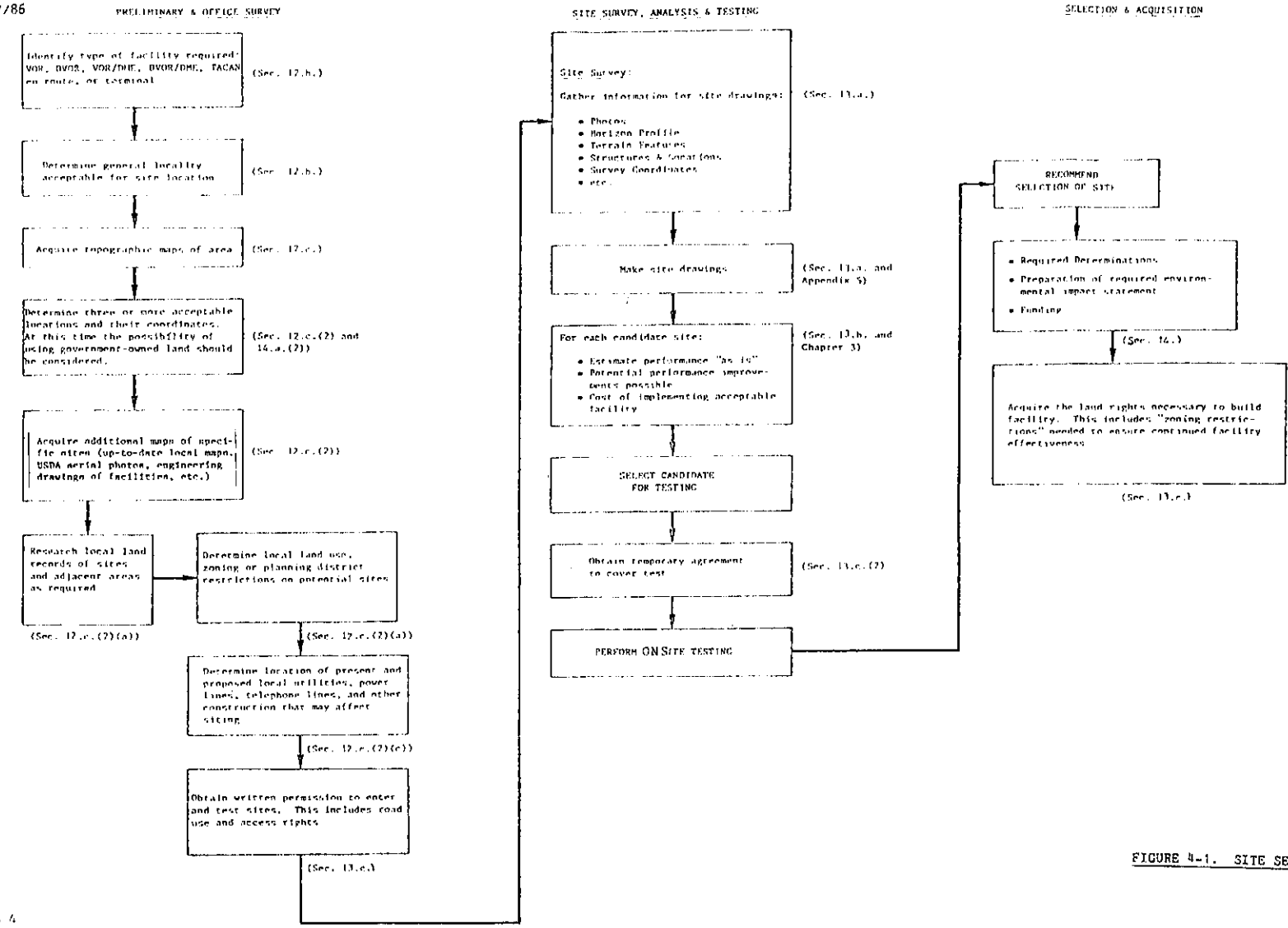

FIGURE 4-1. SITE SELECTION PROCEDURE

(b) The possibility of using Government-owned land should be investigated at this time. See FAA Order 4660.1, Real Property Accountability Handbook.

(c) Location of the proposed facility with respect to any nearby town or airport, roads, utility lines, and boundary lines in the vicinity.

(d) Local utilities' plans for new or upgraded lines near the proposed sites and local planning districts' long-range plans that might impact on these sites.

17. SITE SURVEY, ANALYSIS, AND TESTING.

a. General.

(1) The primary purpose of the site survey is to obtain sufficient information to prepare site drawings (see appendix 6). The site drawings should include a vicinity sketch, site plan, plot layout plan, and horizon profile. The survey will establish (and document in the various drawings) a dimensional description of the site, including the locations and heights of prominent adjacent natural and man-made terrain features and obstructions. Distant terrain features that represent potential obstructions should also be identified. See paragraph 13.c(2) below for information concerning permission to enter the land.

(2) Features to be noted in the survey will include such details as trees, fences, drainage, existing buildings, utility lines, and obstructions within the vicinity of the antenna position out to a distance of 2000 feet. During the survey, other features that may be noted are topographical characteristics, particularly surface variations, that may have an impact on the propagation of signals from the site.

(3) Accurate measurements are required for the coordinates of the location and the horizon profile. The latitude and longitude of the location must be determined to the nearest 15 seconds of arc. The coordinates will later be refined to an accuracy of $\pm$40 feet by the U.S. Geological Survey. The horizon profile is obtained by setting up a transit or theodolite at the correct antenna height and location for the site, and recording the vertical angle of all obstructions in a full circle around the site. These measurements must be accurate to $\pm$0.1 degree in vertical angle and should be given for each 10 degrees around the circle, unless elevation changes warrant more frequent measurements. If the profile taken for an antenna height of 4 feet does not show any object above 0.5 degree, then the profile at 16 feet does not need to be made. A set of accurately registered panoramic photos are an alternative to the horizon profile.

b. Site Evaluation.

(1) After preparation of the site drawings, the techniques discussed throughout chapter 3 should be applied to analyze the characteristics associated with each site under consideration. The evaluation should include:

(a) Estimates of performance that can be expected from each unimproved site.

(b) Improvement of the above performance that can be expected if corrective measures are taken. Such techniques are discussed at length in chapter 5.

(c) Estimated cost of implementing a facility that will provide acceptable performance.

(2) Selection of a tentative VOR, VOR/DME, TACAN, or VORTAC site is then made, based on the above analysis, with the objective of meeting the required performance at the least possible cost. This site should then be field tested to verify the predicted performance. In unusual cases where the site test is unsatisfactory and the performance deviates greatly from expectations, the site should be reanalyzed in light of the new data. If, as a result of a complete reevaluation, one of the alternative sites previously ruled out is now found to be most promising, a new site test will be required. Successful completion of a site test(s) will provide data for the site selection. If more than one site is technically satisfactory, then relative costs will be the determining factor.

c. Preliminary Considerations Before Testing.

(1) At the time of the office survey, it is of prime importance to establish the identity of the owners of the land for all candidate sites and the addresses through which they may be contacted. The legal description of land can usually be obtained locally from city, township, or county clerk's office. If possible, a copy of the deed(s) or other appropriate documentation showing land ownership should be attached to the Site Survey Report. In addition, there may be land adjacent to the proposed sites which would be affected by the site zoning restrictions. These restrictions, discussed in detail in paragraph (3) below, may be determined during the office survey, so that the ownership information of this type land, if required, may also be included in the Site Survey Report.

(2) Once the site surveys are completed and it has been decided to field test a specific candidate site, a temporary agreement must be entered into with the property owner(s). This agreement (Permit to Test, Testing License, etc.) will secure entry and access to the property for setting up a portable VOR and testing the site. These agreements, and the initial permission to enter the land for the site surveys, are governed by FAA Order 4660.1, Real Property Accountability Handbook.

(3) At the time that the temporary agreement is secured, the landowner(s) should be made aware that the following zoning restrictions will be required if the site is actually selected. This will reduce the possibility of complications in this regard at the time of lease negotiations. The restrictions are:

(a) General. All obstructions within 1000 feet of the antenna are to be removed except as noted below. Normal crop raising and grazing operations may be permitted in this area, except at mountain top facilities where antennas are 4-feet high. In these instances, crop raising and grazing must be restricted to areas below and off the counterpoise. No grazing should be permitted in the vicinity of the monitor detectors.

(b) Trees and Forests. Trees close to the VOR antenna can cause severe scalloping. Single trees of moderate height (up to 30 feet) may be tolerated beyond 500 feet, but no closer. No groups of trees should be within a 1000-foot radius or subtend a vertical angle of more than 2 degrees. At mountain top sites, no trees within 1000 feet should be visible from the antenna array.

(c) Wire Fences. Ordinary farm-type wire fences about 4-feet high are not permitted within 200 feet of the antenna; fences of the chain type (6 feet or more in height) are not permitted within 500 feet of the antenna; beyond these distances no wire fence should extend more than 0.5 degree above the horizontal, measured from the antenna. These requirements may be relaxed for fences essentially radial to the antenna. Since there is a large number of possible combinations of fence height and orientation with terrain configuration of various types, each of which may produce a different effect, the foregoing must serve as a general guide only. At many sites, a special study by experienced engineering personnel will be required to permit a judgement as to what fences can be tolerated. At mountain top sites, wire fences may be permitted within 200 feet of the antenna, provided they do not extend above the line of sight from the top of the antenna to the edge of the level area (that is, they are within the shadow area of the ground counterpoise).

(d) Power and Control Lines. Power and control line extensions should be installed underground for a minimum distance of 600 feet from the antenna. Overhead power and control lines may be installed beyond 600 feet but should be essentially radial to the antenna for a minimum distance of 1200 feet. No overhead conductors (including possible future construction), except for extensions serving the site, should be permitted within 1200 feet of the antenna. If a nonradial conductor is so oriented that it does not come within 1200 feet of the antenna, but the perpendicular distance to the antenna from its imaginary extension is less than 1200 feet, then the vertical angle subtended by the uppermost conductor and/or the top of the pole (measured from ground elevation at the antenna site) should not exceed 1 degree; also no conductor should extend above the horizontal plane of the antenna.

Other than the foregoing, there should be no lines or supporting structures so located that they subtend a vertical angle (measured from ground elevation at the site) of greater than 1.5 degrees. In addition, no conductor should extend more than 0.5 degree above the horizontal plane containing the antennas, unless they are essentially radial (within $\pm$10 degrees) to the antenna array. At mountain top sites, the conductors will be permitted within 1200 feet of the antenna, provided they do not extend above the conical surface formed by the top of the antenna and the edge of the leveled area.

(e) Structures. No structures should be permitted within 1000 feet of the antenna, except for buildings such as the transmitter building at a mountain top site located on a slope below the ground level of the antenna so that they are not visible from the antenna. All structures that are partly or entirely metallic shall subtend vertical angles of 1.2 degrees or less, measured from ground elevation at the antenna site. Wooden structures with negligible metallic content and little prospect of future metallic additions (such as roofs and wiring) may be tolerated if subtending vertical angles of less than 2.5 degrees. However, at airports, where a single hangar or line of hangars, administrative buildings, etc., may have considerable length, it is necessary to look upon such structures as producing interference in the same manner (only more severe) as power and telephone lines, and the criteria for power, control, and telephone lines will apply.

(4) Temporary permits to utilize access roads of adjacent property owners shall also be obtained prior to site testing. Easements are very often all that are required to install a permanent access road to a facility after it is established, and the actual purchase of land for this purpose is not necessary. Leases or other agreements, as required, should be entered into with appropriate governing agencies or property owner(s) for the use of existing roads. Appropriate procedures for entering into such agreements are given in FAA Order 4660.1, Real Property Accountability Handbook.

14. LAND ACQUISITION

a. When a site has finally been selected as appropriate for permanent installation of a VOR/DME/TACAN facility, a legal description and plat of the site, access road, utility easements, and zoning restrictions must be obtained prior to requesting the acquisition of the property rights. All transactions for acquiring an interest in property, whether purchase, lease, or use restriction, are governed by FAA Order 4660.1, Real Property Accountability Handbook, and are handled by Real Estate Office personnel. As an aid to planning, several excerpts as well as references to certain sections, are given below:

(1) Funding. When land is to be purchased for a new facility site, funds for the purchase shall be included in the region or center Facilities and Equipment (F&E) budget in the same fiscal year as the funds for the facility equipment, installation, and building, as applicable. This amount will only be an estimate of the value of the land rights to be acquired, plus acquisition costs, plus a 15- to 20-percent contingency. Instructions for including land acquisition funds in the annual F&E budget submission are found in Order 2500.24, Call For Estimates - Facilities and Equipment (RIS: BU-2500-4).

(2) Required Determinations All possible sites which are technically acceptable for the efficient operation of the facility must be considered. Before any action is begun to acquire new land, a determination must be made that the requirements cannot be satisfied by use of property already held by the FAA, property which is excess to other government agencies, public land, exchange of government-owned property for privately owned property, or the use of existing rights-of-way and easements when available at nominal cost or less.

(3) Site Investigation and Testing. Prior to conducting investigations and tests, the legal right to enter and use the land must be obtained in writing from the landowner and, if appropriate, the right to clear or otherwise change the character of the land. If only verbal authority is granted, confirm this in a letter with a return receipt. When a landowner will not grant a right of entry, then a right of entry must be obtained through the U.S. courts. Local U.S. attorneys should be consulted in these instances through Regional Counsel. Contacts with landowners should generally be made by Real Estate personnel, and when contacts are made by others they must be under the direction of the Real Estate Office.

(4) Environmental Impact Statements. Environmental Impact Statements (EIS), or Finding of No Significant Impact (FONSI) shall be approved before negotiations for the acquisition of any land interest. Real Estate files should contain a copy of the EIS or FONSI as applicable, or a reference to the office of record.

(5) General. The above are included to assist site planning personnel in developing the information base and time line needed to implement their activity. Order 4660.1, Real Property Accountability Handbook also contains comprehensive information regarding the actual purchase of land or leasing it. Close coordination with the Real Estate Office will ensure the most efficient handling of this process.

19. RESERVED.

CHAPTER 5. SITE IMPROVEMENT

20. GENERAL.

a. The navaids of interest here are intended to provide reliable service within acceptable performance margins on a continuous basis in spite of extremes of weather and changing terrain caused by seasonal variations in vegetation or the encroachment of new construction. These variations of the environment in which the navaids must perform require that measures for performance improvement be undertaken each time such a change adversely affects performance. When it is determined that additional FAA equipments be located near the VORTAC antenna site, such a colocation may require additional site improvement features relative to the VORTAC. Thus, site improvements may be required throughout the useful lifetime of the site.

b. Site improvements involve two separate and distinct activities. One is the analysis of the performance or the predicted performance of the VORTAC within the site environment. For a proposed new site, such analysis may be a paper-and-pencil exercise primarily of ray tracing to analyze potential interference sources. After substantial commitment to the site, either through actual site acquisition or as alternates are eliminated, the investment in analysis may be more substantial and include computer simulations. Once the VORTAC is installed, the analysis may involve instrumented flights and analysis of flight data. In the latter activity, the measuring instrument is often a commercial receiver. In such situations, the analyst is presented not with raw data, but with data as processed by a specific receiver, and the idiosyncracies of the receiver must be taken into account in the evaluation process.

c. The second aspect of site improvement is the selection and implementation of the improvement features. Specific site improvement actions should not be undertaken until the sources and the nature of potential or actual performance problems have been identified through the process of analysis. Because of the cost and the time delays associated with such improvements, however, the investigator may elect to initiate preventative measures during the site installation phase when construction labor and materials may be conveniently available. Initial attention to potential site problems can prevent expensive delays in service availability to the flying public.

d. There are two general approaches to site improvement. One is through site modification such as removal of an offending structure or by minimizing the multipath by destructive reflection. The second approach is through changes in the VORTAC antenna equipment. Strictly speaking, these latter activities are not site improvements. They will be described as such, however, since the changes are made in response to specific site problems. A larger-than-conventional counterpoise, for example, may be used in a site where distant low angle coverage is not a major problem but where longitudinal multipath is of concern. The installation of the counterpoise at ground level in mountain top sites where height-gain is not a problem but where ground conductivity is of concern is another example of modification of the antenna installation in response to site peculiarities.

e. The VORTAC antenna installation including counterpoise should, whenever possible, conform with one of the several conventional types in use within the FAA. First priority, however, shall be given to the achievement of an

overall VORTAC performance that conforms with FAA requirements. No two sites are alike and the encroachments of suburbia on formerly rural areas creates increasingly severe environments for navaid sites. As a result, in the interest of VORTAC performance, measures may have to be taken in the future which were not required in the past.

21. SITE IMPROVEMENT FOR VOR.

a. Uses of the Counterpoise.

(1) The VOR is the workhorse navigational instrument for en route applications. It is used almost universally for en route applications and at or near many terminal facilities. The DVOR is recommended only for those applications with severe and unavoidable lateral multipath problems.

(2) The large VOR counterpoise is designed to diminish the effects of longitudinal multipath (reduce nulls and signal amplitude minimums). The counterpoise results in the sharp attenuation of radiation at negative elevation angles (see figure 5-1).

(3) The large DVOR counterpoise aids in minimizing longitudinal multipath. In addition, however, the large diameter reduces the asymmetry experienced by the off-center DVOR radiating elements and minimizes modulation created by such asymmetries.

(4) A properly installed counterpoise minimizes the effect upon lateral multipath (course scalloping) of obstacles which do not extend above the horizon of the counterpoise. Further, it minimizes the effect upon longitudinal multipath of those ground areas below its horizon (see figure 5-1).

5) Effective functioning of the counterpoise depends upon good ground conductivity in the vicinity of the counterpoise and good electrical bonding between transmitter "ground", counterpoise, and the surrounding earth ground (see figure 5-2).

(6) Height-gain of the VOR site over the average terrain out to several miles is desirable for distance coverage. It should not be obtained through elevating the counterpoise significantly above the immediate area.

Such elevations create sharp discontinuities for the radiating wavefront in the vicinity of the counterpoise perimeter. The discontinuity can cause wavefront bending resulting in increased ground illumination and more longitudinal multipath. The 12-foot elevation of the counterpoise in conventional installations (see figure 1-3) should not be exceeded if at all possible, and where ground conductivity is poor, ground-level counterpoises are preferable.

b. Diminishing the Effect of Longitudinal Multipath in VOR.

(1) Preliminary to the minimization of longitudinal multipath (amplitude variations) is the task of identifying the specific nature of that multipath and the probable causes. Table 5-1 provides guidance for this process.

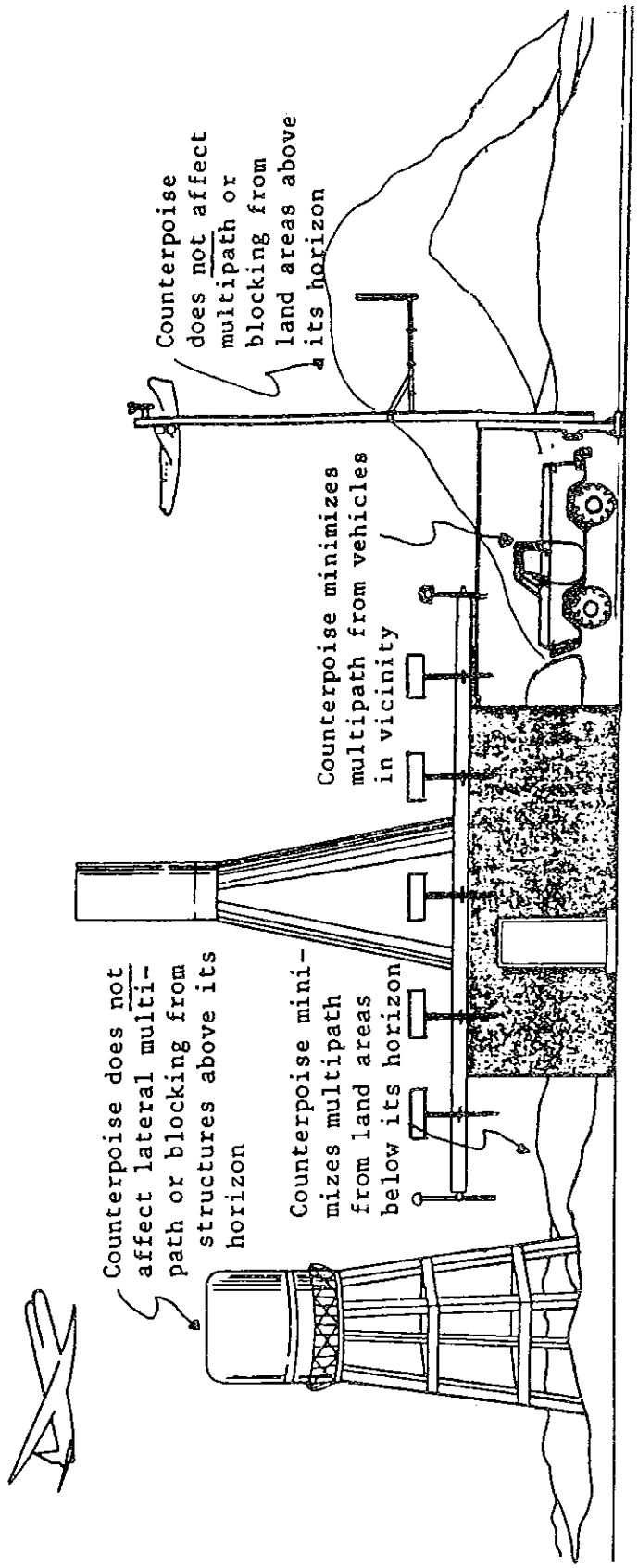

FIGURE 5-1. UTILITY AND SHORTCOMINGS OF THE VOR COUNTERPOISE

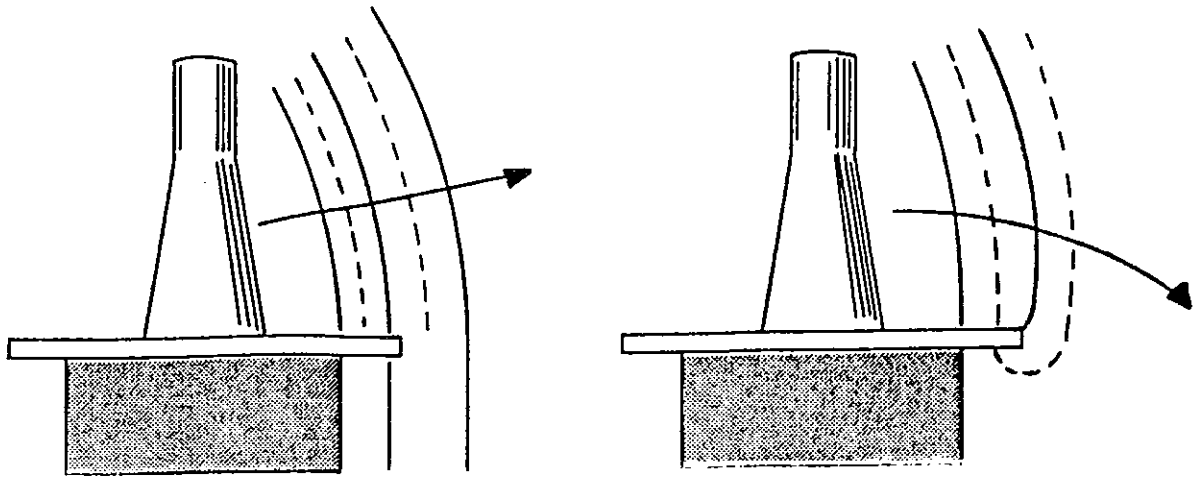

(a) Smooth em interface at perimeter. (b) Discontinuity at perimeter.

FIGURE 5-2. COUNTERPOISE BOUNDARY

TABLE 5-1. EXPLORATION OF MULTIPATH CAUSES

Vertical Angle of Null	Possible Cause	Comment
0° to 8°	Geography conducive to multipath	Consider counterpoise size and shape
More than 8°	Discontinuities experienced by em field at counterpoise boundary	Consider quality of ground connection and of ground conductivity
Null location the same at all azimuths	Cause or solution primarily with the counterpoise	See text
Null location in vertical angle found to be limited to restricted range of azimuths	Cause or solution primarily with the geography	See text

(2) From the viewpoint of geometry and simple ray tracing, the counterpoise prevents all VOR em propagation at vertical angles of declination greater than 8 degrees from illuminating the ground (see figure 2-8). The viewpoint is an oversimplification but does indicate that vertical nulls at angles of 8 degrees or less are susceptible to minimization through increase in counterpoise diameter. Before any such change is considered, however, it is useful to further identify the characteristics of the problem. See paragraph 17.b.(6) for a discussion of sloping the outer edge of the counterpoise as a means of increasing diameter as seen by the em radiation.

(3) The vertical nulls may be in the vertical angular region below 8 degrees but limited in azimuths. Such a characteristic indicates that a particular geographic area is contributing to the multipath. Examination of figure 5-3 reveals that there is a range of ground levels which will contribute destructive VOR longitudinal multipaths. It should be evident from the figure that the site geometry may be conducive to longitudinal multipath in one direction only. Consideration of figure 5-1, of the Rayleigh roughness criterion (see figure 2-6), and of the required Fresnel zone size (see figure 3-3) should assist in identifying the ground area of interest. Cost and other factors then will determine whether the null minimization is most readily accomplished by counterpoise expansion or by modification of the geography. Generally, land close to the VOR site is the only land which can be readily modified.

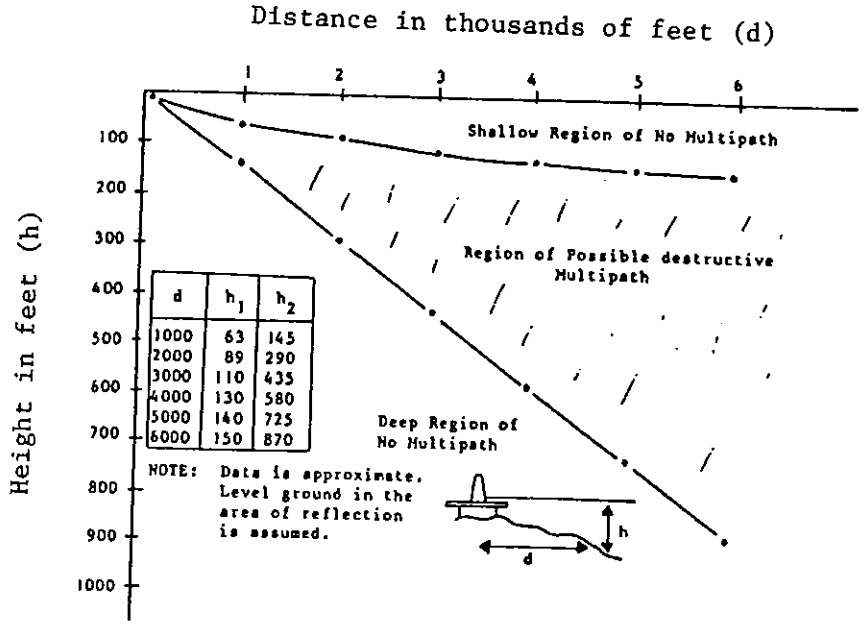

FIGURE 5-3. RANGE OF ELEVATIONS WITHIN WHICH VOR DESTRUCTIVE LONGITUDINAL MULTIPATH (VERTICAL NULLS) CAN OCCUR

(4) Depending upon the geometry and the magnitude of the Rayleigh roughness criterion, a reflecting area of limited extent can be diminished in its effects by plowing, the planting of shrubs, or the deliberate positioning of buildings as part of a site consolidation program. Large and distant reflecting areas associated with low grazing angles are usually less amenable to modification.

(5) For nulls at vertical angles greater than 8 degrees, the investigator should consider the possibility that discontinuities at the perimeter of the counterpoise may be causing the em wave front to bend toward the ground. These discontinuities may be caused by excessive height of the counterpoise above ground, poor connectivity between counterpoise and ground, poor ground conductivity, or a combination of two or more of these factors.

(6) A variety of improvements are possible for the problem of discontinuity at the counterpoise perimeter. In Europe, good results have been obtained by sloping the outer edge of the counterpoise upward. It is claimed, for the particular configuration used in Europe that this modification simulated a counterpoise of approximately double the actual diameter. See Feyer and Nattrodt, IEEE Transactions on Aerospace and Navigational Electronics, March 1965. It has been suggested that sowing metallic filings in the area around the counterpoise will compensate for poor ground conductivity. Finally, it is the usual practice at mountain top sites, where soil conductivity is often poor, to install the counterpoise at ground level.

c. Locating the Contributors to VOR Lateral Multipath.

(1) Lateral multipath creates scalloping, a periodically varying deviation of indicated bearing from true bearing. Locating an object which is a source of scalloping is accomplished by analysis of the course deviation recording taken on an orbital flight. Scalloping characteristics observed over a complete orbit can then be analyzed to identify the bearing to the interfering object from the VOR site and the distance of that object from the site.

(2) Two sets of procedures have been developed for identifying the location of scalloping sources. The first method is based on theoretical considerations and differentiates among three types of interfering objects according to the way in which they interact with the VOR field. The second method is an empirical one, which uses two simple graphic procedures to identify either nearby interfering objects or more distant ones. These two methods are discussed below in general terms, with detailed instructions for both included in appendices 3 and 4.

(3) The theoretical approach requires classification of the interfering object as a nondirectional re-radiator or a directional reflector. Directional reflectors may be either of short length or long length. Classification is accomplished by inspection of the scalloping in the flight record. The determination of the location of the object is based on the fact that the azimuth on which maximum scalloping amplitude occurs is related to the bearing of the object from the VOR. Furthermore, the frequency of the scalloping is a function of the distance of the object from the VOR.

(a) Using the approach based on theory, the relationship of the azimuth of the object to the azimuth of the scalloping source depends upon the type of object involved. For the nondirectional re-radiator, maximum scalloping amplitude will occur along two oppposing radials (180-degree separation) at a right angle (90 degrees) to the radial of the interfering object. A directional reflector will show maximum scalloping on one or two azimuths, depending upon the length of the reflector. Such maxima will be 145 degrees from an azimuth normal to the reflector. If there are two maxima 180 degrees apart, the procedure for locating a nondirectional re-radiator is appropriate. If there are two maxima 70 degrees apart, the procedure for a long-length directional reflector should be used. For a single maximum, or multiple maxima not spaced as above, the procedure for a short-length directional reflector should be used. These procedures are described in detail in appendix 3.

(b) There are several limitations on the use of the theoretically derived method described above. Interference sources may exhibit both re-radiating and reflecting characteristics. This can serve to obscure the identifying characteristics of the actual scalloping observed in the bearing error recording. Furthermore, the flight-check receiver circuits will damp out scalloping that occurs at frequencies greater than about one-half cycle per second. This can be a significant problem for scalloping sources distant from the VOR. The use of a slower aircraft and/or larger orbits can alleviate some, but not all, of this problem. If the scalloping source is very close to the VOR, the scallops may be so long that they may not be apparent on the recordings. Finally, some of the procedures will yield only a general locus of the possible locations of the scalloping source, creating a significant practical difficulty in locating the specific interfering object.

(4) To overcome the practical difficulties in the use of the theoretical method, two empirical procedures for locating VOR scalloping sources were developed and documented in internal FAA memoranda by Earl E. Palmer of the Northwest Region. The first procedure is called the Scallop Counting Method (SCM). It provides satisfactory results for locating scalloping sources from approximately 30 to 6000 feet from the VOR, and is useful for the majority of scalloping problems. The second procedure is called the Center of Symmetry Method (CSM). This procedure uses orbital data or ground error curves and is useful for finding scalloping sources very near the VOR, approximately 100 feet or less. Both methods are described in detail in appendix 4.

(a) The Scallop Counting Method uses the orbital scalloping frequency at several azimuths to determine a locus of points (straight lines) where the scalloping source could be located. The common intersection of three or more of these lines is the location of the scalloping source. Flight inspection recordings are most useful for this method, since higher frequency scalloping that is damped by the receiver may be observed on the recording of the automatic gain control voltage level. Other factors that may impact on the usefulness of the recordings are aircraft speed, altitude, and orbital radius. Consideration of these factors and a discussion of the complete procedures for this method are detailed in appendix 4.

(b) The Center of Symmetry Method relies on the principle that the scalloping source causes scalloping that is symmetrical, but out of phase, on each side of the radial on which the source is located. All scalloping sources exhibit this property; however, as the scalloping source gets farther away from the VOR, the orbital scalloping frequency becomes higher, and will be damped out and lost in the VOR bearing recording process. The CSM uses SAFI Bearing Error Reports or Saberliner orbital error plots on FAA Form 8240-4, and applies the symmetrical and out-of-phase relationship mentioned above. The recordings are taped into a continuous loop representing 360 degrees, and examined on a light table so that each half of the loop can be seen superimposed on the other. The loop is then rolled until the symmetrical scallops are aligned. A full description of the technique, with examples, is given in appendix 4.

d. Minimization of VOR Lateral Multipath.

(1) The horizontally polarized VOR signals are very susceptible to interfering lateral multipath reflection from power lines, metal fences, and metal buildings. The most satisfactory approach to minimization of these reflections is the physical removal of the reflector, the relocation of the VOR site, or the conversion of the facility to DVOR which is resistant to such interference. These methods are often costly and sometimes impractical.

(2) The use of wave-cancellation techniques to reduce the reflections to acceptable levels has proven to be practical in many situations (see figure 5-4). Wave cancellation is accomplished by the use of a secondary reflector placed at such a distance in front of the offending reflector as to create destructive interference.

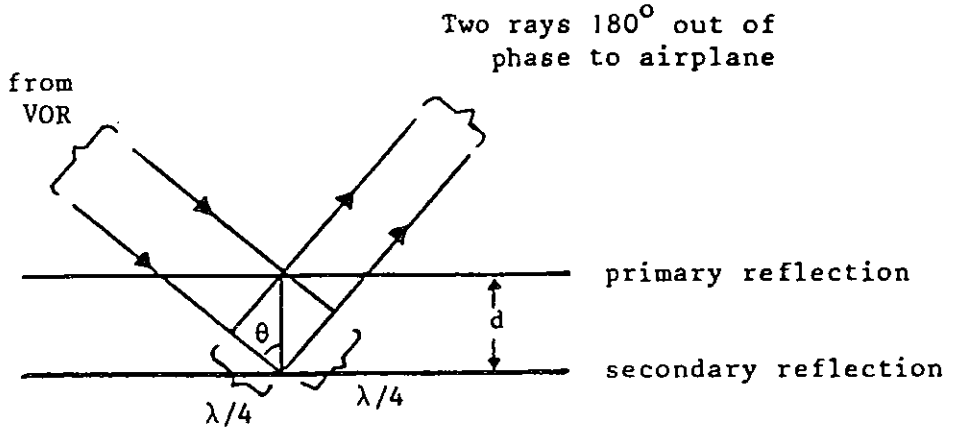

$d \cos \theta = \lambda/4$

FIGURE 5-4. GEOMETRY FOR WAVE CANCELLATION

(3) Wave cancellation techniques can also be used in connection with metallic buildings. In such applications, more than one cancelling conductor is required. The horizontal spacing of the conductors is in accordance with the principles illustrated in figure 5-3. A vertical conductor spacing of one-eighth wavelength has been found to be satisfactory. See Karns, IEEE Transactions on Aerospace and Navigational Electronics, March 1964.

(4) Because of the horizontal polarization of the VOR radiation, telephone lines and power lines are particularly effective sources of disturbance since these conductors are usually installed parallel to the earth. Their effects can be minimized if these conductors are installed along radials of the VOR radiating system. Alternately, they may be buried underground. See figures 7-8 and 7-9 and the associated discussion on short and long conductors.

(5) Fences are in a similar category to telephone and power lines, although the possibility is greater that fences will be below the horizon of the counterpoise.

(6) In areas of severe lateral multipath, which may include metallic buildings and vehicles of a variety of types, the DVOR should be considered as a replacement for the VOR. Because of the poorer low-angle distance performance of the DVOR and its large overhead "cone of confusion", the use of the DVOR has been limited in the past to terminal areas.

(7) The discussion of VOR lateral multipath minimization is summarized in table 5-2.

e. Minimization of DME and TACAN Longitudinal Multipath.

(1) Fading effects due to longitudinal multipath can be expected to be more severe for DME and TACAN than for VOR because of the higher carrier frequency of these two navaids. In addition, the VOR antenna elements are closer to the counterpoise, both in absolute distance and in wavelengths, than is the situation for DME and TACAN. Hence, the counterpoise is more effective in reducing below-the-horizon radiation for VOR than for the antennas more highly elevated above the counterpoise.

(2) There are two features of the DME and TACAN radiators which assist in the minimization of longitudinal multipath. One is the fact that these are multielement antennas designed to provide sharp attenuation for radiation below the horizon. See the cutaway sketch of a DME antenna in figure 1-6. The second feature is the vertical polarization of the radiation which provides a lower coefficient of reflection from the earth than horizontal polarization does. See figure 6-1 and the discussion associated with figures 6-33 through 6-39.

(3) The requirement for co-siting of TACAN and VOR components requires that compromises be made in the site features. It is emphasized, see section 23.b.(8), that the first Fresnel zone be free of obstacles in order to minimize TACAN signal fading. A discussion of Fresnel zones is presented in order to develop the importance of the first Fresnel zone.

TABLE 5-2. MINIMIZATION OF VOR LATERAL MULTIPATH

Source of Lateral Multipath	Method of Minimization of Multipath Effects
Long wires (telephone, power lines)	o Wave cancellation - see figure 5-4 o Bury conductors underground o Install along radial lines from the VOR
Metal fences	o Replace metal with nonconducting material o Wave cancellation o Install along radial lines from the VOR o Keep well below counterpoise horizon
Metallic building surfaces	o Wave cancellation o Keep below counterpoise horizon
Many unavoidable sources	o Replace VOR with DVOR (Provided DVOR characteristics are acceptable to the needs)

In the following paragraph, however, typical calculations are presented, showing the practical difficulty of providing a clear first Fresnel zone. See figure 5-5 and imagine an infinitely large transparent screen in the path of radiation from VORTAC to aircraft and with its plane perpendicular to the direct ray. Concentric circles may be drawn on this screen centered on the point where the direct ray intersects the screen. The radius of the first circle is such that the difference in path length between the direct path from the screen to the aircraft and the path from the circumference of the circle is $\lambda/2$. For this simplified discussion, we assume that the screen is at least 10 times as far from the VORTAC as it is from the aircraft so that all points within the first few Fresnel zones are essentially equidistant from transmitter. The area included within this first circle is the first Fresnel zone. The radii of succeeding circles are such that the corresponding path-length differences are integral multiples of $\lambda/2$. The ring-shaped areas thus formed are the second, third, etc., Fresnel zones. The em fields from the odd-numbered zones are in phase at the aircraft; the em fields from the even-numbered zones are opposite in phase to the fields from the odd-numbered zone. If it were possible to block off all contributions except those from the first Fresnel zone, the em field at the aircraft would be found to be double its free space value. If the contributions from only the first two Fresnel zones are permitted, they almost cancel, resulting in a nearly zero field at the aircraft. The locus of the first Fresnel zone is an ellipse with a circular cross section. The elliptical outline is shown in figure 6-44.

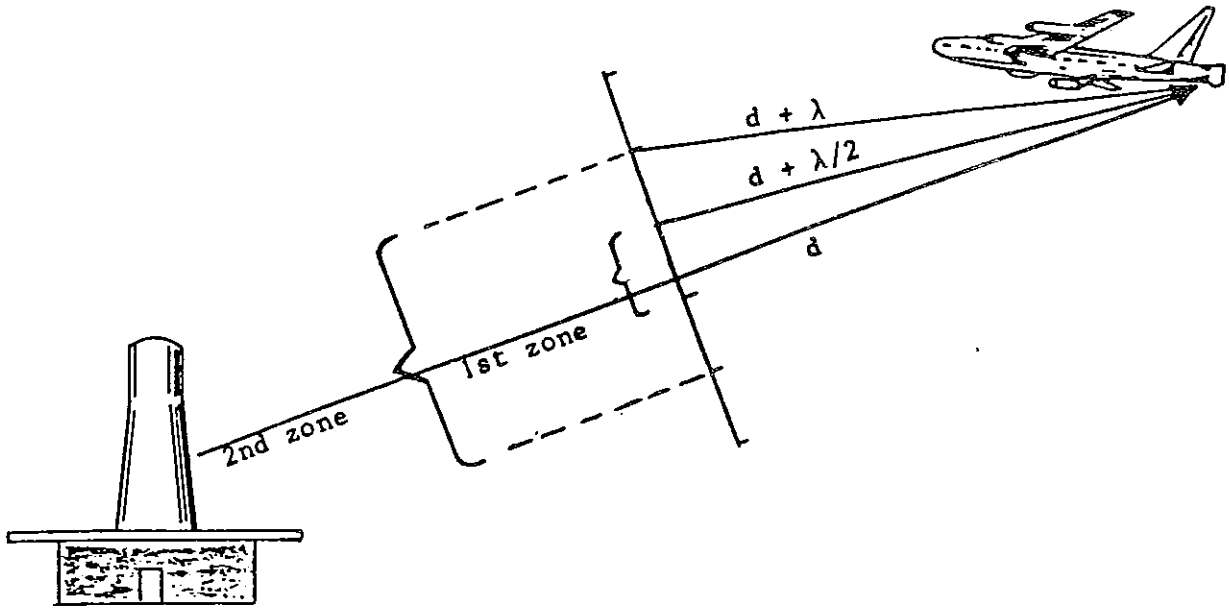

FIGURE 5-5. THE FRESNEL ZONE CONCEPT

(4) Table 5-3 shows the clearance required around the direct ray to the aircraft for first Fresnel zone clearance for an aircraft 40 nautical miles away at an altitude of 1,000 feet. The DME antenna site elevation must be on the order of 5,000 feet above the terrain, which is 20 nautical miles distant in order to provide the required Fresnel zone clearance. It is rare that one is able to obtain a site having these characteristics. The conclusion reached is that considerable reliance must be placed upon the beam shaping characteristics of the antenna and the Brewster angle effect in minimizing the effect of ground blocking or ground reflections. Once the VORTAC equipment is installed, the detailed graphic procedures described in section 23.c. may be used to locate and determine the operational importance of the individual nulls in the vertical pattern. The nature of these nulls can be modified by changes in the ground roughness (see figure 2-6) in the area where the reflection is taking place.

(5) Natural terrain features or specially constructed screens can be used to trap null-producing rays. The techniques are illustrated in figure 5-6. The construction of the screens is described in connection with lateral multipath.

TABLE 5-3. GROUND CLEARANCE REQUIRED FOR FIRST FRESNEL ZONE

$$R = \left\{ \frac{\lambda\, d(r_o - d)}{r_o} \right\}^{\frac{1}{2}} \cong \frac{1}{22.2} \left[d(r_o - d) \right]^{\frac{1}{2}} \text{ for } \lambda = 10^3 \text{ ft, } r_o = 40 \text{ n.m.}$$

(see section 23.b.(8).

d (n.m.)	R (n.m.)	R (feet)	Approx. Elev. * of Ray Center (ft)	Additional ** Ground Clearance Needed (feet)
0.5	0.20	1217	24	1193
1.0	0.28	1710	24	1686
2.0	0.39	2388	26	2362
5.0	0.60	3623	40	2583
10	0.78	4744	88	4656
15	0.87	5303	168	5135
20	0.90	5477	280	5197
25	0.87	5303	424	4879
30	0.78	4744	600	4144
35	0.60	3623	808	2815
38	0.39	2388	948	1440
39	0.28	1710	997	713
39.5	0.20	1217	1022	195

* Based on the approximation for the distance to the radio horizon, see paragraph 21.a.(4).

** These results are approximate only.

NOTE: Rays below 1 in (c) above which could produce nulls are trapped by the screen. Rays above 1 do not produce nulls.

FIGURE 5-6. TECHNIQUES FOR TRAPPING NULL PRODUCING RAYS
(From: TACAN Principles and Siting Criteria, Greco and Reed, Naval Electronic System Test and Evaluations Facility, 1968)

(6) At military installations, the areas causing null-producing rays can sometimes be engineered to be in the region of the Brewster angle through variation in the height of the TACAN antenna installation. This degree of freedom is not usually available to the site investigator concerned with a VORTAC facility.

f. Minimization of DME and TACAN Lateral Multipath.

(1) The important distinguishing feature of lateral multipath for TACAN and DME as contrasted with VOR is the much smaller size of the Fresnel zone. In simple language this means that a much smaller metallic surface than is required for VOR lateral multipath will cause strong side reflections for TACAN and DME. Parked aircraft can, for example, have such an effect.

(2) Because of the smaller size of TACAN-associated Fresnel zones, it is practical to construct relatively small-sized traps to capture and divert the offending signals (see figures 5-7 and 5-8).

(3) Wave cancellation techniques used with VOR and described in connection with figure 5-4 should be effective with TACAN radiation as well. Because of the shorter wavelengths involved, more precision will be required in the placement of the reflecting elements, and the associated support structure should be sufficiently rigid to maintain the spacing.

22.-23. RESERVED

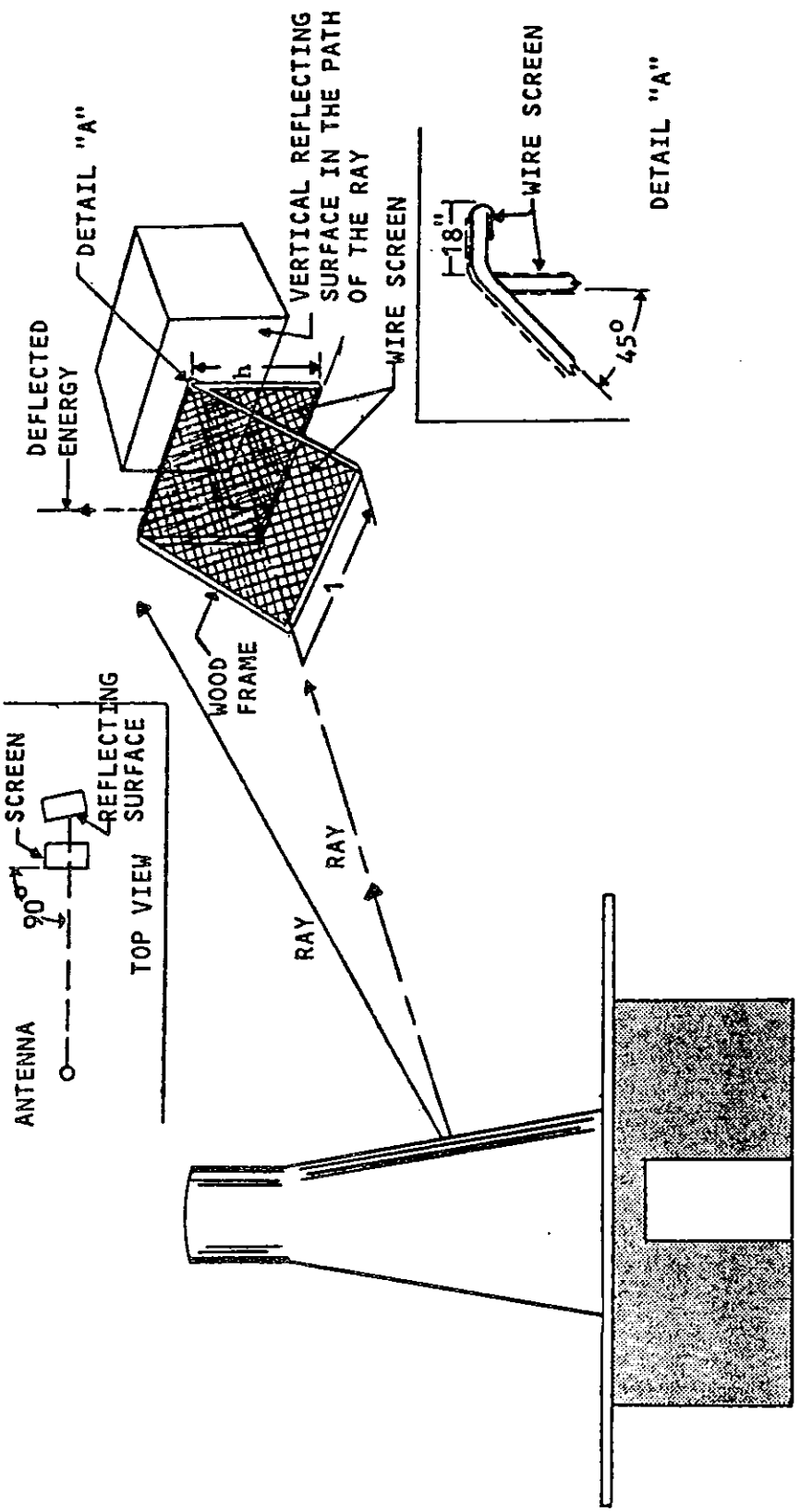

FIGURE 5-7. REFLECTIVE SCREEN CONFIGURATION (From: TACAN Principles and Siting Criteria, Greco and Reed, Naval Electronic System Test and Evaluations Facility, 1968)

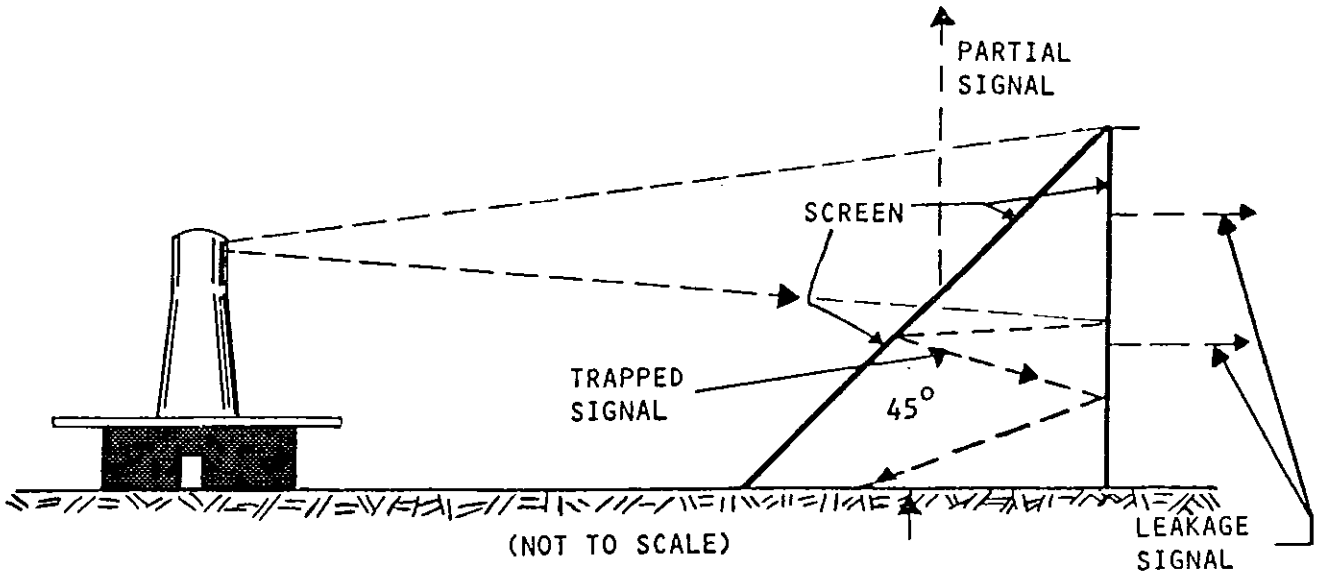

FIGURE 5-8. USE OF REFLECTIVE SCREEN (From: TACAN Principles and Siting Criteria, Greco and Reed, Naval Electronic System Test and Evaluation Facility, 1968)

CHAPTER 6. CONSIDERATIONS OF LONGITUDINAL MULTIPATH

24. GENERAL.

a. The main reason for elimination of VOR longitudinal multipath is that the VOR operation depends on the comparison of two signals, the reference and the variable phase signals, and the destructive interference of either of the two prevents proper system performance. A second reason is that horizontally polarized radiation reflects very readily, particularly at low grazing angles, thus having the capacity for producing deep nulls seriously affecting system operations.

b. The use of the counterpoise, the choice of site geography, and the growth of Fresnel zone requirements with distance all make it possible to minimize VOR longitudinal multipath at most sites.

c. By way of contrast, the longitudinal multipath associated with DME and TACAN cannot readily be eliminated but it is generally less serious in its effects than in the case of VOR. The vertically polarized radiation reflects with a considerably greater attenuation than does horizontally polarized radiation, and the pulsed nature of the modulations provides some multipath protection.

d. In summary, longitudinal multipath exists at all TACAN and DME installations, but its presence may not appreciably deteriorate performance. Hence, considerable analysis of such multipath may be of use in evaluating equipment performance. The longitudinal multipath should not cause problems in the average VOR installation, and analysis is of interest only to the extent necessary to eliminate the effect.

e. In view of the foregoing, the treatment of longitudinal multipath for DME and TACAN is detailed and complete while that for VOR is very brief. Note, however, that all of the geometric considerations discussed in connection with TACAN and DME apply as well to VOR and DVOR.

25. PROPAGATION CONSIDERATIONS IN GENERAL.

a. Propagation Components and Effects.

(1) The four components of a navaid signal radiated from a ground station and received at the airborne receiver are the direct signal, the longitudinal multipath signal, the lateral multipath signal, and the ground wave.

(2) Propagation effects due to the ground wave may be ignored since these effects are limited to the range of 1 to 10 wavelengths above the surface of the earth. Additionally, ground wave effects are of secondary importance at 100 MHz and entirely negligible at 1,000 MHz.

(3) The reflection coefficient for longitudinal multipath differs considerably for vertical polarization, as in DME and VORTAC, and horizontal polarization, as in VOR and DVOR. See figure 6-1.

(4) Radio Horizon. Distance to the radio horizon may be determined from the geometry of figure 6-2. Calculations reveal that the standard service volume as defined in paragraph 21.b is entirely within the radio horizon for VOR, DME, and VORTAC.

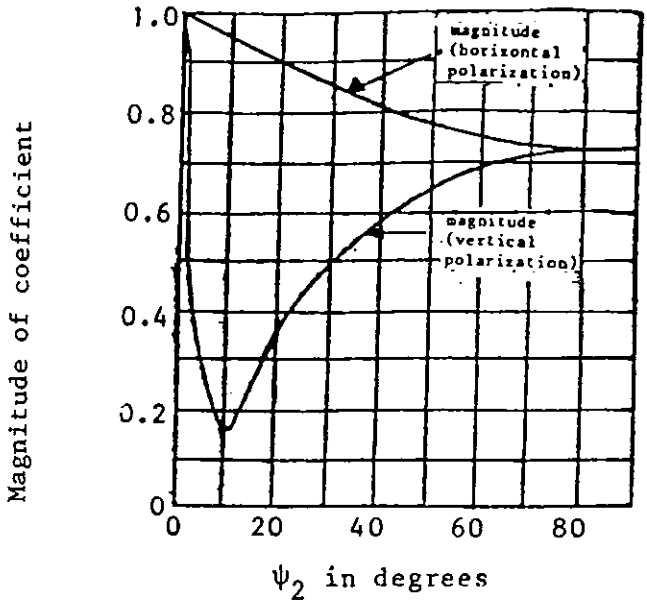

FIGURE 6-1. REFLECTION FROM A PERFECT EARTH

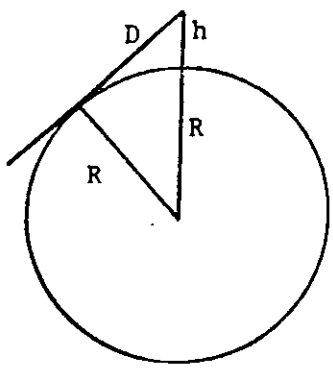

$$D^2 + R^2 = (h + R)^2$$
$$D \simeq [2Rh]^{\frac{1}{2}}$$
$$h << R$$

FIGURE 6-2. RADIO HORIZON GEOMETRY

The conventional simplified relationship for distance to the radio horizon is:

$$D = \sqrt{2h}$$

h in feet

D in statute miles

In the dimensions used in the present order and with h always in feet, this may be written as:

$$D = 1.23\sqrt{h} \cong 5/4\sqrt{h} \text{ nautical miles}$$

$$D = 2.3\sqrt{h} \text{ kilometers}$$

(5) Multipath Fading. Figure 6-3 shows the multipath fading characteristics that can result because the phase difference between direct and reflected rays varies with atmospheric conditions. The geometry of the navaid situation, with the airborne receiver much higher than the transmitter, results in the point of re-radiation being very close to the ground-based transmitter. With this geometry, the phase difference between the two rays is relatively constant, and fading is reduced in importance.

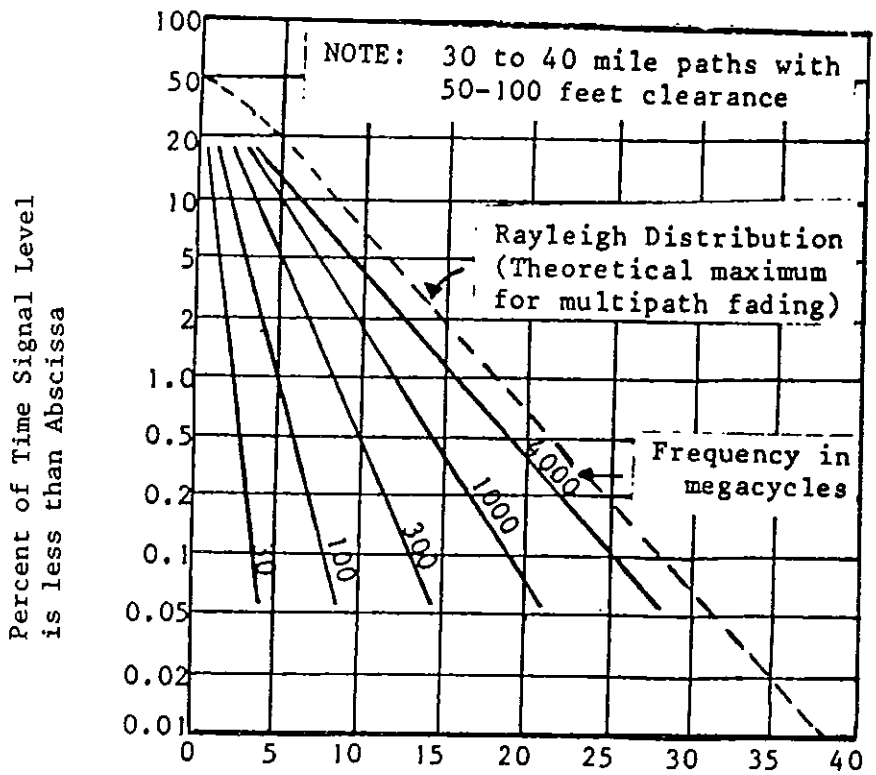

FIGURE 6-3. TYPICAL FADING CHARACTERISTICS

(6) Diffraction Due to Obstacles. The horizontal ray, in the case of low-altitude and high-altitude navaids of the types under consideration here, must provide a usable signal at 1,000 feet altitude (305 m) at a slant range of 40 nautical miles (74 km). This horizontal ray may be considered as propagating in free space only if it has substantial clearance over all obstacles. The signal loss when this ray grazes a hill (see figure 6-4) may be anywhere in the range of 2 to 20 dB, with 6 dB as a probable value.

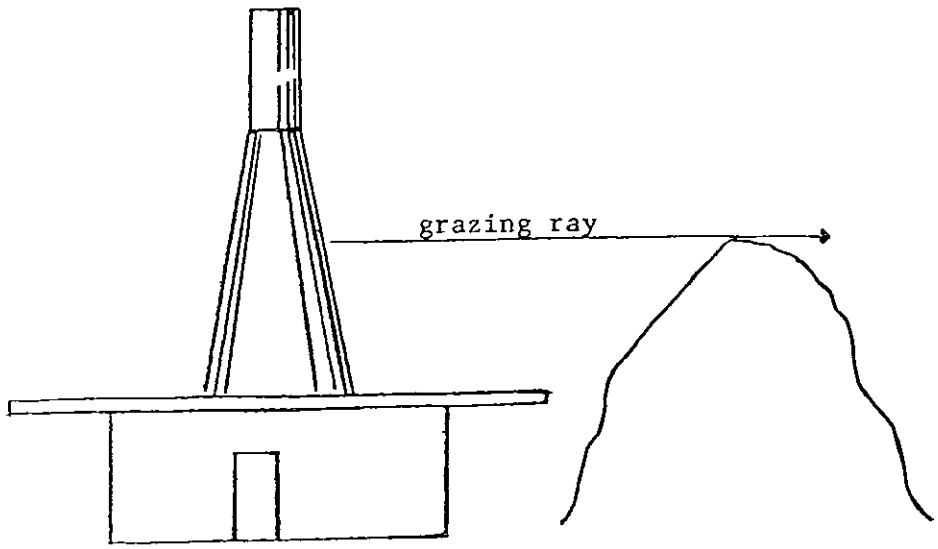

FIGURE 6-4. DIFFRACTION ACROSS A HILL

b. Standard Service Volumes[1/]

(1) Ground stations are classified according to their intended use. These stations are available for use within their service volume. Outside the service volume, reliable service may not be available. For standard use, the airspace boundaries are called standard service volumes. They are defined in table 6-1 below for the three station classes. These SSVs are graphically shown in figures 6-5 through 6-9. The SSV of a station is indicated by using the class designator as a prefix to the station type designation. (Examples: TVOR, LDME, and HVORTAC.)

1/ Text and illustrations for subsection 21.b. from: FAA Advisory Circular No. 00-31A, September 20, 1982.

TABLE 6-1. STANDARD SERVICE VOLUME DESIGNATOR

SSV Class Designator	Altitude and Range Boundaries
T (Terminal)	From 1000 feet (305 m) AGL up to and including 12,000 feet (3,658 m) AGL at radial distances out to 25 nmi (46 km). See figures 6-7 and 6-8.
L (Low Altitude)	From 1000 feet (305 m) AGL up to and including 18,000 feet (5,486 m) AGL at radial distances out to 40 nmi (74 km). See figures 6-6 and 6-9.
H (High Altitude)	From 1000 feet (305 m) AGL up to and including 14,500 feet (4,420 m) AGL at radial distances out to 40 nmi (74 km). See figures 6-5 and 6-9. From 14,500 feet (4,420 m) AGL up to and including 60,000 feet (18,288 m) at radial distances out to 100 nmi (185 km). See figures 6-5 and 6-9. From 18,000 feet (5,486 m) AGL up to and including 45,000 feet (13,716 m) at radial distances out to 130 nmi (241 km). See figures 6-5 and 6-8).

c. Considerations for Extended Coverage.

(1) Introduction. This order is concerned primarily with siting the navaid systems in order to obtain reliable service within the standard service volume. It is, however, useful to be able to determine the extended coverage performance of the various equipments for applications where extended coverage is desired and for determining interference potential between different sites. For additional material refer to FAA Advisory Circular 00-31A.

(2) Radio Line of Site for Low Elevation Angles. From figure 6-10,

$$ha \cong 6080\, r_o \left[\frac{r_o}{2R_1} + \tan\alpha\right]$$

and extending the earth radius by a factor of 4/3 to account for atmospheric diffraction:

$$ha \cong 0.662\, r_o^2 + 6080\, r_o \tan\alpha$$

for

$$\alpha \leq 6^o$$

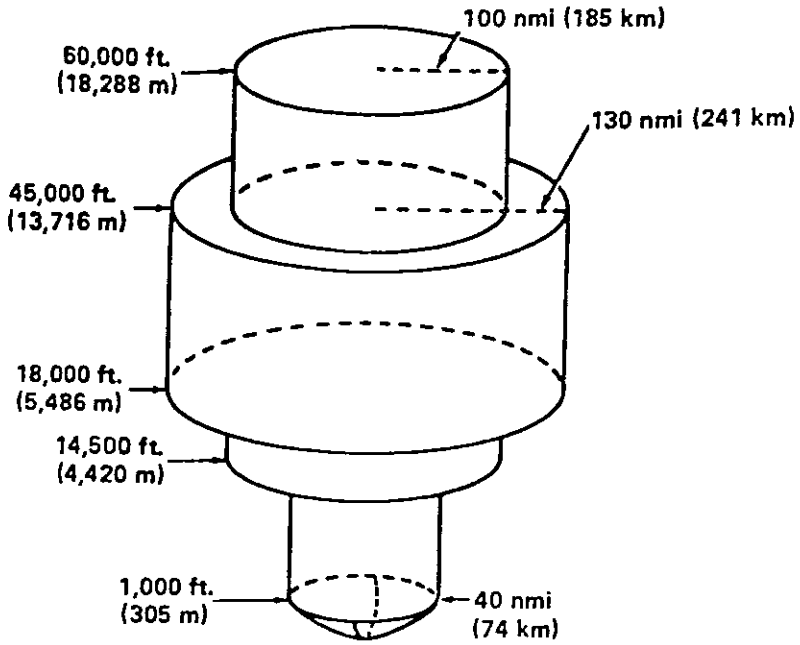

FIGURE 6-5. STANDARD HIGH ALTITUDE SERVICE VOLUME
(Refer to figure 6-9 for altitudes below 1000 feet 305 m)

NOTE 1: All elevations shown are with respect to the station's site elevation (AGL). Metric measurements are given for convenience and are approximations. These figures do not reference the area defined as the Vertical Angle Coverage Limitations (see note 2).

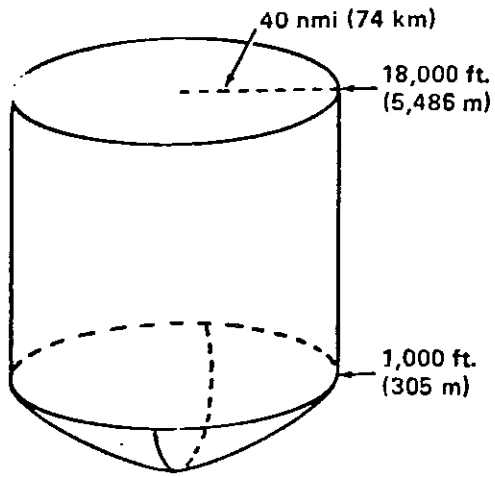

FIGURE 6-6. STANDARD LOW ALTITUDE SERVICE VOLUME
(Refer to figure 6-9 for altitude service volume)

NOTE 2: Azimuth signal information is normally provided from the radio horizon up to elevation angles of approximately 60 degrees for VOR components and 40 degrees for TACAN components. Distance information provided by TACAN and DME will provide satisfactory service from the radio horizon to an elevation angle of not less than 60 degrees.

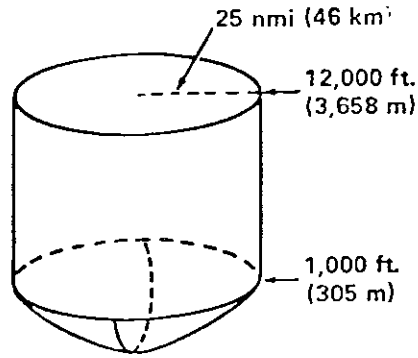

FIGURE 6-7. STANDARD TERMINAL SERVICE VOLUME (Refer to figure 6-8 for altitudes below 1000 feet 305 m)

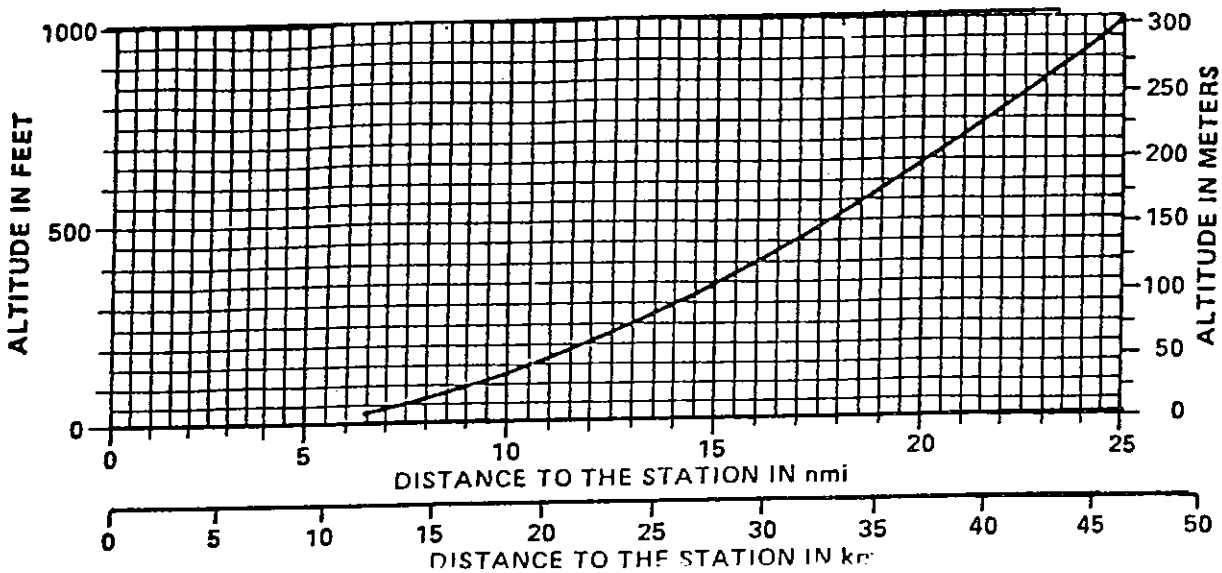

FIGURE 6-8. DEFINITION OF THE LOWER EDGE OF THE STANDARD T (TERMINAL) SERVICE VOLUME

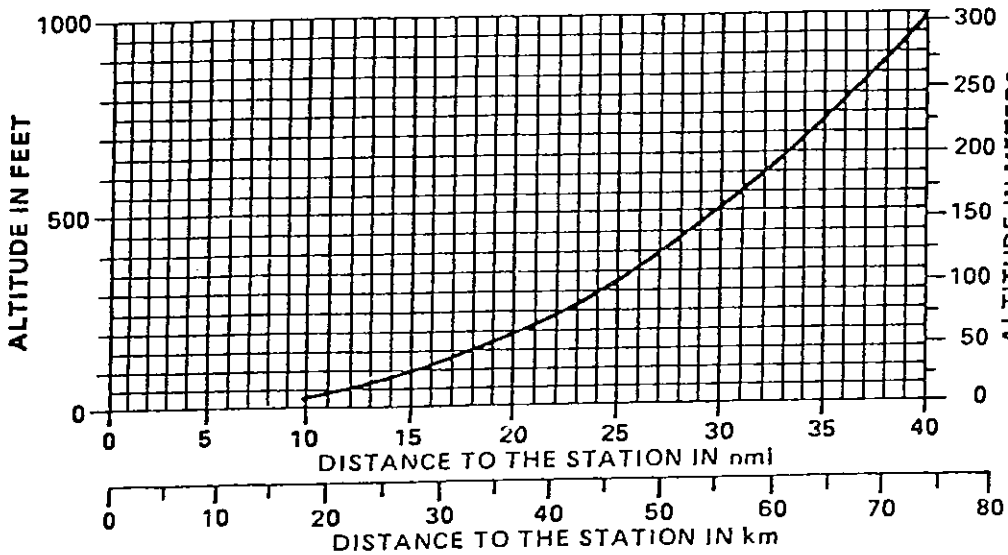

FIGURE 6-9. DEFINITION OF THE LOWER EDGE OF THE STANDARD H (HIGH) AND L (LOW) SERVICE VOLUMES

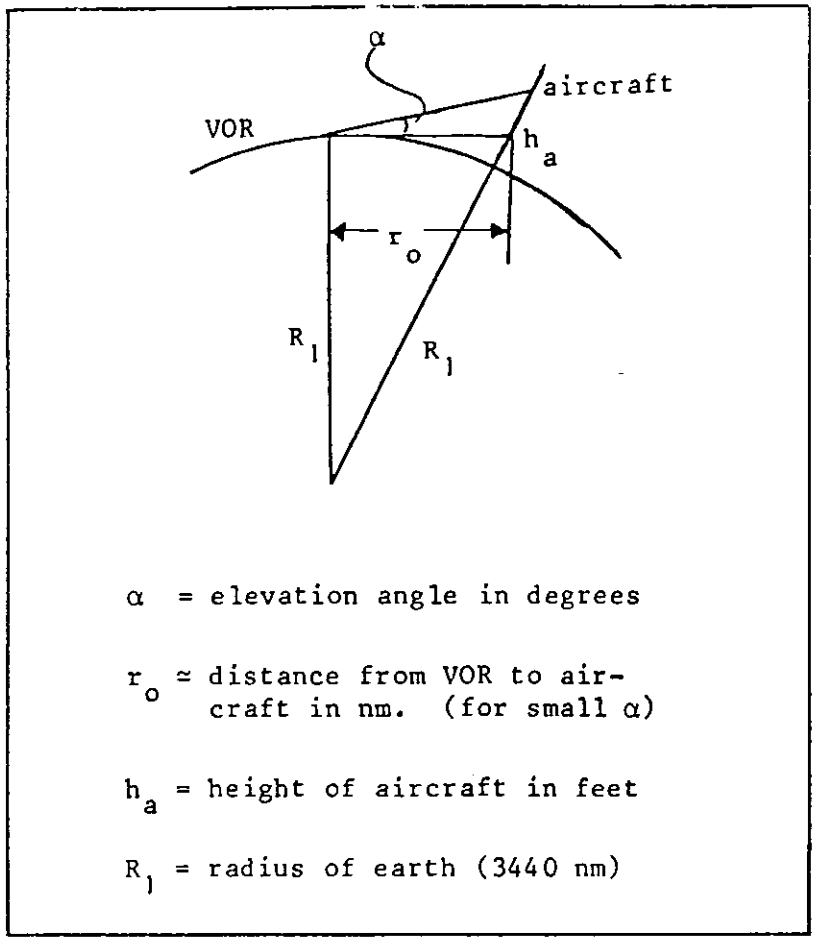

FIGURE 6-10. LINE OF SIGHT RELATIONSHIPS

These results are plotted in figures 6-11 and 6-12.

(3) VOR Coverage. The VOR ground station shall provide a minimum signal power density of -120 dBW/m^2 (95 percent time availability) through the operational service volume. Assuming, as is reasonable, that the VOR transmitting system has the following power budget:

20 dBW	transmitter power
- 3 dB	cable loss
+ 2.2dBi	antenna gain
19.2dBW	effective isotropic radiated power (118 MHz)

Then the curves of coverage of VOR as shown in figures 6-13 and 6-14 are obtained.

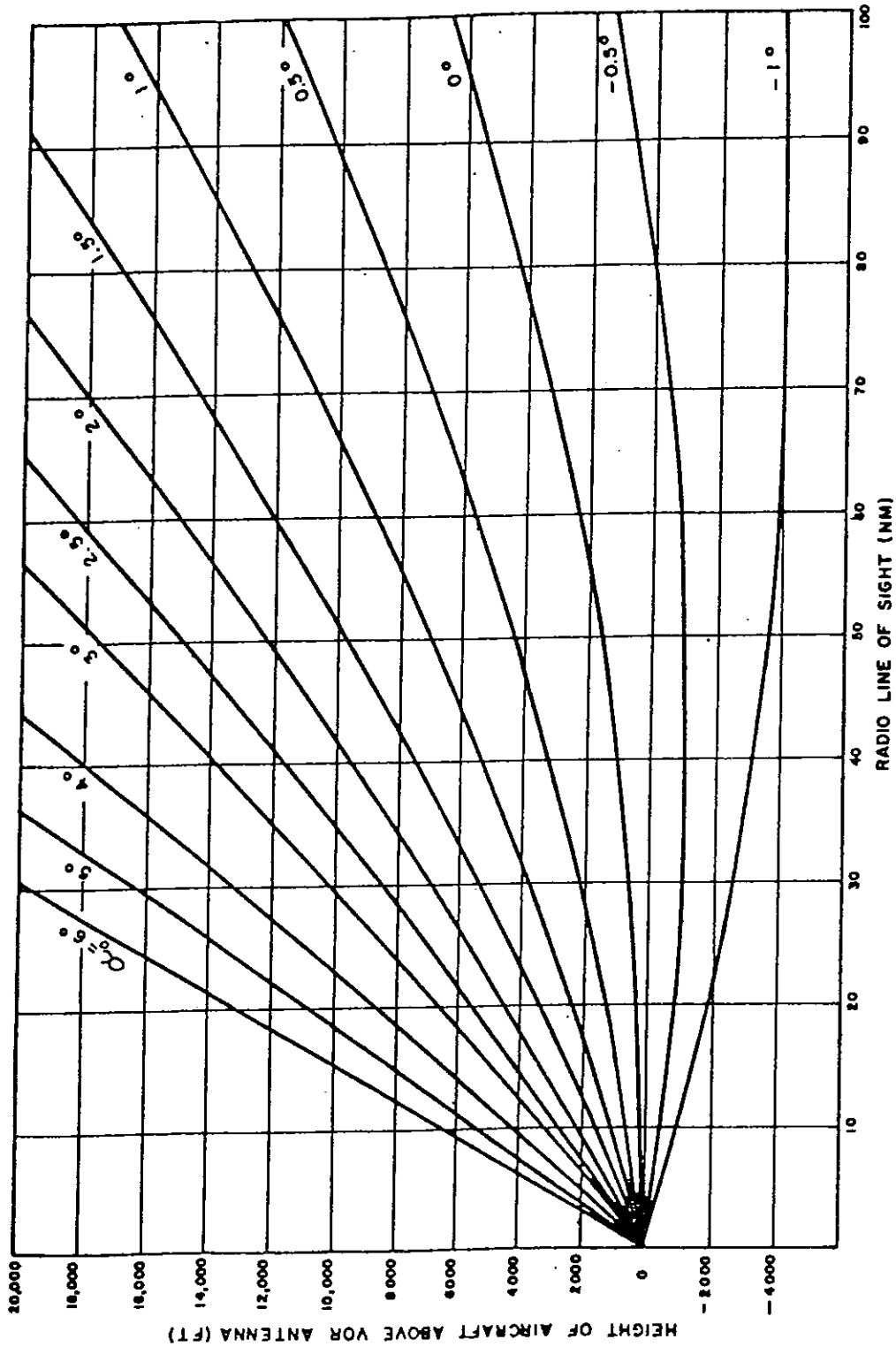

FIGURE 6-11. RADIO LINE OF SIGHT (AIRCRAFT BELOW 20K)

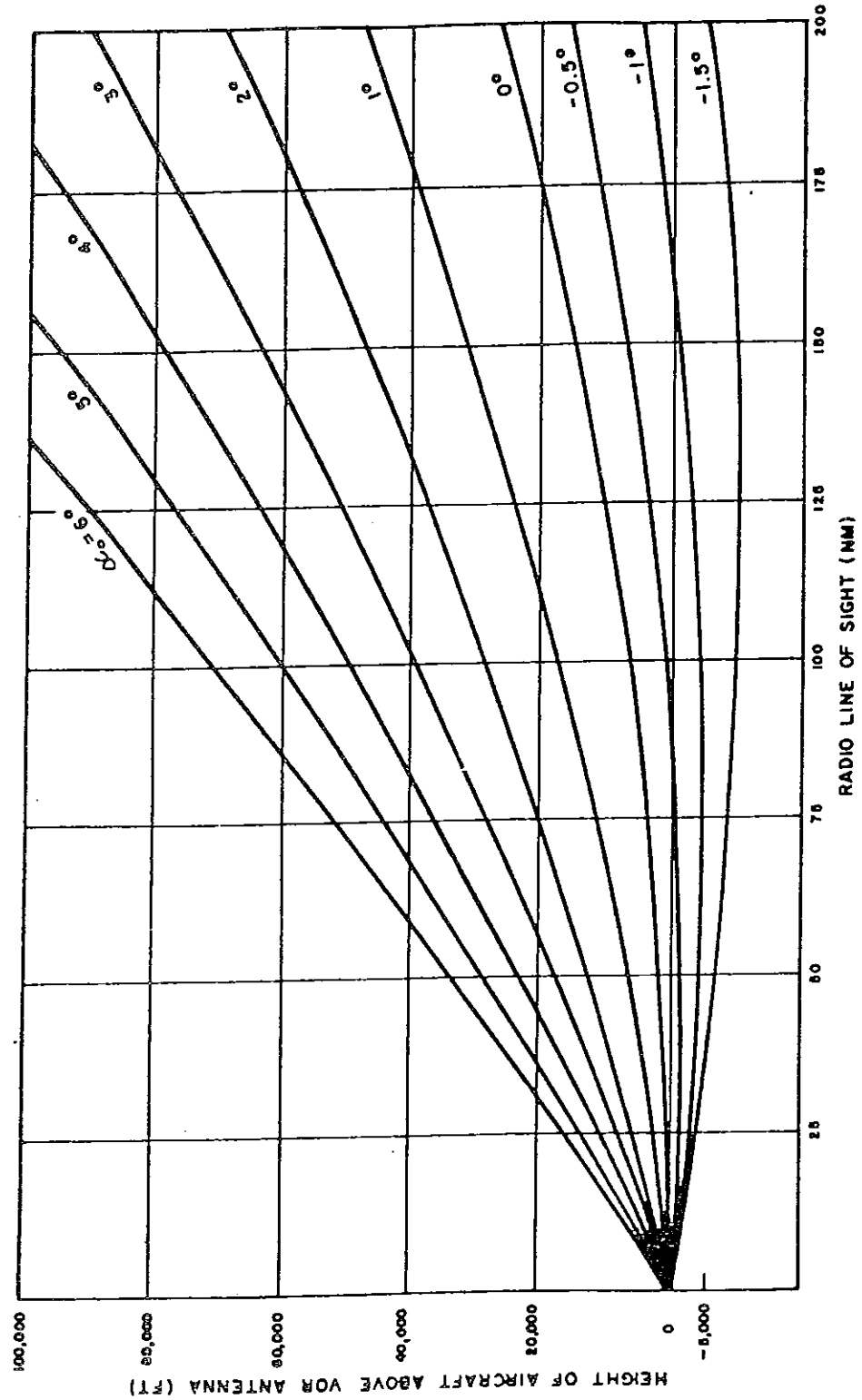

FIGURE 6-12. RADIO LINE OF SIGHT (AIRCRAFT BELOW 100K)
(From: FAA Advisory Circular No. 00-31A, September 20, 1982)

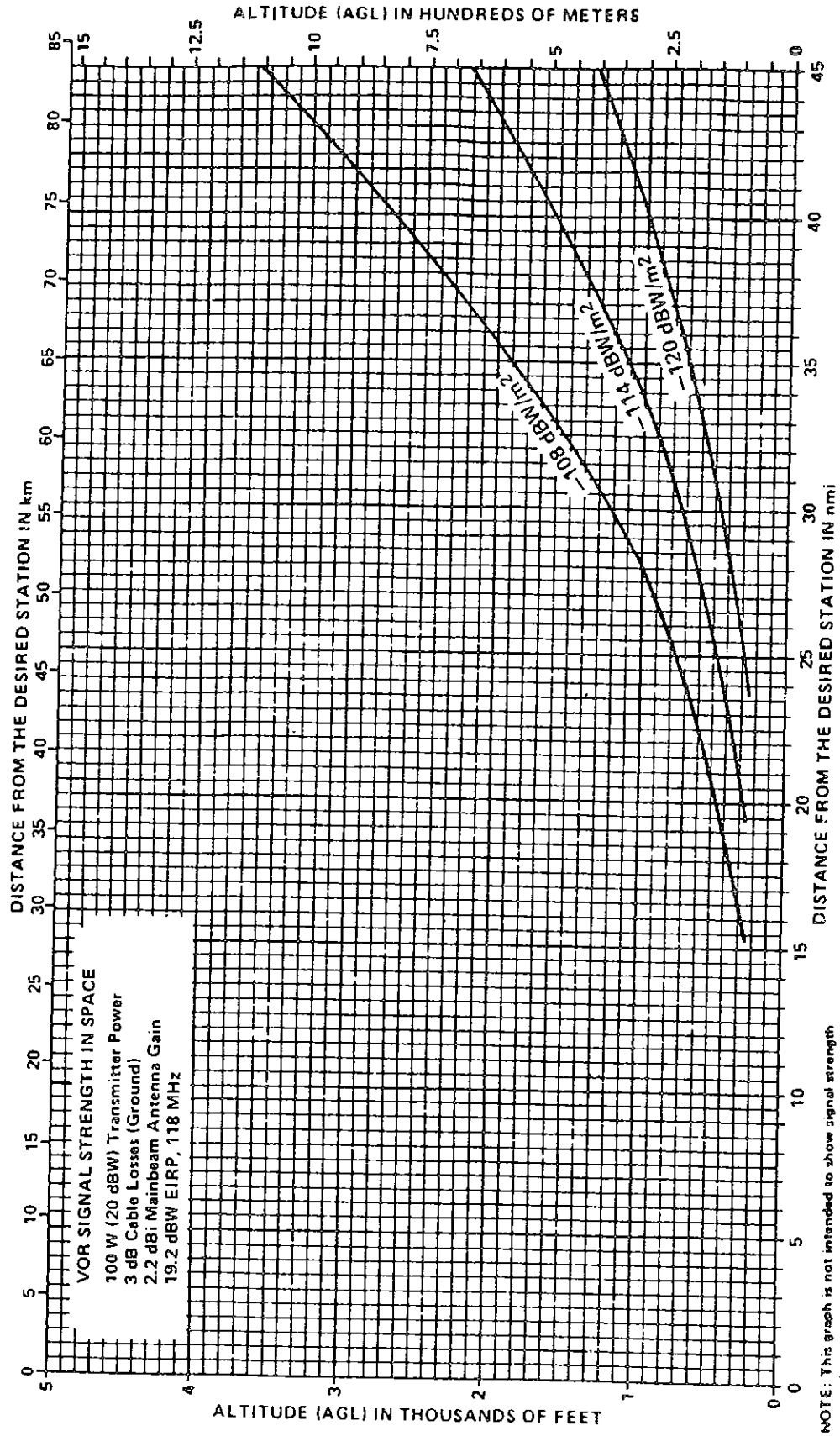

FIGURE 6-13. VOR SIGNAL STRENGTH IN SPACE - SHORT RANGE
(From: FAA Advisory Circular No. 00-31A, Appendix 1)

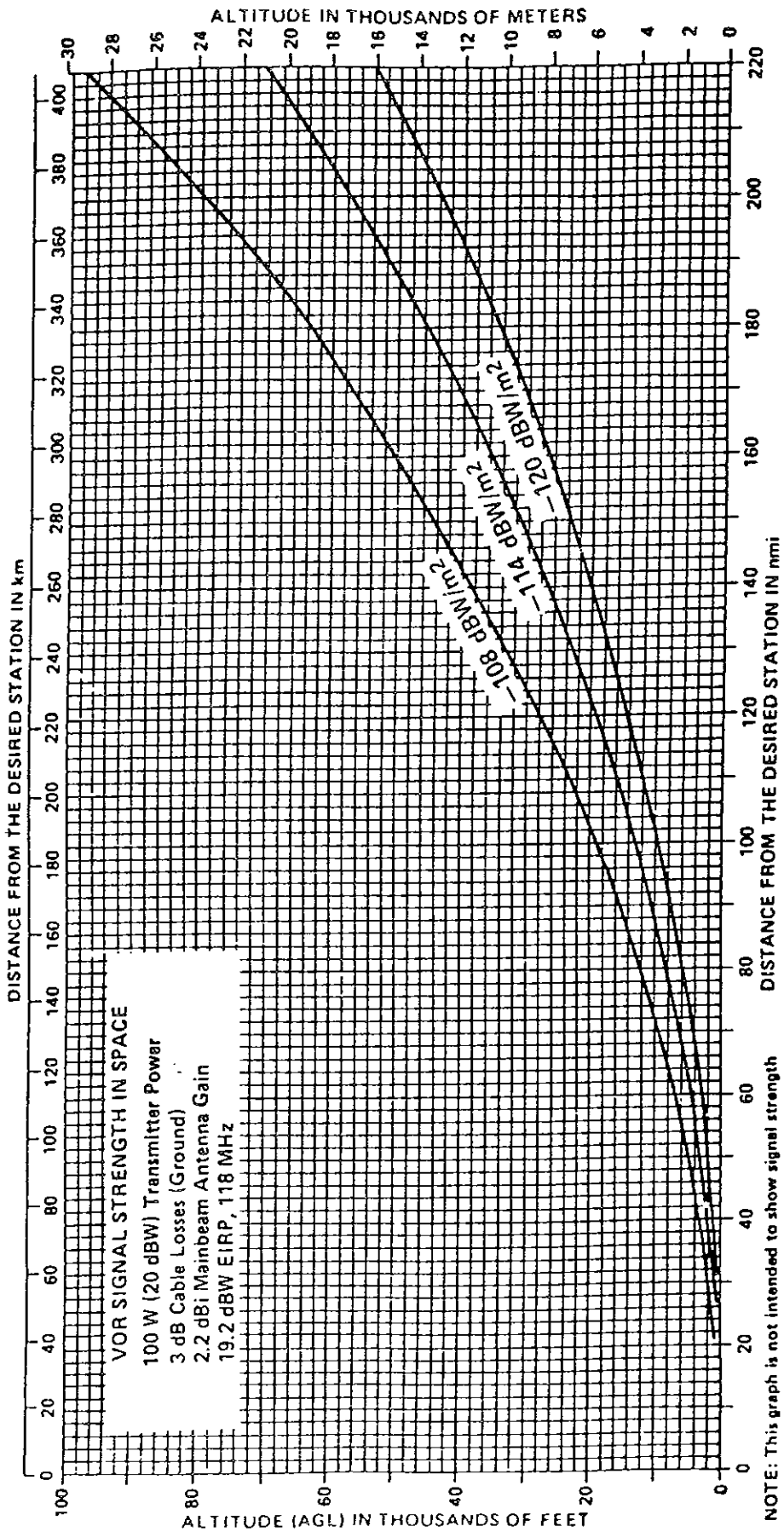

FIGURE 6-14. VOR SIGNAL STRENGTH IN SPACE - LONG RANGE
(From: FAA Advisory Circular No. 00-31A, Appendix 1)

(4) DME Coverage. The DME ground station shall provide a minimum signal power density of -91.5 dBW/m^2 (95 percent time availability) for that part of the operational service volume which is above 18,000 feet (5,486 m). Within that part of the service volume which is below 18,000 feet (5,486 m) a minimum signal power density of -86.0 dBW/m^2 shall be provided. Signal power is determined by the average over one second of the equivalent peak pulse voltage waveform. Assuming, as is reasonable, that the DME transmitting system has the following power budget:

20 dBW	transmitter power
- 1.5dB	cable loss
+11.4dBi	antenna gain
29.9dBW	effective isotropic radiated power (1213 MHz)

Then the curves of coverage of DME as shown in figures 6-15 and 6-16 are obtained.

(5) TACAN Coverage. The TACAN shall provide the same signal coverage as already described for the DME. A reasonable power budget for the TACAN is:

37 dBW	transmitter power
- 1.5dB	cable loss
+ 7.4dBi	antenna gain
42.9dBW	effective isotropic radiated power (1213 MHz)

Then the curves of coverage of DME as shown in figures 6-17 and 6-18 are obtained.

(6) For an additional discussion of coverage see FAA Advisory Circular 00-31A.

26. LONGITUDINAL MULTIPATH FOR VOR.

a. Overview.

(1) An objective in the siting of VOR and DVOR equipments is to completely eliminate any substantial instrumental errors due to longitudinal multipath. It is in furtherance of this objective that the large counterpoise is a feature of every VOR and DVOR installation.

(2) In those situations where longitudinal multipath adversely affects system performance, its effects shall be minimized or, if possible, eliminated by refinements of the engineering of the counterpoise and the characteristics of the ground in the vicinity of the counterpoise. See chapter 5.

(3) In situations where costs or other constraints prevent the minimization of longitudinal multipath to permit equipment performance within standard service volumes and tolerances, appropriate steps shall be taken to inform the flying public of that portion of the standard service volume for which the system is not operational within specifications.

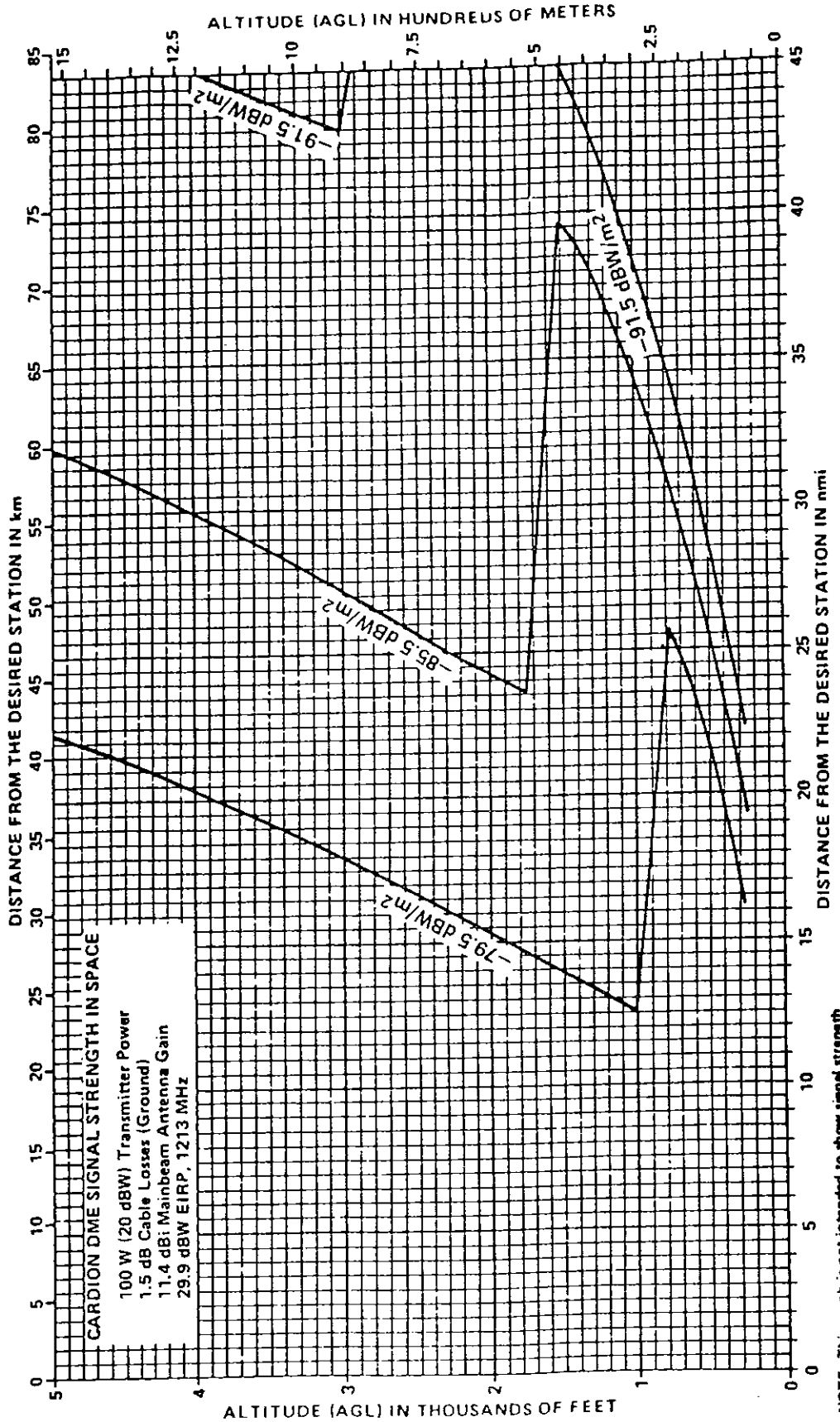

FIGURE 6-15. CARDION DME SIGNAL STRENGTH IN SPACE - SHORT RANGE
(From: FAA Advisory Circular No. 00-31A, Appendix 1)

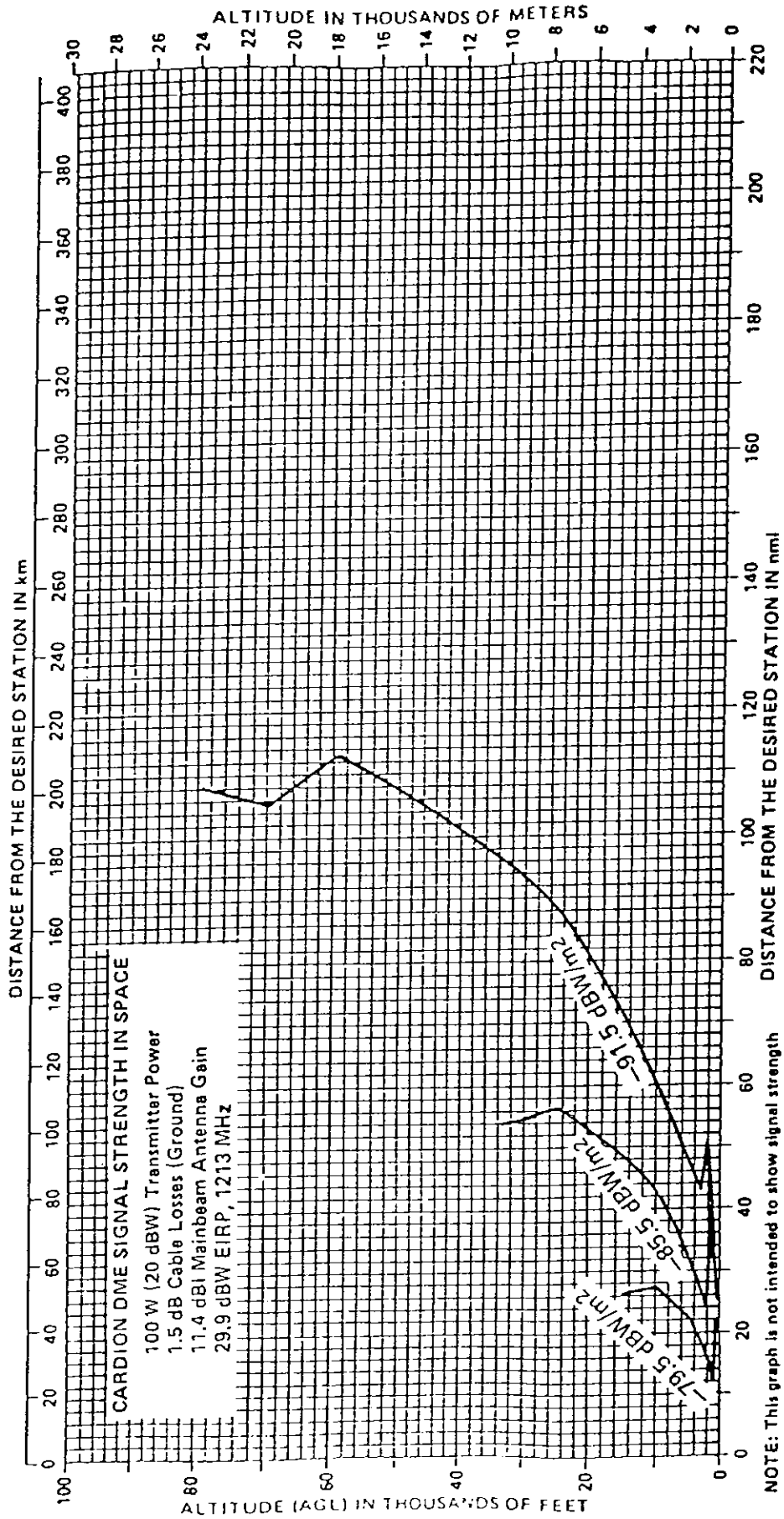

FIGURE 6-16. CARDION DME SIGNAL STRENGTH IN SPACE - LONG RANGE
(From: FAA Advisory Circular No. 00-31A, Appendix 1)

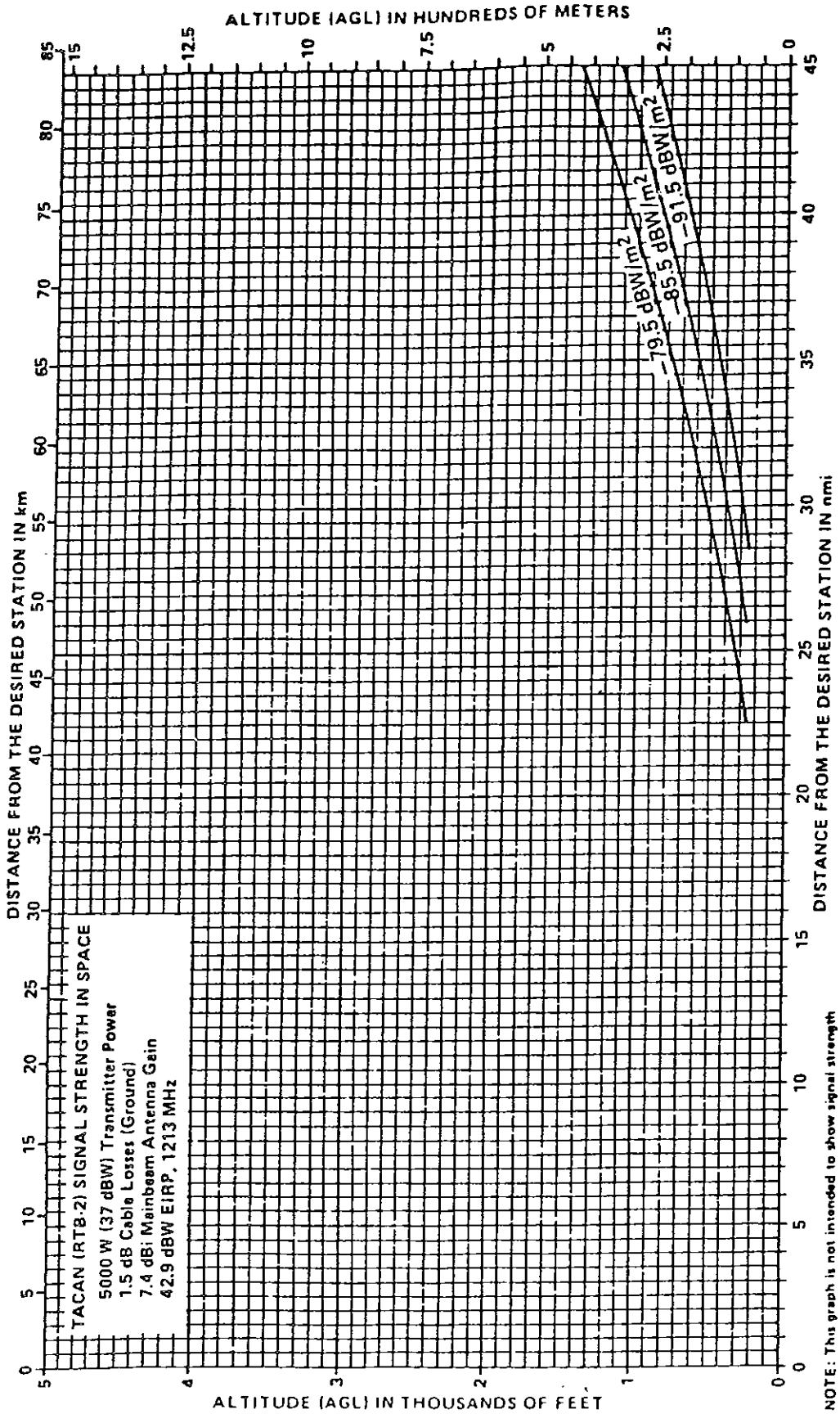

FIGURE 6-17. TACAN (RTB-2) SIGNAL STRENGH IN SPACE - SHORT RANGE
(From: FAA Advisory Circular No. 00-31A, Appendix 1)

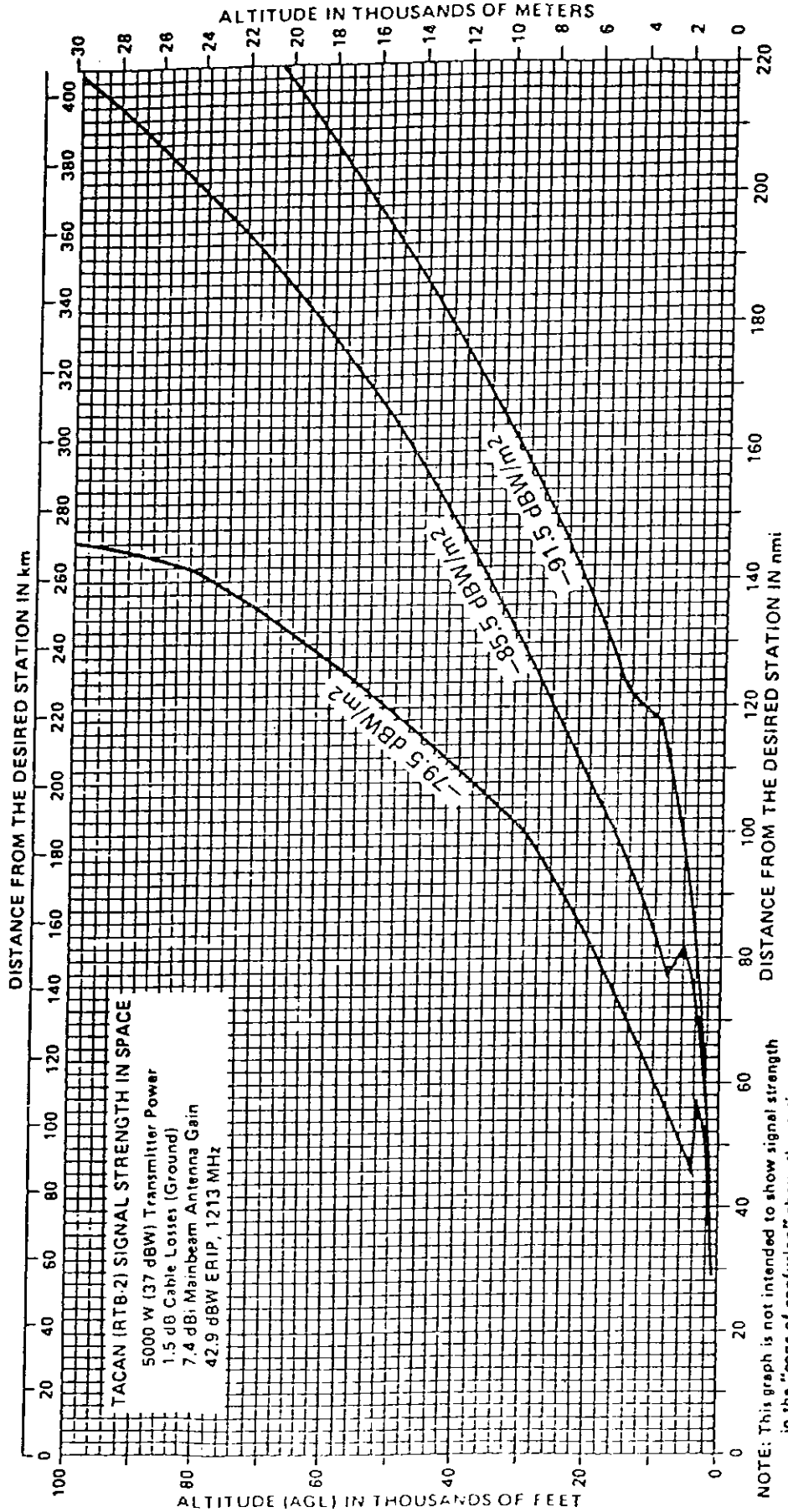

FIGURE 6-18. TACAN (RTB-2) SIGNAL STRENGTH IN SPACE - LONG RANGE
(From Advisory Circular No. 00-31A, Appendix 1)

b. The Effect of Reflecting Surfaces.

(1) The function given in paragraph 5.b.(1) represents the vertical radiation pattern of the VOR in the presence of a perfectly conducting ground.

(2) For the usual height of the VOR radiating loops of 15 feet and at the VOR wavelength of approximately 8 feet, this pattern produced by the source and reflected source has a first null at about 15 degrees.

(3) The depth and severity of the 15-degree null is a function of the ground conductivity, roughness, and slope over the Fresnel zone illuminated by the 15-degree ray. Generally, these physical imperfections, as contrasted with a smooth, perfectly reflecting ground, tend to fill in the null that is predicted by theory.

(4) Considering the 4-foot height of the VOR antenna above the counterpoise and the counterpoise as a reflector yields a radiation pattern null at about 60 degrees. This is at the limit of the standard service volume of the VOR.

(5) Operationally, the equipment performance at angles below about 10 degrees is the most important. The conventional counterpoise provides little protection for angles below about 8 degrees (see figure 2-8). Additionally, the ground is a good reflector for horizontal polarization and low grazing angles at VOR frequencies.

c. Uses of the Fresnel Zone Size.

(1) The VOR is susceptible to the effects of longitudinal multipath primarily in the region of grazing angles below 8 degrees. The principle natural protection of the equipment in this angular region is the size of the Fresnel zone required to support the reflection.

(2) Figure 3-3 demonstrates that the farther the area of reflection can be removed from the VOR site, the larger the Fresnel zone required to sustain the reflections. Hence, it is desirable to select geography sufficiently irregular to place the reflection point at a distance of perhaps a mile or more.

(3) Smooth valley floors around high mesa sites, as may occur in western states, can be expected to provide the required large-area Fresnel zones for grazing angle multipath. The height-gain of such sites, however, affords the possibility for use of a larger-than-conventional counterpoise with no loss in distant coverage.

(4) Ocean surfaces, by their regularity, can provide the large-area Fresnel zones for grazing angle multipath. The single degree of freedom available at locations experiencing such problems is the variation of the height of the radiating antennas. Counterpoises have been used at ground level at such locations.

d. VOR Versus DVOR for Longitudinal Multipath.

(1) The performance of both VOR and DVOR depends upon the near simultaneous arrival at the aircraft receiver of both the reference-phase and the variable-phase signals. The elimination of either of these signals by destructive longitudinal multipath adversely affects performance.

(2) In VOR, the variable-phase signal is relatively vulnerable to the effect of longitudinal multipath, whereas the reference-phase signal, because of the characteristics of fm, is relatively resistant. In DVOR, exactly the reverse is true. It follows that there is no inherent advantage to one over the other in combatting longitudinal multipath, although, in some situations, second-order effects may favor one over the other.

(3) The discussion is summarized in table 6-2 below.

TABLE 6-2. ELIMINATION OF VOR LONGITUDINAL MULTIPATH

Parameter	Comment
Overall Objective	Reduce or eliminate effects of longitudinal multipath
Angular Area of Concern	Operationally, the region of vertical angle of 0 degree to 10 degrees is of most concern; particularly because the effect of the counterpoise is diminished in the 0-degree to 8-degrees region
Effect of Ground	Excellent reflector for low grazing angle VOR radiation
Effect of Fresnel Zone Size	Large Fresnel zone size makes coherent reflection more difficult. Hence, move reflection area as far from site as possible
VOR Versus DVOR	No intrinsic merits of one over the other for longitudinal multipath

27. LONGITUDINAL MULTIPATH FOR TACAN.

a. Calculation of the Basic Parameters.

(1) In an aircraft flying at a constant altitude toward a ground-based VORTAC beacon, the airborne antenna intercepts field strengths which go through a series of maxima and minima as shown in figure 6-19. The lobe formation, in a given geometry, is dependent upon the frequency of the transmitted signal and the characteristics of the reflecting ground or water. Since satisfactory operation of TACAN equipment is dependent upon the strength of the arriving signal, it is desirable to prevent the specular reflection which causes the lobe structure.

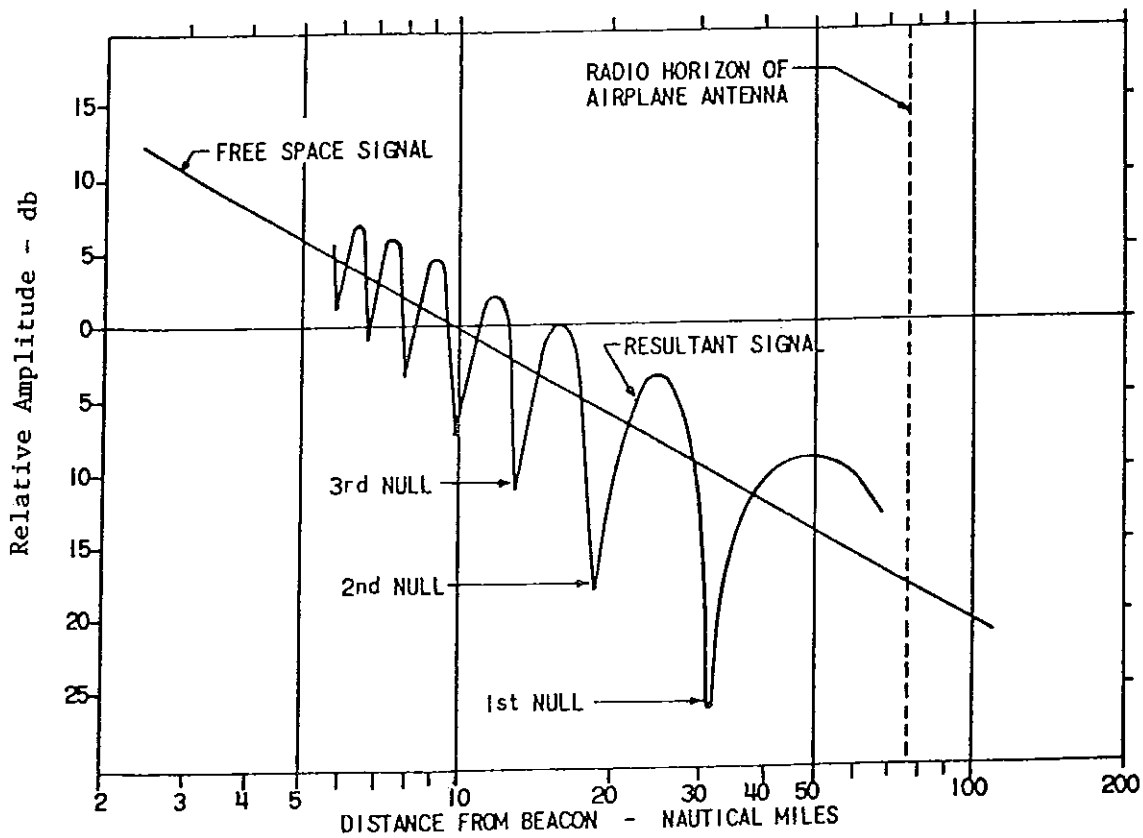

1. Frequency: 1000 Mc.
2. Antenna height above ground: 40 feet
3. Antenna type: AN/GRA-60
4. Aircraft altitude: 3000 feet
5. Terrain: smooth average land with no obstructions; conductivity (σ) of 0.03 mho-m/sq m; and a relative permittivity (ϵ_r) of 15.

FIGURE 6-19. RADIATION PATTERN OF A TWO-PATH INTERFERENCE PHENOMENA

(2) Since the formation of nulls is primarily a geometric problem, their locations may be calculated without regard to the specific antenna to be used. Refer to figure 6-20. A ray leaving the transmitting antenna at height h_1 will strike the ground at a grazing angle ψ and

$$\tan \psi \cong \frac{h_1}{6080 d_1} - \frac{d_1}{9120k}$$

at a distance d_1, from the transmitting antenna measured along the earth's surface. These parameters are related by:

$$d_1 \cong -3445k \tan \psi + \left[(3445 \tan \psi)^2 + 1.14 \, k \, h_1 \right]^{1/2} \text{ (nautical miles)}$$

The height above terrain, h_2, of a receiving antenna which will intercept this reflected ray is given by:

$$h_2 = ka \, \frac{1 - \cos d_2/ka + \sin d_2/ka_1 \tan \psi}{\cos d_2/ka - \sin d_2/ka \tan \psi} \times 6080 \text{ (feet)}$$

(3) The factor k used in the foregoing equations to compensate for atmospheric refraction is given by

$$k = \frac{1}{1 + \frac{a \Delta N}{n(10)^6}}$$

where n is the refractive index and ΔN is the change in refractivity of the atmosphere between the earth's surface and a height of one thousand feet or 0.308 kilometer above the surface. Note that the dimension of a and ΔN must agree. It is sufficient for purposes of this order to consider only three values of k. The value at the location of interest should be calculated, as will be explained, and then for purposes of referring to charts, the standard value nearest to the calculated value should be added. The refractivity, ΔN, is given by

$$N = N_o \, e^{-0.0322 h_s + \Delta N (h - h_s)}$$

where:

h_s = height of the earth's surface above mean sea level in thousands of feet

h = height above earth's surface in thousands of feet

alternatively

$$N = N_o \, e^{0.10577 h_s + \Delta N (h - h_s)}$$

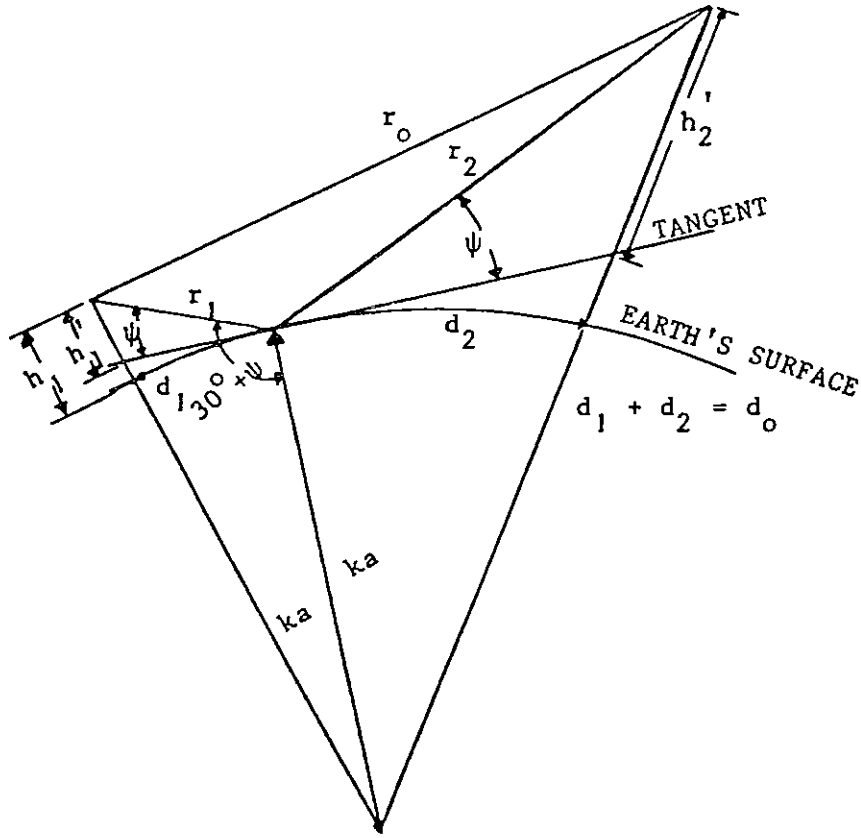

FIGURE 6-20. TWO-PATH PROPAGATION GEOMETRY

where:

d_1 = distance from the transmitting antenna to the earth reflecting point in nmi as measured along the earth surface.

h_1 = transmitting antenna height in feet.

a = earth radius, 3445 nmi.

when h_s is measured in kilometers. Note that the second term on the right above must also be in the appropriate metric units.

From the above equation both N_s, the refractivity at the earth's surface and ΔN can be calculated, since, using English units,

$$N_s = N_o e^{-0.0322h_s}$$

and

$$\Delta N = N_1 - N_s$$

where N_1 = refractivity at 1,000 feet. The value of n is $N_s(10)^{-6}$. The three values of k which are adopted as standard are:

N_s	ΔN (metric)	k
200	-22.33	1.166
301	-39.23	1.333
400	-68.13	1.766

The maps of figures 6-21 and 6-22 may be consulted for the values of N_o for the geographic area of interest.

(4) Divergence factor is defined as the ratio of the field strength obtained after reflection from a spherical surface to that obtained after reflection from a plane surface, where the radiated power, total axial distance, and type of reflecting surface are the same in both cases, and the solid angle is a small elemental angle approaching zero in magnitude. The divergence factor for any grazing angle Ψ is given by

$$D = \frac{1}{\left[1 + \frac{2r_1r_2}{kad_o \tan \Psi}\right]^{\frac{1}{2}}} = \left[\frac{kad_o \tan \Psi}{kad_o \tan\Psi + 2r_1r_2}\right]^{\frac{1}{2}}$$

where:

$$r_1 = \frac{(ka + h_1)\sin d_1/ka}{\cos \Psi}$$

and

$$r_2 = \frac{(ka + h_2)\cos d_2/ka - ka}{\sin \Psi}$$

$$d_o = d_1 + d_2$$

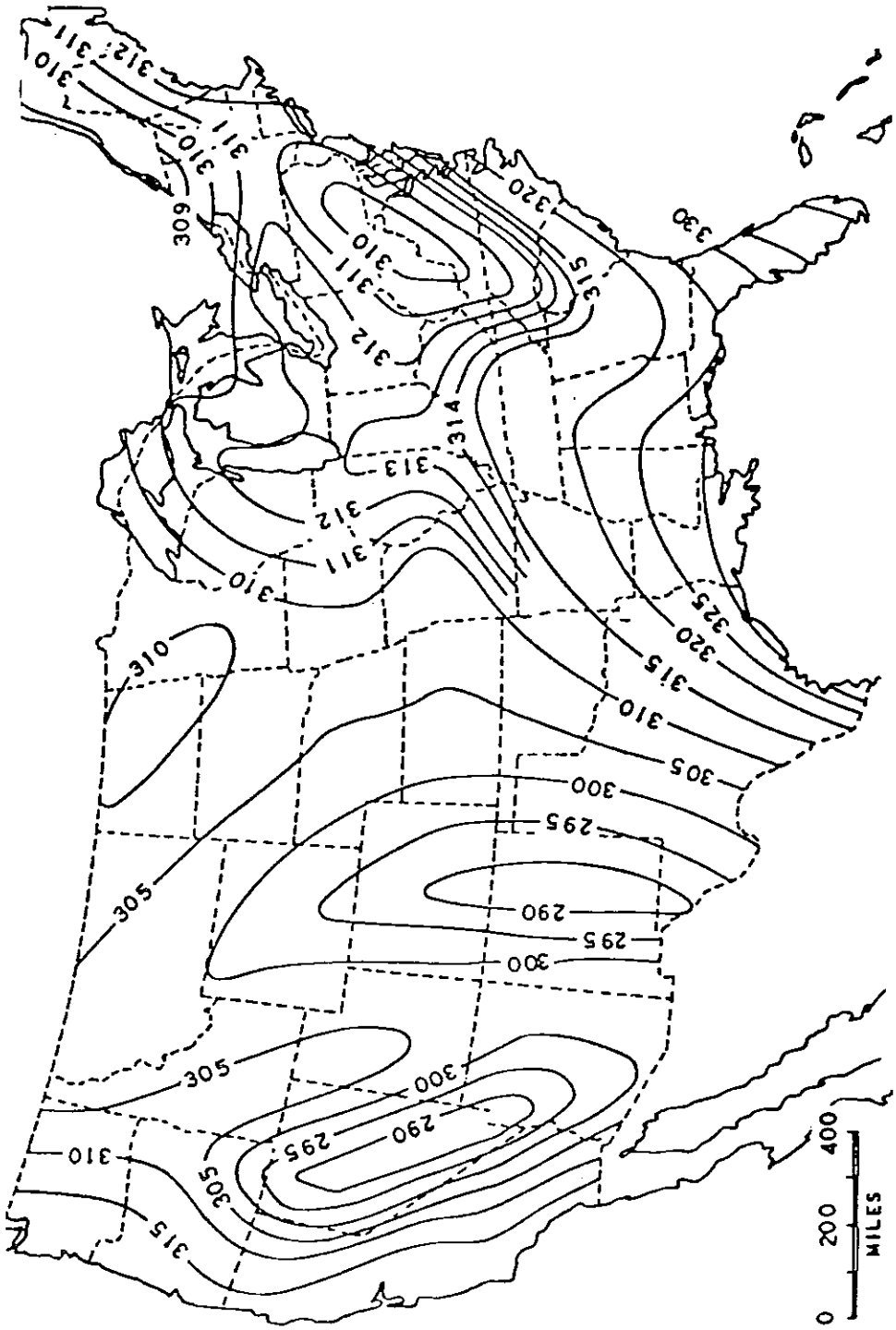

FIGURE 6-21. CONTOURS OF SURFACE REFRACTIVITY REDUCED-TO-SEA-LEVEL VALUES (N_o) FOR THE UNITED STATES

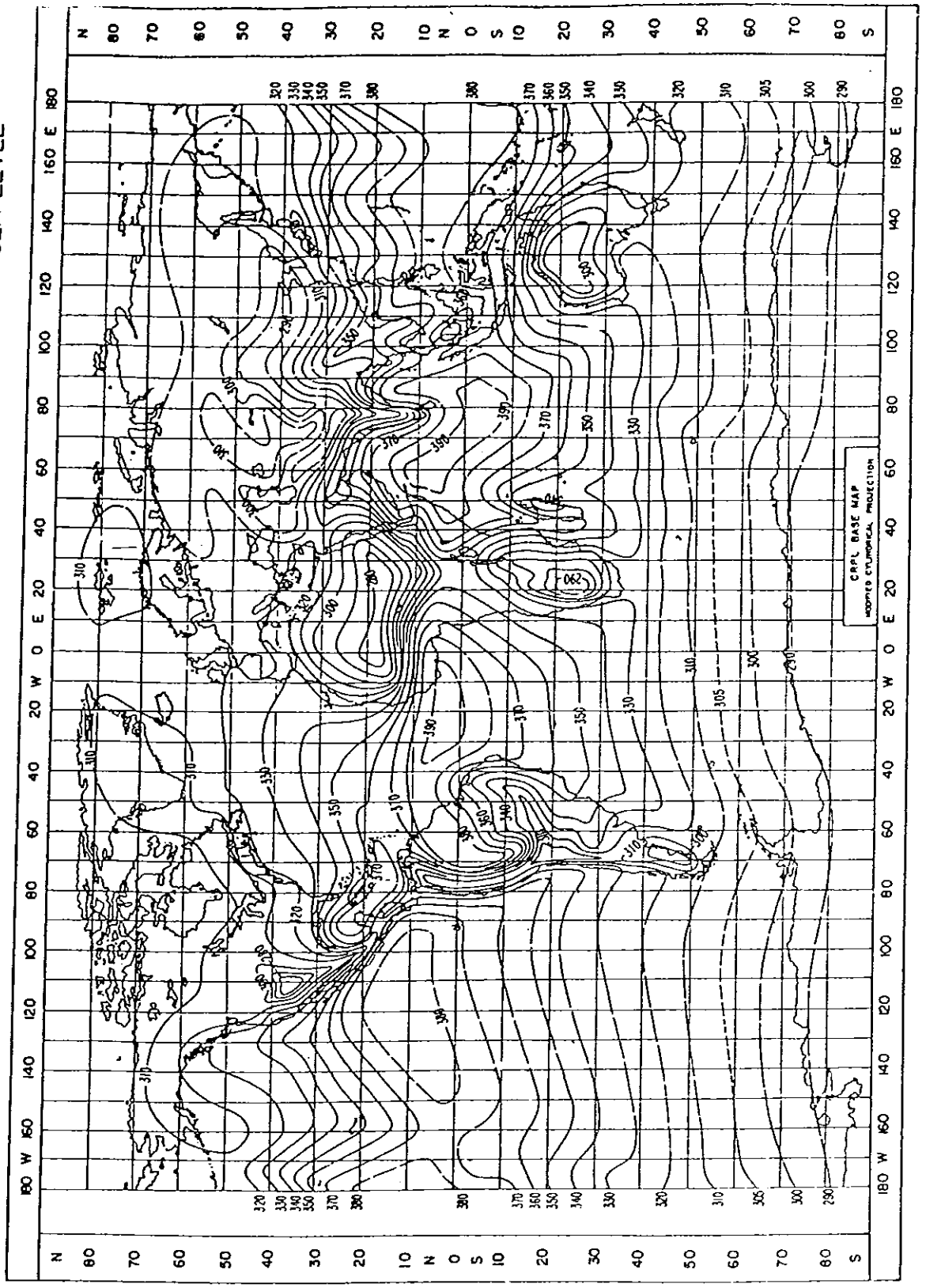

FIGURE 6-22. CONTOURS OF SURFACE REFRACTIVITY REDUCED-TO-SEA-LEVEL VALUES (N°) FOR THE WORLD

Note that d_2 may be obtained in the same manner as d_1 except that h_2 is used as the height in the equation. For reference purposes, note the following:

$$h_1 = h_1 - 0.88{d_1}^2/k \quad h_2 = h_2 - 0.88{d_2}^2/k$$

where h_1 and h_2 are in feet and d_1 and d_2 are in nautical miles.

(5) TACAN antennas use vertical polarization, and the reflection coefficient for vertically polarized waves is given by

$$R_v e^{j\phi v} = \frac{\bar{n}^2 \sin\psi - \sqrt{n^2 - \cos^2\psi}}{n^2 \sin\psi + \sqrt{n^2 - \cos^2\psi}}$$

where n^2 is a complex permittivity coefficient and is given by

$$n^2 = {}_r - j\frac{18000\sigma}{f_{MHz}} = {}_r - jx$$

where

er is the relative permittivity of the earth at the reflecting Fresnel zone,

σ is the conductivity of the reflecting earth in mho-m/sq m,

f_{MHz} is the carrier frequency in megahertz.

For adaptation to the computer operation, these relationships may be expressed in the following form:

$$R_v = \left[\frac{(\epsilon_r^2+x^2)\sin^2\psi+m(\epsilon_r-\cos^2\psi)-\sqrt{2}\sin\psi\sqrt{\epsilon_r-\cos^2\psi}\left[\epsilon_r\sqrt{m+1}+x\sqrt{m-1}\right]}{(\epsilon_r^2+x^2)\sin^2\psi+m(\epsilon_r-\cos^2\psi)+\sqrt{2}\sin\psi\sqrt{\epsilon_r-\cos^2\psi}\left[\epsilon_r\sqrt{m+1}+x\sqrt{m-1}\right]}\right]^{\frac{1}{2}}$$

where $m = \sqrt{1+\frac{x^2}{(\epsilon_r-\cos^2\psi)^2}}$

$$\phi_v = \tan^{-1}\frac{\sqrt{2}\sin\psi\sqrt{\epsilon_r-\cos^2\psi}\left[\epsilon_r\sqrt{m-1}-x\sqrt{m+1}\right]}{(\epsilon_r^2+x^2)\sin^2\psi-m(\epsilon_r-\cos^2\psi)}$$

where $(-90 \leq \phi < 0^\circ)$

$$\phi_v = 180^\circ+\tan^{-1}\frac{\sqrt{2}\sin\psi\sqrt{\epsilon_r-\cos^2\psi}\left[\epsilon_r\sqrt{m-1}-x\sqrt{m+1}\right]}{(\epsilon_r^2+x^2)\sin^2\psi-m(\epsilon_r-\cos^2\psi)}$$

where $(-180 \leq \phi \leq -90^\circ)$

The curves of figures 6-23 through 6-29 show the variation of R and d for a number of ground conditions at 1000 MHz. These curves may be used with negligible error at all TACAN frequencies.

(6) The path-length difference, θ, in degrees is given by:

$$\theta = \frac{\Delta r}{\lambda} \times 360^{\circ} = \frac{\Delta r \times f_{MHz}}{2.733} \text{ degrees}$$

where λ is the wavelength

Δr is the path-length difference, and

$\Delta r = r_1 + r_2 - r_o$ (see figure 6-20)

The direct ray path length, r_o, between transmitter and receiver is

$$r_o = \left[r_1^2 + r_2^2 - 2r_1 r_2 \cos (180^{\circ} - 2\psi) \right]^{\frac{1}{2}}$$

$$= \left[r_1^2 + r_2^2 + 2r_1 r_2 \cos 2\psi \right]^{\frac{1}{2}}$$

(7) The magnitude of the direct ray will be given as E_o, and the magnitude of the reflected ray by DRE_o. This discussion assumes that, for direct and reflected signal magnitudes, the direct and reflected path lengths are the same. This assumption produces negligible error. The total phase difference between the direct and reflected rays is given by $\theta - \phi$, but since the angle ϕ is inherently negative, these angles in effect are additive. The vector sum of the two components is shown in figure 6-30 for the two conditions, (a) where $(\theta - \phi)$ is less than 90° and (b) where $(\theta - \phi)$ is greater than 90°. The resultant field is given by

$$E_d = E_o \left[1 + DR^2 + 2DR \cos (\theta - \phi) \right]^{\frac{1}{2}}$$

The ratio of the magnitude of the field in an earth environment to the magnitude of the free-space field (E_d/E_o) is designated $g(\theta)$ and is called the earth-gain factor or

$$g(\theta) = \frac{E_d}{E_o} = \left[1 + DR^2 + 2DR \cos (\theta - \phi) \right]^{\frac{1}{2}}$$

where D is the divergence factor and R is the absolute value of the reflection coefficient.

The earth, with its many types of land and water surface conditions and, hence, many conductivity and permittivity factors, and the type of wave polarization, cause the earth-gain function to vary from a small value (nearly zero) to a value slightly less than 2.0. With vertical polarization, such as the TACAN

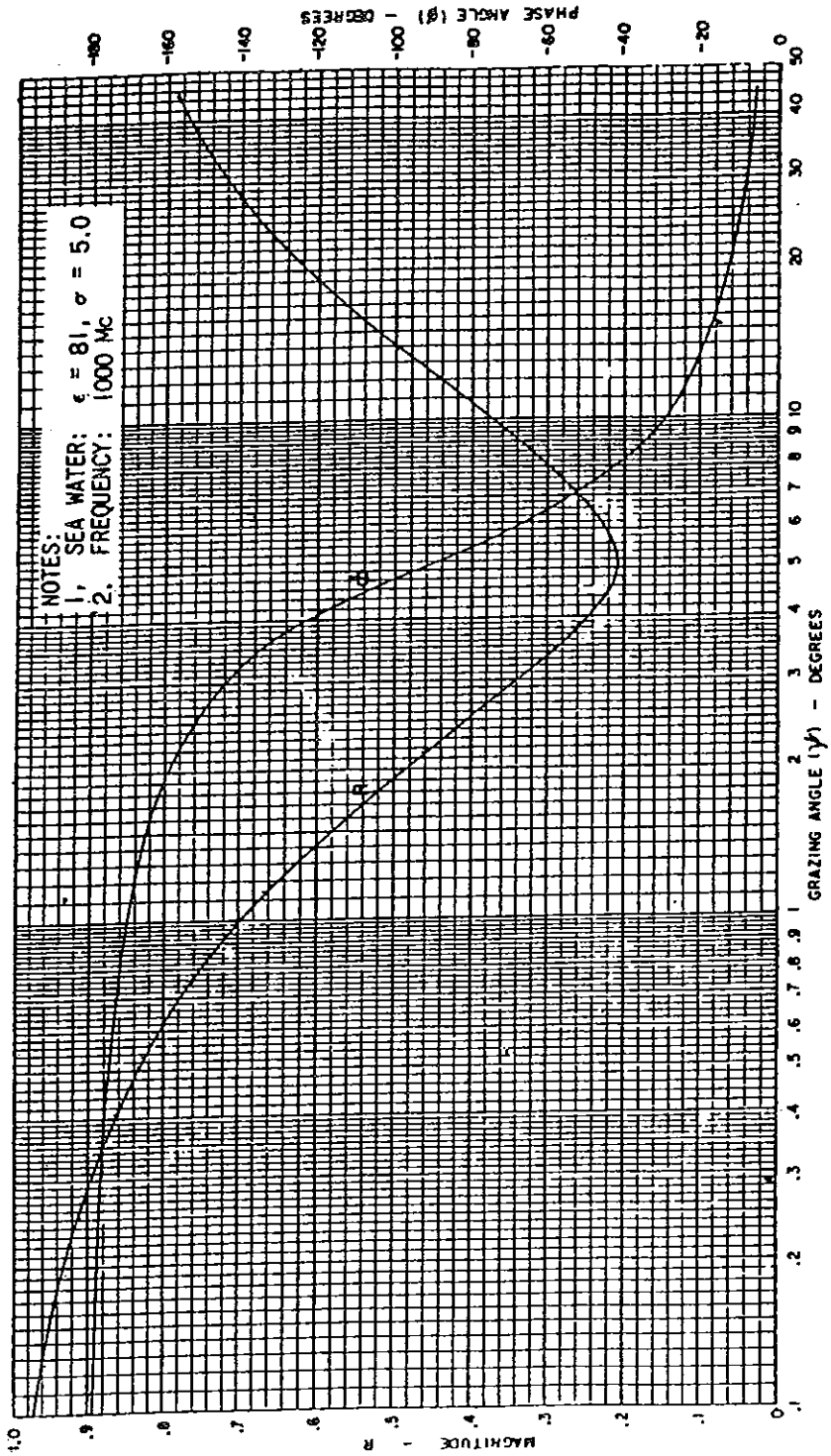

FIGURE 6-23. REFLECTION COEFFICIENT FOR SEA WATER

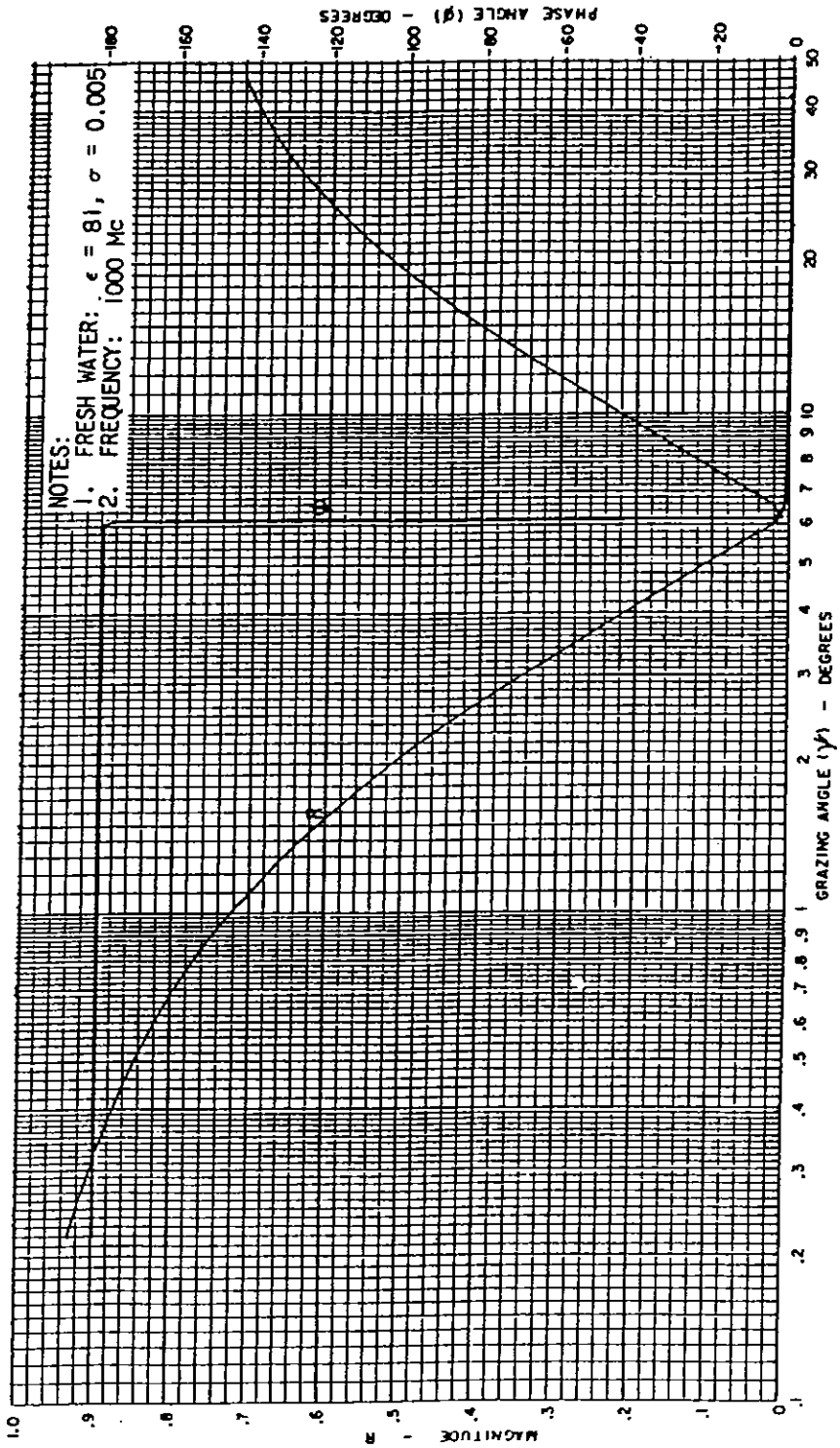

FIGURE 6-24. REFLECTION COEFFICIENT FOR FRESH WATER

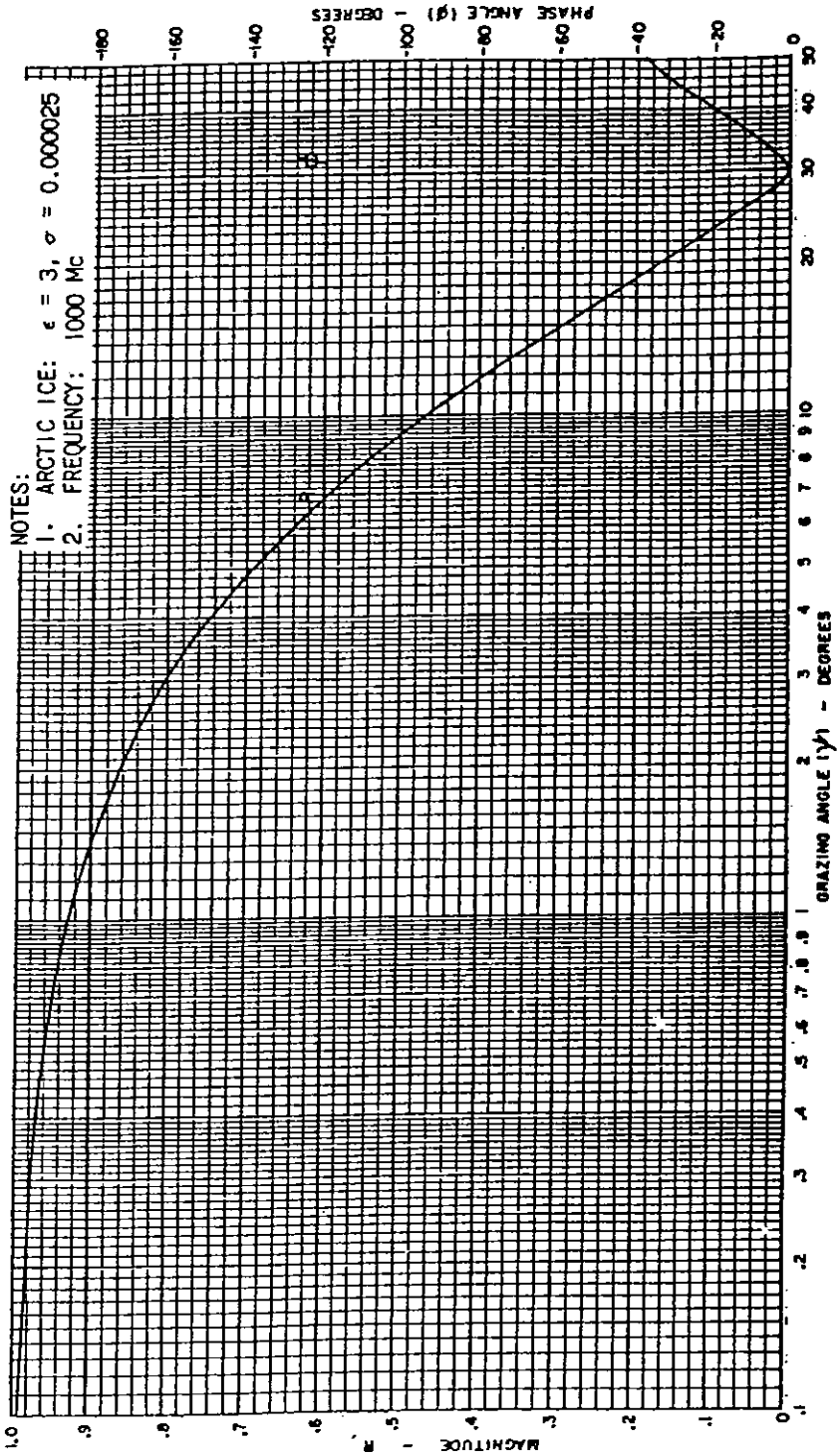

FIGURE 6-25. REFLECTION COEFFICIENT FOR GLACIAL ICE

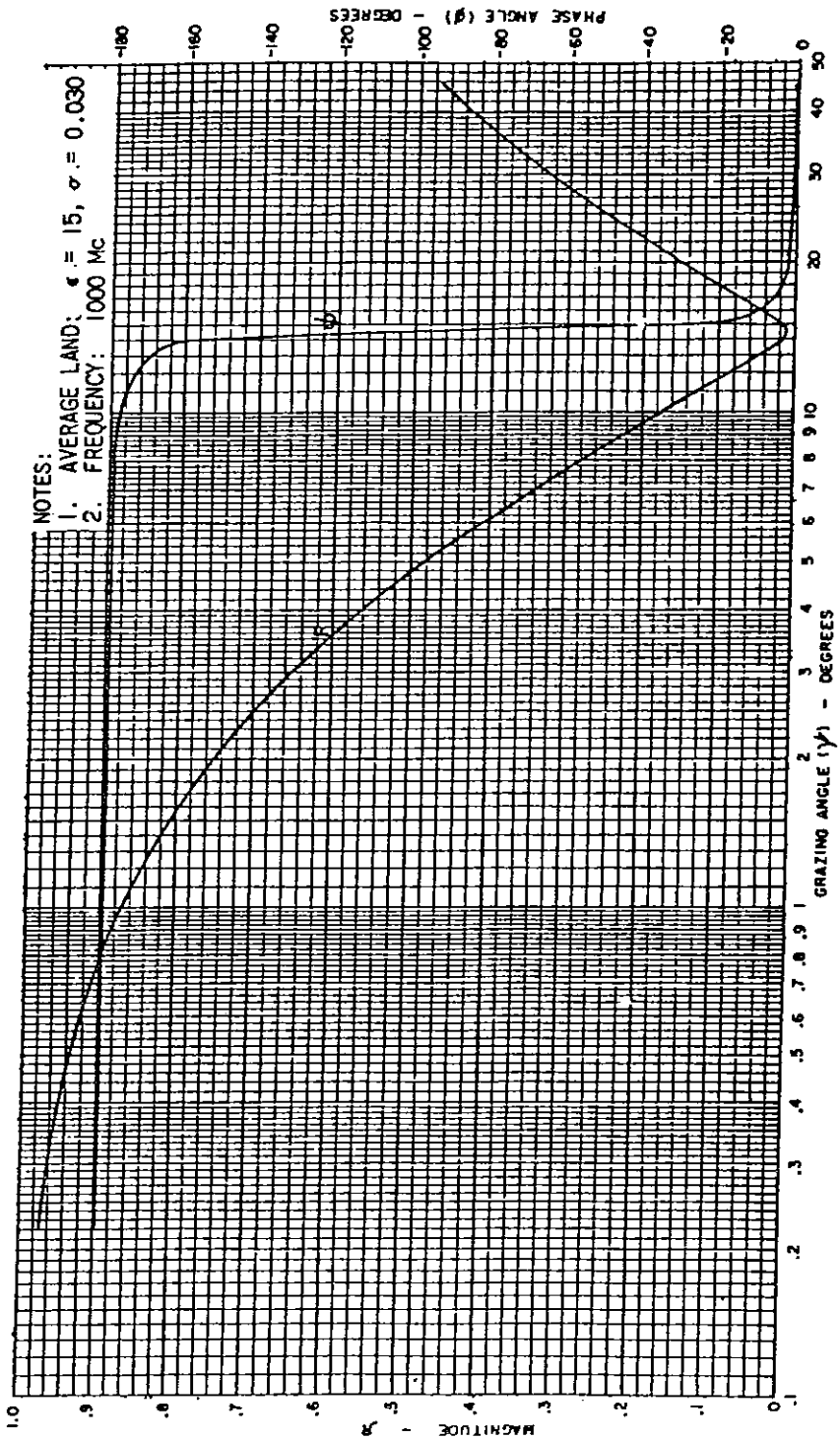

FIGURE 6-26. REFLECTION COEFFICIENT FOR AVERAGE LAND, ε = 15

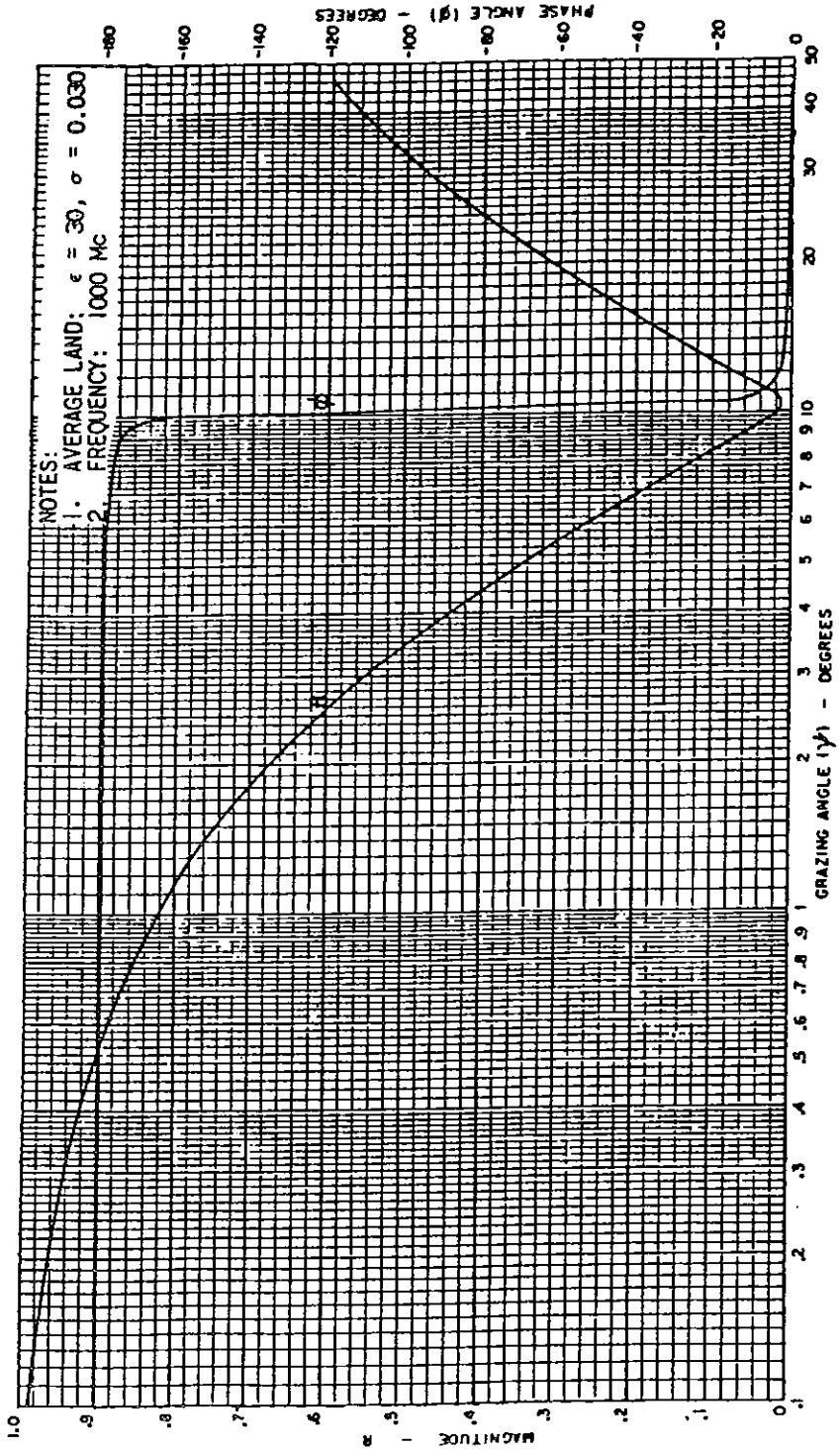

FIGURE 6-27. REFLECTION COEFFICIENT FOR AVERAGE LAND, ε = 30

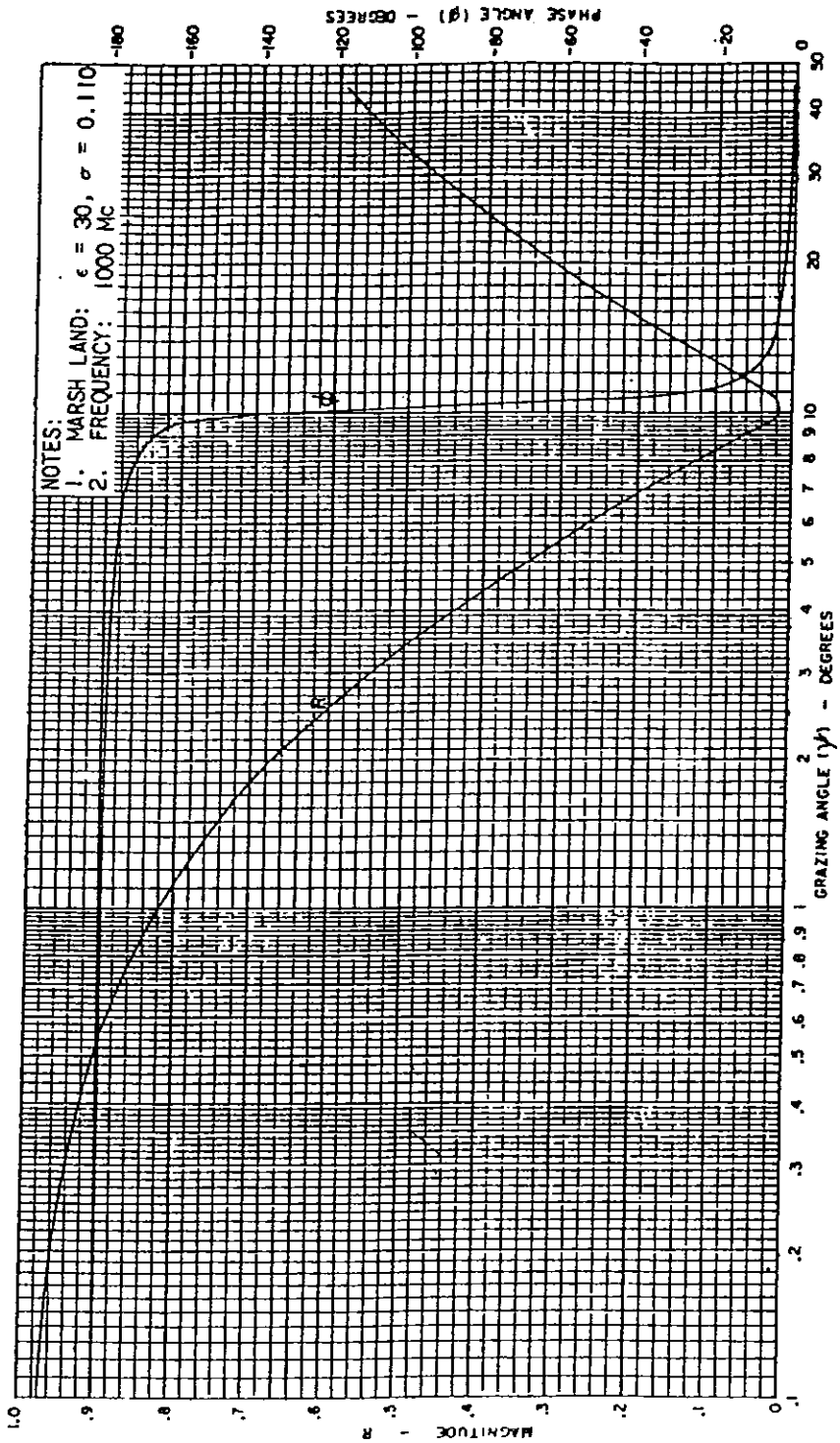

FIGURE 6-28. REFLECTION COEFFICIENT FOR MARSH LAND

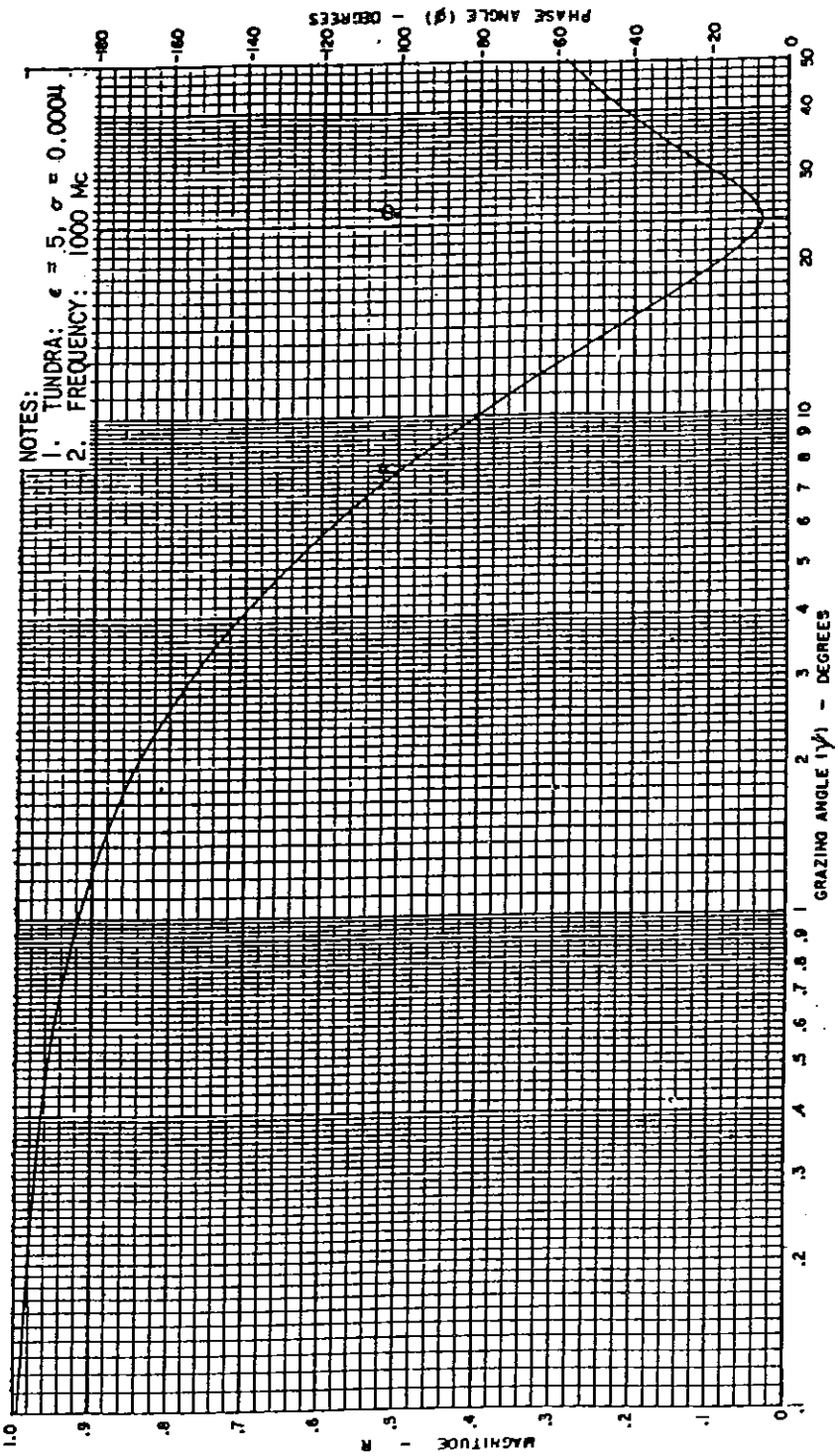

FIGURE 6-29. REFLECTION COEFFICIENT FOR TUNDRA

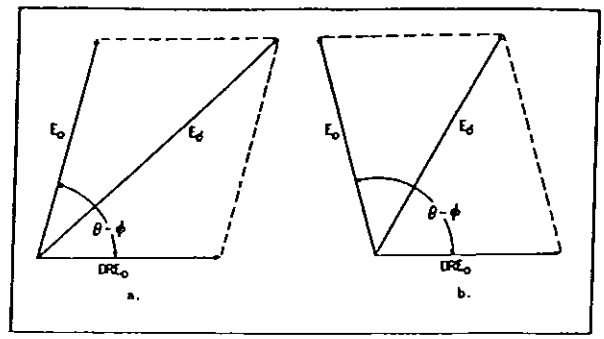

FIGURE 6-30. VECTOR SUM OF DIRECT AND REFLECTED FIELD COMPONENTS

employs, the excursions of the maximums and the depth of the nulls are not as great as they are with horizontal polarization. The earth-gain function, $g(\Theta)$, may be graphically represented as shown in figure 6-31 where $g(\Theta)$ is plotted as the ordinate and height of the receiving antenna, h_2 as the abscissa. Since the physical location in space where the two signals from the transmitter combine is directly related to the grazing angle, Ψ, the abscissa may just as well use Ψ as the variable. The curve depicts the variation of the $g(\Theta)$ function for the simple case of an isotropic transmitting antenna located as a fixed height above ground and radiating vertically polarized waves. A curve, such as figure 6-31, is very useful to the system planner or engineer in locating the position of troublesome nulls.

b. Radiation Characteristics in the Interference Region.

(1) The null positions are numbered consecutively starting from radio horizon, and they are referred to as number of the null. The starting point for the problem of determining null positions is found in the earth-gain or $g(\Theta)$ function,

$$g(\Theta) = \left[1 + DR^2 + 2DR \cos(\Theta - \phi)\right]^{\frac{1}{2}}$$

A null in the radiation pattern occurs when $\cos(\Theta - \phi)$ has the value -1, provided D and R remain constant. Under these conditions,

$$g(\Theta) = \sqrt{1 - 2DR + \overline{DR}^2} = 1 - DR$$

It would now appear to be a simple matter to determine the value of grazing angle Ψ that will produce this condition. However, due to the variation of both D and R with Ψ, a null in the pattern occurs when $\cos(\Theta - \phi)$ has a value slightly different from -1, and the actual minimums of $g(\Theta)$ do not lie on the (1 -DR) locus. When considering grazing angles below Brewster's angle (the neck in the curve of figure 6-31), a minimum is to the left of the point of contact of the $g(\Theta)$ curve with the locus (1 -DR), and for angles above Brewster's angle, a minimum is to the right of the point of contact. Computerized data are used to first determine the minimums of $g(\Theta)$ accurately, and then the corresponding grazing angle, Ψ, and null number, $n_{\sin\Psi}$. This approach is necessary in order to establish a useful parameter by which the position of any particular null may be calculated.

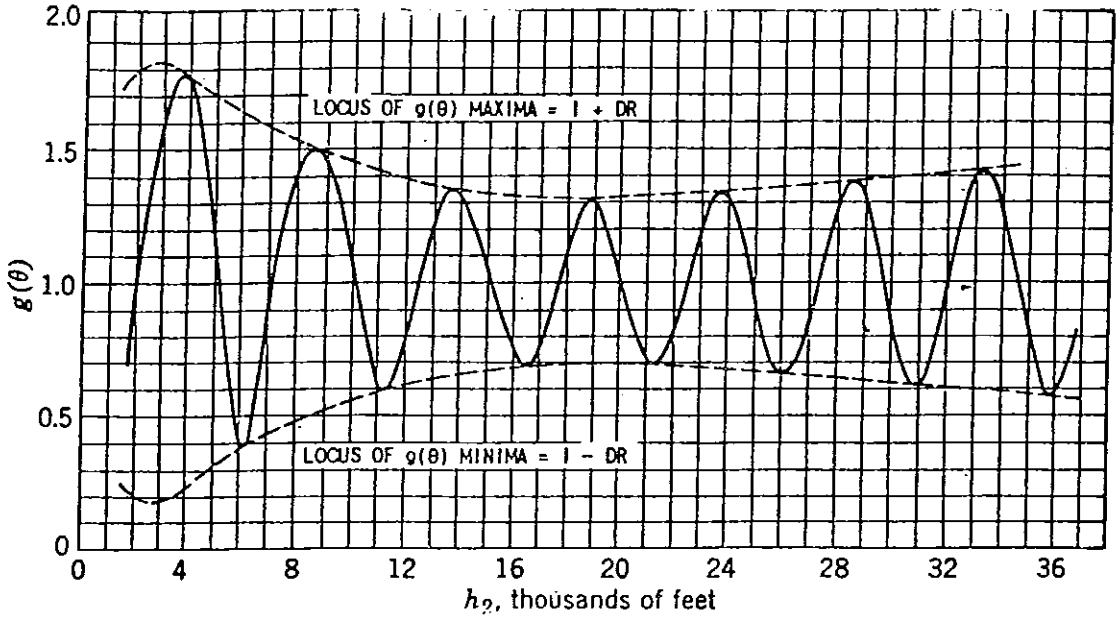

FIGURE 6-31. EARTH-GAIN FUNCTION, g(⊙), OF AN ISOTROPIC RADIATOR

(2) The null number, used to determine the number of nulls within a given grazing angle Ψ, is given very nearly by either of the two following expressions. First by,

$$n_{\Delta r} = \frac{\Delta r \; f_{MHz}}{984}$$

where Δr is the path-length difference in feet. Alternately,

$$n_{\Delta r} = \frac{\Delta r \; f_{MHz}}{300}$$

where Δr is the path-length difference in meters. Secondly, it is given by

$$n_{\sin \Psi} = \frac{h_1 \; f_{MHz} \; \sin \Psi}{492}$$

where h_1 is in feet or alternately

$$n_{\sin \Psi} = \frac{h_1 \; f_{MHz} \; \sin \Psi}{150}$$

where h_1 is in meters

$n_{\sin \Psi}$ will be referred to as the null number.

The null positions can be defined by means of the null numbers and the particular behavior of the null numbers for variations in antenna height, frequency, and environmental conditions makes the null number a useful parameter in the solution for null positions. The null number is an integer plus (or sometimes minus) a decimal; that is,

$$n = y + z$$

where y is the integral number of the null, and z is the difference (a decimal) between n and y.

For nulls that occur at angles greater than Brewster's angle, the decimal (z) is nearly 0.50. For nulls which occur at angles less than Brewster's angle, the decimal is approximately ± 0.05, except for high antenna heights (greater than about 70 feet). Table 6-3 gives the number of nulls in the radiation pattern below Brewster's angle, $_B$, and also the number in the angle between Brewster's angle and a 45° elevation, for a number of selected antenna heights and the two frequencies of 1000 and 1180 megahertz. Table 6-4 contains all the values of n for the nulls in the radiation pattern below Brewster's angle up to number 18. When n exceeds 18 but is less than the Brewster n, use the integral number of the null plus the decimal which is indicated as average z. For nulls which occur at angles greater than Brewster's angle, use the integral number of the null plus z, as further presented in table 6-4. The dashed, stepped line appearing in each table 6-4 variation represents the dividing line between "below and above" Brewster's angle, and the smaller null numbers are always those below Brewster's angle. Table 6-4 also lists a number of earth surface parameters to be expected in TACAN operation, together with the values of Brewster's angle for 1000 and 1180 MHz operation. For low antennas (up to about 20 feet), the first few nulls will have null numbers slightly less than the number of the null, and in these cases, the (z) would be negative. For instance, when propagating at 1000 MHz over fresh water from an antenna height 10 feet above the water surface, we have:

Number of the Null	Null Number	z
1	0.9840	-0.0160
2	1.9288	-0.0712

NOTE: Reference to table 2-1 and figure 2-6 will reveal that for the vast majority of sites there are only a limited number of heights for DME and TACAN antennas that need be used and only a limited range of grazing angles involved.

TABLE 6-3. BREWSTER'S ANGLE, ψ_B, AND NUMBER OF NULLS FOR SELECTED SURFACE CONDITIONS

Surface Type	Surface Constants ϵ_r	σ	Brewster's Angle $f_{Mc} = 1000$	$f_{Mc} = 1180$
Sea Water	81	5.0	5.19	5.42
Fresh Water	81	0.005	6.34	6.34
Marsh Land	30	0.110	10.34	10.34
Average Land	30	0.030	10.41	10.34
Average Land (Dry)	15	0.030	14.47	14.47
Desert Land	3	0.011	30.0	30.0
Glacial Ice	3	0.000025	30.0	30.0
Tundra	5	0.0004	24.0	24.0
Arctic Ice	10	0.0001	32.8	32.8

Conductivity, σ, in mho-m/sq m

NUMBER OF NULLS BELOW BREWSTER'S ANGLE AND IN 45 DEGREES

h_1	ϵ	σ	ψ_B	45°	h_1	ϵ	σ	ψ_B	45°
5	81	5.0	None	6	5	81	0.005	1	6
10	81	5.0	1	13	10	81	0.005	2	13
20	81	5.0	3	19	20	81	0.005	4	28
40	81	5.0	7	57	30	81	0.005	7	42
60	81	5.0	11	85	40	81	0.005	9	56
100	81	5.0	18	143	60	81	0.005	13	85
175	81	5.0	33	250	100	81	0.005	22	143
					175	81	0.005	39	251
5	30	0.110	2	6	5	30	0.030	2	6
10	30	0.110	4	13	10	30	0.030	3	13
20	30	0.110	7	20	20	30	0.030	7	29
40	30	0.110	14	56	40	30	0.030	15	56
60	30	0.110	21	85	60	30	0.030	21	85
80	30	0.110	28	114	100	30	0.030	35	143
100	30	0.110	36	143	175	30	0.030	63	250
175	30	0.110	63	250					

TABLE 6-3. NUMBER OF NULLS BELOW BREWSTER'S ANGLE AND IN 45 DEGREES (continued)

f = 1000 Mc k = 1.333

h_1	ϵ	σ	ψ_B	45°	h_1	ϵ	σ	ψ_B	45°
5	15	0.030	3	6					
10	15	0.030	5	13					
20	15	0.030	10	28					
30	15	0.030	15	42					
40	15	0.030	20	56					
50	15	0.030	25	71					
60	15	0.030	30	85					
80	15	0.030	40	114					
100	15	0.030	50	143					
175	15	0.030	88	250					

f = 1180 Mc k = 1.333

5	81	5.0	None	7	5	81	0.005	1	7
10	81	5.0	2	16	10	81	0.005	2	16
20	81	5.0	4	33	20	81	0.005	5	33
40	81	5.0	8	67	30	81	0.005	8	50
60	81	5.0	13	101	40	81	0.005	11	67
100	81	5.0	22	169	60	81	0.005	16	101
175	81	5.0	39	296	100	81	0.005	26	169
					175	81	0.005	46	296
5	30	0.110	2	7	5	30	0.030	2	7
10	30	0.110	4	16	10	30	0.030	4	16
20	30	0.110	8	33	20	30	0.030	9	33
30	30	0.110	12	50	30	30	0.030	13	50
40	30	0.110	17	67	40	30	0.030	17	67
60	30	0.110	25	101	60	30	0.030	25	101
80	30	0.110	34	135	100	30	0.030	42	169
100	30	0.110	42	169	175	30	0.030	74	296
175	30	0.110	76	296					

TABLE 6-3. NUMBER OF NULLS BELOW BREWSTER'S ANGLE AND IN 45 DEGREES (continued)

f = 1180 Mc k = 1.333

h_1	ϵ	σ	ψ_B	45°
5	15	0.030	3	7
10	15	0.030	6	16
20	15	0.030	11	33
30	15	0.030	17	50
40	15	0.030	23	67
50	15	0.030	29	84
60	15	0.030	35	101
80	15	0.030	47	135
100	15	0.030	59	169
175	15	0.030	104	296

TABLE 6-4. NULL NUMBERS BELOW AND ABOVE BREWSTER'S ANGLE AT 1000 and 1180 MC FOR SELECTED SURFACE CONDITIONS AND k = 1.333

Sea Water ($\epsilon = 81, \sigma = 5.0$)

$f_{Mc} = 1000$

Nulls below Brewster's angle are above dashed enclosure

h_1=5	10	20	40	60	100	175
1.3955	1.0809	1.0362	1.0335	1.0535	1.1361	1.3842
2.4491	2.3446	2.0882	2.0493	2.0579	2.1225	2.3640
3.4642	3.4164	3.1924	3.0707	3.0681	3.1199	3.3438
4.4714	4.4399	4.3147	4.0995	4.0805	4.1218	4.3302
5.4759	5.4522	5.3769	5.1393	5.0963	5.1261	5.321?
6.4790	6.4595	6.4062	6.1927	6.1161	6.1317	6.316?
	7.4649	7.4242	7.2534	7.1405	7.1392	7.312?
	8.4683	8.4351	8.3065	8.1698	8.1474	8.311?
	9.4709	9.4429	9.3461	9.2055	9.1573	9.311?
	10.4730	10.4491	10.3737	10.2443	10.1693	10.312?
	11.4744	11.4533	11.3928	11.2824	11.1818	11.313?
	12.4758	12.4571	12.4068	12.3162	12.1970	12.316?
	13.4766	13.4599	13.4179	13.3441	13.2140	13.3191
		14.4621	14.4259	14.3663	14.2332	14.3224
		15.4640	15.4325	15.3833	15.2537	15.3268
		16.4655	16.4377	16.3975	16.2757	16.3315
		17.4668	17.4423	17.4085	17.2981	17.3368
		18.4678	18.4459	18.4173	18.3200	18.3424

Average ϵ 3688

Nulls Above Brewster's Angle

h_1=5	10	20	40	60	100	175
0.4559	0.4611	0.4384	0.4527	0.4539	0.4752	0.5675

TABLE 6-4. NULL NUMBERS BELOW AND ABOVE BREWSTER'S ANGLE AT 1000 and 1180 MC FOR SELECTED SURFACE CONDITIONS AND k = 1.333 (continued).

Sea Water ($\epsilon = 81, \sigma = 5.0$)

$f_{Mc} = 1180$

Nulls below Brewster's angle are above dashed enclosure

h_1=5	10	20	40	60	100	175
1.3362	1.0506	1.0283	1.0329	1.0604	1.1626	1.4514
2.4404	2.2451	2.0591	2.0423	2.0591	2.1434	2.4355
3.4590	3.3923	3.1152	3.0562	3.0651	3.1361	3.4121
4.4682	4.4276	4.2192	4.0734	4.0723	4.1342	4.3937
5.4734	5.4447	5.3212	5.0963	5.0823	5.1349	5.3809
6.4767	6.4540	6.3760	6.1271	6.0935	6.1372	6.3717
7.4790	7.4603	7.4044	7.1674	7.1078	7.1411	7.3652
	8.4645	8.4214	8.2184	8.1243	8.1451	8.3607
	9.4677	9.4326	9.2713	9.1446	9.1509	9.3577
	10.4702	10.4406	10.3164	10.1697	10.1573	10.3558
	11.4721	11.4466	11.3504	11.1996	11.1649	11.3545
	12.4735	12.4512	12.3748	12.2328	12.1729	12.3542
	13.4747	13.4548	13.3931	13.2675	13.1821	13.3546
	14.4756	14.4579	14.4061	14.3001	14.1930	14.3555
	15.4763	15.4603	15.4161	15.3282	15.2054	15.3570
	16.4769	16.4621	16.4267	16.3523	16.2189	16.3583
		17.4637	17.4310	17.3720	17.2343	17.3609
		18.4651	18.4365	18.3874	18.2510	18.3632
Average z					0.1936	0.4043

Nulls Above Brewster's Angle

h_1=5	10	20	40	60	100	175
0.4476	0.4593	0.4564	0.4514	0.4545	0.4805	0.5881

TABLE 6-4. NULL NUMBERS BELOW AND ABOVE BREWSTER'S ANGLE AT 1000 and 1180 MC FOR SELECTED SURFACE CONDITIONS AND k = 1.333 (continued)

Fresh Water ($\epsilon = 81$, $\sigma = .005$)

$f_{Mc} = 1000$

Nulls below Brewster's angle are above dashed enclosure

h_1=5	10	20	30	40	60	100	175
0.9047	0.9840	0.9986	1.0064	1.0149	1.0411	1.1282	1.3786
1.5399	1.9288	1.9941	2.0034	2.0117	2.0336	2.1078	2.3544
2.5062	2.5660	2.9864	3.0006	3.0097	3.0307	3.0980	3.3304
3.5010	3.5105	3.9567	3.9974	4.0074	4.0282	4.0920	4.3130
4.4993	4.5033	4.6306	4.9913	5.0045	5.0262	5.0885	5.3000
5.4984	5.5006	5.5198	5.9712	6.0029	6.0247	6.0853	6.2904
6.4975	6.4992	6.5080	6.7432	6.9980	7.0239	7.0833	7.2826
	7.4984	7.5043	7.5319	7.9851	8.0223	8.0812	8.2768
	8.4977	8.5023	8.5136	8.8628	9.0196	9.0797	9.2715
	9.4969	9.5010	9.5086	9.5472	10.0173	10.0780	10.2674
	10.4964	10.4997	10.5060	10.5210	11.0136	11.0771	11.2644
	11.4957	11.4988	11.5044	11.5144	12.0074	12.0757	12.2611
	12.4952	12.4982	12.5034	12.5110	12.9764	13.0747	13.2583
	13.4947	13.4973	13.5023	13.5094	13.6375	14.0732	14.2558
		14.4967	14.5016	14.5080	14.5425	15.0721	15.2530
		15.4963	15.5006	15.5071	15.5304	16.0700	16.2513
		16.4956	16.4999	16.5062	16.5273	17.0683	17.2491
		17.4950	17.4992	17.5055	17.5245	18.0669	18.2479
Average z						.0770	.2557

Nulls Above Brewster's Angle

h_1=5	10	20	30	40	60	100	175
0.5071	0.5046	0.5020	0.4960	0.4965	0.5015	0.5208	0.6112

TABLE 6-4. NULL NUMBERS BELOW AND ABOVE BREWSTER'S ANGLE AT 1000 and 1180 MC FOR SELECTED SURFACE CONDITIONS AND k = 1.333 (continued)

Fresh Water ($\epsilon = 81, \sigma = .005$)

$f_{Mc} = 1180$

Nulls below Brewster's angle are above dashed enclosure

h_1=5	10	20	30	40	60	100	175
0.9387	0.9878	1.0013	1.0092	1.0196	1.0514	1.1570	1.4471
1.5738	1.9632	1.9975	2.0058	2.0153	2.0417	2.1327	2.4289
2.5090	2.6990	2.9929	3.0036	3.0132	3.0376	3.1200	3.4028
3.5021	3.5203	3.9842	4.0018	4.0117	4.0353	4.1127	4.3822
4.4999	4.5075	4.9364	4.9983	5.0097	5.0335	5.1076	5.3665
5.4986	5.5024	5.5789	5.9924	6.0075	6.0319	6.1041	6.3545
6.4980	6.5003	6.5177	6.9796	7.0059	7.0305	7.1016	7.3454
7.4971	7.4987	7.5082	7.8468	8.0032	8.0297	8.0988	8.3378
	8.4979	8.5045	8.5416	8.9964	9.0281	9.0970	9.3318
	9.4973	9.5126	9.5180	9.9720	10.0263	10.0952	10.3266
	10.4967	10.5009	10.5112	10.6785	11.0247	11.0938	11.3220
	11.4961	11.5000	11.5072	11.5325	12.0226	12.0927	12.3176
	12.4954	12.4992	12.5061	12.5195	13.0202	13.0910	13.3149
	13.4951	13.4986	13.5047	13.5151	14.0156	14.0901	14.3123
	14.4945	14.4977	14.5033	14.5125	14.9984	15.0888	15.3097
	15.4938	15.4969	15.5027	15.5107	15.8354	16.0877	16.3067
	16.4933	16.4963	16.5020	16.5096	16.5609	17.0863	17.3051
		17.4956	17.5013	17.5087	17.5394	18.0848	18.3031
Average z						.0930	.3083

Nulls Above Brewster's Angle

h_1=5	10	20	30	40	60	100	175
0.5112	0.5126	0.4987	0.5028	0.4947	0.4995	0.5244	0.6833

TABLE 6-4. NULL NUMBERS BELOW AND ABOVE BREWSTER'S ANGLE AT 1000 and 1180 MC FOR SELECTED SURFACE CONDITIONS AND k = 1.333 (continued)

Average Land ($\epsilon_r = 15$, $\sigma = 0.030$)

$f_{Mc} = 1000$

Nulls below Brewster's angle are above dashed enclosure

h_1=5	10	20	30	40
0.9886	0.9981	1.0034	1.0083	1.0167
1.9668	1.9952	2.0030	2.0072	2.0138
2.8556	2.9925	3.0036	3.0063	3.0129
3.5011	3.9863	4.0032	4.0056	4.0119
4.5003	4.9259	5.0034	5.0053	5.0116
5.4976	5.5185	6.0032	6.0050	6.0110
6.4970	6.5005	7.0038	7.0043	7.0106
	7.4973	8.0043	8.0041	8.0098
	8.4959	9.0061	9.0041	9.0094
	9.4952	10.0180	10.0044	10.0092
	10.4943	10.4950	11.0039	11.0092
	11.4938	11.5000	12.0046	12.0088
		12.5020	13.0069	13.0086
		13.5020	14.0112	14.0086
		14.5030	15.0906	15.0095
		15.5030	16.4836	16.0107
		16.5040	17.4892	17.0116
		17.5040	18.4903	18.0141

Average z 0170

Nulls Above Brewster's Angle

h_1=5	10	20	30	40
0.4990	0.4994	0.5030	0.4881	0.4880

TABLE 6-4. NULL NUMBERS BELOW AND ABOVE BREWSTER'S ANGLE AT 1000 and 1180 MC FOR SELECTED SURFACE CONDITIONS AND k = 1.333 (continued)

Average Land ($\epsilon_r = 15, \sigma = 0.030$)

$f_{Mc} = 1180$

Nulls below Brewster's angle are above dashed enclosure

h_1=5	10	20	30	40
0.9915	0.9990	1.0037	1.0107	1.0206
1.9809	1.9971	2.0029	2.0088	2.0172
2.8761	2.9944	3.0022	3.0078	3.0154
3.5253	3.9929	4.0010	4.0070	4.0145
4.5037	4.9843	5.0002	5.0067	5.0140
5.4990	5.9073	6.0006	6.0063	6.0133
6.4971	7.5008	7.0001	7.0058	7.0127
7.4967	8.4978	7.9989	8.0059	8.0121
	9.4963	8.9997	9.0048	9.0120
	10.4954	9.9988	10.0048	10.0117
	11.4944	10.9985	11.0039	11.0108
	12.4938	12.4915	12.0046	12.0106
	13.4932	13.4938	13.0046	13.0107
	14.4928	14.4932	14.0042	14.0100
	15.4925	15.4941	15.0053	15.0098
	16.4918	16.4931	16.0069	16.0101
		17.4931	17.0135	17.0104
		18.4922	18.4658	18.0103

Average x 0.0136

Nulls Above Brewster's Angle

h_1=5	10	20	30	40
0.5044	0.4949	0.4904	0.4862	0.4847

TABLE 6-4. NULL NUMBERS BELOW AND ABOVE BREWSTER'S ANGLE AT 1000 and 1180 MC FOR SELECTED SURFACE CONDITIONS AND k = 1.333 (continued)

Average Land ($\epsilon = 15, \sigma = 0.030$)

$f_{Mc} = 1000$

Nulls Below Brewster's Angle

50	60	80	100	175
1.0275	1.0418	1.0785	1.1282	1.3790
2.0232	2.0348	2.0654	2.1080	2.3550
3.0214	3.0321	3.0600	3.0984	3.3308
4.0202	4.0303	4.0568	4.0930	4.3131
5.0194	5.0291	5.0547	5.0892	5.3004
6.0189	6.0285	6.0530	6.0867	6.2910
7.0182	7.0277	7.0519	7.0849	7.2836
8.0175	8.0271	8.0510	8.0830	8.2774
9.0170	9.0267	9.0501	9.0817	9.2727
10.0167	10.0260	10.0494	10.0806	10.2685
11.0165	11.0253	11.0485	11.0794	11.2650
12.0162	12.0248	12.0479	12.0787	12.2621
13.0160	13.0242	13.0476	13.0779	13.2591
14.0156	14.0241	14.0467	14.0769	14.2569
15.0156	15.0238	15.0464	15.0761	15.2547
16.0149	16.0232	16.0459	16.0755	16.2529
17.0152	17.0235	17.0452	17.0746	17.2509
18.0157	18.0229	18.0447	18.0740	18.2493

Average z

0.0191	0.0310	0.0489	0.0786	0.2371

Nulls Above Brewster's Angle

50	60	80	100	175
0.4901	0.4900	0.5026	0.5007	0.5740

TABLE 6-4. NULL NUMBERS BELOW AND ABOVE BREWSTER'S ANGLE AT 1000 and 1180 MC FOR SELECTED SURFACE CONDITIONS AND k = 1.333 (continued)

Average Land ($\epsilon = 15, \sigma = 0.030$)

$f_{Mc} = 1180$

Nulls Below Brewster's Angle

50	60	80	100	175
1.0340	1.0517	1.0969	1.1570	1.4473
2.0280	2.0423	2.0802	2.1327	2.4283
3.0258	3.0390	3.0731	3.1204	3.4023
4.0246	4.0370	4.0690	4.1132	4.3812
5.0235	5.0355	5.0665	5.1085	5.3653
6.0228	6.0344	6.0643	6.1050	6.3534
7.0219	7.0335	7.0628	7.1026	7.3439
8.0215	8.0325	8.0617	8.1002	8.3359
9.0208	9.0320	9.0605	9.0984	9.3296
10.0205	10.0310	10.0595	10.0970	10.3244
11.0199	11.0308	11.0586	11.0961	11.3199
12.0194	12.0301	12.0578	12.0946	12.3159
13.0188	13.0296	13.0572	13.0934	13.3122
14.0185	14.0292	14.0566	14.0928	14.3095
15.0180	15.0286	15.0556	15.0916	15.3065
16.0180	16.0280	16.0549	16.0910	16.3041
17.0173	17.0273	17.0543	17.0900	17.3018
18.0169	18.0274	18.0542	18.0895	18.2997

Average z

0.0219	0.0319	0.0558	0.0898	0.2768

Nulls Above Brewster's Angle

50	60	80	100	175
0.4879	0.4853	0.5061	0.5030	0.5895

TABLE 6-4. NULL NUMBERS BELOW AND ABOVE BREWSTER'S ANGLE AT 1000 and 1180 MC FOR SELECTED SURFACE CONDITIONS AND k = 1.333 (continued)

Average Land ($\epsilon = 30$, $\sigma = 0.030$)

$f_{Mc} = 1000$

Nulls below Brewster's angle are above dashed enclosure

h_1=5	10	20	40	60	100	175
0.9760	0.9952	1.0027	1.0162	1.0415	1.1282	1.3790
1.7896	1.9883	2.0017	2.0132	2.0448	2.1078	2.3546
2.5202	2.9685	2.9998	3.0121	3.0316	3.0984	3.3308
3.5035	3.6946	3.9995	4.0106	4.0298	4.0928	4.3132
4.4998	4.5145	4.9975	5.0103	5.0288	5.0892	5.3004
5.4983	5.5038	5.9919	6.0095	6.0276	6.0865	6.2909
6.4972	6.4997	6.9620	7.0089	7.0267	7.0845	7.2834
	7.4984	7.5587	8.0084	8.0261	8.0828	8.2774
	8.4976	8.5139	9.0074	9.0253	9.0813	9.2723
	9.4964	9.5079	10.0056	10.0248	10.0800	10.2683
	10.4957	10.5077	11.0063	11.0239	11.0791	11.2648
	11.4951	11.5062	12.0046	12.0232	12.0781	12.2618
	12.4946	12.5062	13.0032	13.0228	13.0767	13.2591
	13.4940	13.5062	13.9971	14.0220	14.0763	14.2568
		14.5058	14.6313	15.0220	15.0753	15.2542
		15.5050	15.5086	16.0209	16.0744	16.2526
		16.5000	16.5062	17.0208	17.0735	17.2506
		17.4910	17.5035	18.0203	18.0733	18.2490
verage z				0.0260	0.0809	0.2454

Nulls Above Brewster's Angle

h_1=5	10	20	40	60	100	175
0.5038	0.4990	0.4904	0.4923	0.4947	0.5126	0.5938

TABLE 6-4. NULL NUMBERS BELOW AND ABOVE BREWSTER'S ANGLE AT 1000 and 1180 MC FOR SELECTED SURFACE CONDITIONS AND k = 1.333 (continued)

Average Land (ϵ = 30, σ = 0.030)

f_{Mc} = 1180

Nulls below Brewster's angle are above dashed enclosure

h_1=5	10	20	30	40	60	100	175
0.9821	0.9965	1.0033	1.0102	1.0204	1.0517	1.1570	1.4473
1.9133	1.9916	2.0014	2.0082	2.0164	2.0425	2.1237	2.4285
2.5454	2.9834	3.0003	3.0067	3.0150	3.0387	3.1204	3.4023
3.5082	3.9466	3.9980	4.0059	4.0136	4.0364	4.1132	4.3814
4.5013	4.5656	4.9968	5.0049	5.0131	5.0349	5.1083	5.3653
5.4989	5.5097	5.9937	6.0043	6.0116	6.0338	6.1050	6.3532
6.4976	6.5028	6.9911	7.0033	7.0116	7.0327	7.1023	7.3435
7.4969	7.4992	7.9755	8.0030	8.0110	8.0320	8.1002	8.3357
	8.4982	8.6652	9.0009	9.0098	9.0309	9.0982	9.3294
	9.4972	9.5134	9.9994	10.0089	10.0299	10.0971	10.3242
	10.4965	10.5036	10.9971	11.0084	11.0297	11.0954	11.3194
	11.4957	11.5003	11.9903	12.0084	12.0287	12.0941	12.3157
	12.4949	12.4994	12.8676	13.0075	13.0282	13.0931	13.3122
	13.4944	13.4982	13.5168	14.0068	14.0275	14.0919	14.3093
	14.4938	14.4974	14.5059	15.0051	15.0272	15.0909	15.3061
	15.4935	15.4967	15.5028	16.0034	16.0267	16.0905	16.3038
	16.4930	16.4956	16.5014	16.9830	17.0262	17.0893	17.3015
		17.4984	17.5004	17.5217	18.0255	18.0885	18.2994
Average z					0.0302	0.0915	0.2878

Nulls Above Brewster's Angle

h_1=5	10	20	30	40	60	100	175
0.5006	0.4974	0.4939	0.4919	0.4915	0.4939	0.5153	0.6113

TABLE 6-4. NULL NUMBERS BELOW AND ABOVE BREWSTER'S ANGLE AT 1000 and 1180 MC FOR SELECTED SURFACE CONDITIONS AND k = 1.333 (continued)

Marsh Land ($\epsilon = 30, \sigma = 0.110$)

$f_{Mc} = 1000$

Nulls below Brewster's angle are above dashed enclosure

h_1=5	10	20	40	60	80	100	175
0.9799	0.9964	1.0033	1.0167	1.0420	1.0798	1.1286	1.3790
1.7949	1.9932	2.0021	2.0143	2.0353	2.0663	2.1084	2.3547
2.5088	2.9861	3.0021	3.0137	3.0326	3.0609	3.0988	3.3311
3.4982	3.6700	4.0019	4.0131	4.0312	4.0581	4.0938	4.3137
4.4965	4.4985	5.0028	5.0130	5.0305	5.0557	5.0904	5.3010
5.4955	5.4951	6.0062	6.0132	6.0295	6.0543	6.0875	6.2913
6.4949	6.4941	7.0409	7.0133	7.0291	7.0535	7.0857	7.2843
	7.4938	8.4833	8.0137	8.0292	8.0529	8.0846	8.2781
	8.4935	9.4885	9.0148	9.0289	9.0523	9.0833	9.2735
	9.4930	10.4897	10.0162	10.0288	10.0516	10.0821	10.2694
	10.4929	11.4909	11.0189	11.0289	11.0510	11.0814	11.2660
	11.4925	12.4913	12.0240	12.0293	12.0508	12.0807	12.2631
	12.4924	13.4909	13.0358	13.0302	13.0506	13.0799	13.2606
	13.4918	14.4910	14.0927	14.0302	14.0505	14.0797	14.2585
		15.4909	15.4465	15.0315	15.0505	15.0789	15.2560
		16.4907	16.4755	16.0330	16.0500	16.0789	16.2545
		17.4905	17.4846	17.0358	17.0502	17.0782	17.2527
		18.4901	18.4878	18.0392	18.0509	18.0782	18.2512
Average z				0.0342	0.0573	0.0891	0.1589

Nulls Above Brewster's Angle

h_1=5	10	20	40	60	80	100	175
0.4988	0.4939	0.4898	0.4854	0.4880	0.4944	0.5051	0.5861

TABLE 6-4. NULL NUMBERS BELOW AND ABOVE BREWSTER'S ANGLE AT 1000 and 1180 MC FOR SELECTED SURFACE CONDITIONS AND k = 1.333 (continued)

Marsh Land ($\epsilon = 30, \sigma = 0.110$)

$f_{Mc} = 1180$

Nulls below Brewster's angle are above dashed enclosure

h_1=5	10	20	40	60	80	100	175
0.9874	0.9984	1.0037	1.0208	1.0520	1.0980	1.1572	1.447?
1.9298	1.9964	2.0034	2.0174	2.0431	2.08?2	2.1329	2.428?
2.5292	2.9923	3.0026	3.0163	3.0393	3.0740	3.1207	3.4023
3.5009	3.9780	4.0023	4.0156	4.0372	4.0700	4.1136	4.3816
4.4972	4.5240	5.0020	5.0151	5.0358	5.0674	5.1092	5.3657
5.4964	5.4967	6.0037	6.0146	6.0352	6.0656	6.1059	6.3539
6.4956	6.4960	7.0048	7.0148	7.0344	7.0641	7.1033	7.3443
7.4948	7.4948	8.0186	8.0149	8.0342	8.0627	8.1012	8.3368
	8.4940	9.4810	9.0149	9.0340	9.0618	9.0996	9.3303
	9.4935	10.4878	10.0152	10.0330	10.0609	10.0985	10.3253
	10.4933	11.4908	11.0158	11.0328	11.0602	11.0973	11.3205
	11.4931	12.4907	12.0172	12.0326	12.0598	12.0960	12.3168
	12.4924	13.4912	13.0180	13.0324	13.0592	13.0950	13.3133
	13.4922	14.4914	14.0224	14.0322	14.0586	14.0942	14.3103
	14.4917	15.4912	15.0285	15.0327	15.0584	15.0937	15.3076
	15.4914	16.4915	16.0467	16.0333	16.0584	16.0928	16.3054
	16.4911	17.4912	17.2958	17.0331	17.0578	17.0925	17.3029
		18.4907	18.4630	18.0343	18.0573	18.0918	18.3009
Average z				0.0381	0.0665	0.1028	0.3054

Nulls Above Brewster's Angle

h_1=5	10	20	40	60	80	100	175
0.5023	0.4957	0.4897	0.4853	0.4870	0.4958	0.5082	0.6054

(3) Beacon distance, r_o, is the radio distance from transmitting source to the airborne receiver. The expression for r_o is given in paragraph 23.a.(6).

(4) In order to accurately evaluate the field strength in space, the angle chi, χ, (see figure 6-32) formed by the direct ray and a line parallel to the ground at the transmitting antenna position, must be known.

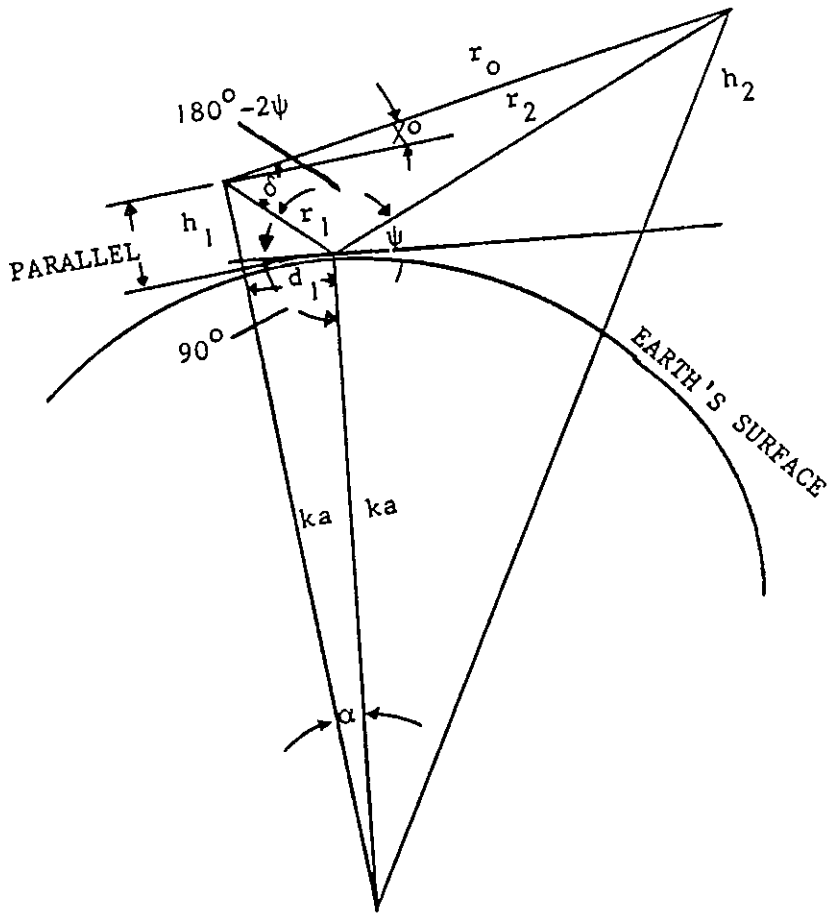

FIGURE 6-32. GEOMETRY FOR THE SOLUTION OF RADIATION ANGLE chi, χ

This angle is used to obtain the relative field strength for the direct ray from the free space antenna directivity pattern. Hence, a method of conversion from ψ^o to χ^o is necessary. The deviation from angle ψ to χ is given by,

$$\text{Deviation, } \Delta^{o} = 2\psi^{o} - \sin^{-1}\left(\frac{r_2 \sin 2\psi}{r_o}\right) + \frac{d_1}{ka}$$

and the angle chi is then given by

$$\chi^{o} = \sin^{-1}\left(\frac{r_2 \sin 2\psi}{r_o}\right) - \psi^{o} - \frac{d_1}{ka}$$

where r_o, r_2, d_1, and ka must be in the same units of measure.

(5) For the case of the TACAN antenna, it is necessary to consider the antenna's directivity in order to calculate the interference field structure. The magnitude of the direct ray will be given as $E_o E_\chi / r_o$, and the magnitude of the reflected ray by $DRE_o E_\psi / r_r$. Then the field strength at any given grazing angle and beacon distance is given by

$$E_{BD} = E_o\,(E)\left[\left(\frac{1}{r_o}\right)^2 + \left(\frac{1}{r_r}\,DR\,\frac{E_\psi}{E_\chi}\right)^2 + \frac{2}{r_o r_r}\,DR\,\frac{E_\psi}{E_\chi}\cos\,(\Theta - \phi)\right]^{\frac{1}{2}}$$

where E_o is the rms field strength at a unit distance, the mile, since r_o, r_1 and r_2 are expressed in statute miles, then,

$$E_o = \frac{\sqrt{30\ P \times G}}{1.609} \text{ rms mv/m at 1 s.m.}$$

where:

P = radiated power in watts

G = power gain of the antenna relative to an isotropic radiator

$r_r = r_1 + r_2$, the reflected path length

E_χ is the normalized value of E as obtained from the free space antenna directivity pattern at the radiation angle χ^{o}

E_ψ is the normalized value of E as obtained from the free space directivity pattern at the grazing angle ψ^{o}

For the range of values of r_o and r_r encountered in TACAN operation it may generally be assumed that the error introduced by letting $r_r = r_o$ will be negligible and then,

$$E_{BD} = E_o\,(E_\chi)\frac{1}{r_o}\left[1 + \left(DR\,\frac{E_\psi}{E_\chi}\right)^2 + 2DR\,\frac{E_\psi}{E_\chi}\cos\,(\Theta - \phi)\right]^{\frac{1}{2}} \text{ mv/m}$$

It is convenient to express the g(Θ) function, illustrated in figure 6-31, in decibels. As such, it is defined as 20 log of the ratio of the resultant field strength corresponding to a given grazing angle ψ and radial distance to the free-space field at the same angle and distance from the transmitter or

$$g(\Theta)_{db} = 20 \log \frac{\frac{E_\chi}{E_o r_o}\left[1 + \left(DR \frac{E_\psi}{E_\chi}\right)^2 + 2DR \frac{E_\psi}{E_\chi} \cos(\Theta - \phi)\right]^{\frac{1}{2}}}{\frac{E_\chi}{E_o r_o}}$$

$$= 10 \log \left[1 + \left(DR \frac{E_\psi}{E_\chi}\right)^2 + 2DR \frac{E_\psi}{E_\chi} \cos(\Theta - \phi)\right]$$

Maximums of g(Θ) occur when cos (Θ - ϕ) = 1 and minimums when cos (Θ - ϕ) = -1

For maximums:

$$g(\Theta)_{db} = 20 \log \left(1 + DR \frac{E_\psi}{E_\chi}\right)$$

For minimums:

$$g(\Theta)_{db} = 20 \log \left(1 - DR \frac{E_\psi}{E_\chi}\right)$$

TACAN antennas are of the tilted array type illustrated by the representative normalized directivity pattern shown in figure 6-33. The pattern is tilted up in order to discriminate against the ground reflected ray. The up-tilt is such that maximum radiation occurs at an angle, χ^o, of approximately 5^o to 15^o. Discrimination against the ground-reflected ray results in a shallow null and a field strength that is close to the free space value.

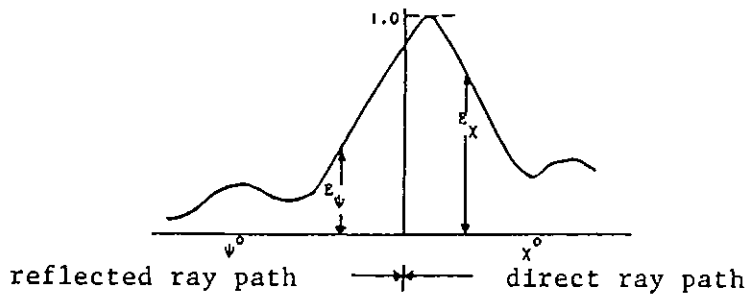

FIGURE 6-33. TYPICAL NORMALIZED FREE SPACE DIRECTIVITY PATTERN

(6) In the consideration of the wave theory of propagation each point on the expanding sphere of radiated energy may be considered as a secondary source which radiates energy in all forward directions. In the transmission of energy in free space from a transmitter to a receiver, there are, in reality, an infinite number of paths to consider. Now suppose a plane is placed perpendicular to the line between T and R (transmitter and receiver), and concentric circles are drawn which represent the loci of the origin of secondary waves traveling to R. When the radii of these circles are so chosen that the total path length from T to R via a point on the circle increases in increments of a half wavelength over the direct path from T to R, then the zones, as represented by the successive areas within the circles, are called Fresnel zones. In the volume of space between T and R, if there are no obstructing bodies such as buildings or hills, a given Fresnel zone outlines an ellipsoid of revolution having a circular cross-section centered on the axis between T and R.

(7) With transmitter and receiver located over a smooth spherical earth, it is evident that the earth will intersect certain of the Fresnel zones, depending on the elevations of T and R. The area of the earth's surface which intersects the zones (now the reflecting area) is elliptical, and most of the reflection occurs within the first Fresnel zone, the zone in which the path length via a point on the circle is one-half wavelength longer than the direct path from T to R. On the assumption that the earth is flat over the relatively small distances involved when using moderate-height transmitting and receiving antennas, the radial limits of the reflecting area (the limits of the major axis of the ellipse) for the first Fresnel zone, as measured from the transmitter location, are given by,

$$\ell_o = d_1 (1 + 2a) - 2d_1 \sqrt{a(1 + a)}$$

in units of d_1

$$\ell_1 = d_1 (1 + 2a) + 2d_1 \sqrt{a(1 + a)}$$

in units of d_1

where

$$a = \frac{\lambda}{4 h_1 \sin \Psi}$$ (dimensionless with λ and h_1 in same units)

$$= \frac{246}{f_{MHz} h_1 \sin \Psi}$$ (with h_1, transmitter height in feet)

The minor axis or width of the ellipse at its center (normal to the radial) is given by,

$$w = 4h_1 \sqrt{a(1 + a)}$$

in units of h_1

(8) In choosing a possible site for a TACAN antenna the system planner must consider the following important rule for the propagation path chosen:

> The first Fresnel zone should be clear of obstructing objects in order to minimize fading.

A vertical plane profile showing the concept of first Fresnel zone clearance over a rough earth terrain is shown in figure 6-34. The radius R on the locus which establishes the ellipse, at any distance d for a path length r_o, is given by,

$$R = \left\{ \frac{\lambda}{4} \left(r_o + \frac{\lambda}{4} \right) \left[1 - \frac{4(2d - r_o)2}{(2r_o + \lambda)^2} \right] \right\}^{\frac{1}{2}}$$

or when the wavelength $\lambda < r_o$, then

$$R = \left\{ \frac{\lambda d(r_o - d)}{r_o} \right\}^{\frac{1}{2}}$$

Whether the obstructions are hills or buildings does not alter the concept. A choice of site such that more than one Fresnel zone is clear of obstructions will not necessarily improve the situation, since reflection from outside the first Fresnel zone could then arrive out of phase, and the familiar lobe structure would be present, especially if these reflecting surfaces were smooth earth or water. Variations in the refractive index would then cause these lobes to shift up and down, thereby causing fading.

c. Graphic Procedure for Determining Distribution and Depth of Nulls

(1) The following nomographic procedure, to be described in detail, is appropriate for determining the distribution and depth of nulls in the TACAN vertical radiation pattern due to earth reflection:

(a) Determine the value of the earth radius factor, k.

(b) Using the curves of figures 6-35 through 6-40, determine the grazing angle ψ for arbitrarily chosen nulls. The first several nulls will usually be the deepest and are likely to be the ones that will create navigation problems.

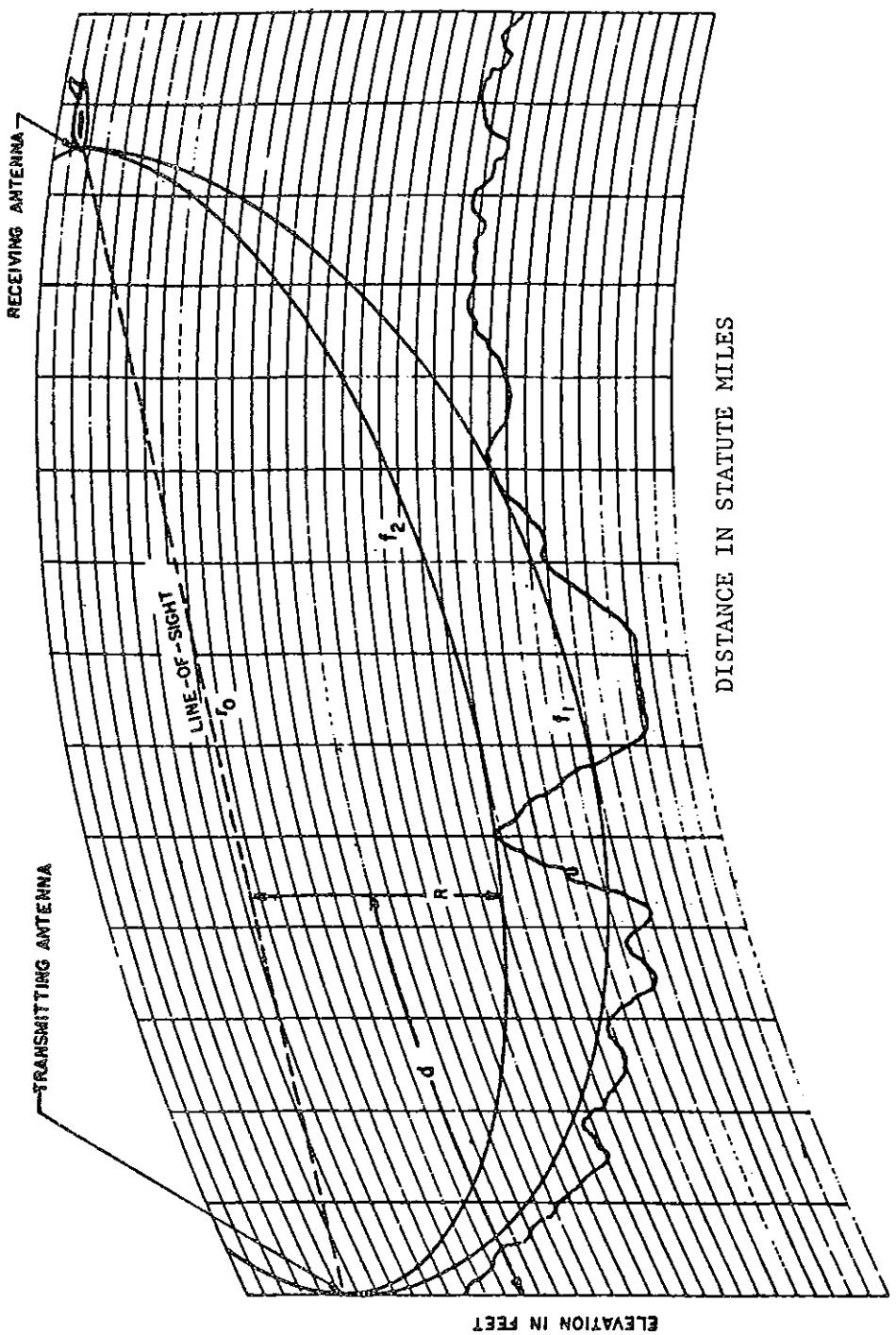

NOTES:

1. Earth radius k used to correct for atmosphere refraction.
2. Antennas located at foci of ellipse.
3. f_2 greater than f_1.
4. d is distance to desired point on the ellipse.

FIGURE 6-34. PROFILE CHART SHOWING FIRST FRESNEL ZONE ELLIPSES

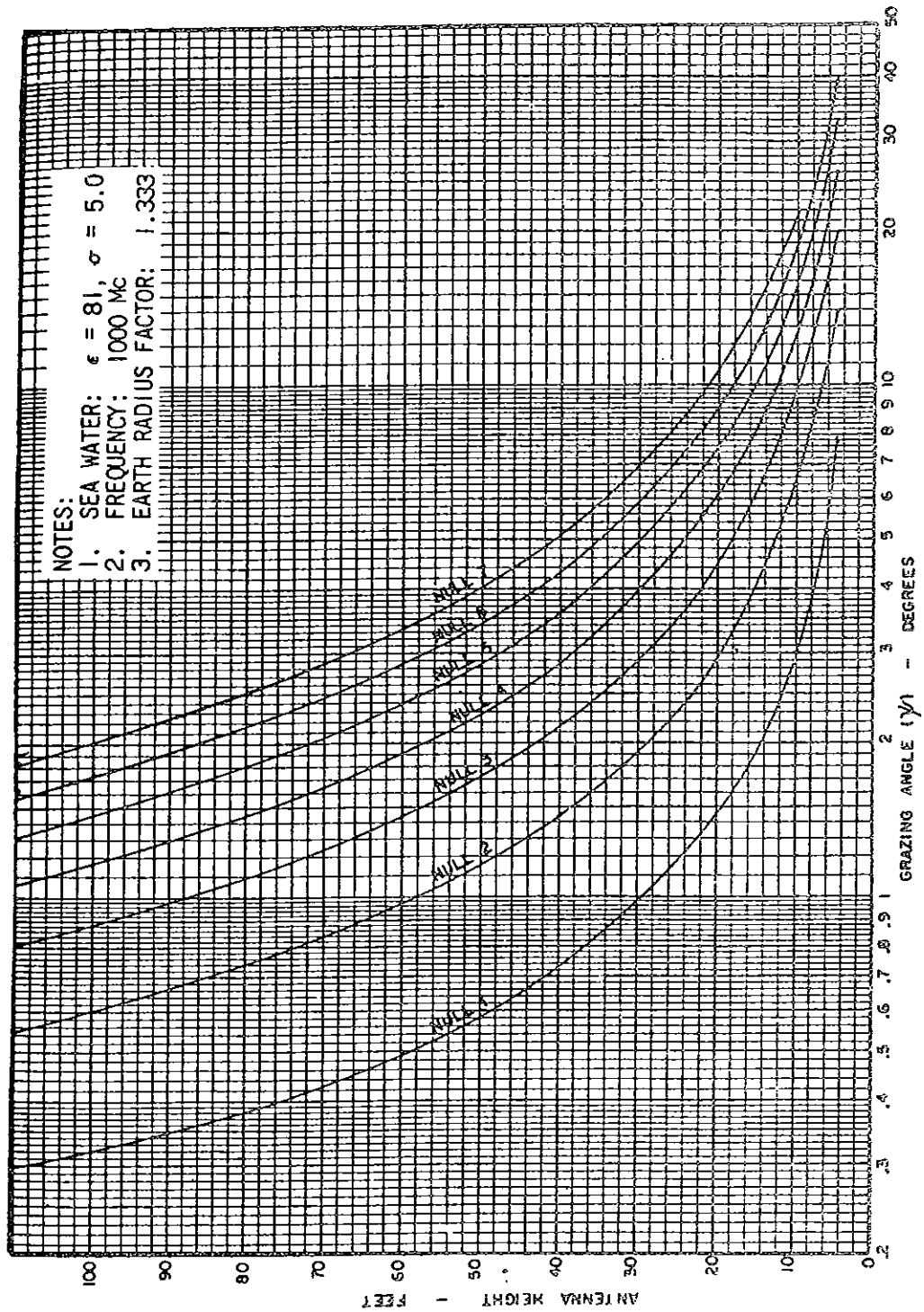

FIGURE 6-35. GRAZING ANGLES FOR NULLS AS A FUNCTION OF ANTENNA HEIGHT (FOR SEA WATER, FREQUENCY = 1000 Mc)

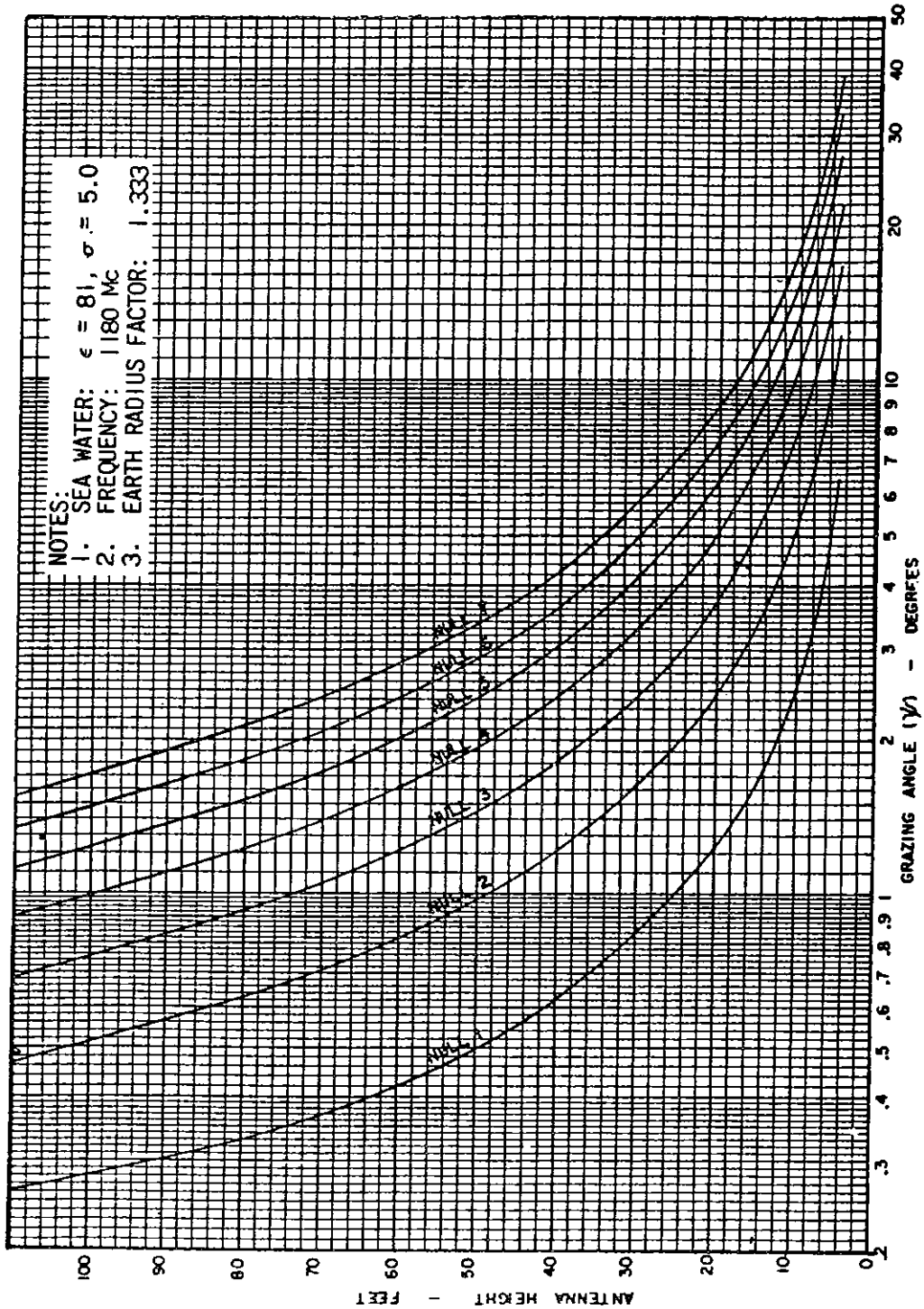

FIGURE 6-36. GRAZING ANGLES FOR NULLS AS A FUNCTION OF ANTENNA HEIGHT (FOR SEA WATER, FREQUENCY = 1180 Mc)

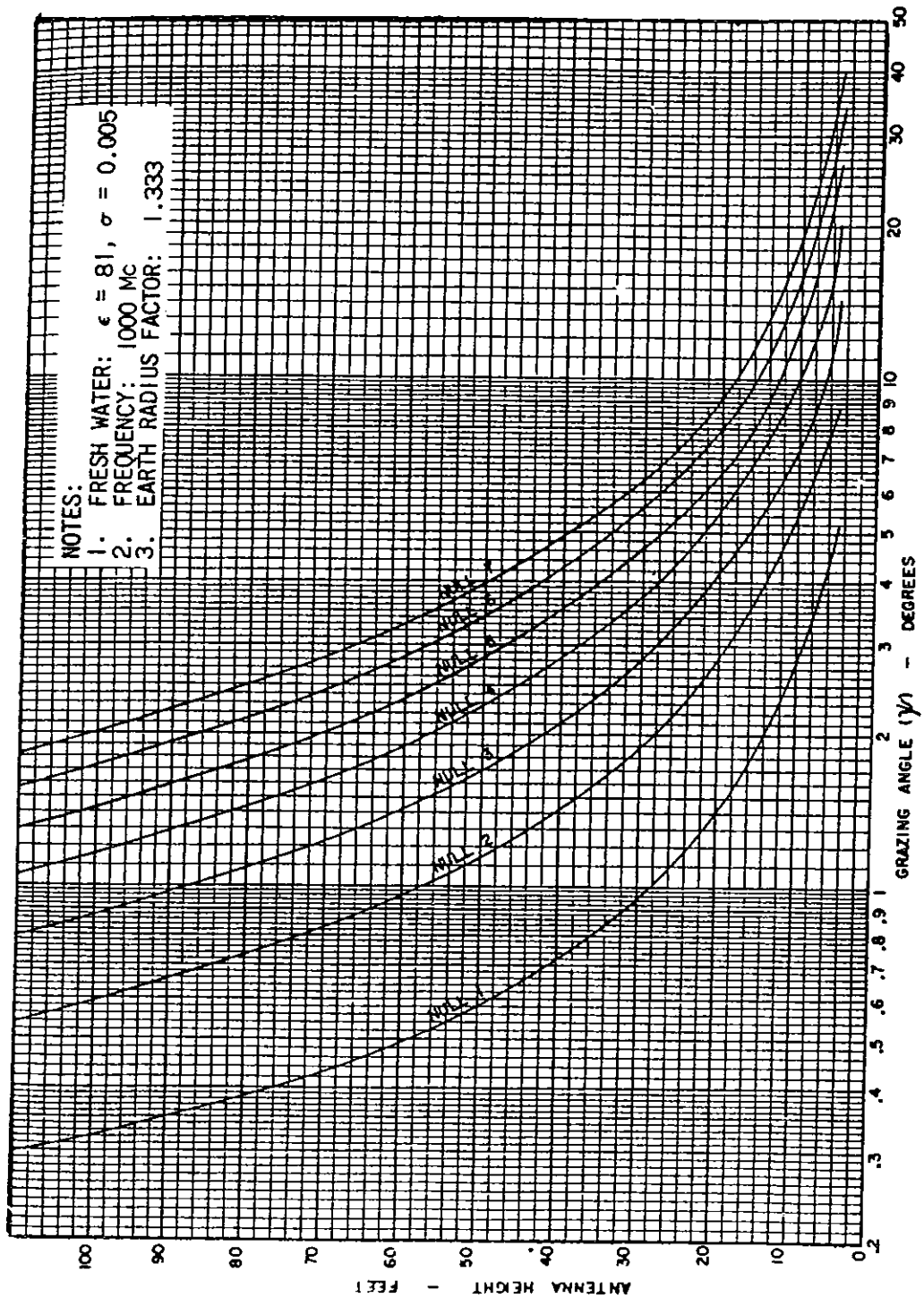

FIGURE 6-37. GRAZING ANGLES FOR NULLS AS A FUNCTION OF ANTENNA HEIGHT (FOR FRESH WATER, FREQUENCY = 1000 Mc)

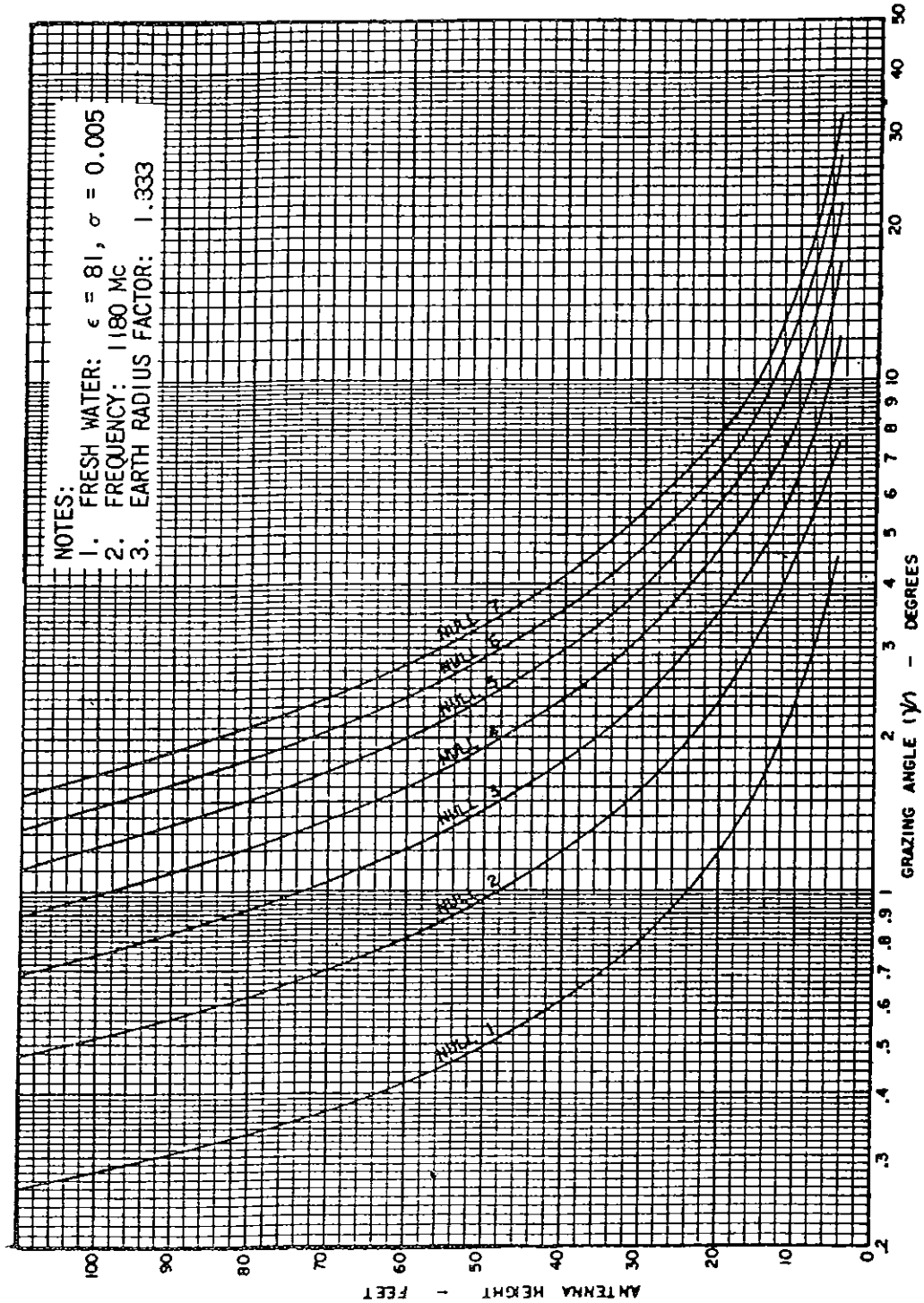

FIGURE 6-38. GRAZING ANGLES FOR NULLS AS A FUNCTION OF ANTENNA HEIGHT (FOR FRESH WATER, FREQUENCY = 1180 Mc)

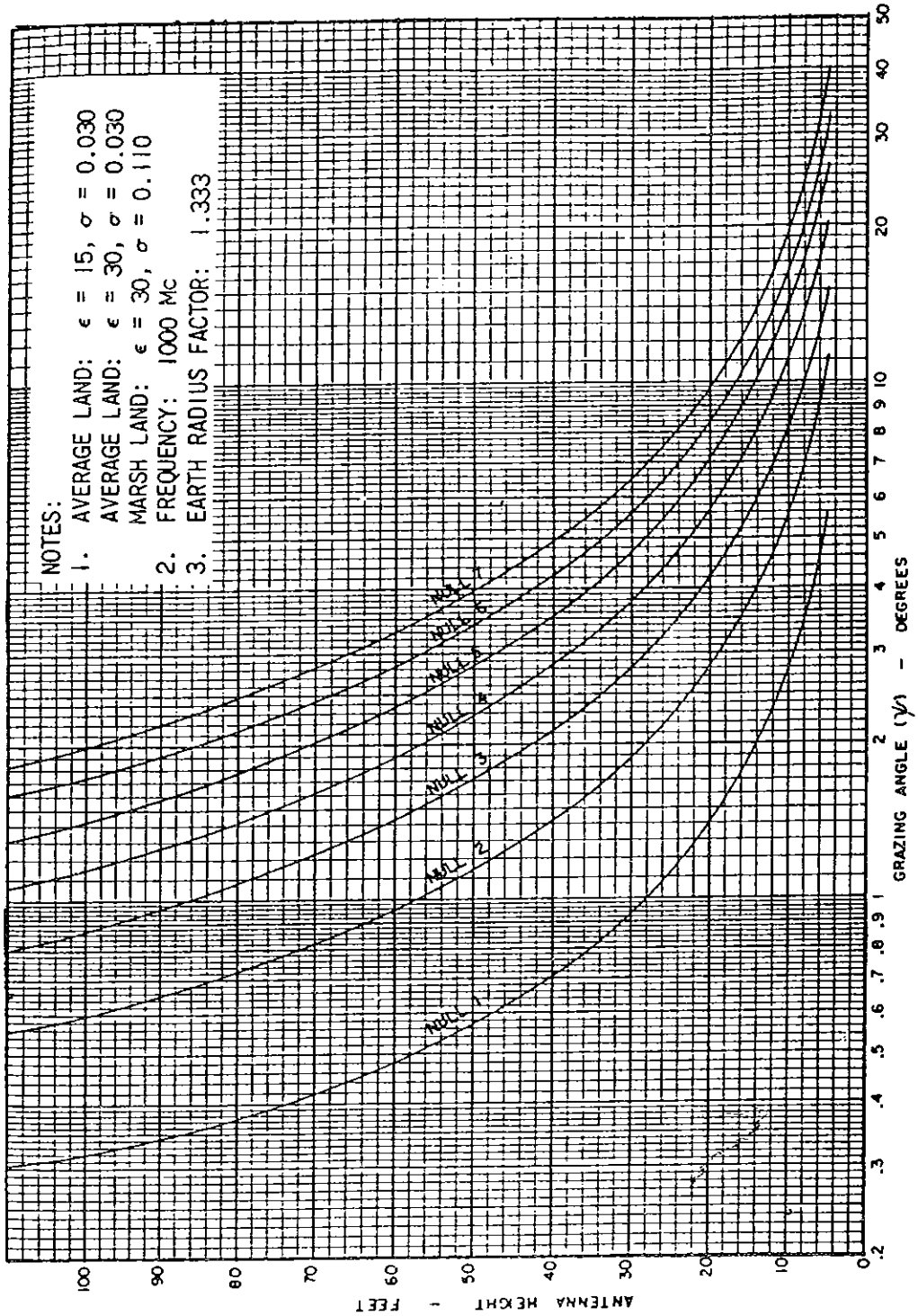

FIGURE 6-39. GRAZING ANGLES FOR NULLS AS A FUNCTION OF ANTENNA HEIGHT (FOR AVERAGE LAND, FREQUENCY = 1000 Mc)

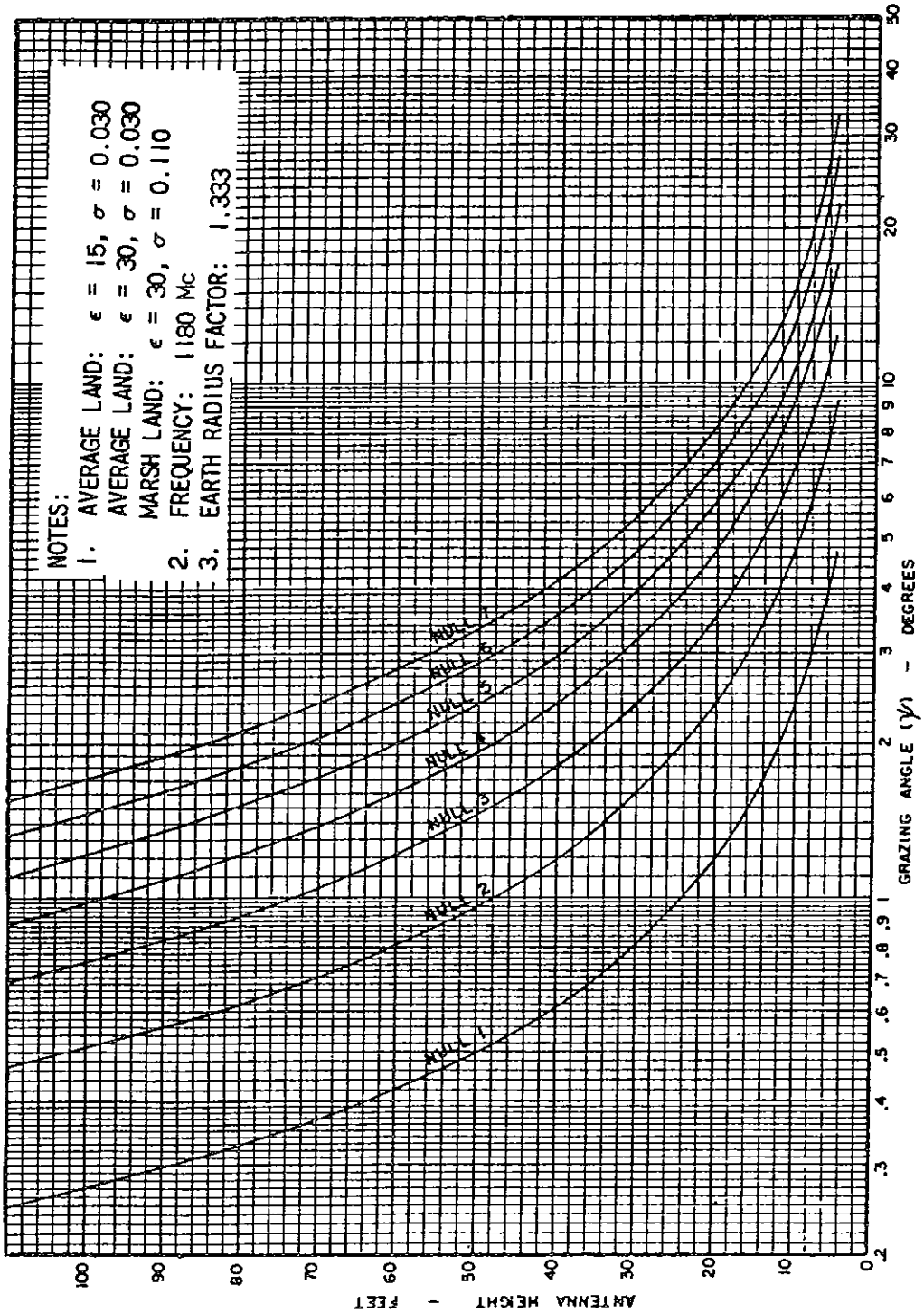

FIGURE 6-40. GRAZING ANGLES FOR NULLS AS A FUNCTION OF ANTENNA HEIGHT (FOR AVERAGE LAND, FREQUENCY = 1180 Mc)

(c) Using the curves of figures 6-41 through 6-46, determine the distance d to the center of reflection of the Fresnel zone for the parameters under consideration.

(d) In this graphical method, obtain the value of the radiation angle χ by assuming that it is approximately equal to the grazing angle ψ. It will be shown that the error introduced by this approximation is negligible.

(e) Determine the free-space directivity of the downward directed ray corresponding to the grazing angle ψ. For this purpose, use the directivity pattern for the antenna used. Typical patterns are shown in figures 6-47 and 6-48. If the pattern for the specific antenna is not available, it is permissible to use the pattern from an antenna having the same number of active elements.

(f) Determine the free-space directivity of the upward directed direct ray using the methods just described for the downward directed ray.

(g) Determine the divergence factor D from figures 6-49a, 6-49b, and 6-49c.

(h) Using figures 6-23 through 6-29, determine the magnitude of the reflection coefficient.

(i) Determine the earth gain factor, $g(\sigma)_{dB}$, <u>for the null under consideration</u> using the equation

$$g(\sigma)_{dB} = 20 \log \left[1 - DR \frac{E_\psi}{E_\chi}\right] (\text{nulls})$$

Note that neither E_ψ nor E_χ need be known - only their relative amplitudes.

(j) Calculate points on the locus of the maxima of $g(\sigma)$ using the equation

$$g(\sigma)_{dB} = 20 \log \left[1 + DR \frac{E_\psi}{E_\chi}\right] (\text{maxima})$$

These points do not locate lobe maxima, they are simply points on the locii of maxima.

(k) Determine the beacon distance corresponding to the grazing angle considered. Refer to figures 6-50 through 6-52.

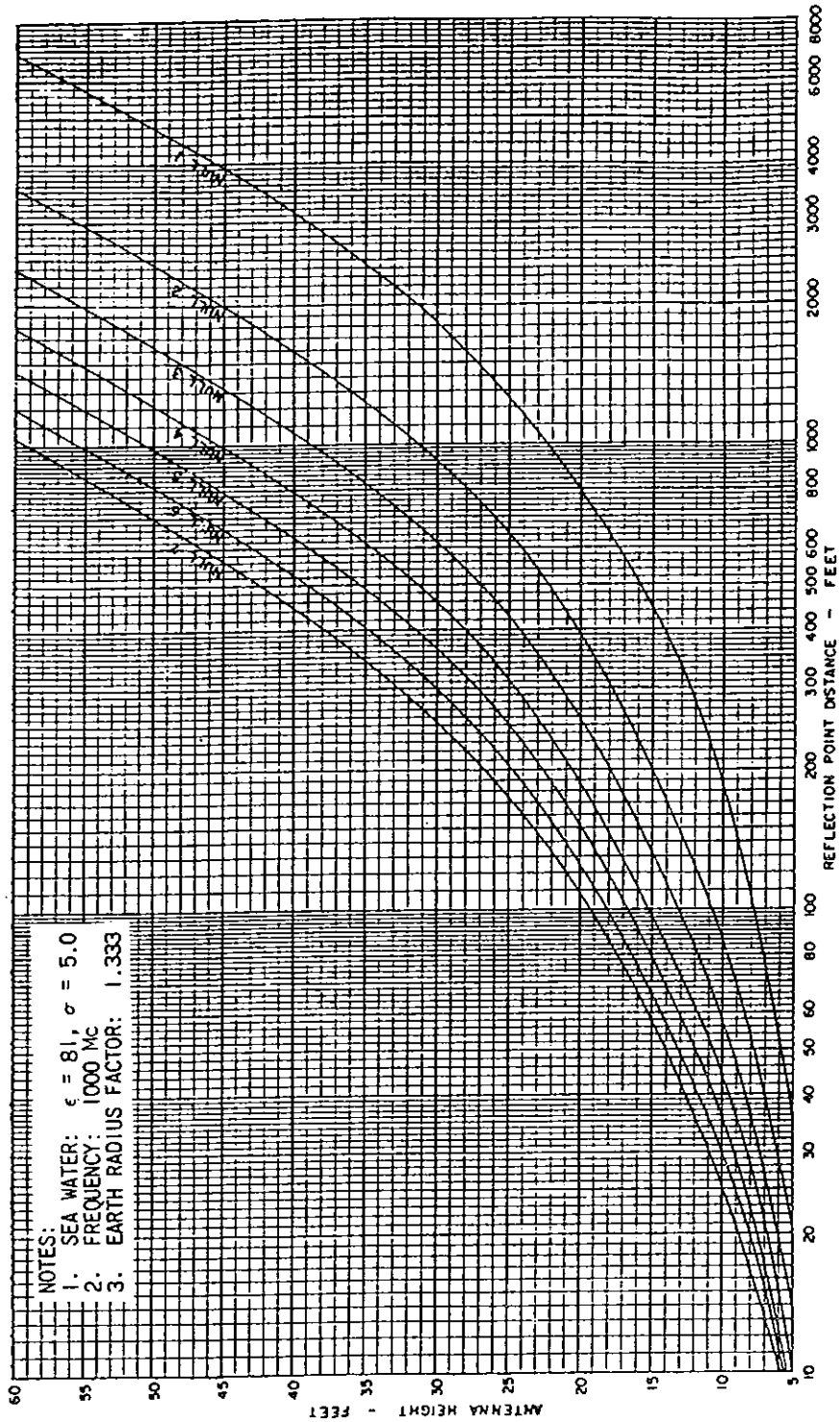

FIGURE 6-41. DISTANCE TO MEAN REFLECTION POINT FOR NULLS AS A FUNCTION OF ANTENNA HEIGHT (FOR SEA WATER, FREQUENCY = 1000 Mc)

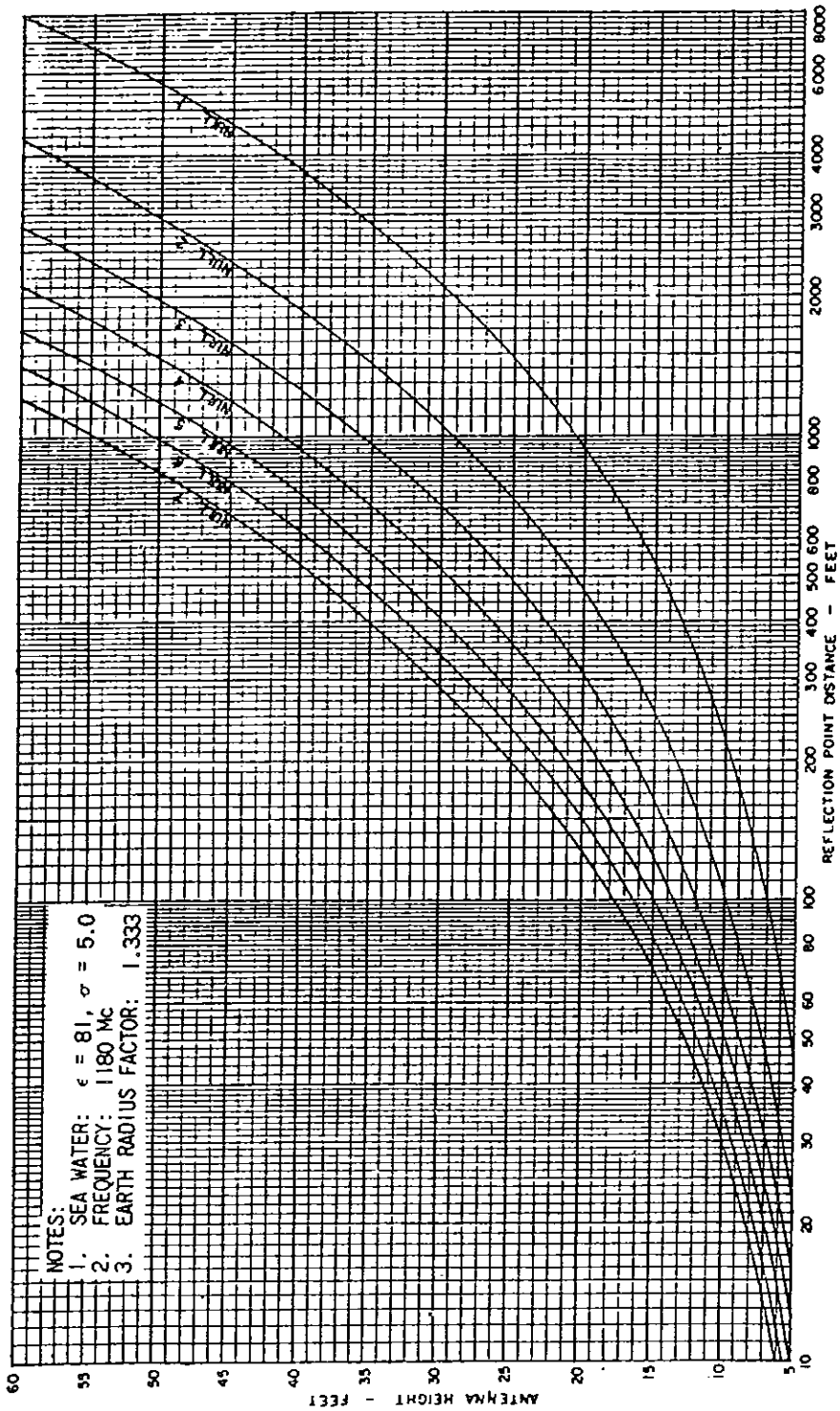

FIGURE 6-42. DISTANCE TO MEAN REFLECTION POINT FOR NULLS AS A FUNCTION OF ANTENNA HEIGHT (FOR SEA WATER, FREQUENCY = 1180 Mc)

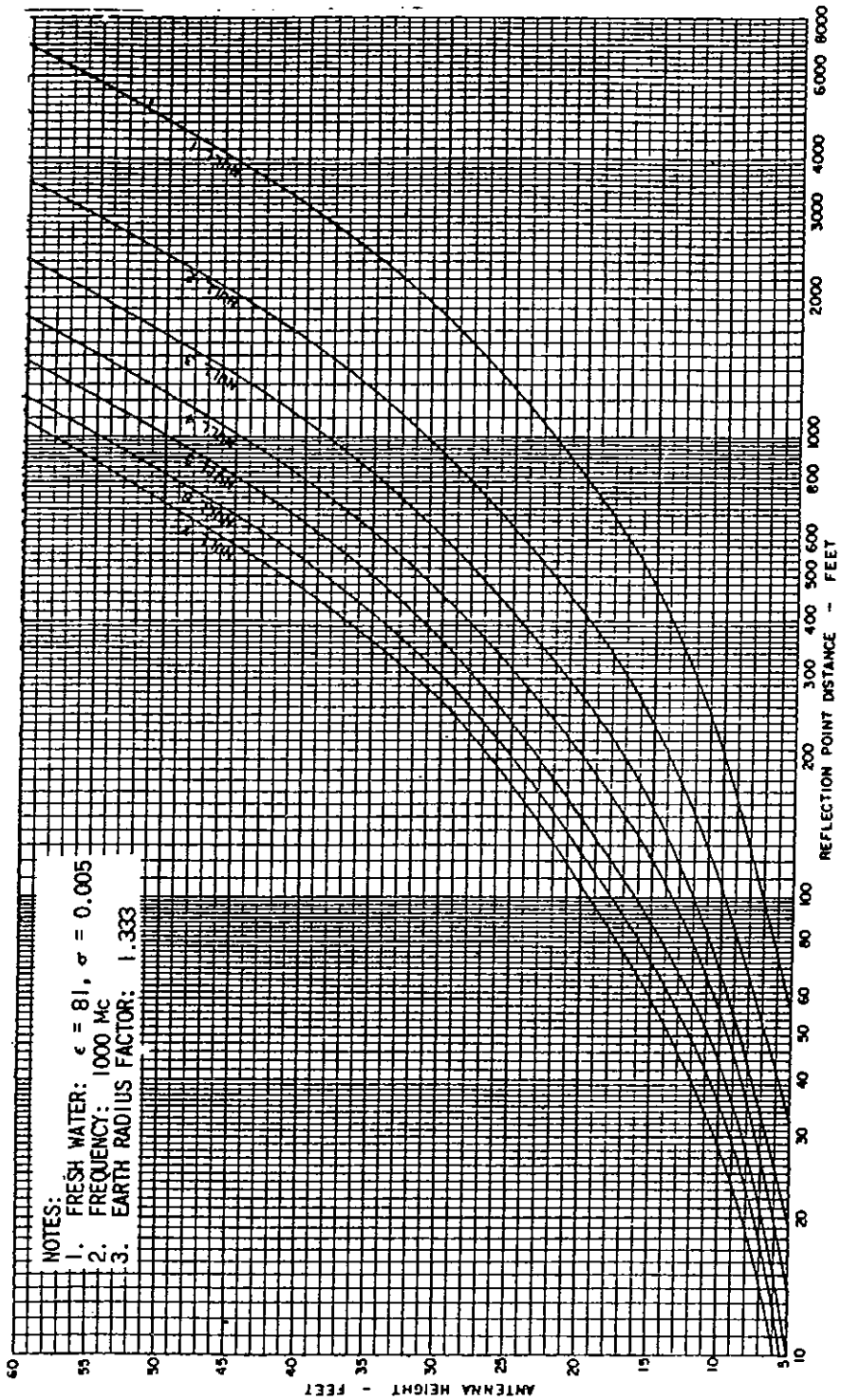

FIGURE 6-43. DISTANCE TO MEAN REFLECTION POINT FOR NULLS AS A FUNCTION OF ANTENNA HEIGHT (FOR FRESH WATER, FREQUENCY = 1000 Mc)

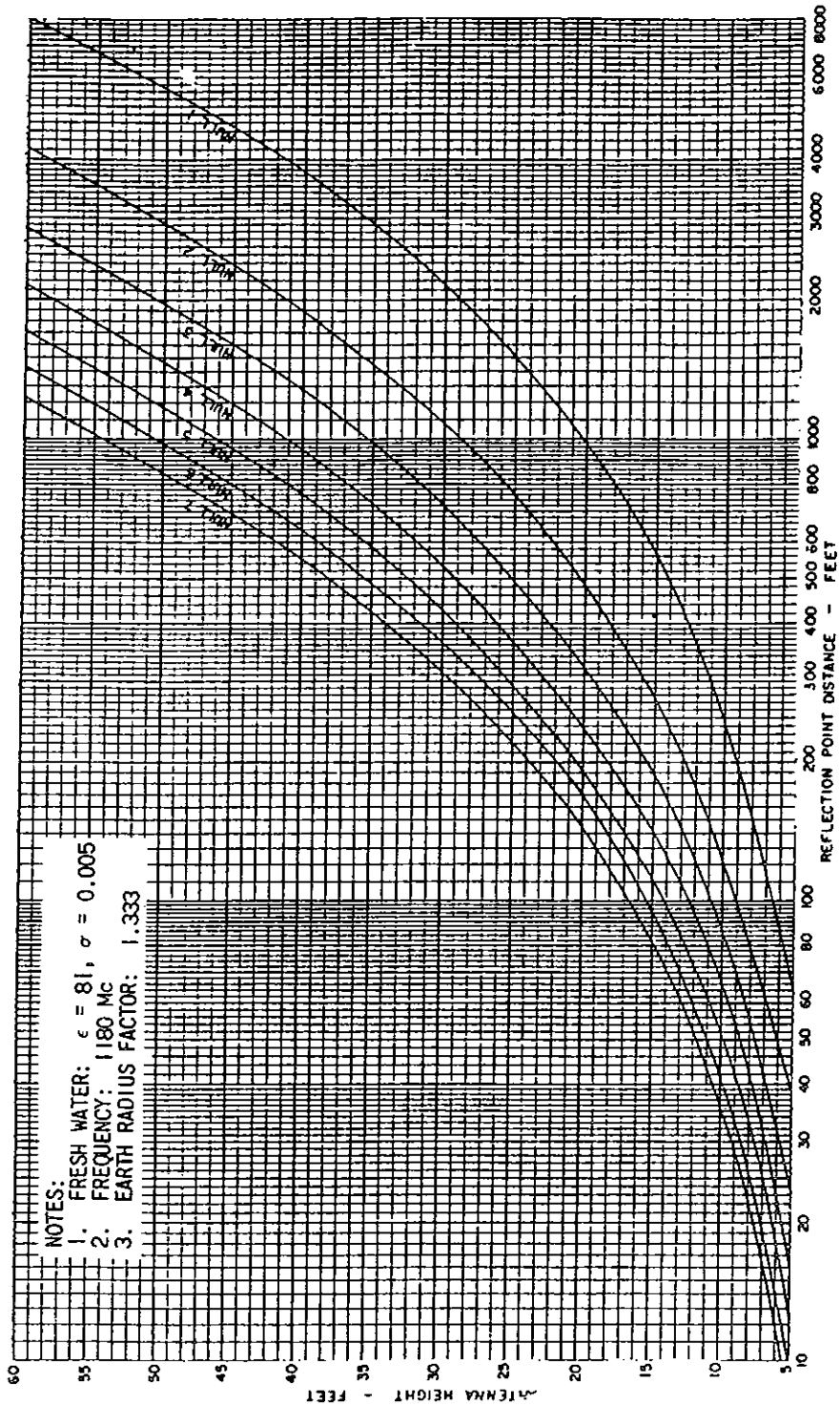

FIGURE 6-44. DISTANCE TO MEAN REFLECTION POINT FOR NULLS AS A FUNCTION OF ANTENNA HEIGHT (FOR FRESH WATER, FREQUENCY = 1180 Mc)

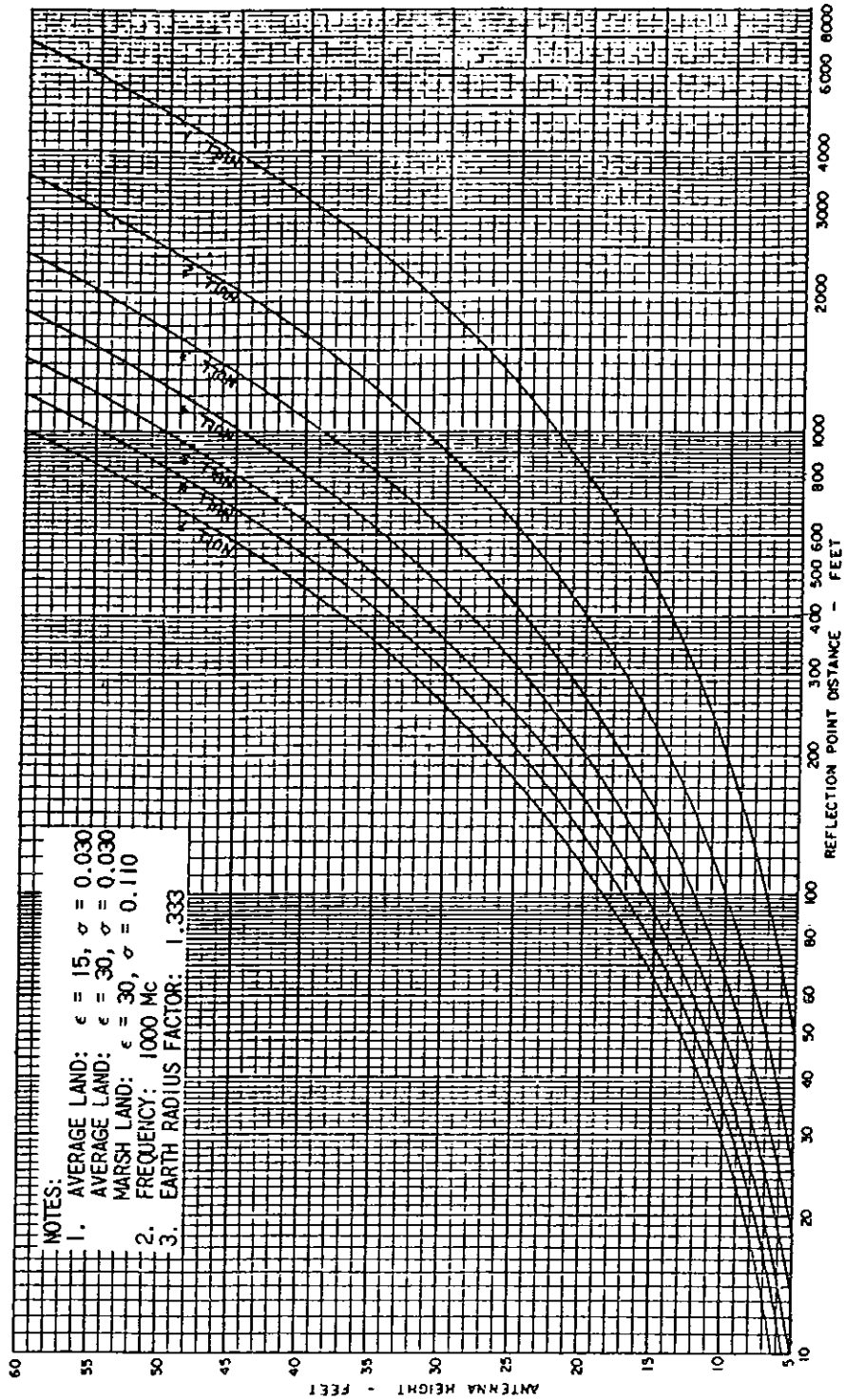

FIGURE 6-45. DISTANCE TO MEAN REFLECTION POINT FOR NULLS AS A FUNCTION OF ANTENNA HEIGHT (FOR AVERAGE LAND, FREQUENCY = 1000 Mc)

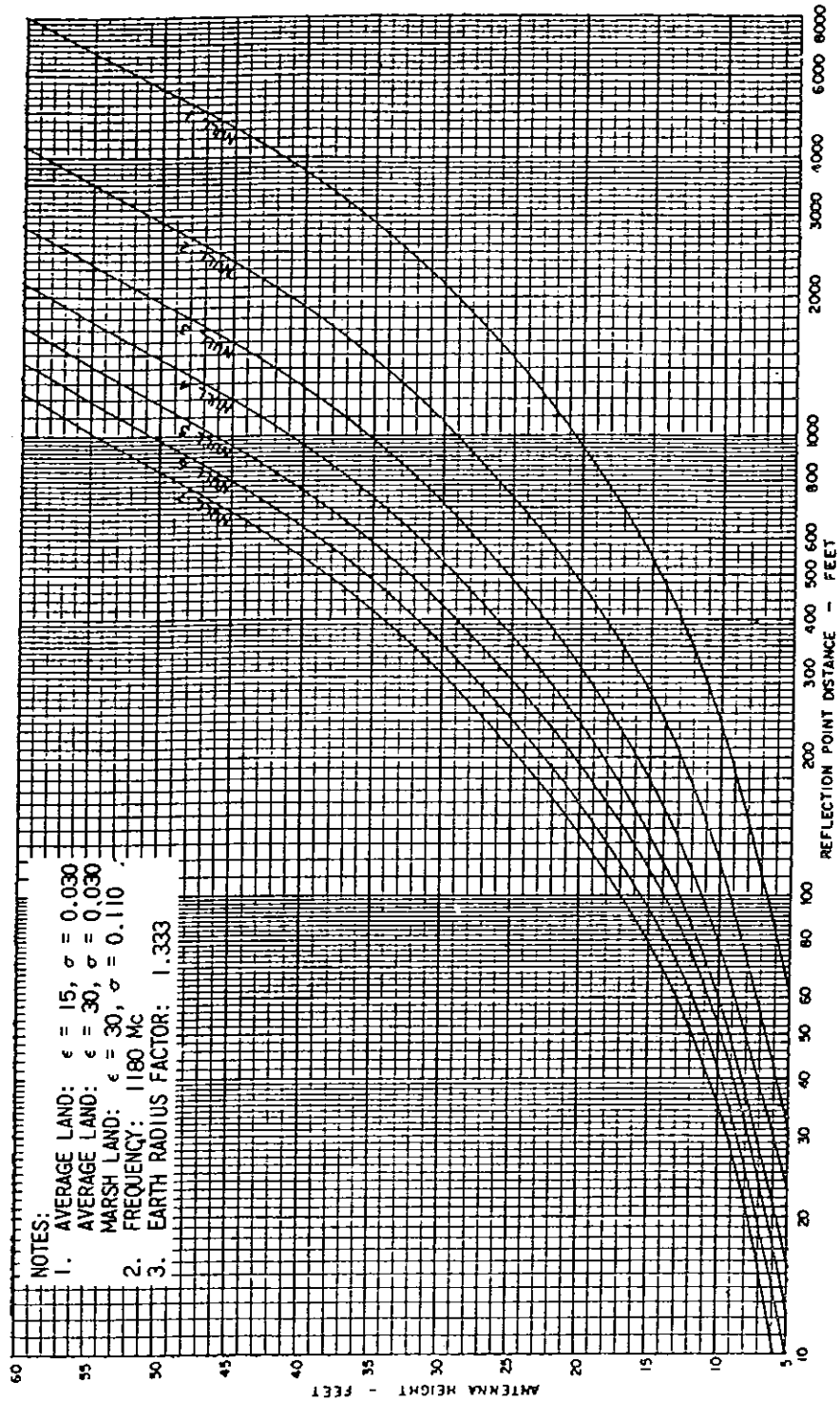

FIGURE 6-46. DISTANCE TO MEAN REFLECTION POINT FOR NULLS AS A FUNCTION OF ANTENNA HEIGHT (FOR AVERAGE LAND, FREQUENCY = 1180 Mc)

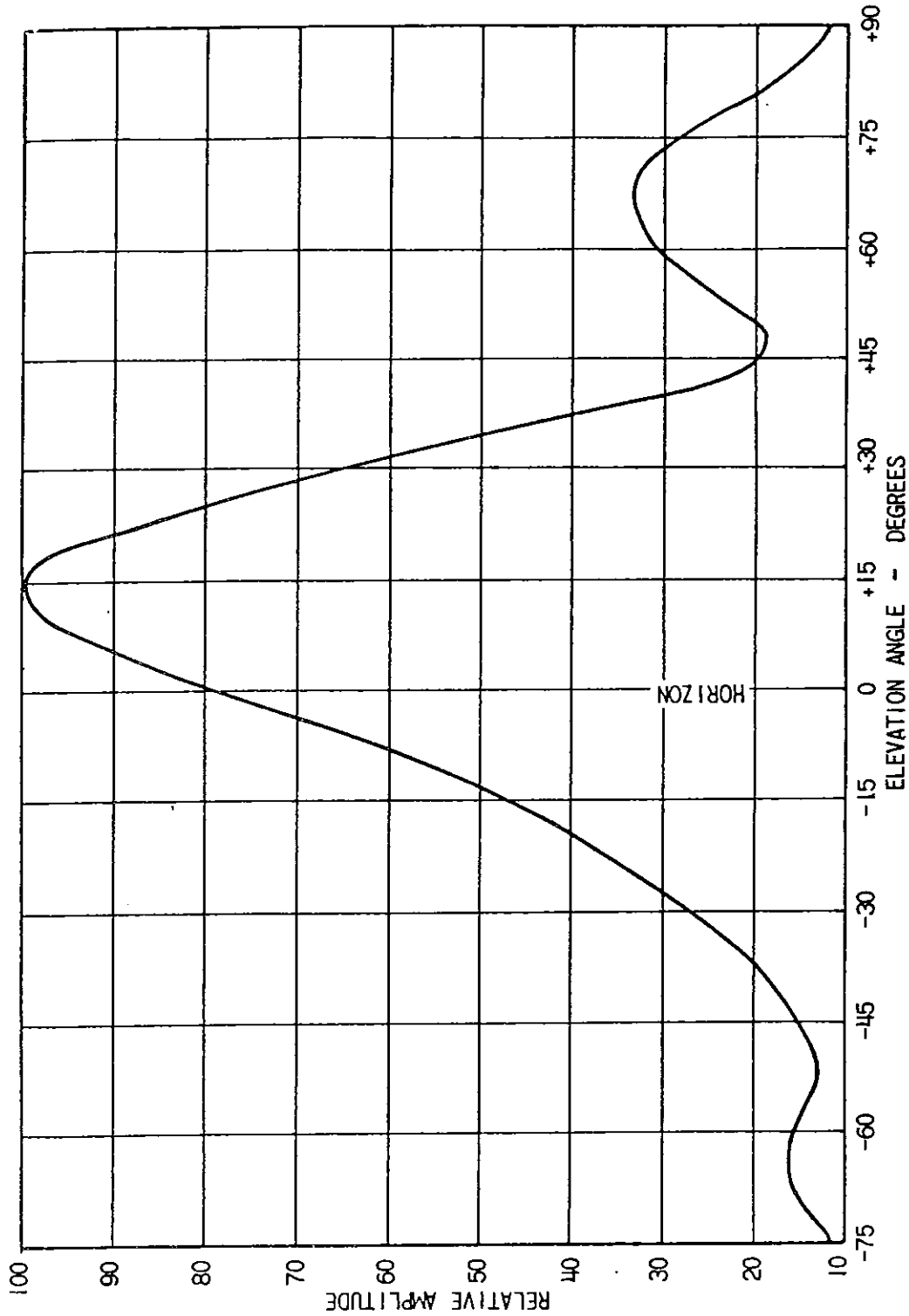

FIGURE 6-47. FREE SPACE DIRECTIVITY PATTERN FOR THE AT-1056/GRA-60 AT 992 Mc

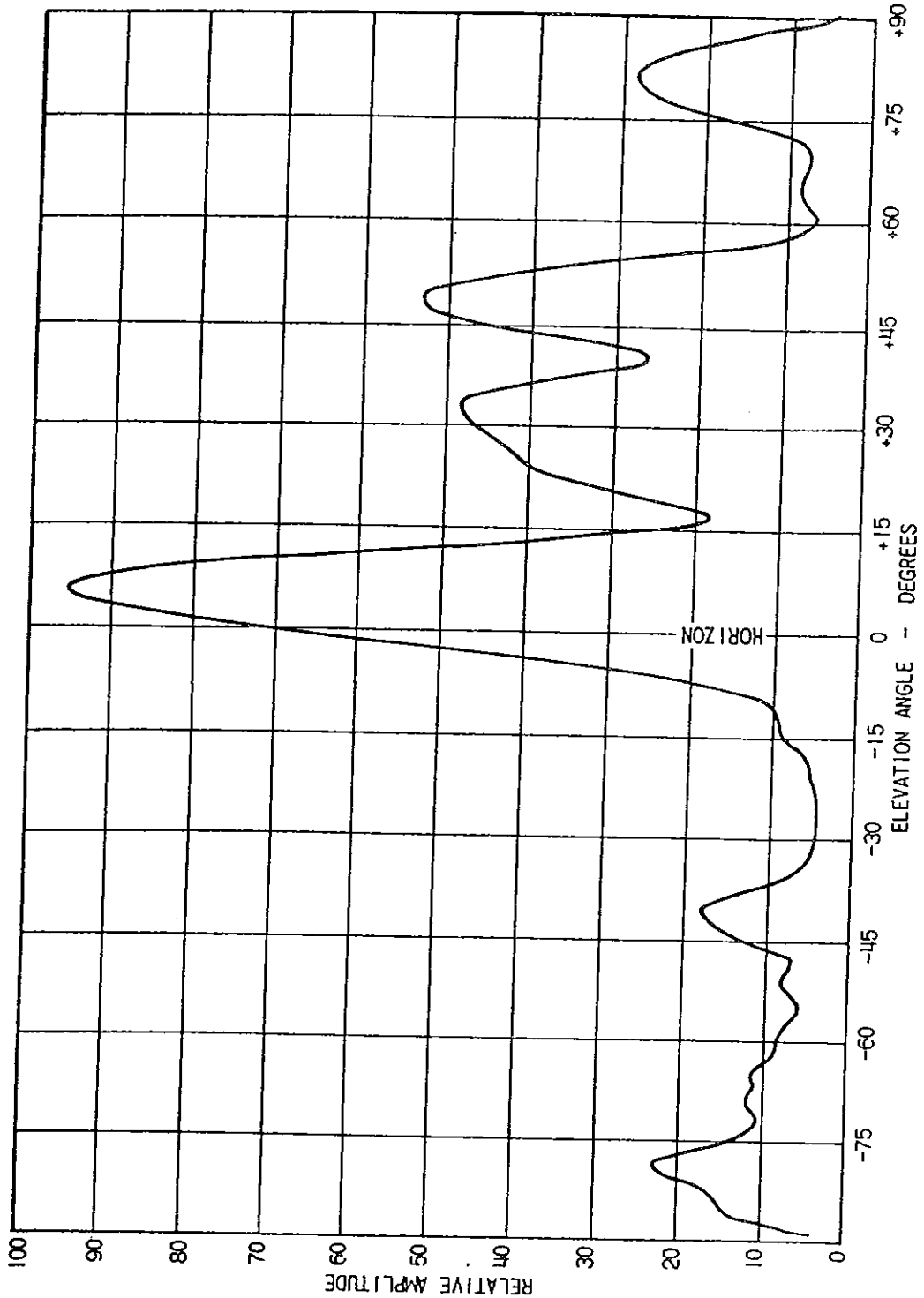

FIGURE 6-48. FREE SPACE DIRECTIVITY PATTERN FOR THE OA-592/URN-3 AT 992 Mc

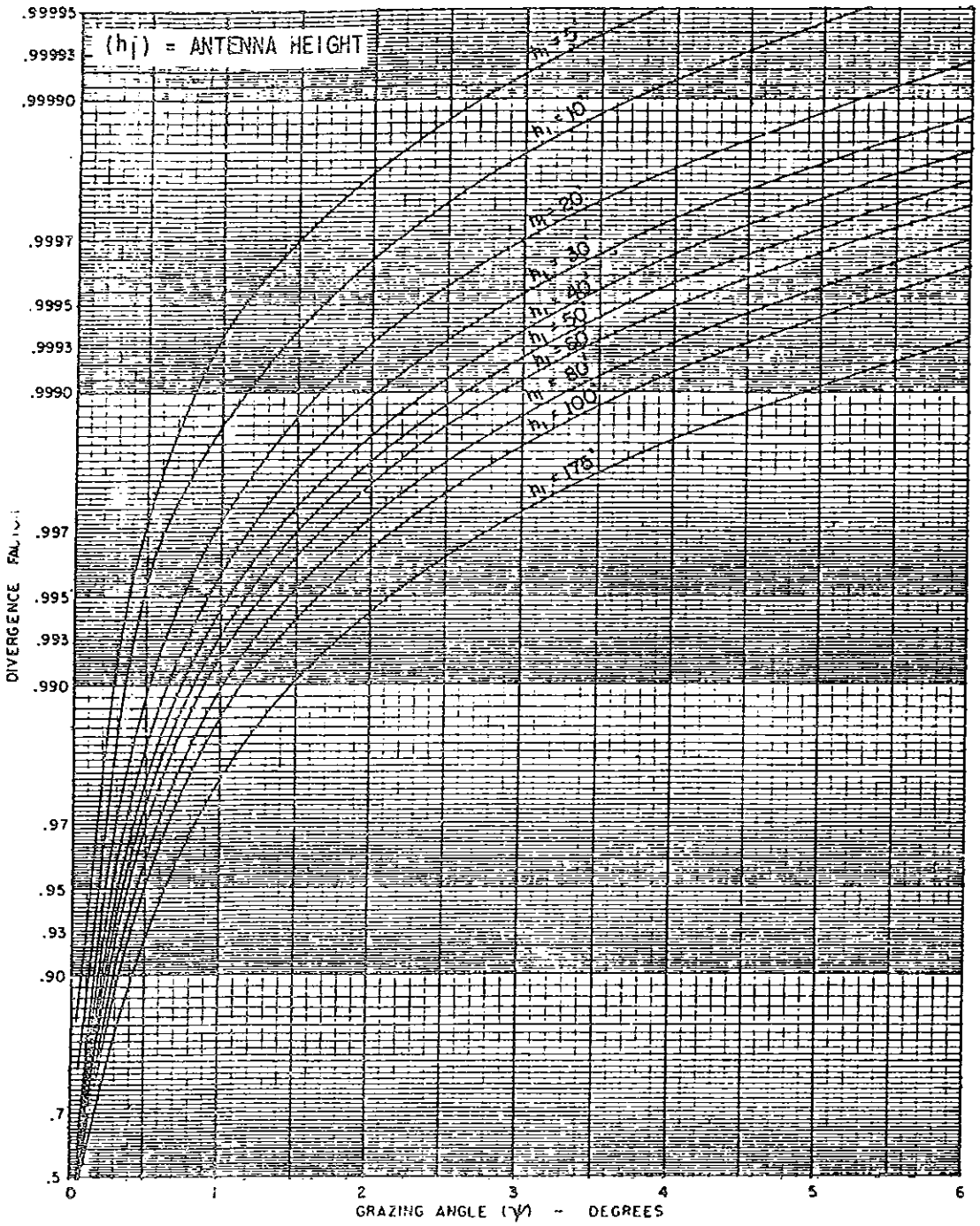

FIGURE 6-49a. DIVERGENCE FACTOR FOR AN EARTH-RADIUS FACTOR OF 1.166

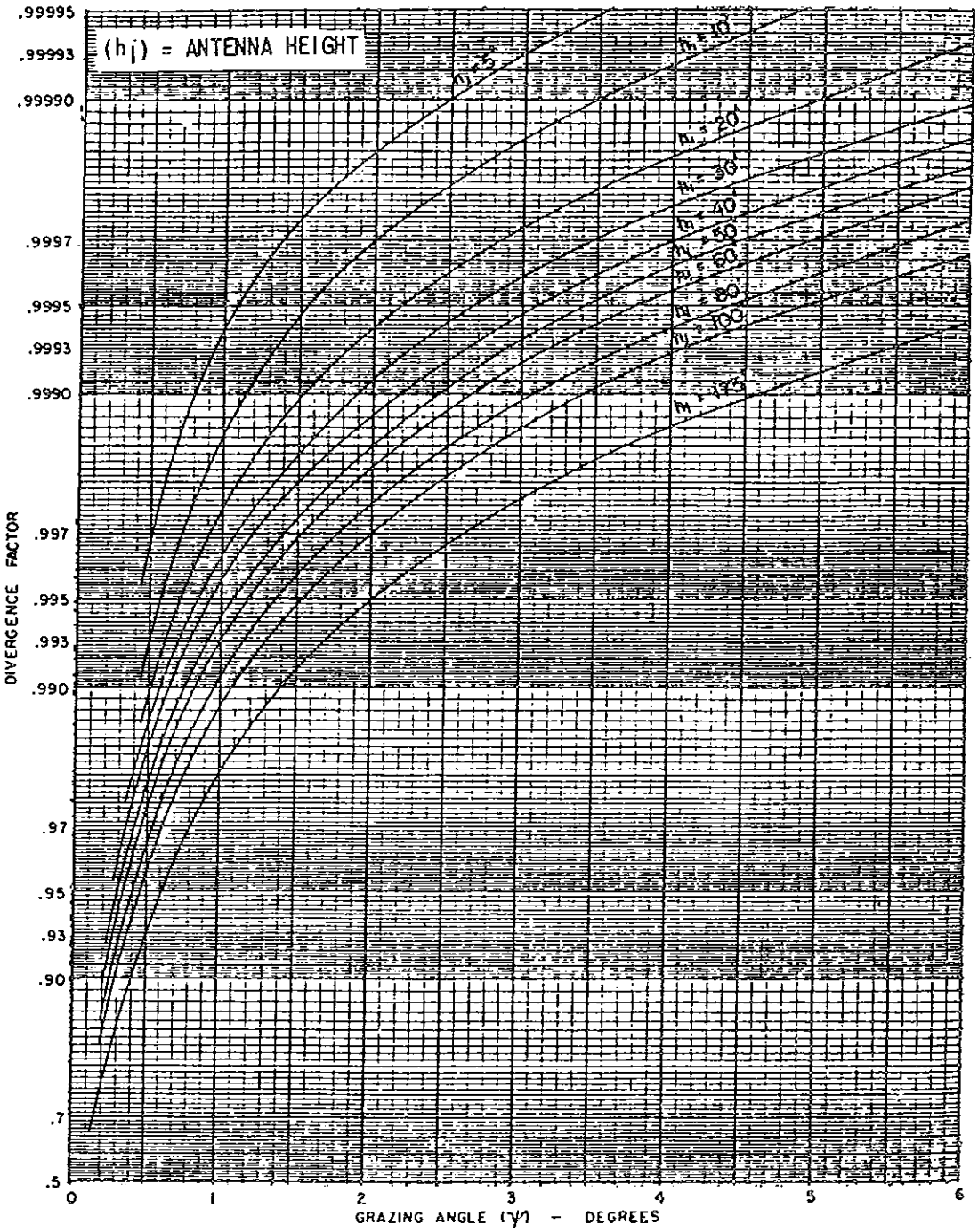

FIGURE 6-49b. DIVERGENCE FACTOR FOR AN EARTH-RADIUS FACTOR OF 1.333

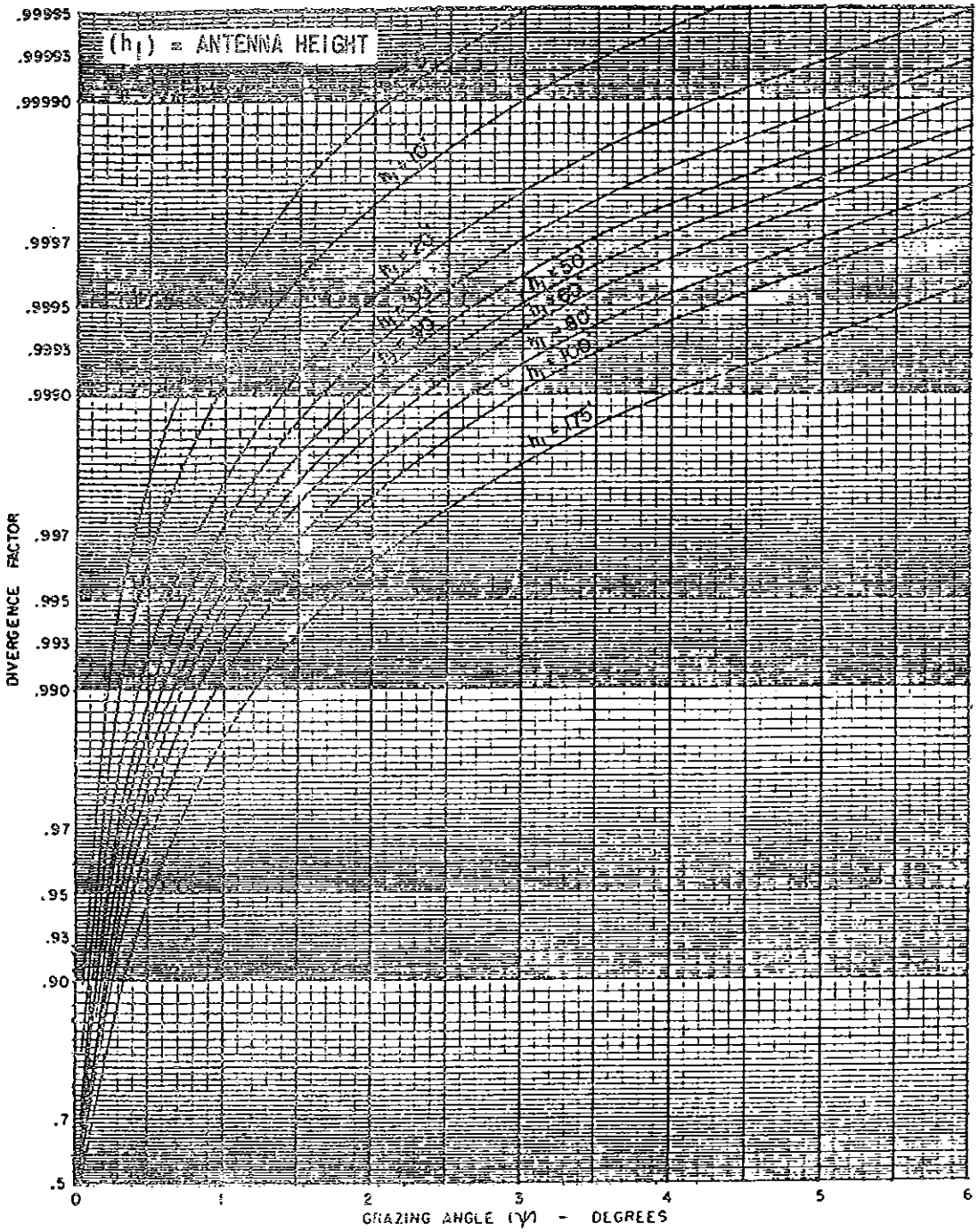

FIGURE 6-49c. DIVERGENCE FACTOR FOR AN EARTH-RADIUS FACTOR OF 1.766

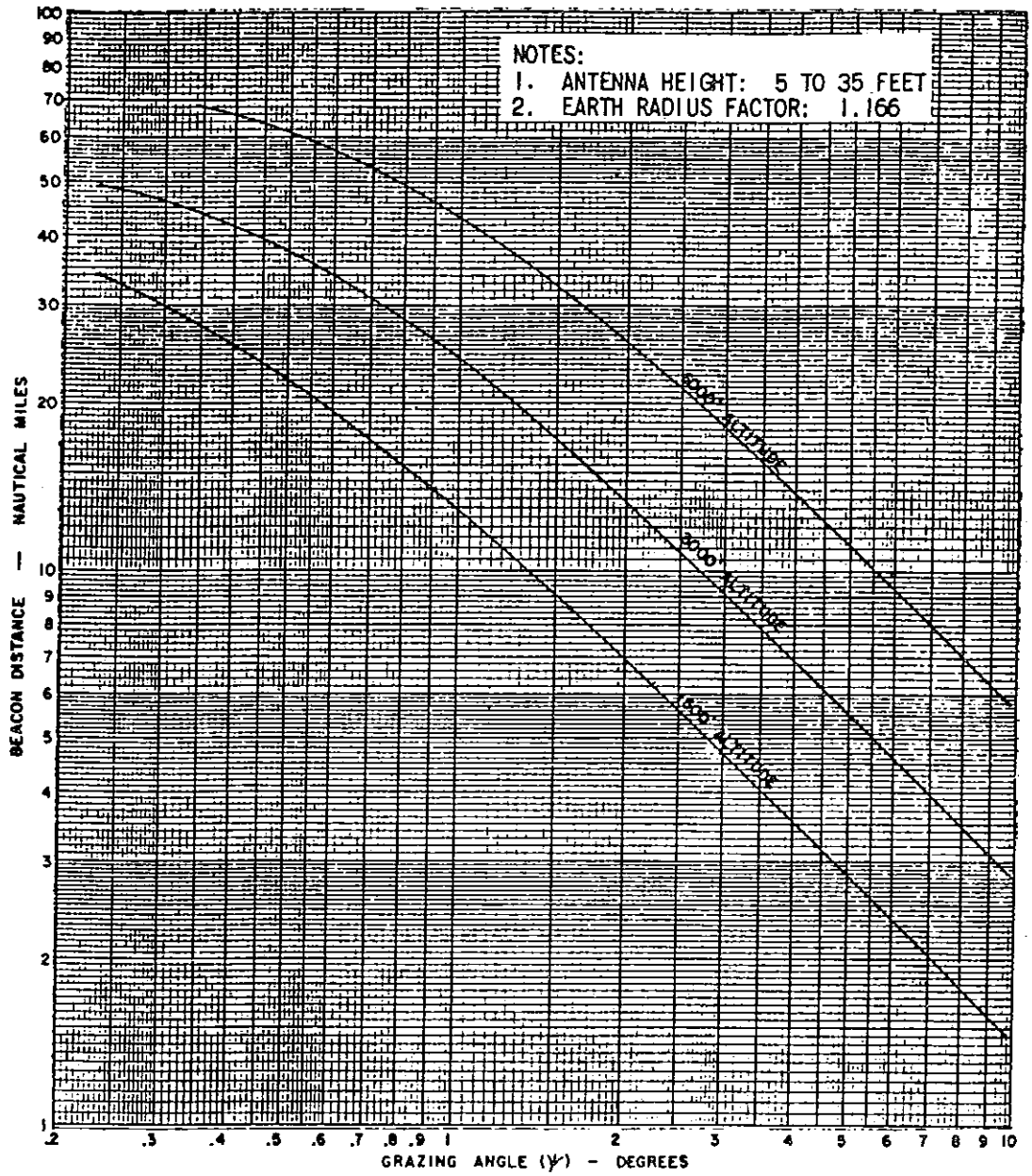

FIGURE 6-50a. BEACON DISTANCE AS A FUNCTION OF GRAZING ANGLE (ANTENNA HEIGHT 5 to 35 FEET, EARTH-RADIUS FACTOR OF 1.166)

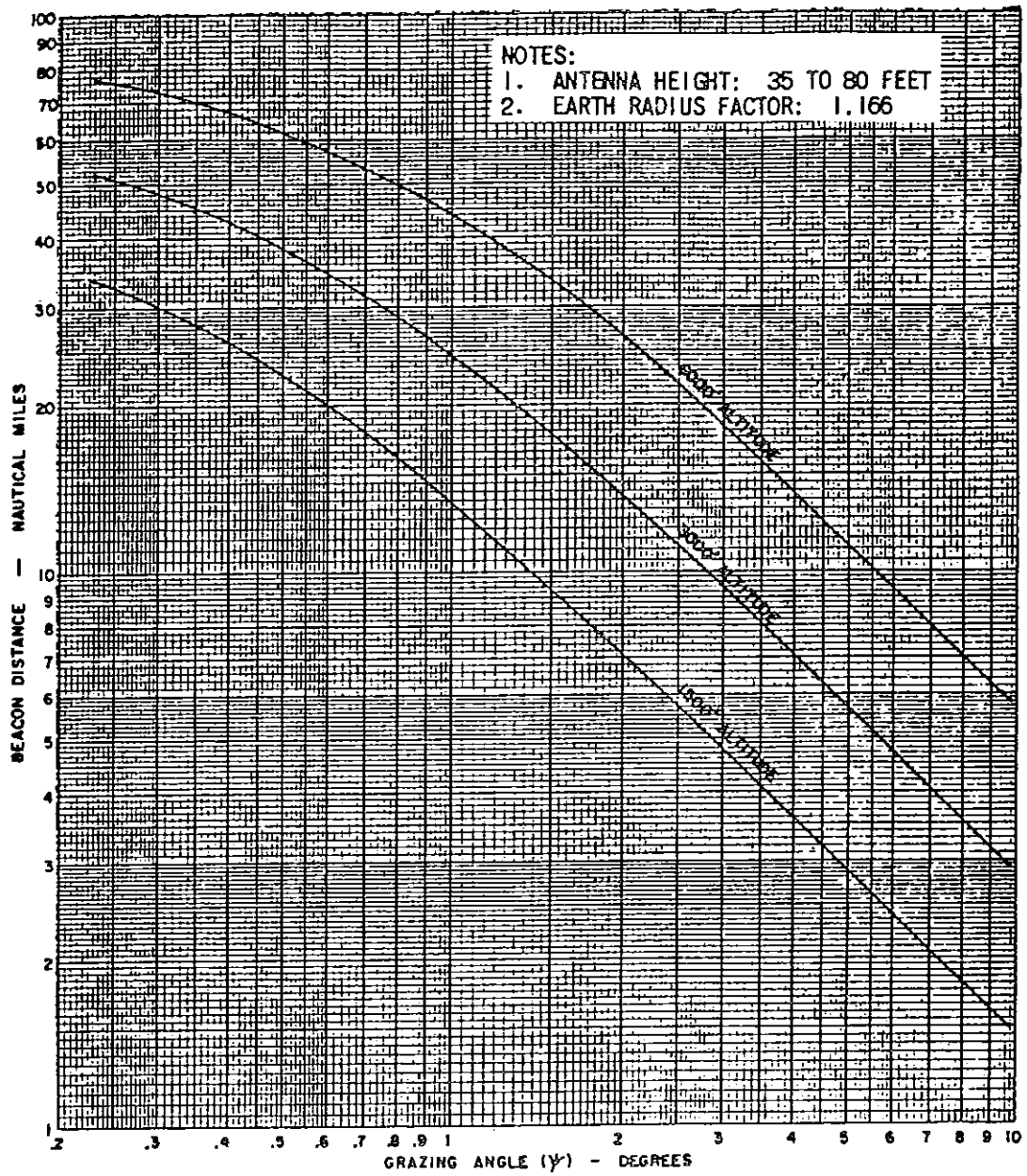

FIGURE 6-50b. BEACON DISTANCE AS A FUNCTION OF GRAZING ANGLE (ANTENNA HEIGHT 35 to 80 FEET, EARTH-RADIUS FACTOR OF 1.166)

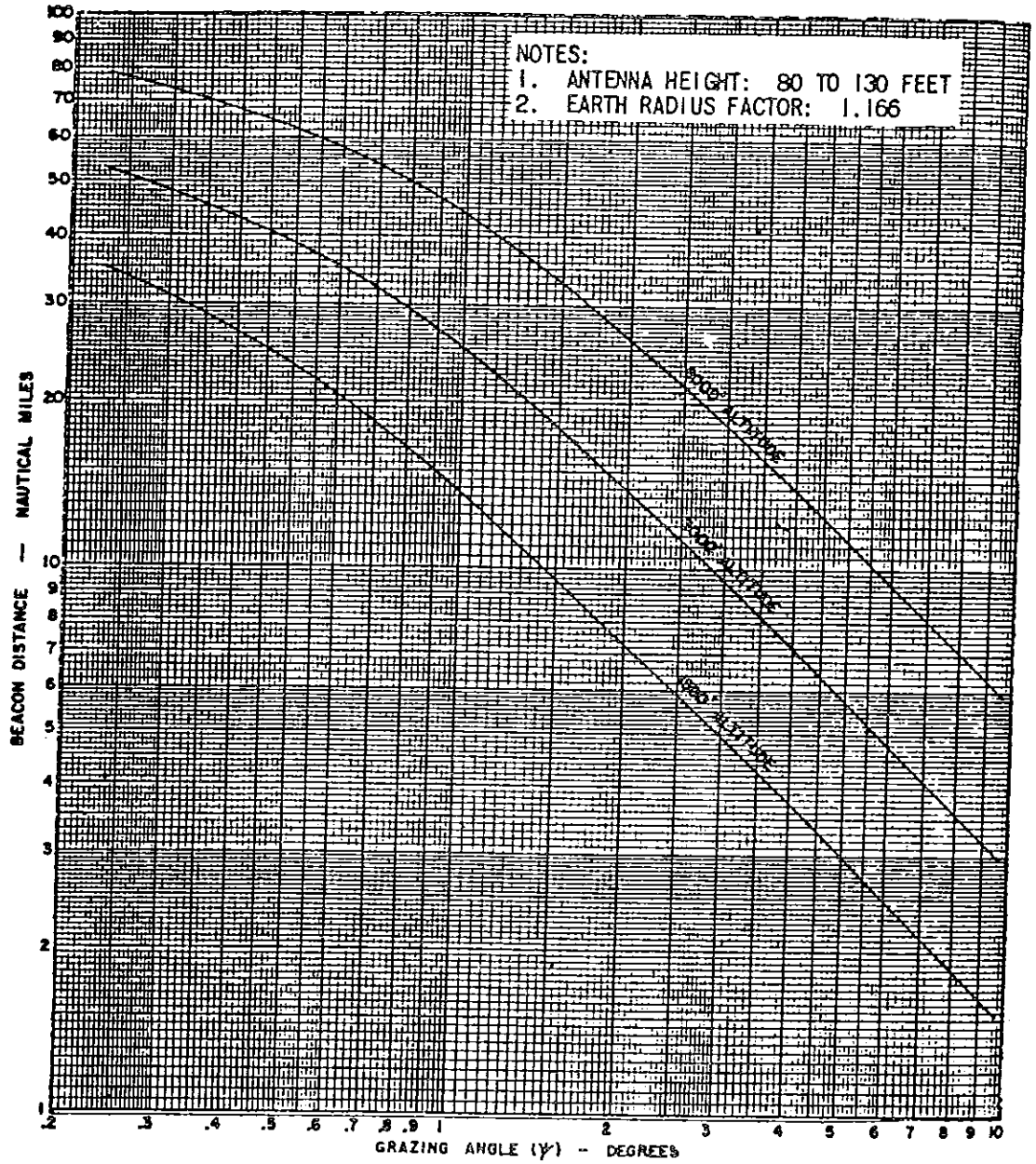

FIGURE 6-50c. BEACON DISTANCE AS A FUNCTION OF GRAZING ANGLE (ANTENNA HEIGHT 80 to 130 FEET, EARTH-RADIUS FACTOR OF 1.166).

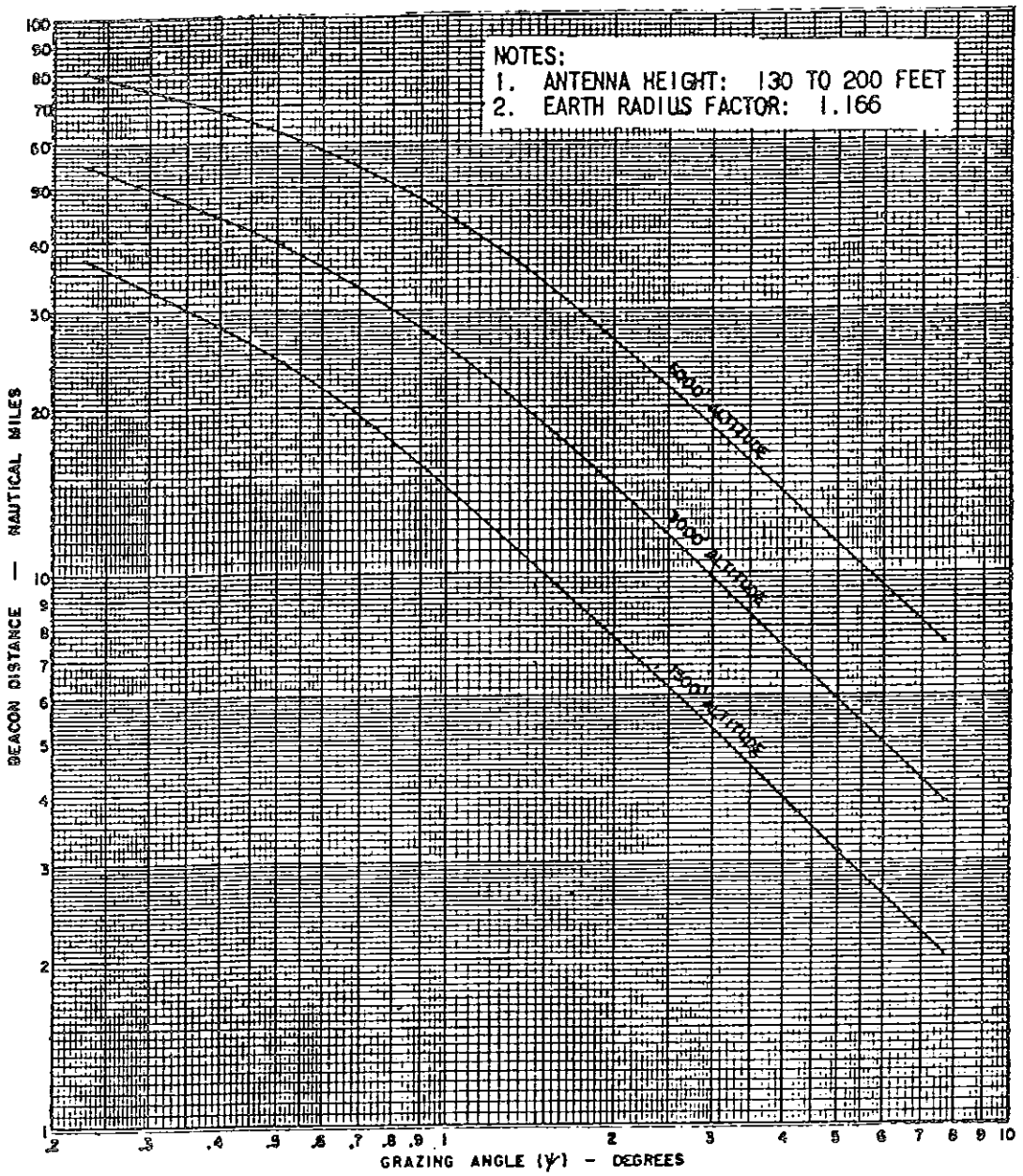

FIGURE 6-50d. BEACON DISTANCE AS A FUNCTION OF GRAZING ANGLE (ANTENNA HEIGHT 130 to 200 FEET, EARTH-RADIUS FACTOR OF 1.166)

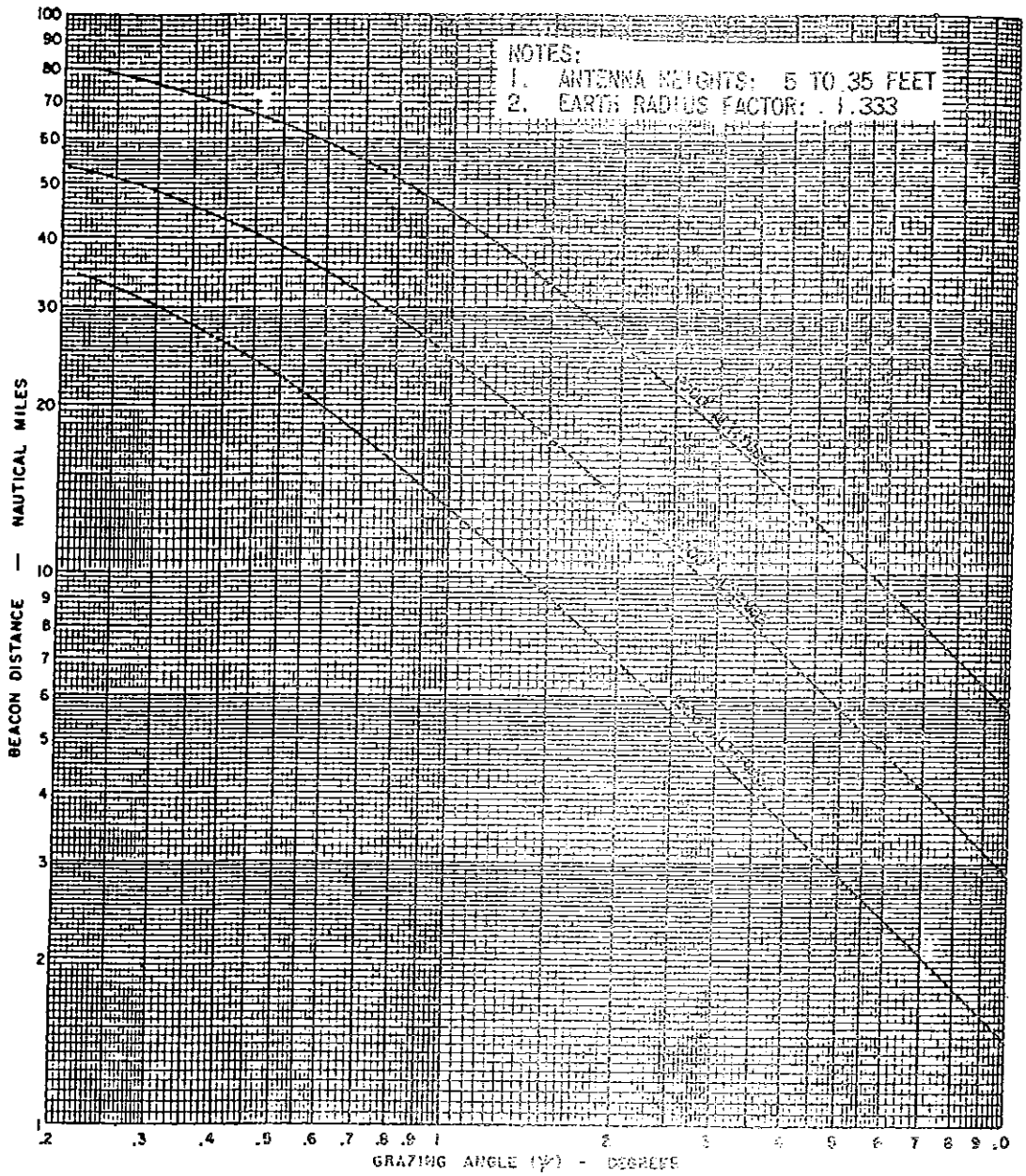

FIGURE 6-51a. BEACON DISTANCE AS A FUNCTION OF GRAZING ANGLE (ANTENNA HEIGHT 5 to 35 FEET, EARTH-RADIUS FACTOR OF 1.333)

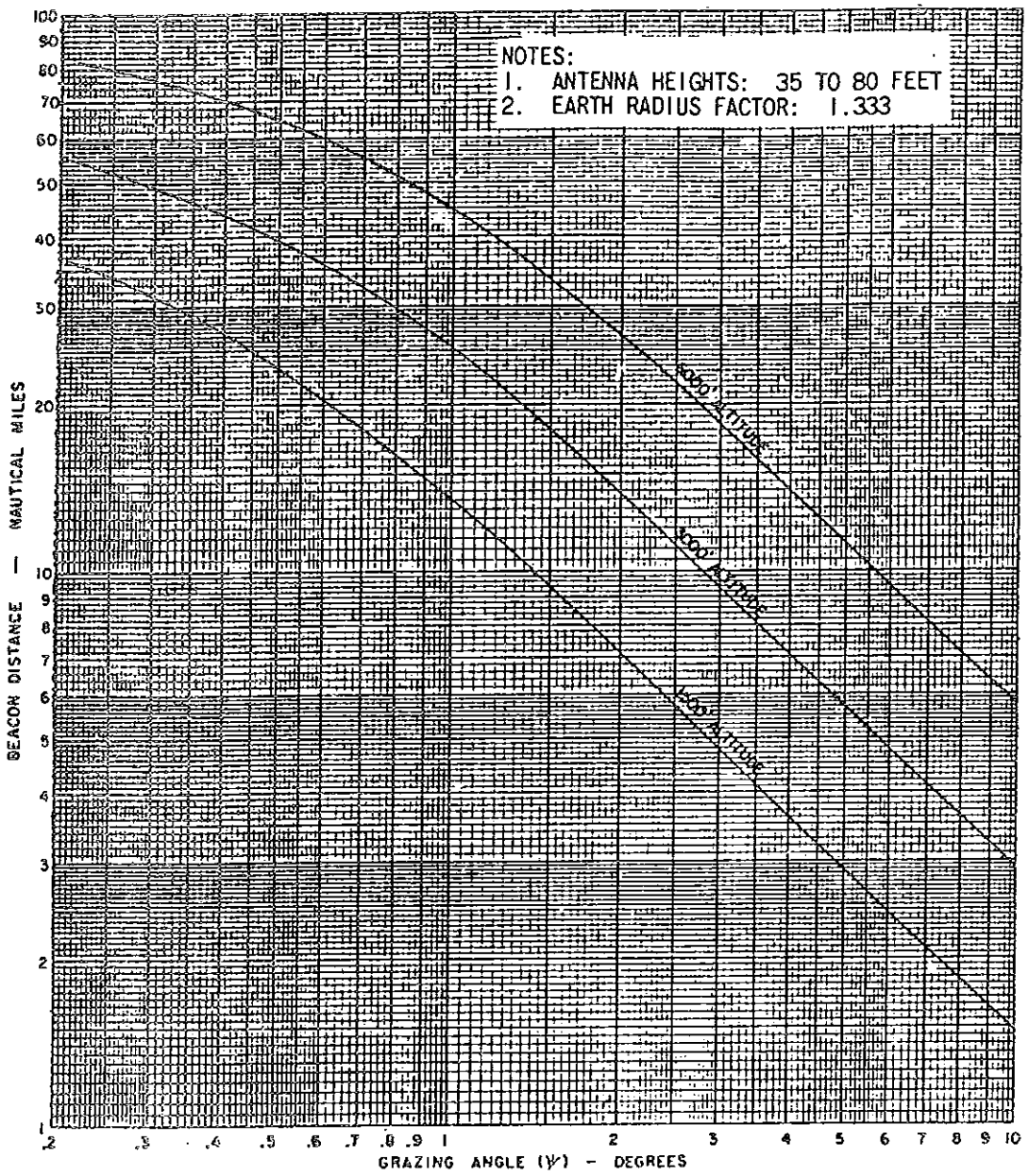

FIGURE 6-51b. BEACON DISTANCE AS A FUNCTION OF GRAZING ANGLE (ANTENNA HEIGHT 35 to 80 FEET, EARTH-RADIUS FACTOR OF 1.333)

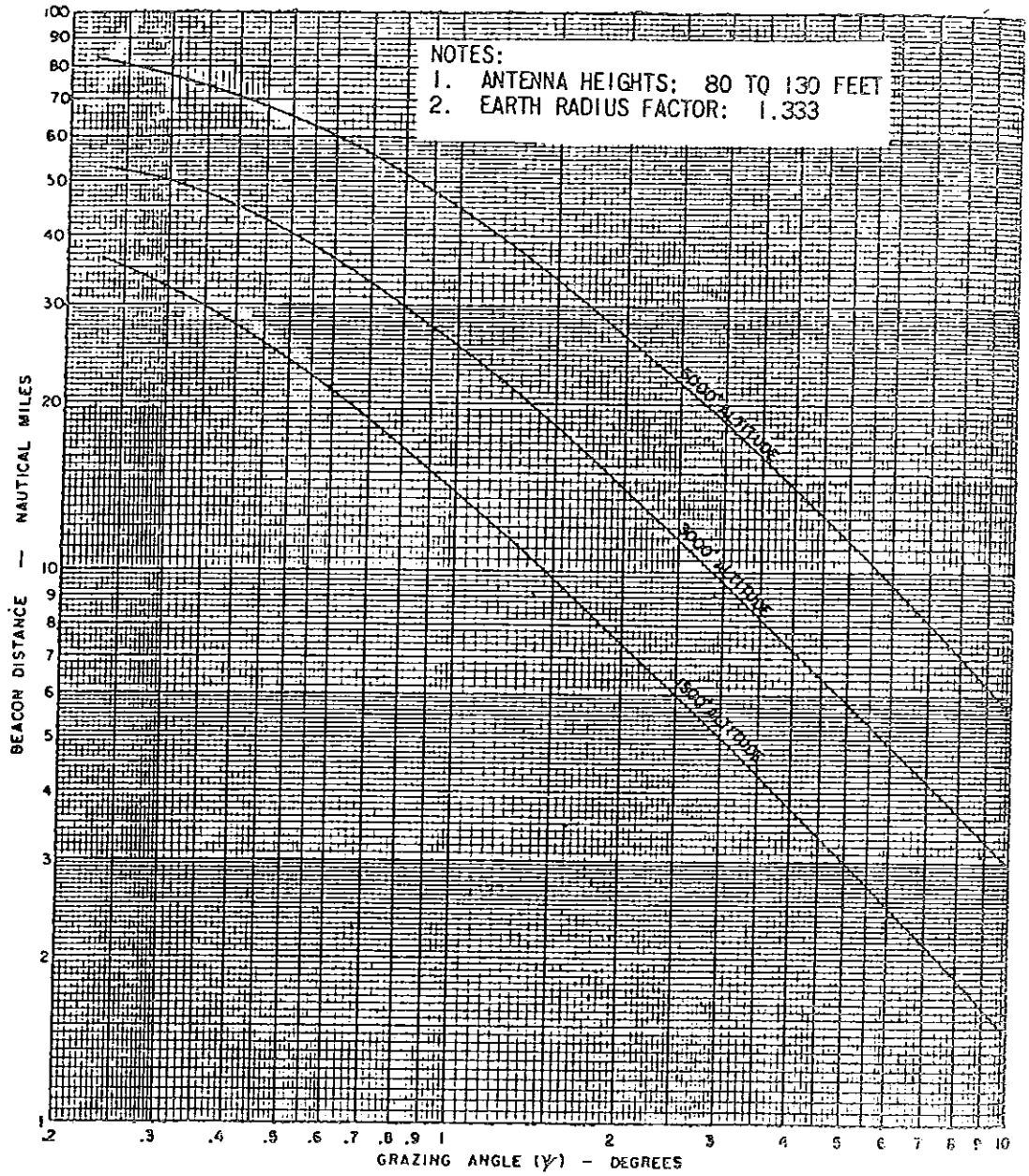

FIGURE 6-51c. BEACON DISTANCE AS A FUNCTION OF GRAZING ANGLE (ANTENNA HEIGHT 80 to 130 FEET, EARTH-RADIUS FACTOR OF 1.333)

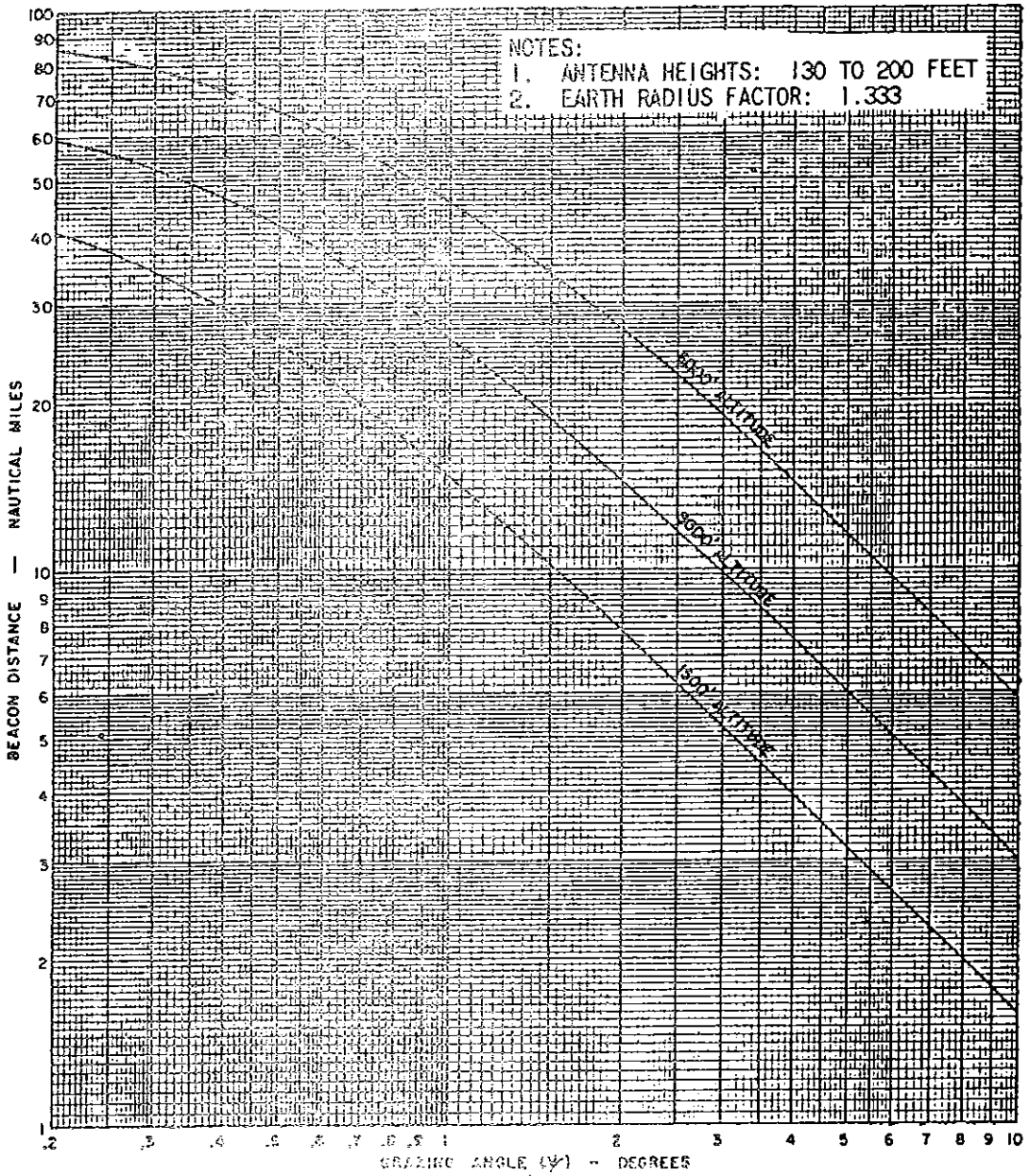

FIGURE 6-51d. BEACON DISTANCE AS A FUNCTION OF GRAZING ANGLE (ANTENNA HEIGHT 130 to 200 FEET, EARTH-RADIUS FACTOR OF 1.333)

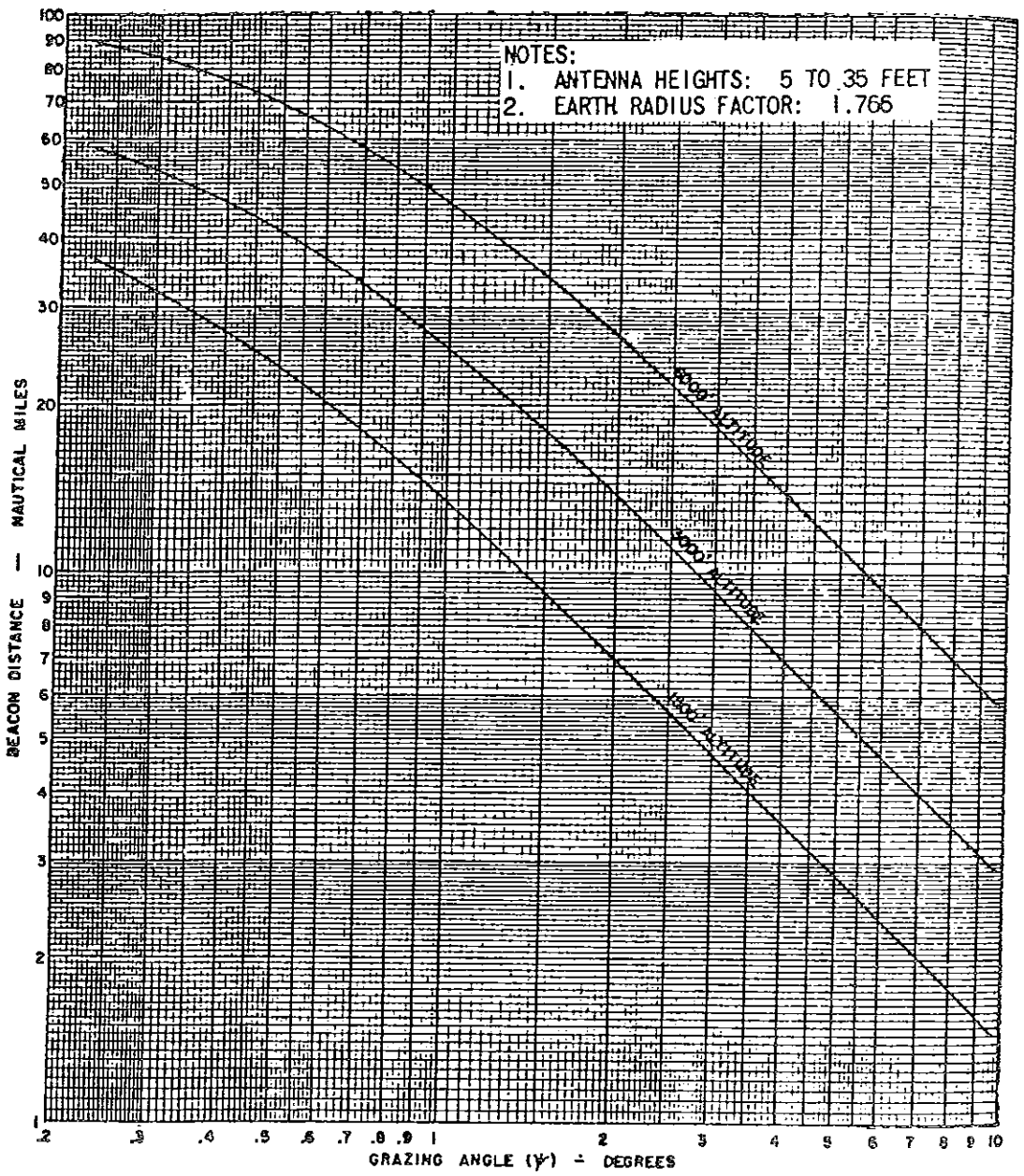

FIGURE 6-52a. BEACON DISTANCE AS A FUNCTION OF GRAZING ANGLE (ANTENNA HEIGHT 5 to 35 FEET, EARTH-RADIUS FACTOR OF 1.766)

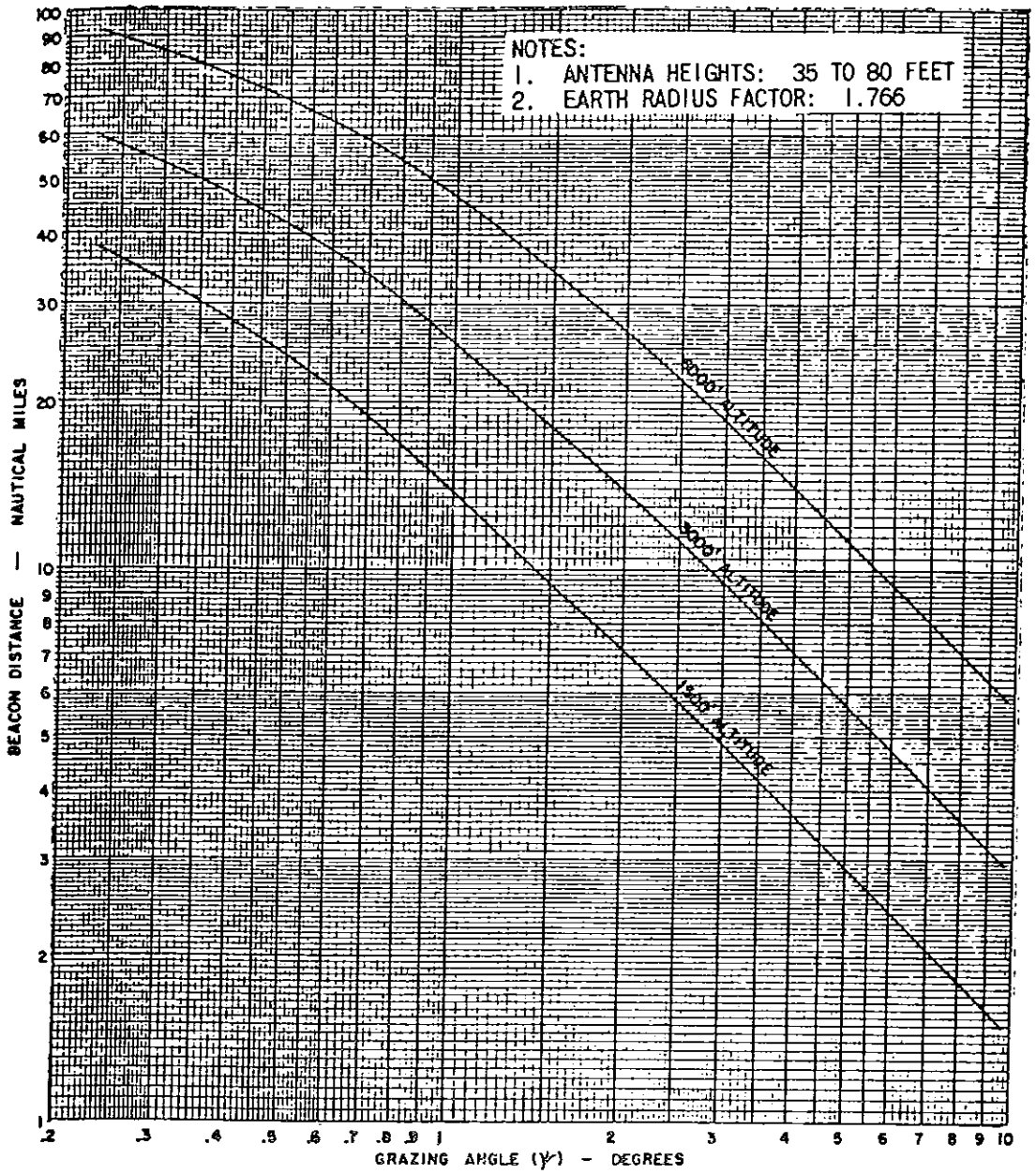

FIGURE 6-52b. BEACON DISTANCE AS A FUNCTION OF GRAZING ANGLE (ANTENNA HEIGHT 35 to 80 FEET, EARTH-RADIUS FACTOR OF 1.766)

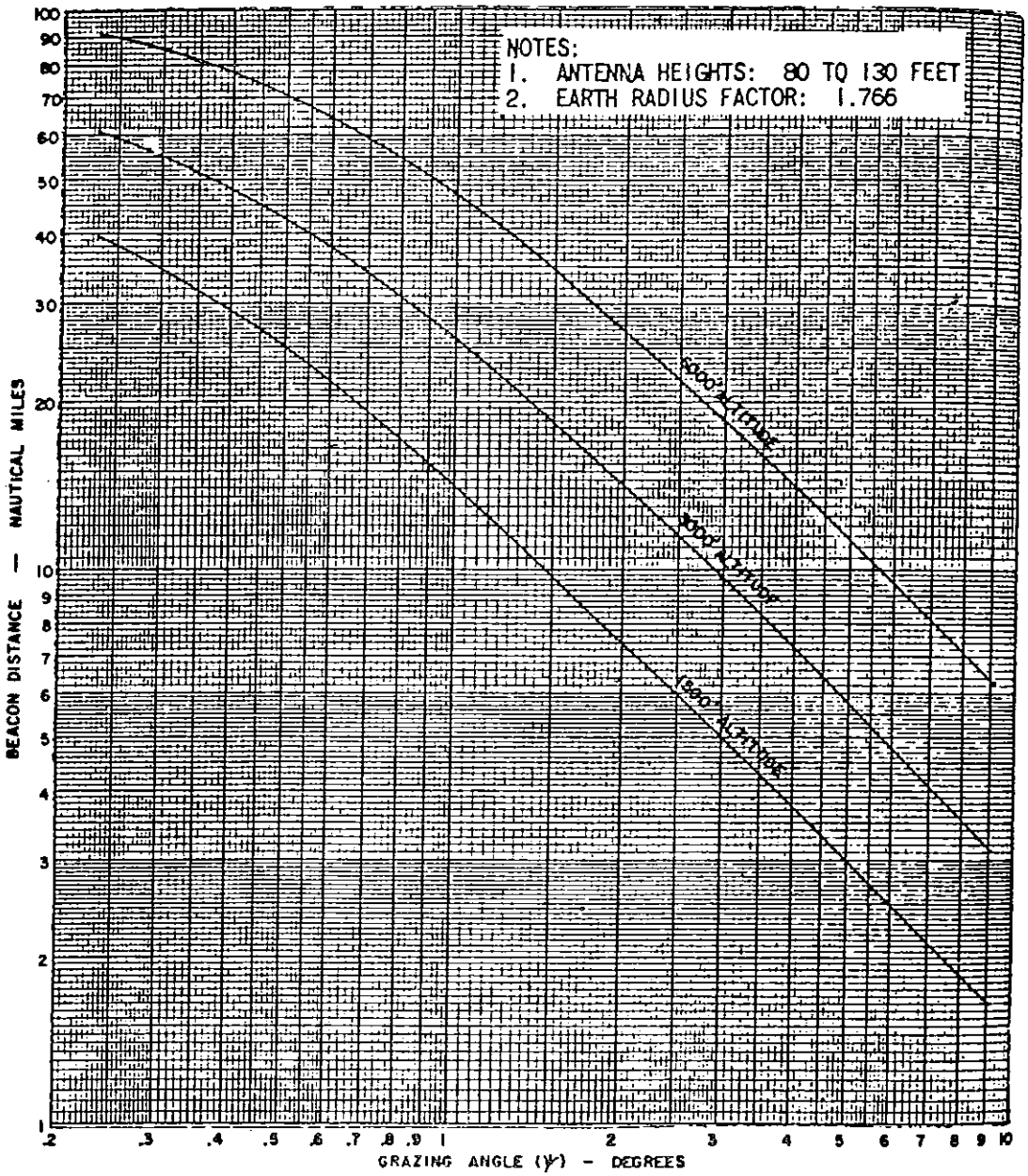

FIGURE 6-52c. BEACON DISTANCE AS A FUNCTION OF GRAZING ANGLE (ANTENNA HEIGHT 80 to 130 FEET, EARTH-RADIUS FACTOR OF 1.766)

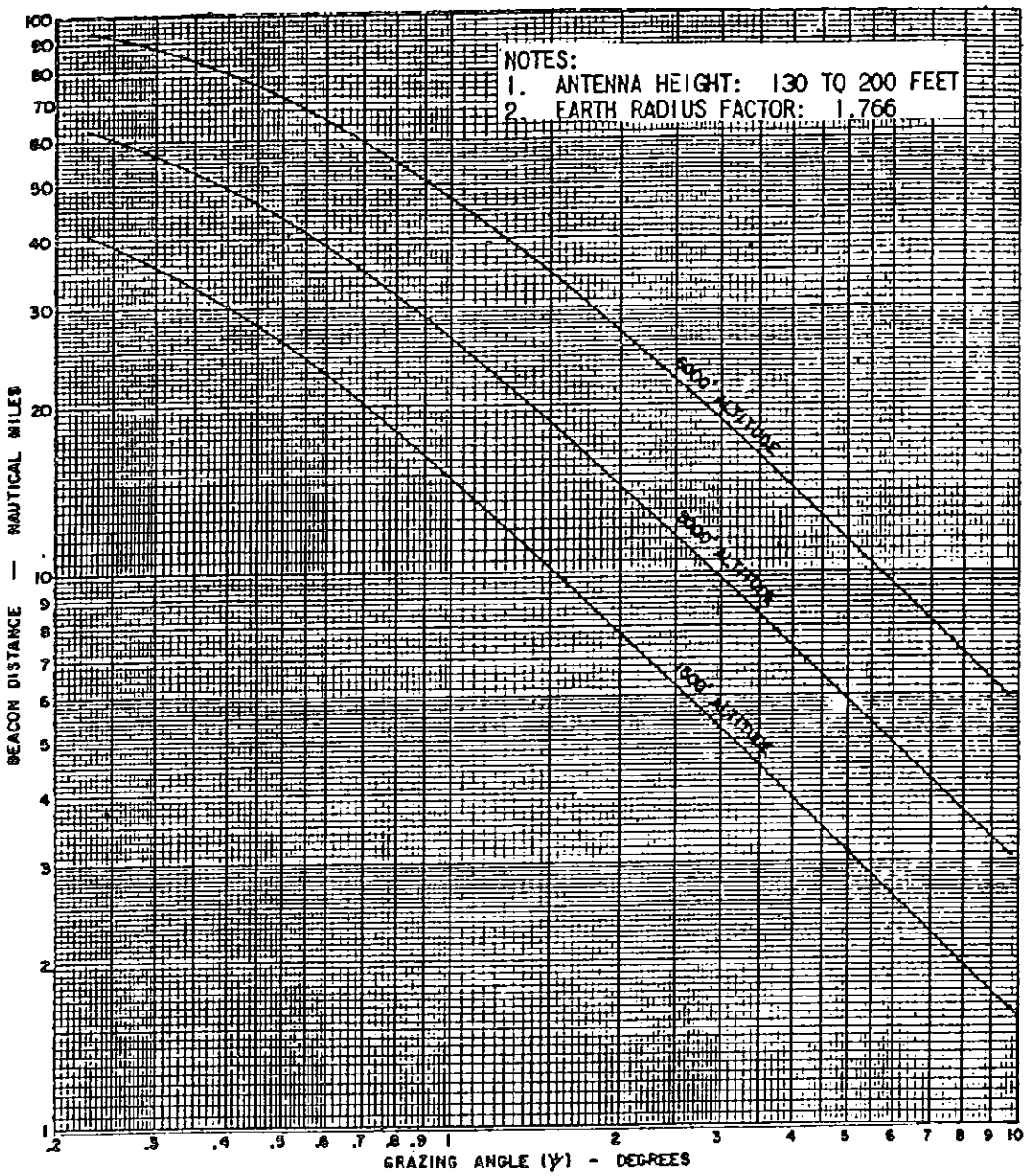

FIGURE 6-52d. BEACON DISTANCE AS A FUNCTION OF GRAZING ANGLE (ANTENNA HEIGHT 130 to 200 FEET, EARTH-RADIUS FACTOR OF 1.766)

CHAPTER 7. CONSIDERATIONS OF LATERAL MULTIPATH

28. GENERAL.

a. Recall the comparison between longitudinal and lateral multipath presented in Section 4. Recall also the overview discussion of lateral multipath presented in Section 6. The material just referenced provides an overview and summary for the subject of lateral multipath.

b. Fundamental to a discussion of reflection and re-radiation is a knowledge of the dimensions required to provide a substantial re-radiated signal. As with longitudinal multipath, the first Fresnel zone is primarily responsible for producing the interfering wave. Figure 7-1 shows the geometry and the equations for calculating the first Fresnel zone size. Figures 7-2, 7-3, and 7-4 provide graphic values of the Fresnel zone dimensions. Interfering wave energy is primarily dependent upon the dimension PD, where P is the point of reflection satisfying the law of reflection; i.e., angle of incidence equals angle of reflection, and D is the forward point at which travel distance from navaid to aircraft is Y/2 longer than along the path involving point P.

c. Distortion of course information due to lateral multipath manifests itself, in the case of VOR, as course scalloping on the aircraft VOR receiver indicator. Course scalloping is a periodic variation of the indicated azimuth about the correct azimuth, where the frequency (or period of oscillation) varies with position in space.

(1) Two terms associated with scalloping are bends and roughness. A bend is a single scalloping cycle, or part thereof, of sufficiently low frequency (a long period in time) to appear as a permanent course displacement on the aircraft receiver indicator. Roughness is a combination of two or more scalloping frequencies originating from separate interfering wave sources. Separating roughness into its individual scalloping frequency components is another complexity in propagation interference analysis.

(2) Course scalloping derives its name from the shape of the curve resulting from a plot (as observed by an airborne receiver) of the magnitude (in degrees) of the deviation of indicated azimuth from true azimuth, as a function of azimuth (in degrees). This curve frequently has a sinusoidal shape, hence the term scalloping. Because of this shape, standard waveform terminology is used in discussing scalloping; i.e., "scalloping amplitude." While the pilot is concerned with the magnitude of his specific course deviation, the ground engineer is concerned with the frequency and amplitude of the scalloping.

d. Re-radiators are divided, for purposes of discussion, into specular and diffuse reflectors. See figure 2-4 for sketches contrasting these types of surfaces. In the material to be presented, specular and directional reflectors will be seen to have the following characteristics with regard to scalloping amplitude.

(1) Scalloping amplitude is a function of the angle of incidence between interfering wave and reflector.

(2) Maximum scalloping amplitude occurs at the angle of incidence approaching 55 degrees.

(3) Half-power scalloping amplitude occurs at angles of incidence of 35 and 73 degrees.

(4) Angles of incidence below 35 and above 73 degrees have relatively small scalloping amplitude compared to the maximum.

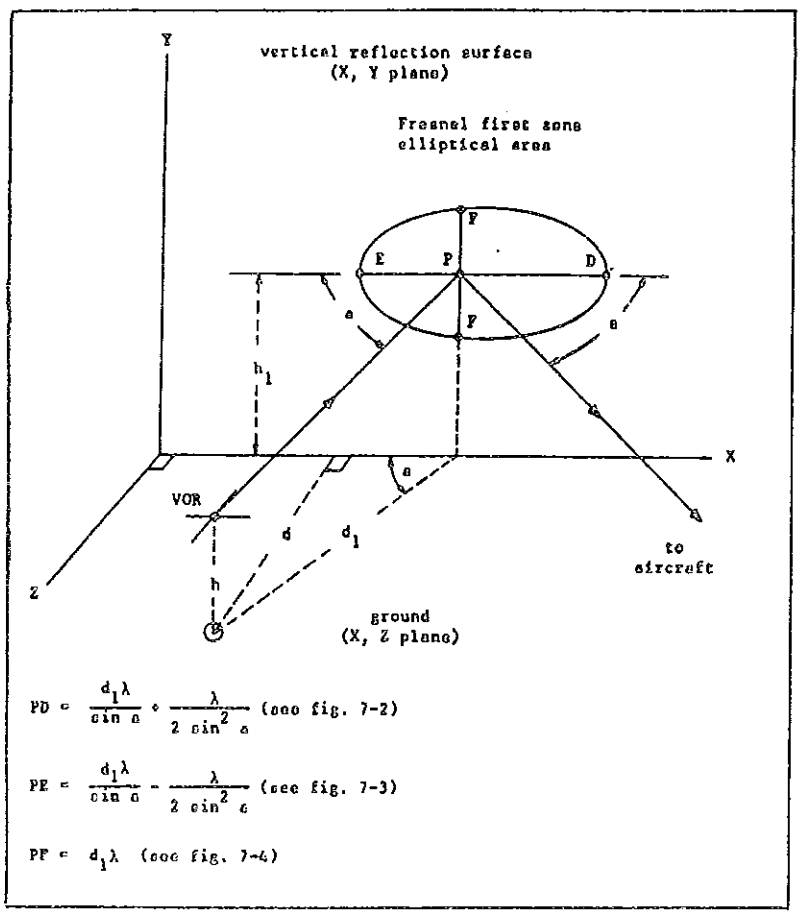

FIGURE 7-1. REFLECTOR SURFACE DIMENSIONS (FRESNEL FIRST ZONE) CONTRIBUTING TO SCALLOPING

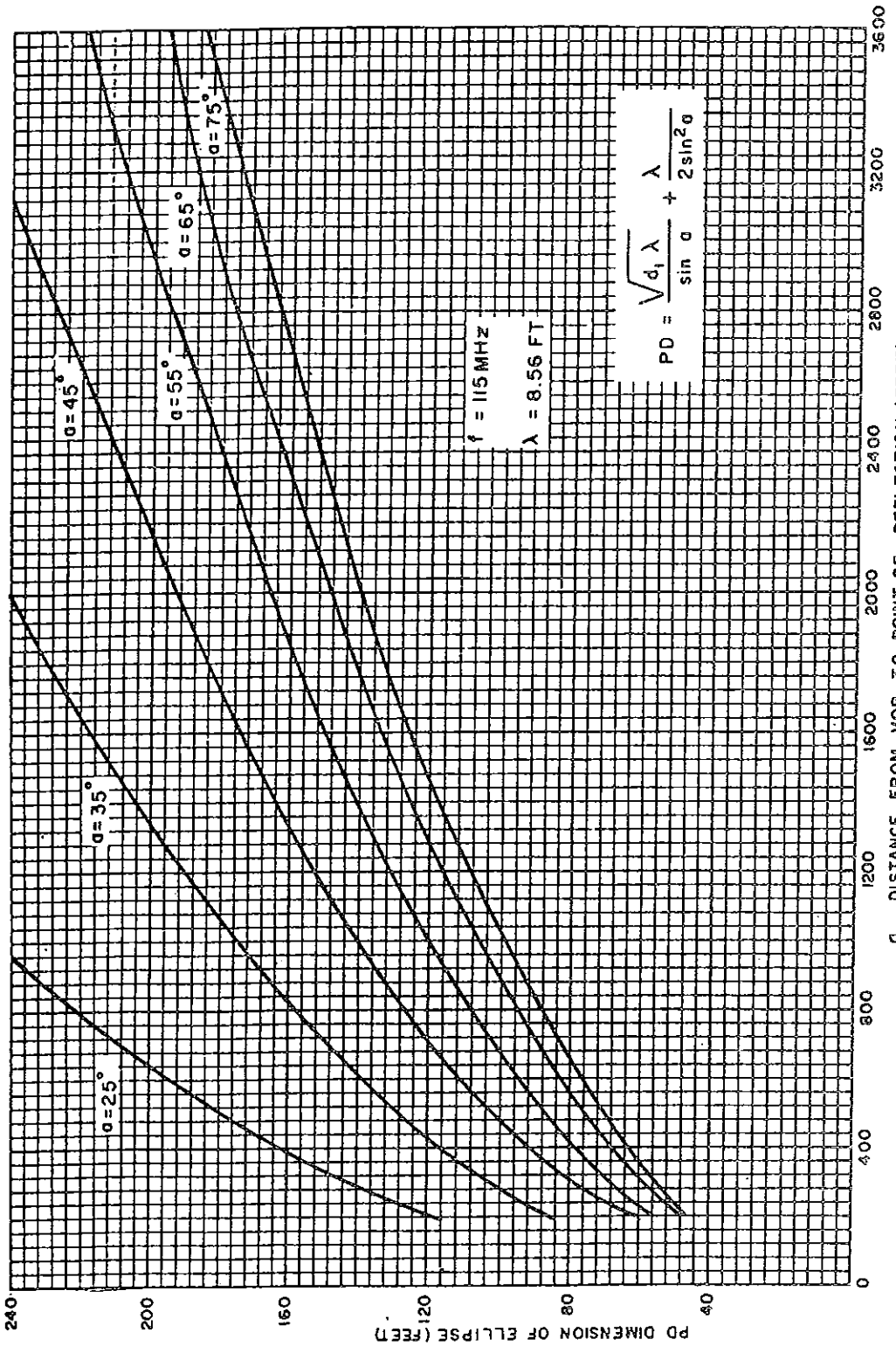

FIGURE 7-2. GRAPHIC VALUES OF PD

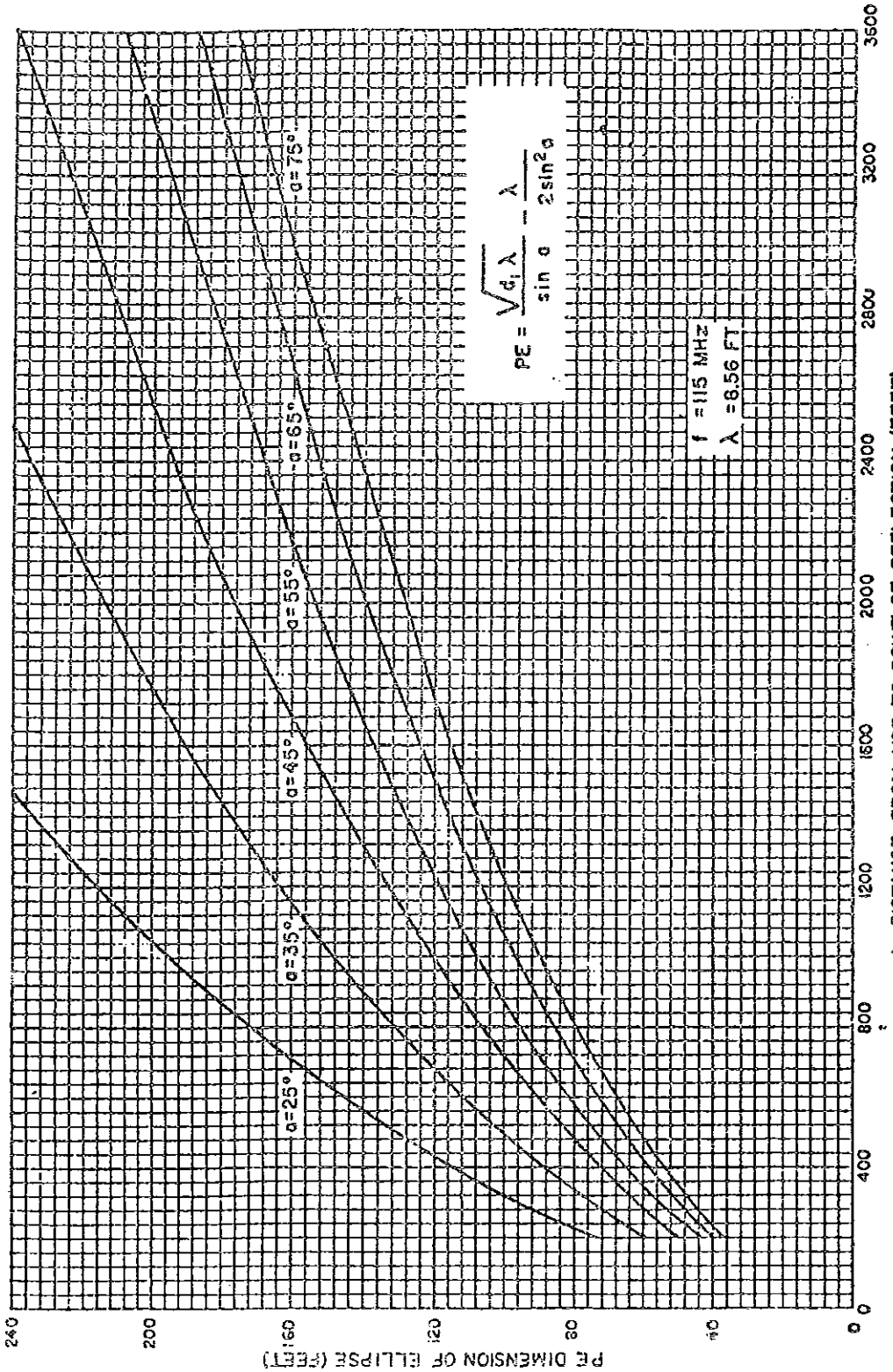

FIGURE 7-3. GRAPHIC VALUES OF PE

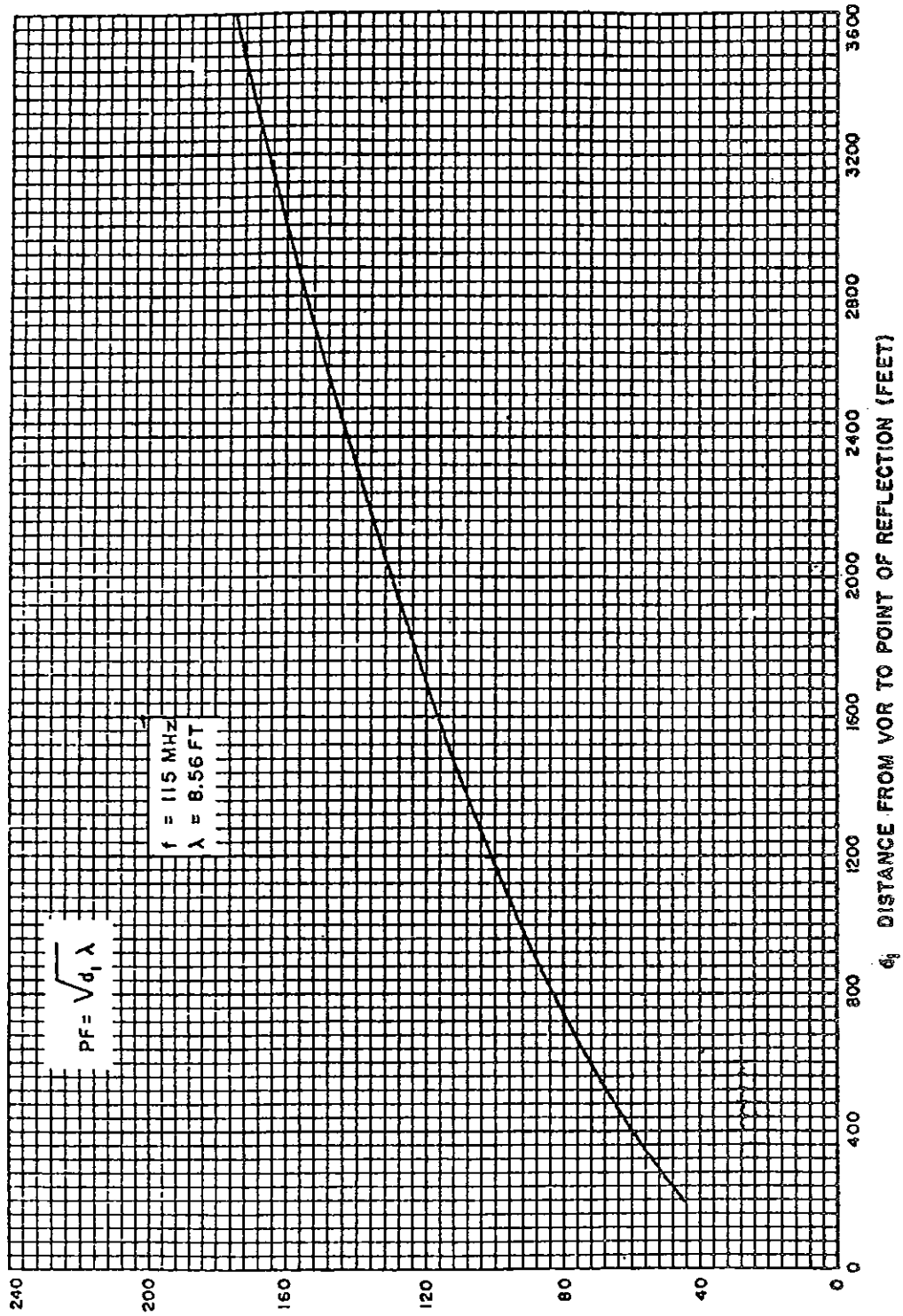

FIGURE 7-4. GRAPHIC VALUES OF PF

(5) Angle of incidence is zero at all points along a reflector in radial alignment with the VOR, thus causing no course scalloping.

(6) Scalloping amplitude is approximately inversely proportional to the square of distances between interfering object and VOR over a large range of distance ratios.

(7) Scalloping amplitude is approximately proportional to the square of heights of interfering objects over a large range of height ratios.

e. Diffuse reflectors have the following characteristics with regard to scalloping amplitudes.

(1) Scalloping amplitude is maximum along a bearing line 90 degrees from the azimuth of the re-radiating object.

(2) Scalloping amplitude decreases in a sinusoidal manner with azimuth displacement from the maximum scalloping bearing line.

(3) Scalloping amplitude approaches zero along the azimuth of the re-radiating object.

(4) Scalloping amplitude is proportional to the ratio of re-radiated signal amplitude to direct signal amplitude at the aircraft receiver.

f. A number of general conclusions with regard to scalloping frequency can be derived from the material to be presented.

(1) When approaching the VOR, the frequency of scalloping is lowest when closest to the re-radiating object.

(2) The frequency of scalloping increases with an increase in distance between the re-radiating object and the VOR.

(3) Scalloping frequency is maximum along a bearing line where:

(a) Angle of reflection ($\theta_o - \theta_1$) equals 90 degrees for a nondirectional re-radiation. Note this is also the angle of maximum scalloping amplitude.

(b) Angle of incidence (a) equals 45 degrees for a directional reflector.

(4) Scalloping frequencies encountered on radial flight are appreciably lower than those on an orbital flight at similar aircraft locations.

g. During radial flight, a zero-frequency scalloping error may be experienced. The magnitude of this error may be determined from a knowledge of scalloping amplitude at other frequencies and the VOR receiver scalloping frequency response curve.

29. AMPLITUDE OF COURSE SCALLOPING

a. General. The amplitude of course scalloping is measured in degrees and, for obvious practical reasons, it is desirable to know this amplitude as presented to the pilot in his Course Deviation Indicator. Re-radiating surfaces have already been discussed as specular and diffuse reflectors (see figure 2-4). In connection with lateral multipath and course scalloping, we use different but related terms for re-radiating surfaces and speak of directional and diffuse re-radiators. Directional radiators include all re-radiators which re-radiate the infringing EM energy in a preferred direction. These include smooth surfaces which support specular reflection, wires and fences which radiate directionally because of resonance effects, and groupings of objects such as trees or wires which radiate directionally because of the interferometer effect. Note that a surface may be smooth for one angle of ray arrival and rough for another angle. Additionally, a surface may be rough for DME and VORTAC frequencies and smooth at the lower frequency of VOR. See figure 2-6 for a summary of the roughness criterion. The interferometer or periodicity effect is presented in figure 2-5.

b. Scalloping Amplitude Due to Directional Radiators.

(1) The equation for amplitude of scalloping is given below. It applies to both short and long directional reflectors. The geometries are illustrated in figures 7-5 and 7-6.

$$S = \pm \arctan \left[\sqrt{2}\ A \sin a \sin 2a\right] \quad \text{(degrees)}$$

Where A = Amplitude of Er/Amplitude of Ed. Figure 7-7 is a plot of this equation for a single value of A.

(2) For short-length reflectors, the spread of azimuths which are susceptible to scalloping will be small. Short is defined as involving a small spread of azimuth coverage as seen from the VOR site. See figure 7-8.

(3) For long reflectors, the ratio of scalloping at any angle compared to that at the angle of maximum scalloping is shown graphically in figure 7-9 for a particular value of A, and is described analytically in the following equation.

$$\frac{S_o}{S_{MAX}} = \frac{\pm \arctan \left[\sqrt{2}\ A \sin \Theta_o \sin 2\ \Theta_o\right]}{\pm \arctan \left[\sqrt{2}\ A \sin \Theta_{o_{MAX}} \sin 2\ \Theta_{MAX}\right]}$$

Note that figure 7-9 may be used to illustrate the scalloping of a long reflector regardless of its orientation to the VOR site. Simply make the appropriate azimuthal correction for the direction of the bearing normal to the reflector and apply that correction to the azimuthal indications on figure 7-9.

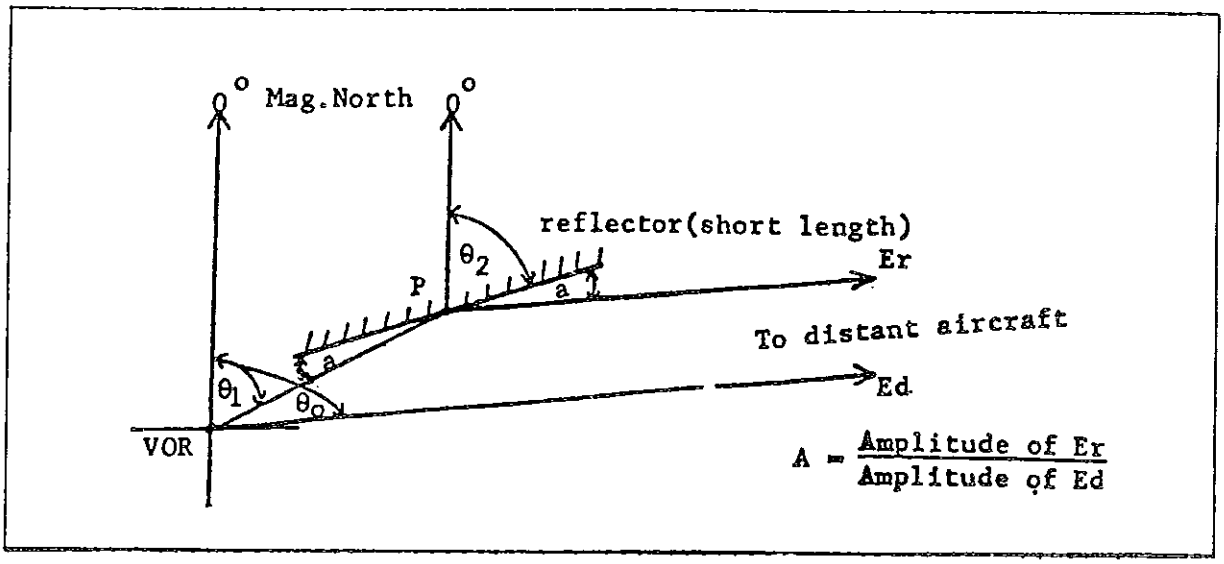

FIGURE 7-5. DIRECTIONAL REFLECTOR (SHORT LENGTH)

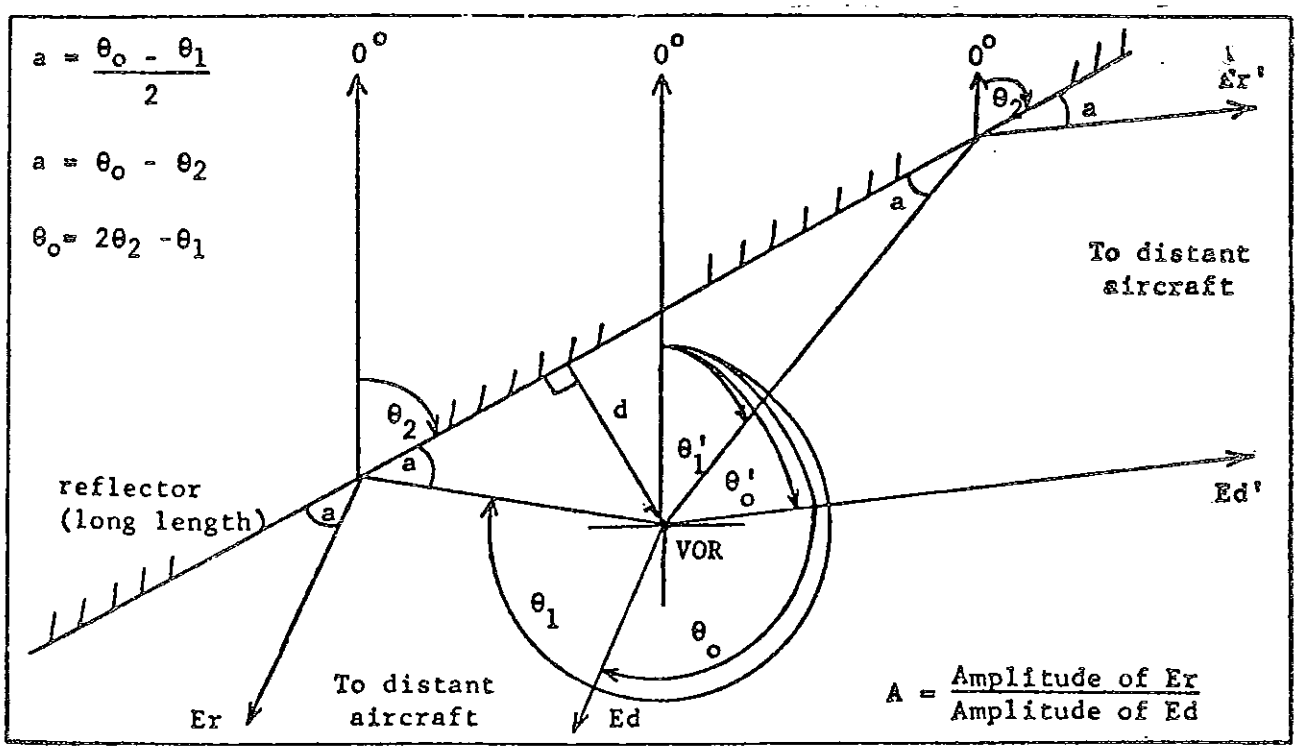

FIGURE 7-6. DIRECTIONAL REFLECTOR (LONG LENGTH)

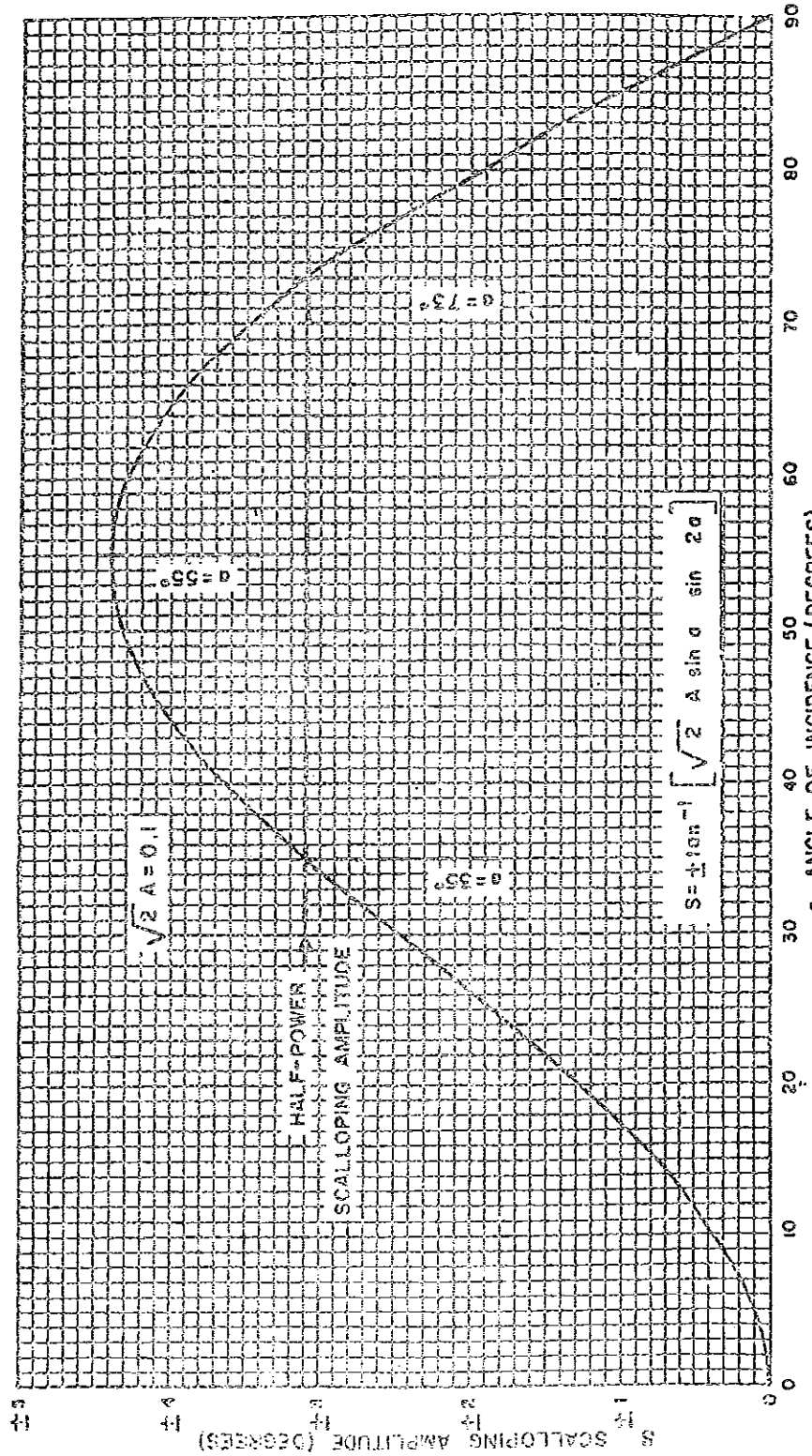

FIGURE 7-7. SCALLOPING AMPLITUDE VERSUS ANGLE OF INCIDENCE

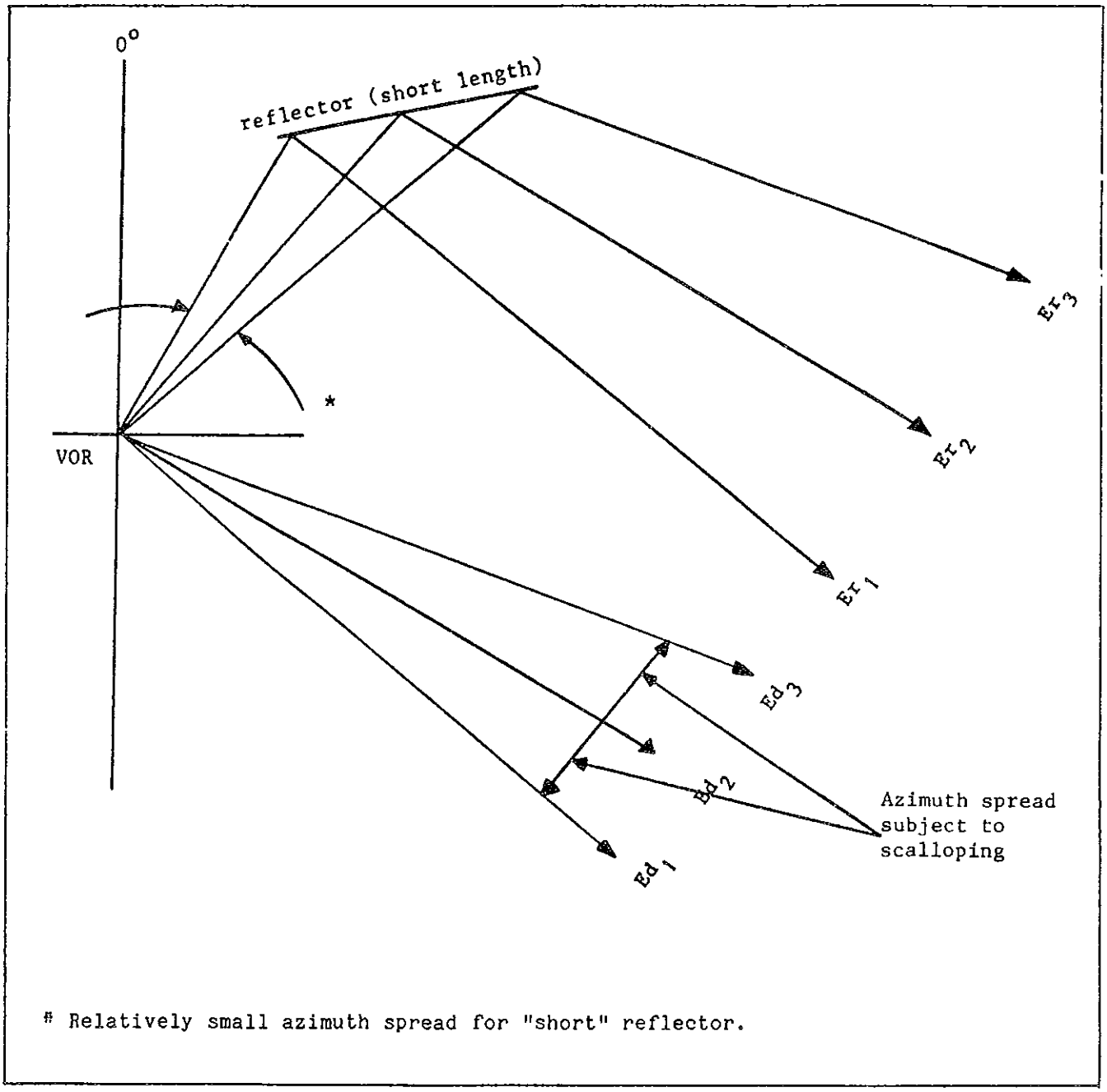

Relatively small azimuth spread for "short" reflector.

FIGURE 7-8. SPREAD OF COURSE SCALLOPING AMPLITUDE

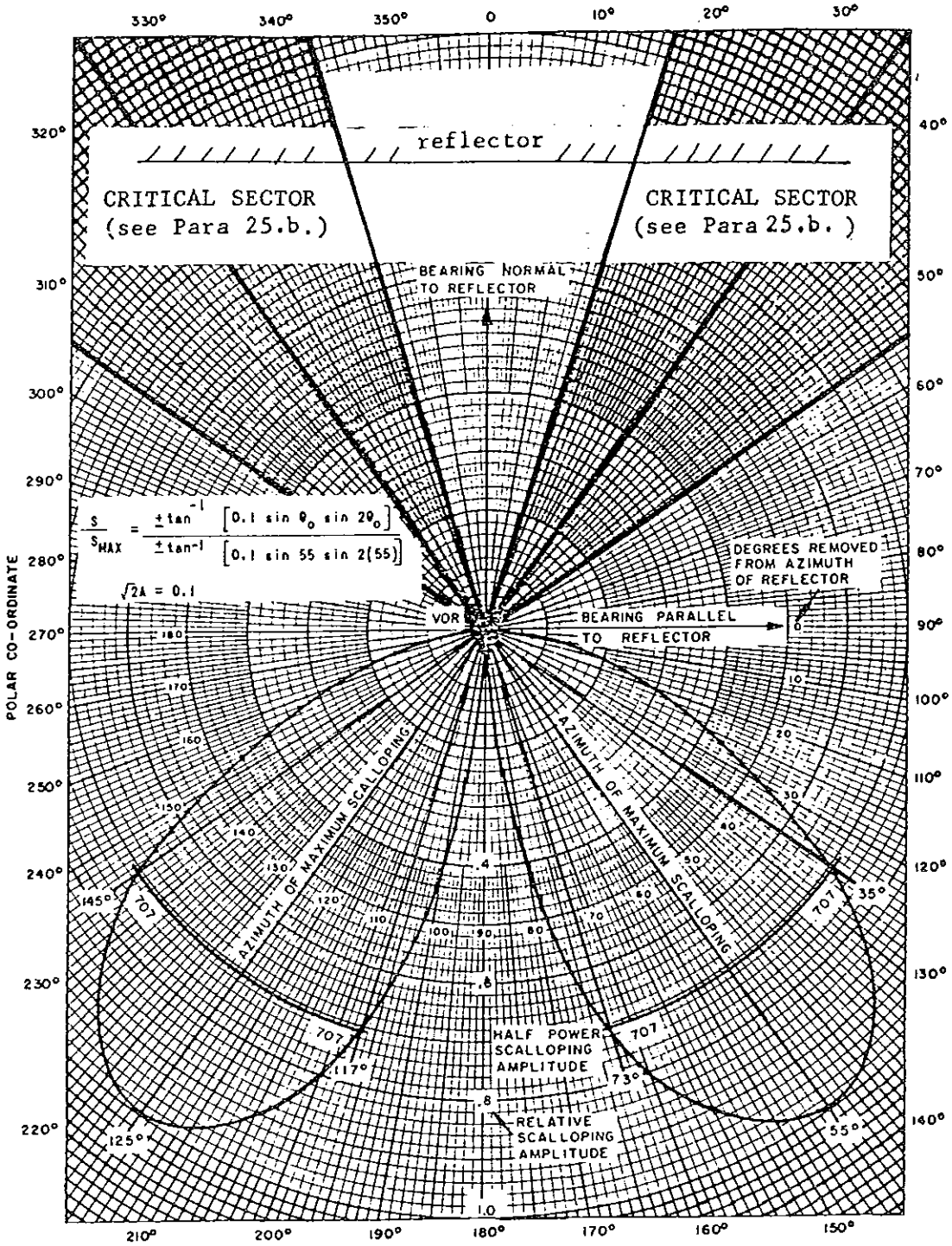

FIGURE 7-9. RELATIVE SCALLOPING AMPLITUDE DUE TO LONG REFLECTORS

c. Diffuse Radiators. Figure 7-10 is a graphic presentation of the amplitude of scalloping for the angular parameters defined in figure 7-11. The analytic relationship is described by the equation below.

$$S = \pm \arctan \left[A \sin (\theta_0 - \theta_1) \right] \text{ (degrees)}$$

where

A = Amplitude of Er/Amplitude of Ed

d. Effect of Geometry on Scalloping Amplitude.

(1) The amount of signal re-radiated from the interfering object is a function of the location of the object with respect to the VOR/VORTAC site. This signal magnitude in turn determines the parameter A which appears in the expressions for scalloping for both directional and diffuse reflectors. It is difficult to determine A in absolute terms, but it is easier and useful to determine A in relative terms for variations in the geometry. Using the parameters defined in figure 7-12, the scalloping amplitude in terms of an undetermined constant can be expressed as shown in the equation associated with that figure. Figures 7-13, 7-14, and 7-15 present graphically the variation in scalloping amplitude as the parameters of the geometry are varied.

(2) The equation presented in figure 7-12 can be used to predict scalloping amplitude under one set of conditions when the amplitude is known for another set of conditions. For example, if scalloping amplitude S (in degrees) is known for d_1, then the amplitude S' for the changed distance d_1' is presented graphically in figure 7-16 and is expressed analytically as shown in the equation included with the figure. Similarly, if a change of height only is involved, the new scalloping amplitude can be determined as shown graphically and in analytic form in figure 7-17.

(3) Additionally and within certain limits, an approximate relationship may be used for changes in both height and distance.

$$S' \simeq S \left[\frac{d_1 h_1'}{d_1' h_1} \right]^2 \text{ (degrees)}$$

when $\frac{h_1}{d_1}$ and $\frac{h_1'}{d_1'}$ are less than 0.1

$\frac{h\, h_1}{d_1}$ and $\frac{h\, h_1'}{d_1'}$ are less than 1.0 foot

(4) In application of these equations and graphs, height of interfering objects is taken as the uppermost portion of the object such as the top of a fence or the peak of a tower. In considering distance changes with directional reflectors, the angle of incidence of the interfering wave is assumed to remain constant. Where this condition does not prevail, an additional factor can be applied in accordance with the basic equation presented in figure 7-12.

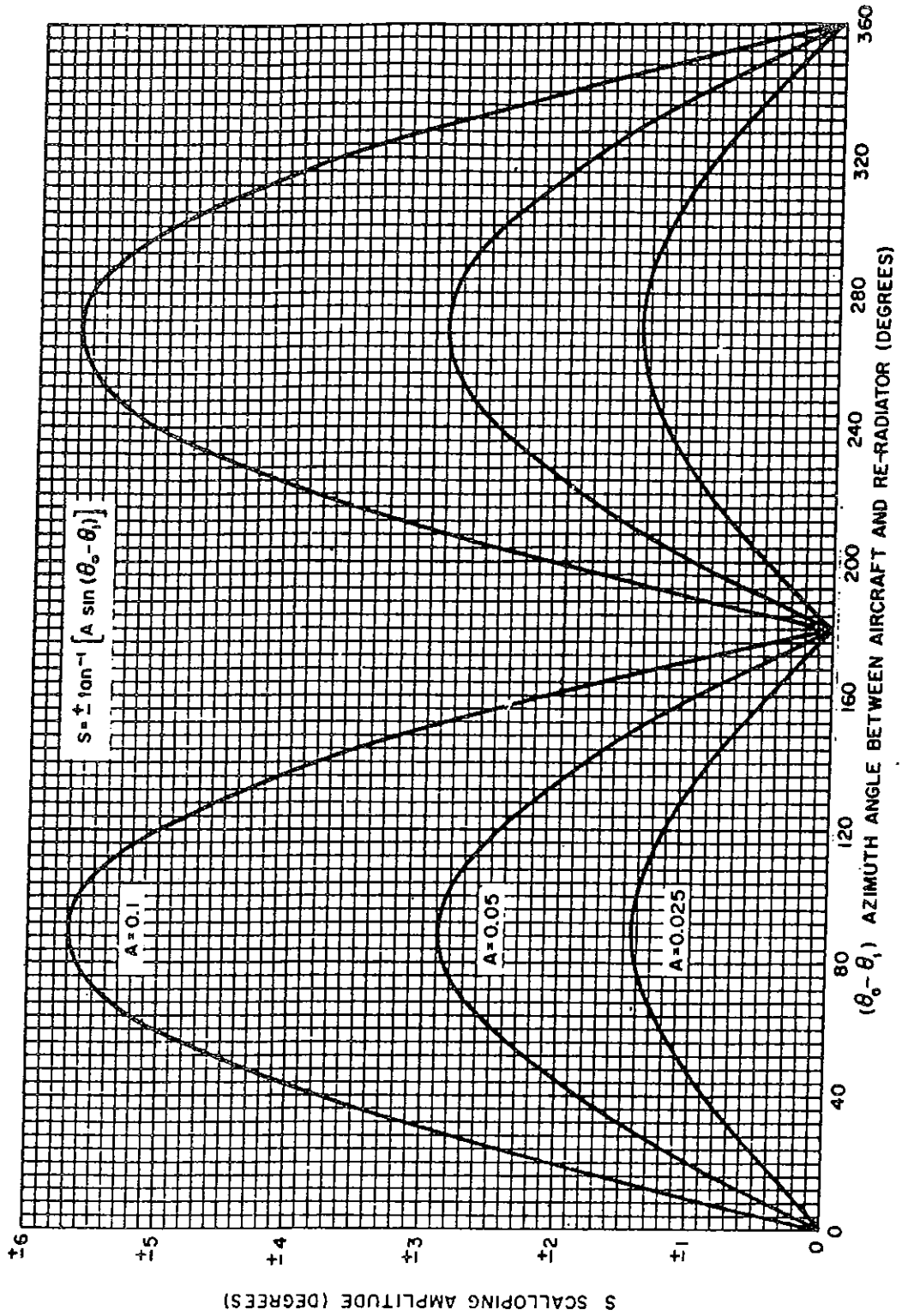

FIGURE 7-10. SCALLOPING AMPLITUDE VERSUS AZIMUTH ANGLE BETWEEN AIRCRAFT AND RE-RADIATOR

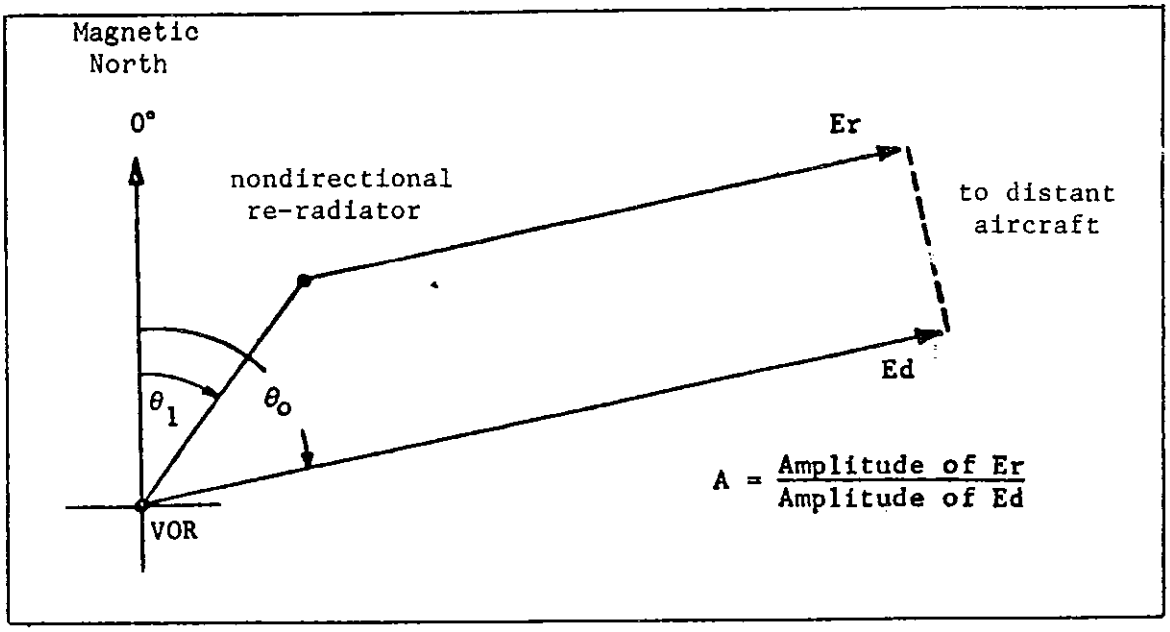

FIGURE 7-11. NONDIRECTIONAL RE-RADIATOR

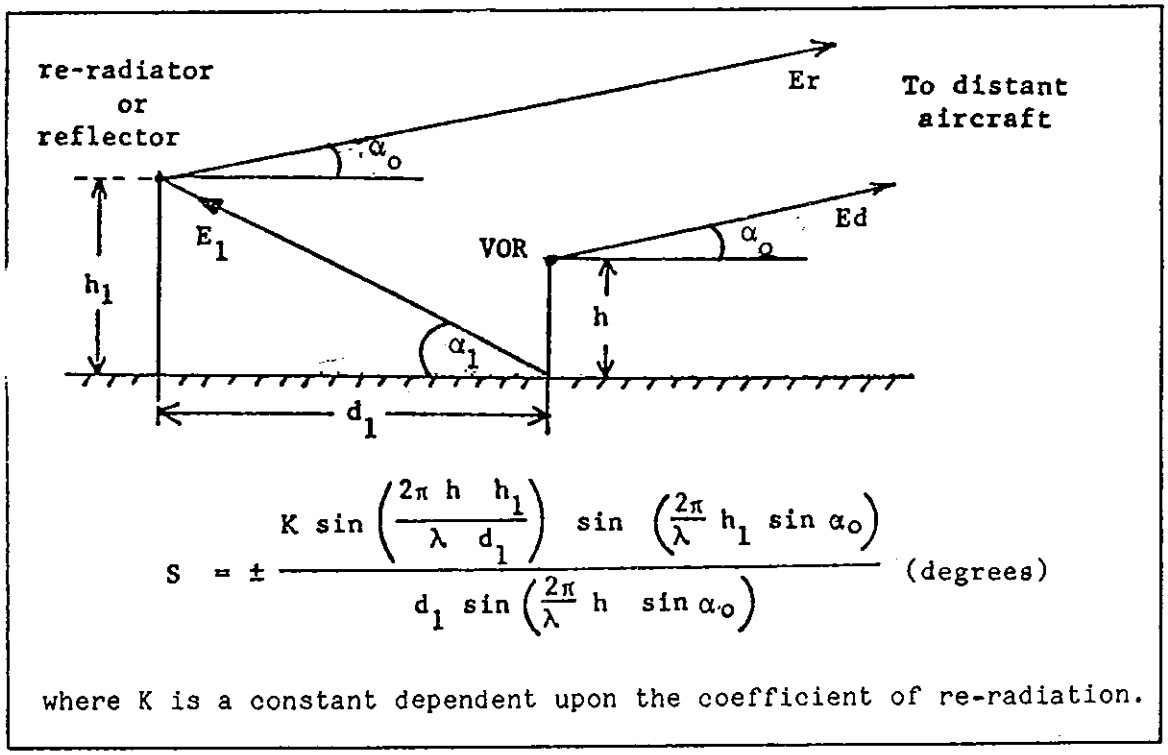

FIGURE 7-12. SCALLOPING AS A FUNCTION OF GEOMETRY

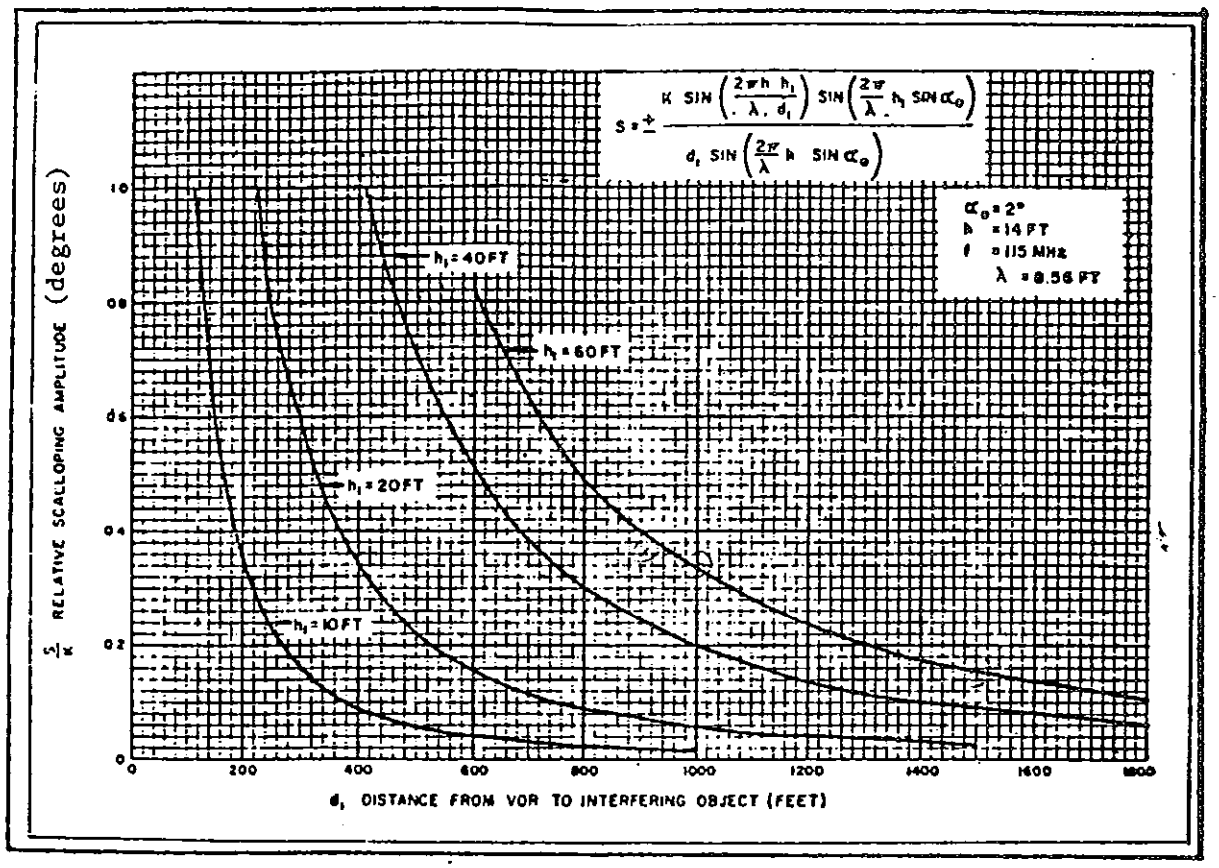

FIGURE 7-13. RELATIVE SCALLOPING AMPLITUDE VERSUS HEIGHT AND DISTANCE OF INTERFERING OBJECT

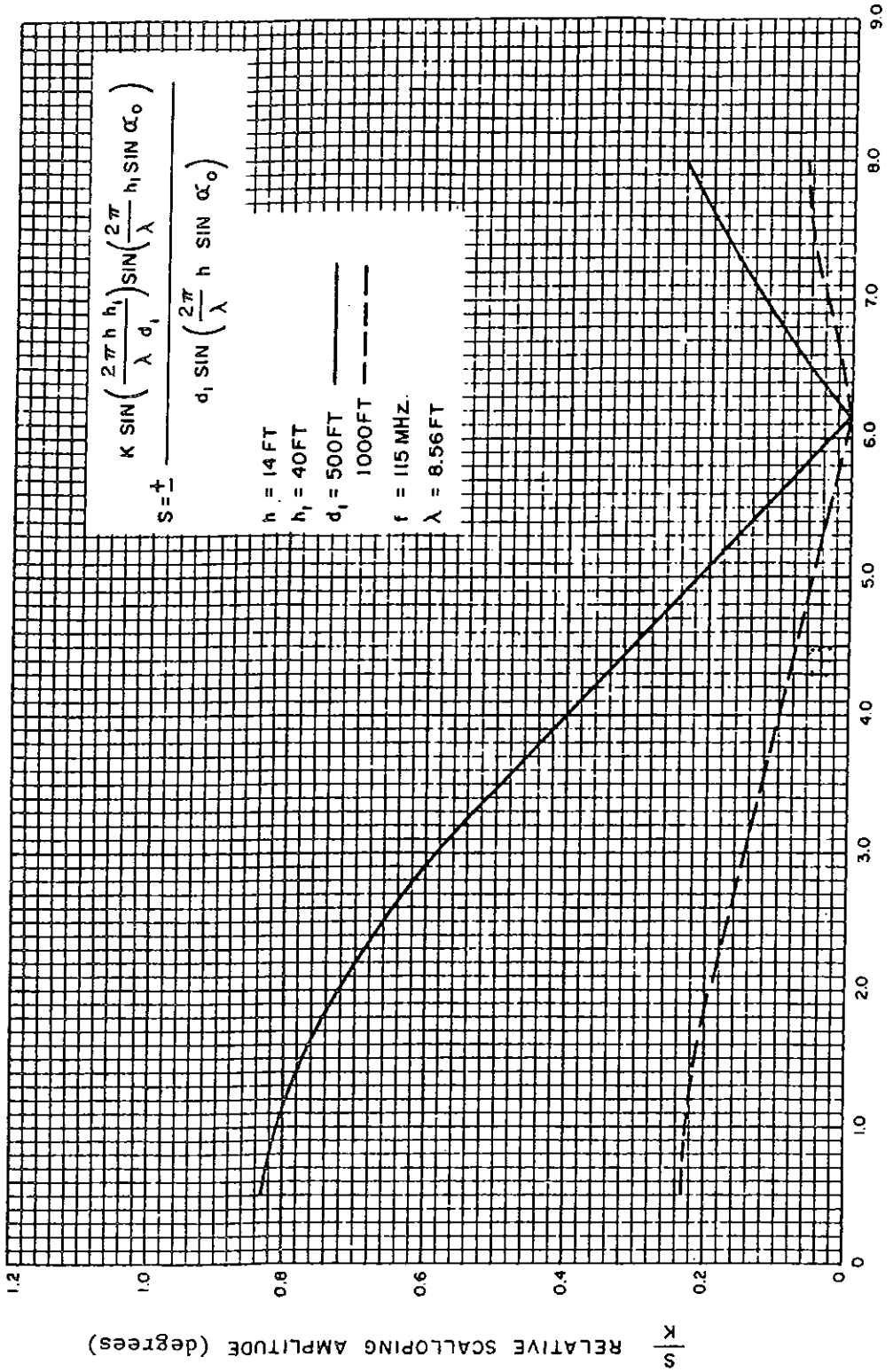

FIGURE 7-14. RELATIVE SCALLOPING AMPLITUDE VERSUS AIRCRAFT ELEVATION ANGLE

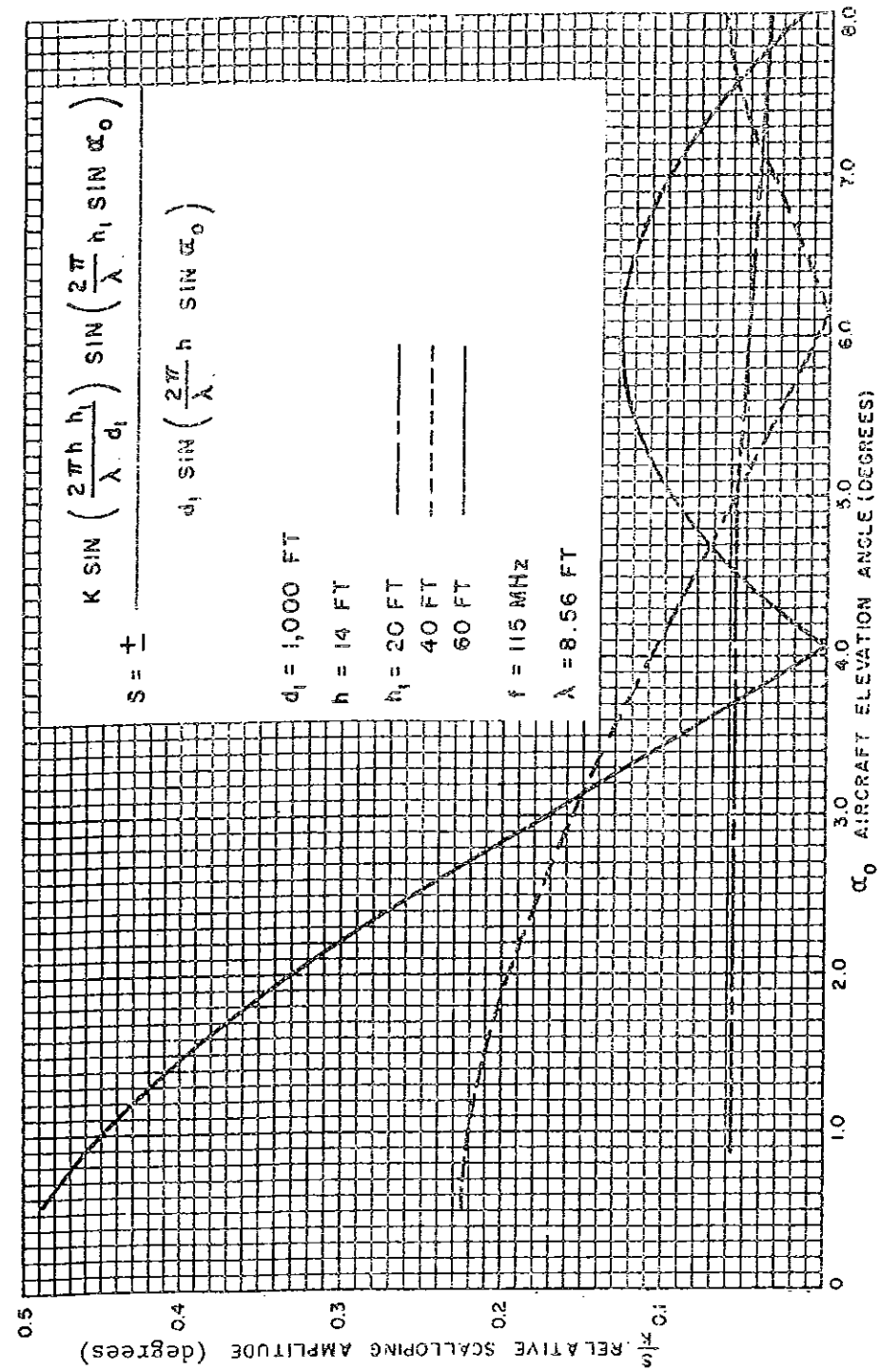

FIGURE 7-15. RELATIVE SCALLOPING AMPLITUDE VERSUS AIRCRAFT ELEVATION ANGLE AND HEIGHT OF INTERFERING OBJECT

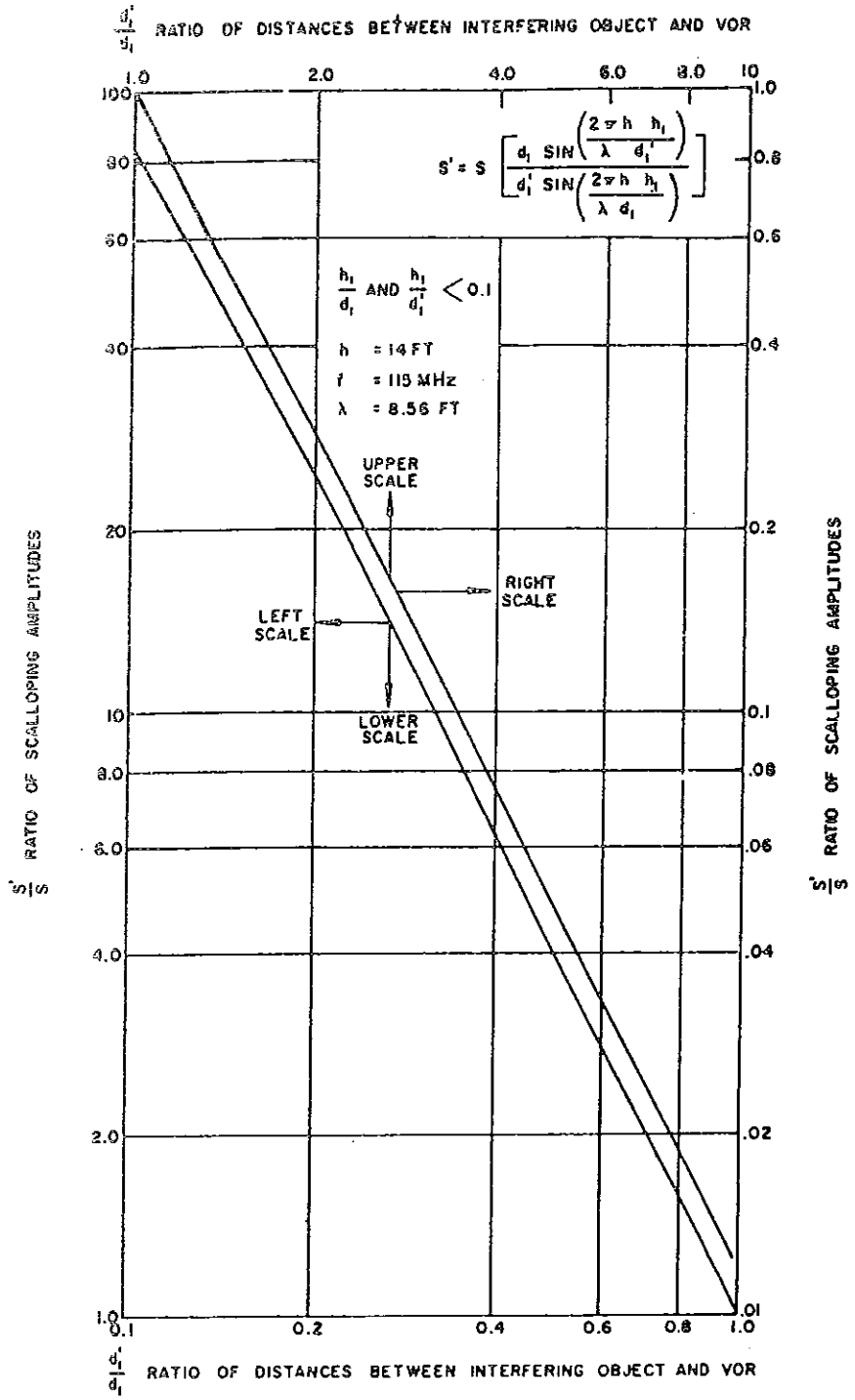

FIGURE 7-16. RELATIONSHIPS BETWEEN DISTANCES AND SCALLOPING AMPLITUDE

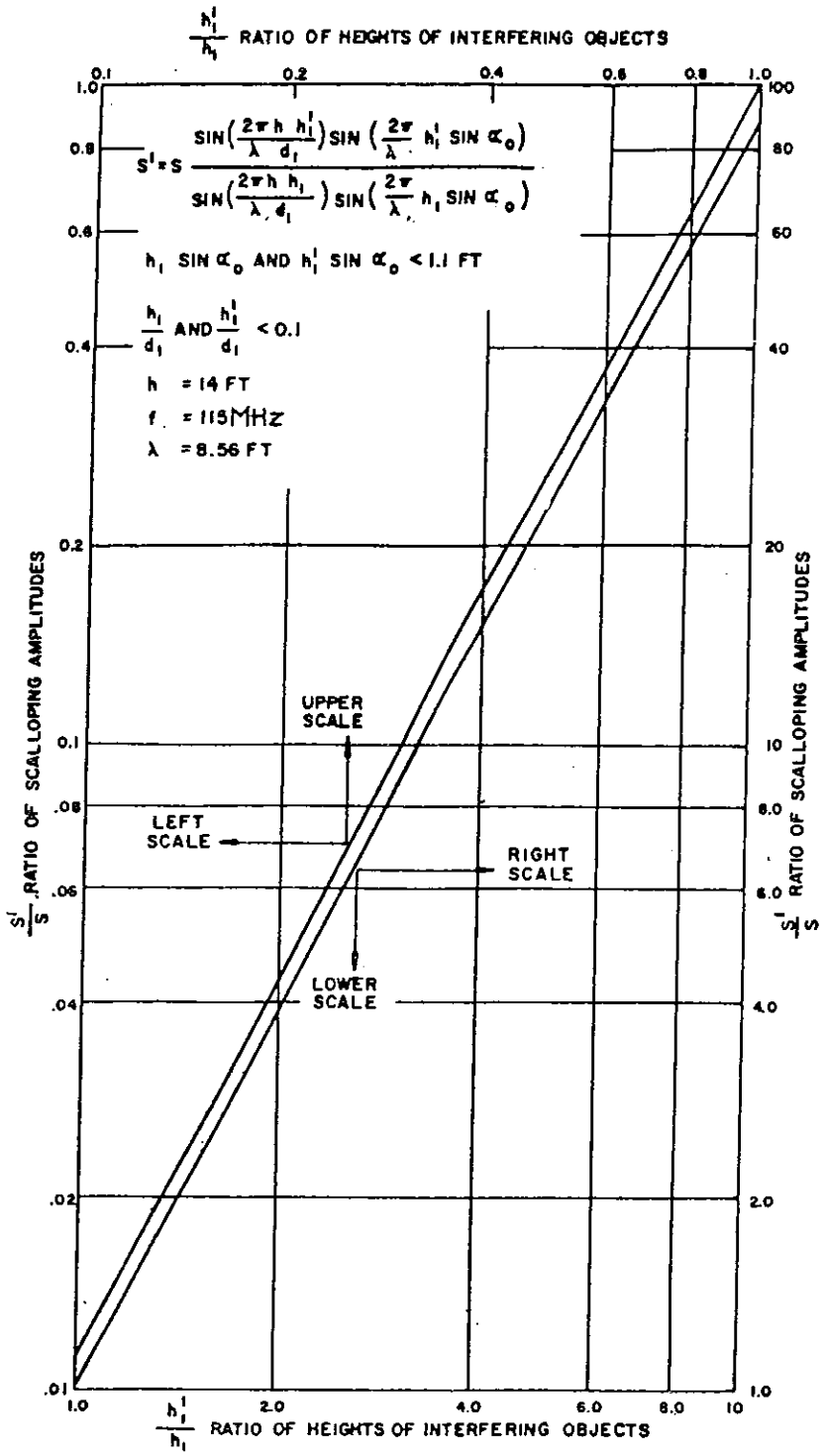

FIGURE 7-17. RELATIONSHIPS BETWEEN INTERFERING OBJECTS HEIGHTS AND SCALLOPING AMPLITUDE

30. FREQUENCY OF COURSE SCALLOPING.

a. General. Scalloping frequency for an aircraft in orbital flight and for an aircraft in radial flight are treated separately in the material which follows. In both discussions it is assumed that the aircraft travels at a constant speed of 140 knots. As already mentioned, the VOR scalloping amplitude presented to the pilot is a function of the scalloping frequency response of the VOR receiver. An illustrative example is developed after the discussion of scalloping frequency to show how to convert scalloping amplitudes at one frequency to another frequency, taking the receiver response into account.

b. Scalloping Frequency - Orbital Flight.

(1) The geometry for a nondirectional re-radiator causing scalloping is shown in figure 7-18, where the analytic expression for f_s, the scalloping frequency, is also presented. By inspection, the scalloping frequency is a maximum when the angle $(\theta_o-\theta_1)$ is 90 degrees or 270 degrees. The analytic expression can be written for a special case as follows:

$$f_s = \frac{27.55 \sin (\theta_o-\theta_1)}{r_o/d_1}$$

where

Va = 140 knots = 140(1.688) ft/sec = 236 ft/sec

λ(115 MHz) = 984/115 = 8.56 ft

N = 236/8.56 = 27.55 wavelengths per sec

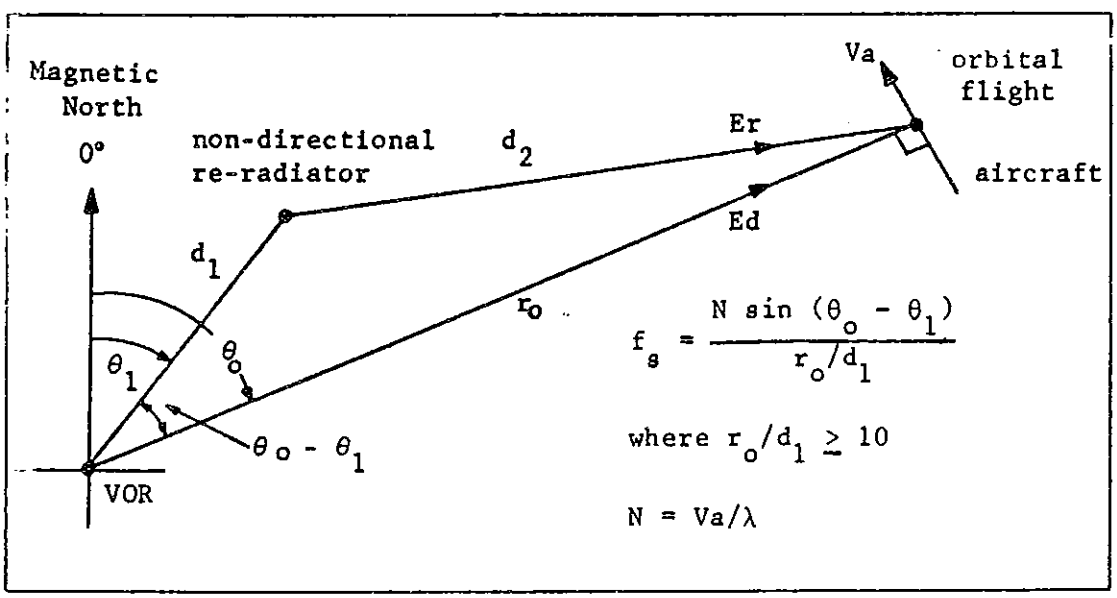

FIGURE 7-18. NONDIRECTIONAL RE-RADIATOR

Using the foregoing numerical expression, graphic presentations of the variation in scalloping frequency are presented in figures 7-19 through 7-22 for variations in r_o/d_1 and for variations in the angle $(\theta_o-\theta_1)$.

(2) The geometry for a directional re-radiator causing scalloping is shown in figure 7-23 where the analytic expression for f_s, the scalloping frequency, is also presented. Using the same numerical parameters as before, the analytic expression may be written:

$$f_s = \frac{27.55 \sin 2a}{r_o/d_1} \quad .$$

where

Va = 140 knots

$\lambda = \lambda(115 \text{ MHz})$

Note that the scalloping frequency is a maximum when a is 45 degrees. Using the numerical parameters above, graphic presentations of the variation in scalloping frequency are presented in figures 7-24 through 7-27 for variations in r_o/d_1 and a.

(3) With respect to course scalloping characteristics, a long-length directional reflector may be viewed as a continuous string of short-length directional reflectors. Course scalloping equations are identical for both types of reflectors, and conclusions pertinent to short reflectors apply as well to long reflectors. However, an angle of incidence between interfering wave and reflector occurring at 55 degrees, corresponding to maximum scalloping amplitude, is more likely with a long-length reflector than with a short one. In situations where a short-length reflector location and orientation are recognized, equations shown in figure 7-23 can be useful in calculating the angle of incidence to be encountered and the VOR courses susceptible to scalloping.

c. Scalloping Frequency - Radial Flight.

(1) Using, for a nondirectional radiator, the same geometry and nomenclature as before, the analytic expression for f_s, the scalloping frequency for orbital flight is as shown in figure 7-28.[8] This expression for an aircraft speed of 140 knots, a VOR carrier frequency of 115 MHz and $(\theta_o-\theta_1)$ of 90 degrees or 270 degrees is as written below.

$$F_s = 27.55 \left[1 - \frac{(r_o/d_1)}{\sqrt{1 + (r_o d_1)^2}} \right]$$

Graphic presentations of the variation of f_s, the scalloping frequency, with variations in r_o/d_1 are included as figures 7-29 and 7-30.

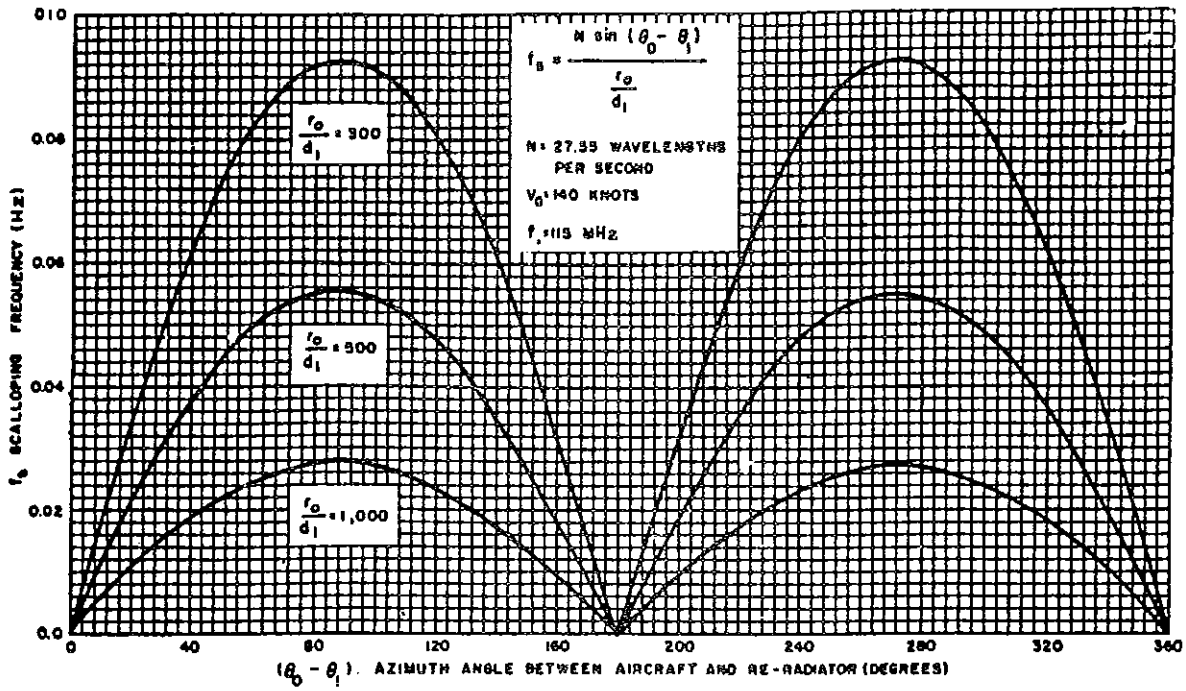

FIGURE 7-19. VARIATION IN SCALLOPING FREQUENCY WITH CHANGE IN VALUE OF r_o/d_1

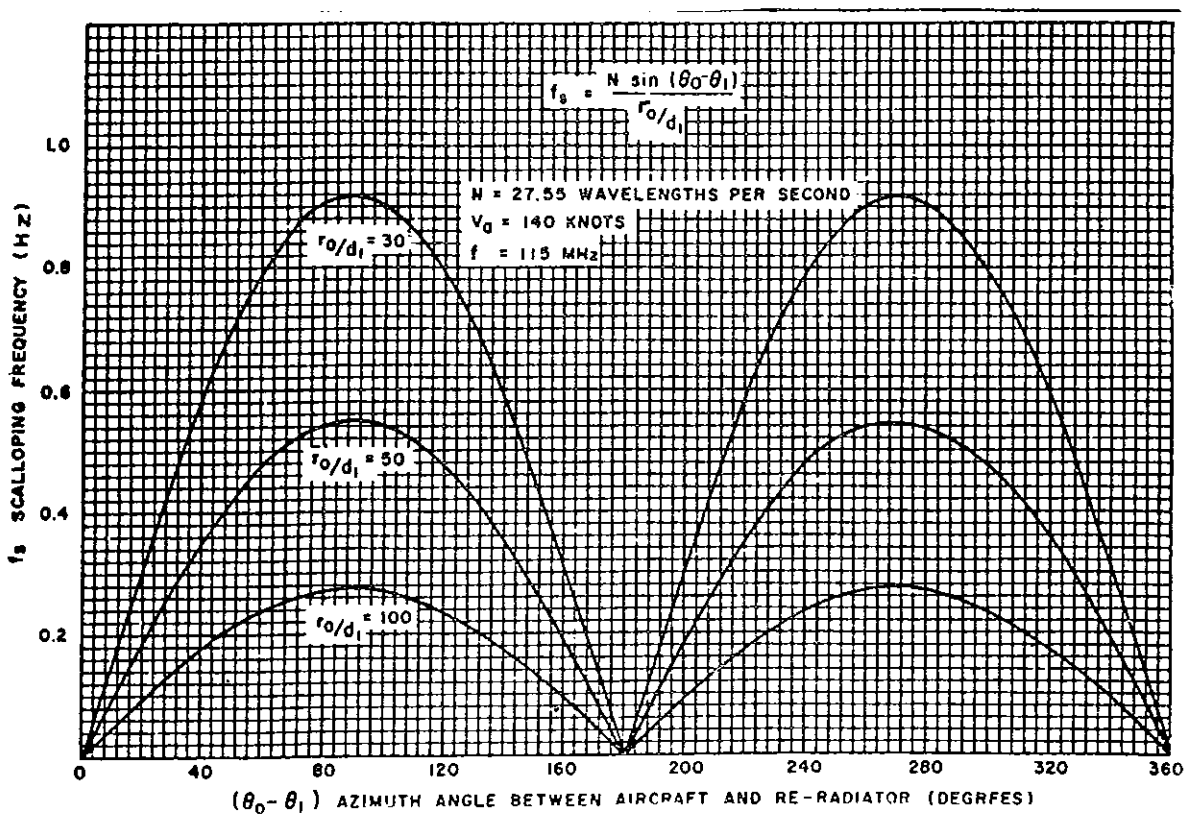

FIGURE 7-20. FURTHER VARIATION IN f_s WITH CHANGE IN VALUE OF r_o/d_1

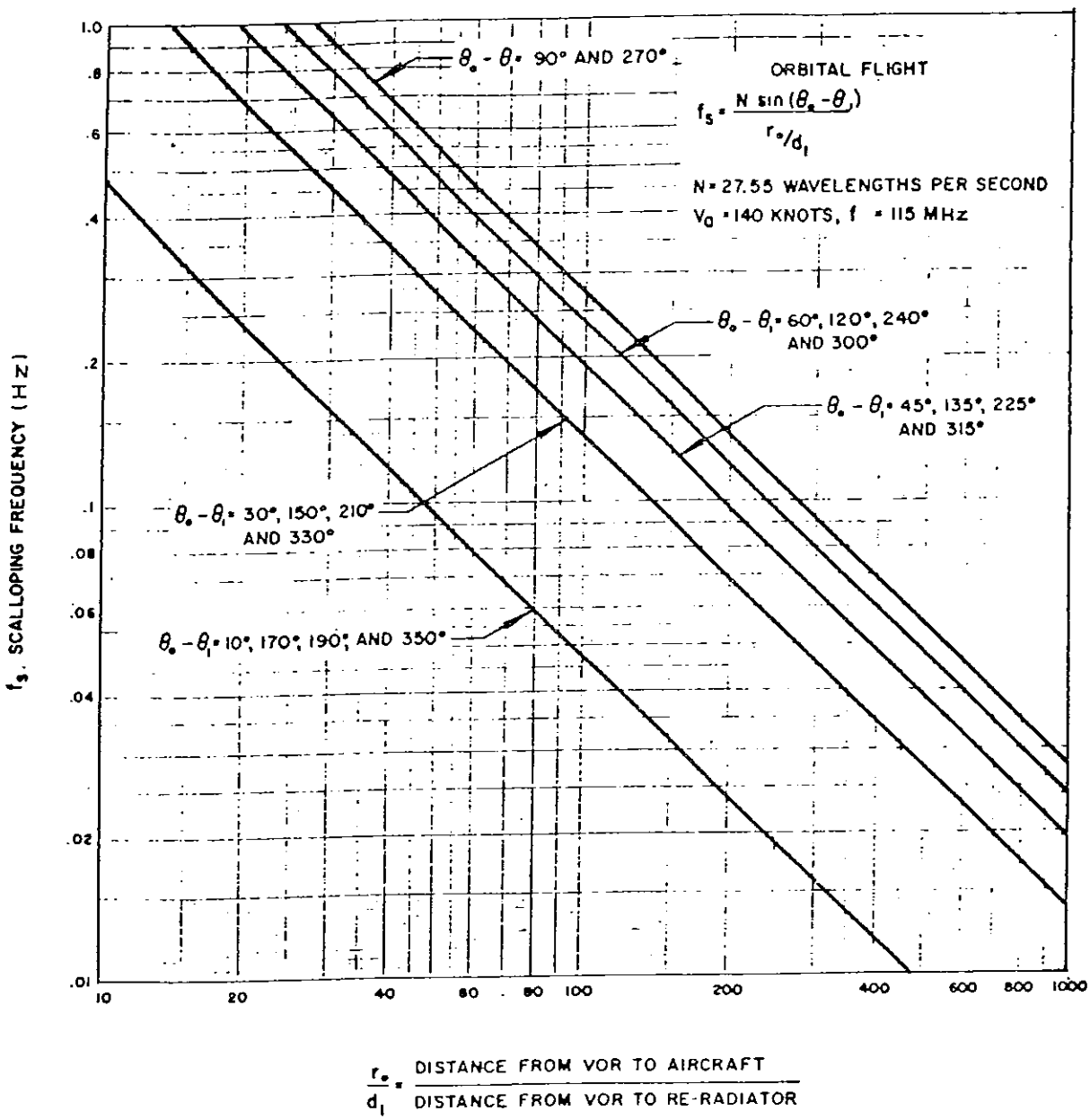

FIGURE 7-21. SCALLOPING FREQUENCY VARIATION WITH CHANGE IN AIRCRAFT AZIMUTH

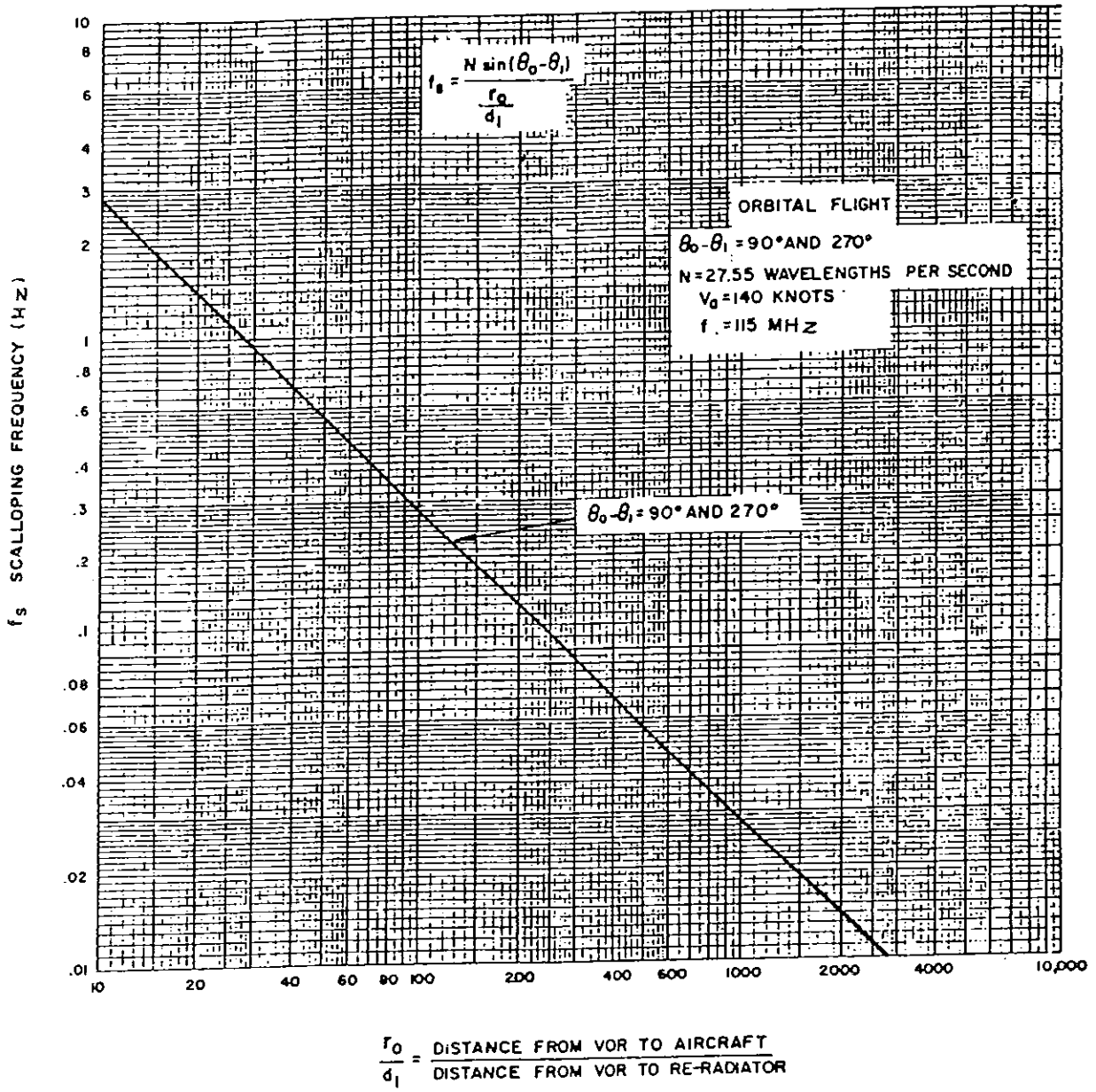

FIGURE 7-22. SCALLOPING FREQUENCY VARIATION ALONG LINE OF MAXIMUM SCALLOPING AMPLITUDE

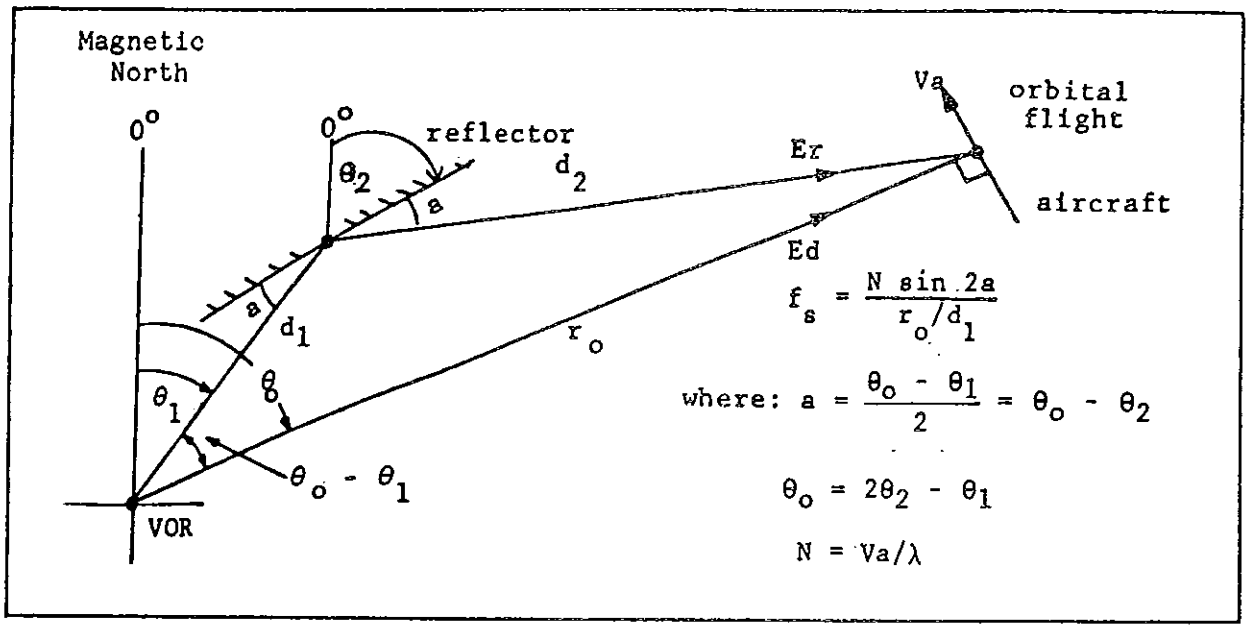

FIGURE 7-23. DIRECTIONAL REFLECTOR

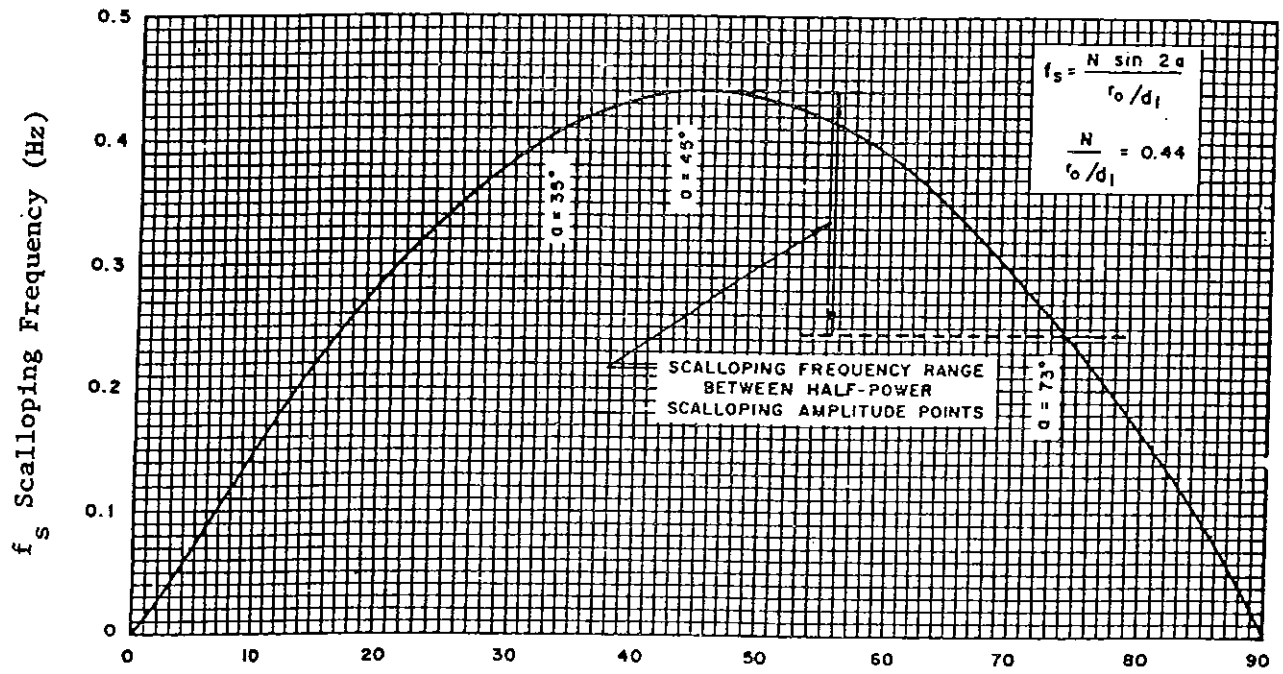

FIGURE 7-24. SCALLOPING FREQUENCY ON ORBITAL FLIGHT AS A FUNCTION OF ANGLE OF INCIDENCE

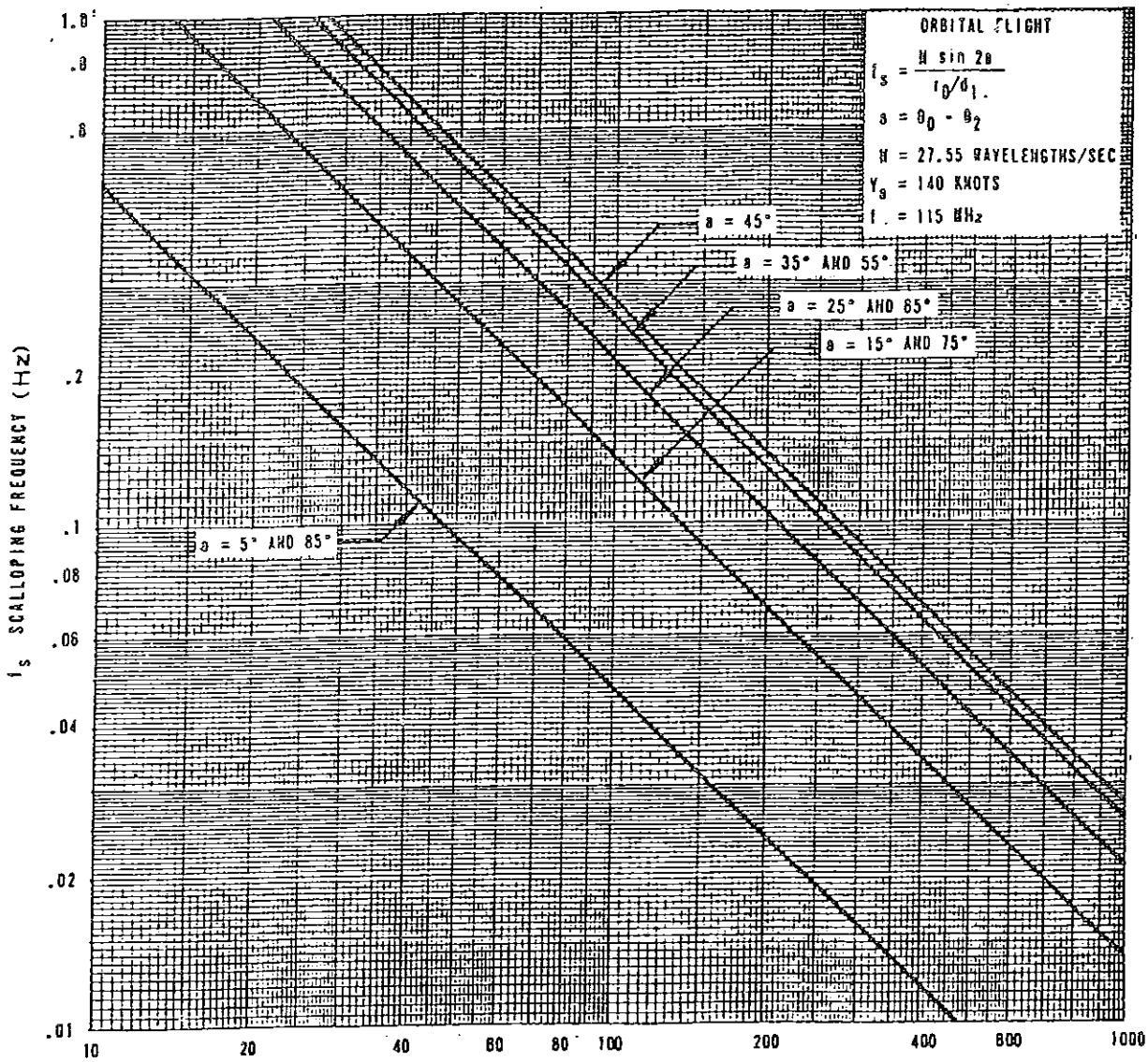

$$r_o/d_1 = \frac{\text{Distance from VOR to aircraft}}{\text{Distance from VOR to point of reflection}}$$

FIGURE 7-25. VARIATION IN SCALLOPING FREQUENCY FOR VARIOUS ANGLES OF INCIDENCE

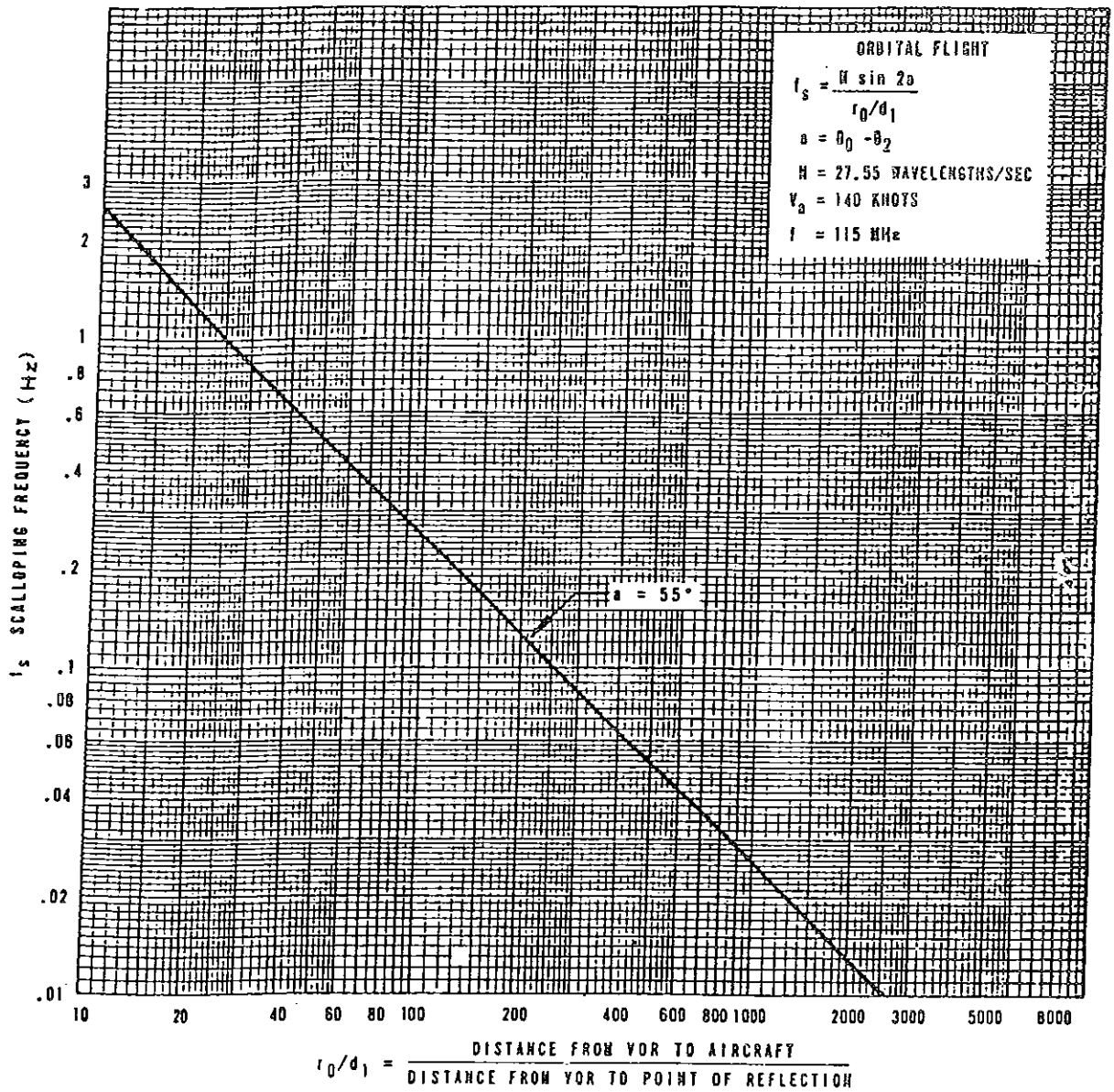

FIGURE 7-26. VARIATION IN SCALLOPING FREQUENCY AT THE ANGLE OF INCIDENCE OF 55 DEGREES

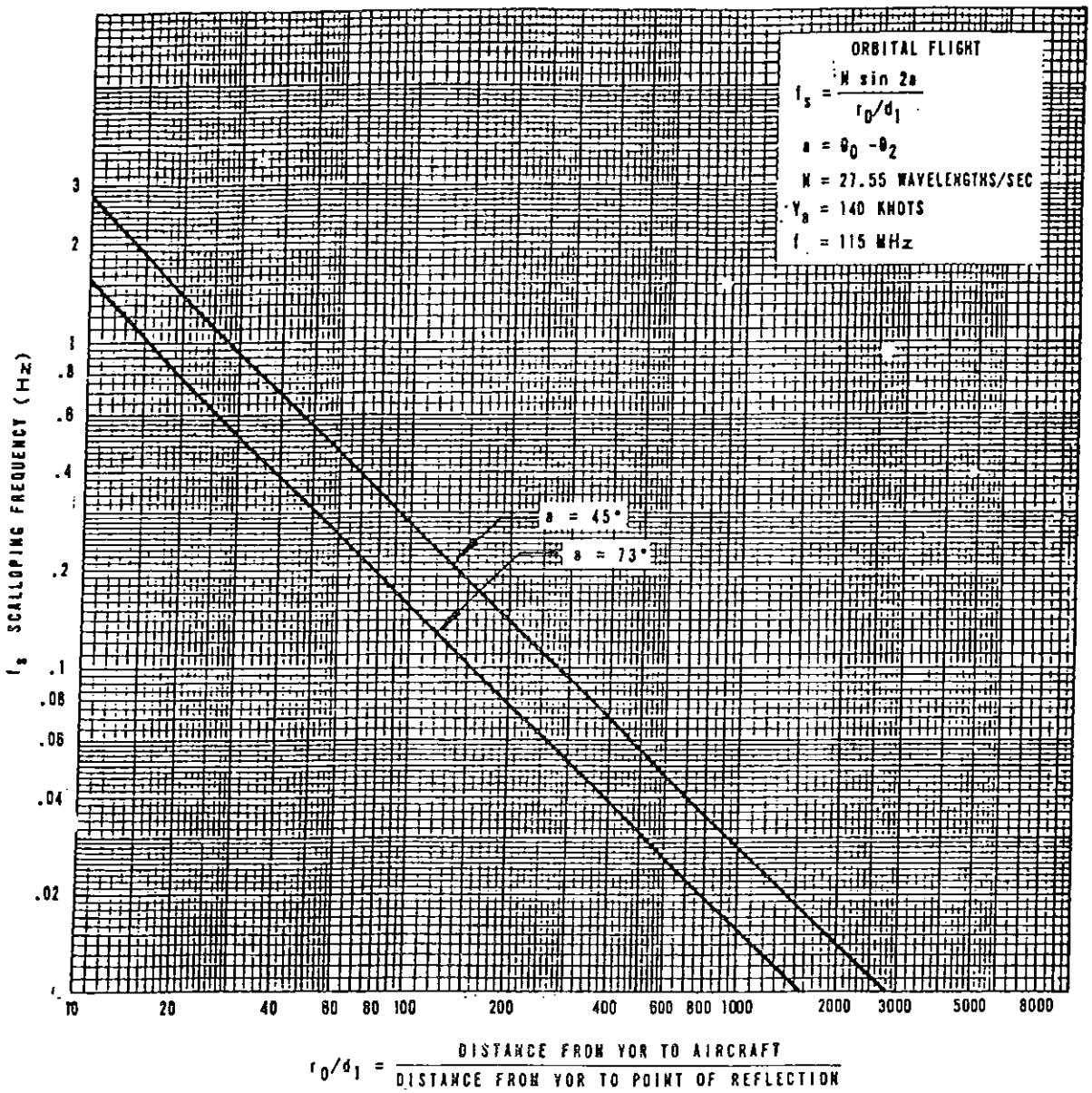

FIGURE 7-27. VARIATION IN SCALLOPING FREQUENCY AT THE ANGLES OF INCIDENCE OF 45 DEGREES AND 73 DEGREES

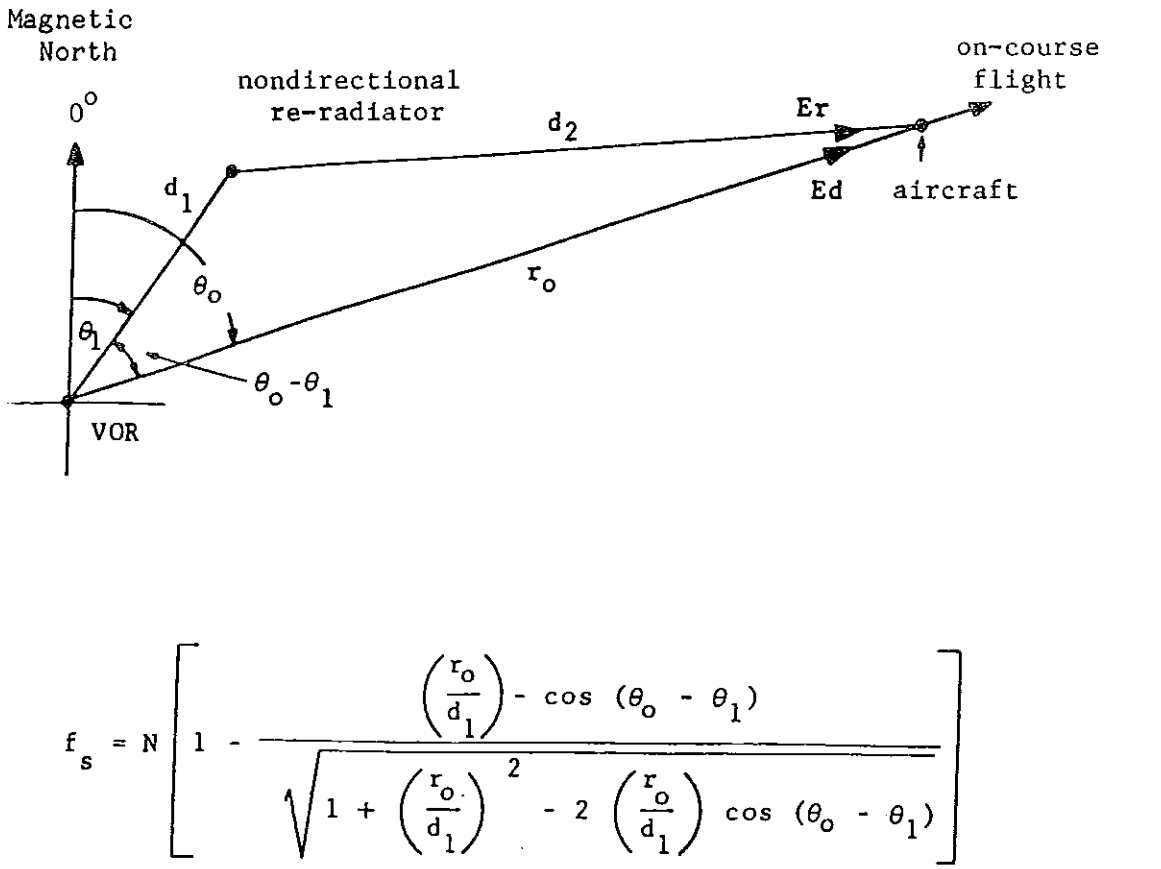

$$f_s = N\left[1 - \frac{\left(\frac{r_o}{d_1}\right) - \cos(\theta_o - \theta_1)}{\sqrt{1 + \left(\frac{r_o}{d_1}\right)^2 - 2\left(\frac{r_o}{d_1}\right)\cos(\theta_o - \theta_1)}}\right]$$

FIGURE 7-28. NONDIRECTIONAL RE-RADIATOR

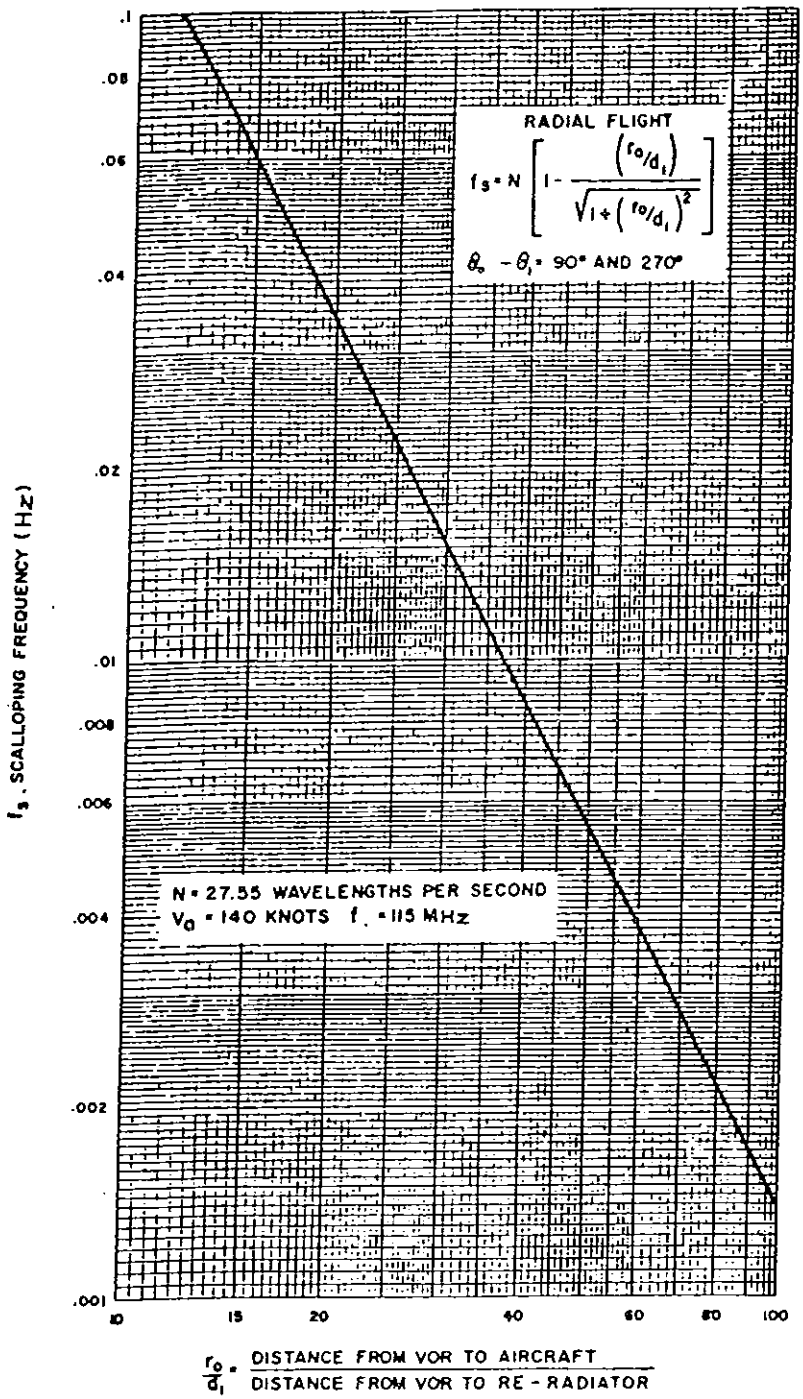

FIGURE 7-29. SCALLOPING FREQUENCY ALONG RADIAL OF MAXIMUM SCALLOPING AMPLITUDE; $r_o d_1$ = 10 TO 100

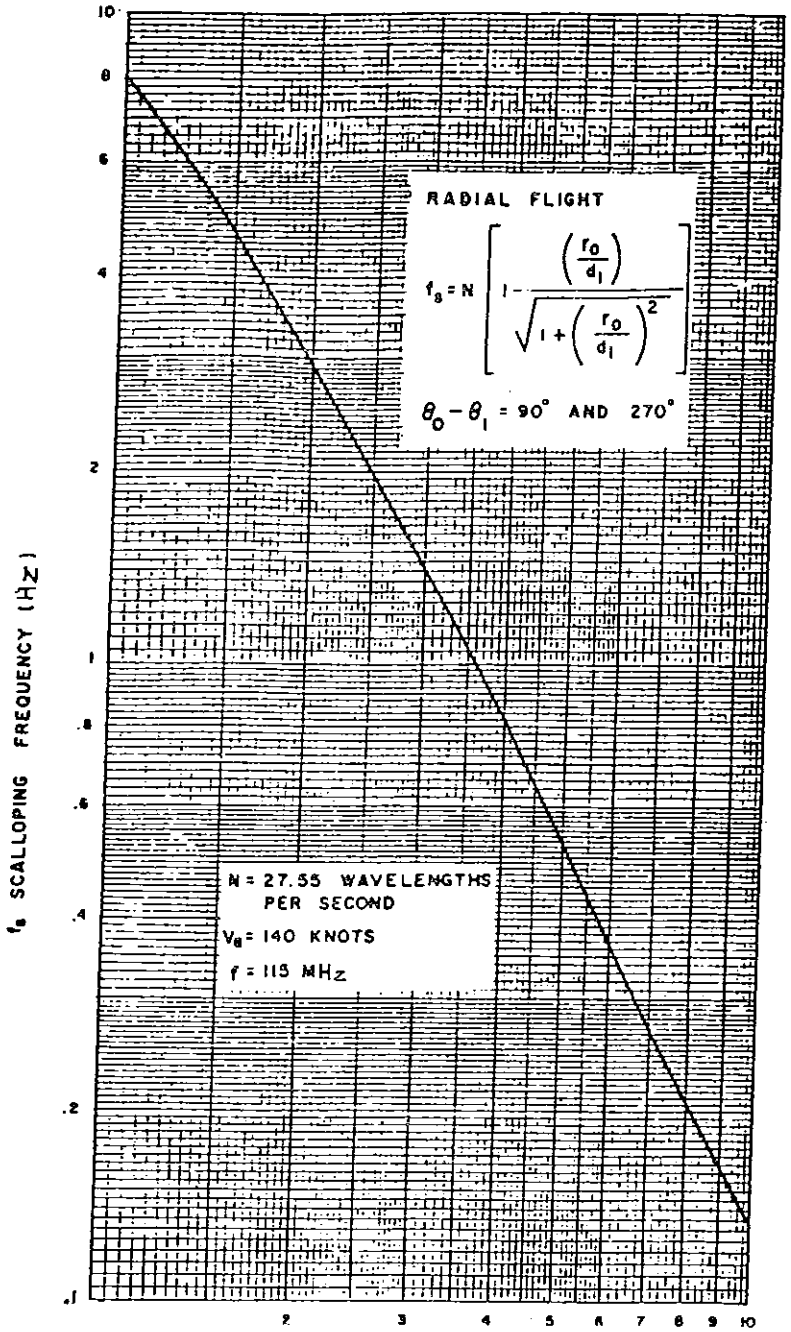

$$\frac{r_o}{d_1} = \frac{\text{Distance from VOR to aircraft}}{\text{Distance from VOR to re-radiator}}$$

FIGURE 7-30. SCALLOPING FREQUENCY ALONG RADIAL OF MAXIMUM SCALLOPING AMPLITUDE; $r_o d_1$ = 1 TO 10

d. Scalloping Amplitudes Presented to the Pilot

(1) Figure 7-31, which is a typical scalloping response curve for a VOR receiver, may be used to estimate the radial flight scalloping frequency response that will be experienced from knowledge of the orbital flight scalloping frequency that has been measured.

(2) During radial flight, a very slow scalloping frequency, approaching zero, will be experienced and it is useful to determine the amplitude of this scalloping. Figures 7-32a and 7-32b reveal that, along the 310-degree radial at the Washington National Airport, a scalloping amplitude and frequency of ± 0.6 degrees and 1.28 Hz, respectively, were measured. From figure 7-31, the VOR receiver has a nine percent response to 1.28 Hz on a scale normalized to zero frequency response. Hence, the zero frequency scalloping amplitude can be expected to be ± 6.67 degrees as shown below.

$$S_{of} = \frac{\text{Scalloping Amplitude}}{\text{Relative Scalloping Amplitude Percent}}$$

$$= \frac{\pm 0.6^{\circ}}{.09} = \pm 6.67^{\circ}$$

(3) The frequency of scalloping, f_s, as seen by an aircraft on a radial flight and in the presence of a directional re-radiator is as shown below.

$$f_s = N\left[1 - \frac{\left(\frac{r_o}{d_1}\right) - \cos 2a}{\sqrt{1 + \left(\frac{r_o}{d_1}\right)^2 - 2\left(\frac{r_o}{d_1}\right)\cos 2a}}\right]$$

Refer to figures 7-5 and 7-6 for the geometry. Along the azimuth of maximum f_s, a = 45 degrees, and for the parameters of 140 knots and 115 MHz, this expression reduced to the one obtained in the previous paragraph is

$$f_s = 27.55\left[1 - \frac{(r_o/d_1)}{\sqrt{1 + (r_o d_1)^2}}\right]$$

which is plotted in figures 7-29 and 7-30.

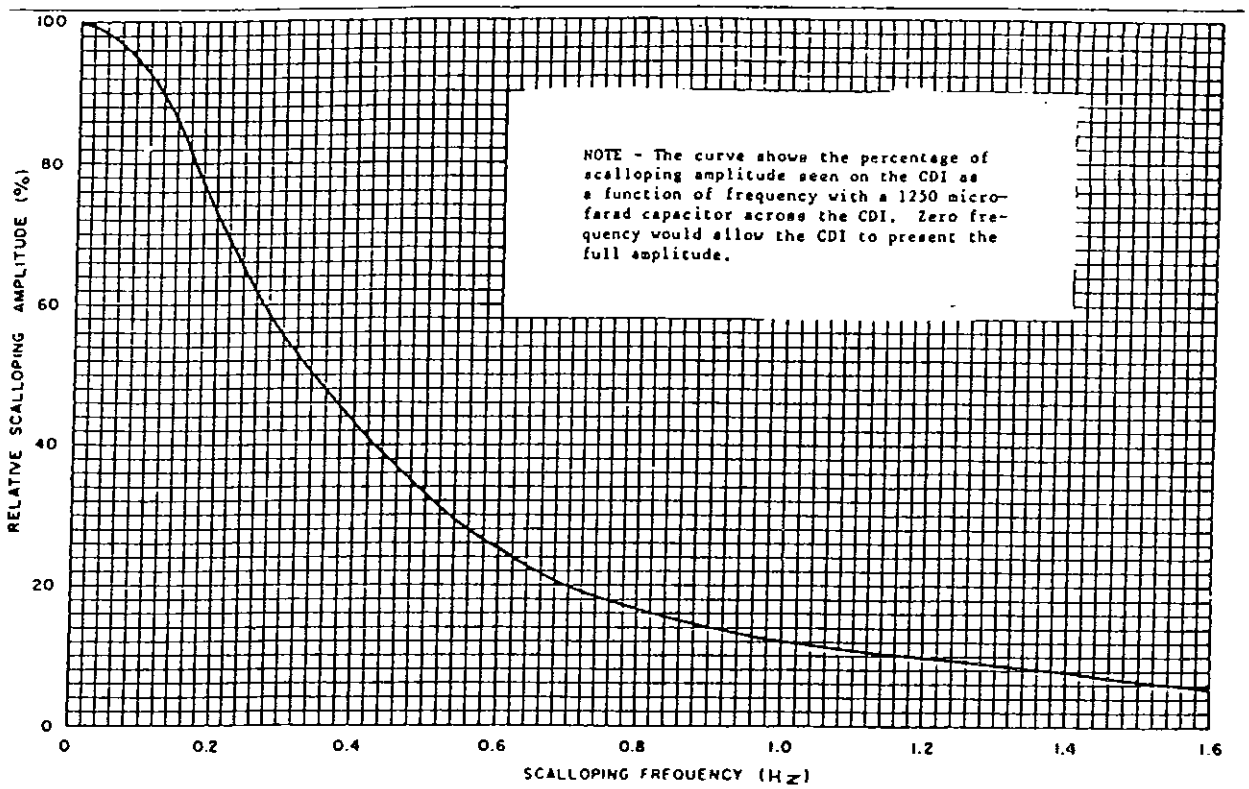

FIGURE 7-31. TYPICAL SCALLOPING RESPONSE FOR VOR RECEIVER

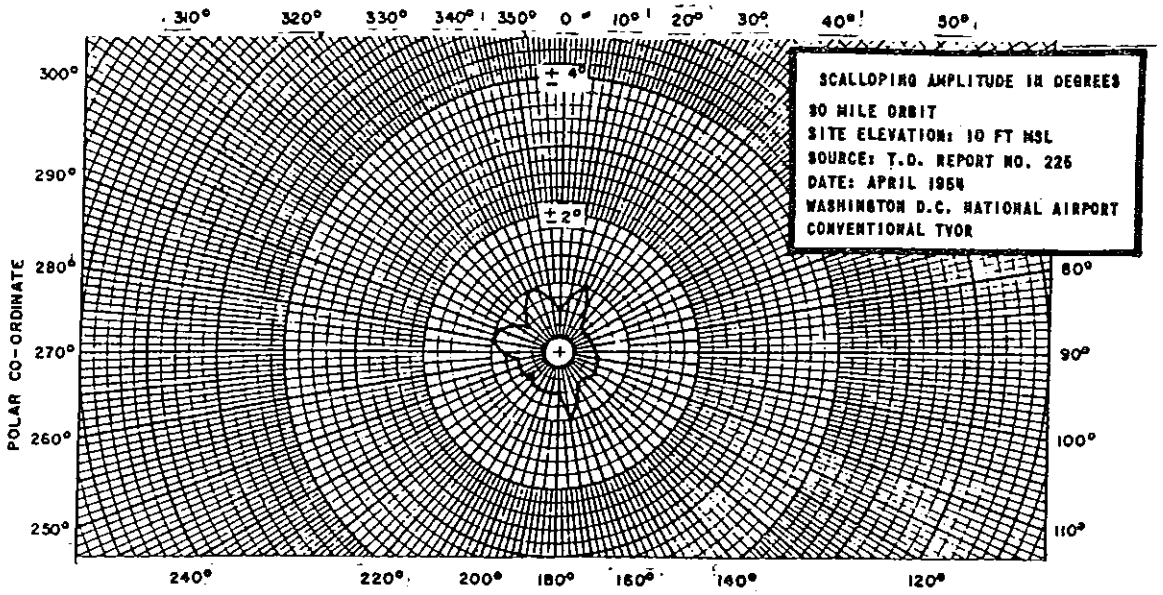

FIGURE 7-32a. SCALLOPING AMPLITUDE

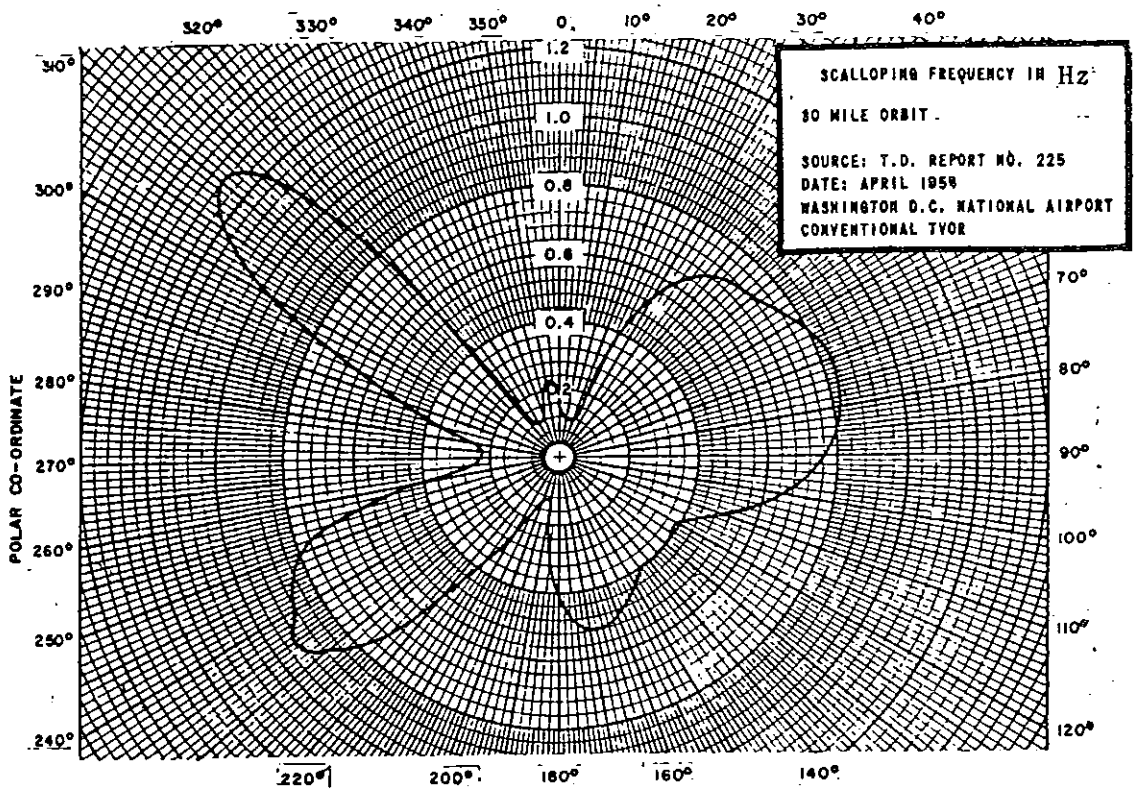

FIGURE 7-32b. SCALLOPING FREQUENCY

CHAPTER 8. SCATTERING SIMULATIONS

31. GENERAL.

a. Previous chapters have presented various practical and theoretical approaches to siting VOR, VOR/DME, and VORTAC facilities. This chapter and its related appendix provide access to simulation tools to assist in evaluating the potential effects of specific types of obstructions on the performance of only the VOR facilities. The types of obstructions considered here are thin-wire obstacles (i.e., utility lines and fences) and metallic obstacles shaped as bodies of revolution (i.e., water tanks and silos).

b. The use of these simulations is most suited for established facilities, particularly where construction of a potential obstacle is planned in the vicinity of the site, or where it is desired to identify the magnitude of error arising from a given obstacle. For new facilities, flight testing of candidate sites provides more comprehensive and reliable information than is presently possible with simulations.

c. The purpose of this chapter is to describe the available programs and to provide guidance on the inputs required to properly utilize each program. Full description of the program methodology and theoretical basis is beyond the scope of this order, but is available in the following reports:

(1) "Effects of Scattering by Obstacles in the Field of a VOR/DVOR," Report No. FAA-RD-74-153, Harry Gruenberg and Bradley J. Strait, July 1974.

(2) "Effects of Scattering by Obstacles in the Field of a VOR/DVOR," Report No. FAA-RD-76-21, Harry Gruenberg and Kazuhiro Hirasawa, February 1976.

The programs were originally run on an IBM 360 and have since been rewritten to be used on the CDC 6600, Scope 3.4, Fortran Extended System which is available to FAA.

d. The programs are available in card decks through:

Navigation Program, APM-420
Federal Aviation Administration
Washington, DC 20591
(202) 426-1944 (Commercial)

e. Appendix 2 contains sample data input cards and the resultant program output for each of the programs described. This will enable users to verify that their installation of the programs is running correctly.

f. The following discussion assumes a basic knowledge of computer programming in general and FORTRAN in particular.

32. LONG-WIRE COMPUTATION PROGRAM (LONGSY).

a. The program LONGSY provides a means for analyzing the scalloping effects of a wire more than 200 feet in length in the field of a VOR. Up to three parallel wires are accommodated by the program, provided that wire-to-wire spacing does not exceed three feet. The input parameters for this program are as follows:

b. Card 1. The number of segments of wires. The variable name in the program is IMP and the input is an integer up to ten digits (I10). Figure 8-1 illustrates a four-segment wire.

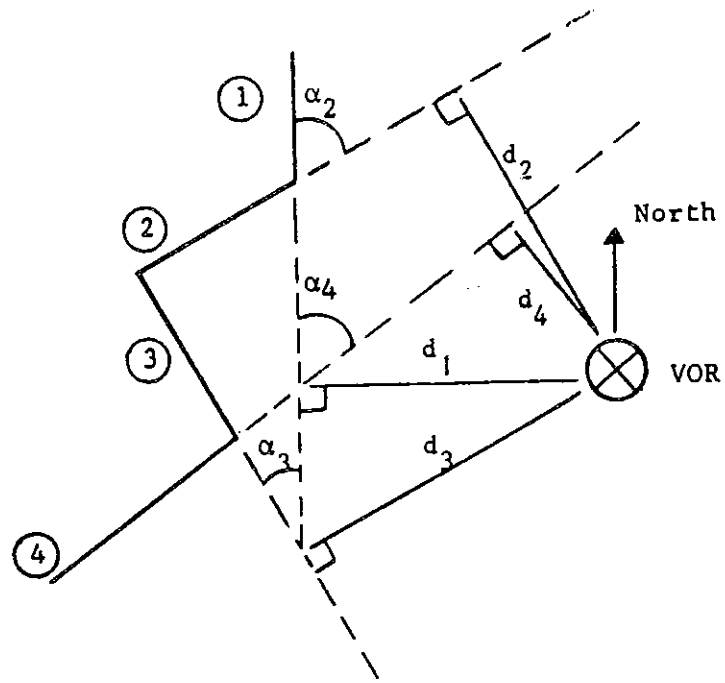

FIGURE 8-1. SAMPLE WIRE PROBLEM

c. Card 2.

(1) The spacing of the wire configuration in feet. The variable name is D3 and requires an F10.4 input field. If wire spacing exceeds three feet, then run the program for a single wire, and multiply the result by the number of wires.

(2) The number of wires in the configuration. The variable name is N and requires an I10 input field. The number of wires can be one to three. If more than three wires are in the configuration, the program will require the following general formula:

$$\left| \sum_{i=1}^{N} (Kh_i)^2 \sin (Kh_d \varepsilon)/Kh_i \varepsilon \exp -j \left[Kd_i(1+\sin\phi)+(Kh_i^2/2D) \right] \right|$$

d. Card 3.

(1) The height of the counterpoise above ground. The variable name is H and requires an F10.2 input field.

(2) The height of the four loops above the counterpoise. The variable name is SH and requires an F10.2 input field.

(3) The radius of the counterpoise in feet. The variable name is R and requires an F10.2 input field.

(4) The carrier frequency in megahertz. The variable name is FRM and requires an input field of F10.2.

e. Card 4.

(1) The radius of the circular aircraft orbit in miles. The variable name is SR and requires an F10.2 input field.

(2) The altitude of the aircraft in feet (HA), with an F10.2 input field.

(3) The aircraft speed in miles per hour (V), with an F10.2 input field.

(4) The time constant of the 30 Hz signal of the receiver, between 0.3 and 0.4. The variable name is FO and requires an input field of F10.2.

f. Card 5. Three inputs, the initial azimuth angle in degrees (SPH), the final azimuth angle in degrees (EPH) (less than 180 degrees) and the increment in degrees (AINC). All use an F10.2 input field.

g. Cards 6 and 7. These cards provide the description of each wire segment, and there should be one pair (cards 6 & 7) for each segment specified in Card 1.

(1) Card 6 contains the normal distance from the VOR to the wire in feet (D), the location of the first endpoint of the wire in feet (AL1), and the location of the second endpoint of the wire in feet (AL2). These each require an input field of F10.2. Figure 8-2 shows how these values are determined. Using wire segments from figure 8-1 as an example, figure 8-2a shows for segment 1 the measurement of AL1 and AL2 as being positive to the north or right of the perpendicular from the VOR. This convention should be followed for each segment. Figure 8-2b illustrates this convention for segment 2, where both AL1 and AL2 are negative.

(2) The remaining two inputs on Card 6 are the radius of the wire in feet (A), which requires an F10.6 input field, and the height of the wire above ground in feet (H1), which requires an F10.2 input field.

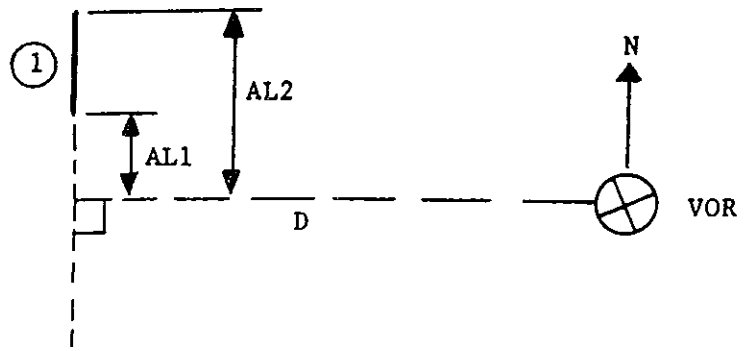

FIGURE 8-2a. LENGTH OF WIRE SEGMENTS (SEGMENT 1)

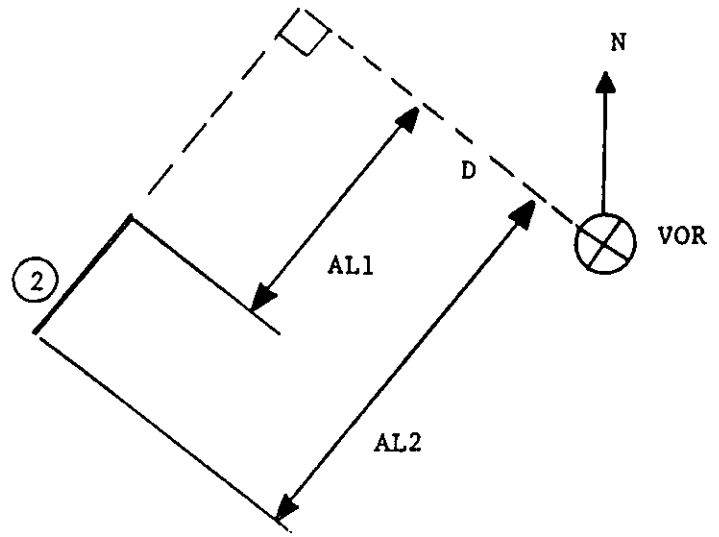

FIGURE 8-2b. LENGTH OF WIRE SEGMENTS (SEGMENT 2)

h. Card 7. This card contains the angular difference of wire position, in degrees from north, for the wire segment described in Card 6. Clockwise is positive and counterclockwise is negative, and the card requires an input field of F10.2. Referring to figure 8-1, segment 1 is oriented north-south, and therefore $\alpha_1 = 0$. Segment 2 will have a positive α_2 rotation, and segment 3 will have a negative α_3 rotation. Running this program for a wire of more than one segment will yield an error prediction for each wire segment. In order to find the total error, the errors for each segment must be summed at each azimuthal point, providing a composite error curve for the entire wire.

33. BODIES-OF-REVOLUTION COMPUTATION PROGRAM (CYLPI and CYLP2).

a. The programs CYLPI and CYLP2 are used to calculate errors in a VOR field due to bodies of revolution; i.e., obstructions such as water tanks or silos. Program CYLPI calculates the admittance matrix of the obstruction, and program CYLP2 uses this matrix to calculate the error due to the obstruction. The obstruction is assumed to have an axis running through its center and perpendicular to the X-axis (90- and 270-degree radials) of the VOR station. It is also assumed that the obstruction is symmetrical about this axis.

b. The program CYLPI requires five input cards.

(1) Card 1 has two inputs. The first is the number of points which define the contour (NP), with an I5 input field. There should be 21 points for each wavelength of the contour. Therefore, if the contour is two wavelengths high, then 42 points must be used. The second input is the VOR frequency in megahertz (FRM), with an F10.2 input field.

(2) Cards 2 and 3 describe the locations of the points that define the contour. The reference is to the first point in the contour and to the central axis, and the unit of measurement is the wavelength of the VOR signal. For a VOR operating at 115 MHz, the wavelength is 2.6 meters, or approximately 8.5 feet. Figure 8-3 illustrates this for a cylinder 0.5 wavelength in diameter and 0.375 wavelength high. Since the body is less than one wavelength high, only 15 points are used to define the contour.

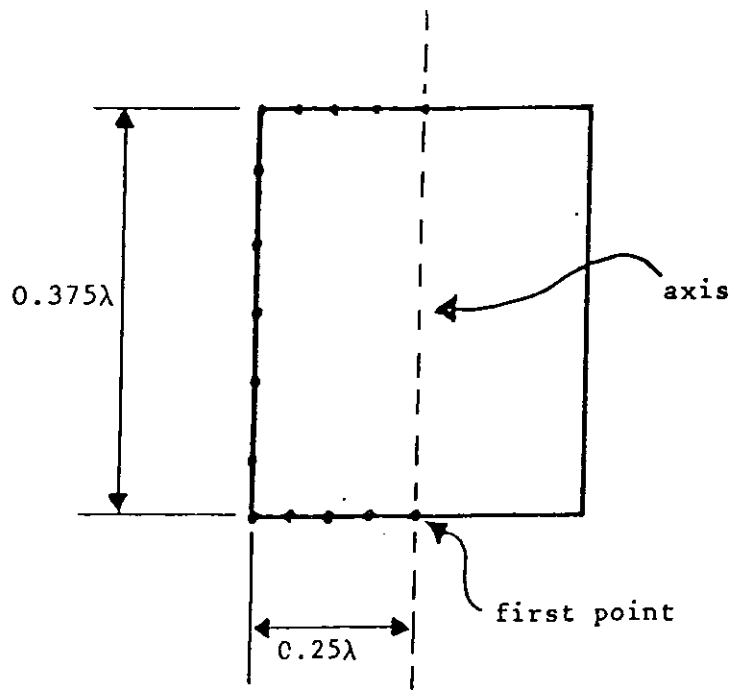

FIGURE 8-3. BODY OF REVOLUTION

(a) Card 2 contains the distance of each specified point on the contour from the central axis. This variable is named RH(I), I = 1 to NP, and requires an input field of 10F8.4. There may be a maximum of 43 points, and since each card contains 10 points, there can be up to five cards of this type.

(b) Card 3 contains the elevation of each point with respect to the first point, and the variable is called ZH(I), and requires an input field of 10F8.4. The limits are the same as for Card 2.

(3) Card 4 is the number of modes, called NTR, and requires an I/O input field. The number of modes should be at least three per wavelength.

(4) Card 5 contains the mode number (NM) in an I5 input field, and the subdivisions of the mode to be used for the calculations (NPHI) also in an I5 input field. The modes and their associated number of subdivisions are:

NM	NPHI
0	8
1	12
2	16
3	20
4	20
.	.
.	.
.	.

c. After the program CYLPI has been successfully run, the resulting admittance matrix, ADDPAR, is stored for use by CYLP2. CYLP2 is then run to calculate the error due to the obstruction. This program requires seven types of input cards:

(1) Card 1.

(a) Number of modes (NX), input field of I10, same as NTR in CYLPI.

(b) Number of points to define the contour (NP), input field of I10, same as NP in CYLPI.

(c) Frequency of VOR in MHz (FRM), input field of F10.2, same as FRM in CYLPI.

(2) Card 2.

(a) The perpendicular distance in feet from the VOR to the centerline of the obstruction (XX), input field of F10.1.

(b) The distance of the obstruction above the ground in feet (ZZ), input field of F10.2.

(3) Card 3.

(a) Height of the counterpoise above the ground in feet (HH), input field of F10.2.

(b) Height of the four-loops above the counterpoise in feet (SH), input field of F10.2.

(c) Radius of the counterpoise in feet (RR), input field of F10.2.

(4) Card 4. Same as type 2 card(s) in CYLPI.

(5) Card 5. Same as type 3 card(s) in CYLPI.

(6) Card 6.

(a) Altitude of the aircraft in feet (HS), input field of F10.2.

(b) Radius of the aircraft orbit in miles (DIT), input field of F10.2.

(7) Card 7.

(a) Starting azimuth in degrees (SPH), input field of F10.2.

(b) Ending azimuth in degrees (EPH), input field of F10.2.

(c) Increment in degrees (AINC), input field of F10.2.

34. SHORT WIRE COMPUTER PROGRAM (FRANK).

a. The program FRANK is designed to estimate the bearing errors introduced into the VOR system when a short wire, less than 200 feet in length, is in the VOR field. The program is generalized so that it can be readily modified to handle up to four wires. The input cards required for this program are described below, with comments regarding variations for multiple wires included where appropriate. Following the input description is a review of the required changes for running analyses of more than four wires, and for variations on configurations.

b. Figure 8-4 provides a schematic description of a wire in a VOR field, and the input descriptions will refer to this figure.

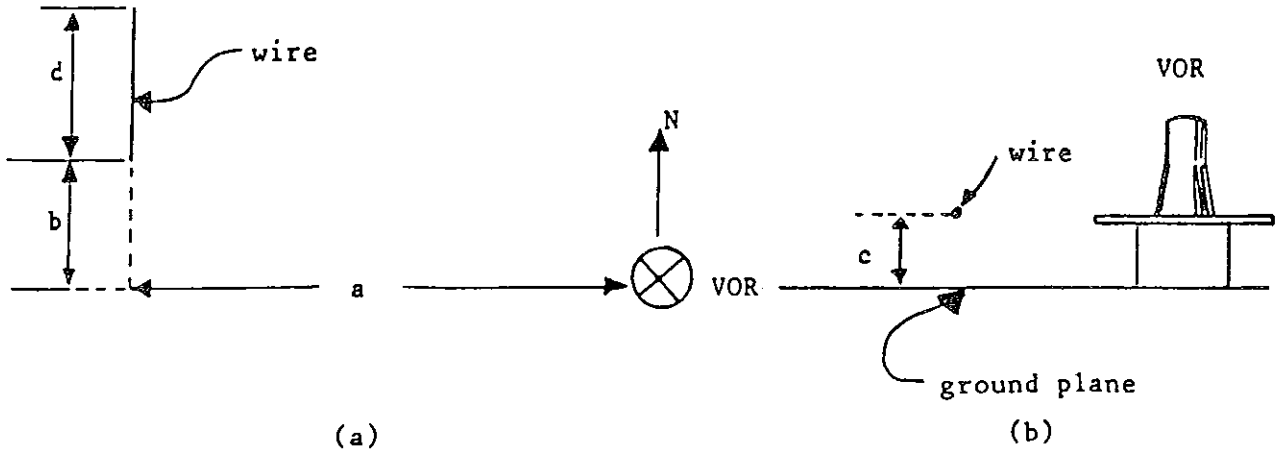

FIGURE 8-4. SHORT WIRE IN A VOR FIELD

(1) Card 1.

(a) The perpendicular distance in feet from the VOR to the wire(s) in question. This is labeled "a" in figure 8-4a. In the program the variable is named XNP1 and requires an input field of F10.4. The first wire is the closest to the VOR, when more than one wire is being considered.

(b) Distance of the wire(s) offset from the X-axis (90- and 270-degree radials) of the VOR. This is labeled "b" in figure 8-4a. In the program the variable is named YNP1 and requires an F10.4 input field.

(c) Elevation of the wire(s) above the ground. This is labeled "c" in figure 8-4b. In the program the variable is named ZNP1 and requires an F10.4 input field.

(d) Length of the wire(s). This is labeled "d" in figure 8-4a. In the program the variable is named XLEN and requires an F10.4 input field.

(2) Card 2.

(a) The number of wires in the configuration (NW), with an I4 input field.

(b) The number of points to describe the wire(s) (NP), with an I4 input field. To determine the number of points required to define the wire(s), divide the length of the wire by the wavelength of the VOR signal, multiply by 20, and add 3. The maximum number that can be used is 281, so if the result is more than that, use 281 points.

(c) The number of different radii encountered on the wire(s) (NR), with an I4 input field.

(d) The frequency of the VOR in MHz (FRM), with an F7.4 input field.

(3) Card 3. First points for each wire (LL(I)), with a 20I4 input field. If more than one wire is being considered, then the number of points must be divided among the wires. This procedure yields a number which is the first point on each wire. For example, if 124 points are being used to describe a two wire configuration, then the first points would be 1 and 62 for the first and second wires, respectively.

(4) Card 4. First points for each radius change (LR(I)), with a 20I4 input field.

(5) Card 5. Radius of wire in meters (RAD(I)), with a 5E14.7 input field. More than one card may be used to complete this input (if NR from Card 2 is more than 5).

(6) Card 6.

(a) Elevation of the aircraft in feet (HS), with an F10.1 input field.

(b) Radius of the orbit of the aircraft in miles (DIT), with an F10.2 input field.

(7) Card 7.

(a) Height of the counterpoise above ground in feet (H), with an F10.2 input field.

(b) Height of the four loops above the counterpoise in feet (SH), with an F10.2 input field.

(c) Radius of the counterpoise in feet (R), with an F10.2 input field.

(8) Card 8. Number of loads (NL), with a 20I4 input field.

(9) Card 9. This card is optional, depending on Card 8. For information, see Report FAA-RD-F4-153.

(10) Card 10.

(a) Starting azimuth in degrees (SPH), with an F10.3 input field.

(b) Ending azimuth in degrees (EPH), with an F10.3 input field.

(c) Increment in degrees (AINC), with an F10.3 input field.

c. The program FRANK is configured to run an error estimate based on one wire in the VOR field. In order to run calculations for more than one wire, several modifications must be made to the program. These are:

(1) Modification of the DO 50 loop. There is a loop in the program that begins with the line "DO 50 I=1, NP" and goes to the line "50 CONTINUE". This loop is generalized for up to four wires and requires only the addition of another data card after Card 2 if more than one wire is being analyzed. This card should contain the distance between the wires in feet (DBW(I)) in an 8F10.4 format, and there may be more than one card for more than nine wires. If there are more than four wires, the loop itself must be modified by the addition of one set of the following four lines for each wire over four:

```
IF (NW.EQ. K-1 ) GO TO 50
IF (I.LE.(LL(K)-1) GO TO 50
PX(I)=(XNP1+DBW( K-1 )*0.3048
PY(I)=YNP1*0.3048+3.5*300.0/FRM*(AI-(LL(K)-1))/(NP/NW)-1)
```

Where K=5,6,etc. is substituted in the underlined places in each expression. The loop will then be generalized for up to that many wires.

(2) Modification of CALZ and ROW subroutines. The subroutines CALZ and ROW are generalized for arbitrary wires. If the wire is a parallel or straight wire, then the CALZ routine for straight or parallel wires must be substituted for the general CALZ routine. If the wire is parallel to the ground plane, then the ROW subroutine for wires parallel to the ground plane must be substituted for the general ROW subroutine.

APPENDIX 1. LIST OF ABBREVIATIONS, ACRONYMS, AND COMMONLY USED TERMS

am	amplitude modulation
BER	Bearing Error Report
beta (β)	deviation ratio in fm. β is the ratio of maximum excursion of the modulated frequency to maximum modulating frequency. In VOR and DVOR, β = 480 Hz/30 Hz = 16
CDI	Course Deviation Indicator
carrier	refers to the radio frequency energy which is modulated with the information-bearing signal
counterpoise	counterpoise is the term commonly used for the metal ground plane used with the VOR/DME/TACAN antenna system
course deviations	errors in VOR bearing indication are detected by means of the Course Deviation Indicator (CDI) and may be recorded on strip recorders. The categories of deviations are itemized below: course roughness - a series of rapid irregular deviations course bends - a series of very slow smooth rhythmic deviations course scalloping - a series of smooth rhythmic deviations scalloping amplitude - is half the peak to peak deviation of the CDI recording, measured in degrees. It is usually measured by taking half the peak to peak value over a ten degree azimuth sector. scalloping frequency - is the number of complete cycles of the CDI pointer (as recorded on the strip recorder) in one second
CSM	Center of Symmetry Method
deviation ratio	see beta (β)
dB	decibel
DME	distance measuring equipment, a navaid
DSB-SC	double sideband suppressed carrier; this is conventional amplitude modulation
DSBDVOR	double sideband Doppler VOR, a navaid

DVOR	Doppler VOR, a navaid
EIS	Environmental Impact Statement
em	electromagnetic
envelope	refers to the information bearing signal which modulates the rf carrier
FAA	Federal Aviation Administration
fm	frequency modulation
fm capture	refers to the capability of fm to selectively reject the weaker of two signals and so improve the signal-to-interference ratio when, initially, the ratio is 6 dB or more
FONSI	Finding of No Significant Impact
GHz	gigahertz, billions of Hertz
ground plane	see counterpoise
Hz	Hertz
ICAO	International Civil Aviation Organization
IFR	Instrument Flight Rules
interferometer	refers to the characteristic of regularly spaced effect objects, such as trees, to re-radiate signal most strongly in specified preferred directions
kHz	kilohertz
LOPs	Lines of Position
LORAN-C	Long Range Navigation (Model C)
MHz	Megahertz
MTBF	Mean Time Between Failures
multipath	multipath usually refers to the phenomenon of a wave of em energy reaching the receiver by reflection or re-radiation from an intermediate object and interfering with the wave that traveled directly from the same source lateral multipath - a wave of em energy radiated at one azimuth which is redirected to another azimuth by interaction with an object such as a tree or a wire-line and which, as a result, contributes to error in the navigational information presented to the pilot

	longitudinal multipath - a wave of em energy which is re-radiated after impacting on the ground. It can, if the geometry is appropriate, interact at the receiver with the direct ray and cause a signal null
NAS	National Airspace System
navaid	navigational aid
nm	nautical mile
NOTAM	Notice to Airmen
reference	refers to that signal in a VOR or DVOR system whose phase phase is azimuth independent
reflection	refers to the re-radiation of em energy from a surface that is sufficiently smooth that the incident and re-radiated energy are in the same plane and, in their angular relationships, satisfy the law of sines. See also re-radiation
re-radiation	refers to the action of em energy in infringing on a surface sufficiently irregular that the em energy radiated back into the atmosphere exhibits a random spatial distribution. In the strict sense, reflected energy is also re-radiated but the more common term reflection is usually applied
rf	radio frequency
SAFI	Semi-Automated Flight Inspection
scalloping	see course deviation
space modulation	the technique used in VOR to create a DSB-LC modulation by radiating three separate signals which combine within the airborne receiver to form the composite carrier plus modulation
SSBDVOR	single sideband Doppler VOR, a navaid
SSV	Standard Service Volume
TACAN	tactical air navigation system, a navaid
variable phase	refers to that signal in a VOR or DVOR system whose phase varies degree for degree with the azimuth
vhf	very high frequency, the radio band from 30 MHz to 300 MHz
uhf	ultra high frequency, the radio band from 300 MHz to 3,000 MHz

Units	Meters (1 foot = 0.305 meters)
	Nautical miles (1 nmi = 1.85 km = 6080 feet = 1.15 statute miles)
	Statute miles (1 mile = 1.60 km = 5,280 feet = 0.87 nmi)
USNO	United States Naval Observatory
VOR	very high frequency omnidirectional radio range, a navaid
VORTAC	VOR tactical air navigation

APPENDIX 2. INPUT AND OUTPUT EXAMPLES FOR COMPUTER SIMULATIONS

1. Chapter 8 provides detailed input instructions for programs that calculate bearing errors resulting from three types of obstructions in a VOR field. This appendix contains sample data input cards and the resultant program output for each of the three types of calculations.

2. The lists of input and output in this appendix were produced from files containing the actual input and output values for each program. The files were edited in order to label the input cards and to conserve space in the printing of the output data. As a consequence, the input card lists contain the correct sequence, number, and values for the input, but the column spacing has been compressed in some cases to facilitate printing. Similarly, the output is compressed into arrays rather than the long single columns that result from an actual computer run. Below are descriptions of the various inputs and their respective outputs, with the edited input and output following as figures 1 through 8.

a. Bodies of Revolution. The programs CLYPI and CYLP2 are used to calculate bearing errors due to objects such as water towers or silos in a VOR field. Figure 1 shows the CYLPI input for a sample problem involving an upright cylinder 3/8 of a wavelength in height and 1/2 a wavelength in diameter, 150 feet from the VOR. The output for CYLPI is not given, as it is an intermediate result for use by CYLP2. The CYLP2 input is given in figure 2. The result of the CYLP2 calculations is given in figure 3. In this example, for each azimuth, from 1 degree to 356 degrees at 5-degree intervals, the bearing error is given in degrees. For the actual output, the results are in two long columns; here the results are folded into two arrays, azimuth above and the corresponding errors below.

b. Short Wires. The program FRANK calculates bearing errors resulting from short wires in the VOR field. Figure 4 shows the input data cards for a single wire. No output is given for this data. Figure 5 gives the input data for a two-wire problem. Figure 6 shows the results of running FRANK with the data of figure 5. As with the CYLP2 output, the results will actually come out as long columns, but for presentation here, the columns have been folded into arrays. For each azimuth given in the upper part of the figure, there is a corresponding bearing error below.

c. Long Wires. The program LONGSY is used for calculating the bearing errors resulting from wires longer than 200 feet in the field of a VOR. Figure 7 shows the input cards for a sample three-segment long-wire problem. Figure 8 is the output resulting from the figure 7 input. In the case of LONGSY, the output is reported by segment: several long columns for each segment. Figure 8 gives the results by segment: at the top, the azimuths reported for segment 1, followed by the bearing errors calculated for each azimuth for segment 1; next, the azimuths reported for segment 2, followed by the calculated errors for each of those azimuths for segment 2; finally, the azimuths reported for segment 3 and the errors calculated for each azimuth for segment 3. The error resulting from the entire wire is the sum of the errors for each segment

at a given azimuth. For example, at an azimuth of 45 degrees, segment 1 shows an error of 0.228 degree, segment 2 shows an error of 0.111 degree, and segment 3 shows an error of -0.569 degree, giving a total bearing error at 45 degrees azimuth of -0.230 degree.

```
 CYLPI.DATA

CARD 1
   NP        FRM
   15      115.00
CARD 2
  RH(I) - 15 ENTRIES
 0.0     0.0625 0.1250 0.1875 0.2500 0.2500 0.2500 0.2500 0.2500 0.2500
 0.2500 0.1875 0.1250 0.0625 0.0
CARD 3
  ZH(I) - 15 ENTRIES
 0.0     0.0     0.0     0.0     0.0     0.0625 0.1250 0.1875 0.2500 0.3125
 0.3750 0.3750 0.3750 0.3750 0.3750
CARD 4
         NTR
          3
CARD 5
   NM   NPHI
    0     8
    1    12
    2    16
```

FIGURE 1. CYLPI INPUT DATA CARDS

CYLP2.DATA

```
CARD 1
        NX          NP      FRM
         3          15      115.
CARD 2
       XX          ZZ
    -150.0       19.00
CARD 3
       HH          SH          RR
     12.00        4.00       26.00
CARD 4 (same as card 2 for CYLPI)
  RH(I) - 15 ENTRIES
 0.0     0.0625 0.1250 0.1875 0.2500 0.2500 0.2500 0.2500 0.2500 0.2500
 0.2500 0.1875 0.1250 0.0625 0.0
CARD 5 (same as card 3 for CYLPI)
  ZH(I) - 15 ENTRIES
 0.0     0.0     0.0     0.0     0.0     0.0625 0.1250 0.1875 0.2500 0.3125
 0.3750 0.3750 0.3750 0.3750 0.3750
CARD 6
       HS          DIT
    4000.0       15.00
CARD 7
       SPH         EPH         AINC
       1.00      360.00        5.00
```

FIGURE 2. CYLP2 INPUT DATA CARDS

CYLP2.OUTPUT.DATA

AZIMUTH (DEGREES)

1.00	6.00	11.00	16.00	21.00	26.00	31.00	36.00	41.00	46.00
51.00	56.00	61.00	66.00	71.00	76.00	81.00	86.00	91.00	96.00
101.00	106.00	111.00	116.00	121.00	126.00	131.00	136.00	141.00	146.00
151.00	156.00	161.00	166.00	171.00	176.00	181.00	186.00	191.00	196.00
201.00	206.00	211.00	216.00	221.00	226.00	231.00	236.00	241.00	246.00
251.00	256.00	261.00	266.00	271.00	276.00	281.00	286.00	291.00	296.00
301.00	306.00	311.00	316.00	321.00	326.00	331.00	336.00	341.00	346.00
351.00	356.00								

ERROR (DEGREES)

0.040	0.234	0.473	0.730	0.813	1.027	1.118	1.178	1.267	1.381
1.532	1.722	1.905	2.093	2.320	2.499	2.667	2.782	2.849	2.860
2.807	2.709	2.545	2.351	2.131	1.862	1.600	1.351	1.110	0.882
0.684	0.538	0.383	0.272	0.157	0.065	0.025	0.121	0.214	0.290
0.466	0.577	0.751	0.982	1.220	1.459	1.698	1.959	2.232	2.431
2.615	2.756	2.834	2.862	2.829	2.741	2.605	2.427	2.239	1.96
1.831	1.657	1.481	1.341	1.241	1.174	1.106	0.919	0.803	0.583
0.451	0.223								

FIGURE 3. RESULTS OF CYLPA CALCULATIONS

```
 FRANK3.DATA

(Sample input for a single-wire problem)

CARD 1
          XNP1         YNP1         ZNP1         XLEN
       -100.00      300.00       30.00       200.00
CARD 2
         NW   NP   NR    FRM
          1  203    1  115.00
CARD 3
       LL(I)
          1
CARD 4
       LR(I)
          1
CARD 5
        RAD(I)
       0.00206
CARD 6
              HS          DIT
         4000.00       15.00
CARD 7
              H           SH           R
          12.00         4.00        26.00
CARD 8
         NL
          0
CARD 9
   (None, since on card 8 NL=0)
CARD 10
             SPH         EPH         AINC
            0.00      360.00         5.00

(Note: Sample output is given only for the two-wire problem.)
```

FIGURE 4. FRANK INPUT FOR A SINGLE SHORT WIRE

FRANK4.DATA

(Sample input for a two-wire problem)

```
CARD 1
          XNP1          YNP1          ZNP1          XLEN
       -150.00        150.00         30.00        35.00
CARD 2
          NW   NP   NR    FRM
           2  122    1  115.00
CARD 2A
           DBW(I)
           5.0000
CARD 3
         LL(I) - 2 POINTS
           1   62
CARD 4
         LR(I)
           1
CARD 5
          RAD(I)
         0.00206
CARD 6
                HS          DIT
           4000.00        15.00
CARD 7
                H           SH           R
            12.00         4.00        26.00
CARD 8
          NL
           0
CARD 9
      (None, since on card 8 NL=0)
CARD 10
               SPH         EPH         AINC
              0.00      360.00         5.00
```

FIGURE 5. FRANK INPUT FOR TWO SHORT WIRES

FRANK.OUTPUT.DATA

TWO-WIRE PROBLEM

AZIMUTH (DEGREES)

0.0	5.00	10.00	15.00	20.00	25.00	30.00	35.00	40.00	45.00
50.00	55.00	60.00	65.00	70.00	75.00	80.00	85.00	90.00	95.00
100.00	105.00	110.00	115.00	120.00	125.00	130.00	135.00	140.00	145.00
150.00	155.00	160.00	165.00	170.00	175.00	180.00	185.00	190.00	195.00
200.00	205.00	210.00	215.00	220.00	225.00	230.00	235.00	240.00	245.00
250.00	255.00	260.00	265.00	270.00	275.00	280.00	285.00	290.00	295.00
300.00	305.00	310.00	315.00	320.00	325.00	330.00	335.00	340.00	345.00
350.00	355.00	360.00							

ERROR (DEGREES)

0.0	0.023	0.162	0.432	0.832	1.336	1.882	2.378	2.716	2.783
2.464	1.704	0.624	0.437	0.983	0.807	0.160	0.533	0.661	0.282
0.248	0.468	0.312	0.029	0.223	0.222	0.103	0.004	0.092	0.210
0.318	0.362	0.331	0.251	0.158	0.077	0.000	0.114	0.302	0.570
0.890	1.185	1.331	1.199	0.732	0.048	0.640	0.932	0.679	0.064
0.553	0.684	0.301	0.277	0.565	0.389	0.099	0.442	0.455	0.151
0.256	0.484	0.423	0.118	0.290	0.626	0.795	0.783	0.638	0.431
0.229	0.076	0.000							

FIGURE 6. FRANK OUTPUT FOR A TWO-WIRE PROBLEM

```
LONGSY.DATA

(Sample input for a three-segment long wire problem)

CARD 1
                IMP
                 3
CARD 2
          D3                  N
          1.5                 2
CARD 3
              H          SH          R          FRM
           12.00       4.00       26.00      114.40
CARD 4
              SR         HA          V          FD
           20.00     3000.00      165.00       0.35
CARD 5
             SPH        EPH        AINC
           00.00      179.00       1.00
CARD 6   (segment 1)
              D          AL1        AL2         A                H1
         1225.00     -400.00    2800.00     0.01910           55.00
CARD 7   (segment 1)
            (alpha)
            00.00
CARD 6   (segment 2)
              D          AL1        AL2         A                H1
         1700.00     -200.00    -1900.00    0.01910           55.00
CARD 7   (segment 2)
            (alpha)
            11.00
CARD 6   (segment 3)
              D          AL1        AL2         A                H1
         1100.00     -600.00    -1300.00    0.01910           55.00
CARD 7   (segment 3)
            (alpha)
            -12.00
```

FIGURE 7. LONGSY INPUT DATA

LONGSY.OUTPUT.DATA

(Sample output for a three-segment long wire problem)

WIRE SEGMENT 1

AZIMUTH (DEGREES)

1.00	2.00	3.00	4.00	5.00	6.00	7.00	8.00	9.00	10.00
11.00	12.00	13.00	14.00	15.00	16.00	17.00	18.00	19.00	20.00
21.00	22.00	23.00	24.00	25.00	26.00	27.00	28.00	29.00	30.00
31.00	32.00	33.00	34.00	35.00	36.00	37.00	38.00	39.00	40.00
41.00	42.00	43.00	44.00	45.00	46.00	47.00	48.00	49.00	50.00
51.00	52.00	53.00	54.00	55.00	56.00	57.00	58.00	59.00	60.00
61.00	62.00	63.00	64.00	65.00	66.00	67.00	68.00	69.00	70.00
71.00	72.00	73.00	74.00	75.00	76.00	77.00	78.00	79.00	80.00
81.00	82.00	83.00	84.00	85.00	86.00	87.00	88.00	89.00	90.00
91.00	92.00	93.00	94.00	95.00	96.00	97.00	98.00	99.00	100.00
101.00	102.00	103.00	104.00	105.00	106.00	107.00	108.00	109.00	110.00
111.00	112.00	113.00	114.00	115.00	116.00	117.00	118.00	119.00	120.00
121.00	122.00	123.00	124.00	125.00	126.00	127.00	128.00	129.00	130.00
131.00	132.00	133.00	134.00	135.00	136.00	137.00	138.00	139.00	140.00
141.00	142.00	143.00	144.00	145.00	146.00	147.00	148.00	149.00	150.00
151.00	152.00	153.00	154.00	155.00	156.00	157.00	158.00	159.00	160.00
161.00	162.00	163.00	164.00	165.00	166.00	167.00	168.00	169.00	170.00
171.00	172.00	173.00	174.00	175.00	176.00	177.00	178.00	179.00	

ERROR (DEGREES)

-0.001	-0.004	-0.009	-0.016	-0.023	-0.027	-0.025	-0.014	0.003	0.018
0.016	0.001	0.001	-0.042	-0.068	0.035	0.144	-0.043	-0.185	0.171
0.034	-0.199	0.239	-0.208	0.167	-0.134	0.091	-0.024	0.014	0.089
-0.180	-0.171	0.213	0.453	0.439	0.371	0.407	0.565	0.650	0.243
-0.525	-0.233	0.516	-0.373	0.228	-0.175	0.121	-0.002	-0.040	0.233
0.328	0.201	0.144	0.357	0.804	0.681	-0.756	-0.291	0.900	-1.035

FIGURE 8. LONGSY OUTPUT

0.803	0.112	-1.219	0.004	0.934	1.118	1.032	0.567	-0.531	-0.771
0.802	-0.506	0.476	-0.622	0.416	0.367	-0.092	-0.242	-0.191	-0.012
0.197	0.070	-0.141	0.112	-0.086	0.049	0.015	-0.024	-0.013	0.0
-0.013	-0.024	0.015	0.049	-0.086	0.112	-0.141	0.070	0.197	-0.012
-0.191	-0.242	-0.091	0.367	0.416	-0.622	0.476	-0.506	0.804	-0.771
-0.531	0.567	1.032	1.118	0.933	0.003	-1.219	0.113	0.802	-1.035
0.899	-0.291	-0.757	0.680	0.804	0.358	0.145	0.201	0.328	0.233
-0.040	-0.001	0.121	-0.175	0.229	-0.374	0.516	-0.233	-0.525	0.249
0.649	0.566	0.408	0.372	0.439	0.453	0.213	-0.171	-0.179	0.089
0.014	-0.024	0.091	-0.134	0.167	-0.208	0.239	-0.199	0.034	0.171
-0.184	-0.043	0.144	0.035	-0.068	-0.042	0.001	0.001	0.016	0.018
0.003	-0.014	-0.025	-0.027	-0.023	-0.016	-0.009	-0.004	-0.001	

WIRE SEGMENT 2

AZIMUTH (DEGREES)

1.00	2.00	3.00	4.00	5.00	6.00	7.00	8.00	9.00	10.00
11.00	12.00	13.00	14.00	15.00	16.00	17.00	18.00	19.00	20.00
21.00	22.00	23.00	24.00	25.00	26.00	27.00	28.00	29.00	30.00
31.00	32.00	33.00	34.00	35.00	36.00	37.00	38.00	39.00	40.00
41.00	42.00	43.00	44.00	45.00	46.00	47.00	48.00	49.00	50.00
51.00	52.00	53.00	54.00	55.00	56.00	57.00	58.00	59.00	60.00
61.00	62.00	63.00	64.00	65.00	66.00	67.00	68.00	69.00	70.00
71.00	72.00	73.00	74.00	75.00	76.00	77.00	78.00	79.00	80.00
81.00	82.00	83.00	84.00	85.00	86.00	87.00	88.00	89.00	90.00
91.00	92.00	93.00	94.00	95.00	96.00	97.00	98.00	99.00	100.00
101.00	102.00	103.00	104.00	105.00	106.00	107.00	108.00	109.00	110.00

FIGURE 8. LONGSY OUTPUT (continued)

111.00 112.00 113.00 114.00 115.00 116.00 117.00 118.00 119.00 120.00
121.00 122.00 123.00 124.00 125.00 126.00 127.00 128.00 129.00 130.00
131.00 132.00 133.00 134.00 135.00 136.00 137.00 138.00 139.00 140.00
141.00 142.00 143.00 144.00 145.00 146.00 147.00 148.00 149.00 150.00
151.00 152.00 153.00 154.00 155.00 156.00 157.00 158.00 159.00 160.00
161.00 162.00 163.00 164.00 165.00 166.00 167.00 168.00 169.00 170.00
171.00 172.00 173.00 174.00 175.00 176.00 177.00 178.00 179.00

ERROR (DEGREES)

-0.000 -0.001 -0.000 0.000 0.002 0.007 0.006 -0.007 -0.022 -0.009
0.022 0.015 -0.017 -0.003 0.002 -0.012 0.002 0.022 -0.044 0.054
-0.042 -0.001 0.061 -0.068 -0.007 0.022 0.007 0.000 -0.032 -0.049
-0.011 0.109 0.188 -0.042 -0.157 0.173 -0.133 0.102 -0.051 0.000
0.060 0.056 -0.012 -0.023 0.111 0.321 0.046 -0.335 0.370 -0.357
0.233 0.147 -0.167 -0.188 -0.124 -0.041 0.007 0.079 -0.174 0.249
-0.262 -0.129 0.325 0.477 0.484 0.144 -0.575 0.254 -0.153 0.434
-0.552 -0.438 -0.201 -0.316 -0.520 0.080 0.228 -0.194 -0.109 0.325
0.241 0.190 0.220 0.058 -0.147 0.119 -0.078 -0.009 0.024 0.0
0.024 -0.009 -0.078 0.119 -0.147 0.058 0.220 0.190 0.241 0.325
-0.109 -0.193 0.228 0.080 -0.520 -0.316 -0.202 -0.439 -0.552 0.434
-0.153 0.254 -0.575 0.144 0.484 0.477 0.324 -0.129 -0.262 0.249
-0.174 0.079 0.007 -0.040 -0.124 -0.188 -0.167 0.148 0.232 -0.357
0.370 -0.335 0.045 0.322 0.112 -0.022 -0.012 0.056 0.060 0.000
-0.051 0.102 -0.133 0.174 -0.157 -0.043 0.187 0.109 -0.011 -0.049
-0.032 0.000 0.007 0.022 -0.007 -0.068 0.061 -0.001 -0.042 0.054
-0.044 0.022 0.002 -0.012 0.002 -0.003 -0.017 0.015 0.022 -0.009
-0.022 -0.007 0.006 0.007 0.002 0.000 -0.000 -0.001 -0.000

FIGURE 8. LONGSY OUTPUT (continued)

WIPE SEGMENT 3

AZIMUTH (DEGREES)

1.00	2.00	3.00	4.00	5.00	6.00	7.00	8.00	9.00	10.00
11.00	12.00	13.00	14.00	15.00	16.00	17.00	18.00	19.00	20.00
21.00	22.00	23.00	24.00	25.00	26.00	27.00	28.00	29.00	30.00
31.00	32.00	33.00	34.00	35.00	36.00	37.00	38.00	39.00	40.00
41.00	42.00	43.00	44.00	45.00	46.00	47.00	48.00	49.00	50.00
51.00	52.00	53.00	54.00	55.00	56.00	57.00	58.00	59.00	60.00
61.00	62.00	63.00	64.00	65.00	66.00	67.00	68.00	69.00	70.00
71.00	72.00	73.00	74.00	75.00	76.00	77.00	78.00	79.00	80.00
81.00	82.00	83.00	84.00	85.00	86.00	87.00	88.00	89.00	90.00
91.00	92.00	93.00	94.00	95.00	96.00	97.00	98.00	99.00	100.00
101.00	102.00	103.00	104.00	105.00	106.00	107.00	108.00	109.00	110.00
111.00	112.00	113.00	114.00	115.00	116.00	117.00	118.00	119.00	120.00
121.00	122.00	123.00	124.00	125.00	126.00	127.00	128.00	129.00	130.00
131.00	132.00	133.00	134.00	135.00	136.00	137.00	138.00	139.00	140.00
141.00	142.00	143.00	144.00	145.00	146.00	147.00	148.00	149.00	150.00
151.00	152.00	153.00	154.00	155.00	156.00	157.00	158.00	159.00	160.00
161.00	162.00	163.00	164.00	165.00	166.00	167.00	168.00	169.00	170.00
171.00	172.00	173.00	174.00	175.00	176.00	177.00	178.00	179.00	

ERROR (DEGREES)

0.000	-0.001	0.001	-0.006	0.013	-0.021	0.023	-0.009	-0.028	0.080
-0.117	0.088	0.023	-0.139	0.118	0.048	-0.123	-0.008	0.055	0.003
-0.034	-0.115	-0.112	-0.013	0.114	0.208	0.234	0.145	-0.109	-0.474
-0.595	-0.047	0.594	0.009	-0.468	0.490	-0.191	0.074	-0.042	0.000
-0.133	0.207	0.191	-0.487	-0.569	-0.103	0.321	0.464	0.223	-0.525

FIGURE 8. LONGSY OUTPUT (continued)

```
-1.299 -Ø.431  1.374 -Ø.623 -Ø.171  Ø.413 -Ø.115 -Ø.655  1.192 -Ø.Ø91
-Ø.987 -Ø.762 -Ø.453 -Ø.416 -Ø.523 -Ø.4Ø9  Ø.1Ø2  Ø.2Ø1 -Ø.124  Ø.Ø22
-Ø.Ø52  Ø.15Ø -Ø.148 -Ø.199  Ø.158  Ø.369  Ø.425  Ø.428  Ø.251 -Ø.255
-Ø.349  Ø.4Ø1 -Ø.258  Ø.223 -Ø.278  Ø.222  Ø.Ø69 -Ø.1ØØ -Ø.Ø67  Ø.Ø
-Ø.Ø67 -Ø.1ØØ  Ø.Ø69  Ø.222 -Ø.278  Ø.223 -Ø.258  Ø.4Ø1 -Ø.349 -Ø.255

 Ø.251  Ø.428  Ø.425  Ø.369  Ø.158 -Ø.199 -Ø.148  Ø.15Ø -Ø.Ø52  Ø.Ø22
-Ø.124  Ø.2Ø1  Ø.1Ø2 -Ø.4Ø9 -Ø.523 -Ø.416 -Ø.453 -Ø.763 -Ø.987 -Ø.Ø91
 1.192 -Ø.655 -Ø.114  Ø.411 -Ø.169 -Ø.625  1.375 -Ø.429 -1.299 -Ø.526
 Ø.222  Ø.463  Ø.32Ø -Ø.1Ø5 -Ø.57Ø -Ø.486  Ø.191  Ø.2Ø7 -Ø.133  Ø.ØØØ
-Ø.Ø42  Ø.Ø74 -Ø.191  Ø.4Ø1 -Ø.468  Ø.ØØ8  Ø.595 -Ø.Ø46 -Ø.595 -Ø.474
-Ø.11Ø  Ø.144  Ø.233  Ø.2Ø7  Ø.113 -Ø.Ø14 -Ø.113 -Ø.115 -Ø.Ø34  Ø.ØØ3
 Ø.Ø55 -Ø.ØØ8 -Ø.123  Ø.Ø48  Ø.118 -Ø.14Ø  Ø.Ø23  Ø.Ø88 -Ø.117  Ø.Ø8Ø
-Ø.Ø23 -Ø.ØØ9  Ø.Ø23 -Ø.Ø21  Ø.Ø13 -Ø.ØØ6  Ø.ØØ1 -Ø.ØØ1  Ø.ØØØ
```

FIGURE 8. LONGSY OUTPUT (continued)

APPENDIX 3. LOCATING SOURCES OF SCALLOPING BY THE THEORETICAL METHOD

1. INTRODUCTION.

a. Locating an object which is a source of scalloping is accomplished by analysis of the course deviation recording taken on an orbital flight. Scalloping characteristics observed over a complete orbit indicate the type of interfering object being encountered; that is, whether it is a nondirectional re-radiator or a directional reflector. The bearing to the interfering object from the VOR site is derived from the azimuth on which maximum scalloping amplitude is recorded. The frequency of scalloping determines the distance that the interfering object lies from the VOR site.

b. Procedures employed for locating the source of scalloping require recognition of the type of interfering object being encountered. For a nondirectional re-radiator, the recording exhibits maximum scalloping amplitude along a bearing line extending from both sides of the VOR station (two azimuths displaced 180 degrees). The scalloping characteristics are symmetrical about this bearing line, as indicated in figures 1 and 2. For a directional reflector, the recording exhibits scalloping over a narrow azimuth segment as shown in figures 3 and 4.

c. Procedural outlines are given for locating nondirectional re-radiators and directional reflectors from observed scalloping. These techniques for locating scalloping sources are based upon theoretical considerations which treat each aspect of the subject in its simplest form. It is assumed that the ground plane is a smooth, level, reflection surface and that a re-radiating object propagates equally in all directions. Some approximation is introduced into the scalloping equations by limits placed on the equation parameters. Allowance may be required for these factors in practical application, and knowledge of their influence is gained with experience.

d. Other techniques and adaptations are available for locating interfering objects from recorded scalloping information. A transparent calculator, used as an overlay on a VOR site drawing, has been developed and employed for locating reflectors.

2. PROCEDURE.

a. Nondirectional Re-Radiator. Figure 5 is to be used in conjunction with the following procedural outline for locating a nondirectional re-radiator from recorded scalloping:

(1) From the aircraft course deviation indicator recording of an orbital flight, locate the azimuth bearing line that exhibits maximum scalloping amplitude. This bearing line, which is designated Line ①, includes two azimuth angles separated by 180 degrees. Where two such azimuth bearing lines exist, they should be considered one at a time.

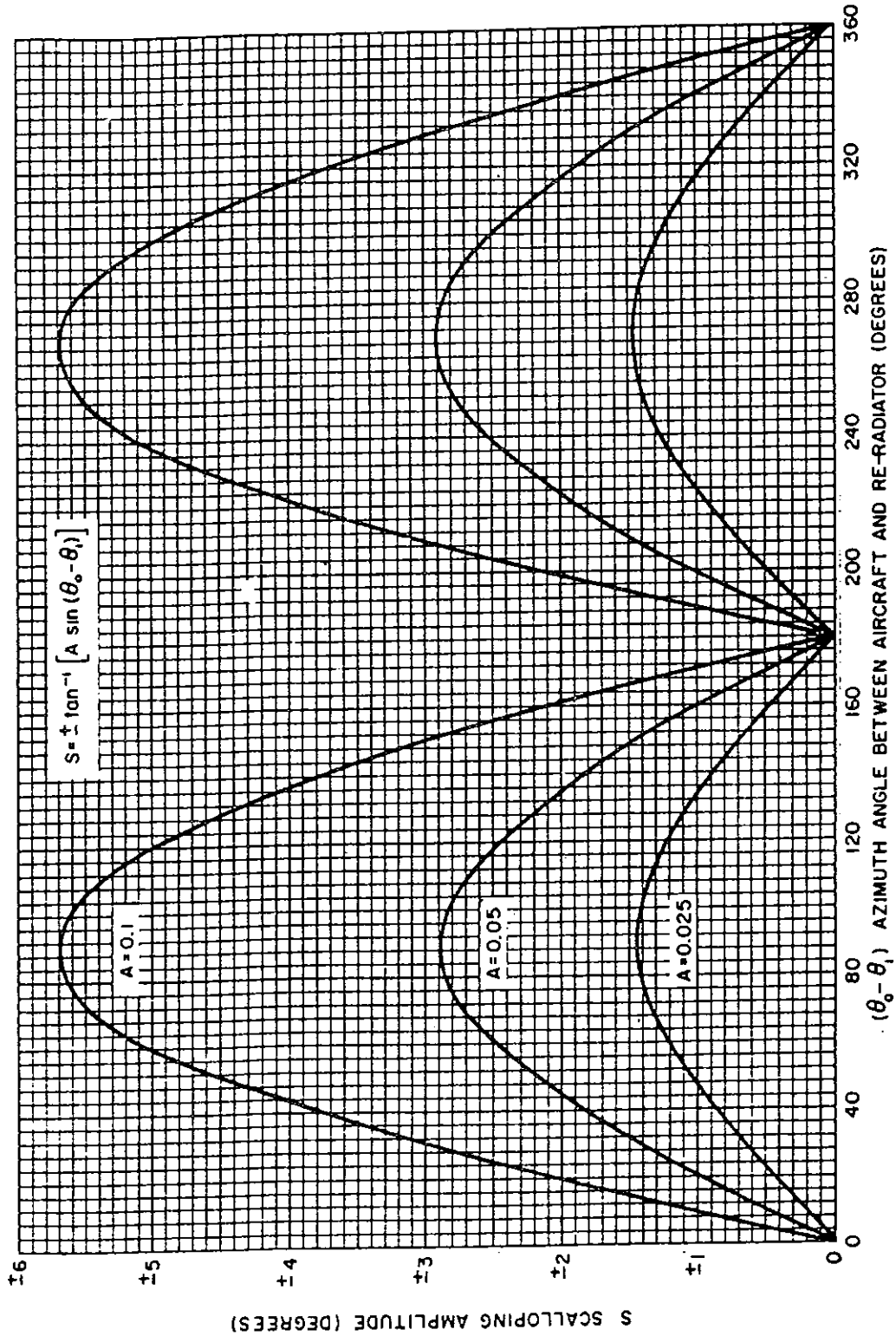

FIGURE 1. SCALLOPING AMPLITUDE VERSUS AZIMUTH ANGLE BETWEEN AIRCRAFT AND RE-RADIATOR

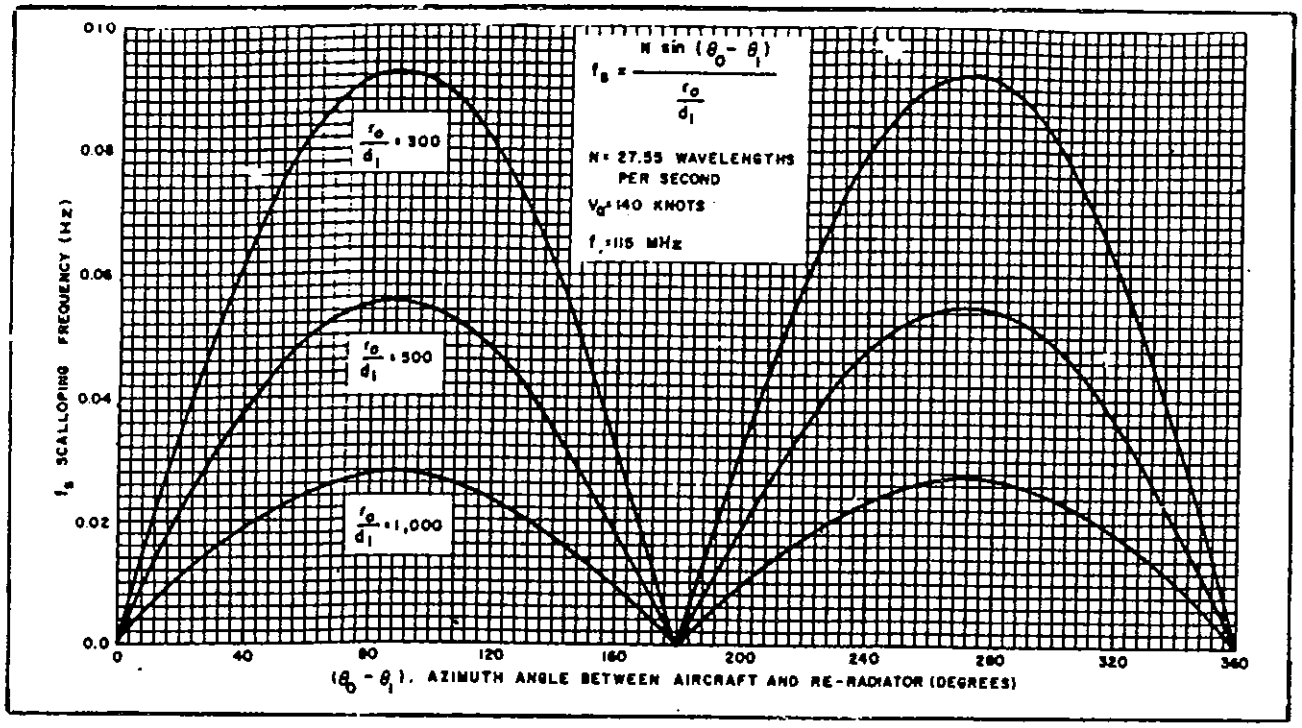

FIGURE 2. VARIATION IN SCALLOPING FREQUENCY WITH CHANGE IN VALUE OF r_o/d_1

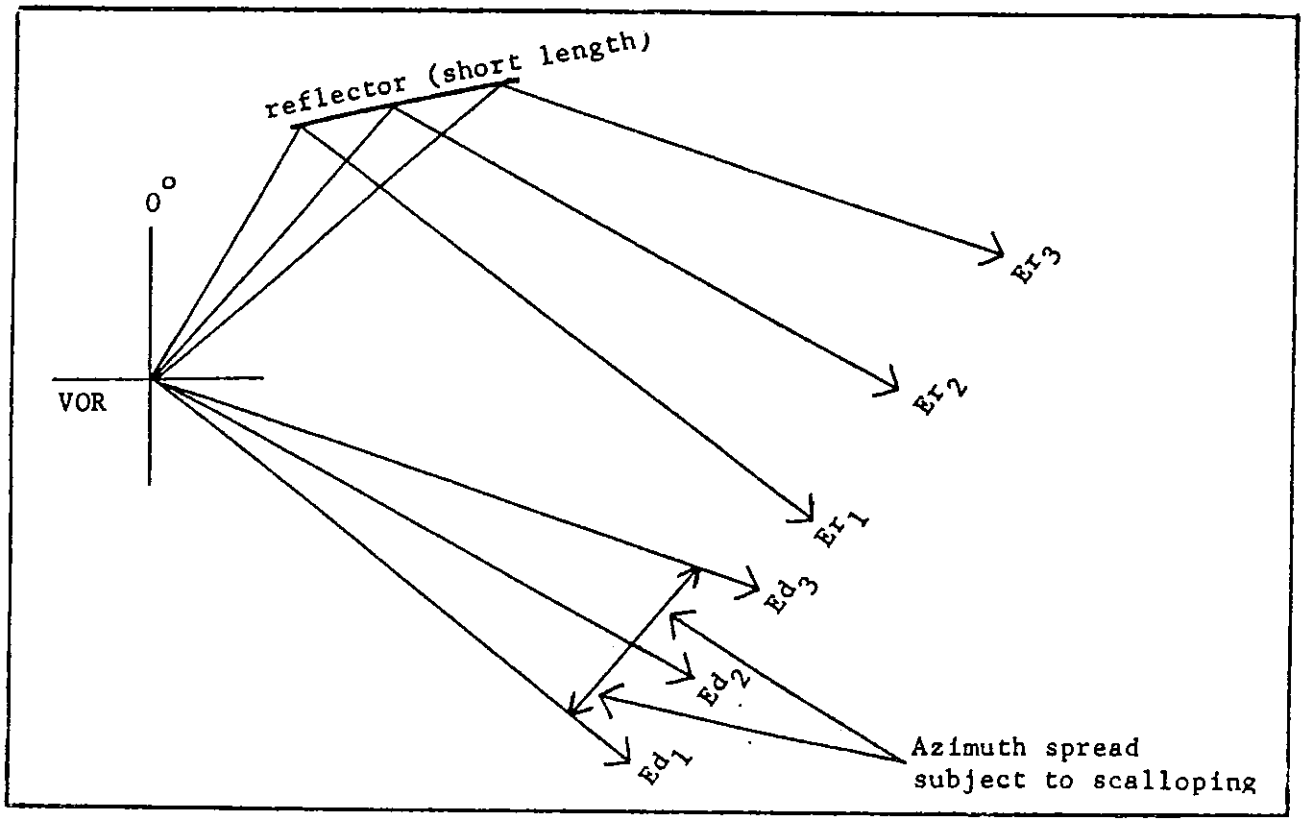

FIGURE 3. SPREAD OF COURSE SCALLOPING AMPLITUDE

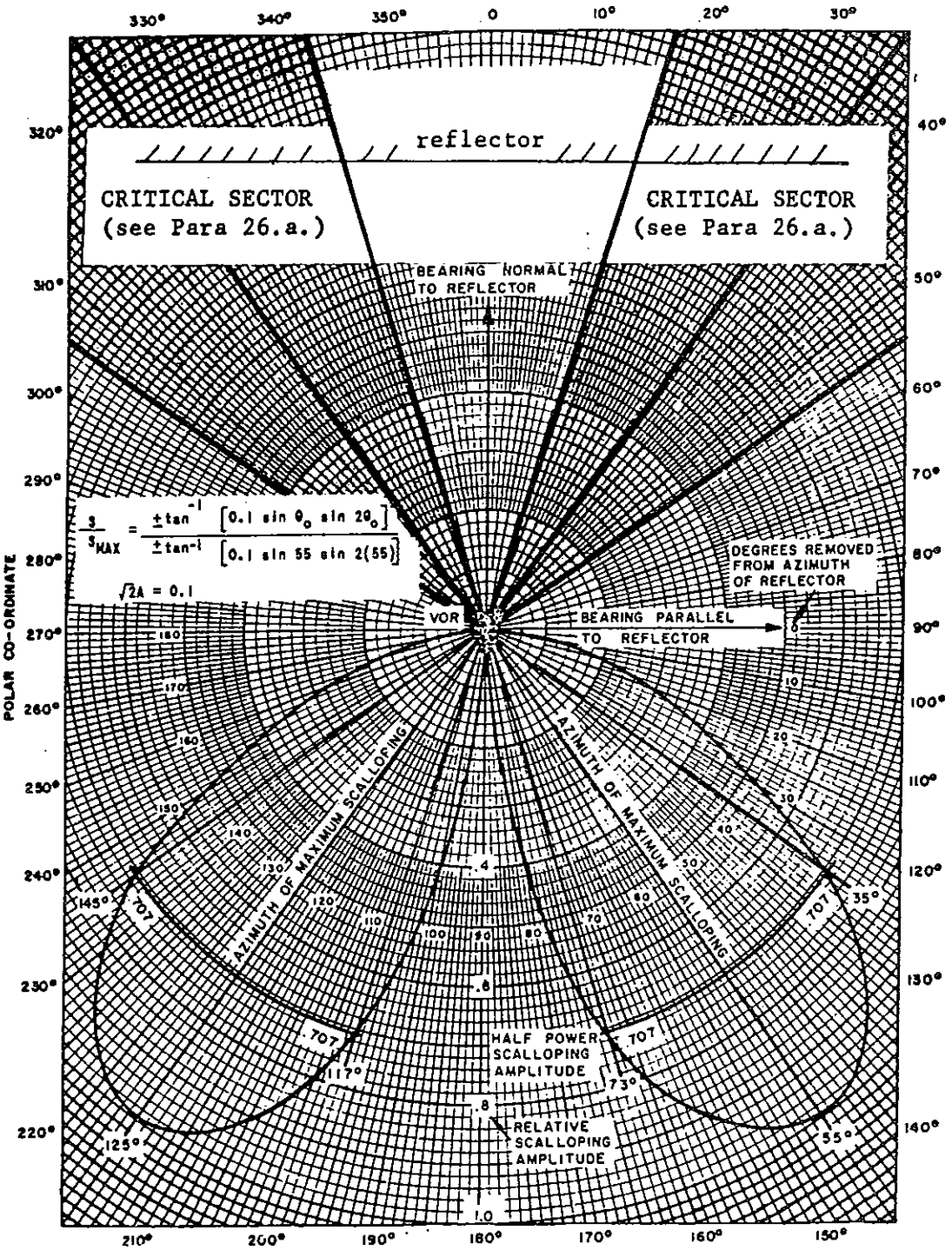

FIGURE 4. RELATIVE SCALLOPING AMPLITUDE DUE TO LONG REFLECTORS

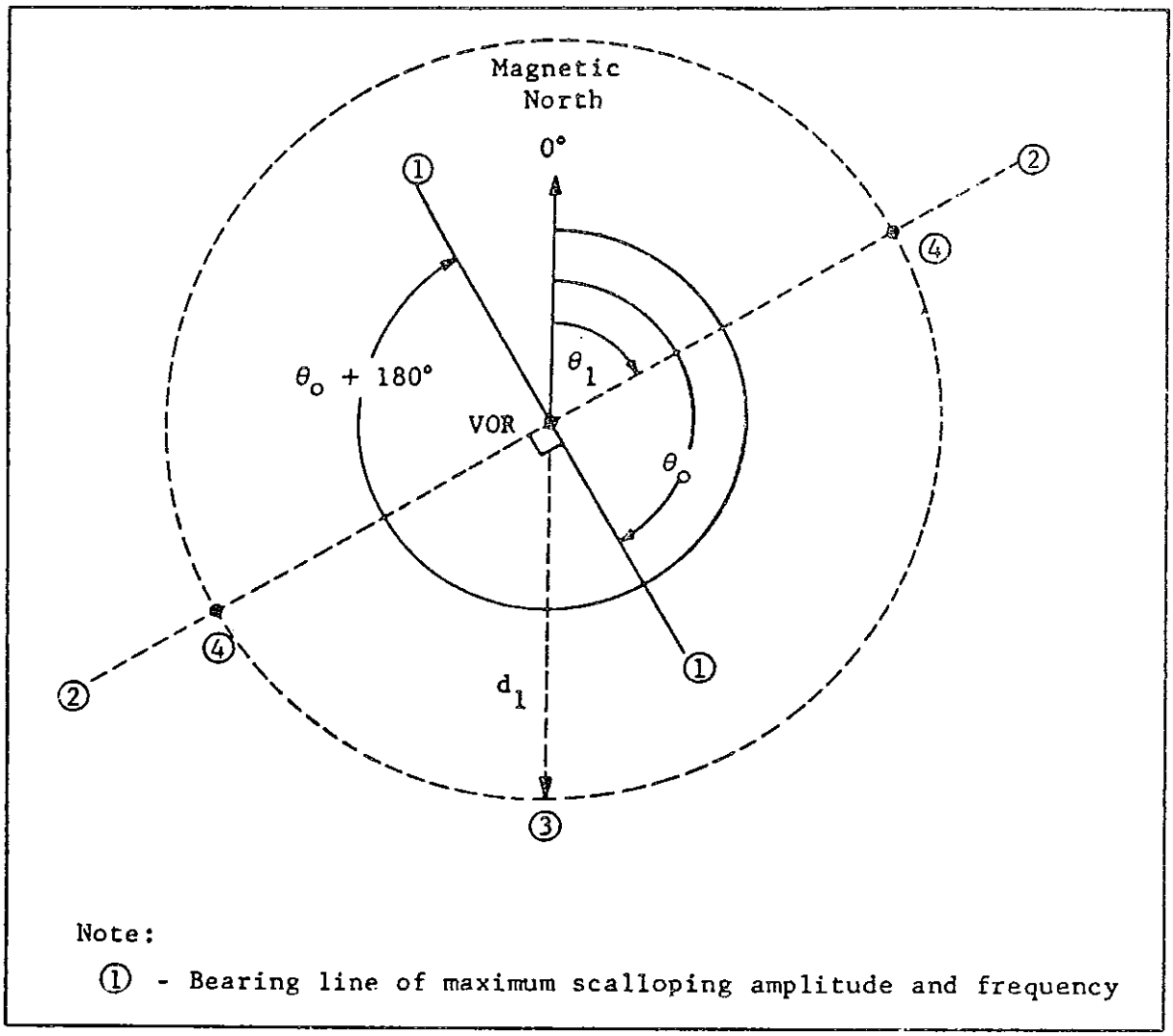

FIGURE 5. LOCATING SOURCES OF SCALLOPING (NON-DIRECTIONAL RE-RADIATOR)

(2) Draw Line ② perpendicular to Line ①.

(3) From the same course deviation recording, determine the scalloping frequency at the maximum scalloping amplitude bearing (Line ①).

(4) Utilizing the scalloping frequency obtained in step (3), determine the ratio r_o/d_1 from figure 6.

(5) Calculate the distance (d_1) and using this as a radius (Point ③), draw a circle around the VOR site.

(6) The points where the circle drawn in step (5) intersect Line ② indicate the two possible locations of the source of re-radiation (designated these points with a ④).

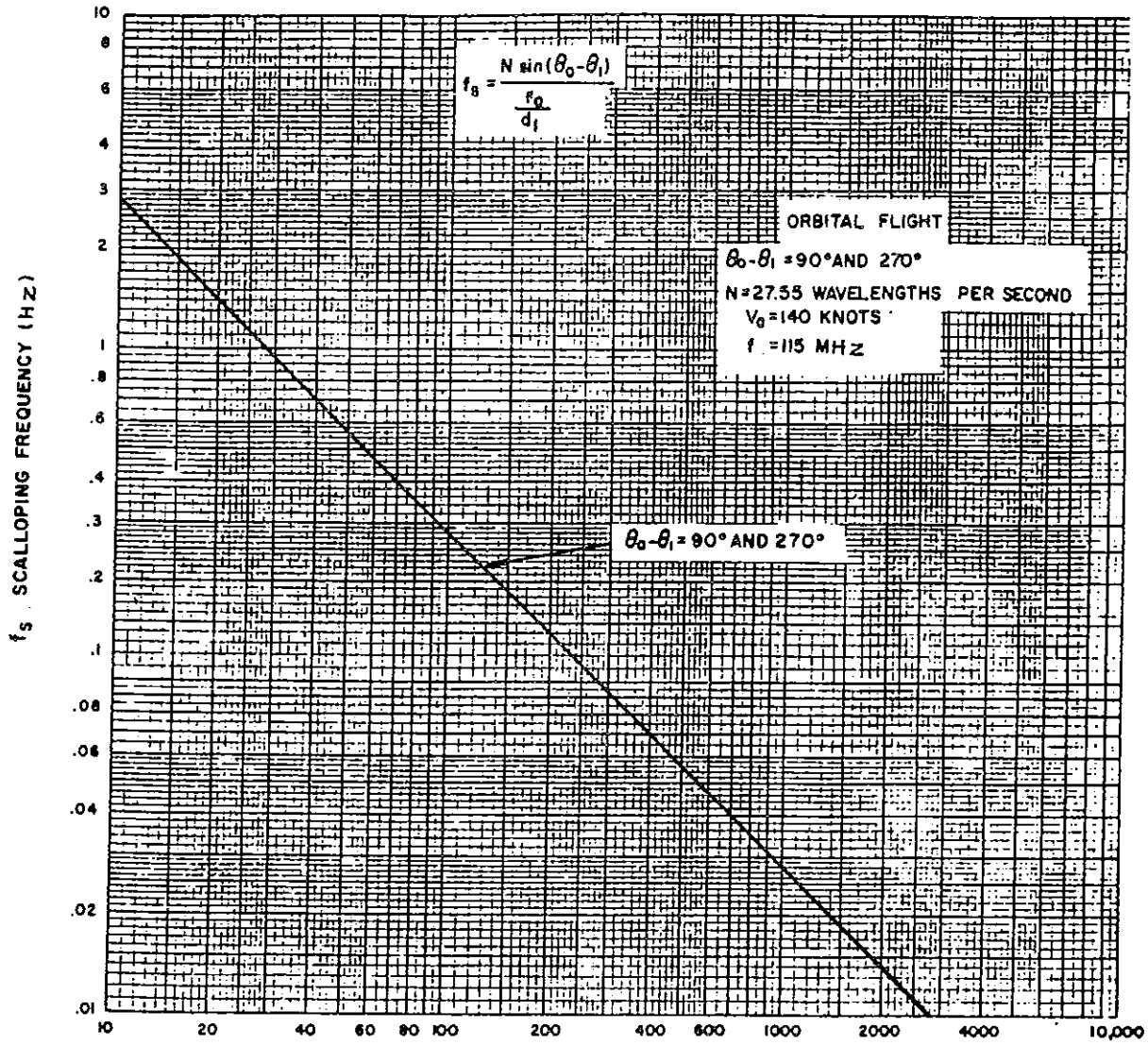

$$\frac{r_o}{d_1} = \frac{\text{Distance from VOR to aircraft}}{\text{Distance from VOR to re-radiator}}$$

FIGURE 6. SCALLOPING FREQUENCY VARIATION ALONG LINE OF MAXIMUM SCALLOPING AMPLITUDE

b. Directional Reflector (long length). Figure 7 is to be used in conjunction with the following procedural outline for locating a directional reflector from recorded scalloping:

(1) From the aircraft course deviation indicator recording of an orbital flight, locate the azimuth angle that exhibits the maximum scalloping amplitude (designate Line ①). Two azimuths separated by about 70 degrees with approximately the same maximum amplitude indicates a long-length reflector (designate one as Line ① and the other as Line ②). Where three or more azimuths of high scalloping amplitude exist, they should be considered separately; also if two azimuths of high scalloping amplitude are not separated by 70 degrees as stated above, they should be considered separately.

(2) From the same aircraft course deviation recording, determine the scalloping frequency at the azimuth of maximum scalloping amplitude (Line ①).

(3) From figure 8, obtain the ratio r_o/d_1 for an incidence angle (a) of 55 degrees.

(4) Calculate the distance (d_1) and draw a circle of this radius (designated as Point ③ around the VOR site).

(5) Draw two lines 110 degrees removed in azimuth from Line ①, and label the point where this line intersects the circle as Point 4 . There are two possible locations for the theoretical point of reflection (a = 55 degrees, see figure 4).

(6) Draw two lines 145 degrees removed from Line ① and label them Lines ⑤. Theoretically, one of these lines is perpendicular to the plane containing the reflector.

(7) Draw two lines (designate as Lines ⑥) perpendicular to Line ⑤ and through their respective Points ④. One of these lines ⑥ represents the plane of the reflector.

(8) Draw two lines 128 degrees removed from Line ①. The two points where these lines intersect Line ⑥ represent the points where a = 73 degrees; label these Points ⑦.

(9) Draw two lines 90 degrees removed from Line ①. The two points where these lines intersect Line ⑥ represent the points where a = 35 degrees; label these Points ⑧.

(10) Lines ⑥ between Points ⑦ and ⑧ show the two possible theoretical locations of the medium-length reflector. These approximate locations should be surveyed to find the actual location.

(11) If two lines of maximum scalloping were drawn in step (1), it is assumed to be a long-length reflector. In this case, there is only one possible plane (Line ⑥) that can contain the reflector. It is the one that is perpendicular to the Line ⑤ that is equidistant from Lines ① and ②.

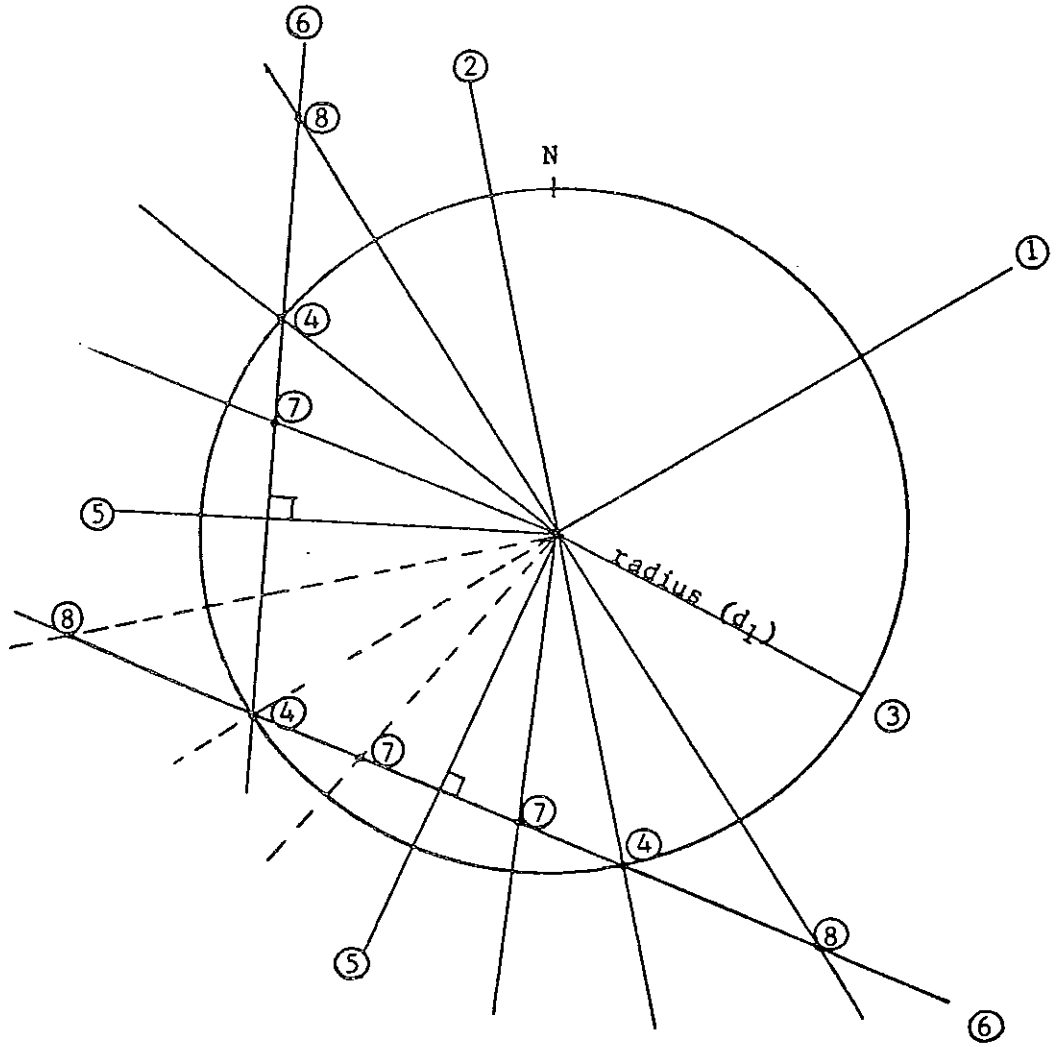

FIGURE 7. LOCATING SOURCE OF SCALLOPING (DIRECTIONAL REFLECTOR) - LONG LENGTH)

(12) The dotted lines drawn 128 degrees, 110 degrees, and 90 degrees from Line (2) and intersecting Line (6) will provide the Points (7), (4), and (8) which correspond to a = 73 degrees, 55 degrees, and 35 degrees, respectively.

(13) Now Line (6) between Point (8) and dotted line Point (8) shows the theoretical location and orientation of the long-length reflector.

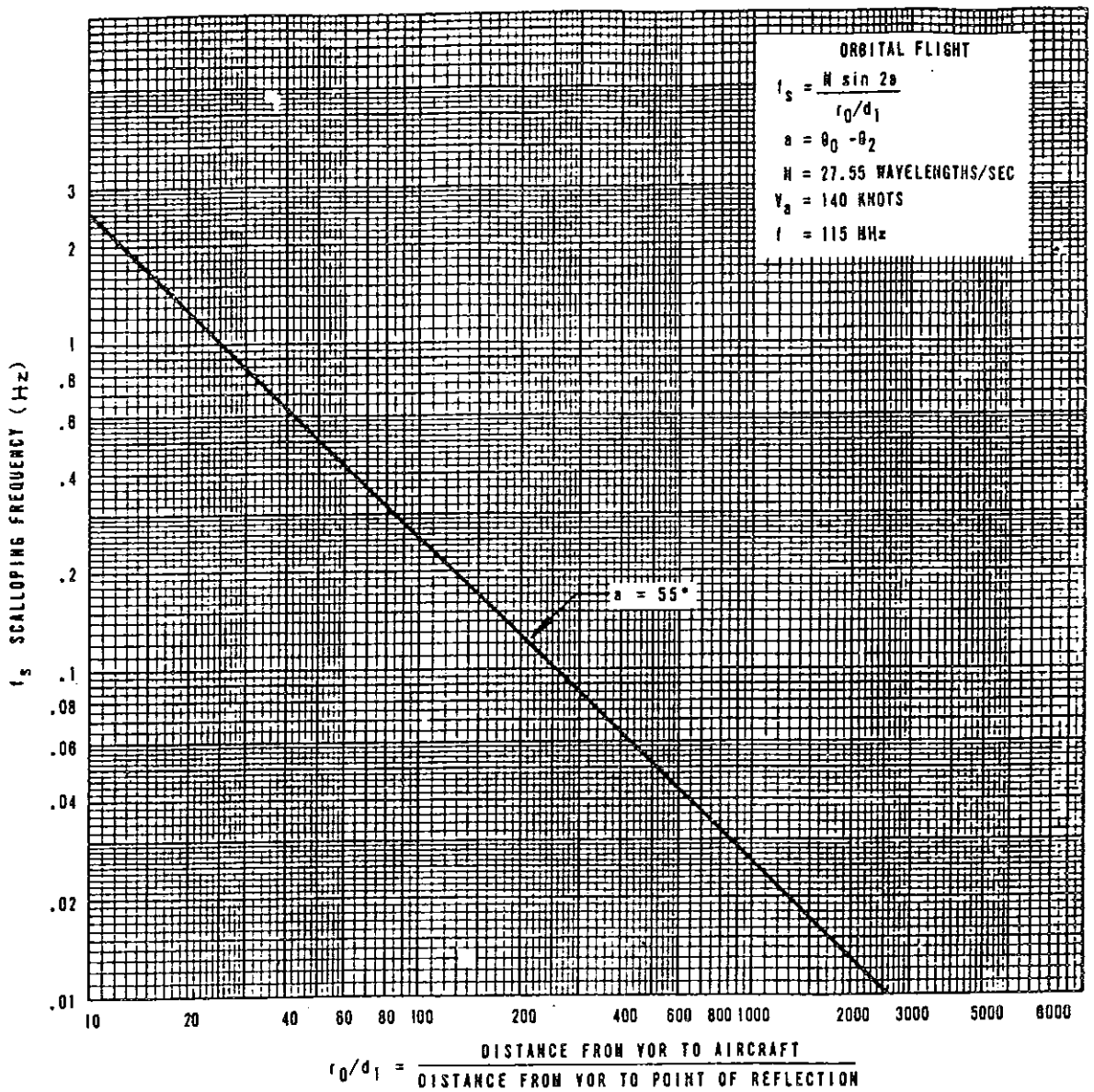

FIGURE 8. PLOT OF EQUATION FOR ANGLE OF INCIDENCE OF 55 DEGREES

c. Directional Reflectors (Short Length). Figure 9 is to be used in conjunction with the following procedural outline for locating a directional reflector from recorder scalloping:

(1) From the aircraft course deviation indicator recording of an orbital flight, locate the azimuth angle that exhibits the maximum scalloping amplitude (designate Line (1)). Where two or more high scalloping amplitude azimuths exist, they should be considered one at a time.

(2) From the same aircraft course deviation recording, determine the scalloping frequency at the azimuth of maximum scalloping amplitude (Line (1)).

(3) From figures 8 and 10 obtain the ratio r_o/d_1 for angles of incidence (a) of 73 degrees, 55 degrees/35 degrees, and 45 degrees.

(4) Calculate the distance (d_1) for each of these r_o/d_1 ratios. Draw three circles about the VOR with radii that are relative to the above distances. These circles represent distance where the angle of incidence (a) equals (73 degrees), (55 degrees/35 degrees), and (45 degrees) and should be designated r_1, r_2, and r_3, respectively.

(5) From figure 4, it can be seen that any azimuth bearing between 125 degrees and 163 degrees removed from Line (1) could possibly be perpendicular to the plane of the reflector. This being the case, any line between 108 degrees and 146 degrees from Line (1) could represent the line where a = 73 degrees.

(6) Draw two lines 146 degrees removed from Line (1) and label the points where they intersect the r_1 radius as Points 2.

(7) Draw two lines 108 degrees removed from Line (1) and label the points where they intersect the radius r_1 as Points (3).

(8) The arc between Points (2) and (3) represents all possible points, where (a) could equal 73 degrees.

(9) Repeat steps similar to (6) and (7) using 128 degrees and 90 degrees to determine Points (4) and (5) on radius r_2. Use 118 degrees and 80 degrees to determine Points (6) and (7) on radius r_3. Use 108 degrees (Line (3)) and 70 degrees to determine Points (8) and (9) on radius r_2.

(10) The arcs between Points (4) and (5) represent all points where a = 55 degrees. The arcs between Points (6) and (7) represent all points where a = 45 degrees. The arcs between Points (8) and (9) represent all points where a = 35 degrees. Connect Points (2), (4), (6), (7), (9), (5), (3) and back to (2) and shade.

(11) The shaded areas should now be surveyed to find the actual point of reflection of the short-length reflector.

(12) Figure 9 can be used as a guide in preparing an overlay drawn to scale for site drawings. In scaling an overlay, the scalloping frequency (f_s) and the site drawing will determine the proper distances for circles r_1, r_2, and r_3.

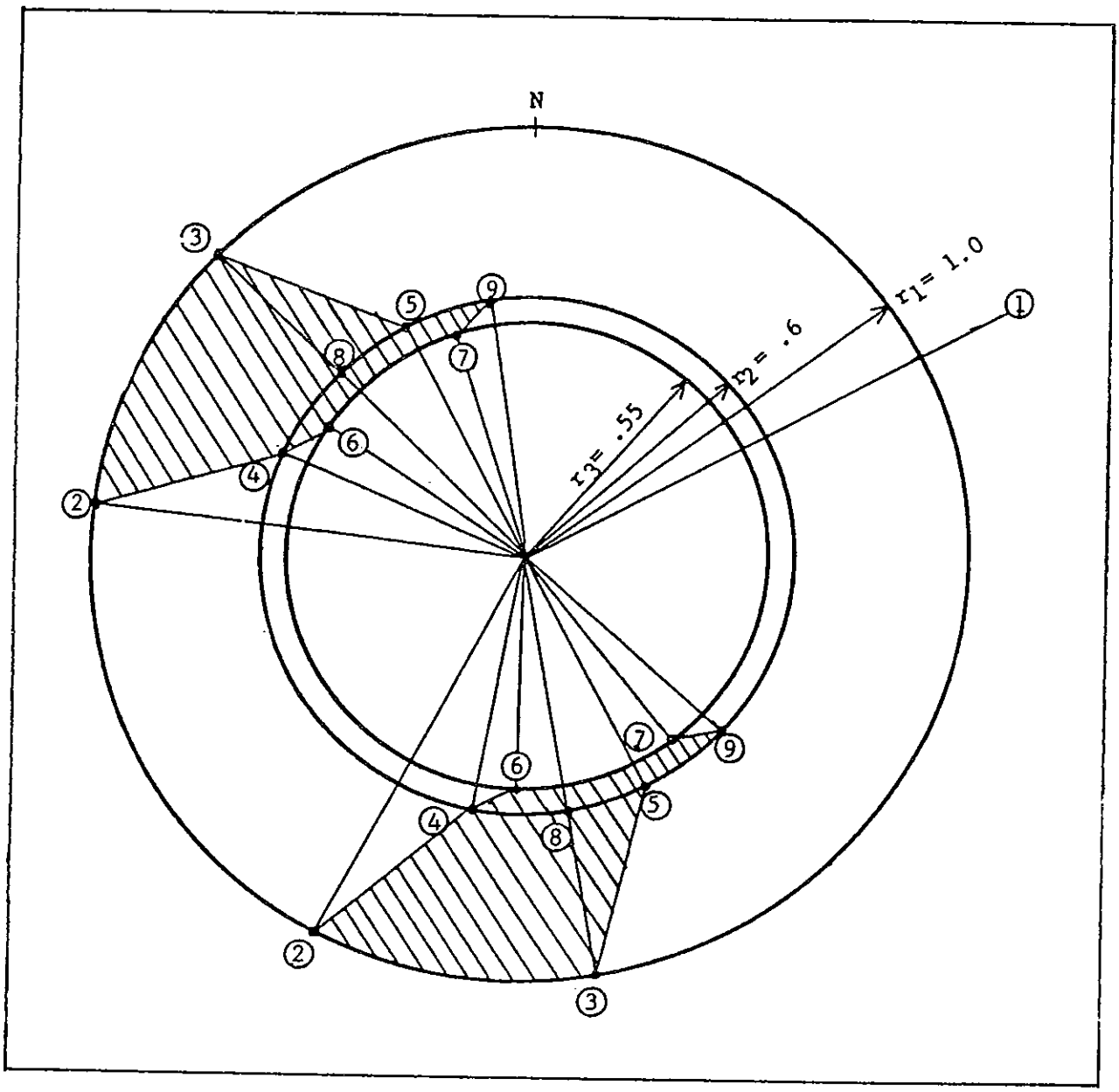

FIGURE 9. LOCATING SOURCES OF SCALLOPING (DIRECTIONAL REFLECTOR - SHORT LENGTH)

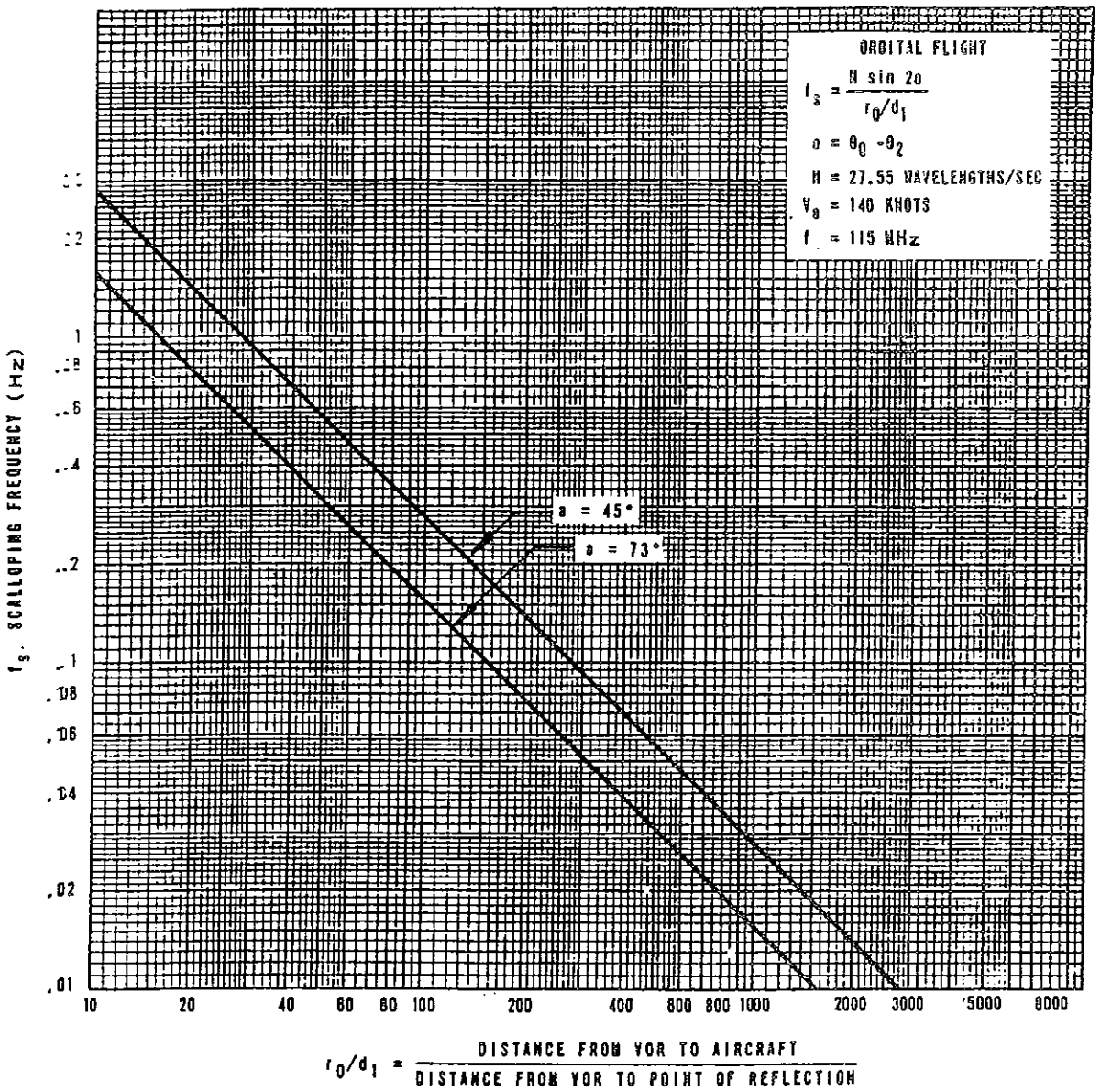

FIGURE 10. PLOT OF EQUATION FOR ANGLES OF INCIDENCE OF 45° AND 73°

LOCATING VOR SCALLOPING SOURCES

by Earl E. Palmer, ANM-431B
FAA Northwest Mountain Region

1. PURPOSE.

Locating an object which is the source of VOR scalloping is a difficult and time consuming task. This report describes two simple, analytical, and accurate methods which will conclusively locate a source of VOR scalloping. These methods have been used successfully in the Northwest Mountain Region for the past 7 years and have located sources as close as 10 feet and as far away as 6000 feet from the VOR. By using a BASIC program and the TI-771 Intelligent Terminal (available in each region Frequency Management Section) or any CP/M base microcomputer and printer, the source of VOR scalloping can usually be located in minutes, instead of hours.

VOR problems which are caused by factors other than reflectors are not discussed in this report. They include improper antenna tuneup, multiple counterpoise effect (common at mountaintop VOR's) or frequency interference. These problems must be resolved by other means. Contrary to what some believe, a VOR does not radiate scalloping. It is the environment around the VOR which causes the scalloping.

The procedures described in this report have been developed independently by the author, with assistance from other engineers in the Northwest Mountain Region. Any resemblance to other methods, if they exist, is purely coincidental.

2. DISCUSSION.

a. General Comments. The methods described in the VOR Siting Handbook, AF P 6700.11, for locating scalloping sources are difficult to use and often give inconclusive results. The methods described in this report use only orbital flight inspection data, either from Semiautomatic Flight Inspection (SAFI) or Saberliner recordings. The limitations of the recordings in locating scalloping sources will be discussed later. Both methods are graphical but provide sufficient accuracy. It should be noted that the terms reflectors, re-radiator, and scalloping source are used synonymously in this report. No distinction is required for the purpose of scalloping analysis.

The first procedure is called the Scallop Counting Method (SCM). It provides satisfactory results for reflectors from approximately 30 to 6000 feet from the VOR, and will be used for the majority of scalloping problems. The SCM is much more convenient when used with a BASIC program and a microcomputer; however, hand-plotted solutions are satisfactory. The microcomputer eliminates the human error and hand plotting. The use of the BASIC program for the TI-771 Intelligent Terminal is described in detail in Section 3 of this report. A BASIC program listing for the Compustar Model 30 is included in Enclosure 5b.

The second procedure described is the Center of Symmetry Method (CSM). This procedure uses orbital data or ground error curves and is useful for finding reflectors very near the VOR, approximately 100 feet or less. Examples are when portions of the VOR counterpoise are re-radiating, or when a VOR monitor antenna or TACAN monitor pole re-radiates. The CSM relies on the principle that the reflector (or re-radiator) causes scalloping that is symmetrical, but out of phase, on each side of the radial on which the reflector is located. All scalloping sources exhibit this property; however as the scalloping source gets farther away from the VOR, the orbital scalloping frequency becomes higher, and will be damped out and lost by the VOR bearing recording process. For VOR ground check curves, the reflector must be on or very near the counterpoise, typically less than 30 feet from the center of the antenna array. For SAFI bearing error reports the scalloping is lost when the scalloping frequency exceeds 3 or 4 scallops in a 10-degree segment. This will allow locating scalloping sources up to approximately 200 feet from the center of the VOR antenna array.

b. Description of the Scallop Counting Method. The mathematical analysis of the SCM is given in Enclosure 5a. Simply stated, the SCM uses the orbital scalloping frequency at several azimuths to determine a locus of points (straight lines) where the scalloping source could be located. The common intersection of three or more of these lines is the location of the scalloping source.

(1) Twin Falls, Idaho, Example. This is the first location where the SCM was successfully used. A hand plotted example will be described.

The procedure is to plot parallel lines on polar paper at a calculated distance each side of the VOR, which is located in the center of the paper. These lines are parallel to the VOR radial where the scallops were counted. As the flight check VOR orbital recordings incremented every 10 degrees with the DC-3 aircraft, it was arbitrarily decided to count the scallops in 10-degree segments of the orbit. At Twin Falls, severe scalloping was reported by users on the airway using the 112-degree radial. Subsequent flight checks confirmed the scalloping, and the airway was removed. Extensive analysis of the radial flight check recordings was inconclusive.

A 20-mile orbit at 4000 feet above the site elevation was flown by flight inspection. Due to the speed to the Saberliner aircraft and the damping of the VOR bearing recording, scalloping was not observed. Analysis of the VOR receiver AGC voltage recordings did show amplitude changes which were uniformly spaced and which could be counted over 10-degree segments of the orbit.

The following data were obtained from the recordings and the formula D=49N (see Enclosure 5a):

Radial in Degrees	Number of Scallops N	Distance D in Feet
20	7	343
115	44	2156
180	21	1029
295	46	2254

As shown in Figure 2-1, two lines were plotted on polar graph paper at the calculated distance D from the center of the polar graph paper, and parallel to the radial. In other words, A and A1 are parallel to the 20-degree radial, and scaled 343 feet from the 20-degree radial. The common intersection of three or more lines is the solution to the problem. Note that two solutions exist, at approximately 2200 feet from the VOR on reciprocal radials of 28 and 208 degrees. At Twin Falls the ATCT is located 2220 feet from the VOR on the 31 degree radial. Subsequent screening of the ATCT reduced the scalloping to an acceptable level, and the airway using the 112 degree radial was restored to service. A computer plot is given in Example 3e(2) of this report.

(2) Analysis of Flight Inspection Recordings. The most critical part of location scalloping sources using the SCM is the analysis of the flight inspection recordings. Many limitations of the recordings mask the scalloping and make analysis difficult. The primary limitation is the damping of the bearing recording in the flight check receiver. As the reflector gets farther away from the VOR, the scalloping frequency increases. A scallop, which is defined as one complete periodic waveform (a distorted sine wave), is damped out by the flight check receiver circuits if its rate is greater than approximately 1/2 cycle per second. To prevent this, either a larger orbit or a slower aircraft is required. Figure 2-2 is an example of VOR bearing scalloping. Note that the two bearing recordings do not track. This has been traced to the auto-calibrate circuit in the Bendix RNA-26CF (FA-4165.3A) flight inspection receiver, which realigns the receiver bearing circuits for 1 second out of every 5. When this circuit is disabled, excellent tracking of two receivers usually occurs.

Analysis of the VOR receiver AGC voltage is also useful, and can be used as the basis for locating the scalloping source. Usually much higher scalloping frequencies can be observed on the AGC recording. Figure 2-3 is an example of scalloping on the VOR AGC voltage recording.

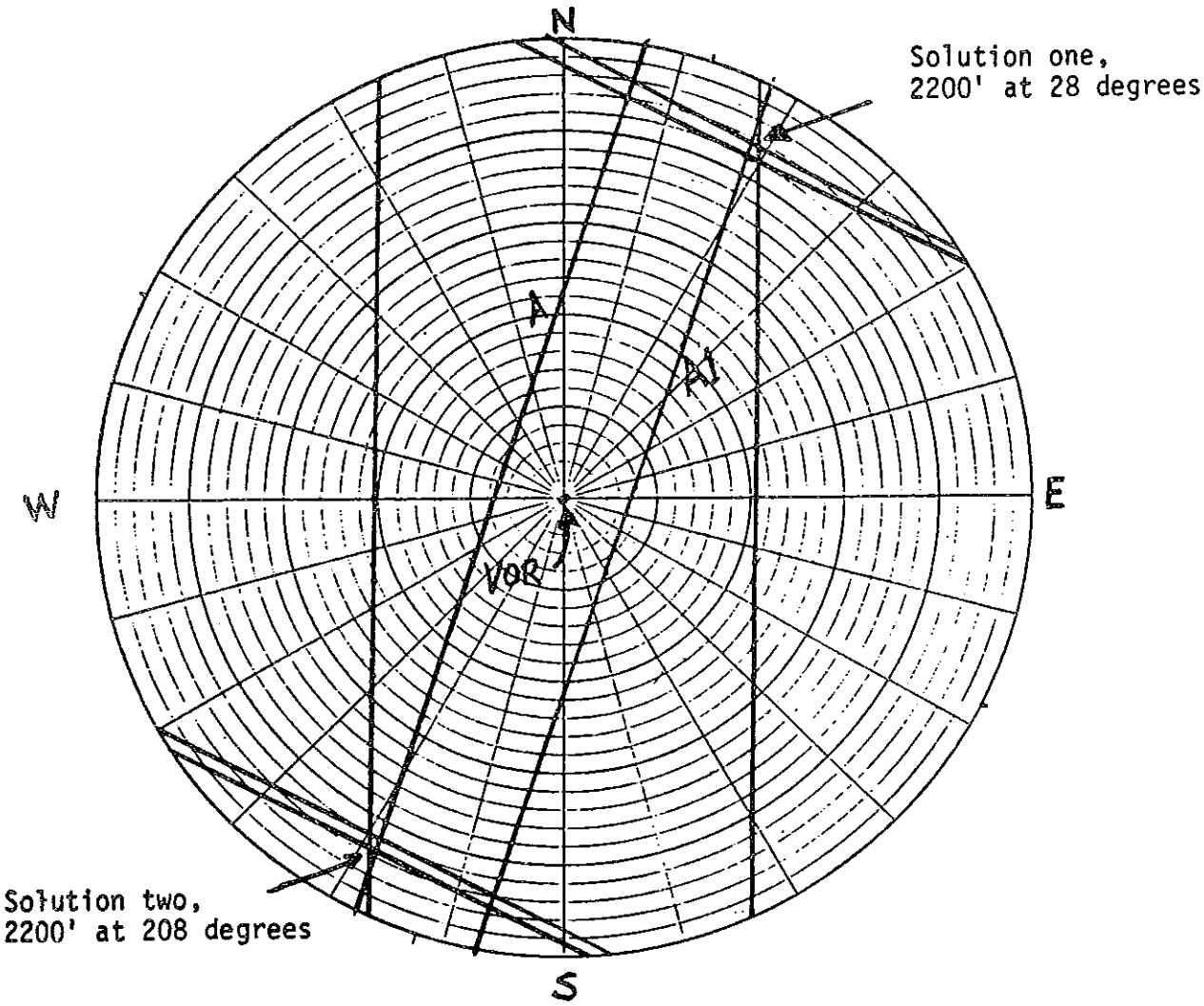

Scale 1" = 1000'

FIGURE 2-1

Figure 2-2 Example of VOR bearing scalloping. Note that the scalloping is approximately the same on both receivers, and that the distance between the scallops is approximately equal. The vertical lines are drawn at the peak of the computed bearing error trace, which is slightly delayed from the raw data.

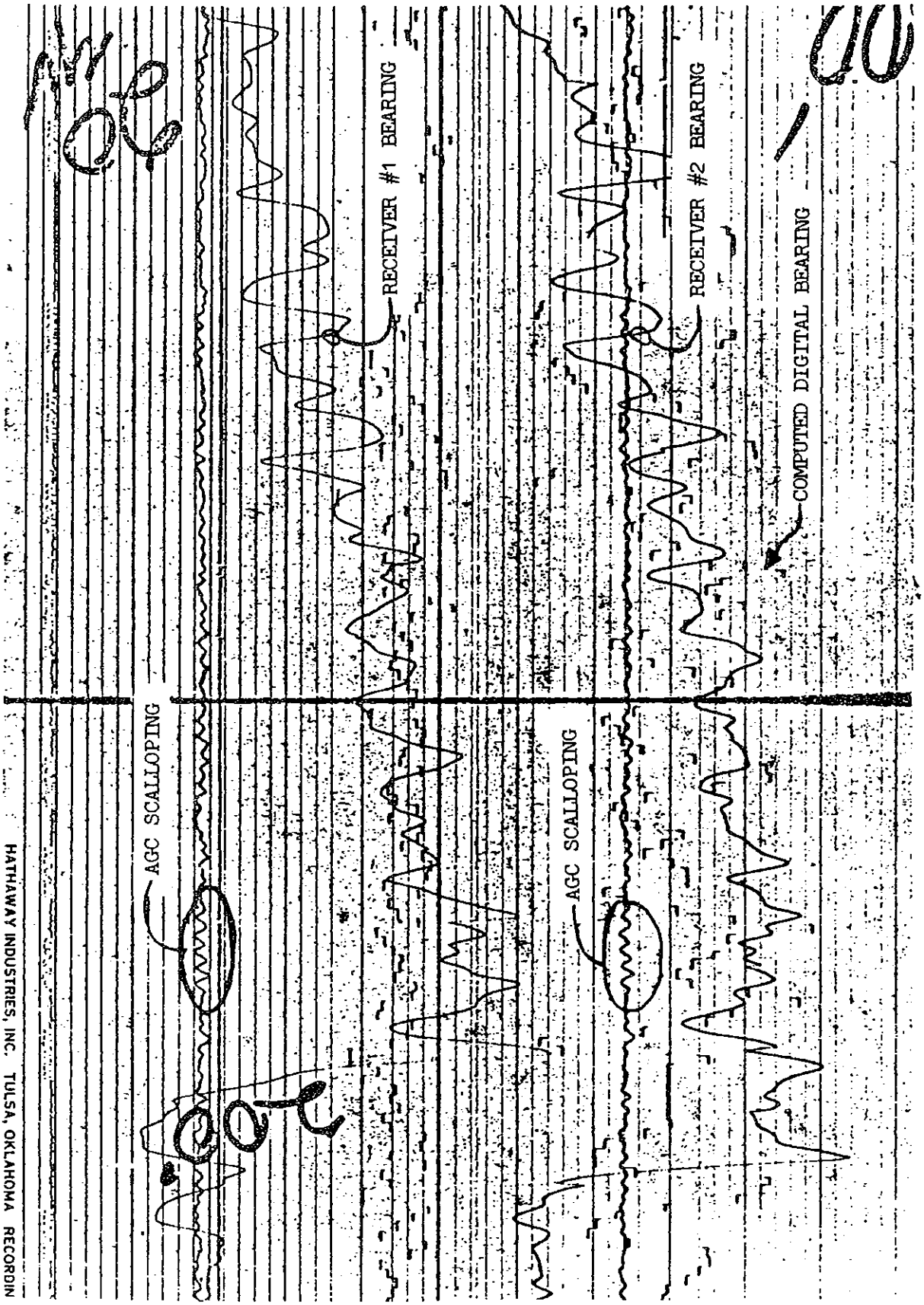

Figure 2-3 Example of VOR receiver AGC scalloping. The number of scallops is counted over a few degrees and then extrapolated out to 10 degrees. Note that the VOR bearing traces are different on each receiver. This indicates that the scalloping frequency is beyond the cutoff frequency of the filters in the bearing indicator circuits.

A similar problem occurs if the scalloping source is within 100 feet of the VOR. Then the scallops are so long that they are not apparent on the recordings. In this case, analysis of SAFI BER's will provide the best results. Scalloping analysis of BER's is shown in Examples 3e(1) and 3e(5).

Analysis of flight inspection recordings requires proper judgment as to what a scallop is, and some experience. In general, the following guidelines should be followed:

(a) Make sure the scalloping has a periodic waveform, and has a constant frequency over several cycles.

(b) If the scalloping is periodic but the duration is less that 10 degrees of the orbit, determine the number of scallops in a portion less than 10 degrees, and extrapolate the data for the full 10 degrees.

(c) If the scallop is very long, as occurs on SAFI BER's, the length of the scallop can be determined in degrees. Then the fractional part of a scallop (occurring) in 10 degrees can be determined. See Example 3e(5).

(d) Scallops should be counted on as many radials as possible. It takes a minimum of three to get a solution; however all significant scallops should be plotted.

(3) Flight Inspection Preplanning. In most cases, a special flight inspection is required. As flight inspections are expensive, preflight planning should be accomplished to insure that satisfactory recordings are obtained. In general the DC-3 was preferable to the Saberliner as it flew slower, and more scallops could be observed for the same orbit radius. A light aircraft with the portable flight inspection package probably would be satisfactory; however this option has not been available in the Northwest Mountain Region. With proper planning Saberliner recordings are usually acceptable.

The orbital altitude and distance are of primary concern. As the radius of the orbit is increased, scalloping from a reflector at a greater distance from the VOR can be observed. The table below gives the approximate maximum distance that scalloping can be observed on either the bearing or AGC recording.

Orbit Radius	10	20	30	40	50	Miles
DC3 Bearing	1100	2200	3300	4400	5500	Feet
DC3 AGC	2200	4400	6600	8800	11000	"
Jet Bearing	600	1200	1800	2400	3000	"
Jet AGC	1200	2400	3600	4800	6000	"

The above table is based on an air speed of 140 knots for the DC-3, 260 knots for the jet, a maximum bearing scalloping frequency of 0.5 Hz, and a maximum AGC scalloping frequency of 1.0 Hz.

The altitude of the aircraft is also very important. In general, if the altitude of the orbit is very high the scalloping is reduced as the direct signal from the VOR tends to increase in amplitude more than the signal from the scalloping source which receives a low angle VOR signal. Conversely, if the aircraft altitude is low, the signal levels are reduced and the recordings become noisy. Then it is difficult to separate the scalloping from the noise. As a general rule it is better to fly lower, where the scalloping is more apparent, as is done on a minimum coverage orbit, and then spend a little more time separating the scalloping from the noise.

Another method to determine the optimum orbit altitude is to locate where maximum scalloping exists on a radial flight. The angle of maximum scalloping can then easily be determined and extrapolated out to obtain the orbital radius altitude. It should be noted that the scalloping sources have characteristic radiation patterns, which can include nulls, minimums, and maximums. Therefore, it is possible that the flight path could be in a reflection null or minimum, and no scalloping would be observed.

With the Automatic Flight Inspection System (AFIS) of the Saberliner aircraft it is not necessary that an orbit be flown. The distance between the VOR and the aircraft does not enter into the calculations. As long as the bearing of the aircraft from the VOR is known, straight or even curved segments are satisfactory. With AFIS, several segments around the VOR may be recorded during routine travel on flight inspections when the aircraft is in the vicinity of the VOR. These may be at a greater distance than an orbit would normally be flown, and the scalloping will possibly be more apparent. Depending on the urgency of the scalloping problem, this approach may be satisfactory, and a special and expensive orbit may not be required.

c. Description of the Center of Symmetry Method (CSM). The CSM uses SAFI BER's, or Saberliner orbital error plots made on FAA Form 8240-4, to locate reflectors that are less than approximately 75 feet from the VOR. For very close reflectors, the VOR ground check error curve may be used. This graphical method is very simple and usually quite conclusive. It is based on the principle that bearing errors produced by a reflector are symmetrical and out-of-phase on each side of the radial on which the reflector is located. No proof is given here for this statement; however, it is intuitive that an object will reflect a signal which has the audio phase of the space modulated 30 Hz AM signal of the particular azimuth on which it is located. This reflected signal will add to the phase of the space modulated signal at azimuths on one side of the reflector, and subtract on the other.

To accomplish a CSM analysis, a bearing error plot must be prepared on transparent paper. The plot is then cut out and taped together at the 0-, 180-, and 360-degree points to make a

continuous loop. The loop is then examined on a light table so that each half can be seen superimposed on the other. For example, 0 to 180 degrees would be visible from the front half of the loop, and 180 to 360 degrees would be visible from the back half of the loop through the front half of the loop. The loop is then rolled so that the front and back halves move in opposite directions.

As the patterns of the curves are observed it will be obvious when the bearing errors are out-of-phase and symmetrical as shown in Figures 2-4, 2-5, and 2-6. The lobes formed are rounded and have a distinctive shape. When this pattern is observed, the scalloping source is located at the azimuth at either end where the paper is folded. Usually the scalloping source will be at the azimuth represented by the fold where the error lobes are the largest. It is possible to develop a computer analysis of the CSM; however the graphical method is very simple and quick. A computer solution would probably take a great deal of time to input all the flight inspection data unless it was automatically done by the flight inspection aircraft computer.

The CSM should only be used after a standard Fourier Analysis of the VOR error curve has been made, especially if the error curve has only a few cycles of error over the full 360 degrees. A bearing error from a reflector will often show up as an unusual harmonic component of the VOR Fourier Analysis. Typically it will appear as third, fifth or higher order components, if the analysis method is capable of producing them.

d. Distance to the Scalloping Source. A very simple and useful relationship exists to determine the distance to close-in reflectors. This relationship only is useful when one predominate reflector causes scalloping which is observable on the entire SAFI or Flight Inspection FAA Form 8240-4 bearing curves. See Figure 2-7 for an example. The distance to the reflector, from the center of the VOR array, is calculated using the formula:

$$D = (\lambda N) / 4 \text{ or } D = 2.15N \text{ @ } 115 \text{ MHz}$$

where λ = wavelength and N = the total number of scallops produced in a 360-degree orbit.

In the example shown in Figure 2-7, 23 scallops are counted in 360 degrees, which indicates that the reflector is 49.22 feet (2.14 x 23) from the antennas radiation center. Some of the scallops are difficult to determine, however, this is not an exact science. An error of $\pm$ three scallops would still give a reasonably accurate answer. This same location is also analyzed in Example 3e(6) with the Compustar microcomputer using the scallop counting method. This procedure indicates the source is at 50 feet on the 43- or 223-degree radial. The Tacan monitor pole is located at 50 feet on the 45-degree radial at this location.

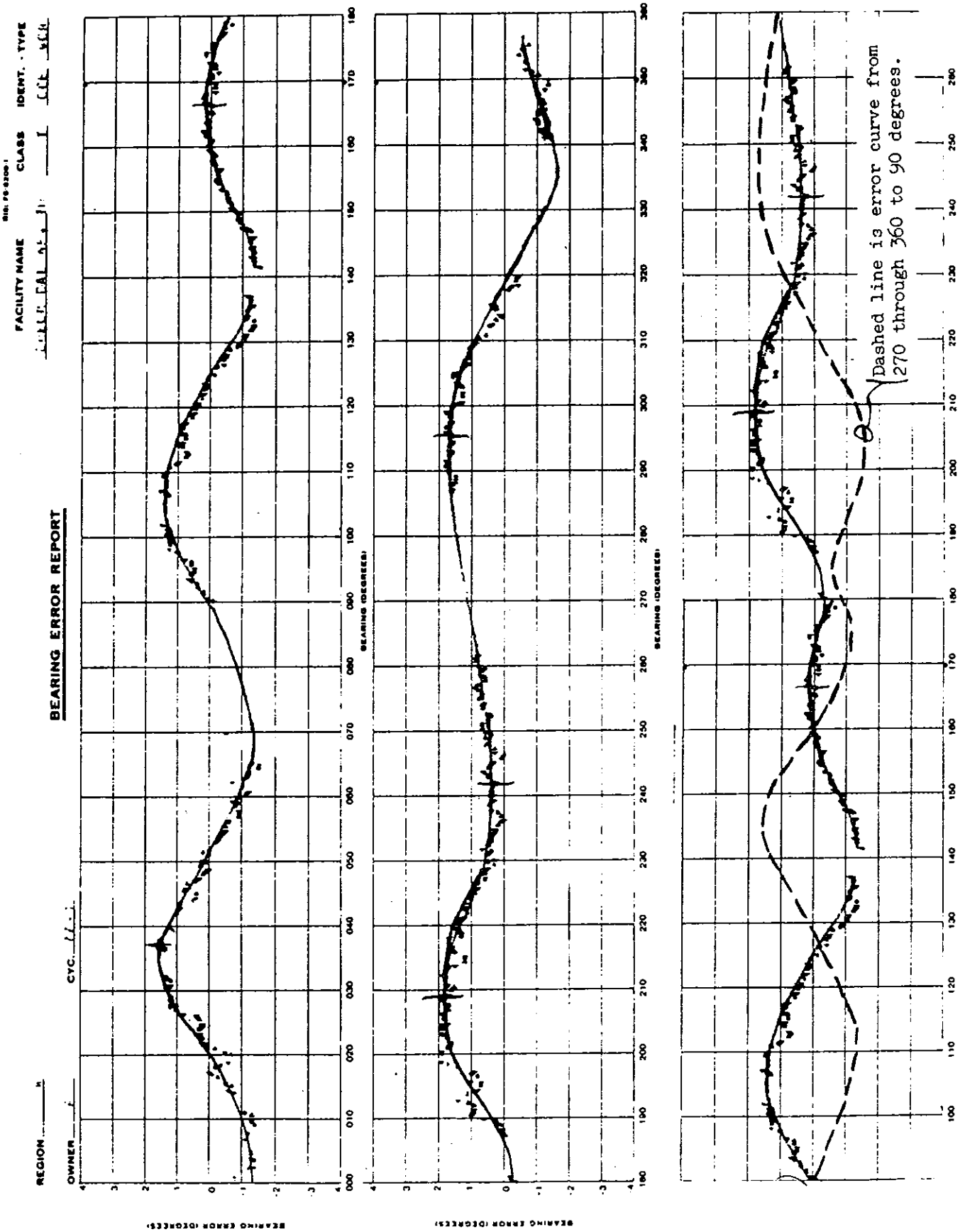
BEARING ERROR REPORT
FACILITY NAME
CLASS
IDENT. - TYPE
REGION
OWNER
CYC.
BEARING (DEGREES)
BEARING ERROR (DEGREES)
Dashed line is error curve from 270 through 360 to 90 degrees.

FIGURE 2-4

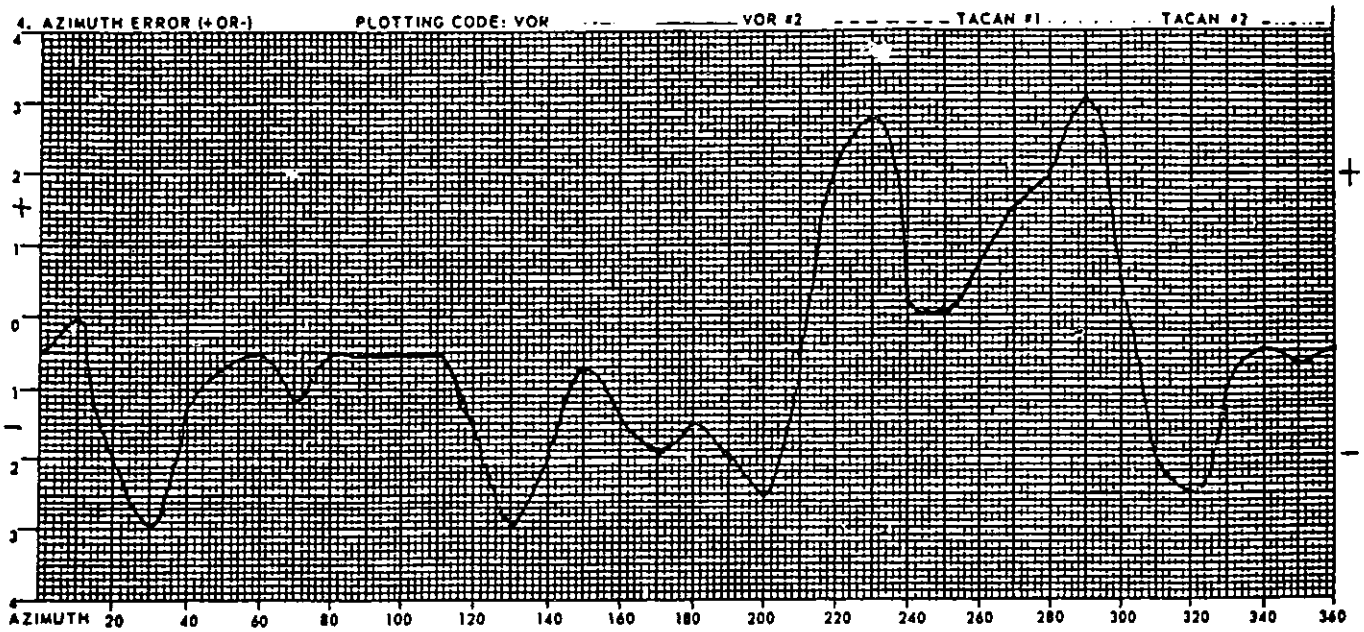

Mountain Home, Idaho, VOR error curve obtained from a FIFO Saberliner Automatic Flight Inspection, Form FAA 8280-4.

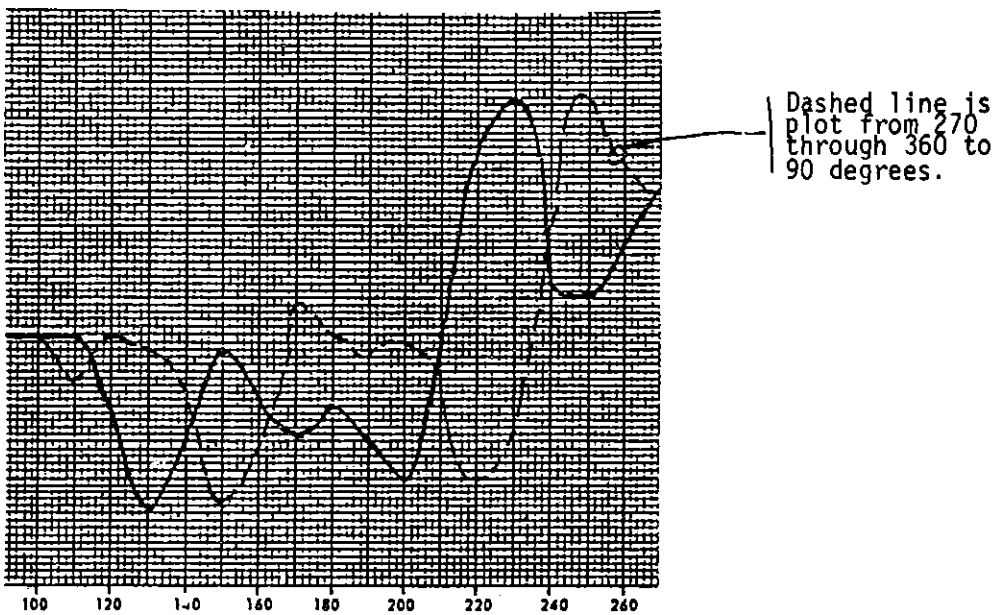

Center of symmetry solution shows the reflector is either at 90 or 270 degrees. Note that the two error curves (dashed and solid lines) are symmetrical and out of phase about 90 or 270 degrees. At Mountain Home this error curve occurred on a new Wilcox VOR facility when a large 36-inch monitor dipole was used on the 270-degree radial. Reducing the size of the dipole eliminated the problem.

FIGURE 2-5

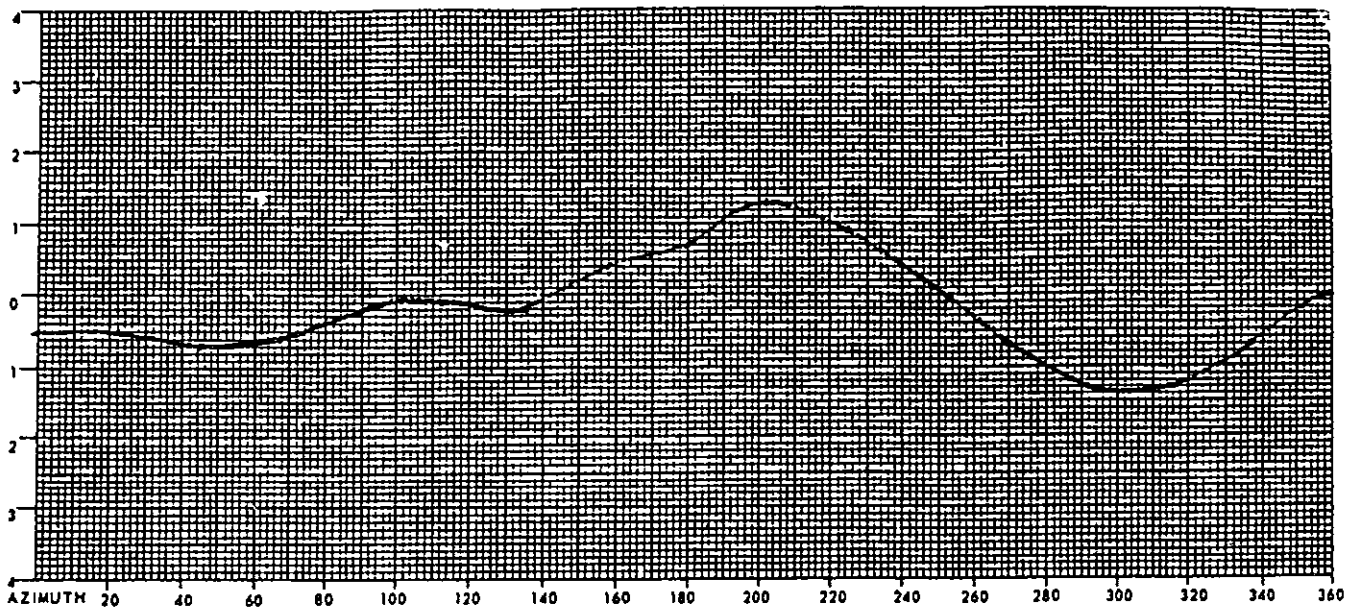

Pasco, Washington, VOR ground error curve, obtained after antenna optimization. This curve could be brought into tolerance, only by maladjusting the antenna system.

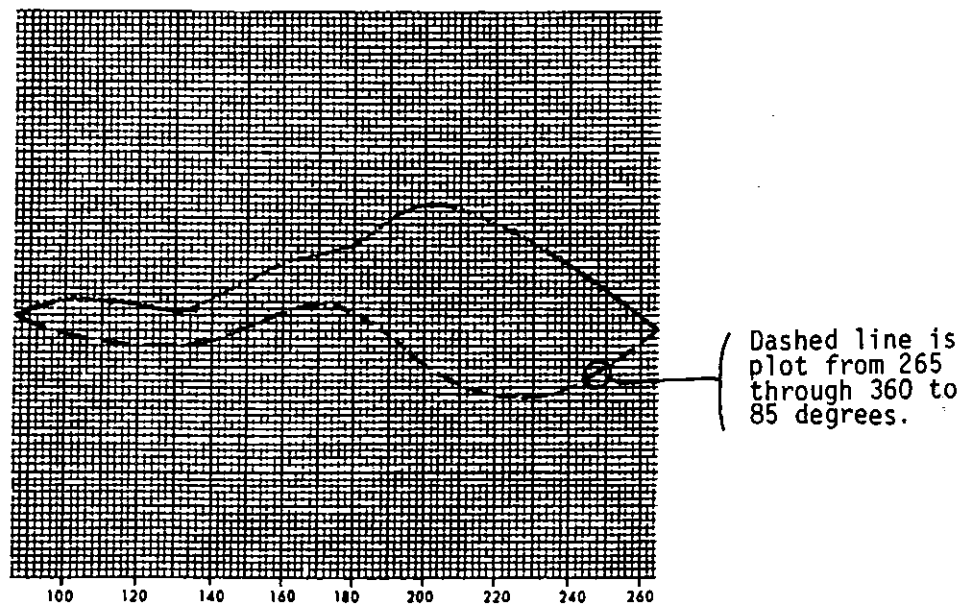

Center of symmetry solution shows a reflector is either at 85 or 265 degrees. Removal of a ladder bracket on the TACAN radome at 260 degrees completely changed the shape of the ground error curve to well within tolerance, without maladjusting the antenna system.

FIGURE 2-6

BEARING ERROR REPORT

REGION NW OWNER F CYC 81-1 FIFO SEA CLASS L IDENT BYI TYPE VOR

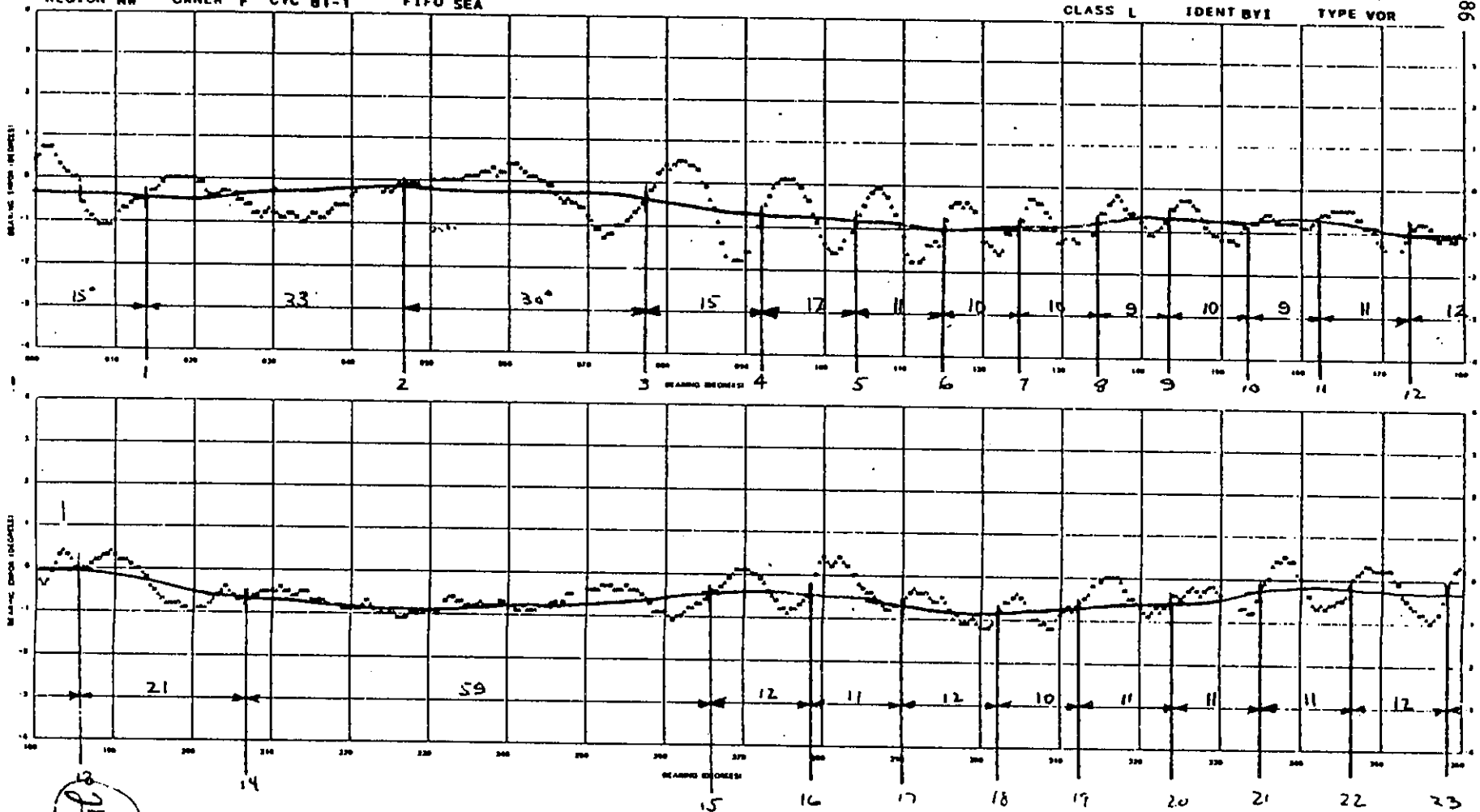

SUMMARY HISTORY BY SECTORS

DATE	FLIGHT NO	AIRCRAFT	ALTITUDE	BEARING START	BEARING DIR	BEARING END	DISTANCE MAX	DISTANCE MIN	DIST BEAM ERROR	AVG AIR	AVG SCH
08-03-81	613	092	25000	180.5	CW	276.0	74	49		31	27
02-04-81	609	091	23100	270.5	CW	5.5	103	69			
08-19-80	625	091	23100	186.5	CCW	91.5	71	47			
07-18-80	604	091	23100	96.5	CCW	1.5	104	70			

FACILITY CHARACTERISTICS

BEAM ERROR (DEG)	DISPERSION RANGE 68%	95%	99.7%
-0.5	-0.0	-0.4	-0.7
	-1.0	-1.5	-1.8

Figure 2-7

3. COMPUTER ANALYSIS USING THE SCALLOP COUNTING METHOD.

a. General Comments. Computer analysis using BASIC programs with the TI-771 Intelligent Terminal has evolved from several more primitive methods. The first was a plot on graph paper as described in Section 2 of this report. The second method was a program on a Monroe 1666 desk top programmable calculator and PL-1 plotter. This was very satisfactory and was used successfully in the Northwest Region for 3 years. However, the Monroe calculator is generally not available to other regions. The TI-771 Intelligent Terminal and BASIC interpreter resolves this problem. The Northwest Mountain Region has two TI-771 systems available, one in Frequency Management, and the other available through Management Services. Compustar Model 30 microcomputers are also available in many sectors and regions. A Microsoft BASIC program has been written for these computers.

The BASIC program has the filename VORSCAL. The program is written in the simplest form of BASIC possible. It has been run with only minor syntax changes on a Heathkit home computer system. The Northwest Mountain Region will provide a copy of the VORSCAL program on a disc provided by any FAA user (either an 8-inch disk for the TI-770 or a 5 1/4-inch disk for the Compustar Model 30). The program is written to work with most any printer, however it should print with 10 characters per inch and 6 lines per inch for the plot scale to be correct.

b. Running the Program. Don't be awed by a microcomputer. It won't blow up if you make a mistake. It is impossible to harm the program stored on the disc from the keyboard while running the program. So if for some reason you have trouble, reset the computer and start again from the beginning. A review of the computer instruction book may be helpful, but is really not required to run the VORSCAL program.

Extreme care should be used in handling the program storage discs. Prior to using them you should be checked out by someone familiar with their use. The recording surfaces on the disc should never be touched. A minute particle of dirt or grease on the disc can destroy a program which has taken hours to produce. Also the discs should be stored in an appropriate container, not in a desk drawer or anywhere they will collect dust or dirt.

c. Using the TI-770. After the flight check recordings have been analyzed and the scallops counted at several azimuths, the VORSCAL program is run as follows:

(1) Turn on the power to the video terminal, printer, and dual disc drive.

(2) Insert the BASIC disc into disc drive 1 (the left hand drive) and the VORSCAL disc into disc drive 2. The computer will now read disc 1 and start to prompt you through the program.

(3) Press the "D" and "return" keys when asked what mode of operation is required.

(4) Enter the date and time as requested by the computer. Use the exact format as requested. When asked to give a station number, press the return key. A station number is not required in this program.

(5) Type in exactly as shown the following statement:

"DSC2:VORSCAL"

Then press the return key. The BASIC program will now prompt you through the program.

(6) Enter the location, VOR frequency, and other data as requested by the program.

(7) Analyze the plot as described on the printout. If the solution is unsatisfactory, the plot can be run again with the necessary data changes. The program automatically scales the plot; however, the scale may not be satisfactory. At the end of each plot the program asks if the scale was satisfactory. If not, the scale can be changed and another plot made.

(8) The program will print out the best solutions, based on the coincidence of three or four lines. These are solved by trial and error during the execution of the program. These answers usually are valid but may not be if a large number of scalloping bearings were entered. Visual analysis of the plot is required to verify the scalloping source location.

(9) Upon completion of the program, remove both discs and turn the power off to all three units.

d. Using the Compustar Model 30. After the flight check recordings have been analyzed and the scallops counted at several azimuths, the VORSCAL program is run:

(1) Turn on the power to the Compustar and printer.

(2) Insert the program disc with the program VORSCAL.COM recorded on it into disc drive A (the lefthand drive).

(3) Type "VORSCAL" and then press the "RETURN" key.

(4) The computer will now prompt you through the program.

(5) Analyze the computer printout as described in Steps 3b(7,8) above.

e. Examples. Five computer generated plots from actual scalloping problems are included as examples. All plots except the Port Angeles example were originally done with earlier plotting methods. Examples on the following pages are:

```
VOR SCALLOPING PROGRAM DEVELOPED BY E.E. Palmer, P.E.
FAA NORTHWEST REGION, SEATTLE, WASHINGTON
CP/M VERSION 1.0, 3-MARCH-83

LOCATION:       EPHRATA, WASHINGTON
FREQUENCY:      112.6
ENGINEER:       EEP
F/C AIRCRAFT:   SAFI
DATE:           5-15-80
SCALE OF PLOT:  20  FEET PER INCH

THE NUMBER OF SCALLOPS COUNTED FOR EACH AZIMUTH IS:
DATA  NUMBER OF SCALLOPS  AZIMUTH
====  ================  =======
 1          1              10
 2          1.2           250
 3          .8            280
```

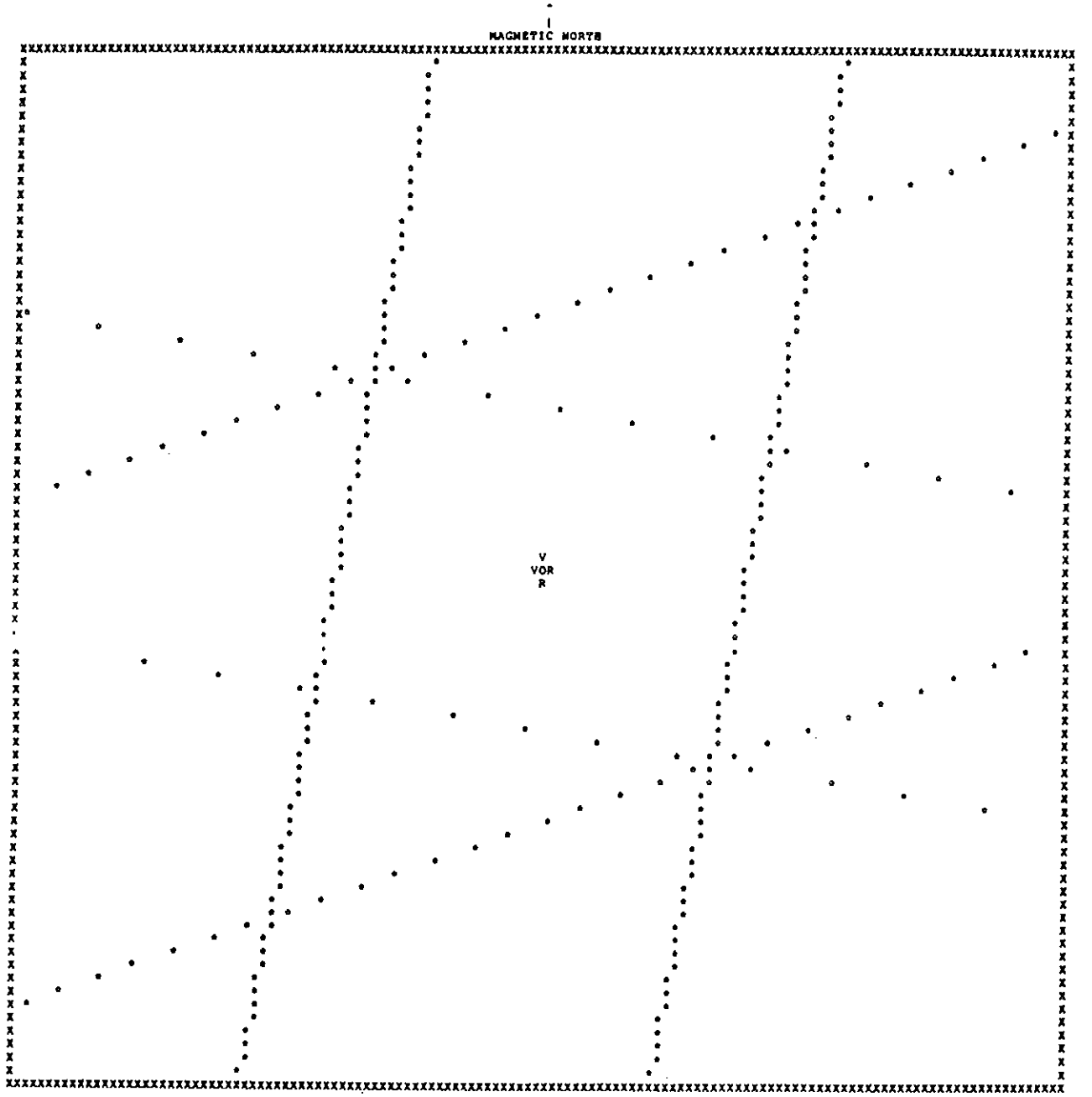


```
THE PLOT SCALE IS 20 FEET PER INCH.
```

PHOTO REDUCED

```
A POSSIBLE SOLUTION USING 3 INTERSECTING LINES IS 67 FEET FROM THE VOR ON THE 139 OR 319 DEGREE RADIAL.

THE ABOVE SOLUTION(S) MAY NOT BE VALID AND SHOULD BE VERIFIED BY GRAPHICAL ANALYSIS, ESPECIALLY IF MORE THAN 4 BEARINGS ARE PLOTTED.

THE LOCATION OF THE SCALLOPING SOURCE IS AT THE COMMON INTERSECTIONS OF THE LINES OF ASTERISKS.  TWO POSSIBLE
SOULTIONS ARE FOUND, ONE CORRECT AND THE OTHER INCORRECT.  THE TWO SOLUTIONS ARE LOCATED ON RECIPROCAL VOR BEARINGS,
THE SAME DISTANCE FROM THE VOR.  THE CORRECT SOLUTION MUST BE DETERMINED BY INSPECTION OF THE FACILITY.

THE ABOVE PLOT SHOULD HAVE A CONTINUOUS ROW OF X'S IN THE VERTICAL COLUMNS ON EACH SIDE OF THE PAPER.  IF NOT
AN ERROR IN THE PLOT HAS OCCURED.

TO MAKE THE LINES OF ASTERISKS MORE VISIBLE, USE A FELT TIP MARKER.  AT ANGLES NEAR 90 OR 270 DEGREES ONLY A FEW
ASTERISKS PER INCH ARE PRINTED.
```

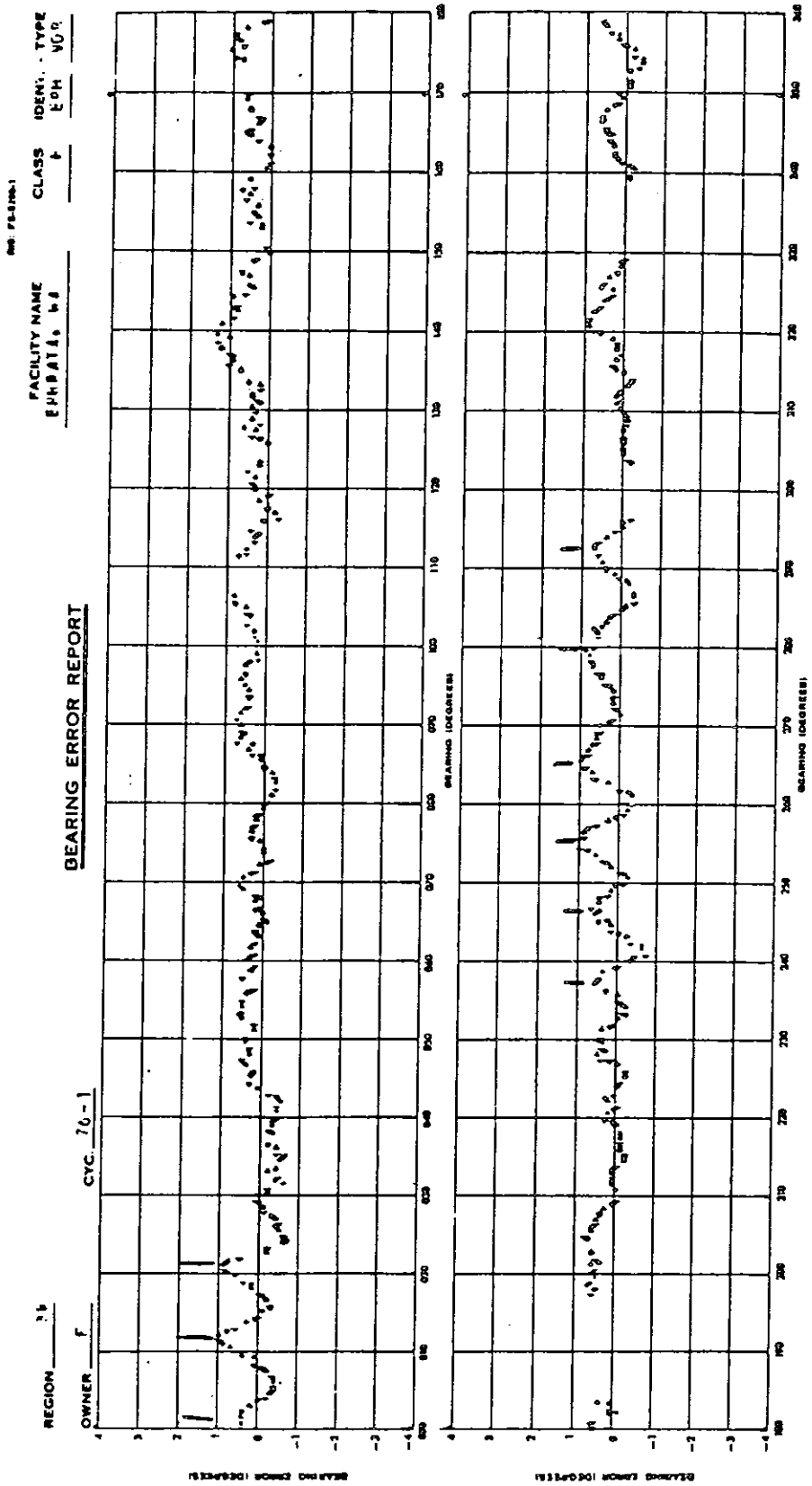

FACILITY CHARACTERISTICS

MEAN ERROR (DEG)	DISPERSION RANGE		
	68%	95%	99.7%
+0.2	+0.5	+0.9	+1.2
	-0.2	-0.5	-0.5

SUMMARY HISTORY BY SECTORS

DATE	FLIGHT NO	AIR-CRAFT	ALTITUDE	START BEARING	DIRECTION	END BEARING	DISTANCE MAX	DISTANCE MIN	AVERAGE POL	AVERAGE AM	AVERAGE PM
12-1[illegible]-75	614	C92	23100	22[illegible].0	CCW	[illegible]2.5	76	40	1.2		
12-26-75	612	C90	19000	87.5	CCW	[illegible]5.5	51	3[illegible]	.5	3[illegible]	2[illegible]
1[illegible]-17-76	616	C90	21400	221.5	CCW	17[illegible].[illegible]	[illegible]0	45	.5	29	2[illegible]
3[illegible]-05-76	600	090	21300	177.[illegible]	CCW	[illegible]2.6	32	21	.[illegible]	26	27
27-2[illegible]-76	621	C91	23100	24[illegible].0	CW	100.3	43	30	.[illegible]	28	31

Example 3c(1)

```
VOR SCALLOPING PROGRAM DEVELOPED BY S.E. Palmer, P.E.
FAA NORTHWEST REGION, SEATTLE, WASHINGTON
CP/M VERSION 1.0, 3-MARCH-83

LOCATION:       TWIN FALLS, IDAHO
FREQUENCY:      115.8
ENGINEER:       SEP
F/C AIRCRAFT:   H-47
DATE:           5/15/80
SCALE OF PLOT:  500  FEET PER INCH

THE NUMBER OF SCALLOPS COUNTED FOR EACH AZIMUTH IS:
DATA  NUMBER OF SCALLOPS  AZIMUTH
----  ------------------  -------
 1            45             290
 2            44             120
 3            44             110
 4            48             300
 5             7              20
 6            21             180
```

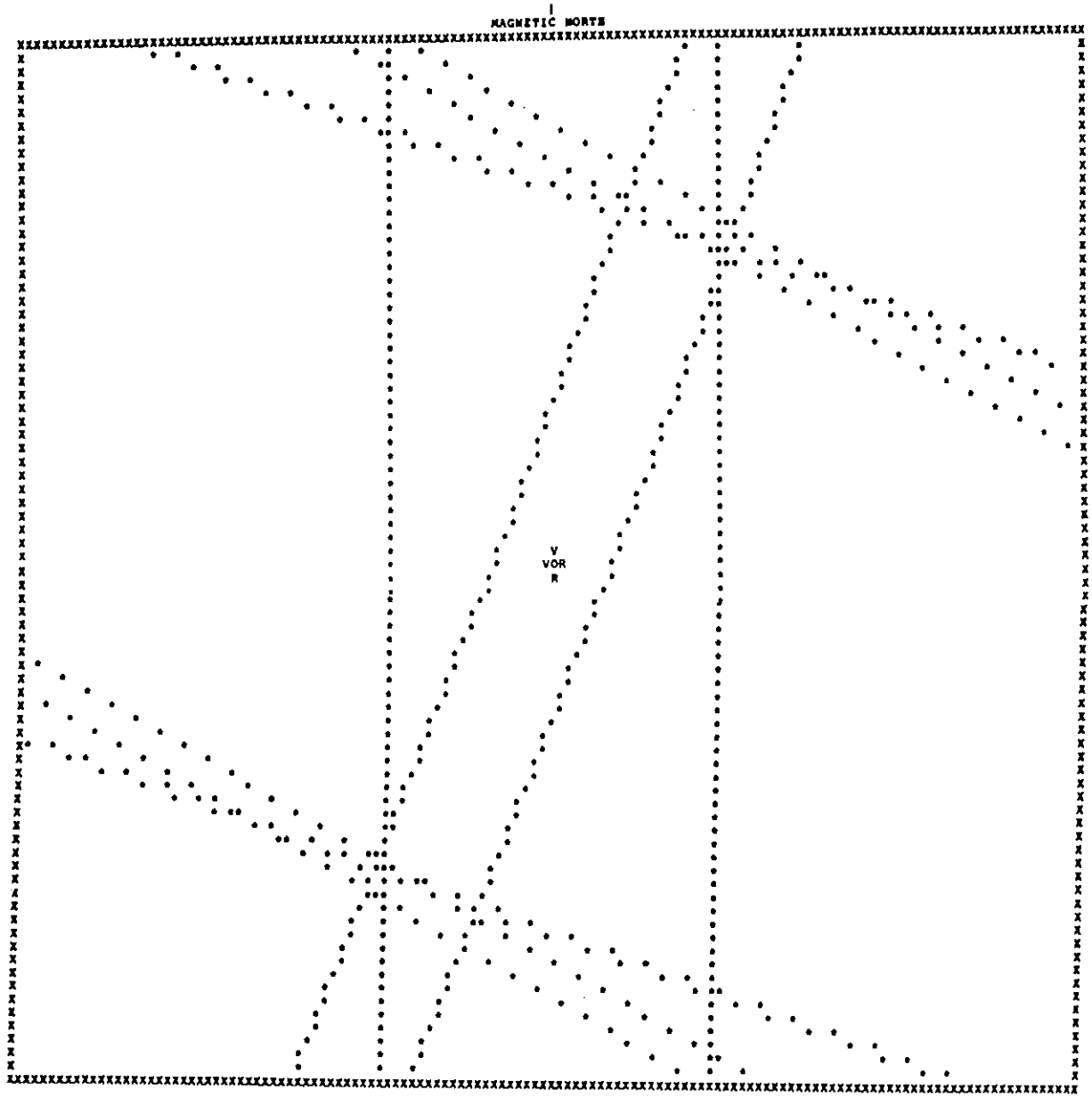


```
THE PLOT SCALE IS 500 FEET PER INCH.

A POSSIBLE SOLUTION USING 4 INTERSECTING LINES IS 2126 FEET FROM THE VOR ON THE 28 OR 208 DEGREE RADIAL.

THE ABOVE SOLUTION(S) MAY NOT BE VALID AND SHOULD BE VERIFIED BY GRAPHICAL ANALYSIS, ESPECIALLY IF MORE THAN 4 BEARINGS ARE PLOTTED.

THE LOCATION OF THE SCALLOPING SOURCE IS AT THE COMMON INTERSECTIONS OF THE LINES OF ASTERISKS.  TWO POSSIBLE
SOULTIONS ARE FOUND, ONE CORRECT AND THE OTHER INCORRECT.  THE TWO SOLUTIONS ARE LOCATED ON RECIPROCAL VOR BEARINGS,
THE SAME DISTANCE FROM THE VOR.  THE CORRECT SOLUTION MUST BE DETERMINED BY INSPECTION OF THE FACILITY.

THE ABOVE PLOT SHOULD HAVE A CONTINUOUS ROW OF X'S IN THE VERTICAL COLUMNS ON EACH SIDE OF THE PAPER.  IF NOT
AN ERROR IN THE PLOT HAS OCCURRED.

TO MAKE THE LINES OF ASTERISKS MORE VISIBLE, USE A FELT TIP MARKER.  AT ANGLES NEAR 90 OR 270 DEGREES ONLY A FEW
ASTERISKS PER INCH ARE PRINTED.
```

PHOTO REDUCED

4/17/86

VOR SCALLOPING PROGRAM DEVELOPED BY E.E. Palmer, P.E.
FAA NORTHWEST REGION, SEATTLE, WASHINGTON
CP/M VERSION 1.0, 3-MARCH-83

LOCATION: PORT ANGELES, WASHINGTON
FREQUENCY: 108.4
ENGINEER: EEP
P/C AIRCRAFT: H-61
DATE: 9-15-80
SCALE OF PLOT: 1000 FEET PER INCH

THE NUMBER OF SCALLOPS COUNTED FOR EACH AZIMUTH IS:

DATA	NUMBER OF SCALLOPS	AZIMUTH
1	90	210
2	75	125
3	60	155
4	76	5
5	86	105
6	86	225
7	76	350

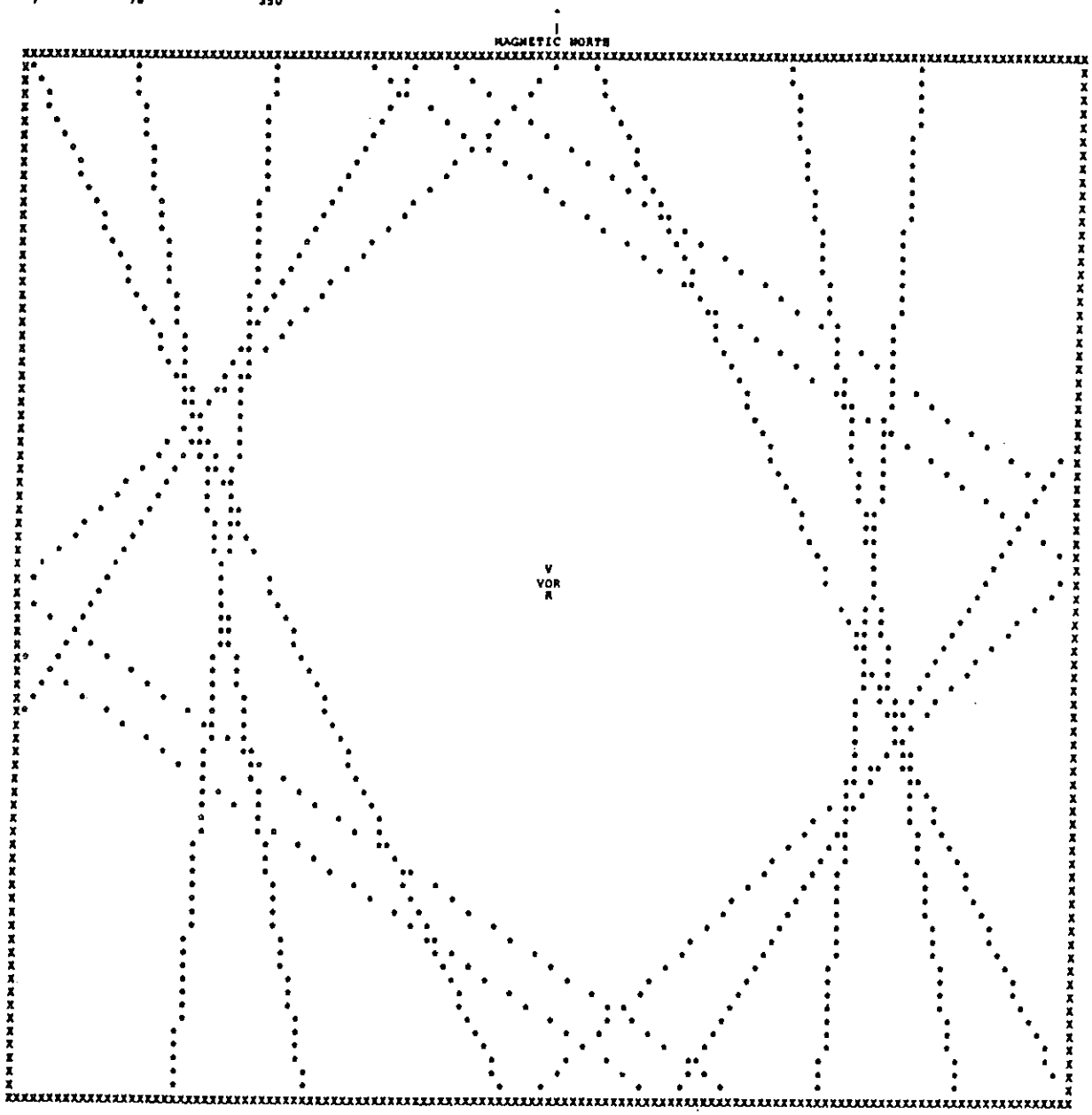

THE PLOT SCALE IS 1000 FEET PER INCH.

A POSSIBLE SOLUTION USING 4 INTERSECTING LINES IS 4857 FEET FROM THE VOR ON THE 115 OR 295 DEGREE RADIAL.

PHOTO REDUCED

THE ABOVE SOLUTION(S) MAY NOT BE VALID AND SHOULD BE VERIFIED BY GRAPHICAL ANALYSIS, ESPECIALLY IF MORE THAN 4 BEARINGS ARE PLOTTED.

THE LOCATION OF THE SCALLOPING SOURCE IS AT THE COMMON INTERSECTIONS OF THE LINES OF ASTERISKS. TWO POSSIBLE SOULTIONS ARE FOUND, ONE CORRECT AND THE OTHER INCORRECT. THE TWO SOLUTIONS ARE LOCATED ON RECIPROCAL VOR BEARINGS, THE SAME DISTANCE FROM THE VOR. THE CORRECT SOLUTION MUST BE DETERMINED BY INSPECTION OF THE FACILITY.

THE ABOVE PLOT SHOULD HAVE A CONTINUOUS ROW OF X'S IN THE VERTICAL COLUMNS ON EACH SIDE OF THE PAPER. IF NOT AN ERROR IN THE PLOT HAS OCCURED.

TO MAKE THE LINES OF ASTERISKS MORE VISIBLE, USE A FELT TIP MARKER. AT ANGLES NEAR 90 OR 270 DEGREES ONLY A FEW ASTERISKS PER INCH ARE PRINTED.

Example 3e(3)

VOR SCALLOPING PROGRAM DEVELOPED BY E.E. Palmer, P.E.
FAA NORTHWEST REGION, SEATTLE, WASHINGTON
CP/M VERSION 1.0, 3-MARCH-83

LOCATION: BAYVIEW, WASHINGTON
FREQUENCY: 108.2
ENGINEER: EEP
F/C AIRCRAFT: H-47
DATE: 5/15/80
SCALE OF PLOT: 400 FEET PER INCH

THE NUMBER OF SCALLOPS COUNTED FOR EACH AZIMUTH IS:

DATA	NUMBER OF SCALLOPS	AZIMUTH
1	18	70
2	22	115
3	21	130
4	24	305
5	20	140

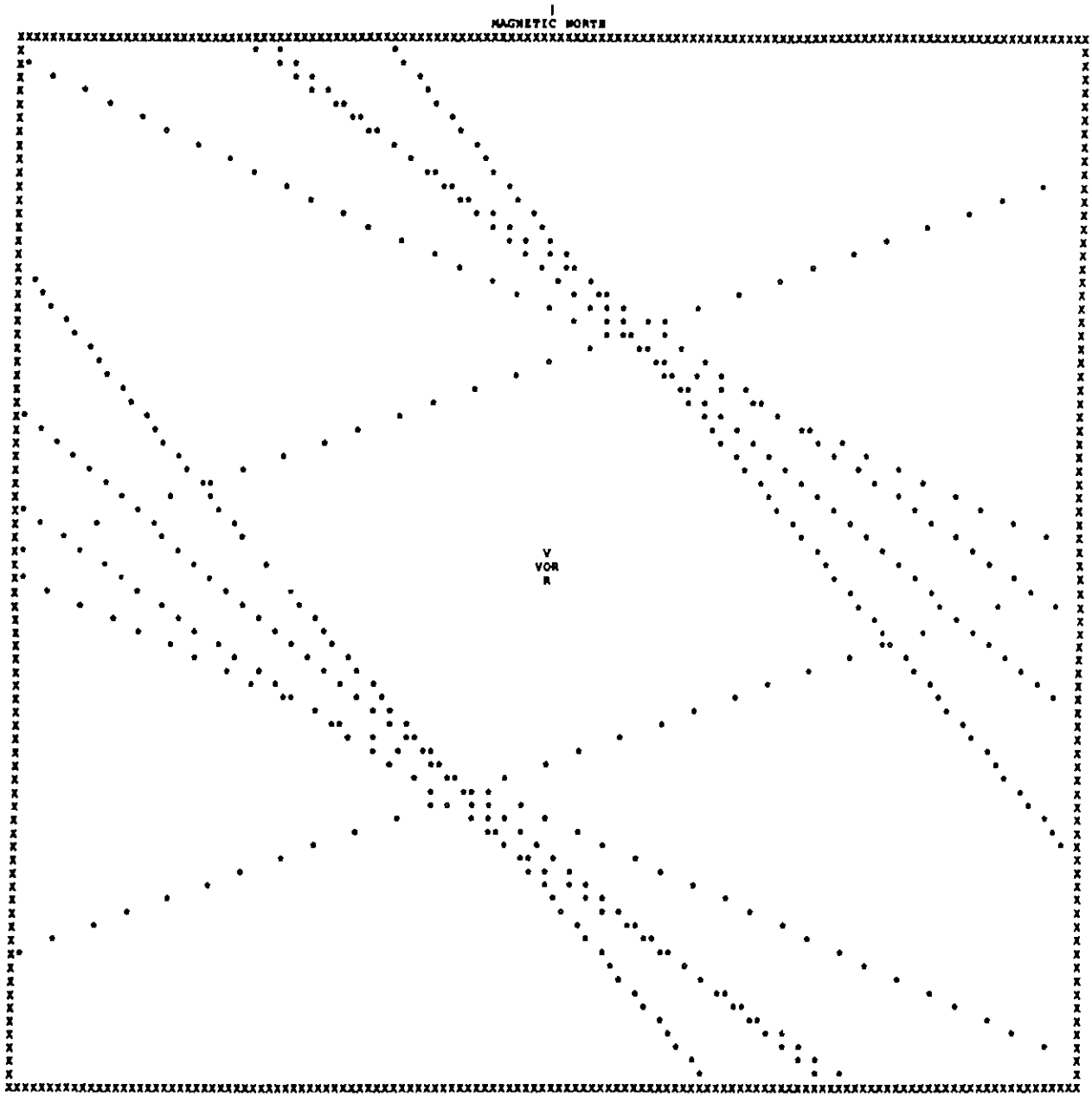

THE PLOT SCALE IS 400 FEET PER INCH.

A POSSIBLE SOLUTION USING 4 INTERSECTING LINES IS 1144 FEET FROM THE VOR ON THE 17 OR 197 DEGREE RADIAL.

PHOTO REDUCED

THE ABOVE SOLUTION(S) MAY NOT BE VALID AND SHOULD BE VERIFIED BY GRAPHICAL ANALYSIS, ESPECIALLY IF MORE THAN 4 BEARINGS ARE PLOTTED.

THE LOCATION OF THE SCALLOPING SOURCE IS AT THE COMMON INTERSECTIONS OF THE LINES OF ASTERISKS. TWO POSSIBLE SOULTIONS ARE FOUND, ONE CORRECT AND THE OTHER INCORRECT. THE TWO SOLUTIONS ARE LOCATED ON RECIPROCAL VOR BEARINGS, THE SAME DISTANCE FROM THE VOR. THE CORRECT SOLUTION MUST BE DETERMINED BY INSPECTION OF THE FACILITY.

THE ABOVE PLOT SHOULD HAVE A CONTINUOUS RON OF X'S IN THE VERTICAL COLUMNS ON EACH SIDE OF THE PAPER. IF NOT AN ERROR IN THE PLOT HAS OCCURED.

TO MAKE THE LINES OF ASTERISKS MORE VISIBLE, USE A FELT TIP MARKER. AT ANGLES NEAR 90 OR 270 DEGREES ONLY A FEW ASTERISKS PER INCH ARE PRINTED.

VOR SCALLOPING PROGRAM DEVELOPED BY E.E. Palour, P.E.
FAA NORTHWEST REGION, SEATTLE, WASHINGTON
CP/M VERSION 1.0, 3-MARCH-83

LOCATION: SALMON, IDAHO
FREQUENCY: 113.8
ENGINEER: EEP
P/C AIRCRAFT: BAPI
DATE: 5/15/80
SCALE OF PLOT: 10 FEET PER INCH

THE NUMBER OF SCALLOPS COUNTED FOR EACH AZIMUTH IS:

DATA	NUMBER OF SCALLOPS	AZIMUTH
1	.5	40
2	.55	210
3	.6	160

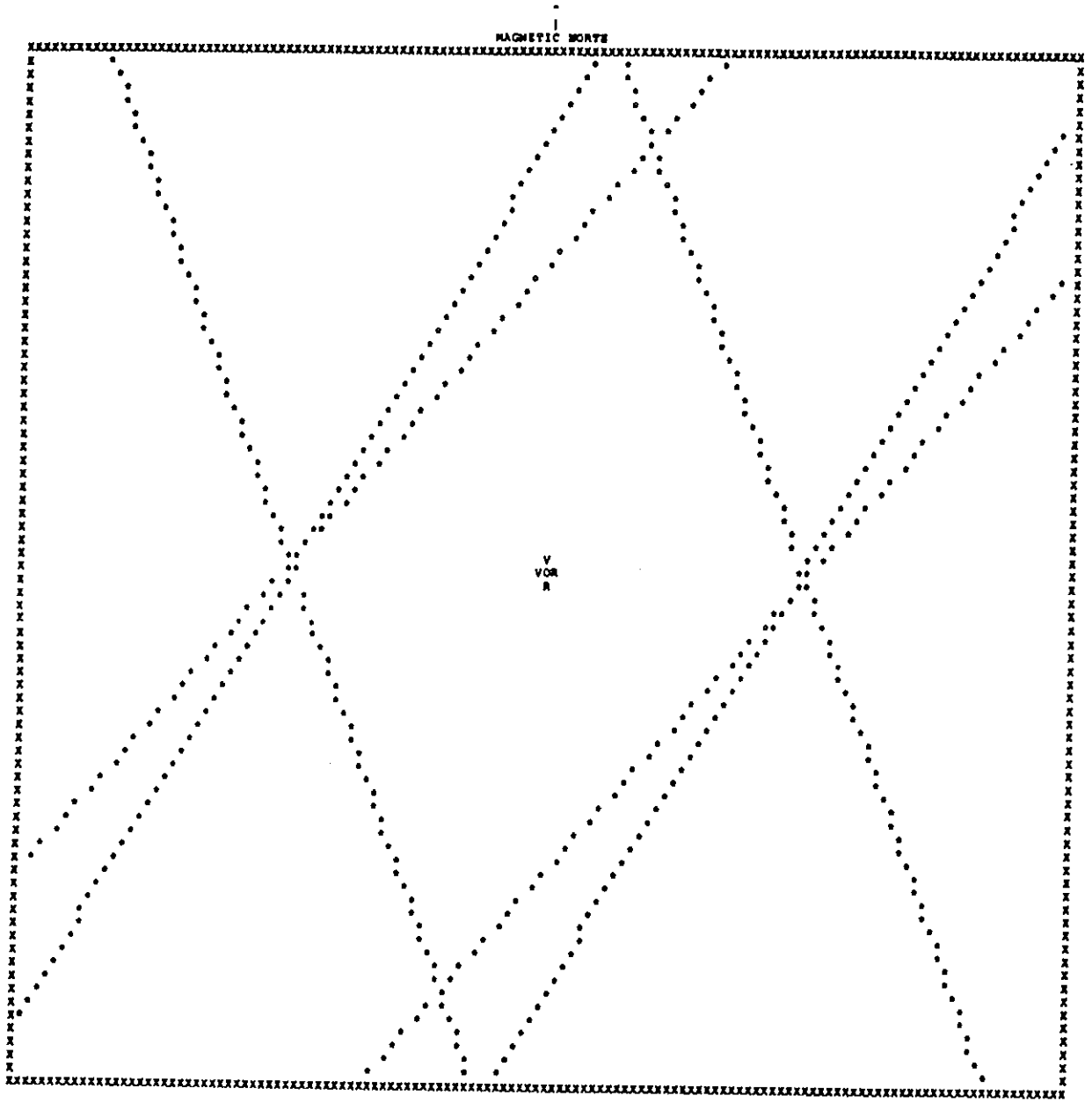

THE PLOT SCALE IS 10 FEET PER INCH.

PHOTO REDUCED

A POSSIBLE SOLUTION USING 3 INTERSECTING LINES IS 31 FEET FROM THE VOR ON THE 93 OR 273 DEGREE RADIAL.

THE ABOVE SOLUTION(S) MAY NOT BE VALID AND SHOULD BE VERIFIED BY GRAPHICAL ANALYSIS, ESPECIALLY IF MORE THAN 4 BEARINGS ARE PLOTTED.

THE LOCATION OF THE SCALLOPING SOURCE IS AT THE COMMON INTERSECTIONS OF THE LINES OF ASTERISKS. TWO POSSIBLE SOULTIONS ARE FOUND, ONE CORRECT AND THE OTHER INCORRECT. THE TWO SOLUTIONS ARE LOCATED ON RECIPROCAL VOR BEARINGS, THE SAME DISTANCE FROM THE VOR. THE CORRECT SOLUTION MUST BE DETERMINED BY INSPECTION OF THE FACILITY.

THE ABOVE PLOT SHOULD HAVE A CONTINUOUS ROW OF X'S IN THE VERTICAL COLUMNS ON EACH SIDE OF THE PAPER. IF NOT AN ERROR IN THE PLOT HAS OCCURED.

TO MAKE THE LINES OF ASTERISKS MORE VISIBLE, USE A FELT TIP MARKER. AT ANGLES NEAR 90 OR 270 DEGREES ONLY A FEW ASTERISKS PER INCH ARE PRINTED.

```
VOR SCALLOPING PROGRAM DEVELOPED BY E.E. Palmer, P.E.
FAA NORTHWEST REGION, SEATTLE, WASHINGTON
CP/M VERSION 1.0, 3-MARCH-83

LOCATION:       BURLEY, IDAHO
FREQUENCY:      112.6
ENGINEER:       EP
F/C AIRCRAFT:   BAPI
DATE:           3-MAR-83
SCALE OF PLOT:  20  FEET PER INCH

THE NUMBER OF SCALLOPS COUNTED FOR EACH AZIMUTH IS:
DATA  NUMBER OF SCALLOPS  AZIMUTH
----  ------------------  -------
1           .3              30
2           .333            63
3           .91             110
4           1.              139
5           .83             180
```

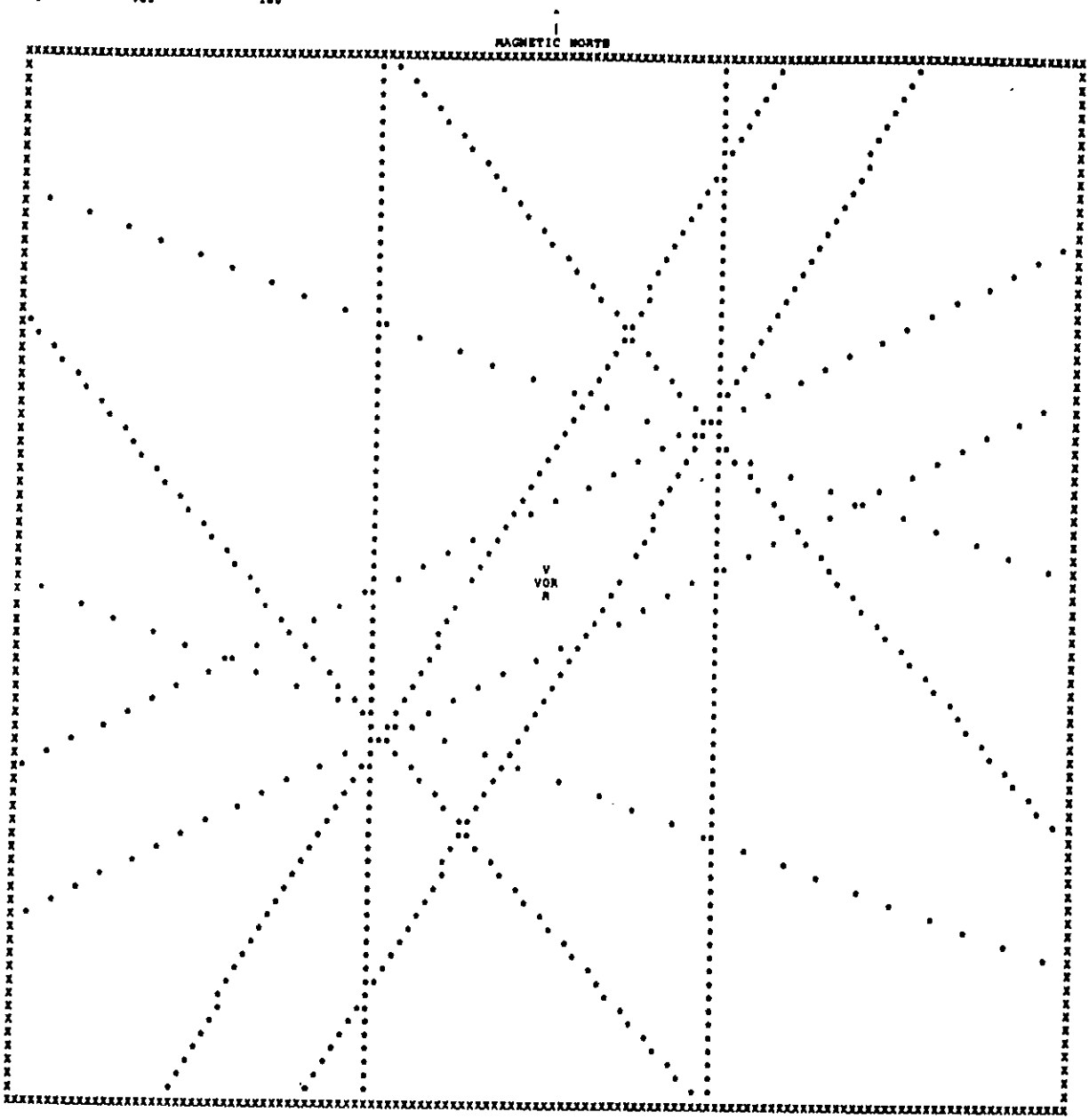


```
THE PLOT SCALE IS 20 FEET PER INCH.
                                  PHOTO REDUCED
A POSSIBLE SOLUTION USING 4 INTERSECTING LINES IS 56 FEET FROM THE VOR ON THE 45 OR 225 DEGREE RADIAL.

THE ABOVE SOLUTION(S) MAY NOT BE VALID AND SHOULD BE VERIFIED BY GRAPHICAL ANALYSIS, ESPECIALLY IF MORE THAN 4 BEARINGS ARE PLOTTED.

THE LOCATION OF THE SCALLOPING SOURCE IS AT THE COMMON INTERSECTIONS OF THE LINES OF ASTERISKS.  TWO POSSIBLE
SOULTIONS ARE FOUND, ONE CORRECT AND THE OTHER INCORRECT.  THE TWO SOLUTIONS ARE LOCATED ON RECIPROCAL VOR BEARINGS,
THE SAME DISTANCE FROM THE VOR.  THE CORRECT SOLUTION MUST BE DETERMINED BY INSPECTION OF THE FACILITY.

THE ABOVE PLOT SHOULD HAVE A CONTINUOUS ROW OF X'S IN THE VERTICAL COLUMNS ON EACH SIDE OF THE PAPER.  IF NOT
AN ERROR IN THE PLOT HAS OCCURED.

TO MAKE THE LINES OF ASTERISKS MORE VISIBLE, USE A FELT TIP MARKER.  AT ANGLES NEAR 90 OR 270 DEGREES ONLY
ASTERISKS PER INCH ARE PRINTED.
```

THE FOLLOWING DERIVATION IS FOR THE DISTANCE "D" FROM THE VOR TO A LINE PARALLEL TO THE RADIUS WHICH PASSES THROUGH THE SCALLOPING SOURCE. (SEE BELOW) THE DISTANCES ARE DRAWN OUT OF PROPORTION WHICH EXAGGERATES THE APPARENT ERROR.

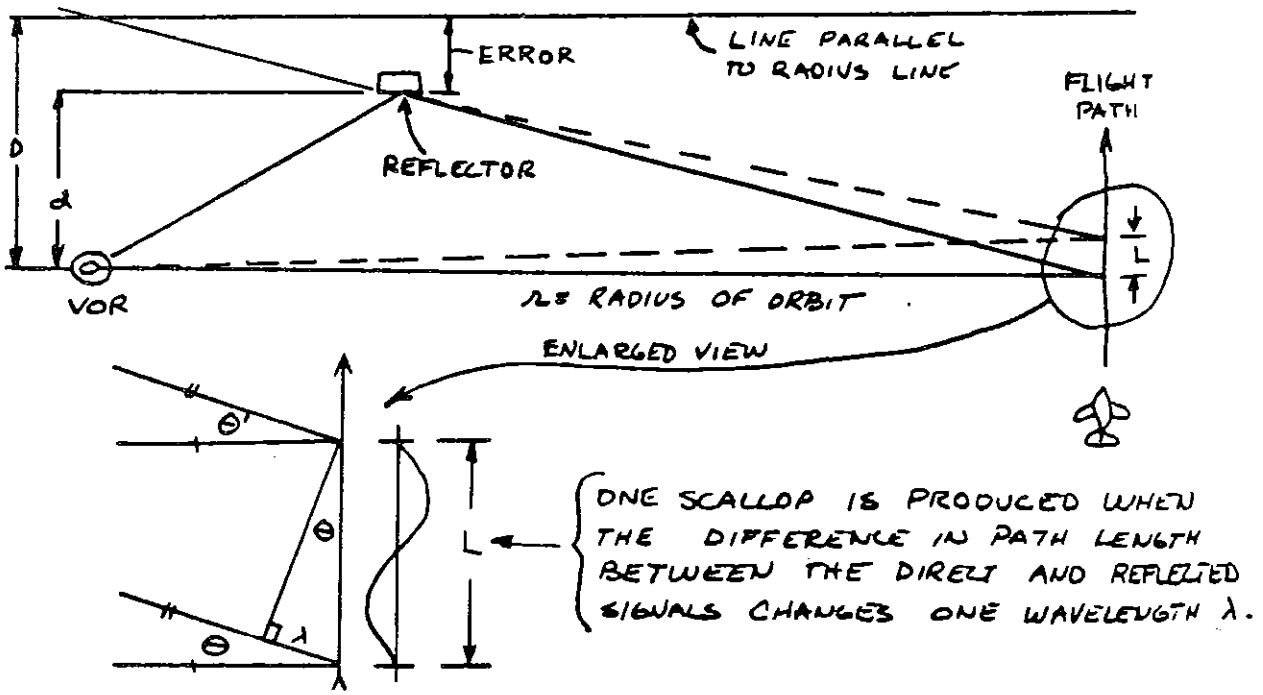

FROM THE ABOVE IT CAN BE SEEN THAT:

1. $\theta = \theta'$ 2. $\sin\theta = \frac{\lambda}{L}$ 3. $\sin\theta = \tan\theta = \frac{D}{r}$ (FOR SMALL ANGLES)

WHERE $D << r$ AND:

L = LENGTH OF ONE SCALLOP IN FEET
λ = WAVELENGTH IN FEET
r = ORBITAL RADIUS DISTANCE IN FEET
θ = ANGLE BETWEEN THE DIRECT AND REFLECTED SIGNALS IN DEGREES
D = APPROXIMATE DISTANCE FROM THE RADIUS LINE TO THE REFLECTOR

PREPARED BY	CHECKED BY	DATE
Earl Palmer		10-18-77
SUBJECT: CALCULATION OF VOR SCALLOPING SOURCES		FILE NO. 6790-1
		SHEET 1 OF 2 SHEETS

FAA Form 6000-4 (4-73) FORMERLY FAA FORM 2067 CALCULATION SHEET

SOLVING EQUATION 3. FOR D

4. $D = r \sin\theta' = r \sin\theta$, $\sin\theta = \frac{\lambda}{L}$, THEN $\boxed{D = \frac{r\lambda}{L}}$

AS FLIGHT CHECK ORBIT RECORDINGS ARE CALIBRATED IN DEGREES, NOT FEET, IT IS MORE CONVENIENT TO COUNT THE NUMBER OF SCALLOPS PER DEGREE. THE FLIGHT CHECK RECORDER BEARING INCREMENTS EVERY 10 DEGREE, IT IS CONVENIENT TO COUNT THE NUMBER OF SCALLOPS IN 10 DEGREE SEGMENTS.

THEN: L IN DEGREES $= \frac{10}{n}$, WHERE n = NUMBER OF SCALLOPS

THE LENGTH OF ONE SCALLOP IN FEET CAN BE FOUND FROM THE FOLLOWING RELATIONSHIP:

$$\frac{L_{FEET}}{2\pi r} = \frac{L_{DEGREES}}{360} \quad \text{OR} \quad L_{FT} = L_{DEG.} \times \frac{2\pi r}{360}$$

(CIRCUMFERENCE)

$$L_{FT} = \frac{10}{n} \times \frac{2\pi r}{360} = \frac{\pi r}{18n}$$

FROM EQUATION 4, $D = \frac{r\lambda}{L}$, THEN $D = r\lambda \times \frac{18n}{\pi r} = \boxed{\frac{18n\lambda}{\pi} = D}$ EQ. 5

NOTE THAT THE RADIUS OF ORBIT IS NOT IN EQUATION 5.

IF THE VOR FREQUENCY IS ASSUMED TO BE 115 MHz,

THE EQUATION CAN BE FURTHER SIMPLIFIED TO:

$$\boxed{D = 49n}$$

PREPARED BY Earl Palmer	CHECKED BY	DATE 10-18-77
SUBJECT CALCULATION OF VOR SCALLOPING SOURCES		FILE NO. 6970-1
		SHEET 2 OF 2 SHEETS

FAA Form 6000-4 (4-73) FORMERLY FAA FORM 2067

CALCULATION SHEET

```
'VORSCAL.BAS'  -  MARCH 1983

100 CL$=CHR$(12):PRINT CL$
110 PRINT
120 DEFINT J,K,N,X,Y,Z
130 PRINT TAB(20)"VOR SCALLOPING PROGRAM"
140 PRINT
150 PRINT"IS WIDE 132 COLUMN PAPER INSTALLED IN THE PRINTER? (Y/N)  <Y>"
160 X$=INPUT$(1)
170 IF (X$<>"N" AND X$<>"n") THEN GOTO 200
180 PRINT:PRINT"SORRY, YOU MUST RECONFIGURE YOUR PRINTER!!!!!!!!"
190 GOTO 150
200 PRINT CL$
210 PRINT "VOR SCALLOPING PROGRAM"
220 PRINT:PRINT"Developed by E.E. Palmer, P.E., FAA"
230 PRINT:PRINT"Northwest Region, Seattle, WA., 3/30/80; Revised 3/3/83"
240 PRINT
250 DEFINT Q
260 DIM Q(40),S(15),A(15)
270 LINE INPUT"LOCATION ";LO$:PRINT
280 LINE INPUT"DATE ";D$:PRINT
290 LINE INPUT"ENGINEER ";EN$:PRINT
300 LINE INPUT"FLIGHT CHECK AIRCRAFT ";AC$:PRINT
310 INPUT"FACILITY FREQUENCY IN MHZ";F:PRINT
320 PRINT CL$
330 INPUT"NUMBER OF BEARINGS TO BE PLOTTED ";X%:PRINT
340 IF X%<3 THEN PRINT "THREE OR MORE ARE REQUIRED":GOTO 320
350 PRINT"TYPE IN THE NUMBER OF SCALLOPS COUNTED, THEN A COMMA FOLLOWED BY"
360 PRINT"THE AZIMUTH (OR AVERAGE AZIMUTH) WHERE THE SCALLOPS WERE COUNTED."
370 PRINT"DO NOT USE AZIMUTHS BETWEEN 85 AND 95, OR BETWEEN 265 AND 275 DEGREES.
380 FOR N%=1 TO X%
390 PRINT
400 INPUT"NUMBER OF SCALLOPS IN 10 DEG., AZIMUTH ";S(N%),A(N%)
410 IF A(N%)>=85 AND A(N%)<= 95 THEN PRINT A(N%);" IS BETWEEN 85 AND 95 DEGREES!"
    :GOTO 400
420 IF A(N%)>=265 AND A(N%)<=275 THEN PRINT A(N%);" IS BETWEEN 265 AND 275 DEGRE
ES!":GOTO 400
430 NEXT N%
440 LT=0:BT=20:PT=20
450 FOR N%=1 TO X% : REM ESTIMATE PLOT SCALE
460 LT=LT+S(N%)
470 NEXT N%
480 LT=(LT/X%)*(2000/F)
490 IF LT<10 THEN C=10 : GOTO 580
500 IF LT<25 THEN C=25 : GOTO 580
510 IF LT<50 THEN C=50 : GOTO 580
520 IF LT<100 THEN C=100 : GOTO 580
530 IF LT<200 THEN C=200 : GOTO 580
540 IF LT<400 THEN C=400 : GOTO 580
550 IF LT<1000 THEN C=1000 : GOTO 580
560 IF LT<2000 THEN C=2000 : GOTO 580
570 IF LT>=2000 THEN C=4000
580 PRINT "THE SCALE OF THE PLOT WILL BE";C;"FEET PER INCH. "
590 PRINT "IS THIS SATISFACTORY?   Y OR N ?"
600 INPUT SC$
610 IF SC$="Y" OR SC$="y" THEN 630
620 INPUT "WHAT IS THE DESIRED SCALE IN FEET PER INCH";C
630 PRINT "SET THE PRINTER TO THE TOP OF PAGE: PRESS ANY KEY TO START";:INPUT X$
640 PRINT CL$ : PRINT "STANDBY, THE SCALLOP PLOT IS IN PROCESS"
650 LPRINT:LPRINT CHR$(27)+CHR$(31)+CHR$(13)
```

'VORSCAL.BAS' - MARCH 1983

```
660 REM THE ABOVE LINE CONFIGURES THE DIABLO 630 PRINTER FOR 10CPI PRINTING
670 REM AND 6INE PER INCH VERTICAL SPACING.  CHANGE FOR OTHER PRINTERS
680 LPRINT "VOR SCALLOPING PROGRAM DEVELOPED BY E.E. Palmer, P.E."
690 LPRINT "FAA NORTHWEST REGION, SEATTLE, WASHINGTON"
700 LPRINT "CP/M VERSION 1.0, 3-MARCH-83"
710 LPRINT :LPRINT "LOCATION: ";TAB(16);LO$
720 LPRINT "FREQUENCY:";TAB(15);F;"MHZ"
730 LPRINT "ENGINEER: ";TAB(16);EN$
740 LPRINT "F/C AIRCRAFT: ";TAB(16);AC$
750 LPRINT "DATE: ";TAB(16);D$
760 LPRINT "SCALE OF PLOT:";INT(C);" FEET PER INCH":LPRINT
770 LPRINT "THE NUMBER OF SCALLOPS COUNTED FOR EACH AZIMUTH IS:"
780 LPRINT "DATA  NUMBER OF SCALLOPS  AZIMUTH"
790 LPRINT "====  ==============  ======"
800 FOR N%=1 TO X%
810 LPRINT N%;TAB(13);S(N%);TAB(29);A(N%)
820 NEXT N%
830 LPRINT TAB(66);"^"
840 LPRINT TAB(66);"|"
850 LPRINT TAB(59);"MAGNETIC NORTH"
860 FOR Y%=1 TO 130
870 LPRINT "X";
880 NEXT Y%
890 LPRINT "X"
900 FOR L=2 TO 78:REM L = LINE NUMBER
910 FOR N%=1 TO X%
920 TA=66+(SIN(A(N%)*3.142/180)/COS(A(N%)*3.142/180))*(40-L)*(10/6)
930 TB=563801*S(N%)/(F*C*COS(A(N%)*3.142/180))
940 W=TA+TB+.5 :REM W=TAB VALUE FORM 2 TO 132
950 W=INT(W)
960 IF (W<2 OR W>129) THEN 980
970 M=M+1:Q(M)=W:REM M = NUMBER OF TAB VALUES PER LINE
980 W=TA-TB+.5
990 W=INT(W)
1000 IF (W<2 OR W>129) THEN 1020
1010 M=M+1:Q(M)=W:REM ARRAY OF TAB VALUES TO BE PLOTTED
1020 NEXT N%
1030 FOR K%=1 TO M-1:REM START OF TAB VALUE SORT
1040 FOR J%=1 TO M-K%
1050 IF Q(J%)<Q(J%+1) THEN 1070
1060 V=Q(J%):Q(J%)=Q(J%+1):Q(J%+1)=V
1070 NEXT J%
1080 NEXT K%
1090 IF X%=<3 THEN 1190
1100 REM START OF BEST INTERSECTION CALCULATION FOR 4 LINES.
1110 FOR K% = 1 TO M-3
1120 KS=Q(K%+3)-Q(K%)
1130 IF KS>20 THEN 1180
1140 IF KS>BT THEN 1180
1150 BT=KS:REM BT=BEST TAB WIDTH VALUE
1160 BL=L:REM BL=BEST LINE VALUE
1170 BV=(Q(K%+3)+Q(K%+2)+Q(K%+1)+Q(K%))/4:REM BV=BEST AVERAGE TAB VALUE
1180 NEXT K%
1190 IF X%=>4 THEN 1290
1200 REM START OF BEST INTERSECTION CALCULATION FOR 3 LINES.
1210 FOR K%=1 TO M-2
1220 KS=Q(K%+2)-Q(K%)
1230 IF KS>20 THEN 1280
```

'VORSCAL.BAS' - MARCH 1983

```
1240 IF KS>PT THEN 1280
1250 PT=KS
1260 PL=L
1270 PV=(Q(K%+2)+Q(K%+1)+Q(K%))/3
1280 NEXT K%
1290 E=0:REM SORT TO DISCARD EQUAL TAB VALUES
1300 FOR B%=1 TO M-1
1310 IF Q(B%)=Q(B%+1) THEN 1330
1320 E=E+1:Q(E)=Q(B%):M=E
1330 NEXT B%
1340 IF Q(B%)=0 THEN 1360
1350 E=E+1:Q(E)=Q(B%)
1360 M=E
1370 LPRINT "X";:REM PUTS X ON LEFT BOUNDARY OF PLOT
1380 IF L=39 THEN 1460
1390 IF L=40 THEN 1560
1400 IF L=41 THEN 1660
1410 FOR R=1 TO M
1420 IF Q(R)<2 THEN GOTO 1440
1430 LPRINT TAB(Q(R));"*";
1440 NEXT R
1450 GOTO 1750
1460 FOR R=1 TO M/2
1470 IF Q(R)=66 THEN GOTO 1500
1480 LPRINT TAB(Q(R));"*";
1490 NEXT R
1500 LPRINT TAB(66);"V";
1510 FOR R=M/2+1 TO M
1520 IF Q(R)=66 THEN GOTO 1540
1530 LPRINT TAB(Q(R));"*";
1540 NEXT R
1550 GOTO 1750
1560 FOR R=1 TO M/2
1570 IF (Q(R)=65 OR Q(R)=66 OR Q(R)=67) THEN GOTO 1600
1580 LPRINT TAB(Q(R));"*";
1590 NEXT R
1600 LPRINT TAB(65);"VOR";
1610 FOR R=M/2+1 TO M
1620 IF (Q(R)=65 OR Q(R)=66 OR Q(R)=67) THEN GOTO 1640
1630 LPRINT TAB(Q(R));"*";
1640 NEXT R
1650 GOTO 1750
1660 FOR R=1 TO M/2
1670 IF Q(R)=66 THEN GOTO 1700
1680 LPRINT TAB(Q(R));"*";
1690 NEXT R
1700 LPRINT TAB(66);"R";
1710 FOR R=M/2+1 TO M
1720 IF Q(R)=66 THEN GOTO 1740
1730 LPRINT TAB(Q(R));"*";
1740 NEXT R
1750 LPRINT TAB(131);"X"
1760 FOR R=1 TO M
1770 Q(R)=0
1780 NEXT R
1790 M=0
1800 NEXT L
1810 FOR Z%=1 TO 131
```

```
1820 LPRINT "X";
1830 NEXT Z%
1840 LPRINT : LPRINT
1850 LPRINT TAB(54)"THE PLOT SCALE IS";C;"FEET PER INCH."
1860 LPRINT
1870 IF X%=<3 THEN 1950
1880 IF BT>10 THEN 2090
1890 BL=(40-BL)/6 : BV=(BV-66)/10 : BA=ATN(BV/BL)*180/3.14159 + .5
1900 BR=BV*C/SIN(BA*3.14159/180)+.5 : BR=ABS(INT(BR)) : BA=INT(BA)
1910 IF BA < 0 THEN BA=BA+180
1920 BB=BA+180
1930 LPRINT "A POSSIBLE SOLUTION USING 4 INTERSECTING LINES ";
1940 LPRINT "IS";BR;"FEET FROM THE VOR ON THE";BA;"OR";BB;"DEGREE RADIAL."
1950 IF X%=>4 THEN 2040
1960 IF PT > 10 THEN 2090
1970 PL=(40-PL)/6 : PV=(PV-66)/10 : PA=ATN(PV/PL)*180/3.14159 + .5
1980 PR=PV*C/SIN(PA*3.14159/180)+.5 : PR = ABS(INT(PR)) : PA = INT (PA)
1990 IF PA < 0 THEN PA=PA + 180
2000 PB=PA+180
2010 LPRINT
2020 LPRINT "A POSSIBLE SOLUTION USING 3 INTERSECTING LINES ";
2030 LPRINT "IS";PR;"FEET FROM THE VOR ON THE";PA;"OR";PB;"DEGREE RADIAL."
2040 LPRINT
2050 LPRINT "THE ABOVE SOLUTION(S) MAY NOT BE VALID AND SHOULD BE VERIFIED ";
2060 LPRINT "BY GRAPHICAL ANALYSIS, ESPECIALLY IF MORE THAN 4 BEARINGS ARE ";
2070 LPRINT "PLOTTED."
2080 LPRINT
2090 LPRINT "THE LOCATION OF THE SCALLOPING SOURCE IS AT THE COMMON ";
2100 LPRINT "INTERSECTIONS OF THE LINES OF ASTERISKS.  TWO POSSIBLE "
2110 LPRINT "SOULTIONS ARE FOUND, ONE CORRECT AND THE OTHER INCORRECT.  ";
2120 LPRINT "THE TWO SOLUTIONS ARE LOCATED ON RECIPROCAL VOR BEARINGS, "
2130 LPRINT "THE SAME DISTANCE FROM THE VOR.  THE CORRECT SOLUTION MUST BE ";
2140 LPRINT "DETERMINED BY INSPECTION OF THE FACILITY. "
2150 LPRINT
2160 LPRINT "THE ABOVE PLOT SHOULD HAVE A CONTINUOUS ROW OF X'S IN THE ";
2170 LPRINT "VERTICAL COLUMNS ON EACH SIDE OF THE PAPER.  IF NOT "
2180 LPRINT "AN ERROR IN THE PLOT HAS OCCURED."
2190 LPRINT
2200 LPRINT "TO MAKE THE LINES OF ASTERISKS MORE VISIBLE, USE A FELT ";
2210 LPRINT "TIP MARKER.  AT ANGLES NEAR 90 OR 270 DEGREES ONLY A FEW "
2220 LPRINT "ASTERISKS PER INCH ARE PRINTED. "
2230 LPRINT CHR$(12)
2240 BT=20:PT=20
2250 LPRINT :LPRINT
2260 PRINT"DO YOU WANT TO CHANGE SCALE AND MAKE ANOTHER PLOT? (Y OR N)  <YES>"
2270 SC$=INPUT$(1)
2280 IF SC$="N" THEN 2310
2290 INPUT"SCALE IN FEET PER INCH= ";C
2300 GOTO 640
2310 PRINT"DO YOU WANT TO CHANGE ANY OF THE SCALLOP DATA?  (Y/N)  <YES>"
2320 DS$=INPUT$(1)
2330 IF DS$="N" THEN 2350
2340 GOTO 320
2350 PRINT"DO YOU WANT TO PLOT ANOTHER FACILITY?  (Y/N)  <YES>"
2360 AF$=INPUT$(1)
2370 IF AF$="N"THEN 2400
2380 GOTO 270
2390 PRINT CL$
```

```
'VORSCAL.BAS'  -  MARCH 1983

2400 PRINT"THIS ENDS THE SCALLOPING ANALYSIS PROGRAM.  HOPE YOU FIND THE SOURCE.
2410 END
```

APPENDIX 5. DESCRIPTION OF SITE DRAWINGS

1. Vicinity Sketch. The following detailed information should be included in this site drawing: (1) location of the facility with respect to any nearby town or airport, if possible, (2) all roads, utility (railroad, power, telephone) lines within the immediate site area, (3) section, county, township or other boundary lines in the vicinity. It should be drawn to include as much area as practicable, and may include general topography. The vicinity sketch is usually combined with the site plan or plot layout.

2. The Site Plan Sketch. This site drawing should show the property ties (easements, rights of way, etc.), natural features, and other important details of the site such as trees, fences, drainage, existing buildings, utility lines, and obstructions within the adjacent terrain (out to 2000 feet, if necessary) of the antenna position. An additional topography map of the site showing more detail than those provided by the geological survey may be required for evaluating sites shown to be especially troublesome. This expansion of the Site Plan is referred to as a "Data of Reflecting Surfaces" and usually is limited to a radius of one mile; particular care should be taken to show the location and orientation of all objects with precision. Correlation with aberrations found on the flight readings will then be possible, and corrective action required will be more easily determined. Plans and profiles of access roads, if applicable, should be included also as supplementary sketches or details.

3. The Plot Layout Plan.

a. The plan should show the layout of the building, the access road, and the location of field detectors, communications antenna, utility terminal pole, other poles, lines of power and control cables, location and log of borings, location of all stakes, marks, and reference points which have been set, and other important details.

b. On the same drawing sheet with the Plot Layout Plan, location data should be noted as follows:

(1) Latitude/Longitude: In degrees, minutes, and seconds, obtained by solar or stellar observations or by referral to a true and correctly known position. The coordinates established for the location should be determined to the best accuracy feasible, but must be at least accurate to the nearest fifteen seconds. This minimum value of accuracy was selected since it is not practical to provide greater accuracy in the majority of instances. (The coordinates for all facilities in the United States will be determined to an accuracy of $\pm$40 feet by the United States Geological Survey.)

(2) Elevation: Nearest 50 feet.

(3) Location: State, Township, Section, County, City, etc.

(4) Power Company: Address and power characteristics.

(5) Telephone Company: Address and type of services available.

(6) Area Type: (desert, farm, etc.).

4. Horizon Profile shall be prepared for each facility. This is to be accomplished by setting up the transit or theodolite at the correct antenna height and location proposed for that particular facility. (A truck roof and/or temporary platform should be used when setting the instrument at 16 feet.) If it has not yet been determined which antenna height is to be used (4 feet or 16 feet), then two profiles should be made. If, however, the horizon profile for an antenna height of 4 feet does not show any object above 0.5° then the profile using the 16 feet does not have to be made. It is very important to ensure that the accuracy of the vertical angle is at least $\pm 0.1^{\circ}$. Plotting this information each 10 degrees throughout the 360 degrees is to be considered nominal; however, where significant changes occur above zero elevation, it is desirable that more frequent readings be taken. The "line of sight" elevation angles thus obtained shall then be used to prepare "Line of Sight Coverage Polar Plots" for aircraft at various altitudes by utilizing figures 6-11 and 6-12. These coverage polar plots are usually prepared for an aircraft altitude of 1500 feet. Identification of the site, elevation, simulated antenna height, and altitude for which the computations were made should be included on the "Coverage Plot."

APPENDIX 6. PANORAMIC MOSAIC PHOTOGRAPHS OF VOR SITES

This appendix provides panoramic mosaic photographs of several VOR sites. These mosaics show the visual horizon profile for each site, with a grid on the photograph to indicate the angular height of obstructions in the field of view. In addition to the visual horizon photos, the Semi-Automated Flight Inspection Bearing Error Reports (SAFI BERs) for each site have been stripped in to show how bearing errors correlate with observed obstructions.

In figure 1, the horizon and BER for the Florence, SC VOR is shown. The scalloping that peaks at an azimuth of 48 degrees appears to arise from the monitor support south of the VOR antenna, in the middle of the extended counterpoise. Another potential source of interference is the line of trees north and east of the antenna, particularly the tall cluster at about 28 degrees azimuth. However, the BER does not have sufficient resolution to verify that these trees are a source of scalloping.

Figure 2 shows the horizon profile and BER for the Toccoa, GA VOR. This is representative of mountaintop VOR installations, and suggests some of the problems with this type of site. Note the twin hilltops at the 325-degree azimuth. This feature of the terrain is intrusive to the VOR field and yet, is too large to be removed or significantly altered. The BER does not have sufficient resolution to identify what impact these hilltops have on the VOR signal.

Figure 3 is the horizon profile seen from the St. Thomas, VI VOR. This is another mountaintop site, although with an unusually clear field of view except for the mountaintops to the east-southeast (95° to 100° azimuth). Some of the blank segments of the BER are suggestive of interference from this ridge, but the actual flight recordings would be required to determine the precise effect of these mountaintops.

Figure 4 is the panoramic view from the Atlanta, GA Doppler VOR, as well as a SAFI BER for that station. This horizon is very clear, the only obstructions being the airport control tower at 46 degrees azimuth, a water tower at 217 degrees azimuth, and a tall tree at 245 degrees azimuth. The BER has too much smoothing to permit identification of the scalloping that may arise from these obstructions.

See appendix 4 for a description of the use of flight recordings in determining the specific location of scalloping sources.

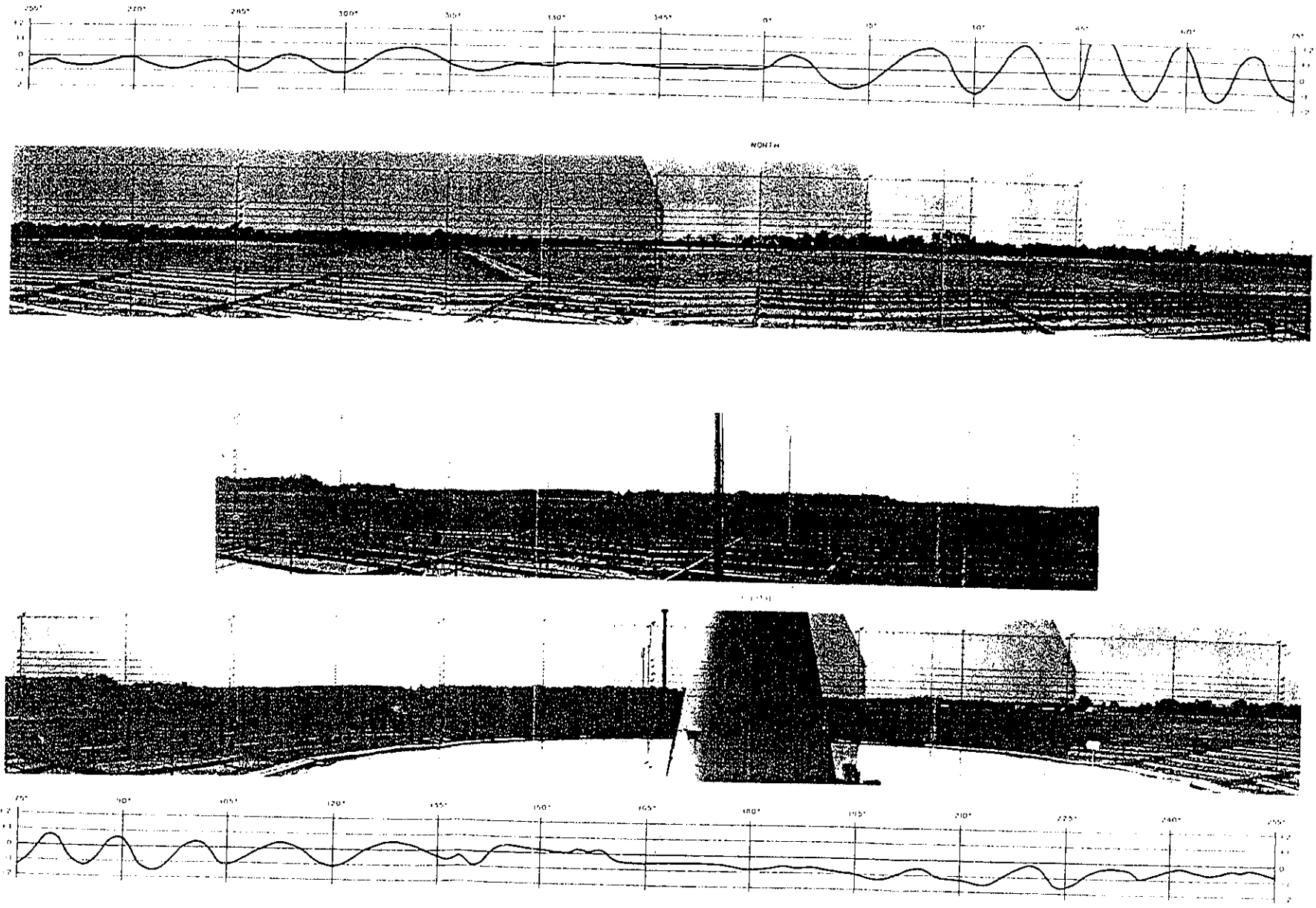

FIGURE 1. FLORENCE, S.C. VOR Page 3(and 4)

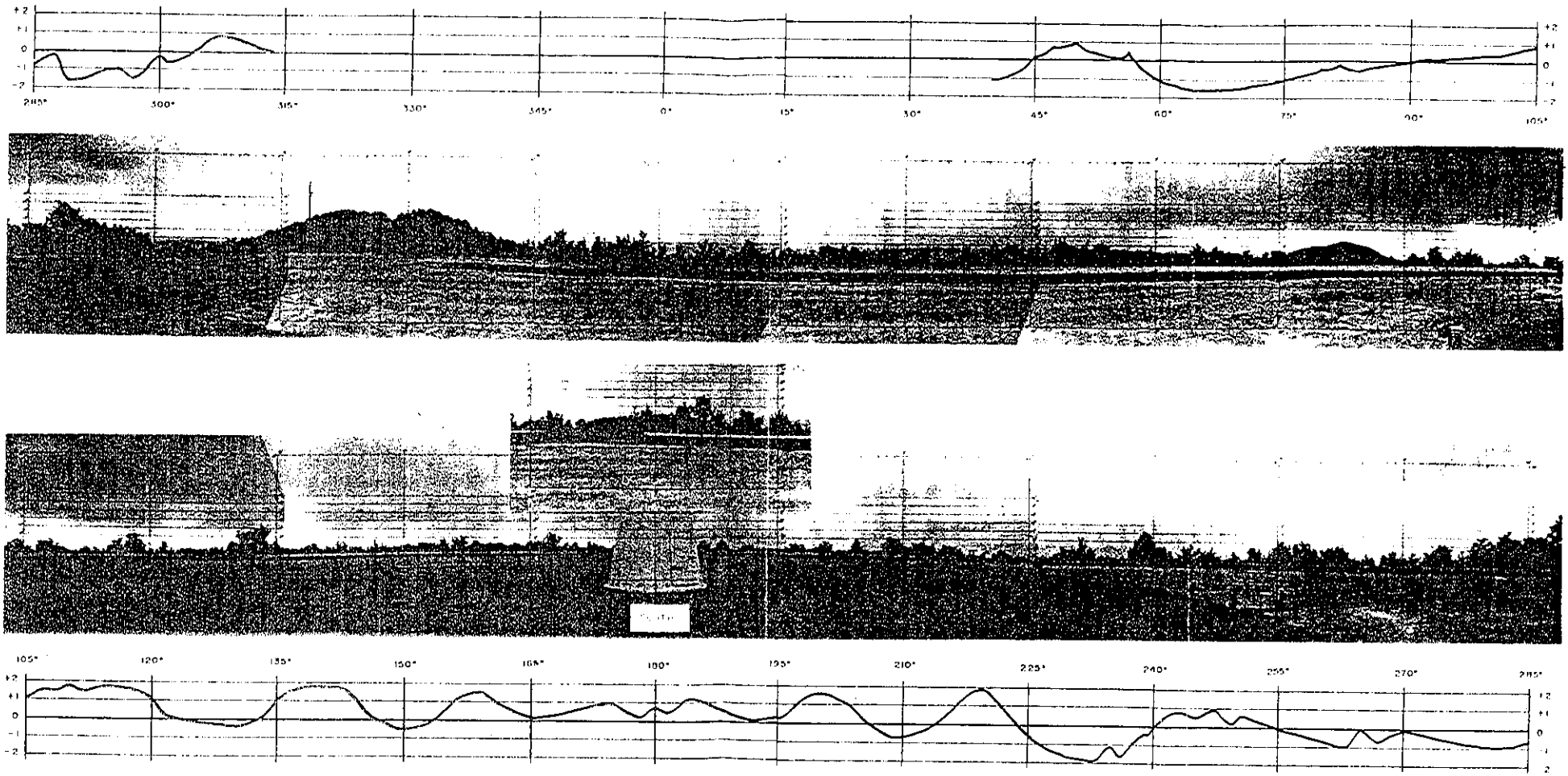

FIGURE 2. TOCCOA, GA. VOR

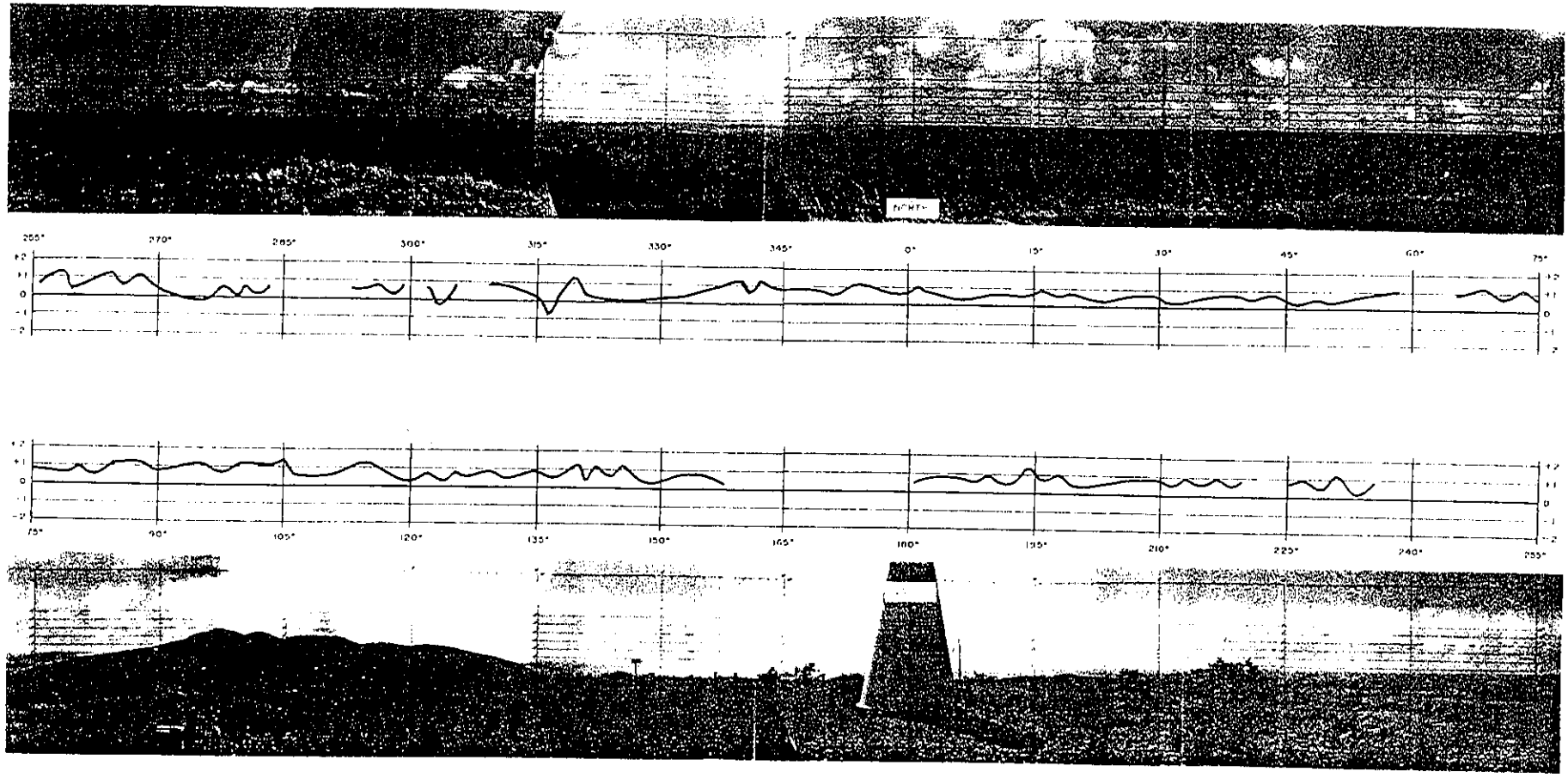

FIGURE 3. ST. THOMAS, V.I. VOR

Page 7(and 8)

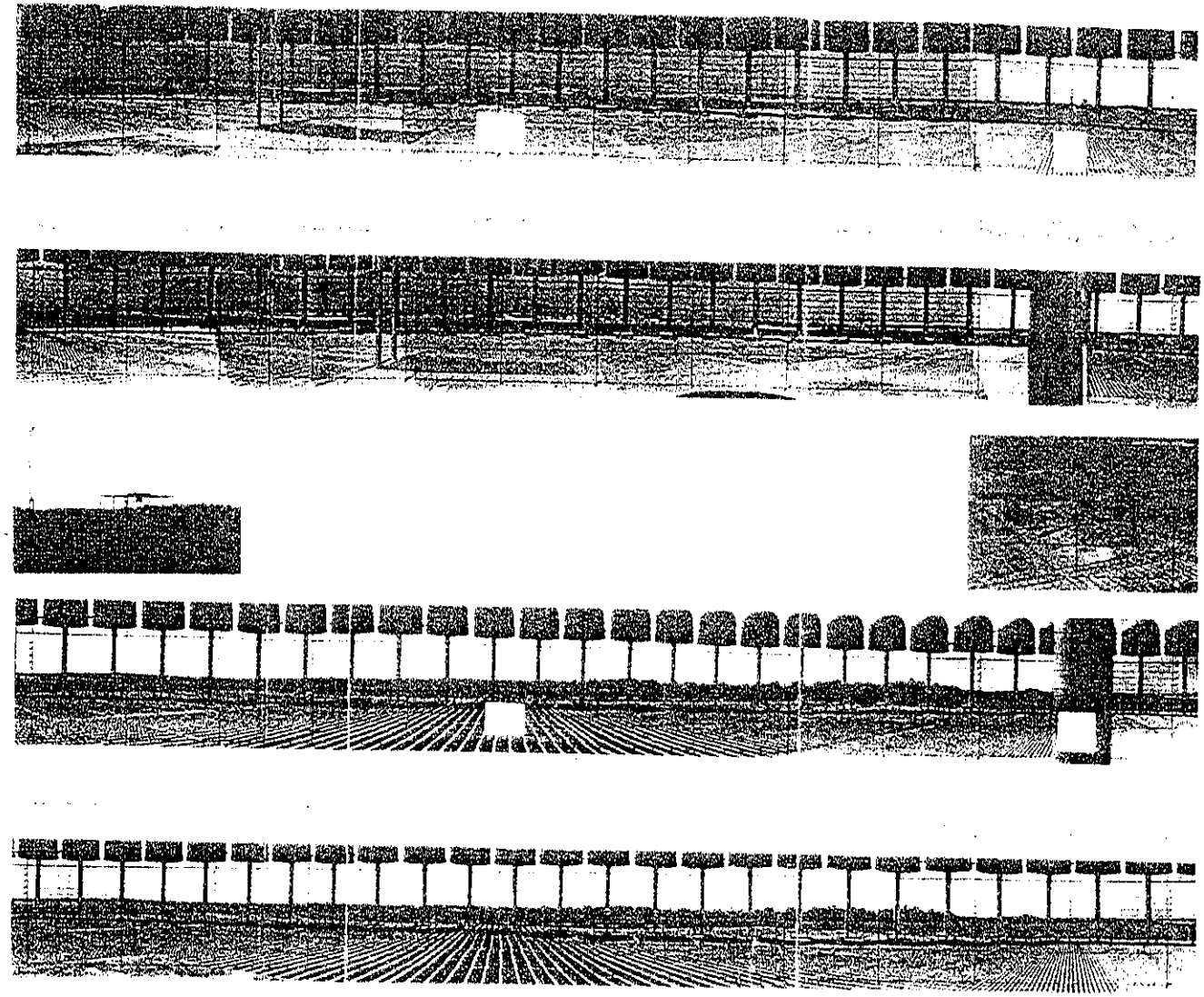

FIGURE 4. ATLANTA, GA. DVOR Page 9(and 10)

APPENDIX 7. TYPICAL VOR SITES

Section 1. General

1. INTRODUCTION. Presented in this appendix are the measured performances and plan views of a series of typical VOR sites of varying complexity accumulated by the FAA over the years. Included are a number of mountaintop facilities. Data were selected on the basis of what was deemed most useful to the siting engineer.

Section 2. Alma, Georgia

COMMENTS: This is a good site inasmuch as the terrain is flat and the trees and reflecting objects have been cleared to a radius of approximately 2000 feet. A study of the course scalloping from the recordings of the 20-mile-radius calibration showed that most of the scalloping is nonsinusoidal, a characteristic of scalloping caused by trees.

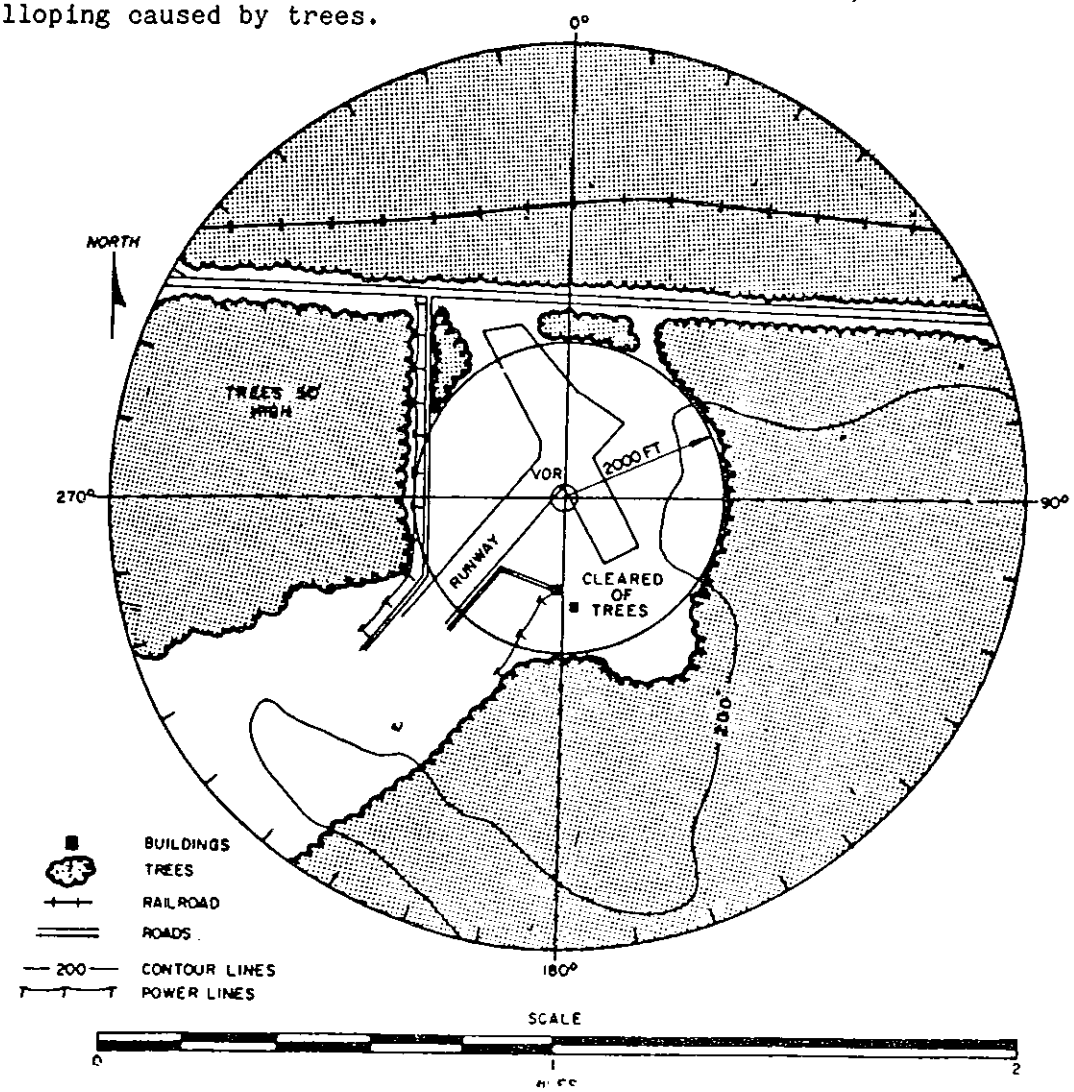

FIGURE 1. VICINITY SKETCH (1-Mile Radius) ALMA, GEORGIA

Section 2. Alma, Georgia (continued)

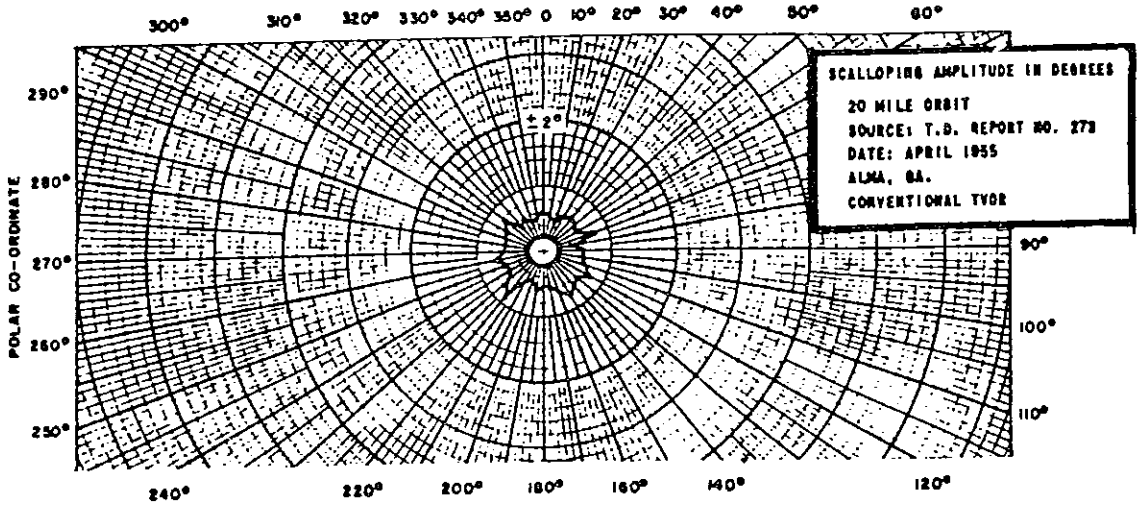

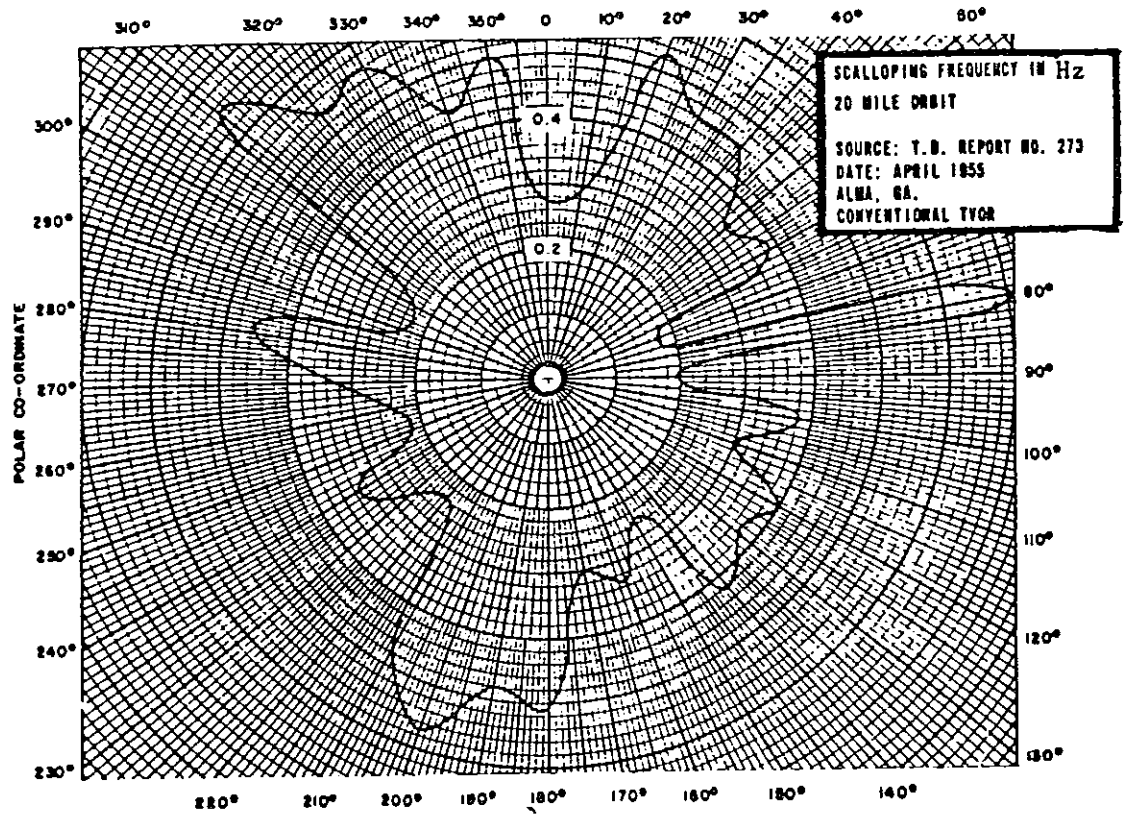

FIGURE 2. SCALLOPING AMPITUDE AND FREQUENCY

Section 3. Atlantic City, New Jersey (FAA Technical Center)

COMMENT: Tests were conducted at the experimental VOR to determine the effects of isolated forest areas. The data obtained during these tests are also shown in Figure 3.5.

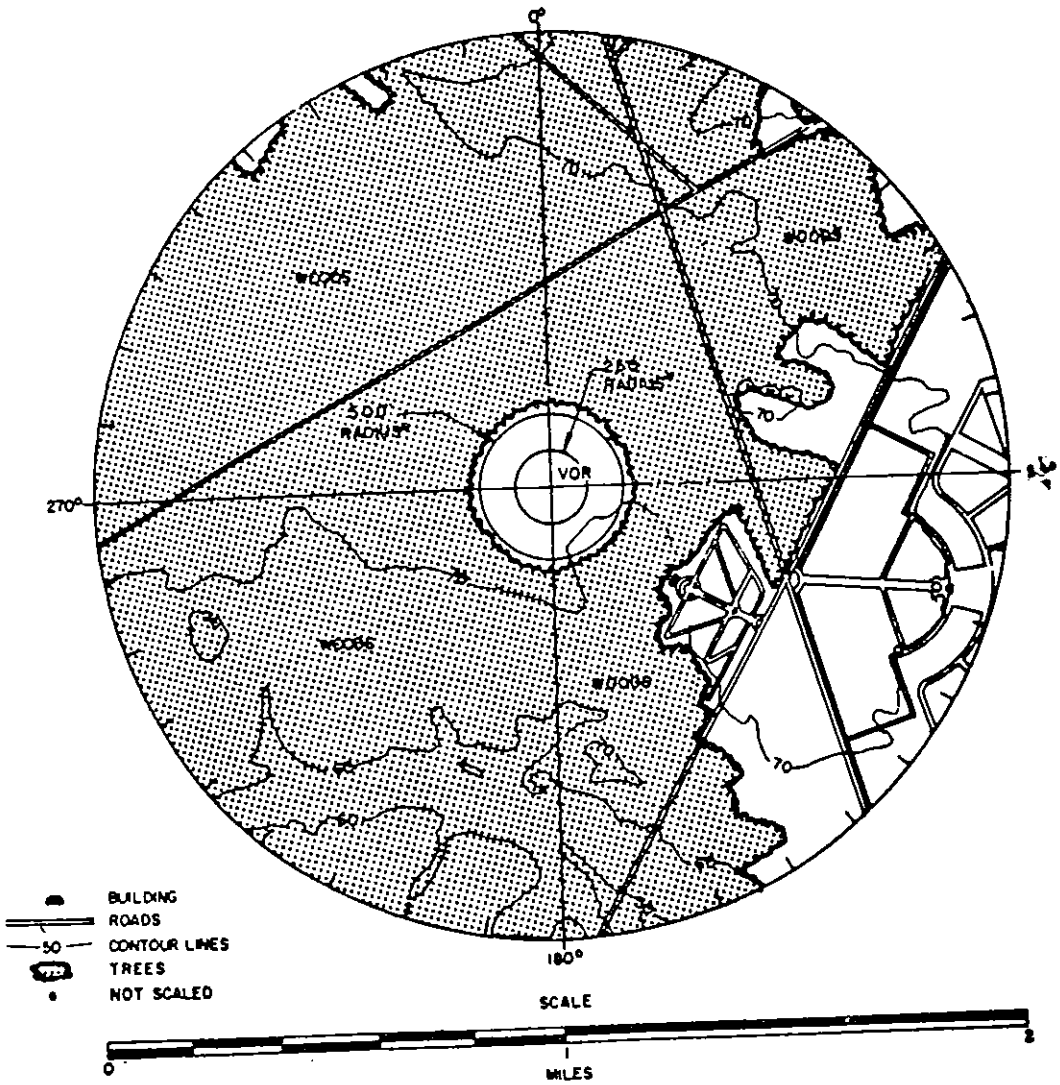

FIGURE 3. VICINITY SKETCH (1-MILE RADIUS) ATLANTIC CITY, NEW JERSEY EXPERIMENTAL VOR

Section 3. Atlantic City, New Jersey (FAA Technical Center) (continued)

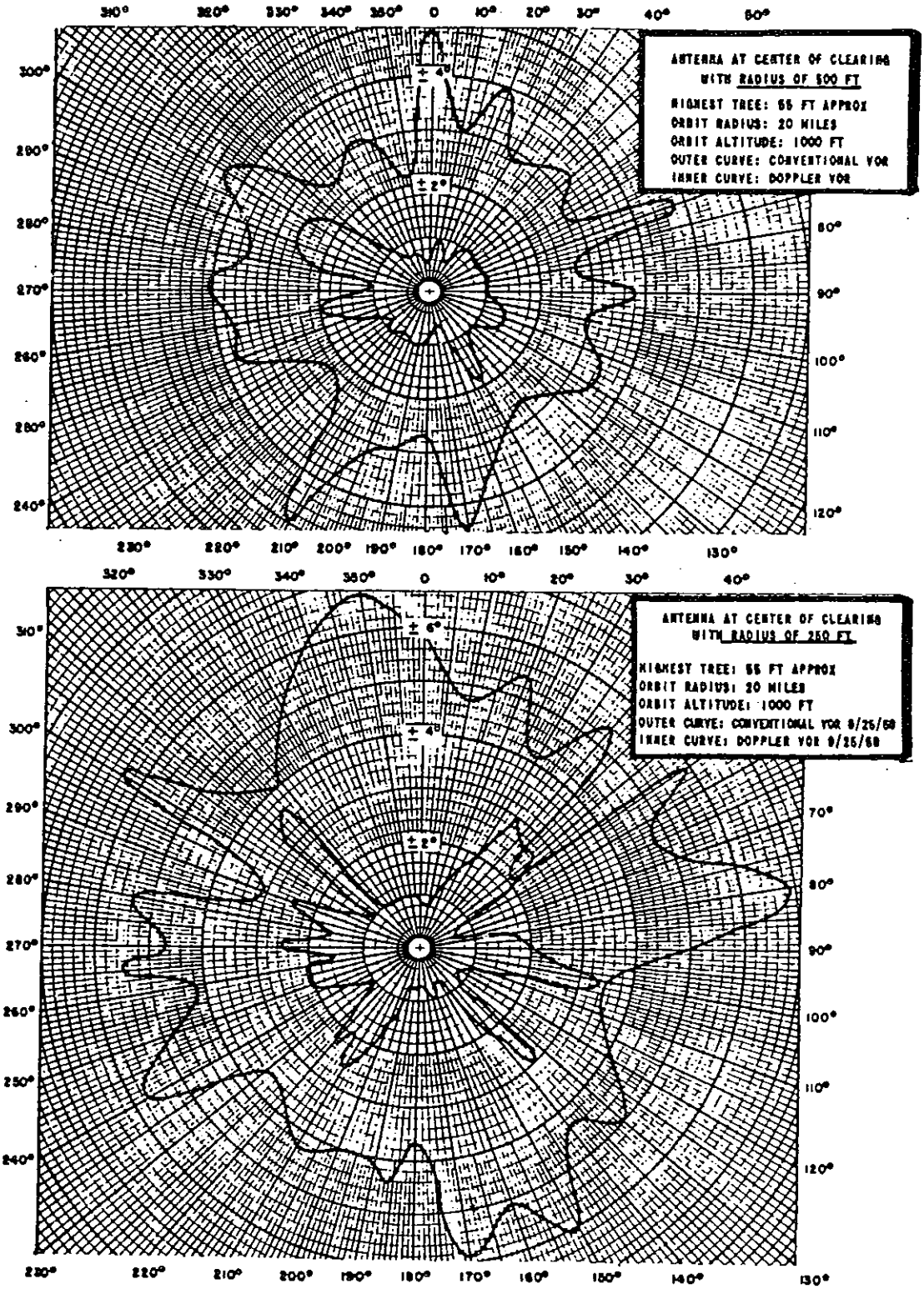

FIGURE 4. SCALLOPING AMPLITUDE

Section 4. Augusta, Maine

COMMENT: This airport site serves as an en route as well as a terminal navigational aid facility.

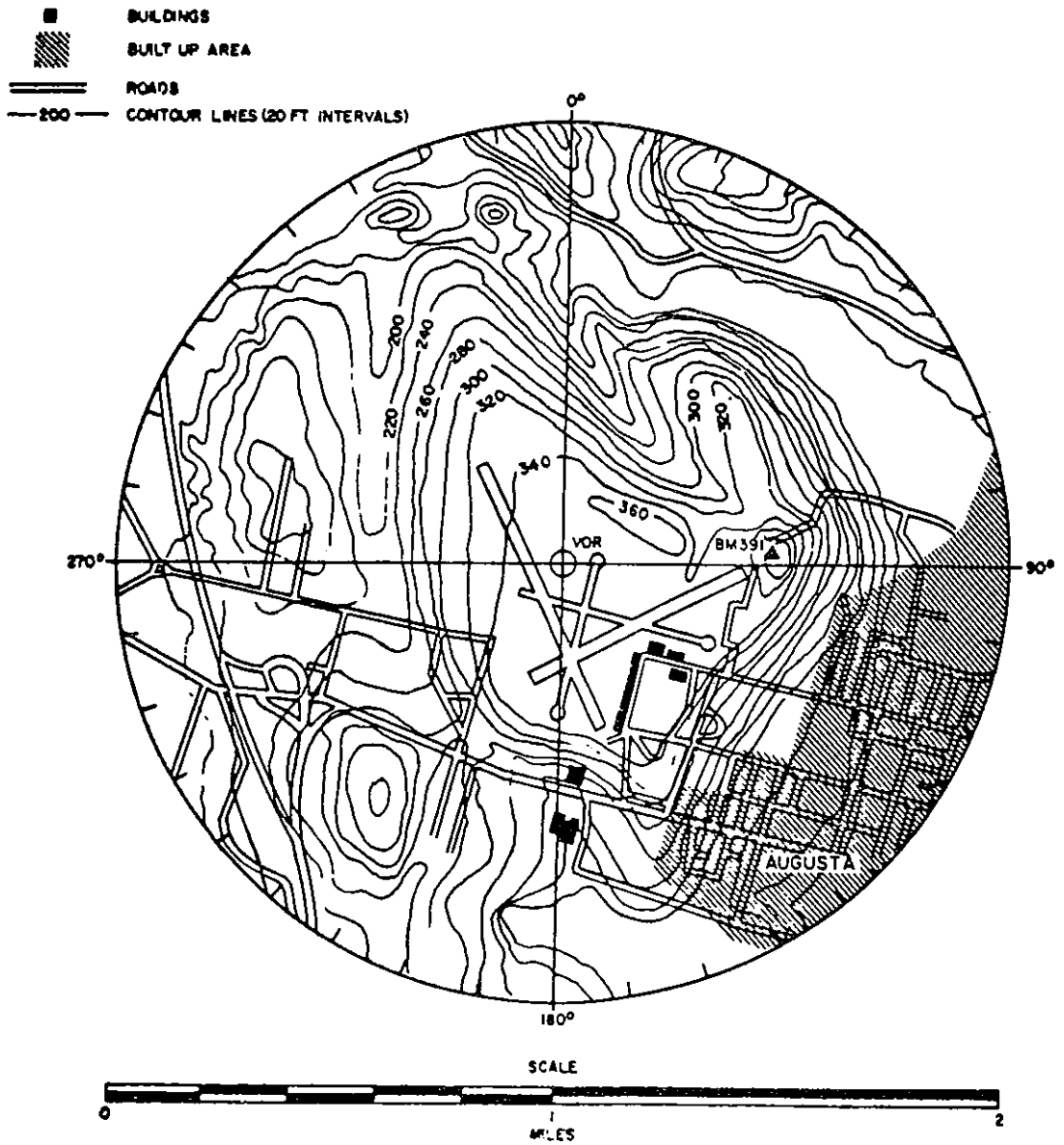

FIGURE 5. VICINITY SKETCH (1-MILE RADIUS) AUGUSTA, MAINE (VORTAC)

Section 4. Augusta, Maine (continued)

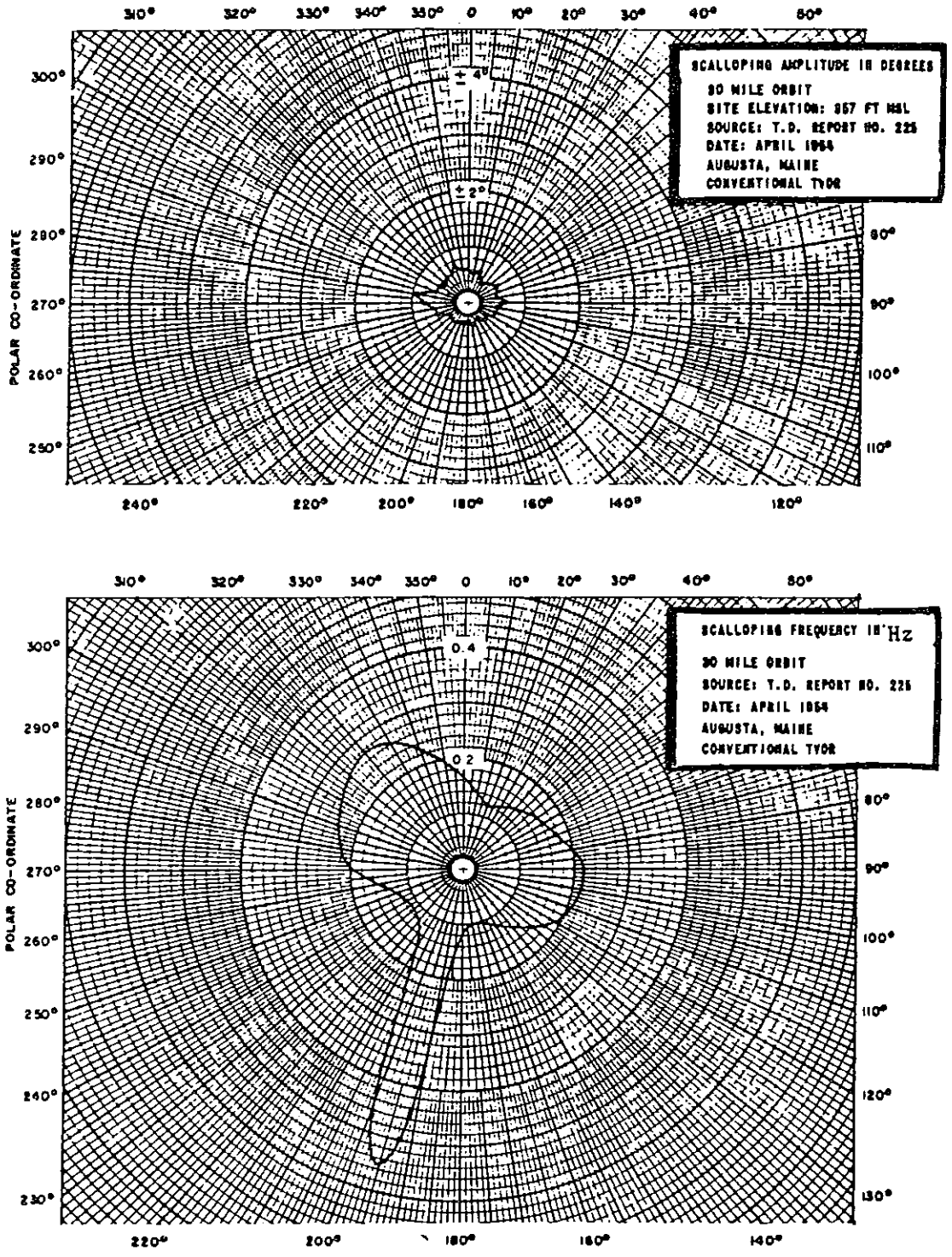

FIGURE 6. SCALLOPING AMPLITUDE AND FREQUENCY

Section 5. Biscayne Bay, Florida

COMMENTS: Experience has shown that ships and large aquatic structures within 2500 feet and aircraft within a mile of the facility are capable of causing significant VOR scalloping or errors. Beyond the one-mile radius mapped, tower extending 1000 feet or more above the VOR site may account for the measured scalloping and roughness.

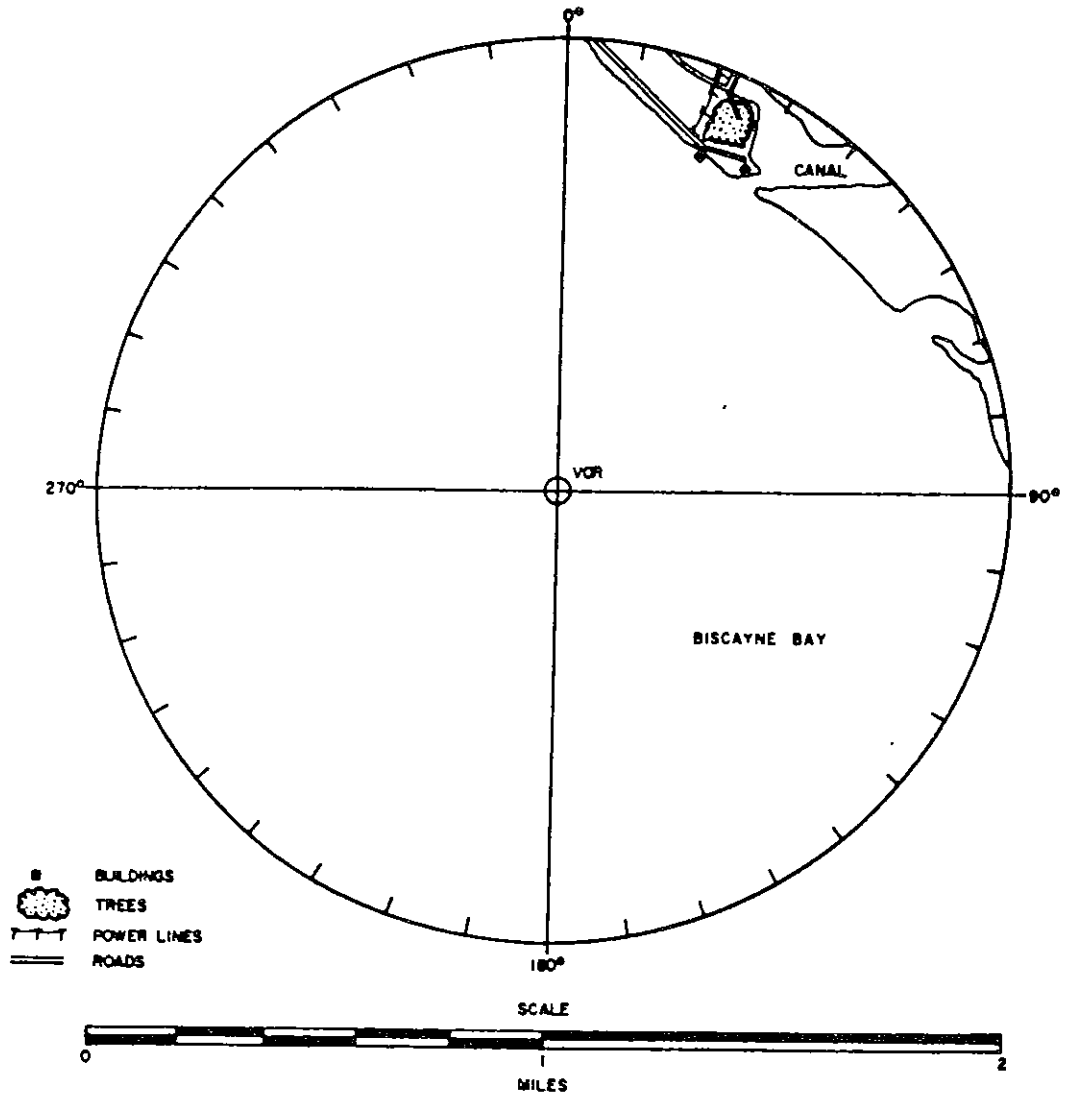

FIGURE 7. VICINITY SKETCH (1-MILE RADIUS) BISCAYNE BAY, FLORIDA VOR

Section 5. Biscayne Bay, Florida (continued)

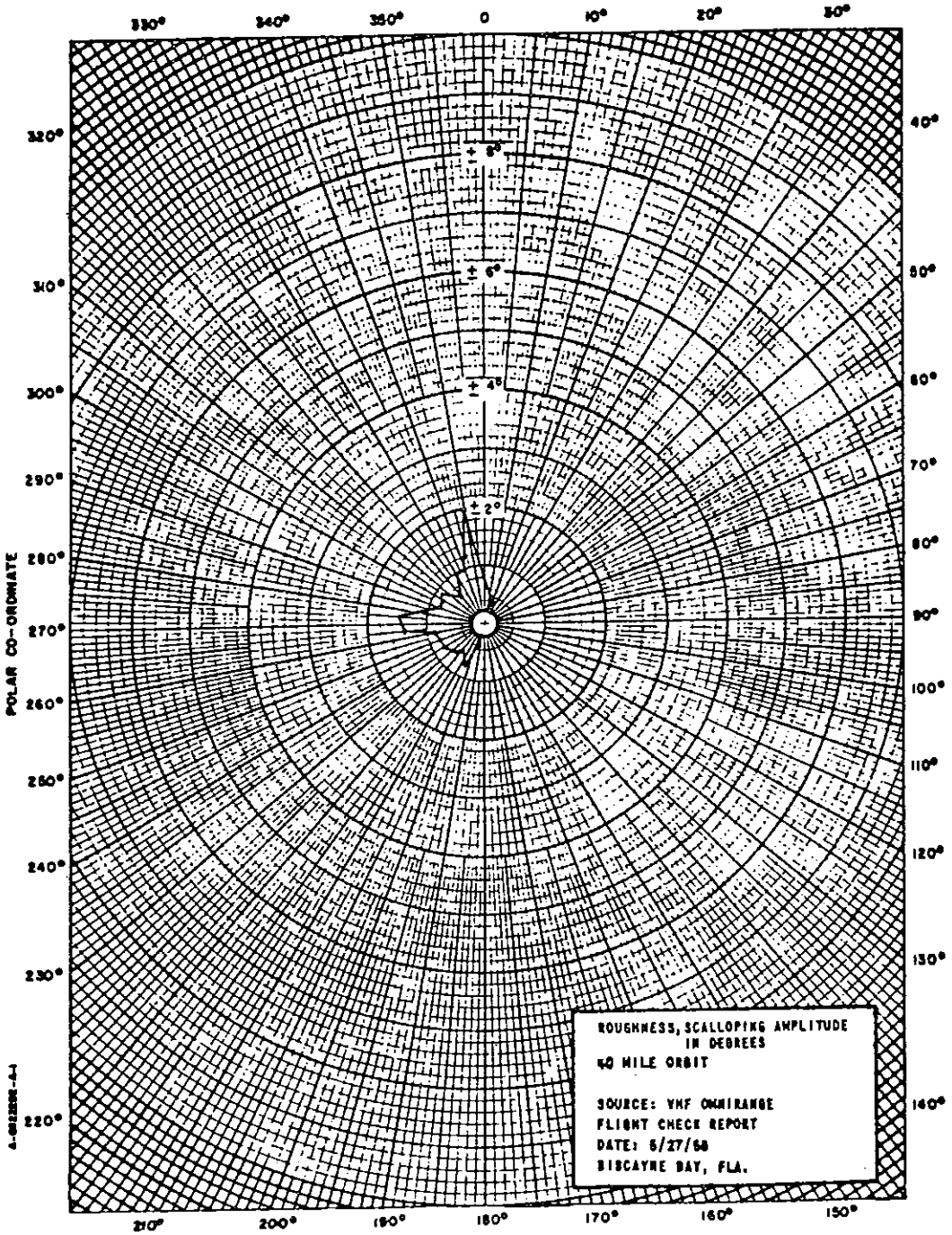

FIGURE 8. ROUGHNESS AND SCALLOPING

Section 6. Boulder City, Nevada

COMMENT: This is an example of a satisfactory "Conventional" VOR in very difficult terrain. Successful operation was achieved by use of a very large counterpoise (200-foot diameter). For additional information see VORTAC Facility Plot Plan.

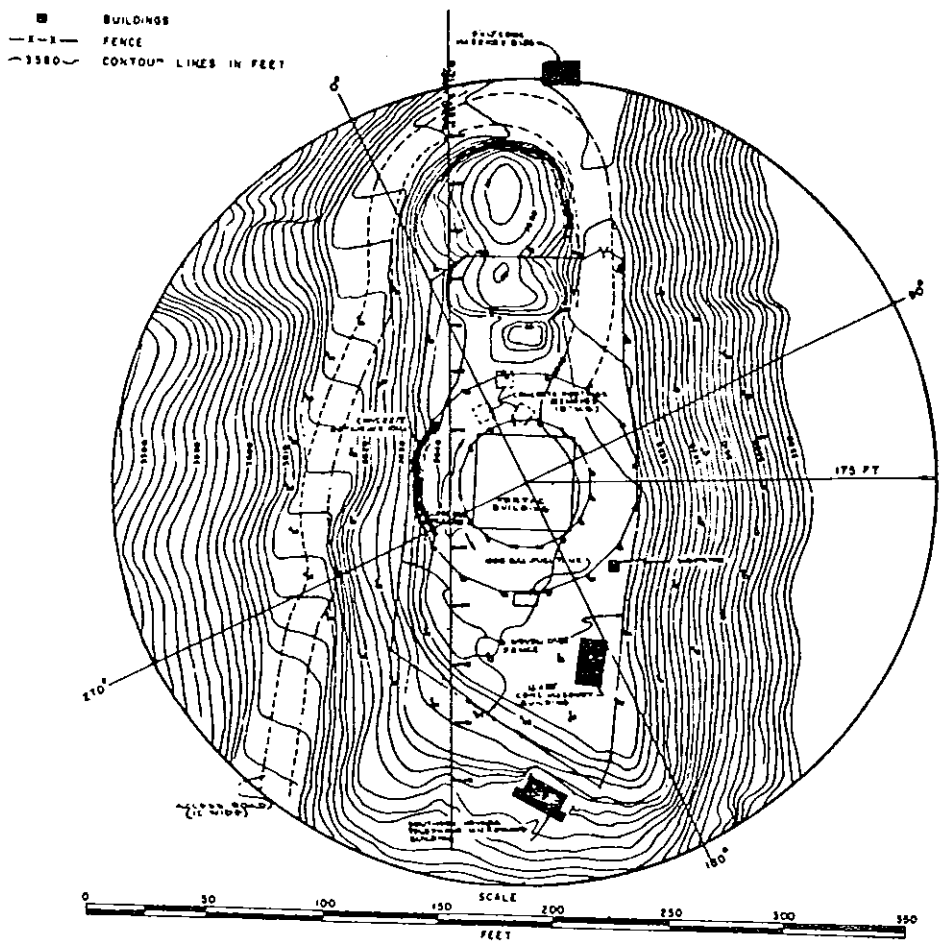

FIGURE 9. VICINITY SKETCH (175-FOOT RADIUS) BOULDER CITY, NEVADA VORTAC

Section 6. Boulder City, Nevada (continued)

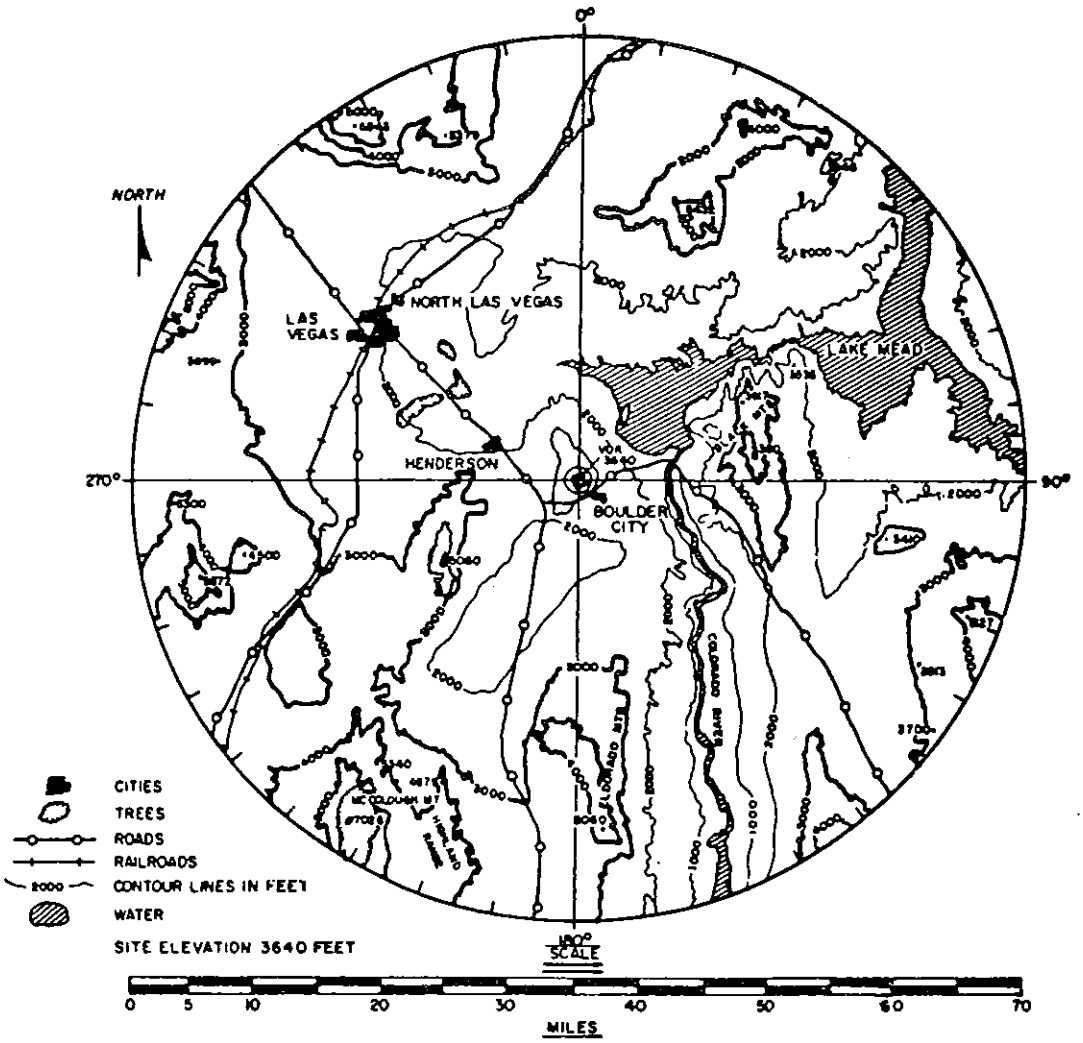

FIGURE 10. VICINITY SKETCH (35-Mile Radius) BOULDER CITY, NEVADA VORTAC

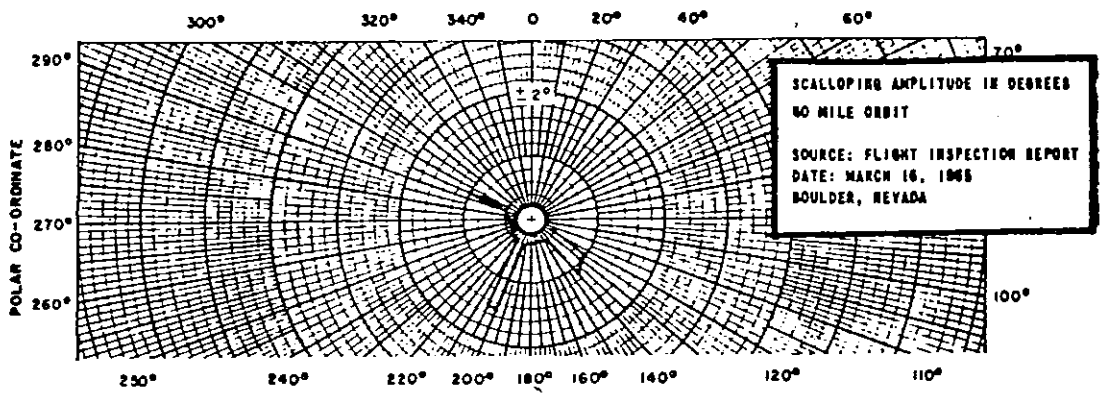

FIGURE 11. SCALLOPING AMPLITUDE

Section 7. Chattanooga, Tennessee

COMMENTS: This is a satisfactory site located in very rugged terrain. The site for the VOR antennas was prepared with very little earth-moving. The station is sited on a knob approximately as high as or higher than the nearby mountainous terrain.

The large scalloping at 16 degrees azimuth is believed to be caused by energy reflected off an inclined plane formed by the ridge running northeast, which redirects the signal to the 16-degree azimuth. It is also quite possible that reflected energy from below the site causes nulls in the vertical plane field intensity pattern at 16 degrees azimuth resulting in the course roughness and scalloping.

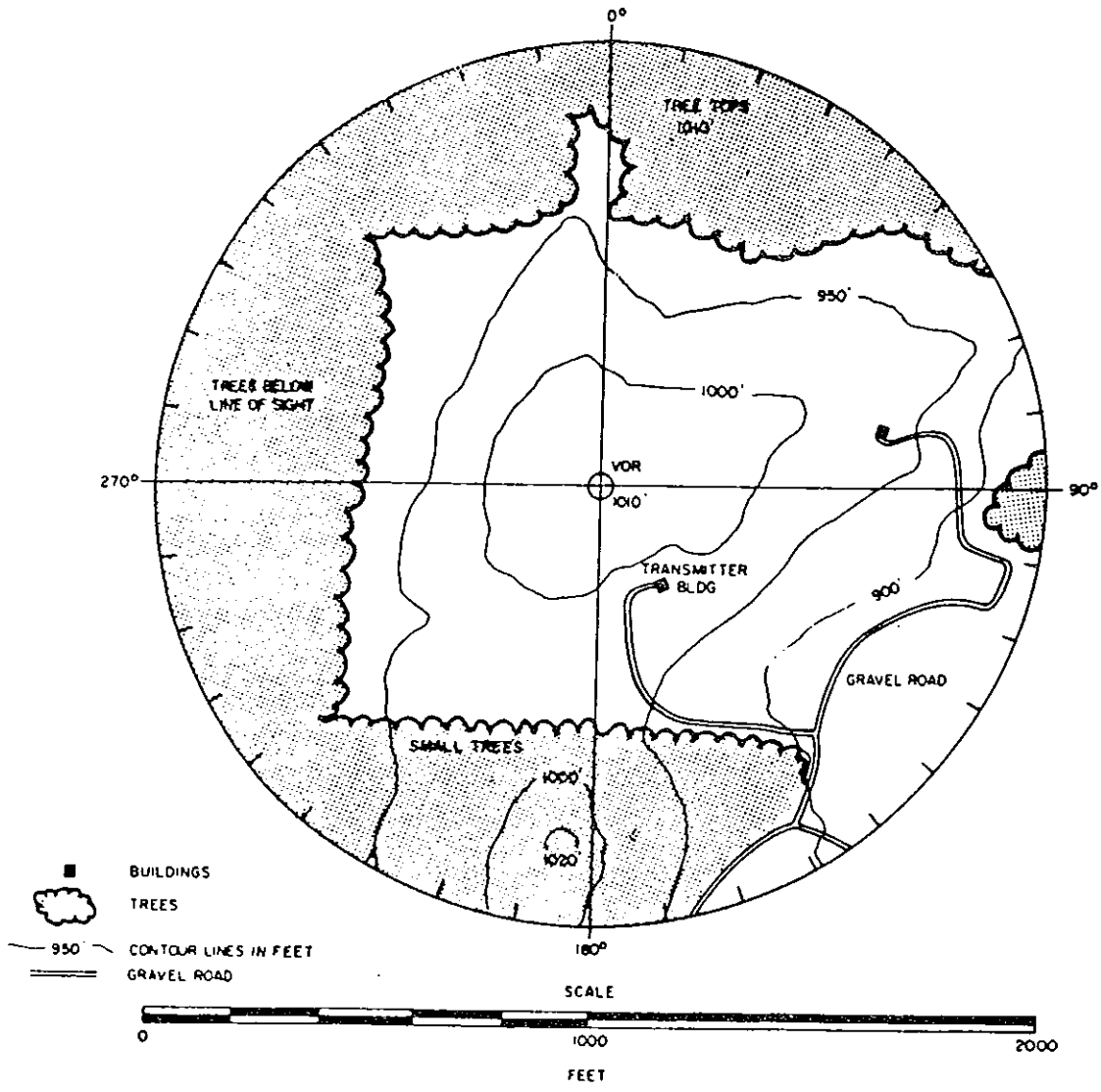

FIGURE 12. VICINITY SKETCH (1000-FOOT RADIUS) CHATTANOOGA, TENNESSEE (VORTAC)

Section 7. Chattanooga, Tennessee (continued)

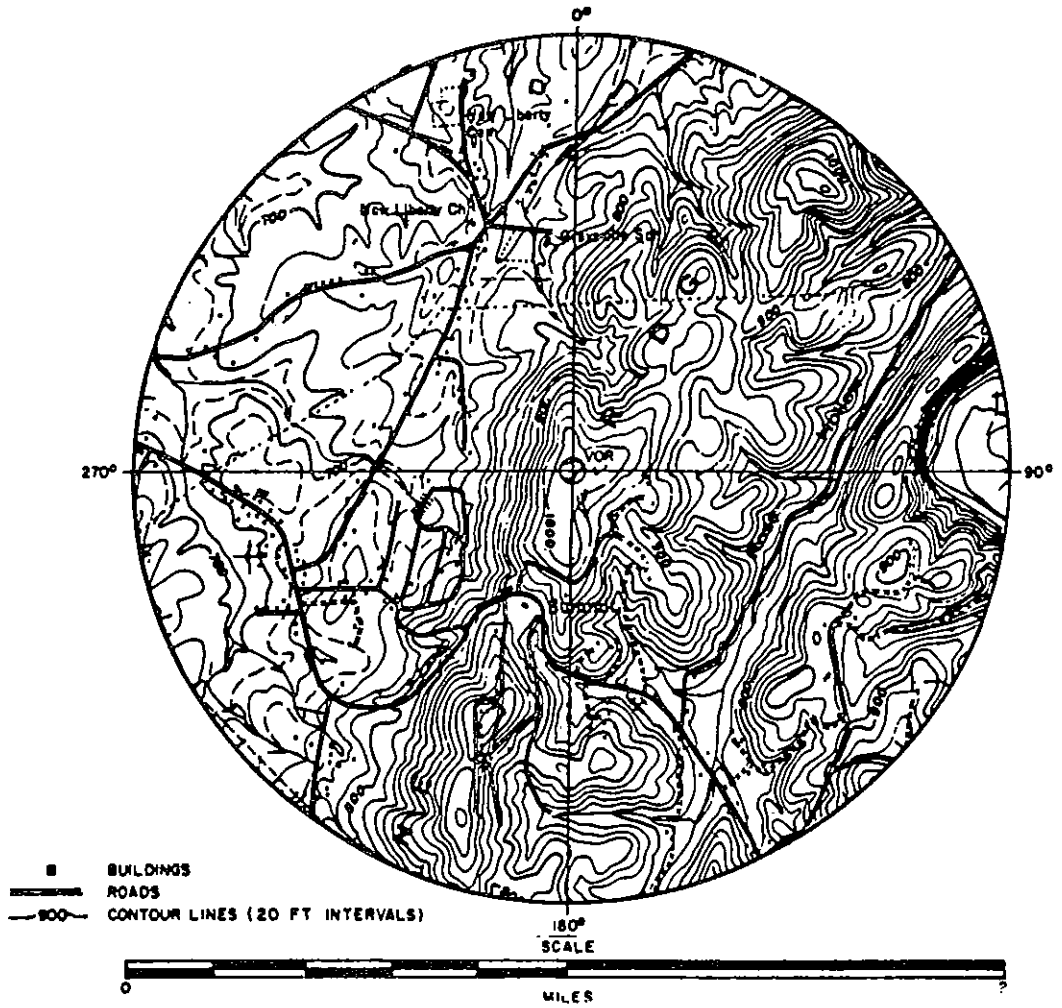

FIGURE 13. VICINITY SKETCH (1-Mile Radius) CHATTANOOGA, TENNESSEE (VORTAC)

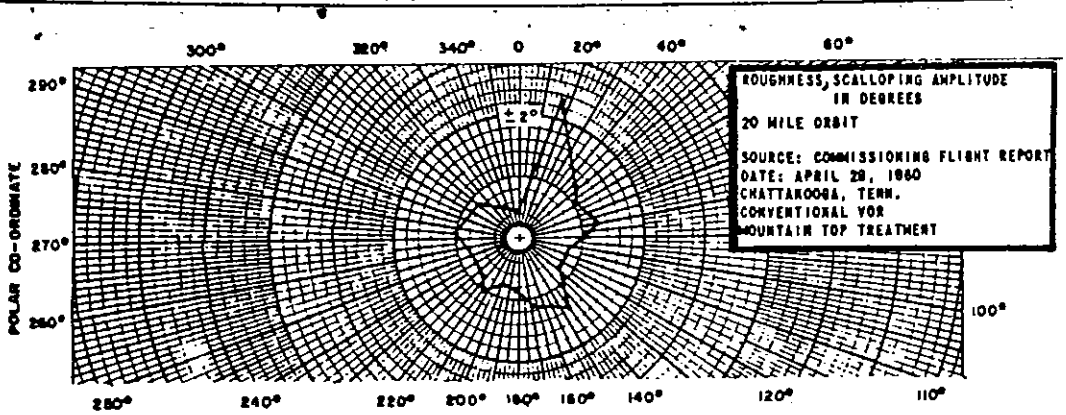

FIGURE 14. ROUGHNESS AND SCALLOPING

Section 8. Columbia, South Carolina

COMMENT: This is an example of an unsatisfactory VOR site test. Excessive bearing errors and severe scalloping on many radials (not shown) were the principal deficiencies. The surrounding forests and the irregular nearby terrain contours were the specific conditions necessitating selection of an alternate site for the VOR.

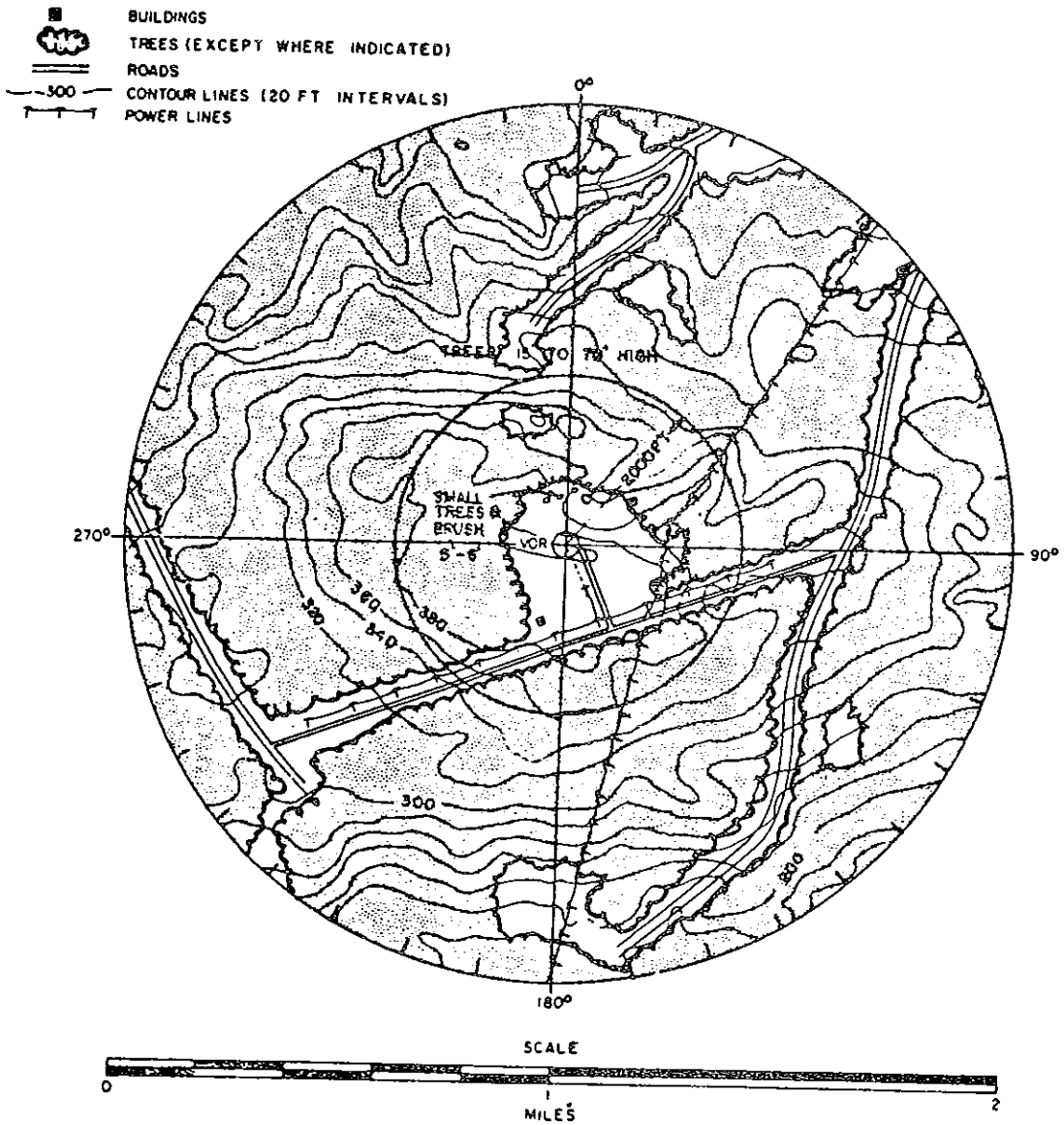

FIGURE 15. VICINITY SKETCH (1-MILE RADIUS) COLUMBIA, SOUTH CAROLINA (TEST SITE FACILITY)

Section 8. Columbia, South Carolina (continued)

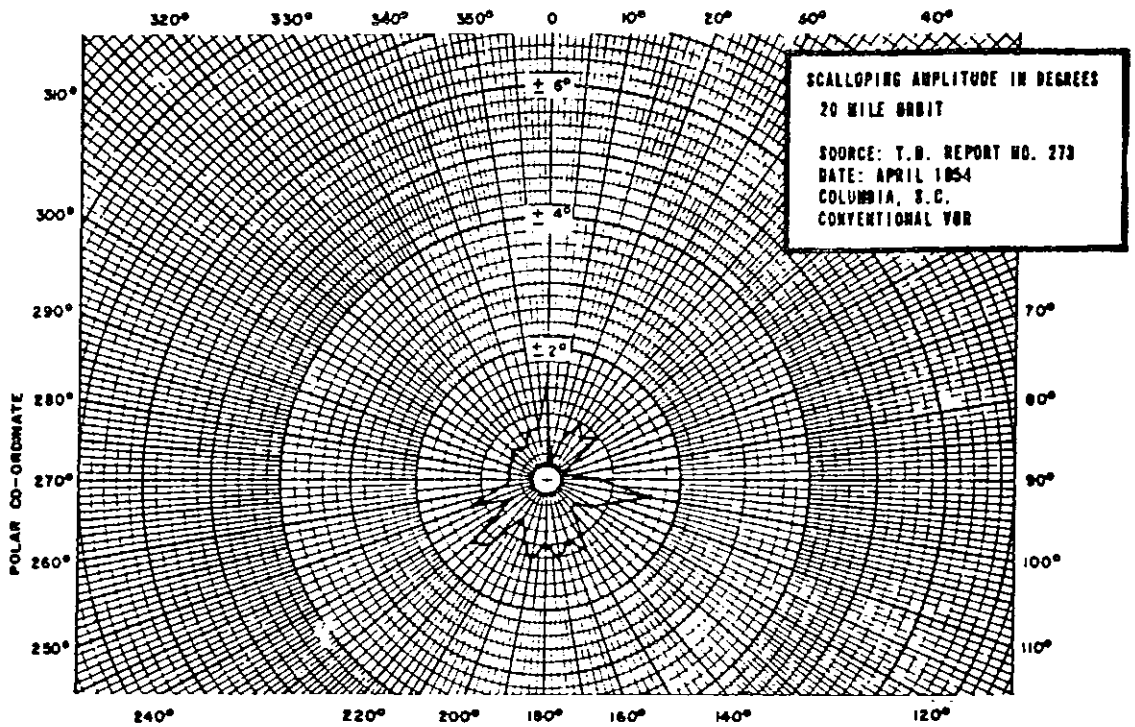

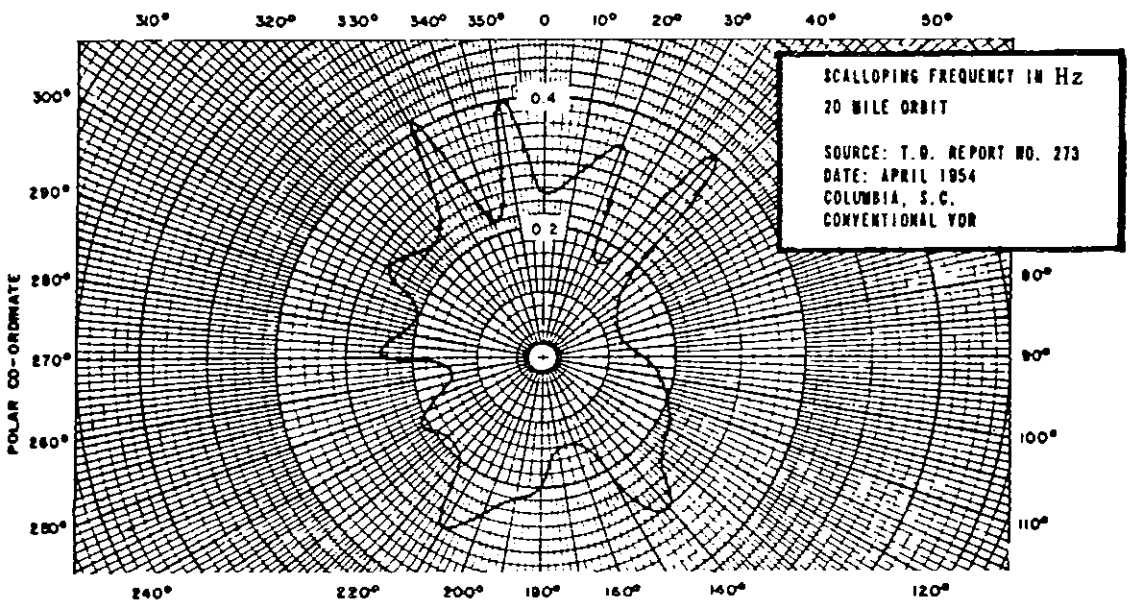

FIGURE 16. SCALLOPING AMPLITUDE AND FREQUENCY

Section 9. Dayton, Ohio

COMMENT: This site is unacceptable as a VOR facility because of scalloping and bending on many radials due to trees. The maximum course scalloping was caused by the wooded section shown on the map approximately 1000 feet south of the VOR. Considerable course scalloping was also caused by the small woods northwest of the VOR.

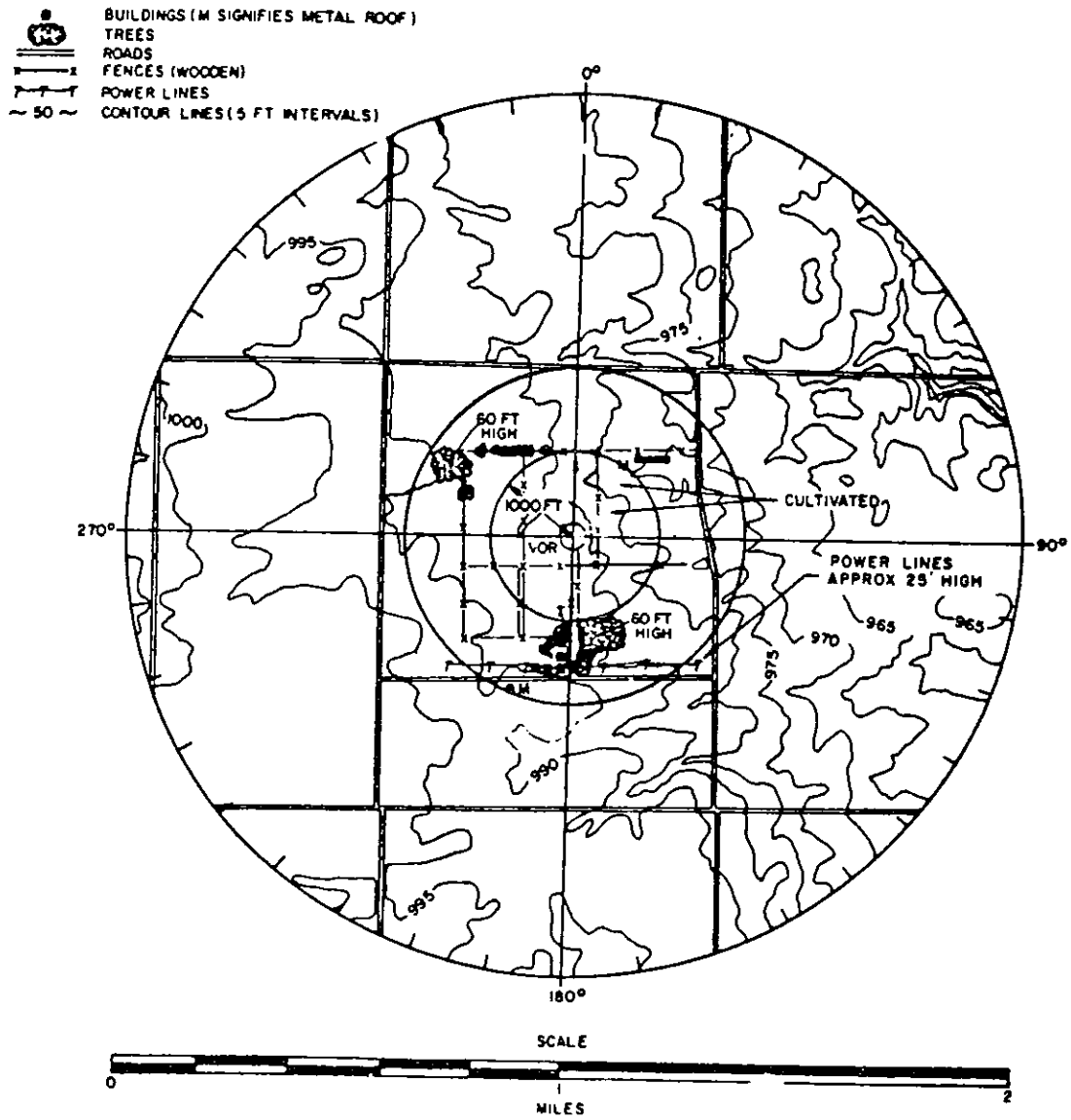

FIGURE 17. VICINITY SKETCH (1-MILE RADIUS) DAYTON, OHIO

Section 9. Dayton, Ohio (continued)

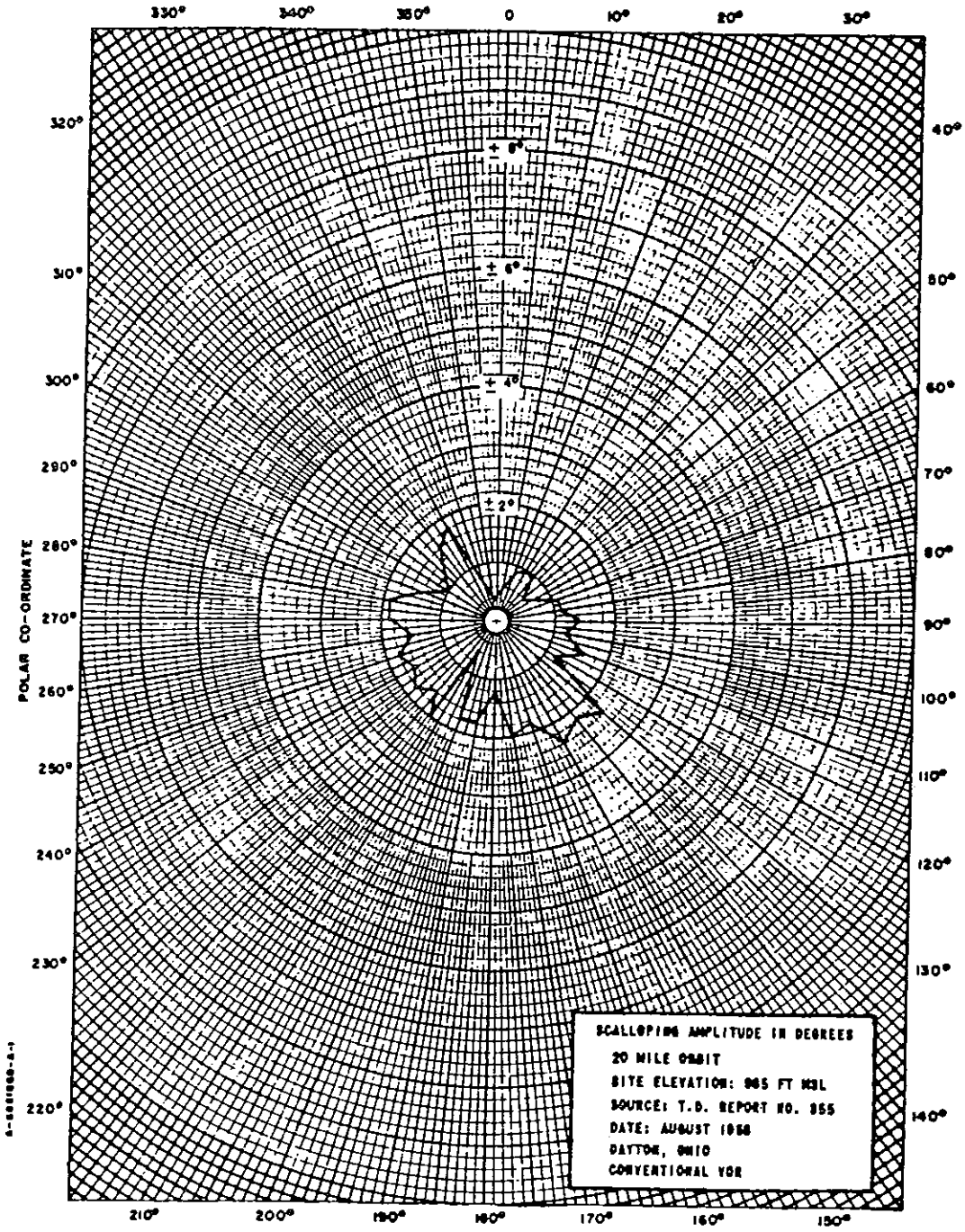

FIGURE 18. SCALLOPING AMPLITUDE

Section 10. Elizabeth City, North Carolina

COMMENTS: The Elizabeth City, North Carolina VOR is located on flat terrain which is free of obstructions for a minimum radius of 1500 feet. A dense wooded area having trees 90 feet high is located approximately 2250 feet from the VOR at an azimuth of 240 degrees. Power lines 20 to 40 feet high enclose three sides of the site at distances of 1500 feet or more.

Woods produce nonsinusoidal course scalloping (course roughness) making it difficult to analyze the scalloping by measuring frequency. Since woods cause scalloping in their approximate direction, the scalloping in the sector from 180 to 250 degrees is no doubt caused by the 60- to 90-foot trees.

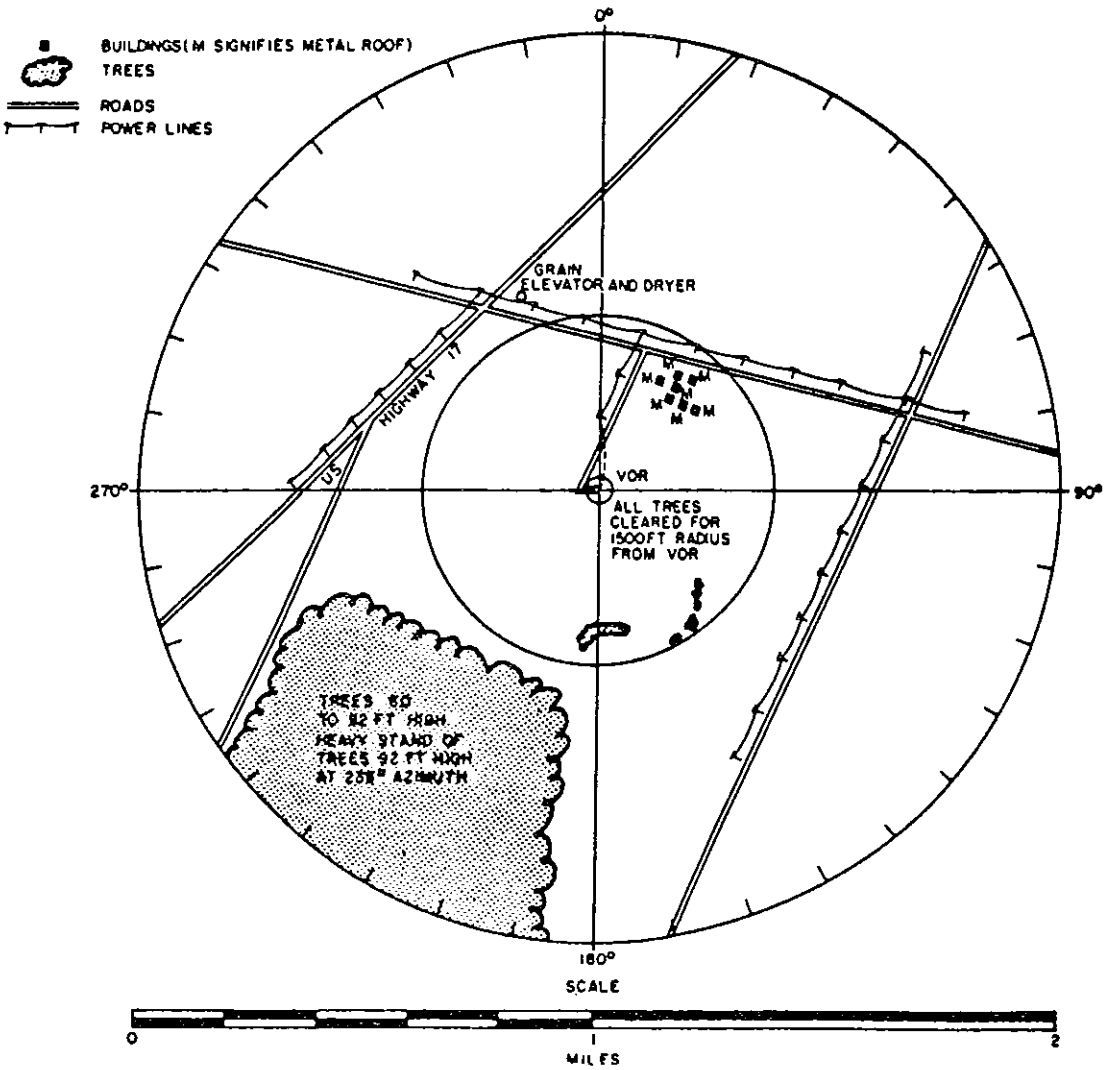

FIGURE 19. VICINITY SKETCH (1-MILE RADIUS) ELIZABETH CITY, NORTH CAROLINA VOR

Section 10. Elizabeth City, North Carolina (continued)

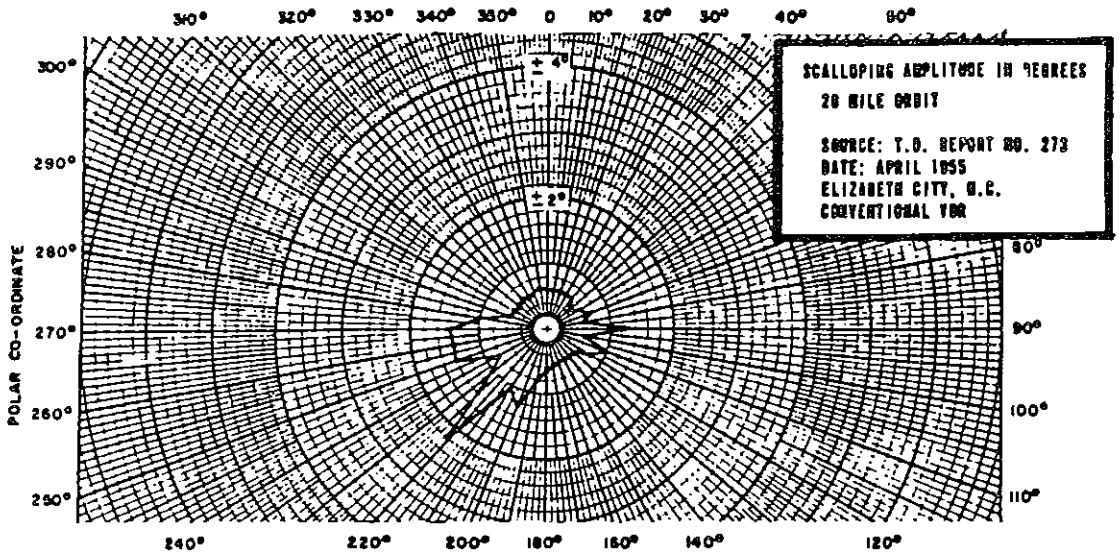

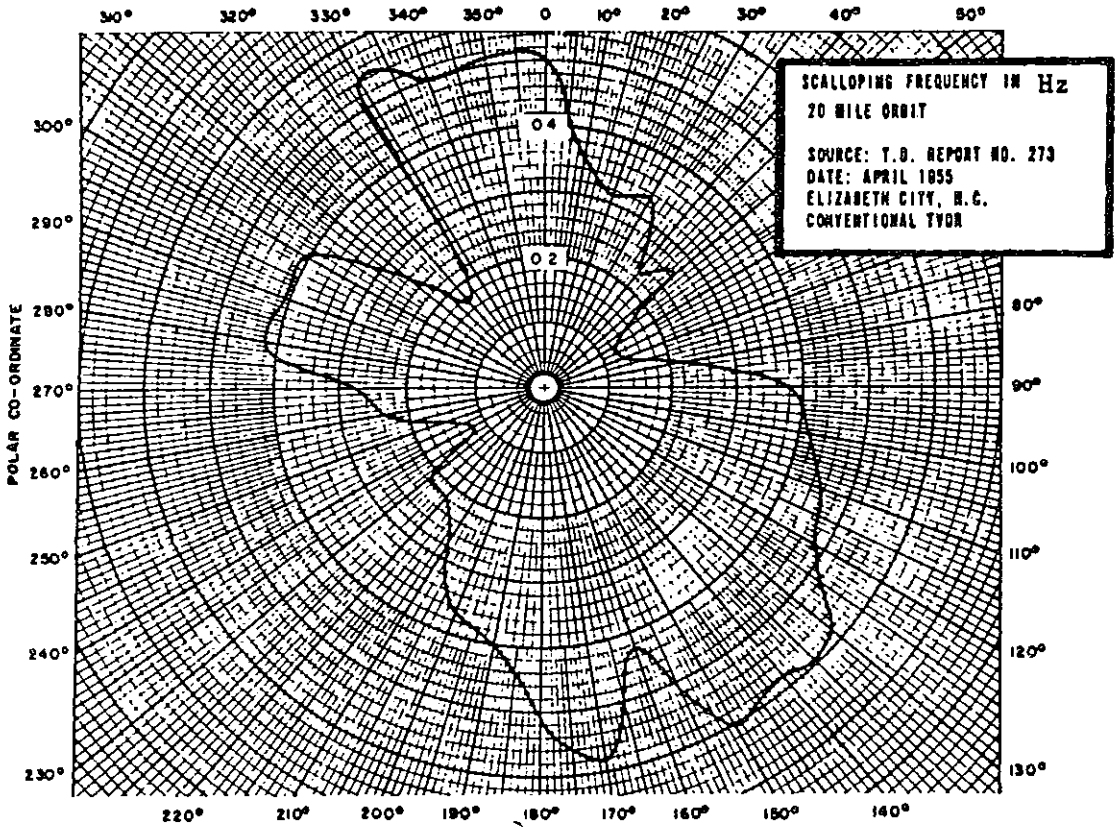

FIGURE 10. SCALLOPING AMPLITUDE AND FREQUENCY

Section 11. Florence, South Carolina

COMMENTS: When operating as a conventional VOR, the power line and trees cause marginal performance. As a Doppler VOR, considerable improvement is realized.

A comparison of orbital and radial scalloping measured on the 248 degrees azimuth at 20 miles distance is very instructive. The conventional VOR produced ±1.2-degrees scalloping on the orbital flight and ±2.5 degrees on the radial flight test. The higher value is a result of the much lower scalloping frequency normally evidenced on all radial flights and the attendant reduced effectiveness of the course deviation indicator filter.

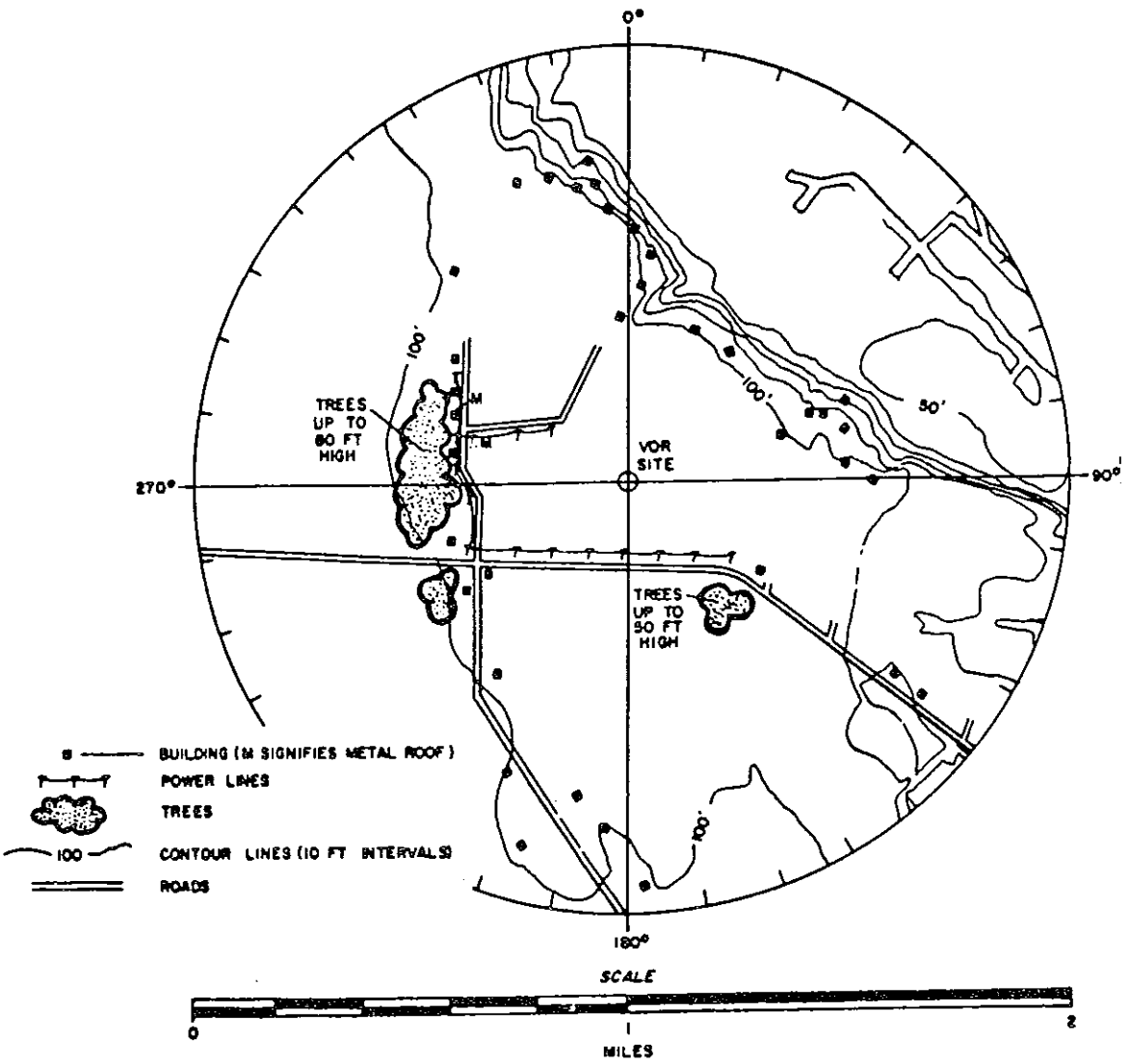

FIGURE 21. VICINITY SKETCH (1-MILE RADIUS) FLORENCE, SOUTH CAROLINA VOR

Section 11. Florence, South Carolina (continued)

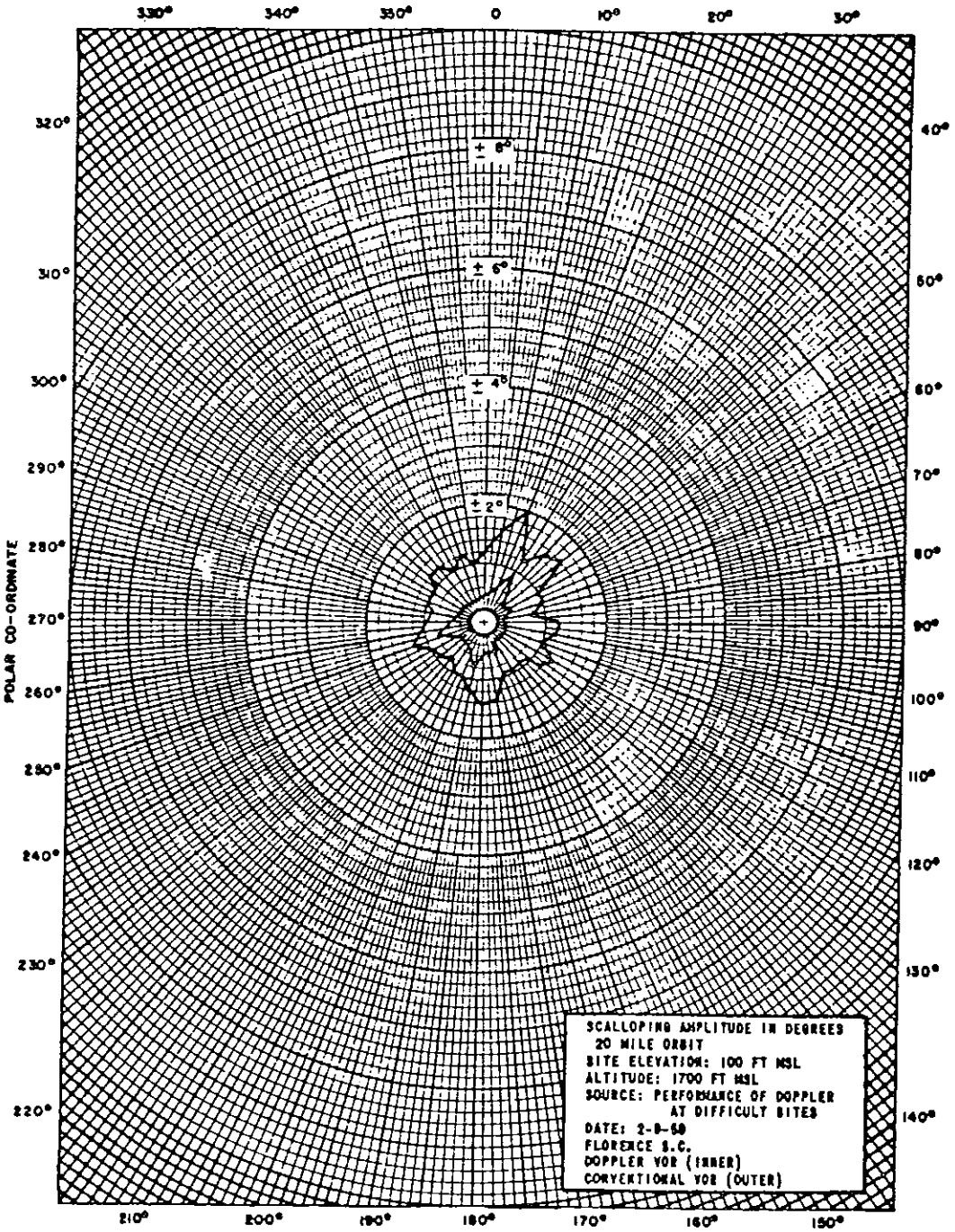

FIGURE 22. SCALLOPING AMPLITUDE

Section 12. Herndon, Virginia

COMMENTS: The towers of the power line 2500 feet northeast of the facility probably cause the 40-degrees azimuth scalloping lobe and the trees 1000 feet southwest of the VOR cause the scalloping in the sector from 200 to 240 degrees azimuth.

The reflections from the northeast power line probably cause the scalloping near 180 degrees azimuth and near 270 degrees azimuth. Fortunately, the wave angle of incidence to the power line that causes maximum scalloping, infringes on the part of the line that is located at a considerable distance (approximately 400 feet) from the VOR.

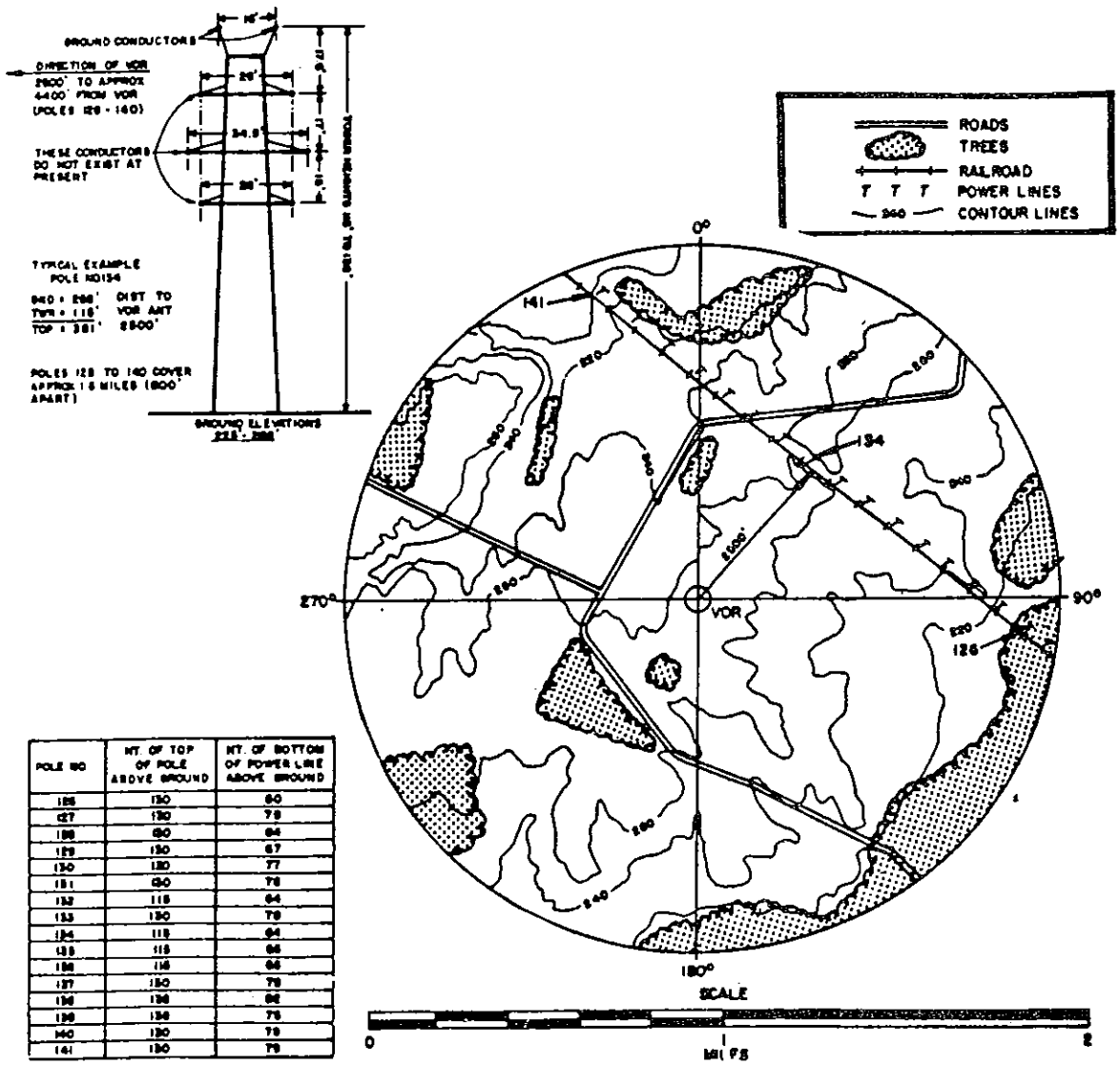

POLE NO	HT. OF TOP OF POLE ABOVE GROUND	HT. OF BOTTOM OF POWER LINE ABOVE GROUND
126	130	80
127	130	78
128	130	84
129	130	87
130	130	77
131	130	78
132	118	84
133	130	78
134	118	84
135	118	86
136	116	86
137	130	78
138	138	86
139	138	78
140	130	78
141	130	78

FIGURE 23. VICINITY SKETCH (1-MILE RADIUS) HERNDON, VIRGINIA VOR

Section 12. Herndon, Virginia (continued)

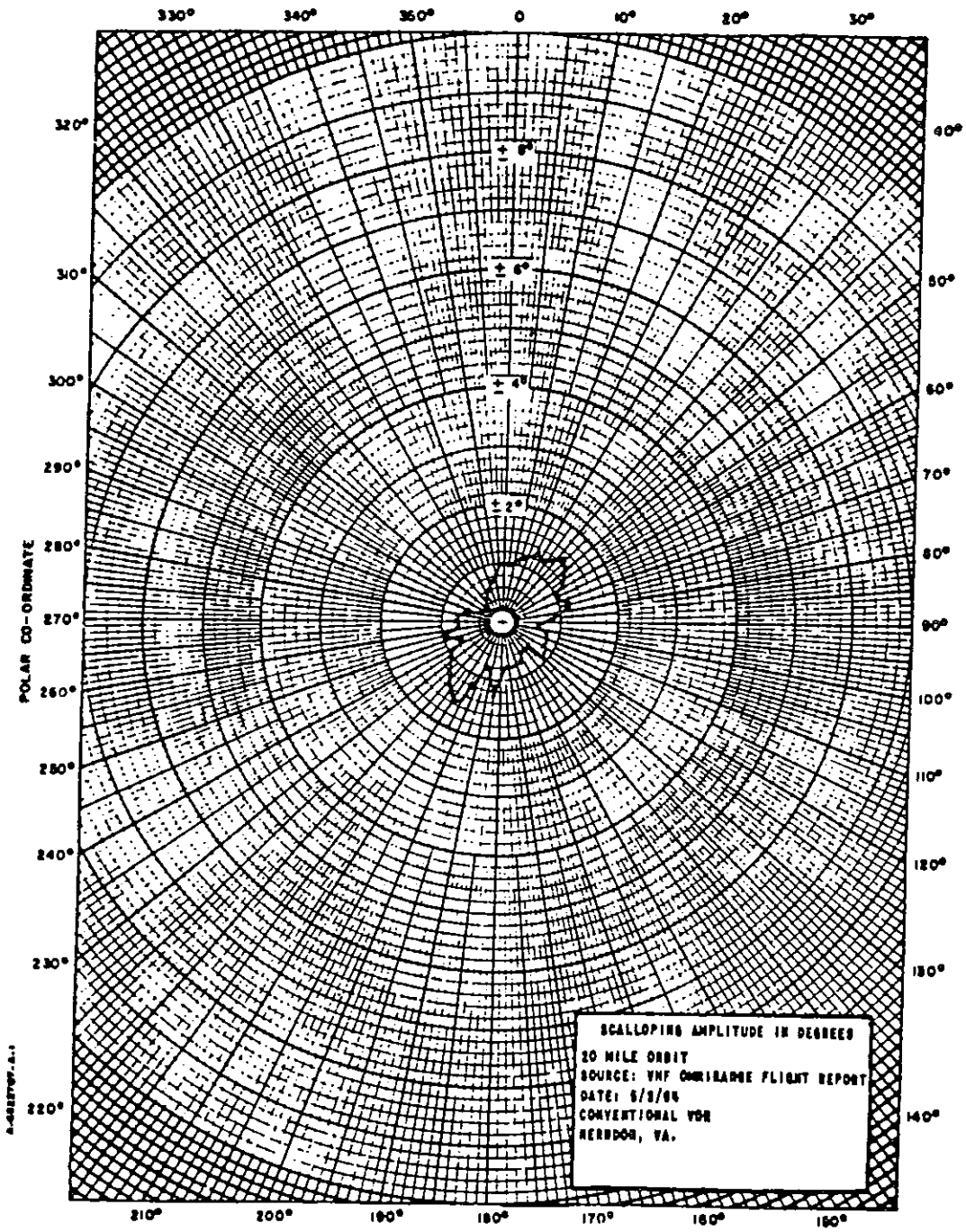

FIGURE 24. SCALLOPING AMPLITUDE

Section 13. Jackson, Michigan

COMMENTS: This information was obtained during the site testing prior to commissioning of the Jackson, Michigan VOR, which is an urban site with power and telephone lines on three sides. The most likely offending reflector, because of proximity and the number of conductors, is a 31-wire line generally running east and west. Its poles are 35 feet high with the part nearest to the VOR being about an 1800-foot distance where the vertical angle is 2.1 degrees. The closest line is a 3-wire line, 35 feet high, located at an azimuth of 180 degrees. It is about a 1600-foot distance, making a vertical angle of 0.9 degree. There are trees in all directions with some as close as 1800 feet with a vertical angle of 2.1 degrees. In addition, there are many hangars, buildings, and industrial plants located within a 1-mile radius.

The Jackson site was used for a considerable amount of Doppler VOR testing. The facility was commissioned with a standard 4-loop antenna system and a Doppler-type counterpoise.

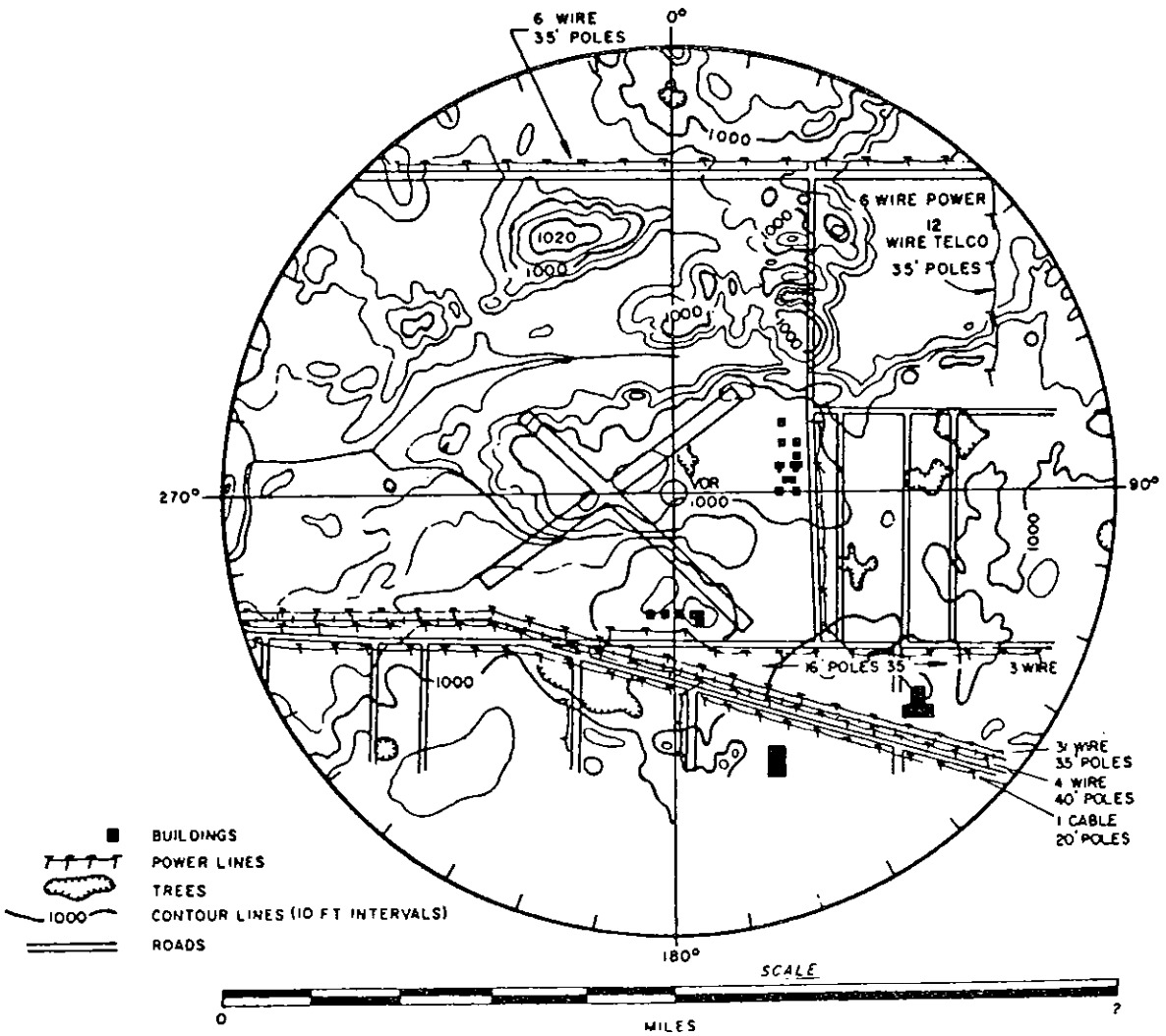

FIGURE 25. VICINITY SKETCH (1-MILE RADIUS) JACKSON, MICHIGAN VOR

Section 13. Jackson, Michigan (continued)

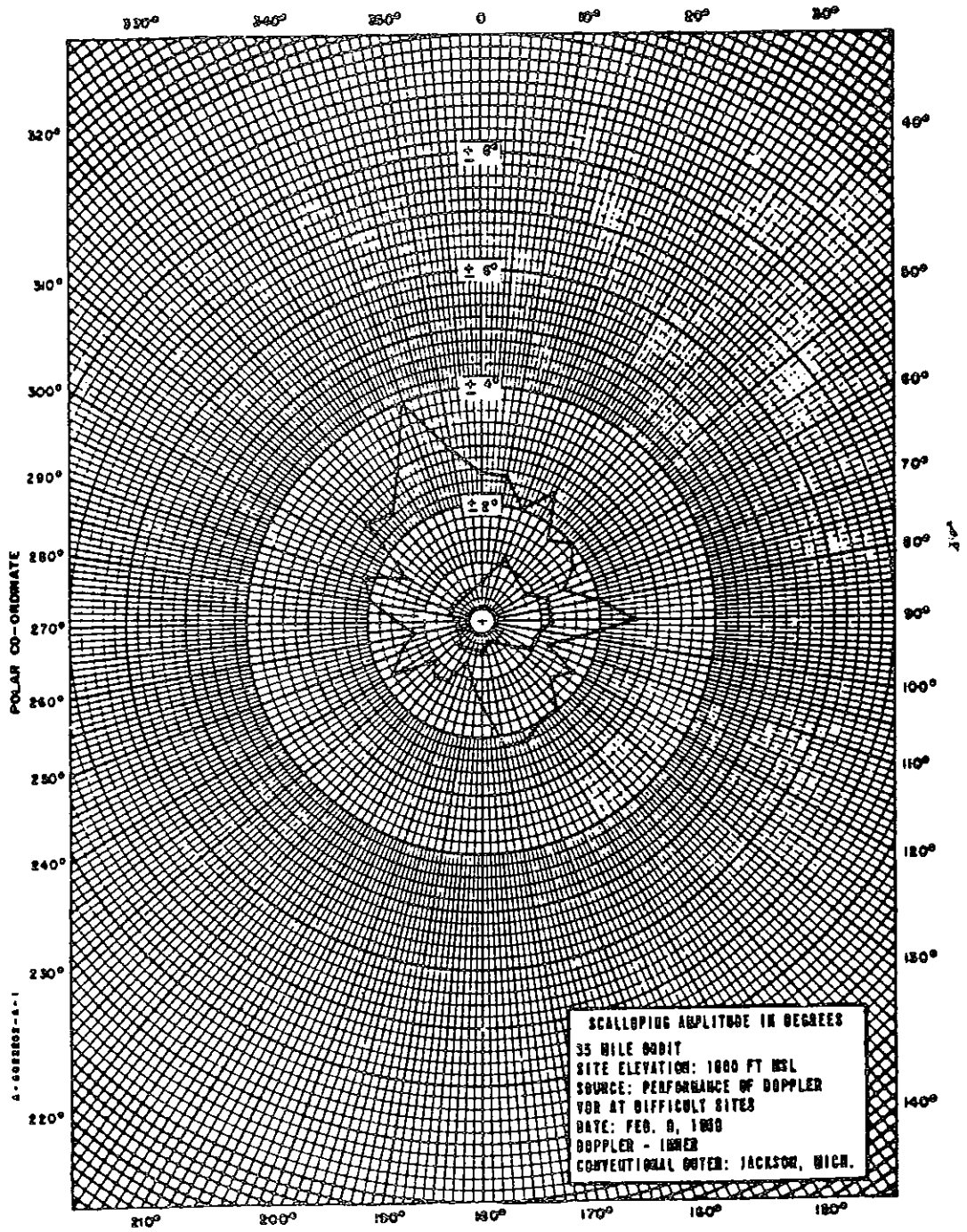

FIGURE 26. SCALLOPING AMPLITUDE

Section 14. Kansas City, Missouri

COMMENTS: The large scalloping in the azimuthal region of 140 degrees is caused by large buildings on high ground and a bridge, all in the city area. The proximity of the PAR to the DVOR is probably the cause of some scalloping in the 30- to 60-degrees sector; however, the buildings and towers in this sector probably cause most of the error. The grain elevator, buildings, and tank farm structures in the 260- to 300-degrees sector are undoubtedly responsible for most of the large scalloping at 255- and 308-degrees azimuth areas. The metal hangars in the 320- to 360-degrees sector probably account for some of the scalloping to the west and northwest.

Probably the main factor responsible for this being a poor site is its location on terrain below the elevation of the surrounding countryside. This also accounts for the poor coverage, undoubtedly due to shadowing.

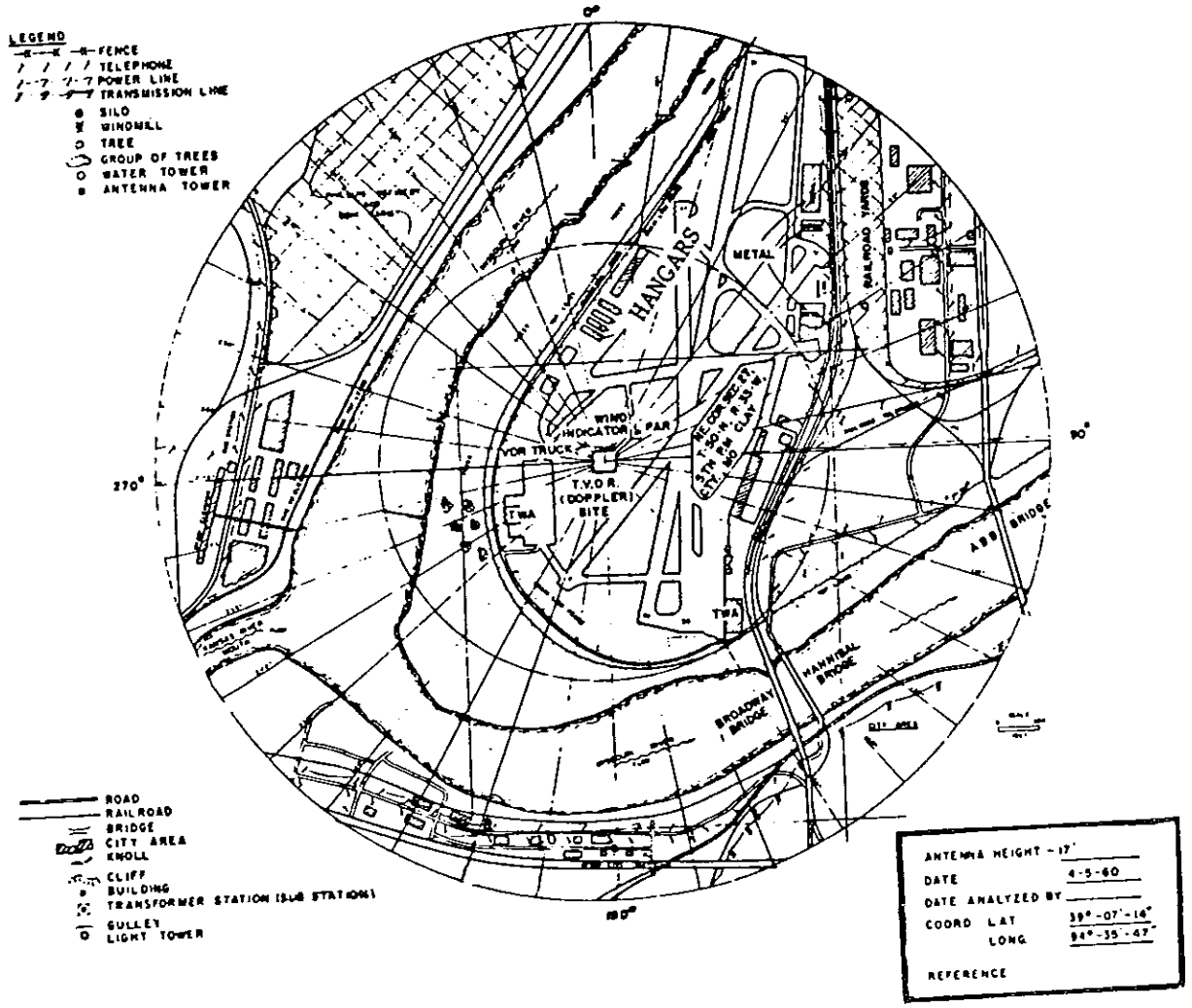

FIGURE 27. VICINITY SKETCH (1-MILE RADIUS) RIVERSIDE, MISSOURI TVOR

Section 14. Kansas City, Missouri (continued)

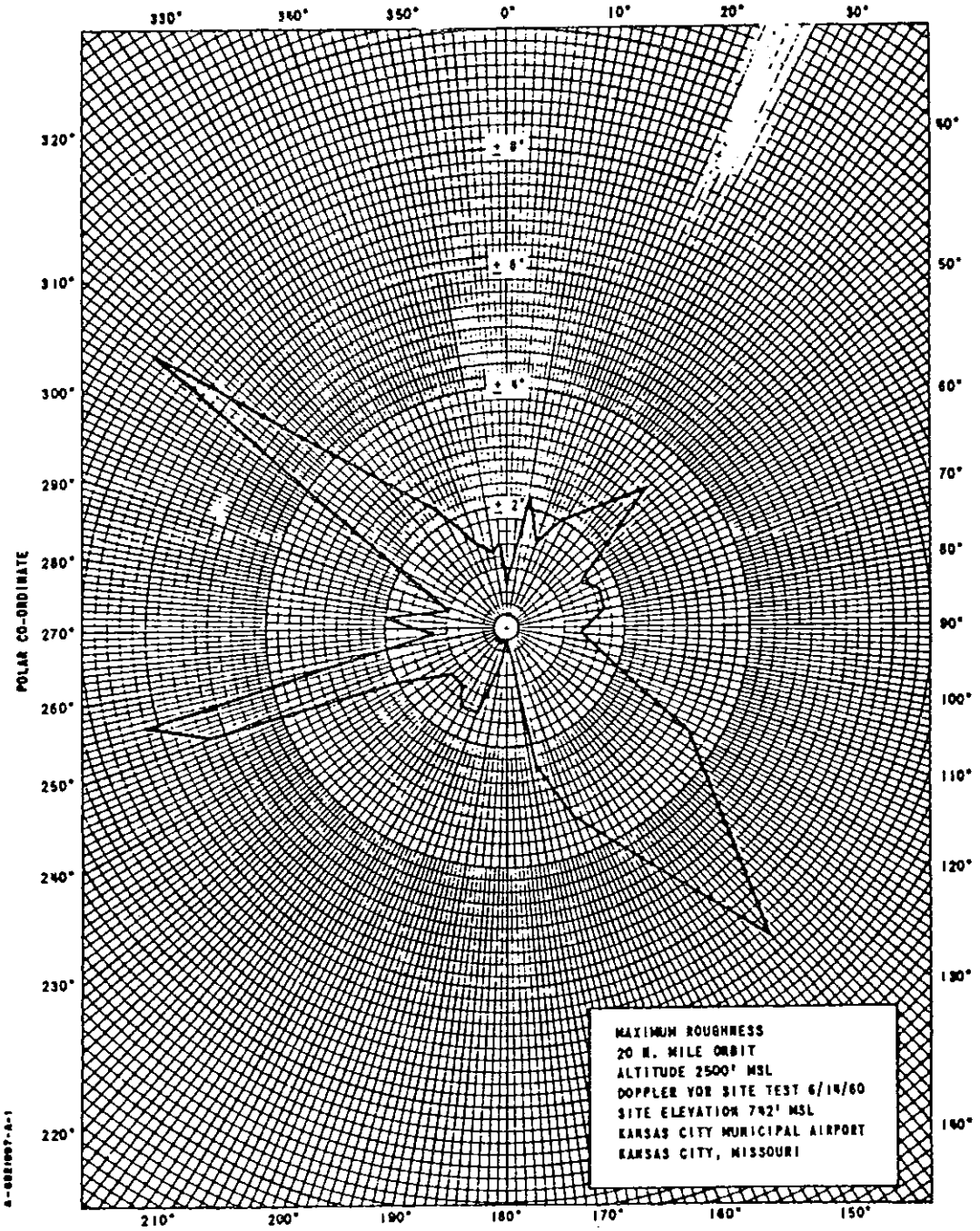

FIGURE 28. ROUGHNESS AMPLITUDE

Section 15. Lake Tahoe, California

COMMENT: This is a good example of a unique mountain top site.

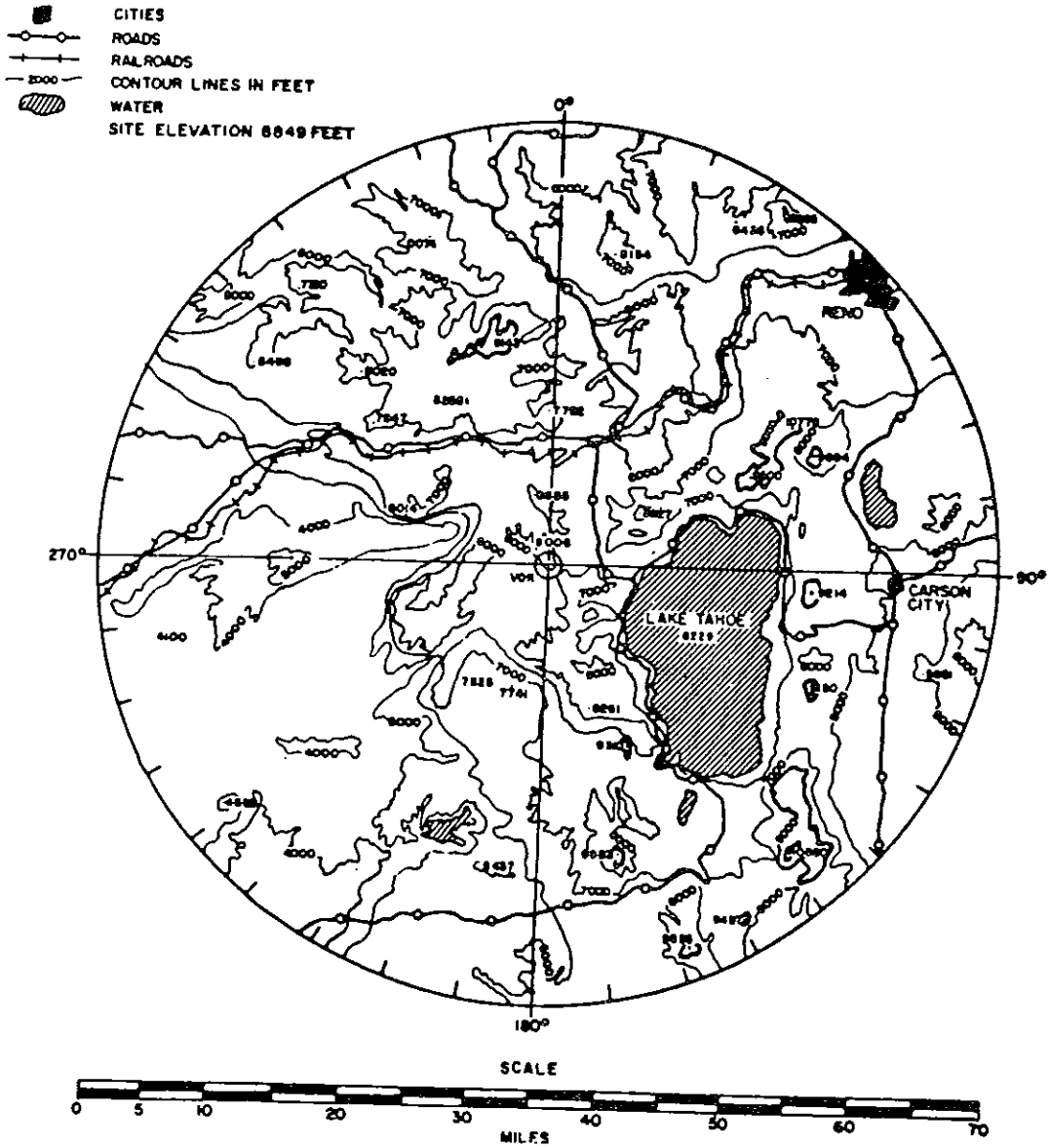

FIGURE 29. VICINITY SKETCH (35-MILE RADIUS) LAKE TAHOE, CALIFORNIA VOR

Section 15. Lake Tahoe, California (continued)

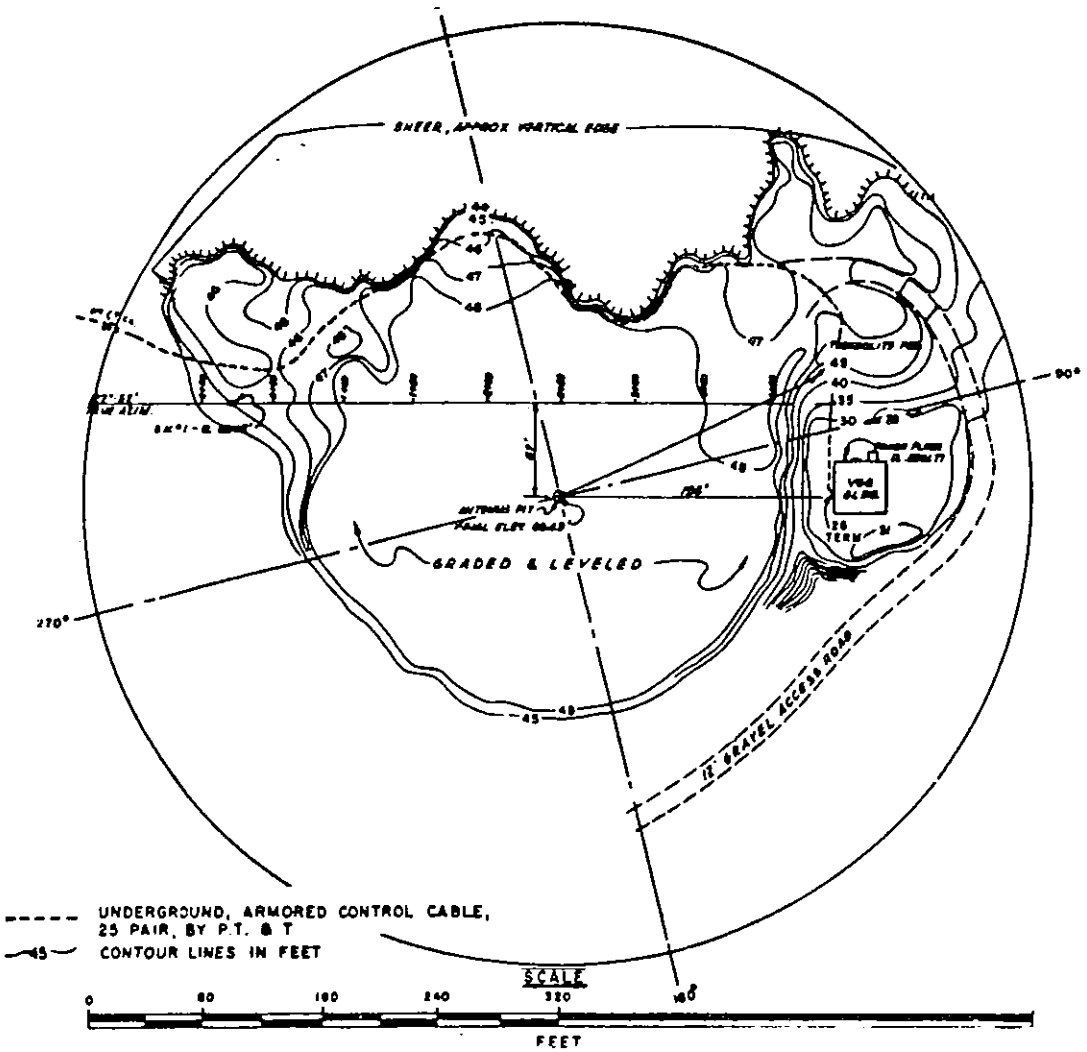

FIGURE 30. VICINITY SKETCH (320-FOOT RADIUS) LAKE TAHOE, CALIFORNIA VOR

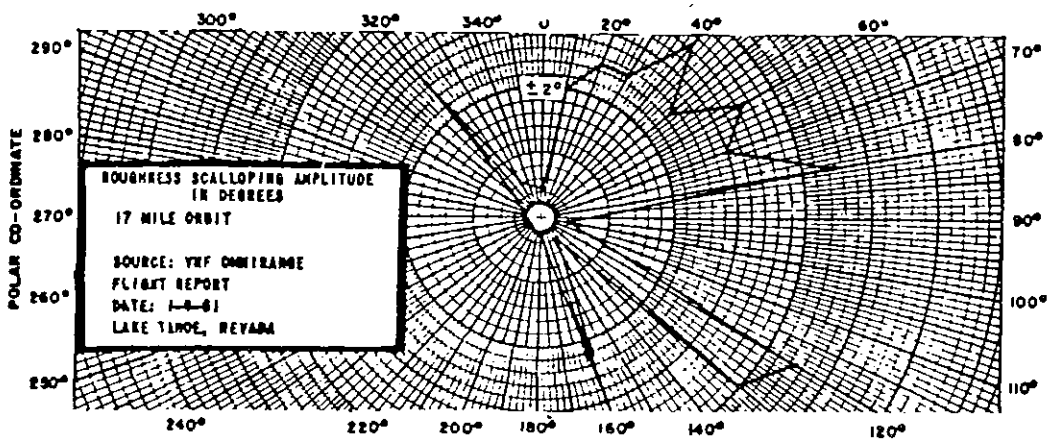

FIGURE 31. SCALLOPING AND ROUGHNESS AMPLITUDE

Section 16. Malad City, Idaho

COMMENT: The 7-mile orbit scalloping amplitude plots show that very satisfactory VOR performance can be obtained in mountainous terrain by careful selection and preparation. Both curves represent results obtained with ground-mounted, 5-loop antennas. The solid line curve was obtained after the site was leveled. A later installation using the FAA 4-loop antenna resulted in a further improvement of VOR performance.

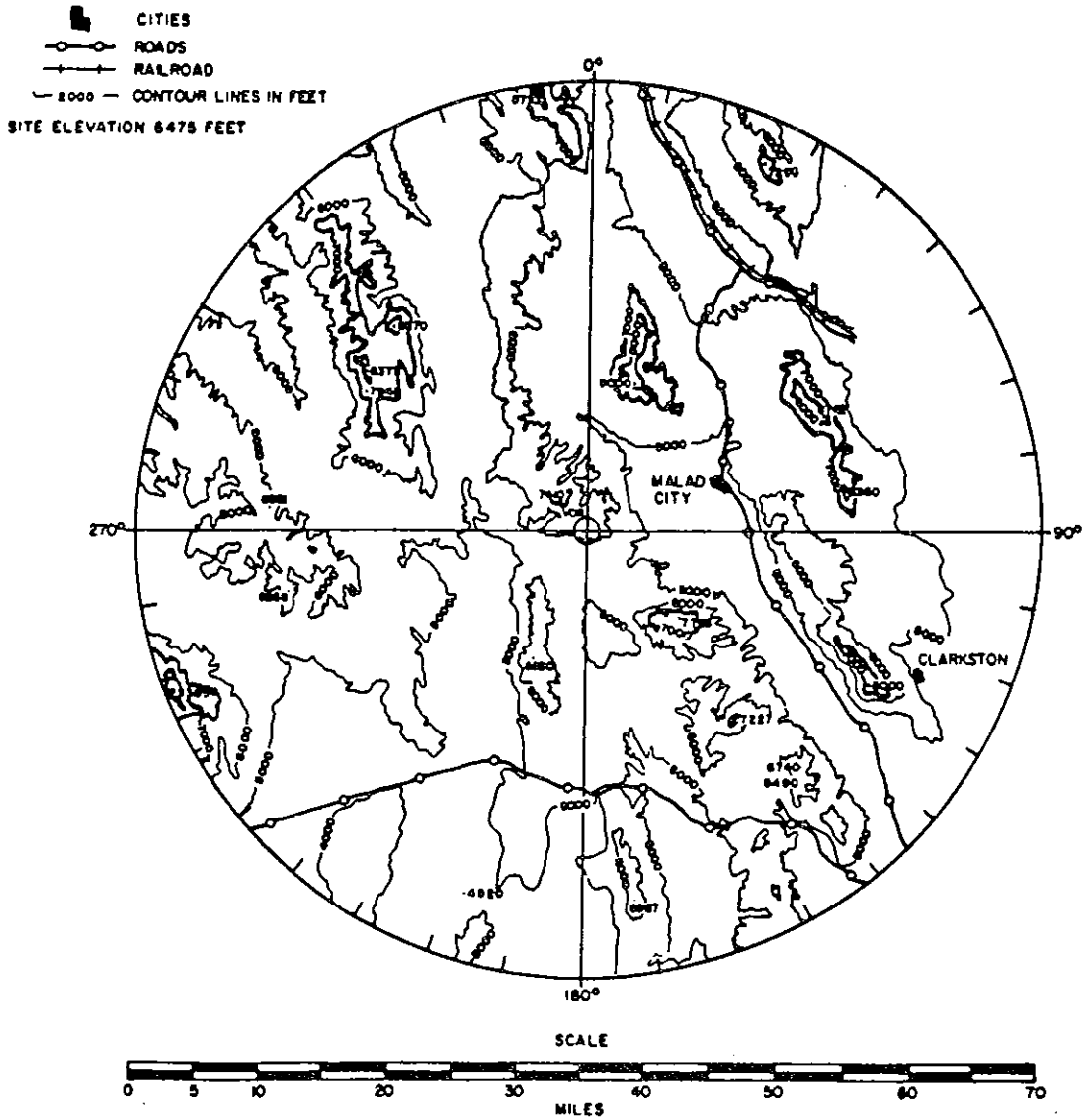

FIGURE 32. VICINITY SKETCH (35-MILE RADIUS) MALAD CITY, IDAHO VOR

Section 16. Malad City, Idaho

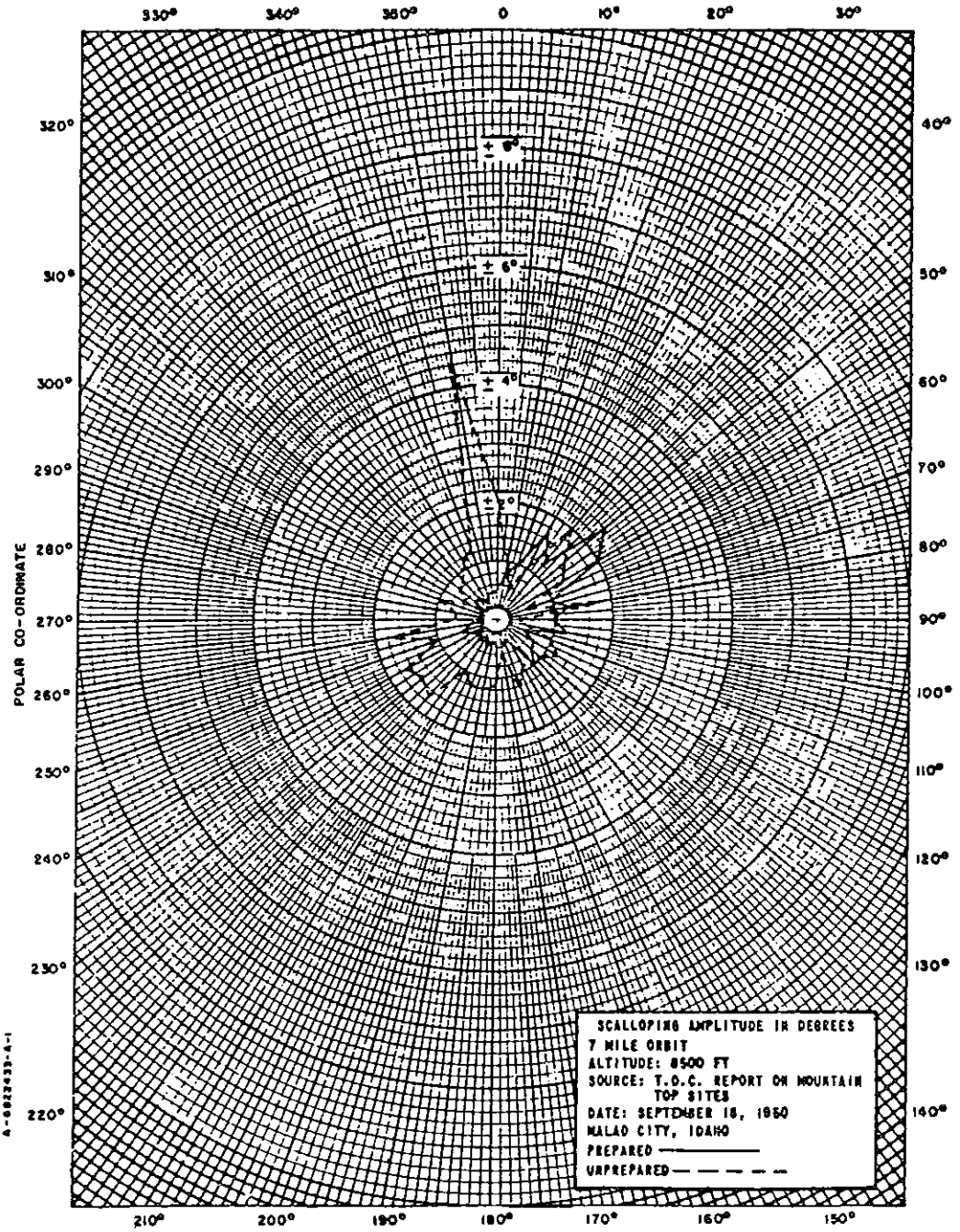

FIGURE 33. SCALLOPING AMPLITUDE

Section 17. Oklahoma City, Oklahoma

COMMENT: The scalloping amplitude curve maxima at 60 and 280 degrees azimuth are believed to be caused by reflections from hangar No. 50 and from the administration building, respectively.

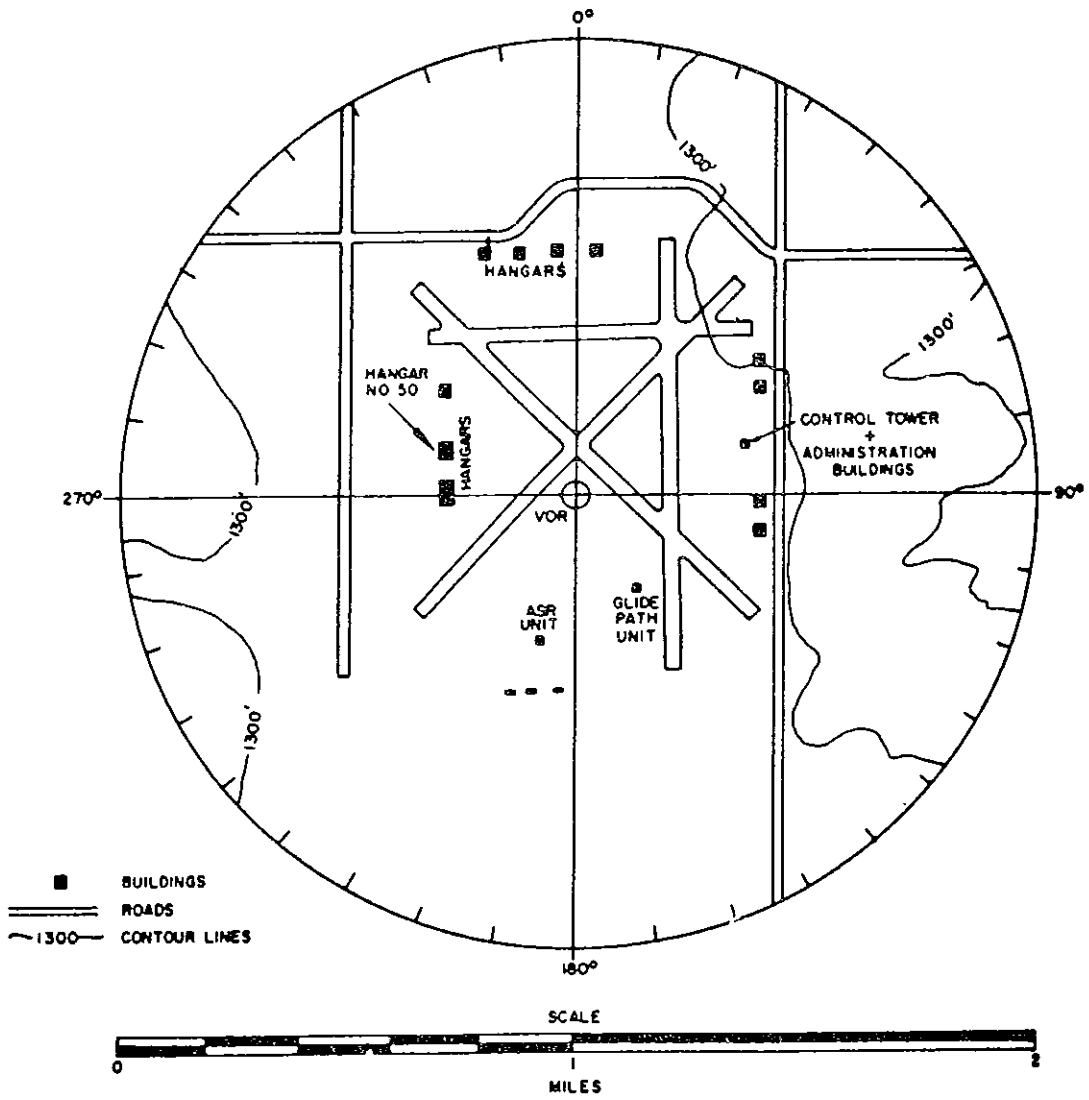

FIGURE 34. VICINITY SKETCH (1-MILE RADIUS) OKLAHOMA CITY, OKLAHOMA VOR)

Section 17. Oklahoma City, Oklahoma (continued)

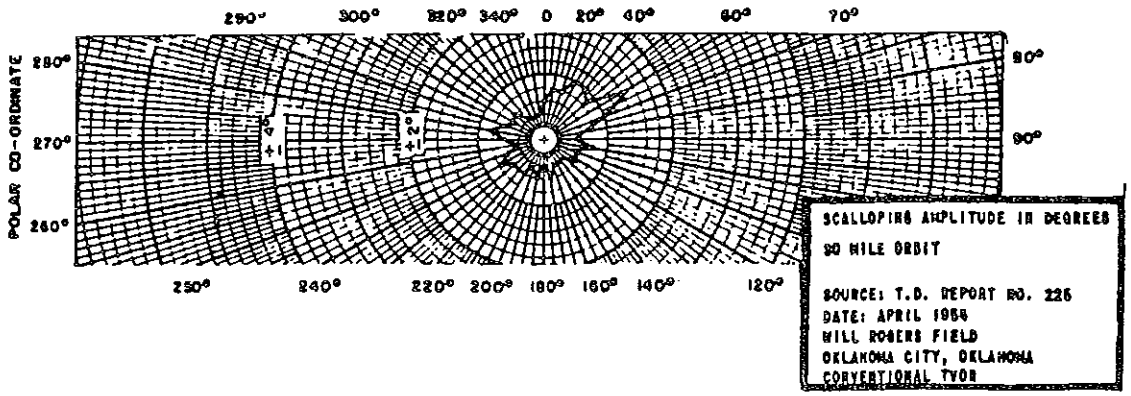

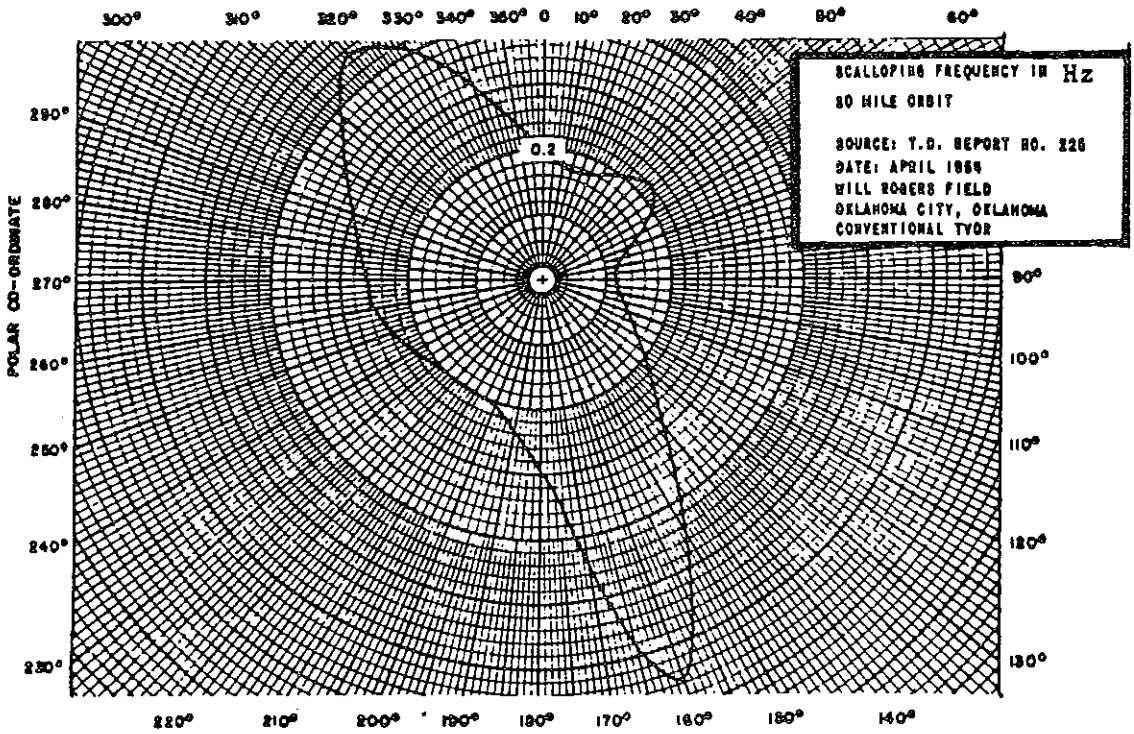

FIGURE 35. SCALLOPING AMPLITUDE AND FREQUENCY

Section 18. Roanoke, Virginia

COMMENT: This a poor site since the ground only 200 feet from the antenna is approximately 15 feet higher than the terrain supporting the antenna. Serious scalloping would be expected on each side of this mound and limited coverage (propagation) in the sector of the higher-than-antenna-site terrain. On a 20-mile circle, the scalloping frequency due to the mound would be so low (0.04 cps) that the scalloping would appear only as a bearing error. This could be measured by obtaining a station bearing error curve with the aircraft at a 20-mile radius.

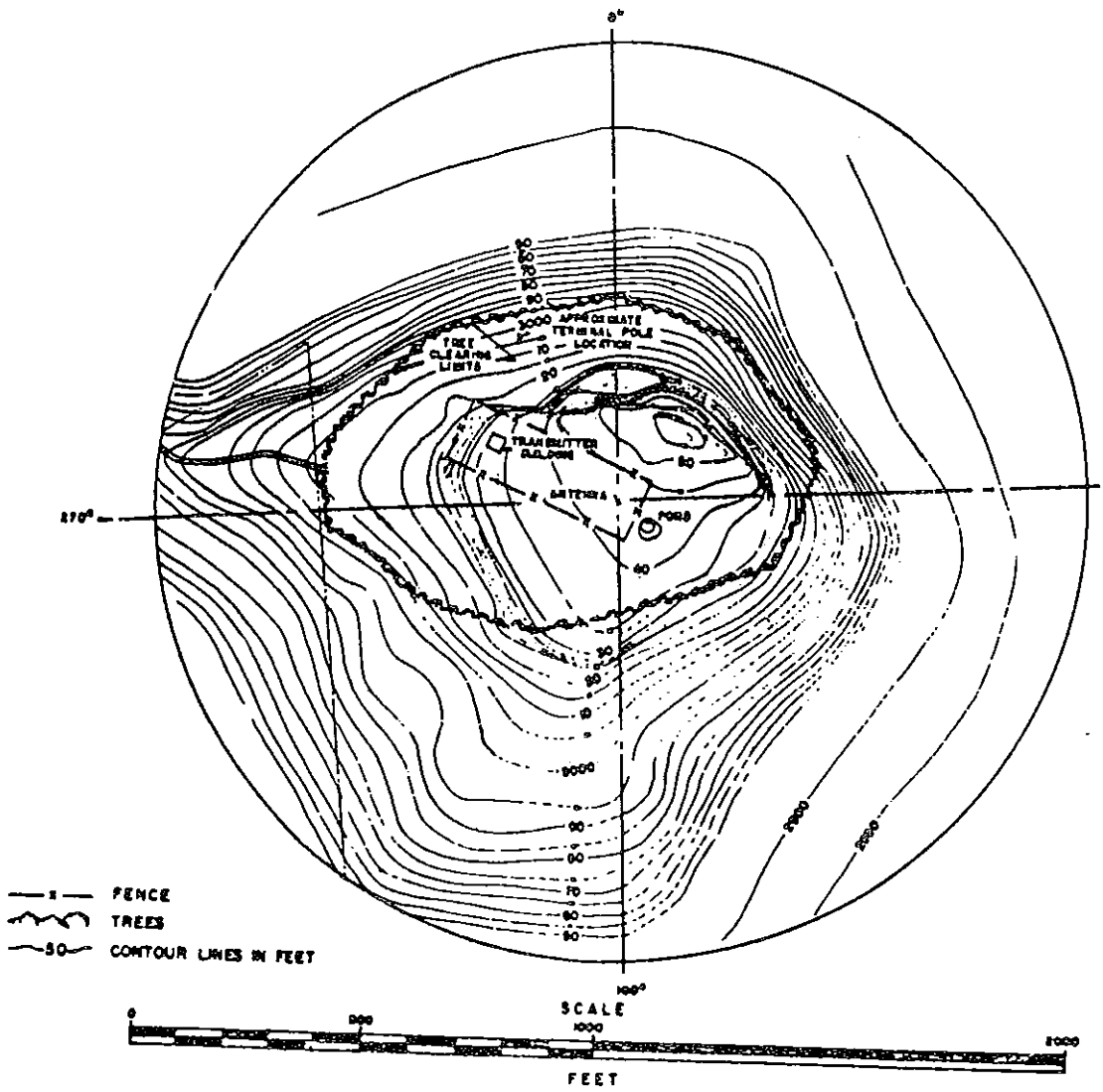

FIGURE 36. VICINITY SKETCH (1000 FOOT RADIUS) ROANOKE, VIRGINIA VOR

Section 18. Roanoke, Virginia (continued)

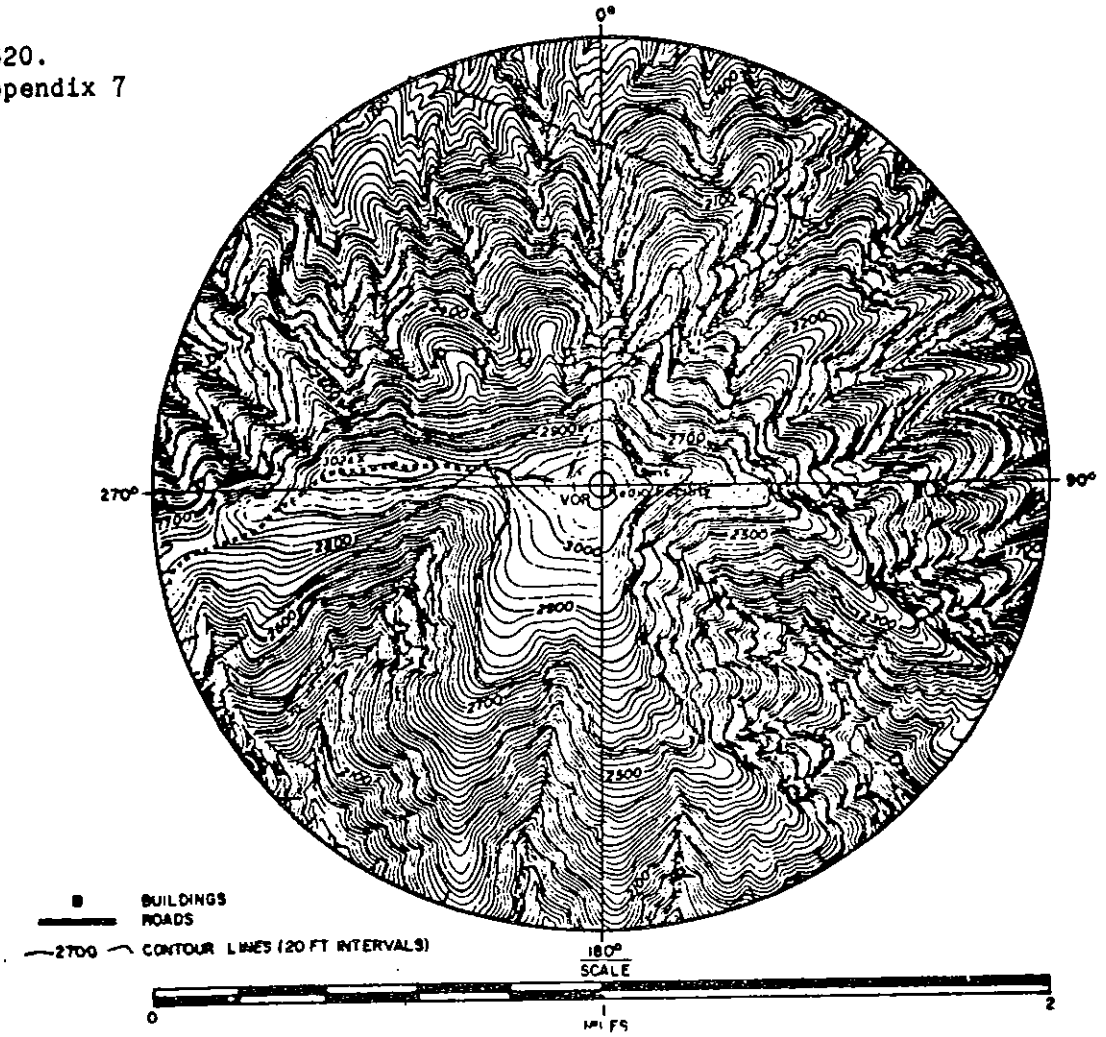

FIGURE 37. VICINITY SKETCH (1-MILE RADIUS) ROANOKE, VIRGINIA VOR

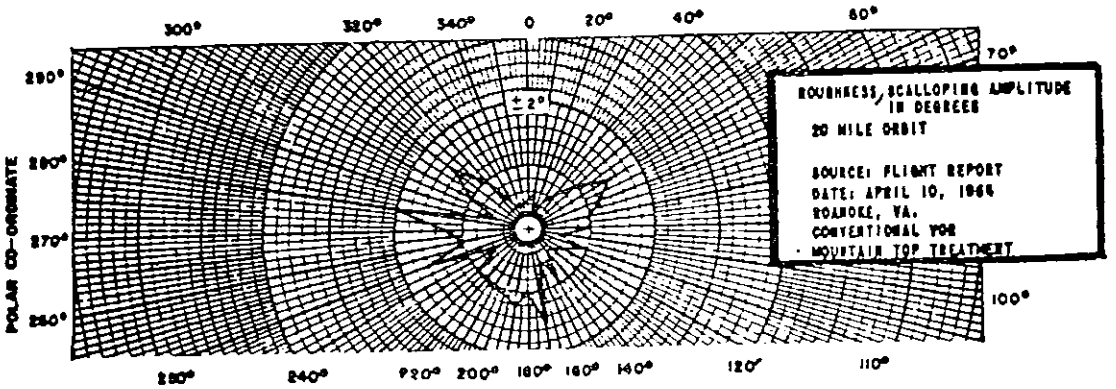

FIGURE 38. SCALLOPING AND ROUGHNESS AMPLITUDE

Section 19. Sisters Island, Alaska

COMMENT: The electrical height of the antennas above the sea is approximately 2100 degrees causing deep vertical plane nulls at intervals of 5 degrees. The surrounding terrain, strongly illuminated by the first signal maximum, reflected energy into the null areas causing course roughness and scalloping.

This is an excellent example of the benefits of the DVOR over the conventional VOR in reducing the effects of deep nulls caused by sea water reflection.

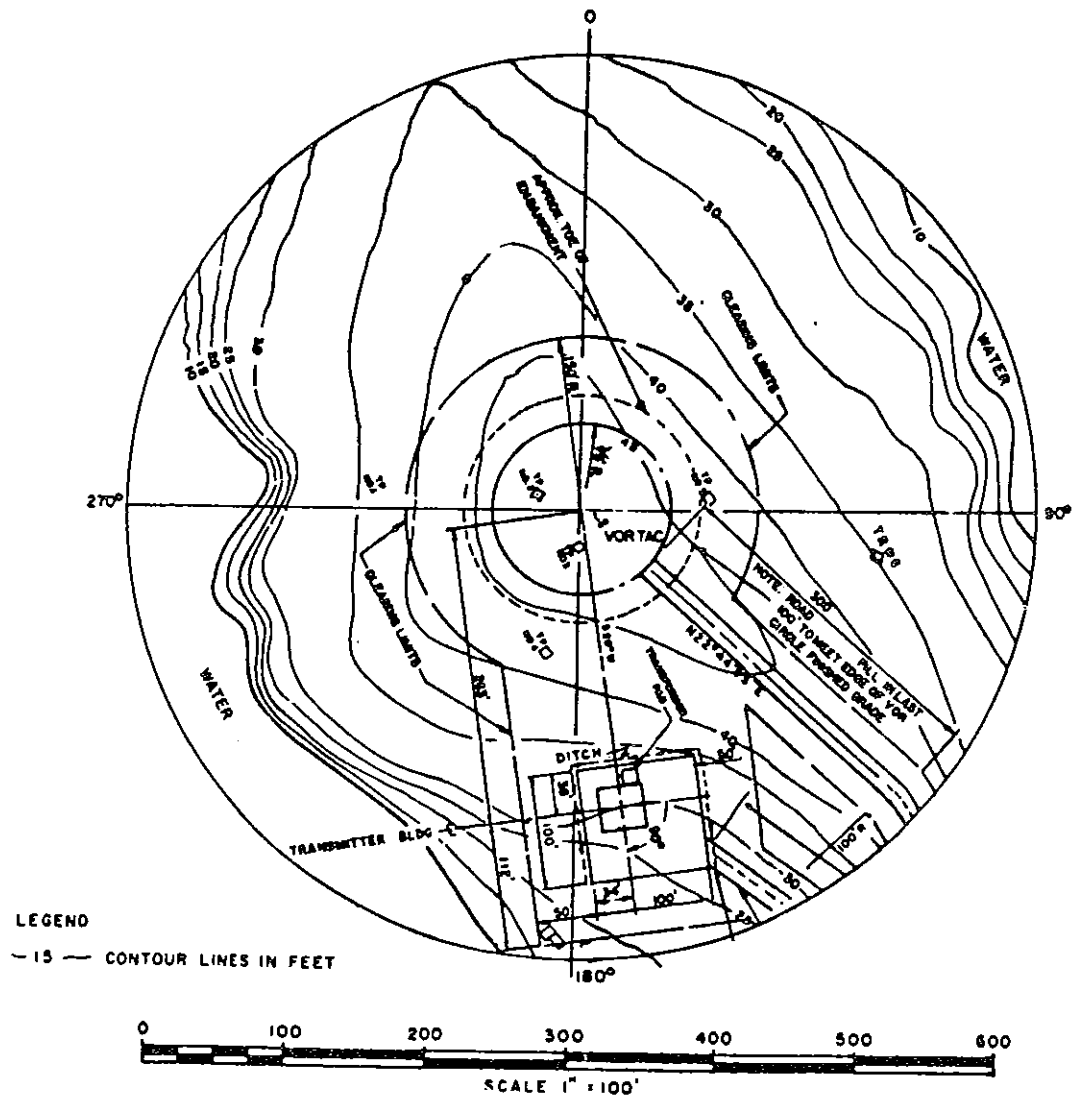

FIGURE 39. VICINITY SKETCH (300-FOOT RADIUS) SISTERS ISLAND, ALASKA VOR

6820.10
Appendix 7

Section 19. Sisters Island, Alaska (continued)

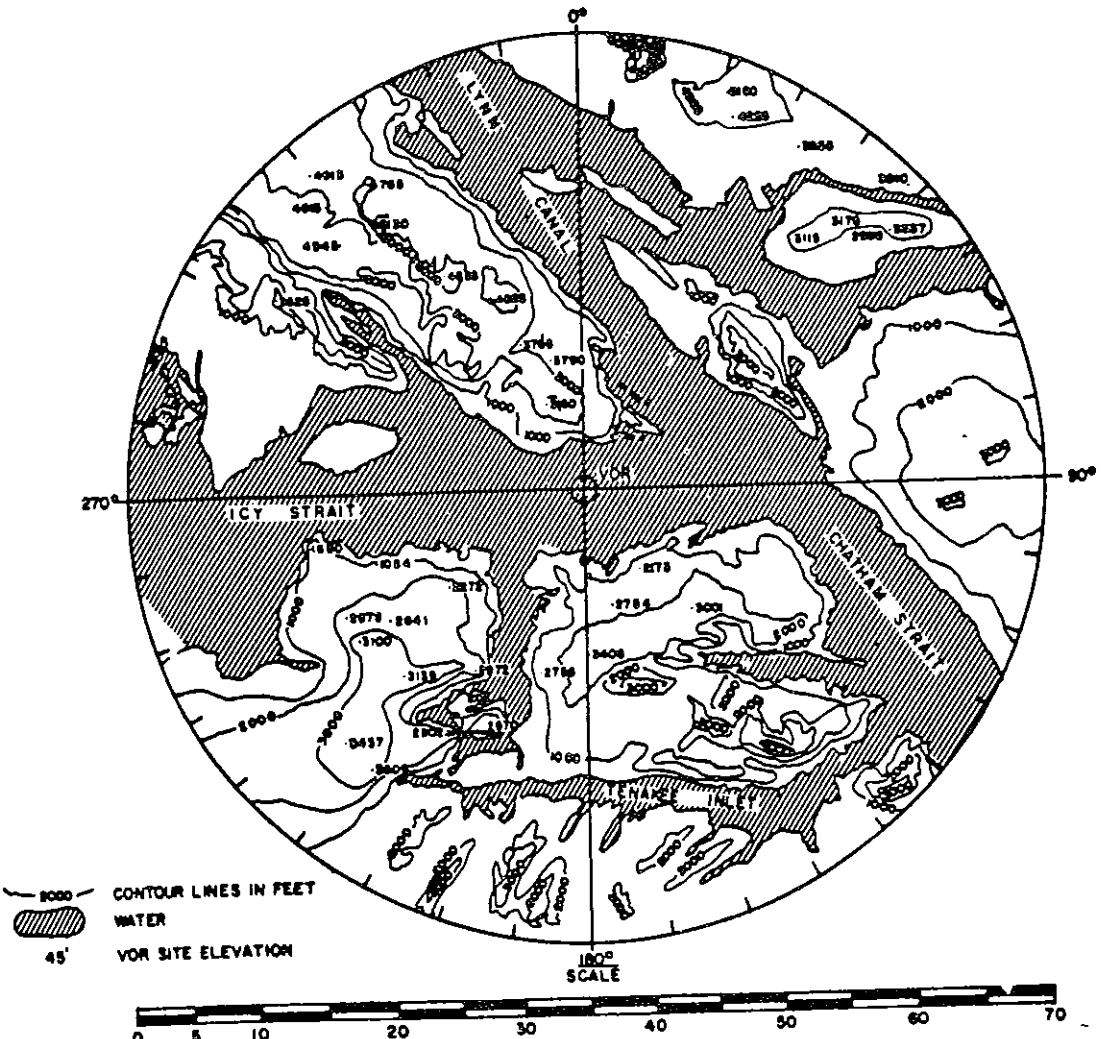

FIGURE 40. VICINITY SKETCH (35-MILE RADIUS) SISTERS ISLAND, ALASKA VOR

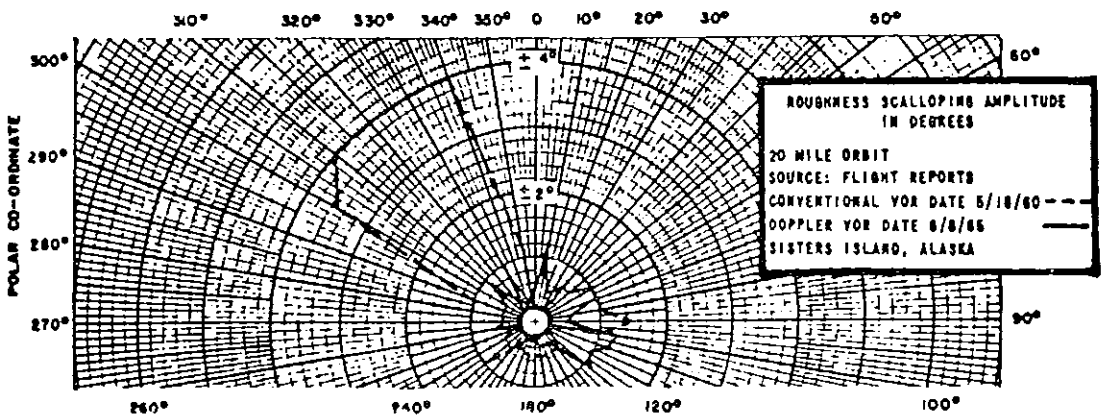

FIGURE 41. SCALLOPING AND ROUGHNESS AMPLITUDE

Section 20. TDC Indianapolis, Indiana

COMMENT: The terrain is flat for miles in all directions from the station. The conventional VOR scalloping in the vicinity of 50 and 230 degrees azimuth is caused by the hangar's north face and west face, respectively; the two towers cause scalloping in the 240 to 260 degrees azimuth sector and the 300 to 320 degrees azimuth sector.

The two vertical towers cause the DVOR scalloping in the vicinity of the 250 and 270 degrees azimuths.

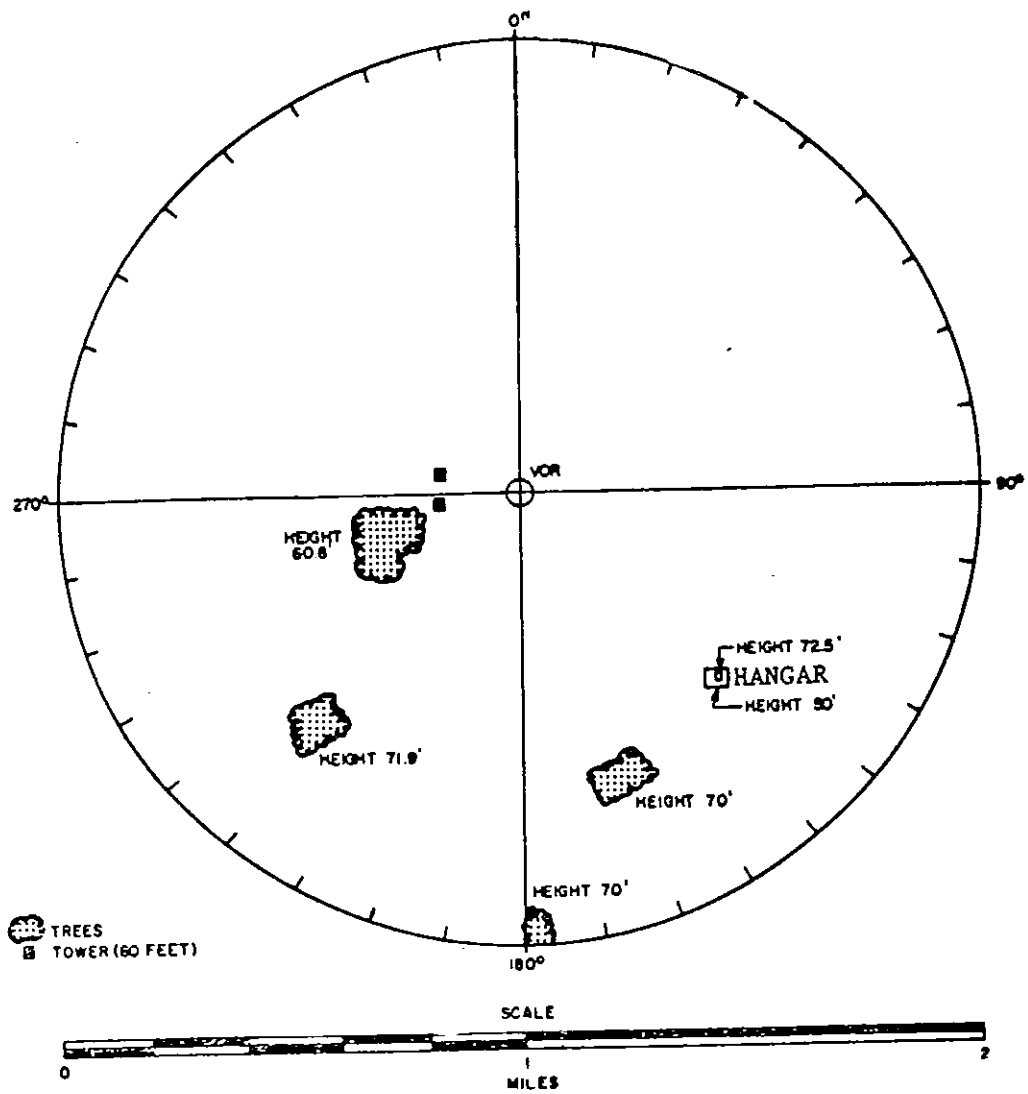

FIGURE 42. VICINITY SKETCH (1-MILE RADIUS) TDC INDIANAPOLIS, INDIANA EXPERIMENTAL VOR

Section 20. TDC Indianapolis, Indiana (continued)

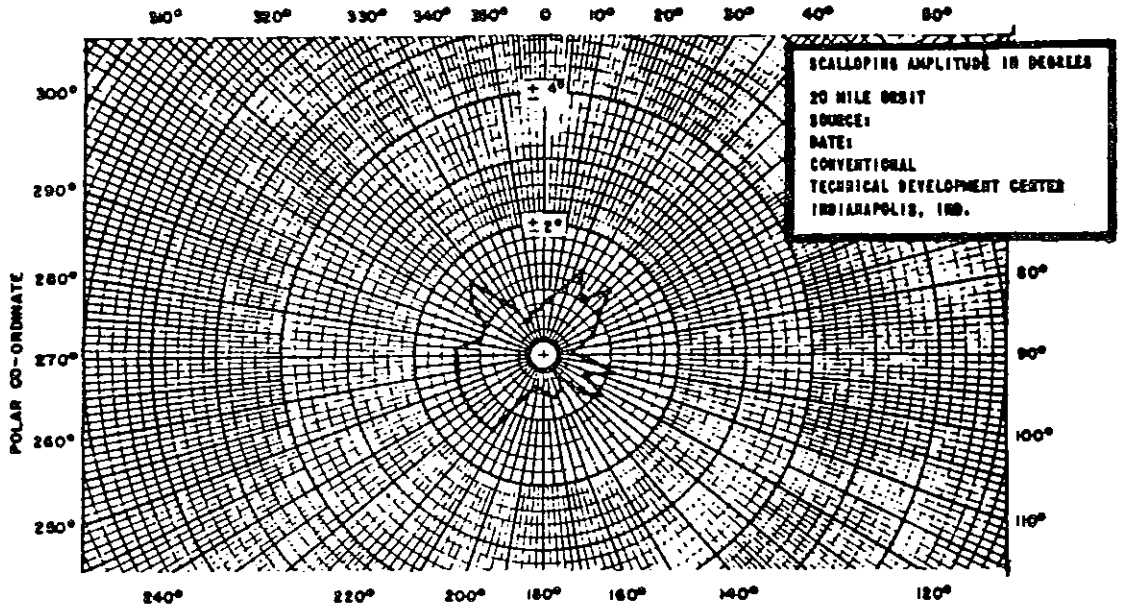

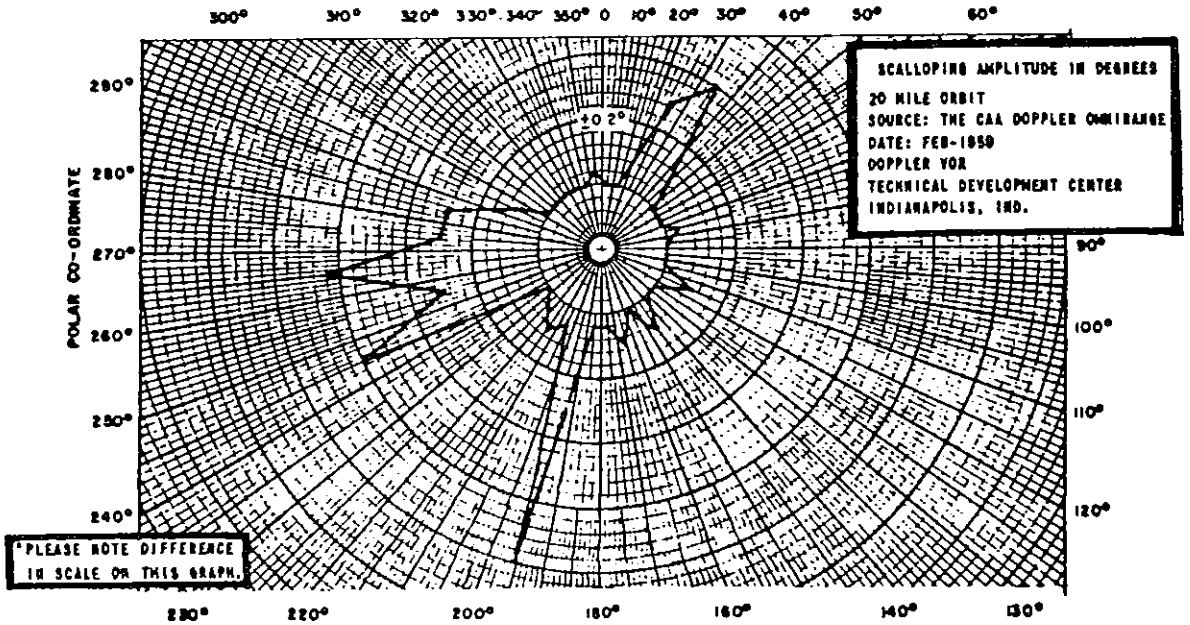

FIGURE 43. SCALLOPING AMPLITUDE

Section 20. TDC Indianapolis, Indiana (continued)

COMMENT: Tests were conducted to determine the performance of a VOR located at various distances from a single tree. The tests were conducted with the horizontal limbs of the tree removed. As the distance between the VOR and the tree is increased, you will note that the scalloping amplitude decreases. The scalloping frequency, however, increases as the distance between the VOR and tree increases. The information obtained during these tests was summarized in Figure 3-5.

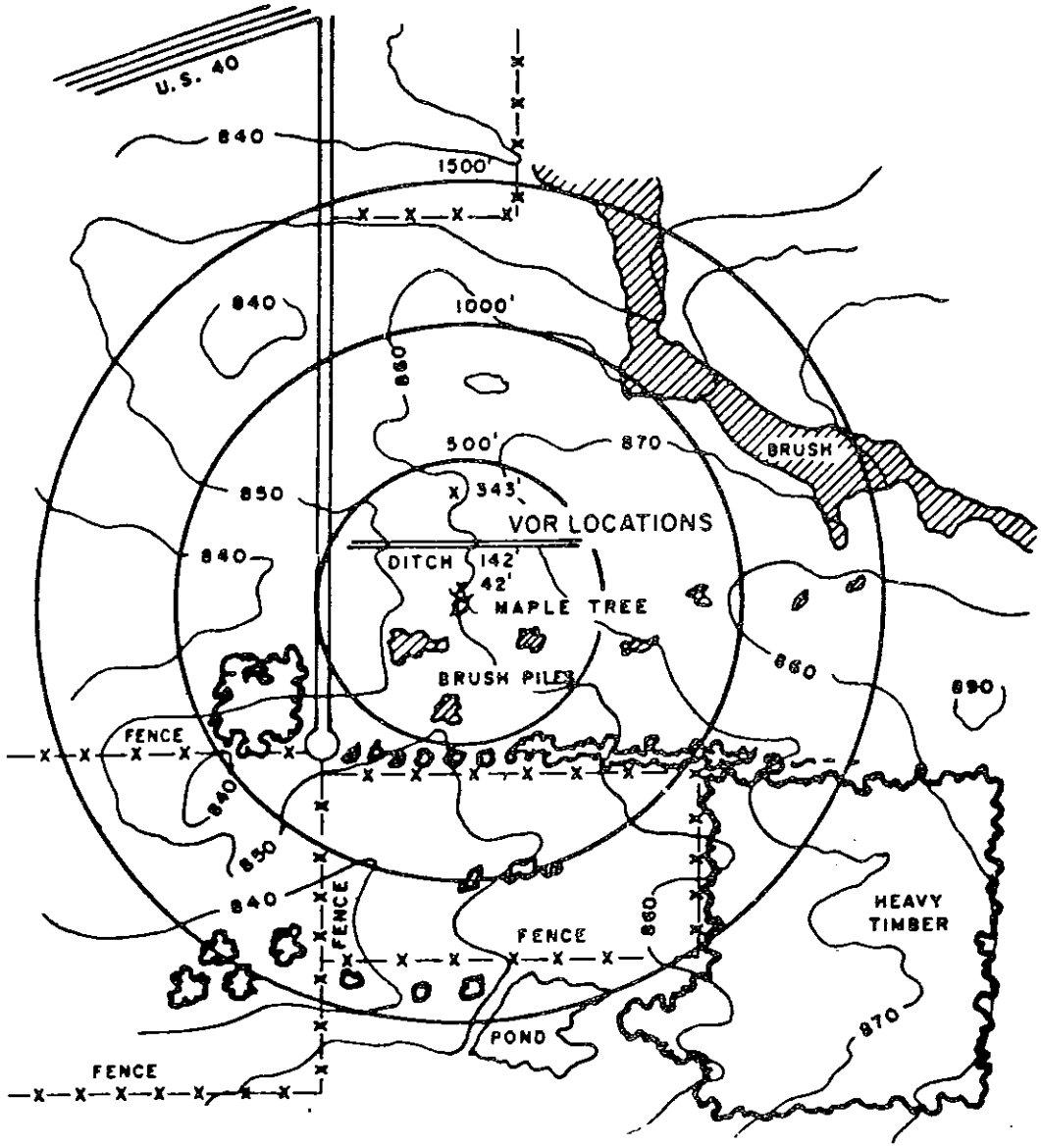

FIGURE 44. VICINITY SKETCH (1500-FOOT RADIUS) TDC INDIANAPOLIS, INDIANA SITE TEST AREA

Section 20. TDC Indianapolis, Indiana (continued)

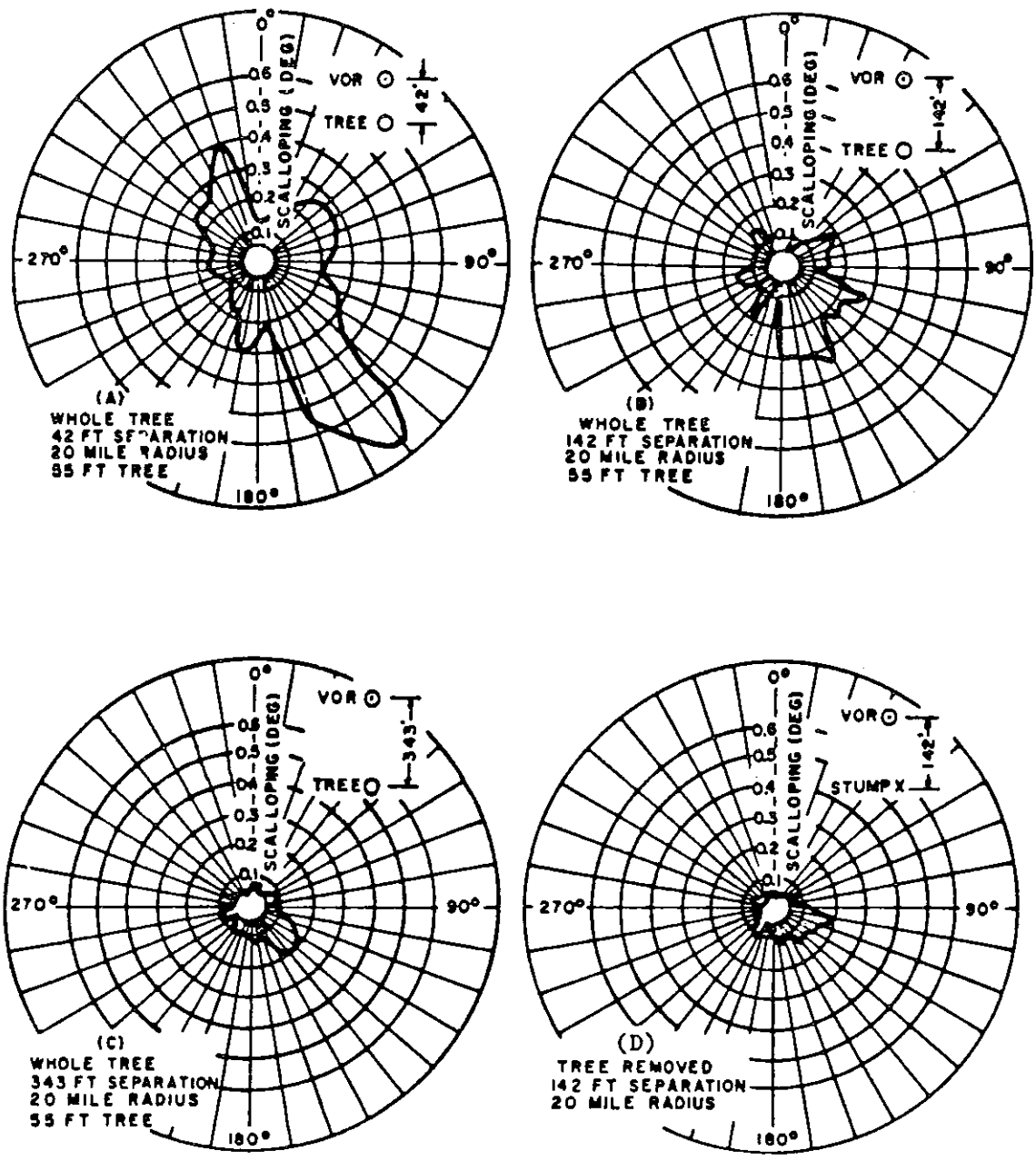

FIGURE 45. SCALLOPING AMPLITUDE

Section 21. Traverse City, Michigan

COMMENT: The site is generally flat with rising land four to six miles distant. Maximum scalloping in the 190 to 210 degrees sector is believed to be due to reflections from the control tower/airport terminal structure.

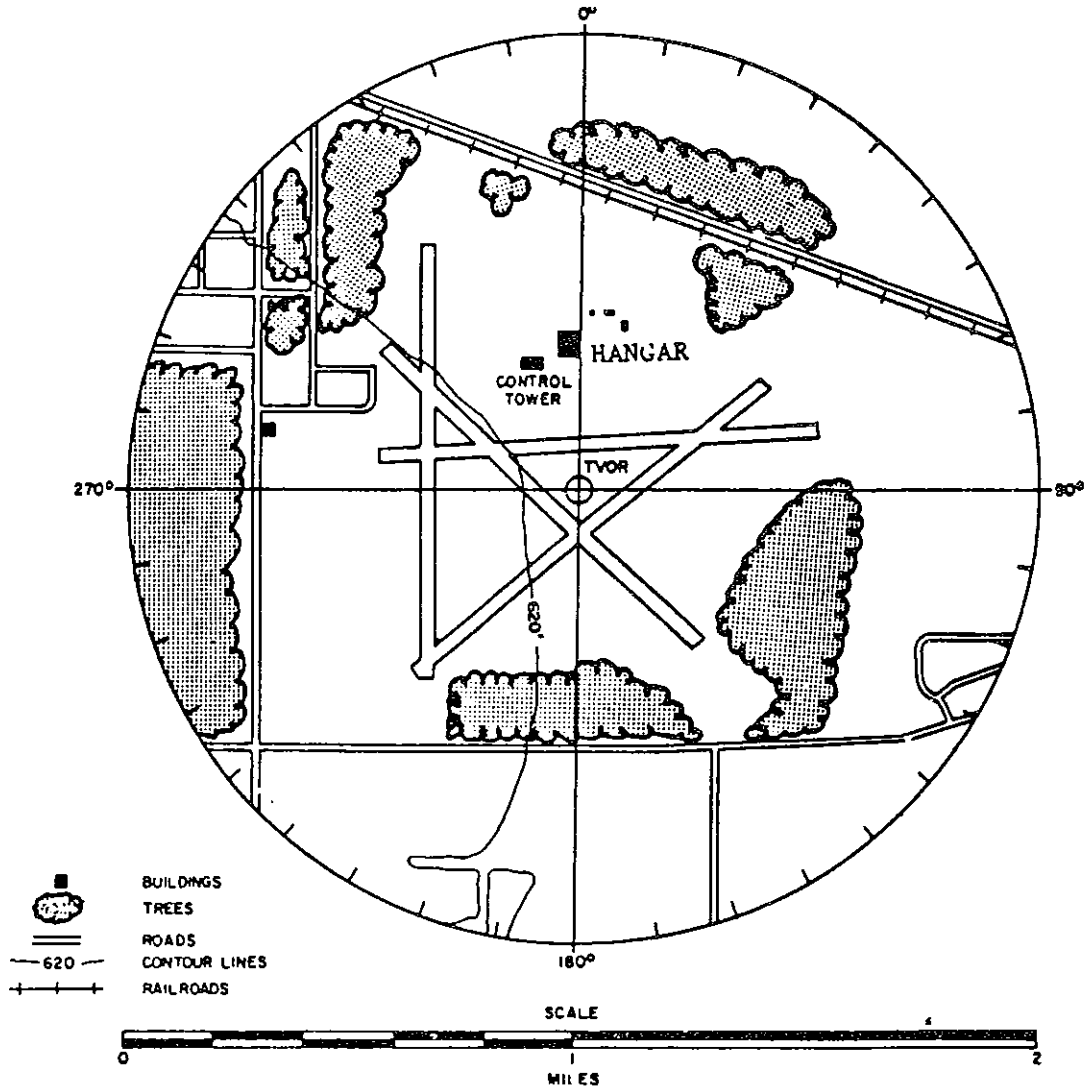

FIGURE 46. VICINITY SKETCH (1-MILE RADIUS) TRAVERSE CITY, MICHIGAN VOR

Section 21. Traverse City, Michigan (continued)

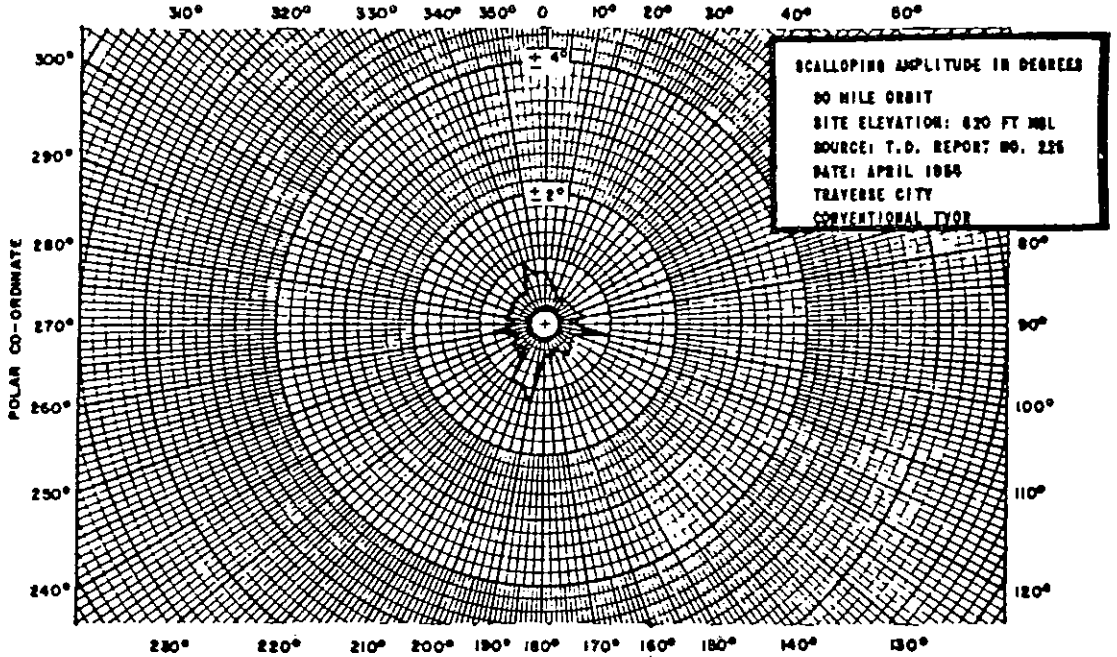

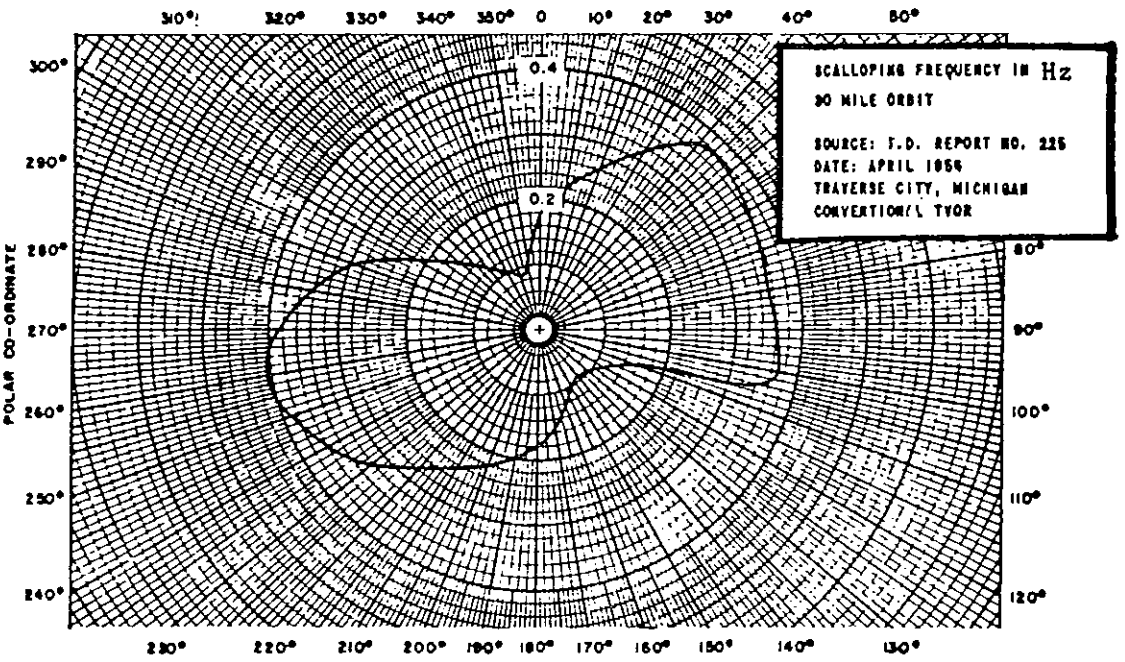

FIGURE 47. SCALLOPING AMPLITUDE AND FREQUENCY

Section 22. Ukiah, California

COMMENT: Performance of this mountain top VOR is very satisfactory. The scalloping graphs indicate the large improvement due to the mountain top VOR configuration when compared to an elevated counterpoise (conventional) installation).

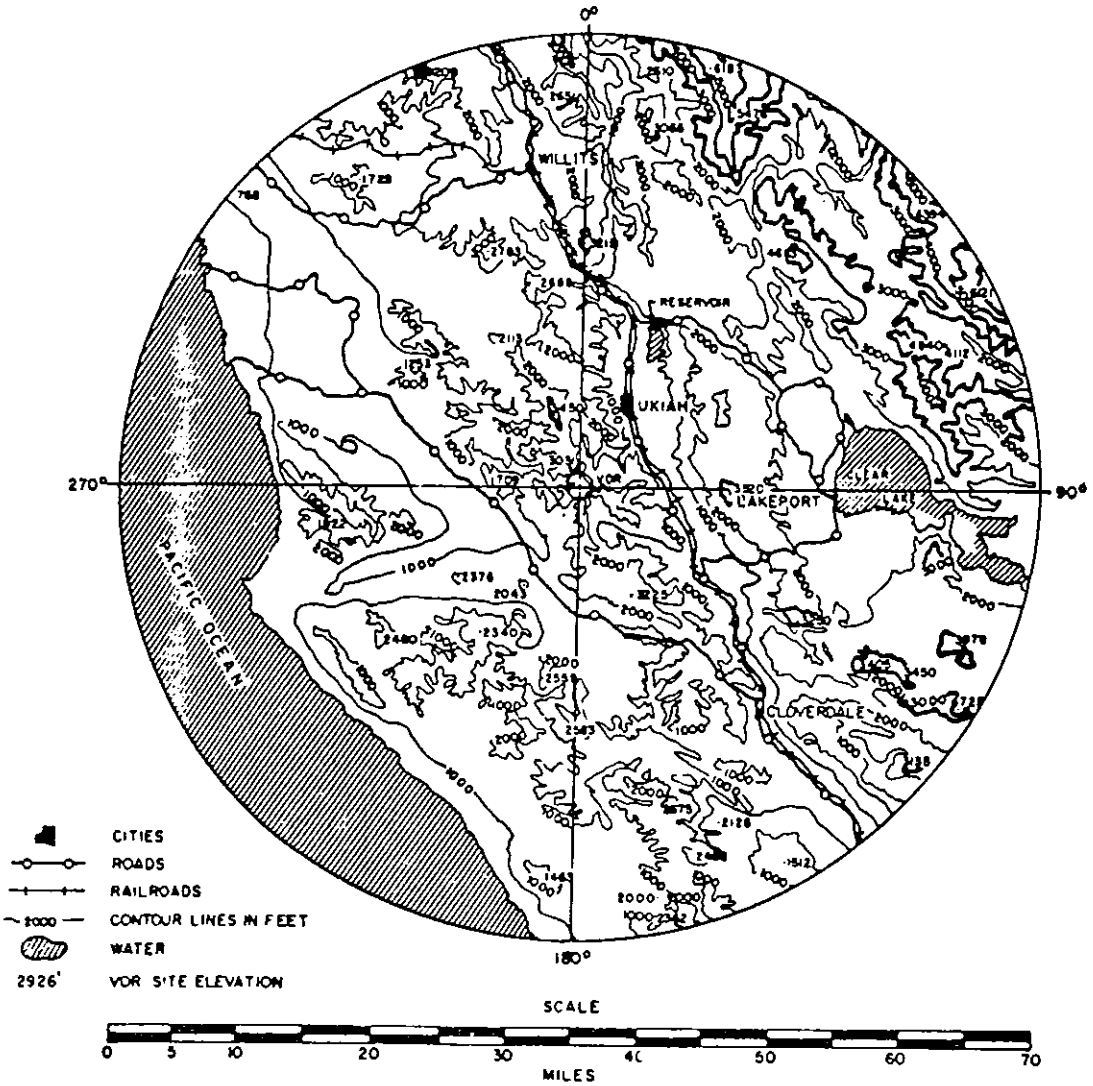

FIGURE 48. VICINITY SKETCH (35-MILE RADIUS) UKIAH, CALIFORNIA VOR

Section 22. Ukiah, California (continued)

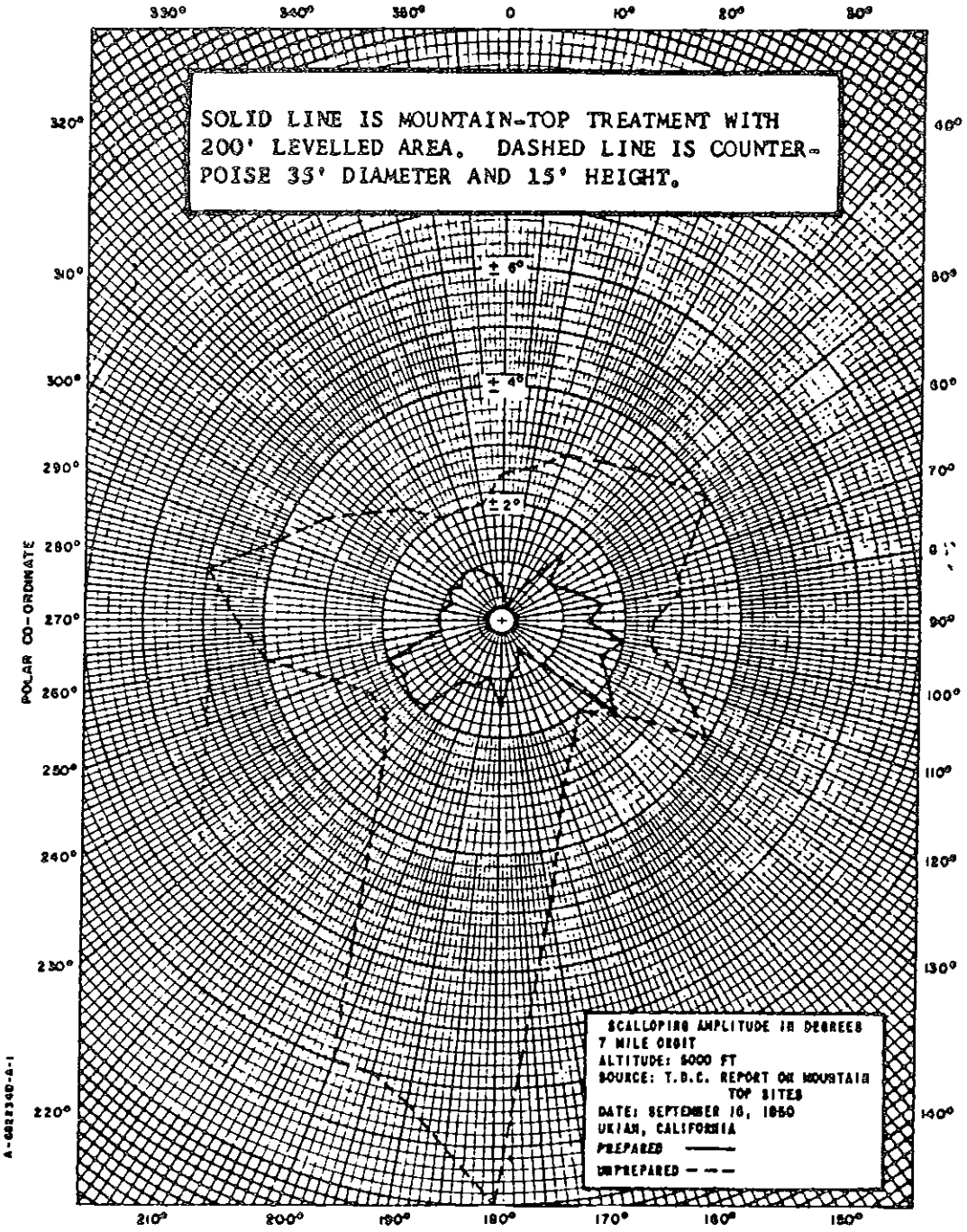

FIGURE 49. SCALLOPING AMPLITUDE

Section 23. Washington, DC

COMMENT: Indicator circuitry filters out the higher frequency scalloping signal thereby minimizing the importance of certain scalloping. The signals that caused the 1.28-Hz scalloping frequency at 310 degrees azimuth and the 0.51 Hz at 170 degrees azimuth are capable of causing course deviation indicator errors of ±6.7 degrees and ±3.7 degrees, respectively, for special cases of flying. Development of the airport and surrounding area has caused continued deterioration of VOR performance and has led to the need for conversion to Doppler.

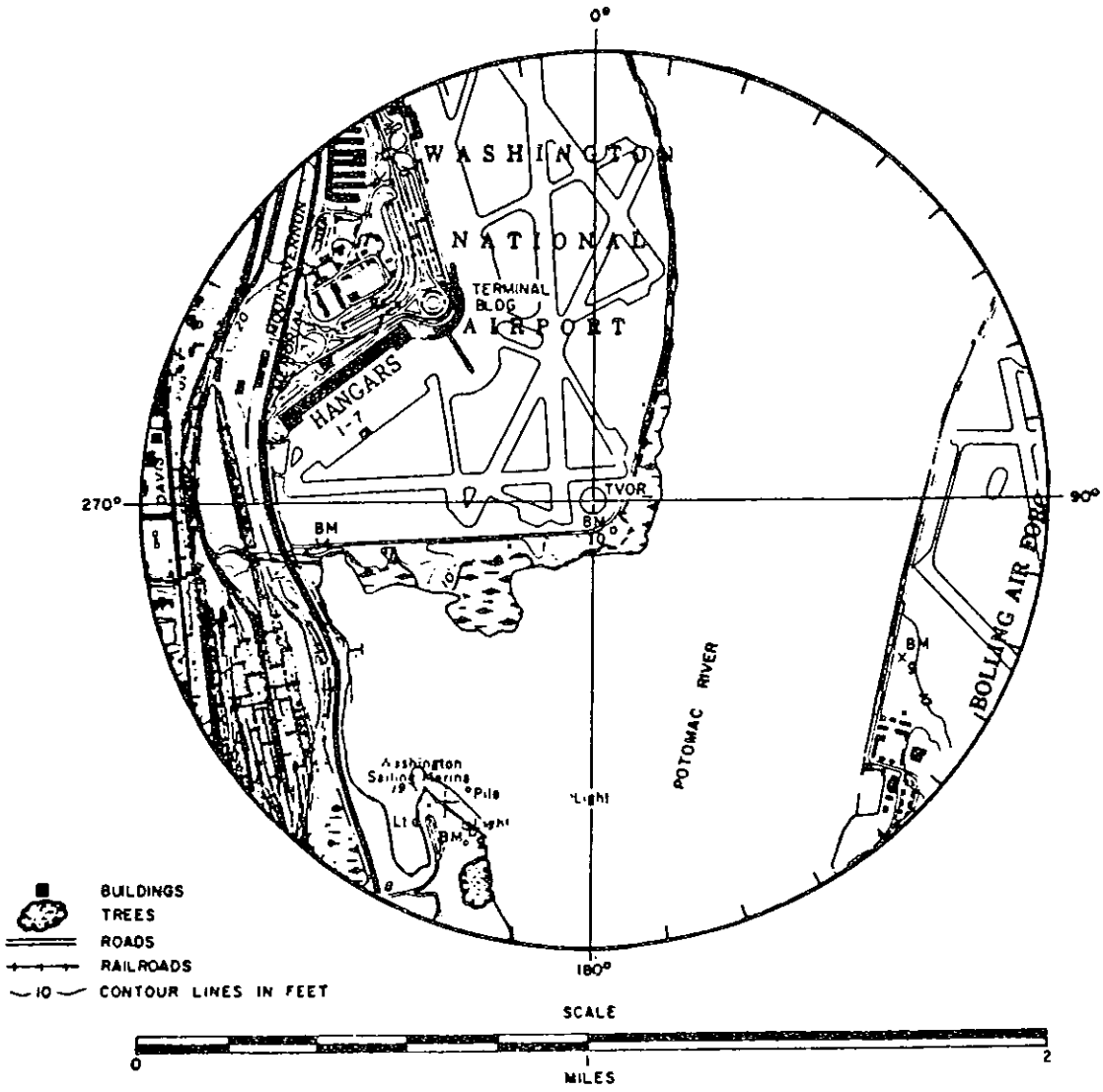

FIGURE 50. VICINITY SKETCH (1-MILE RADIUS) WASHINGTON, DC VOR

Section 23. Washington, DC (continued)

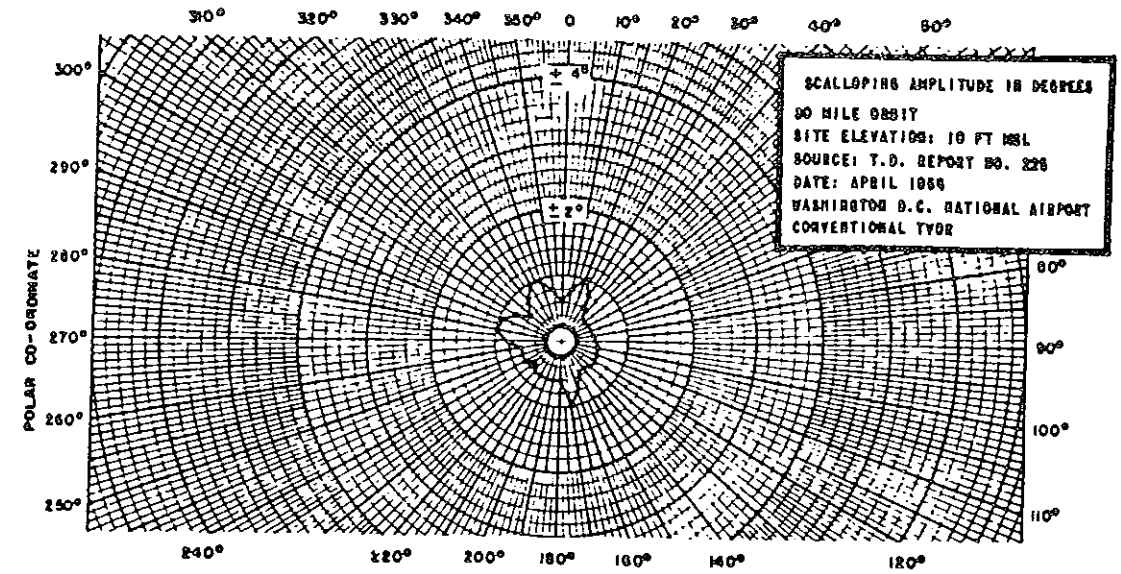

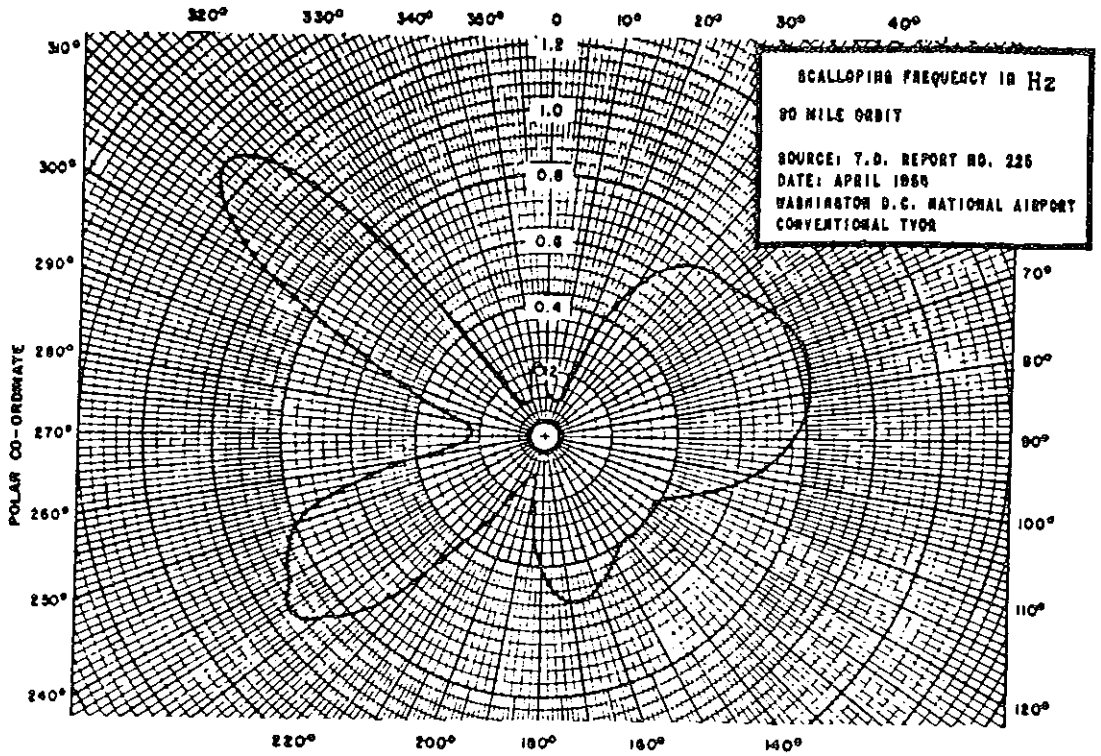

FIGURE 51. SCALLOPING AMPLITUDE AND FREQUENCY

Section 24. Wilmington, North Carolina

COMMENT: This is a good site. It would be an excellent site except for the power line 1100 feet north. The source of course scalloping can often be isolated and attributed to prominent objects in the vicinity of the facility such as power lines, buildings, or towers. A comparison is made between the course scalloping frequency observed and the computed course scalloping frequency of an assumed source of reflections.

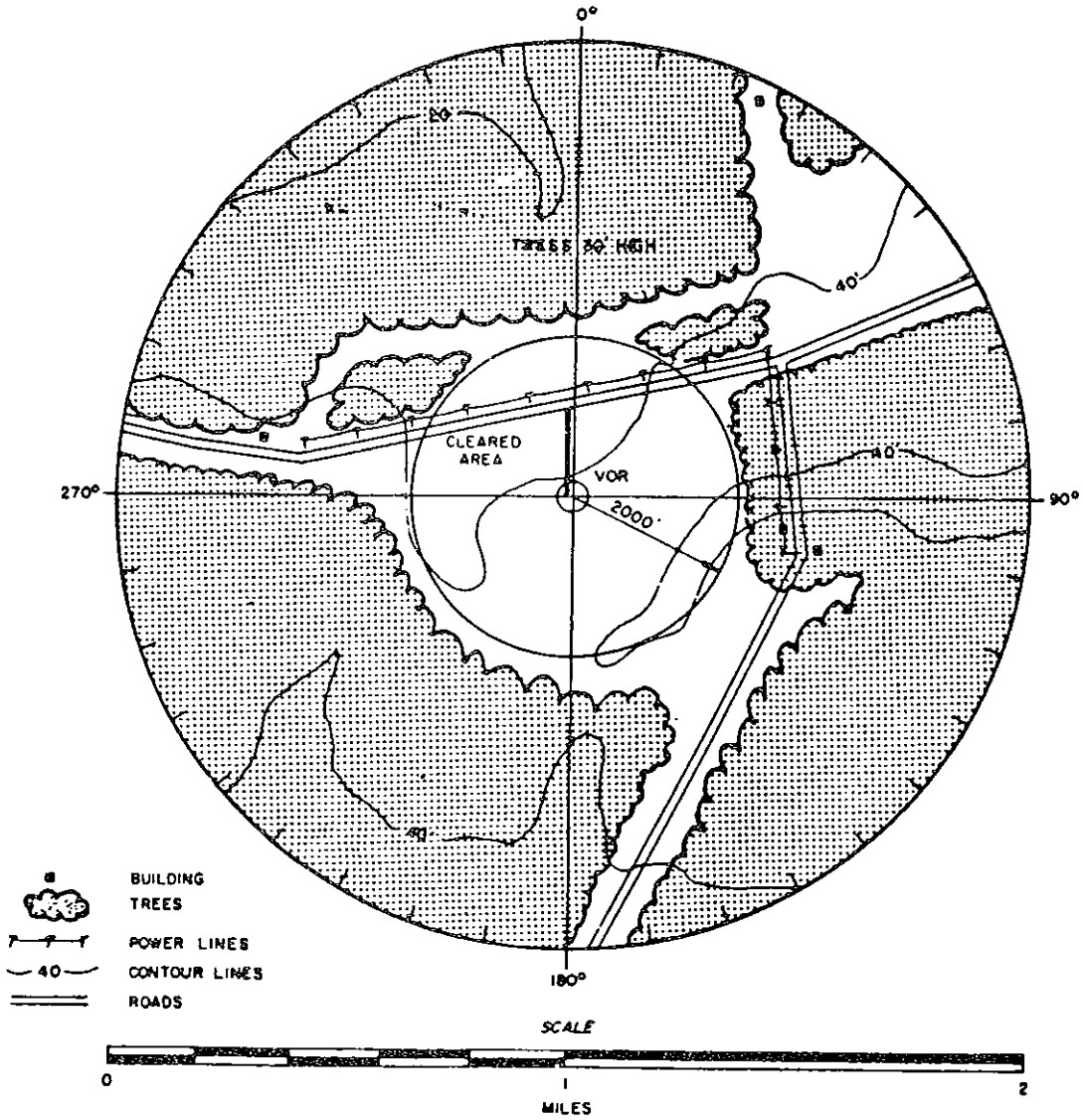

FIGURE 52. VICINITY SKETCH (1-MILE RADIUS) WILMINGTON, NORTH CAROLINA VOR

Section 24. Wilmington, North Carolina (continued)

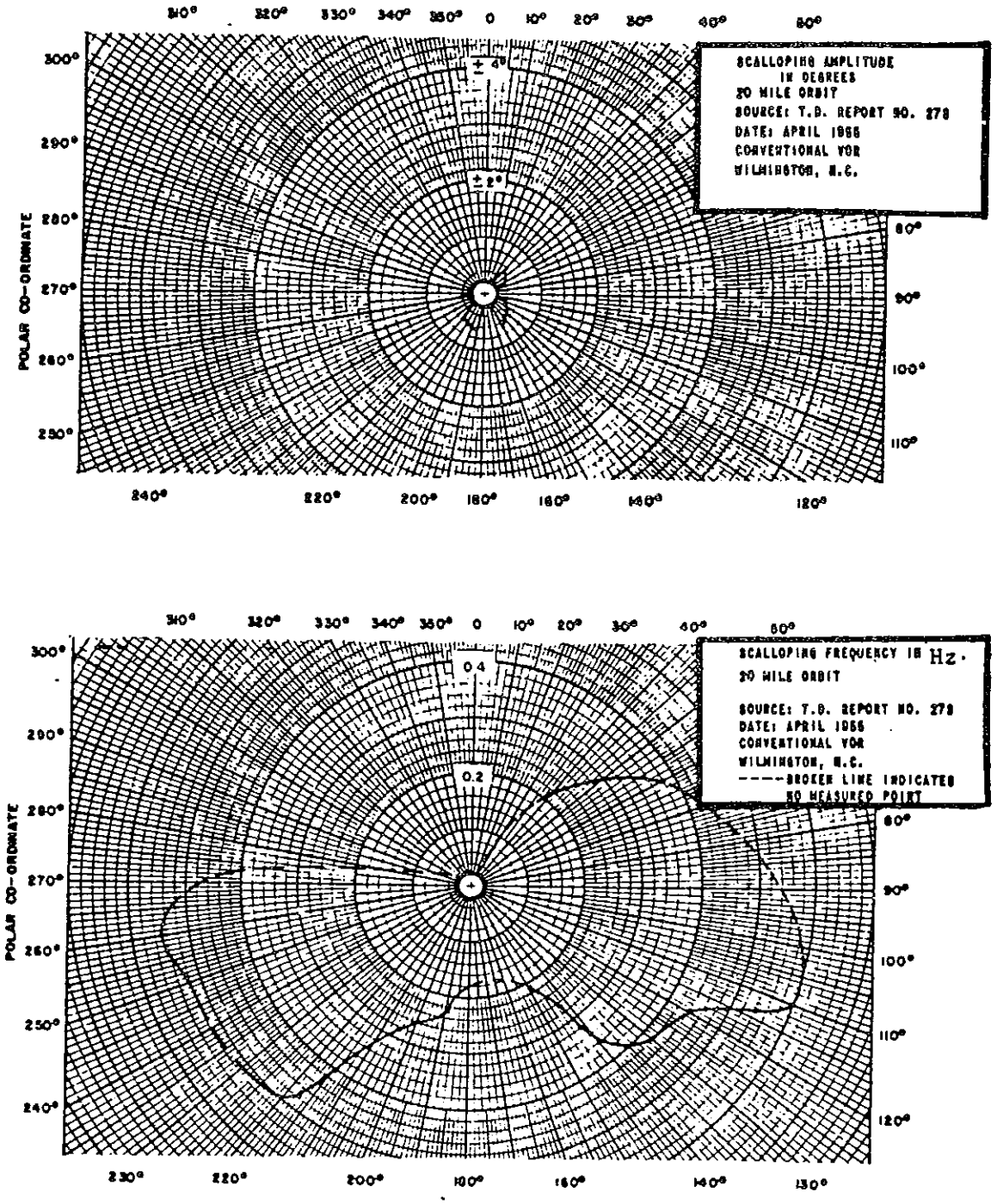

FIGURE 55. SCALLOPING AMPLITUDE AND FREQUENCY

Section 25. Summary of T.D. Report No. 278 (Effect of a Ground Discontinuity of VOR)

1. Introduction and Site Description. In the past, VOR sites have been chosen so that they are located far from large ground discontinuities. Because this practice limits the choice of sites, it was deemed desirable to conduct tests near a large ground discontinuity to determine more precisely its effects on the accuracy of the VOR. This report presents the results of such tests which were conducted near Port Washington, Wisconsin, along the shore of Lake Michigan, where a reasonably straight length of shoreline presented an almost vertical drop of approximately 125 feet from ground-to-water level. The site was relatively flat and devoid of trees and other obstructions for approximately 1000 feet in all directions. Approximately one-third of the site nearest the edge of the lake bank was plowed ground and the remainder was in a natural state. The surface of the lake was calm during the tests.

2. Summary.

a. These tests were conducted on top of a high bluff to determine the effect of an abrupt ground discontinuity on the course accuracy of a VHF omnirange. The results of these tests indicated that satisfactory operation of a VOR located in proximity to a sharp ground discontinuity is attained when the antenna is located 4 feet above the terrain and not less than 63 feet from the ground discontinuity. The tests also showed that the distance from the antenna to the ground discontinuity must be increased to 125 feet for satisfactory operation if the antenna is raised to a height of 14 feet above the terrain (see Table 1).

b. Deep nulls were evident in the vertical plane radiation patterns, and large variations of the course-deviation indicator and the TO-FROM indicator were observed in the nulls when the antenna was placed 13 feet from the discontinuity at a height of 14 feet. These variations were greatly decreased as the antenna was lowered to 4 feet above the terrain and when the distance of 13 feet from the ground discontinuity was maintained. When the antenna was moved away from the ground discontinuity, the nulls of the vertical radiation pattern were filled in and the variations of the course-deviation indicator were further decreased. The surface of the lake was calm during the tests, and flight recordings failed to reveal any irregularities which might be attributed to changes in the surface conditions of the lake.

3. Conclusions.

a. The errors caused by the ground discontinuity were small when:

(1) The VOR antenna was placed 14 feet above ground and 125 feet from the discontinuity, and

(2) The VOR antenna was 4 feet above ground and 63 feet from the discontinuity.

TABLE 1. BEARING ERRORS MEASURED IN THE NULLS*

Distance of Antenna From Ground Discontinuity (Feet)	Null Angle (Degrees)	Antenna Height (Feet)	Maximum Bearing Error in Nulls (± degrees)
13	1.5	14	7.0
13	3.0	14	2.5
13	4.5	14	5.0
13	6.0	14	2.5
13	1.5	4	0.25
13	3.0	4	0.375
13	4.5	4	0.5
13	6.0	4	0.5
125	1.5	14	0.25
125	3.0	14	0.00
63	1.5	4	0.25
63	3.0	4	0.00

* Altitude 1000 feet above ground.

b. The magnitude of the bearing error or scalloping becomes greater as the depth of the nulls in the vertical plane radiation pattern increases.

c. A close correlation was found between calculated and observed location of the lowest null in the vertical plane radiation pattern.

d. The vertical plane radiation patterns show that the effect of the ground discontinuity appears as a multiple-lobe structure superimposed on the normal pattern between elevation angles of approximately 0 to 10 degrees.

e. The depth of the lowest null decreases slowly with an increase in the distance between the VOR antenna and a ground discontinuity.

f. Higher angle nulls produced by the ground discontinuity filled in rapidly as the VOR antenna was moved from the ground discontinuity.

☆U.S. GOVERNMENT PRINTING OFFICE:1990 -273 -439/20575